How Hot is Hot? Tropical Ocean Temperatures and Plankton Communities in the Eocene Epoch

Emanuela Piga

School of Earth and Ocean Sciences

Cardiff University

Submitted in partial fulfilment of the requirements for the degree of:

Doctor of Philosophy (PhD)

February 2020

Al mio Tino e alla mia Mami,

Vi Voglio un Infinito di Bene

Abstract

Sea surface temperatures approach but rarely exceed 30°C in the Indo-Pacific Warm Pool, the hottest region of the modern open ocean. Climate models with reconstructed continental configurations and elevated CO_2 concentrations suggest that an Indo-Pacific Warm Pool has existed since the Mesozoic but virtually no reliable paleotemperature proxy data from the region exist, partly due to the rarity of finding exceptionally preserved foraminifera from deep time. Models suggest that temperatures in the Warm Pool may have become extremely hot, up to 40°C, during warm climate phases such as the early Eocene, potentially exceeding the tolerance limit of eukaryotic life.

As part of this study, a thorough exploration of "legacy" samples archived in the British Petroleum (BP) foraminiferal collections at the Natural History Museum, London, was conducted to search for material suitable for geochemical analysis. This yielded an important sample from the early Eocene of Papua New Guinea which was analysed as well as material from the late Eocene of Java that was collected in a previous expedition.

New oxygen and carbon isotope data are presented from both the early and late Eocene planktonic foraminifera, alongside Mg/Ca for paleotemperature reconstructions from the early Eocene. The study samples contained exceptionally well-preserved ("glassy") foraminifera but suffered from diagenetic infilling by late stage calcite. By the innovative method of crushing the samples and carefully separating foraminiferal test fragments from the infill it was possible to obtain reliable geochemical data from a variety of mixed layer and thermocline species, as well as one data point from benthic foraminifera for both the early Eocene and late Eocene. The successful outcome of the separation was confirmed by the infill consistently having lower $\delta^{18}O$ values than its associated original test, which is indicative of the influence of meteoric waters.

Eocene sea surface temperatures were derived from Papua New Guinea, and measured ~32-35°C, which is several degrees warmer than comparable early Eocene data from a similar latitude in Tanzania. Thus, the data support the presence of a moderately hot Warm Pool in the early Eocene which supported an abundant and diverse eukaryotic plankton community. Considering that modelled palaeogeographies positioned early Eocene Papua New Guinea at ~29°S, the results are still several degrees warmer than modern Warm Pool temperatures. This suggests there were even higher temperatures at the core of the early Eocene Warm Pool. Late Eocene temperatures were retrieved

from Java which was positioned in the tropics (0.54°N), and recorded sea surface temperatures of 37°C while still hosting a diverse and abundant foraminiferal assemblage.

When simulating the Eocene temperatures on the palaeoclimate models under 1120 ppm of atmospheric CO_2, the results from late Eocene Java matched the model outputs better than early Eocene Papua New Guinea, as the temperatures of the latter were underestimated to a greater extent by the models. This may be due to either the presence of higher than 1120 ppm atmospheric CO_2 concentrations in the early Eocene, which would have increased the simulated temperatures of the climate model, or a higher climate sensitivity during the early Eocene due to the intensified hydrological cycle typical of this interval which would have increased the amount of tropical cyclones transferring heat from the tropics to higher latitudes.

Acknowledgements

I would like to start my acknowledgements by thanking my supervisors. First, my supervisor Paul Pearson. It has been an incredibly enriching experience carrying out this project with you and your remarkably immense knowledge on the subject! It has also been very fun doing fieldwork together in Tanzania, including the "accidental" adventures that made it all more colourful and memorable. Many thanks also to my supervisor Carrie Lear, especially with your help on the trace metal data. I am also very grateful to my co-supervisors Tom Hill and Stephen Stukins who are based at the Natural History Museum in London and with whom I spent the first 1.3 years of this project. Thank you for warmly welcoming into the PhD world and for all the help on accessing the microfossil collection of the NHM, as well as all the morning coffee sessions of the team, complaining about the London traffic and putting up with my coffee-induced euphoria! I must also thank my co-supervisor from the University of Bristol Dan Lunt, who kindly hosted me in Bristol for two months during my last year and introduced me to palaeoclimate modelling so that I could run my own simulations.

Secondly, I want to especially thank two people who have been both moral and academic mentors to me and have become very close friends of mine. They have followed me through all the happy and difficult moments of this project and I am very, very grateful that they have entered my life! I would like to call them the NHM mentor, and the Cardiff mentor. The former is Lyndsey Fox, you have always been so kind and generous with me since the first day we met. Only we know how much fun we had in the NHM office, talking about anything and surely also a bit of foraminiferal taxonomy. Even when I left Cardiff you have been a great friend and a shoulder to lean on when I needed a chat. You are truly wonderful. The Cardiff mentor is, obviously, Sindia Sosdian. Thank you for being just you, so gentle, patient, and a great listener. You have also persistently stood by me during the last phase hence the most difficult part of this project, and I cannot thank you enough for all your moral support, you might never know how much it has helped me. I am very excited to going back and sharing fun memories with you soon!

Another person that has been extremely awesome, patient and selflessly helpful is Alexander Farnsworth at the University of Bristol. You have helped me so much on the modelling part while in Bristol and after I left, always being genuinely available when I was frustratingly stuck with the code and always willing to share exciting discussions together, thank you so much Alexander. Excited for more Science together soon! You

are the clearest example to me to what scientific collaborations should look like, and it has been very inspiring to experience it.

I also want to express my gratitude to all the technicians who helped me in different ways during the project. Thank you Alex Ball and Tomasz Goral from the NHM and Duncan Muir from Cardiff University for teaching me how to use an SEM machine and take beautiful images of the foraminiferal samples and make them look amazing, even when they were infilled! Many thanks to Sandra Nederbragt for all the stable isotope analyses, Anabel Morte-Ródenas for the trace metal analyses, and Lindsey Owen for providing equipment in the picking laboratory and for letting me move to a warmer laboratory towards the end!

Massive thanks to the Cardiff PhD community, it has been very fun sharing the Palaeo-office and the unimaginable amount of gossip, tea, and biscuits with you all! An especially deep gratitude goes to Emma Bennett, thank you so much, you only know how much of a moral and physical support you have been in these last few months of writing up!

Thank you also to the Postdocs of Cardiff University Eleanor and Flavia with whom I exchanged enlightening conversations on the Eocene. El thank you so much also for your help in the laboratory discussing Eocene taxonomy and Flavia, grazie mille per aiutarmi con l'identificazione dei foraminiferi bentonici! Thank you also to Rehemat for chats on the Eocene and checking up I was not going more mad than I usually am. I am obviously super grateful to all my friends scattered around the world that have had to put up with me throughout this challenging journey, you are all so very special and I am so excited to become a fun person with you again!

I would like to thank also non-human beings and things that, without knowing, have really helped me and made me giggle in the last months of the project. Thank you, scarily massive popcorn bag that I found after an Open Day at the weekend at University, you have literally lasted so long in the office and I could crunch you whenever I was feeling like eating anything! You have also caused a lot of laughter to the people that entered the office and saw you. Thank you also to the lovely newly moved in neighbour's cat who has been in the house in the last few days of my write-up and kept me company quietly, without any judgement and ready for cuddles anytime!

Lastly and most importantly, I am eternally grateful to my Parents, whom I love very much. Their unconditional love and belief in me have supported me morally and mentally throughout my life. Thank you for instilling in me the determination and tenacity since a

young age, and reminding me of both during the difficult times of a PhD student. Thanks to you I have embarked the study and work journey abroad from a young age, supporting me on every decision I made and making me believe in myself a bit more. You are truly my favourite people on this planet, and not only as wonderful Parents, but also as the bestest friends anyone could ask for!

List of Abbreviations, Acronyms, Initials, and Symbols

$[CO_3^{2-}]$	Carbonate ion concentration
BWT	Bottom water temperature
CH_4	Methane
CO_2	Carbon dioxide
DI H_2O	De-ionised water
DIC	Dissolved inorganic content
DSDP	Deep Sea Drilling Project
E.E.	Early Eocene
EECO	Early Eocene Climatic Optimum
EOGM	Eocene-Oligocene Glacial Maximum
EOT	Eocene-Oligocene Transition
ICP-MS	Inductively coupled plasma mass spectrometer
IODP	International/Integrated Ocean Drilling Program
IPWP	Indo-Pacific Warm Pool
K/Pg	Cretaceous/Paleogene boundary
Ma	Million years ago
Mg/Ca_{sw}	Mg/Ca composition of seawater
Myr	Million years
OMZ	Oxygen minimum zone
pCO_2	Atmospheric carbon dioxide level measured as partial pressure
PETM	Paleocene-Eocene Thermal Maximum
PNG	Papua New Guinea
ppm	Parts per million
PSU	Practical salinity unit
RSD	Relative standard deviation
SEM	Scanning Electron Microscope
SMOW	Standard Mean Ocean Water
SST	Sea surface temperature
VPDB	Vienna Pee Dee Belemnite
$\delta^{13}C$	Carbon isotope composition
$\delta^{13}C_{DIC}$	Carbon isotope composition of dissolved inorganic carbon
$\delta^{13}C_{sw}$	Carbon isotope composition of seawater
$\delta^{18}O$	Oxygen isotope composition
$\delta^{18}O_{sw}$	Oxygen isotope composition of seawater

Table of contents

Chapter 4: Sea surface temperatures and water column reconstruction from the early Eocene of the Moogli mudstones, Papua New Guinea …………......................51

Chapter 1

Introduction

Chapter 1

1 Introduction

1.1 Background to the Project

Simulating past climates with fully coupled atmosphere-ocean general circulation models (GCMs) is of paramount importance given the current and projected rise in atmospheric carbon dioxide (CO_2), as their ability to predict the future climate can be tested against geological data (Kiehl and Shields, 2013; Lunt et al., 2015). Projections indicate that if humans continue to burn fossil fuels at the current rate, then atmospheric CO_2 levels will reach 800–1100 ppm by the year 2100 (Solomon et al., 2007; Kiehl, 2011). Studying the Earth's warm past climates therefore provides rich observational and modelling opportunities to better understand how the Earth operates in a warm climate regime (McInerney et al., 2011). Particular attention has been drawn to modelling the Eocene Epoch and particularly the early Eocene, being the time interval within the Eocene that shows most climatic similarities to projections of the end of the 21st century and beyond (Lunt et al., 2012), and with global mean surface temperatures much warmer than modern (John et al., 2013). Moreover, CO_2 concentrations were higher than present and estimate from as low as 300 ppm to more than 4400 ppm (Royer et al., 2001; Yapp, 2004; Pagani et al., 2005; Sluijs et al., 2006; Pearson et al., 2007; Beerling and Royer, 2011) and as high as ~4700 ppm (Fletcher et al., 2008).

In particular, the tropics (30°N–30°S) make up half of Earth's surface area and play a pivotal role in determining past variations in global mean temperature and the sensitivity of the latter to forcing factors such as greenhouse gas (hereinafter GHG) concentrations (Huber, 2012). In fact, global climate patterns are especially sensitive to tropical sea surface temperature (SST) distributions, as the atmosphere-global ocean circulation is driven by temperature gradients, whose strength determines the global heat distribution (Schneider et al., 1997; Cane, 1998; Rind, 1998; Huber and Sloan, 2000). Thus, knowledge of how hot such crucial areas of the planet were during the Eocene greenhouse and how SST gradients have changed through time is central to understanding long-term global climate patterns, including modes of heat transport and the effects of different levels of radiative forcing (Pierrehumbert, 2002; Caballero and Langen, 2005). Previous work suggested that if SSTs were truly ~35°C in the tropical

regions during the Eocene (Pearson et al., 2007), then the currently warmest tropical region known as the Indo-Pacific Pacific Warm Pool (IPWP) must have been much hotter (Huber, 2008; Inglis et al., 2015).

Earlier Eocene model-data comparisons yielded a significant mismatch whereby geochemical proxies recorded mid-to-high latitudes warmer than today and winters above freezing (Huber, 2008; Huber and Caballero, 2011), while the extent of warmth for SSTs was not as accentuated (Shackleton and Kennett, 1975; Zachos et al., 1994; Bralower et al., 1995; D'Hondt and Arthur, 1996; Crowley and Zachos, 2000; Dutton et al., 2005). An excessive heat flux would therefore be required to flatten latitudinal gradients sufficiently (Pearson et al., 2001), and all climate models to date have failed to simulate such a climate regime without overheating the tropics that characterises this time interval, and which is also known as the Early Eocene equable climate problem (Sloan and Barron, 1990; Caballero and Huber, 2013; Lunt et al., 2013; Sagoo et al., 2013). Strong radiative forcing in simulations (Shellito et al., 2003; Kump and Pollard, 2008) produces tropical SSTs warmer than traditional reconstructions (Zachos et al., 1994; Crowley and Zachos, 2000) and even hotter than these revised reconstructions (Pearson et al., 2007; Huber, 2008).

1.2 The Eocene Epoch

The "Greenhouse" world of the Eocene Epoch (~55.5-33.7 Million Years Ago, hereinafter Ma) was characterised by global mean temperatures significantly higher than today (Wing and Greenwood, 1993; Zachos et al., 2001; Huber, 2012), ice-free poles (Port and Claussen, 2015) reduced temperature seasonality (Eldrett et al., 2009; Huber and Caballero, 2011), higher than modern GHG concentrations (DeConto and Pollard, 2003; Doria et al., 2011), weaker latitudinal temperature gradients (Greenwood and Wing, 1995; Huber and Sloan, 2001), and warmer tropical temperatures (Pearson et al., 2001, 2007; Huber, 2008), as recorded by a wide variety of records in both terrestrial and marine realms. The very different-from-modern land-sea distribution (Ramstein et al., 1997; Sewall et al., 2000) was the result of the major physical changes the Earth was undergoing by the end of the Paleocene and onset of the early Eocene (Anderson et al., 2007); a mode of maximum continental dispersion (Anderson et al., 2007); major tectonic events such as the collision of India with Asia, and the subsequent uplift of the Himalayas and Tibetan plateau (Barron and Peterson, 1991; Raymo and Ruddiman, 1992; Berner, 1994; Mikolajewicz and Crowley, 1997; Zachos et al., 2001) (Fig. 1.1).
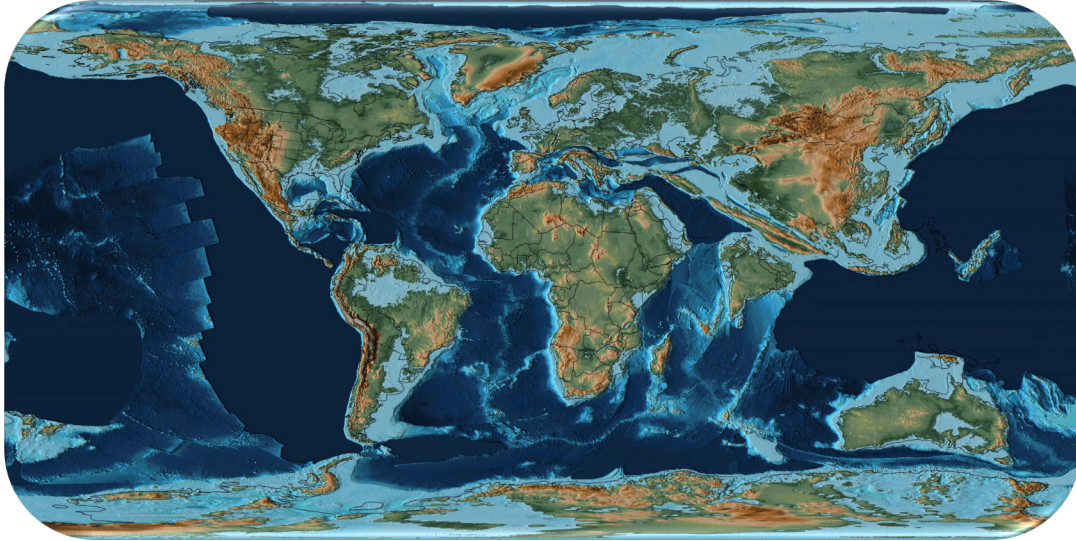
Figure 1.1: Global reconstruction of the tectonic distribution of the Earth during the early Eocene (~52.2 Ma) (Image taken from: Scotese, 2013).

A general trend of relatively constant tropical temperatures and more sensitive high-latitudes during the Eocene (Zachos et al., 1993; Pearson and Palmer, 2000; Bijl et al., 2009) was interrupted by various climatic aberrations, with the most pronounced warming trend occurring in the early Eocene characterized by the Palaeocene-Eocene Thermal Maximum (PETM, ~56 Ma), and peaking with the Early Eocene Climatic Optimum (EECO, ~53 to 51 Ma) (Zachos et al., 2001; Bohaty and Zachos, 2003; Edgar et al., 2010; Anagnostou et al., 2016) (Fig. 1.2). The EECO was followed by a 17-My-long cooling trend, which ultimately resulted in the present glaciated Earth with the onset of the early Oligocene (~35 to 34 Ma) (Pearson and Palmer, 2000).
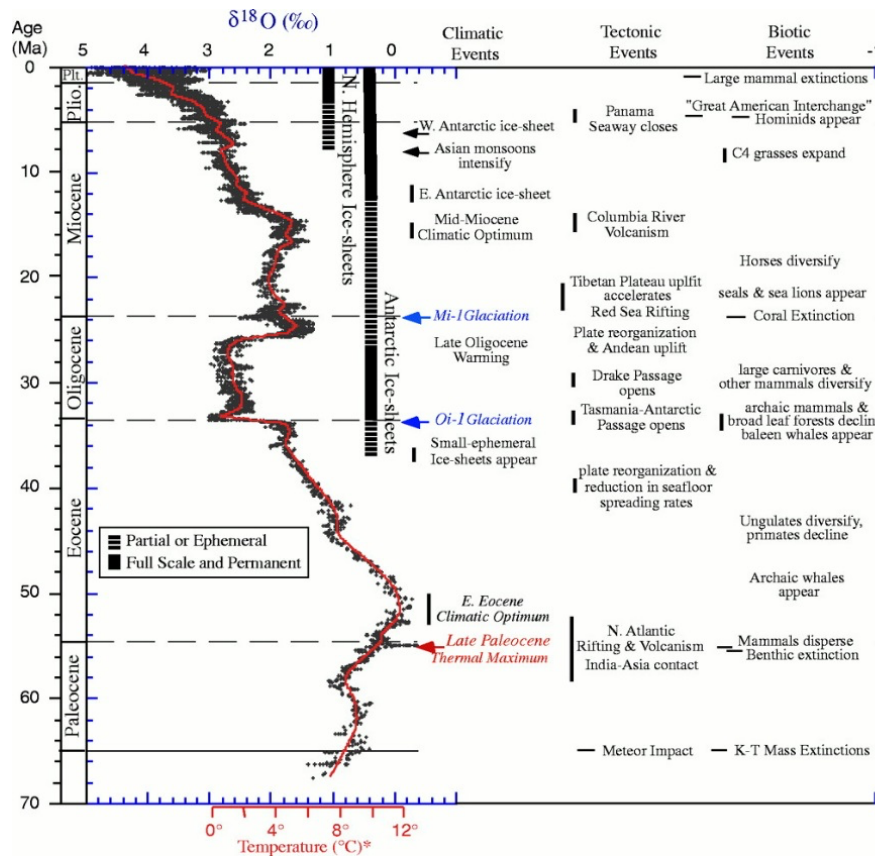
Figure 2.2: Global deep-sea oxygen and carbon isotope records based on data compiled from more than 40 DSP and ODP sites. The purpose of this figure is to simply give an overview of the mean climate pattern before the Eocene, during the Eocene, and following this Epoch (Image taken from Zachos et al., 2001).

This erratic trend is also reflected by CO_2 concentrations which, despite declining over this interval (Pagani et al., 2005), were significantly higher than modern (Royer et al., 2001) (Fig. 1.3). According to recently revisited estimates, CO_2 levels peaked during the EECO at concentrations ≥1000 ppm (Jagniecki et al., 2015; Anagnostou et al., 2016). After this, they experienced an erratic decline between 55 Ma and 40 Ma that may have been caused by reduced CO_2 outgassing from ocean ridges, volcanoes and metamorphic belts, as well as increased carbon burial (Barron, 1985; Creber and Chaloner, 1985).

Enhanced volcanic outgassing of CO_2 may have been supplied by regional metamorphism and magmatism in parts of the Himalayan belt (Pearson and Palmer, 2000), and North America (Kerrick and Caldeira, 1998). Another source of CO_2 may have been the oxidation of methane released from storage either in wetlands (Sloan et al., 1992) or from large seafloor gas hydrate reservoirs, as may have occurred during the PETM and in the early Eocene (Dickens et al., 1995).
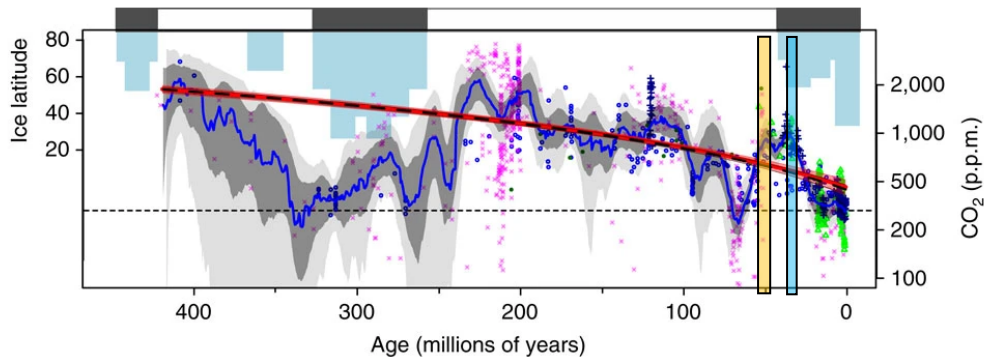
Figure 1.3: Global CO_2 record for the last 420 million years. Image taken and modified from Foster et al. (2017), who compiled latitudinal extent of continental ice deposits (blue bars), as well as multi-proxy atmospheric CO_2 (in ppm; symbols) from the literature (the different authors with the associated displayed data in Supplementary Data 1 of Foster et al., 2017). Each different proxy for CO_2 reconstructions is represented by a specific symbol and colour: leaf stomata (blue circles); pedogenic carbonate $\delta^{13}C$ (pink crosses); boron isotopes in foraminifera green triangles); liverwort $\delta^{13}C$ (dark blue filled circles); and $\delta^{13}C$ of alkenones (dark blue crosses). The purpose of this figure is to simply give an overview of CO_2 concentration evolution in the last 420 million years (for more information on the meaning of each line, please refer to Figure 1's caption in Foster et al., 2017). The vertical shaded bars represent the two main focus intervals of this PhD Study: the Ypresian Stage (~56 to 47.8 Ma) in the early Eocene (orange shaded bar), and the Priabonian Stage (~37.71 to 33.9 Ma) in the late Eocene (blue shaded area).

1.2.1 Modelling the Eocene Epoch

Most model-data comparisons focus on temperature because this is the primary climate variable (Anderson et al., 2007; Lunt et al., 2012). Half of Earth's surface area is in the tropics, so changes and uncertainties in tropical temperatures dominate any climate sensitivity estimate (Huber, 2008). Full complexity climate models simulate the dynamics and magnitude of change of the three-dimensional ocean-atmosphere circulation, and are referred to as atmosphere-ocean general circulation models (AOGCMs). They have become increasingly sophisticated in recent years and their approach is advantageous when the physics governing the important dynamics are unclear, in which case, it is best to include all potential processes for the most complete window into past dynamics. Models require boundary conditions in order to run, and these can be derived from geological observations or proxy-based reconstructions, as well as inferences or calculations based on physical, biological or geochemical arguments (Anderson et al., 2007).

Over the years one major challenge has been to reproduce the small equator-to-pole temperature gradients indicated by the early Eocene palaeoclimate proxies (Barron and

Peterson, 1991; Huber and Sloan 2000; Huber and Sloan, 2001; Huber and Caballero, 2011), that is a means of warming the polar regions more than warming the tropics under Eocene conditions, in the absence of strong snow, sea ice, terrestrial ice feedbacks, and the presence of reduced high-latitude seasonality (Barron, 1987; Huber and Sloan, 2001; Huber, 2008; Tindall et al., 2010; Sagoo et al., 2013), since solely increasing greenhouse gases significantly warms both equatorial and polar regions (Barron, 1987; Huber, 2008). Due to the lack of consistency between model results, oceanic data, and terrestrial data alongside the interpretative uncertainties associated with the proxies, many physical mechanisms have been proposed to solve the early Eocene equable climate problem in climate models, which include increased ocean heat transport, polar stratospheric clouds related to enhanced atmospheric methane (CH_4), as well as opening passageways in the Arctic (Kiehl and Shields, 2013).

In particular, increased poleward heat transport by the ocean or atmosphere has long been considered a solution to these problems (Barron, 1987; Huber, 2012; Lunt et al., 2012). However, the supposition of low thermal gradients propelled by enhanced heat transport is recognized as a climate conundrum: that is, enhanced poleward heat transport is necessary to maintain low meridional temperature gradients, but small meridional temperature gradients reduce rates of poleward heat transport. Moreover, considering that the newer reconstructions have raised polar temperatures (Sluijs et al., 2006; Bijl et al., 2009; Hollis et al., 2009) even more than tropical ones, a mystery still persists. This failure represents one of the greatest challenges in palaeoclimate dynamics because it suggests that climate models fail to reproduce the leading order feedbacks in a warmer world (Valdes, 2011).

However, it has also been argued that tropical temperatures may have been higher than previously considered, which would allow for a purely enhanced greenhouse gas explanation for warmer climates (Huber, 2008; Heinemann et al., 2009; Huber and Caballero, 2011). Following this, the studies which confirmed warmer tropical Eocene temperatures were more in line with GCM simulations even if CO_2 forcing was set very high (Huber, 2008; Tindall et al., 2010; Huber and Caballero, 2011; Robert et al., 2011). With this thought in mind, different studies set CO_2 levels to 16 times pre-industrial concentrations of CO_2 (Lunt et al., 2012; Sagoo et al., 2013) and found that the results matched the proxy data to a greater extent. Huber and Caballero (2011) run a model simulation referred to as EOCENE-4480, with 4480 ppm CO_2 that was meant to represent the early Eocene, even if it does not imply that 4480 ppm was considered to be the actual value for the early Eocene; it was just the radiative forcing necessary for a climate model with a weak climate sensitivity to achieve climate conditions close to those

of the early Eocene. The results were SSTs about 35°C, in strong agreement with proxies (Pearson et al., 2007; Schouten et al., 2007; Huber, 2008; Jaramillo et al., 2010) and winter temperatures in the EOCENE-4480 case remained above freezing, as one of the "features" of the equable climate problem in regions where both quantitative and qualitative proxy data indicate frost intolerance (Markwick, 1998; Collinson and Hooker, 2003; Markwick, 2007; Kvacek, 2010).

Recently, Lunt et al. (2012) carried out an Eocene coupled model inter comparison project (EOMIP), which comprises of a total of four models: 1) HadCM3L (Lunt et al., 2010), 2) ECHAM5/MPI-OM (Heinemann et al., 2009), 3) CCSM3 (Hollis et al., 2009; Liu et al., 2009; Huber and Caballero, 2011), and 4) GISS ModelE-R (Roberts et al., 2009). Each group used different palaeogeographic boundary conditions, multiple CO_2 levels to simulate Eocene climates, and a reduced meridional surface temperature gradient compared with pre-industrial, which reduced further as CO_2 increases (polar amplification). The best Eocene model simulations that best match the proxies vary between 2 times and 16 times pre-industrial CO_2 concentrations, demonstrating the need for better constraints on the actual CO_2 concentrations during the early Eocene. The best match to Eocene proxy data was found at 16 times pre-industrial CO_2 concentrations, although the model and SST data only just overlap for their area ($\delta^{18}O$ and TEX_{86}). However, if a seasonality bias in the proxies is taken into account as well as a more realistic representation of the vegetation, the model-data agreement improves further (Hollis et al., 2012; Lunt et al., 2012). Moreover, they found that the differences in climate sensitivity due primarily to a combination of GHG effect, surface albedo effect, and cloud feedbacks explained the differences between models, rather than solely by CO_2. In fact, even though studies relied on the radiative forcing in the form of very high CO_2 levels which seemed to resolve the equable climate problem without running too far afoul of other constraints, this does not necessarily mean that CO_2 was the only major forcing factor (Pagani et al., 2005; Huber and Caballero, 2011). They did not address whether the enhanced radiative forcing was due to CO_2, CH_4, other GHGs, novel cloud feedbacks, or other "missing" factors (Heinnemann et al., 2009; Huber and Caballero, 2011). Methane concentrations, for example, could have been much higher in the early Eocene and clouds may have functioned differently (Sloan et al., 1992). There are currently no proxies for either of these factors, which is one reason why relatively few studies have incorporated them, and for example in their model simulations Sagoo et al. (2013) simply assumed the other GHGs to be the same as present-day values. Thus, the lack of constrained CO_2 concentrations in this interval has paved the way for searching other significant parameters that affect the temperatures and help maintain

the conditions set by the equable climate problem. This is also because climate sensitivity comprises of both long-term feedbacks, which are related to slow processes such as ice sheets and vegetation, and those processes which adjust on the time scale of decades, such as clouds, water vapour, snow cover, and sea ice, also known as fast feedbacks (Caballero and Huber, 2013). Palaeo-data estimate will include a fraction of both fast and slow feedbacks and this is the challenge of models to find the compromise on the influence of both feedbacks. Over very long time scales, all feedbacks will respond and so long-term data will inform us about the Earth System sensitivity. In fact, Caballero and Huber (2013) run different early Paleogene simulations and showed that the changes in the boundary conditions such as removal of ice sheets and replacement with vegetation as well as changes in aerosols (fast feedbacks) have large impacts on global mean temperature (Caballero and Huber, 2013). They have also found that while slow feedbacks play an important role in maintaining high temperatures during the early Paleogene, fast feedbacks sharply increase in importance as the climate warms (Caballero and Huber, 2013).

Another study by Kiehl and Shields (2013) indicates that past differences in cloud properties may be an important factor in accurately simulating past warm climates; the additional warming resulting from this incoming radiation from such a mechanism would imply lower required atmospheric CO_2 concentrations which may help alleviate the current disparities with CO_2-proxy data for the Eocene (Tindall et al., 2010; Huber, 2012). In light of these results, Lunt et al. (2015) confirmed with their model simulations that strong albedo and emissivity feedbacks amplify the initial forcing, meaning that CO_2 levels do not have to be set very high as cloud cover and cloud albedo lead to warming both globally and at the poles, as well as reducing the equator-to-pole temperature gradient.

Sagoo et al. (2013) has also explored the impact of variables such as uncertain orography on Eocene climate, suggesting that uncertain palaeogeography tends to increase regional uncertainty in modelled climate. In fact, a number of modelling studies have demonstrated that the ocean's overturning circulation, heat transport, and resulting temperature distribution are somewhat sensitive to changes in ocean gateways (Mikolajewicz and Crowley, 1997; Huber, 2000).

1.3   The Indo-Pacific Warm Pool

The Pacific ocean-atmosphere system is governed by a delicately complex balance of dynamical feedbacks (Dijkstra and Neelin, 1995; Jin, 1996, Liu and Huang, 1997). Conceivably, the region's climate could undergo major, long-term reorganizations (Pierrehumbert, 2000), which could strongly modulate global change. The Indo-Pacific Warm Pool (IPWP) is the warmest body of open-ocean water on Earth (Stott et al., 2004; Cheng et al., 2008; Wang and Mehta, 2008; Abram et al., 2009). Defined as the region where mean SST is higher than 28°C (Yan et al., 1992), 29°C (McPhaden and Picaut, 1990; Cravatte et al., 2009; Lin et al., 2013; Holstein et al., 2017) or averaging 30°C during the modern northern hemisphere summer (Stott et al., 2004), the IPWP spans from the western tropical Pacific Ocean, through the Indonesian archipelago, and across the eastern tropical Indian Ocean (Abram et al., 2009). The vigorous atmospheric convection that occurs over the warm pool influences the global distribution of heat and water vapour as it stores a vast amount of thermal energy, and therefore serves as a thermal engine to drive the ocean-atmosphere circulation (Lin et al., 2013) (Fig. 1.4).
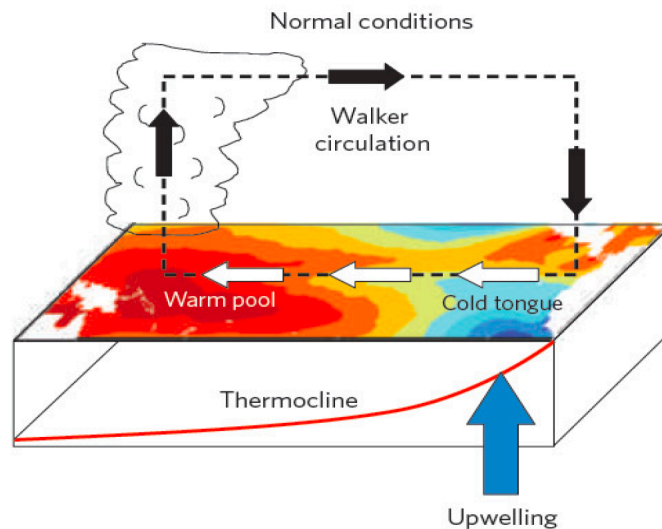
Figure 1.4: A schematic showing the mean climate conditions of the Tropical Pacific and its ocean-atmosphere system during normal conditions. The red colour represents the warm areas, while the blue colour stands for the cold areas. The trade winds and Walker circulation are shown in white arrows and the descending black arrows, respectively. The arrows also indicate the mean position of convection (ascending and descending black arrows) and the mean upwelling position (blue arrow). The red line represents the thermocline, which is shallower in the eastern Pacific Ocean, and progressively becomes deeper towards the western Pacific Ocean.

In fact, studies argue that the Pacific may have been responsible for ~90% of global ocean heat transport during the Palaeogene (Huber and Sloan, 2001; Hollis et al., 2009). The prevailing easterly surface winds drive an east-west tilting of the thermocline, which causes cool sub-thermocline water to upwell in the east, and no upwelling in the west due to the build-up of warmer hence lighter waters at the surface (Huber and Caballero, 2003). The resulting gradient in SST between the Cold Tongue in the east and the Warm Pool in the west drives an east-west overturning circulation in the atmosphere, known as the Walker cell, which enhances surface easterlies and produces further upwelling (Huber and Caballero, 2003). This positive feedback, first recognized by Bjerknes (1969), controls both the time-mean state (Dijkstra and Neelin, 1995; Jin, 1996; Liu and Huang, 1997) and the interannual variability (Neelin et al., 1998) of the tropical Pacific.

Furthermore, climate variability in the IPWP region is influenced by major climate systems such the El Niño-Southern Oscillation (ENSO) (Rasmusson and Wallace, 1983; Trenberth and Shea, 1987; Abram et al., 2009) and the Asian–Australian monsoon (Webster et al., 1998). Because of this, changes in the temperature, size and position of the IPWP have a profound effect on global climate (Gagan et al., 2004), therefore understanding their behaviour and interplay as part of such a complex coupled ocean-atmosphere system is crucial for a better climate prediction. This is particularly relevant for predictions of 21st century climate state, as there is still considerable uncertainty in climate model assessments as to how these tropical climate systems as well as the IPWP will respond to anthropogenic greenhouse warming (Conway et al., 2007; Vecchi and Soden, 2007). For instance, model simulations performed by Lin et al. (2013) confirmed the hypothesis that the alteration of the SST patterns of the warm water in IPWP play an important role in the onset of El Niño event (Cane, 1983) whose modern climate impacts include higher global mean temperatures (Trenberth et al., 2002), increased heat export to the extratropics (Sun and Trenberth, 1998), and continental warmth over parts of North America (Cane, 1998).

1.3.1 Modelling the Indo-Pacific Warm Pool

Assessing the robustness of the tropical Pacific climate is thus a key issue for understanding both past and future climate change. Under this perspective, Huber and Caballero (2003) affirmed that the Eocene provides a particularly exacting test of the robustness of ENSO and the mean east-west thermocline tilt, therefore they run Eocene El Niño simulation. According to their model-proxy comparison, tropical temperatures are only up to 3°C warmer than modern temperatures, with eastern equatorial Pacific SST up to 1°C colder than modern values, suggesting that that their model was capable of

reproducing the general pattern of weakened meridional temperature gradients characteristic of the Eocene. Moreover, they also suggested that the presence of wide-open Panamanian and Indonesian seaways weakly impacts the Intertropical Convergence Zone (ITCZ) location, eastern equatorial upwelling, and thermocline depth. The east-west SST difference across the equatorial Pacific is 7°C therefore only slightly higher than the modern structure of the spectrum and the specific ENSO frequencies are essentially identical to those observed today (Ghil et al., 2002), with only the spatial structure greater than it is today (Huber and Caballero, 2003). The resulting similarity of the simulated Eocene tropical mean state to that of today leads to suggest that ENSO should not be fundamentally different from that of today, as it had also been observed by previous studies (Fedorov and Philander, 2000) and recent model simulations (Kiehl and Shields, 2013). In particular, Kiehl and Shields (2013) obtained Warm Pool temperatures in excess of 40°C in the palaeo-region on either side of India during the PETM, indicating the lack of an ocean thermostat to keep these waters close to present-day values. Warm waters extend far into the extra-tropics with 32°C water off the coast of present-day New Jersey, which greatly matches with the proxy data for this region (Zachos et al., 2006) (Fig. 1.5).
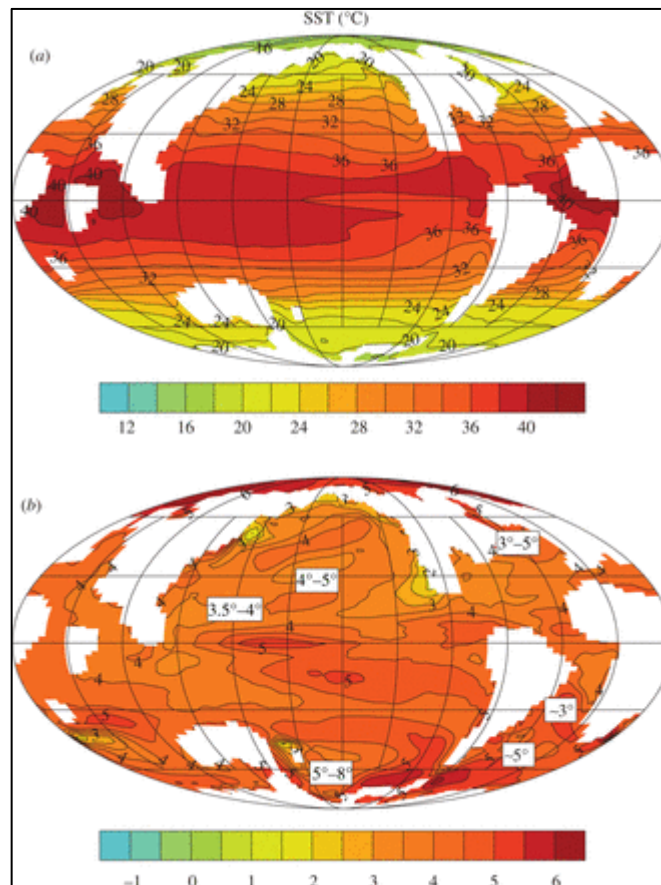
Figure 1.5: SSTs (°C) and (*b*) change in SST (°C) from pre-PETM to PETM climate. Numbers in boxes are observed range in temperature changes. The white regions represent land (Maps taken from: Kiehl and Shields, 2013).

Very recent modelling simulations by Inglis et al. (2015) indicate that the IPWP (~34°C) was ~3–4°C warmer than Eocene samples coming from tropical areas (~30–31°C, Pearson et al., 2007). Moderately higher tropical temperatures relative to today (>2°C) will significantly increase evaporation rates, latent heat transport (Huber and Sloan, 2000), as well as the frequency and strength of tropical cyclones (Sriver and Huber, 2007). Tropical cyclones help to induce ocean mixing which enhances meridional overturning and ocean heat transport. This can reduce the latitudinal temperature gradient by up to 6°C and warm high-latitude oceans by as much as 10°C (Sriver and Huber, 2007; Thomas et al., 2014).

However, research into the underlying mechanisms driving the complex ocean-atmosphere system of this area is limited by the temporal coverage of climate data and the currently available Eocene proxy data are insufficient to directly test these El Niño hypotheses: sparse spatio-temporal coverage renders SST gradients poorly known (Huber and Sloan, 2000) and serious questions have been raised about the accuracy of

the estimates themselves (Schrag, 1999; Pearson et al., 2001). In addition, following the identification of the processes that can highly bias geochemical proxies when reconstructing past climate (e.g. Pearson et al., 2001), there is hope that this information will act as a spur for the targeting of Palaeogene hemipelagic muds from tropical areas that are likely to contain well-preserved planktonic foraminiferal shells. The exceptional preservation of foraminiferal tests from "hemipelagic" clay-rich settings has been attributed to the impermeable nature and low porosity of the clay-rich sediments preventing interaction of the foraminiferal calcite with surrounding pore fluids (Norris and Wilson, 1998; Wilson and Norris, 2001; Sexton et al., 2006; Pearson et al., 2015), which can reduce the accuracy of geochemical proxy-based SST reconstructions, as further in the successive Chapters.

1.4 Multi-proxy Eocene sea surface temperature reconstructions

A multi-proxy approach is ideal in order to reduce the degrees of freedom when determining palaeoenvironmental conditions. Every proxy has its limitations, so the combined application of multiple proxies is essential if important variables, such as SSTs, are to be determined (Pearson, 2012). Besides, using proxies together can help highlight when one or another is compromised.

There have been different attempts at reconstructing Eocene tropical SSTs (e.g. Tripati et al., 2003; Zachos et al., 2003; Sexton et al., 2006a). Most mismatches on palaeotemperature reconstructions between the proxies include $\delta^{18}O$ records as also observed by Liu et al. (2009). Their evidence suggests that Mg/Ca and $\delta^{18}O$-derived SST estimates from well-preserved early and late Eocene planktonic foraminifera are broadly consistent with TEX_{86} estimates but about 10°C warmer than other $\delta^{18}O$ estimates from the tropics (Bijl et al., 2009) and high latitudes (Hollis et al., 2009), suggesting that the primary planktonic $\delta^{18}O$ values were altered by primary diagenesis (Zachos et al., 1994; Bijl et al., 2009). Comparison by Sexton et al. (2006a) of $\delta^{18}O$ and Mg/Ca at individual sites revealed consistent discrepancies of 2°C to 9°C in glassy foraminifera, partially attributing this to uncertainties with the Mg/Ca_{sw} value used (Sexton et al., 2006a). By considering the same value for $\delta^{18}O_{sw}$ (-1‰ for an ice-free planet), Zachos et al. (2003) found that the planktonic foraminiferal temperatures derived for the earliest Eocene at high-latitudes were essentially identical to the TEX_{86} temperatures, except for a temperature anomaly registered by TEX_{86} of 33°C, versus about 22°C by $\delta^{18}O$, which they attributed to a decrease in local sea surface salinity (hence $\delta^{18}O_{sw}$) due to higher runoff during the PETM. Similar early Eocene tropical SSTs were also found by Tripati

et al. (2003) whose data were retrieved from the western central equatorial Pacific Ocean. Using similar Mg/Ca$_{sw}$ values, Mg/Ca-derived SST estimates give values >30°C, with a peak of 34°C. These values are several degrees warmer than those that had been previously calculated using diagenetically altered foraminiferal δ^{18}O values from the same site (Bralower et al., 1995) and other low-latitude sites (Zachos et al., 1994).

Hollis et al. (2009) found tropical conditions (annual SSTs >25°C) in the high-latitude southwest Pacific (about 55°S) for the early to middle Eocene (~50.7 – 46.5 Ma), with a peak in SSTs of 30-35°C at ~50.7 Ma. The values of all the three proxies employed were in good agreement, even though Mg/Ca was found in closer agreement with the relatively higher TEX$_{86}$ values when Mg/Ca$_{sw}$ was set to >35% lower than present, as also indicated by Dickson (2002) since this would make Mg/Ca-derived SST estimates warmer too. The planktonic δ^{18}O was generally consistent with the trend, despite some variability due to the changing state of preservation of foraminifera and its likely effect on the δ^{18}O. Pearson et al. (2007) suggest that the general cooling trend through the Eocene caused the bottom waters to become more undersaturated hence more corrosive, increasing the diagenetic overprint in planktonic tests.

The conversion of TEX$_{86}$ values to SST by Hollis et al. (2009) was performed using the calibration of Kim et al. (2008) which is linear to 30°C, while Pearson et al. (2007) used the equation of Schouten et al. (2003) for SSTs >20°C in the open ocean areas of the tropical early Eocene, and they show that both δ^{18}O and TEX$_{86}$ records from Tanzania were consistently warmer than modern, where maximum SSTs were mostly >30°C and other areas would have probably been warmer (Huber and Sloan, 2001; Pearson et al., 2001). Results by other studies (Bijl et al., 2009; Creech et al., 2010) suggest high-latitude tropical SSTs in the south west Pacific in the range of 30-35°C too, which would indicate a thermal gradient <10°C between low- and high-latitudes (Pearson et al., 2007; Hollis et al., 2009). This presents a challenge for ocean circulation models and different studies put forward different hypotheses; perhaps the early Eocene high-latitude southwest Pacific was influenced by the penetration of the subtropical East Australian Current as well as increased transport by tropical cyclones (Emanuel, 2002; Pearson et al., 2007), or polar stratospheric clouds, which would warm the poles and reduce the latitudinal gradient (polar amplification) (Pearson et al., 2007). According to evidence, most plants and especially the C3 plants that comprised Eocene floras, have physiological mechanisms that break down in the 35° to 40°C range (Huber, 2008). This means that floras may have been thermally stressed, and perhaps undergoing water stress in the warmest intervals (Huber, 2008). There is some evidence of tropical floral extinctions during the warmest periods (Jaramillo et al., 2006; Harrington and Jaramillo,

2007), while forests thrived at higher latitudes. During warming, many taxa may have been forced to flee poleward, innovate, or face extinction (Tewksbury et al., 2008). A study conducted by Frieling et al. (2017) suggested that when tropical SSTs reached values higher than 36°C during the PETM, waters became uninhabitable even for dinoflagellate taxa too, which are among the most temperature-tolerant eukaryotic plankton groups (Hallegraeff et al., 1997).

In conclusion, even if recently most studies that focused on reconstructing the tropical SSTs of the early Eocene show a remarkable congruence and consistent SSTs >35°C, caveats remain in the reliability of the different proxies, which impedes a better match when dealing with a multi-proxy approach. More SSTs records from tropical areas and new experiments with different partition coefficients alongside calibration equations should therefore be further explored in order to improve comparisons among proxies.

1.5 Aims and Objectives of the Study

The primary aim of this study is to reconstruct the sea surface and water column temperatures of the area encompassing the Indo-Pacific Warm Pool in order to assess whether a Warm Pool existed in deep time, and if so be able to investigate how warm the currently warmest ocean region of the world can become under the extreme warmth of greenhouse climates such as the Eocene Epoch. Palaeoclimate modelling is also carried out to test the performance of climate models in representing greenhouse climates by comparing the model outputs with the geological data retrieved from this study. Moreover, the composition, diversity and abundance of plankton communities back in the Eocene is also investigated as it can help assess how and whether species are able to survive and develop adaptation strategies under extreme pressure from the rapidly changing climatic conditions occurring both on the planet and within the water column.

The following objectives listed show how the mentioned aims will be achieved:
- The sites analysed will be the waters around Papua New Guinea for the early Eocene, and around Java for the late Eocene, as both islands currently sit in the core of the Warm Pool.

- The sea surface and water column temperatures will be reconstructed with a multi-proxy approach using both oxygen isotopes ($\delta^{18}O$) and Mg/Ca proxies derived from planktonic foraminiferal tests.

- The palaeoecology and diversity of the species will be assessed by selecting all the species present in the sample and occupying distinct depth habitats through the water column so that the temperatures of the entire water column can be reconstructed.

- A model-data comparison will be carried out, and feedback mechanisms underlying any potential model-data mismatches will be discussed.

Thus, the overarching research questions and hypotheses of this PhD project can be outlined as follows (in chronological order):

- Is it possible to successfully manually separate the infill from the original foraminiferal test wall in a way that the latter is suitable for geochemical analyses and reliable palaeotemperature as well as palaeothermocline reconstructions?

- Considering that today the IPWP is the warmest surface region of the oceans, was there a similar pattern in past greenhouse climate intervals such the early and late Eocene?

  - If so, how hot could the temperatures get to and were they likely regulated by a thermostat-like mechanism like previous studies suggest for similarly hot ocean areas?
  - Were the plankton communities able to adapt to high temperatures and have a higher heat tolerance upper limit?

- Have the most up-to-date climate models been able to improve the existing mismatch between proxy-derived and modelled temperatures?

  - Out of the currently available CO_2 simulations, which better suits the early and late Eocene for proxy-model comparisons?
  - What could mostly be causing a possibly remaining mismatch as climate models continuously strive to better represent the atmosphere-ocean system by including a greater number of feedbacks?

1.6 Declaration

Initially, this study was supposed to find a greater range of Eocene foraminiferal samples in the vast microfossil collection of the Natural History Museum in London, but only one sample of infilled foraminifera from Papua New Guinea was found. Attempts were made at collecting more samples from around the Warm Pool, such as India, Philippines, Borneo, and Tanzania. However, the samples we received from India were assessed and found to be recrystallised, and an additional sample collection would have surpassed the deadline of this project; the samples from Philippines turned out not to be possible in the time frame of this project; the Borneo fieldwork had to be cancelled due to health and safety concerns in accordance with the School's rules and procedures; and lastly, the samples collected during the fieldwork that was carried out in Tanzania in August 2018 are currently still retained by the Tanzania Petroleum Development Corporation in Dar es Salaam and thus it has not been possible to include them in this study.

Chapter 2

Materials and Methods

Chapter 2

2 Materials and Methods

This chapter focuses on the materials studied and methodology used for all the samples under study. Any additional materials or methodologies used for a specific sample will be described in its associated chapter.

2.1 Geochemical proxies

An increasing number of geochemical proxies relying on inorganic and organic compounds has been developed during the last few decades (Eglinton and Eglinton 2008; Castañeda and Schouten, 2011; Nieto-Moreno et al., 2015), and numerous studies currently apply these proxies to reconstruct environmental conditions in marine sedimentary sequences from around the world.

In the present study, the calcareous shells of fossil foraminiferal assemblages were used to reconstruct sea surface temperatures, and the water column temperature gradients of the Indo-Pacific Warm Pool area during the early Eocene and late Eocene.

2.2 Planktonic Foraminifera: our useful time machines

Foraminifera are unicellular eukaryotic organisms that are abundant in oceanic environments and have been widely used because of their abundance and diversity in marine sediments (Schiebel, 2002; Pearson, 2012; John et al., 2013; Pearson et al., 2015). They have been called "armoured amoebae" because they secrete a shell (also known as "test") that can be formed from either secreted organic matter (tectin), secreted minerals (calcite, aragonite or silica) or agglutinated particles. In this study, only those species that secrete calcite tests are considered. These tests, which are made of calcium carbonate ($CaCO_3$), also incorporate trace metals such as magnesium (Mg) and strontium (Sr) as well as different ratios of stable isotopes (e.g. oxygen and carbon) (Hemleben et al., 1989). Thus, this suite of geochemical proxies can be extracted from foraminiferal tests to provide information about the composition and history of the water

and the environmental conditions in which the foraminifer lived at the time it secreted its test. Even though foraminifera have been found to secrete $CaCO_3$ close to isotopic equilibrium with respect to oxygen and carbon (Berger and Wefer, 1991), there is considerable potential for biological and kinetic fractionation of the various isotopes and trace metals incorporated into the calcite (Bijma et al., 1999; Zeebe et al., 2008). Even if small, these significant disequilibrium effects need to be acknowledged when using foraminiferal geochemistry as a palaeoenvironmental proxy.

2.2.1 Foraminiferal Biology and Ecology

Planktonic foraminiferal life cycles generally last weeks or months, and their reproduction is synchronised with the lunar cycle (Hemleben et al., 1989; Spero, 1998; Jonkers et al., 2015), which enables a synchronised release of gametes and thus a higher chance of successful reproduction. When two gametes fuse together, they form a zygote and the first chamber, also known as the proloculus, is established (Schiebel and Hemleben, 2005). Later, a second chamber is formed as the cytoplasm continues to develop, followed by the calcification of progressively larger chambers of uniform morphology that altogether form the test (Brummer et al., 1986). The test seems to have different roles, such as protecting the foraminifer from predation, damage by abrasion or turbulence and controlling water chemistry (extreme ranges of salinity, pH, CO_2, or O_2). Foraminifera feed by trapping organic particles as well as small organisms such as bacteria, diatoms, and copepods with a network of thin pseudopodia (Armstrong and Brasier, 2005). Pseudopodia are foot-like extensions of the cell wall and cytoplasm that cover a foraminifer's skeletal spines (if present). They are also composed of granular ectoplasm, and they radiate out from the central cytoplasm inside the cell (endoplasm) (Armstrong and Brasier, 2005). The ectoplasm connects with the endoplasm via an aperture, which acts as an entrance for the passage of cytoplasm, food, excretory products, and reproductive cells (Armstrong and Brasier, 2005). Benthic foraminifera may also use their pseudopodia for locomotion (Wetmore, 1988).

Foraminifera inhabit different levels of the water column and are principally divided into two categories: planktonic and benthic. Planktonic foraminifera can indicate the temperature of the mixed layer, upper and lower thermocline seawater, while benthic foraminifera are used to measure bottom-water temperature, as well as the environmental conditions at the water-sediment interface (Corliss, 1985). Following the pioneering oxygen isotope "ranking" of foraminifera by different studies including Emiliani (1954) and Poore and Matthews (1984), Pearson et al. (1993) plotted the oxygen and carbon isotope dataset derived from different species of foraminifera in order to

represent a typical year-round pattern of Eocene foraminiferal distribution through the water column for an open-ocean site (Fig. 2.1). The resulting J-shaped graph suggests the fauna distribution is controlled by depth habitat first and then by seasonal abundance, which divides the foraminiferal distribution into three major groups, namely the mixed layer dwellers which live in the uppermost part of the water column; the thermocline dwellers characterised by intermediate carbon and oxygen ratios; and the sub-thermocline dwellers with the lowest carbon and highest oxygen ratios.
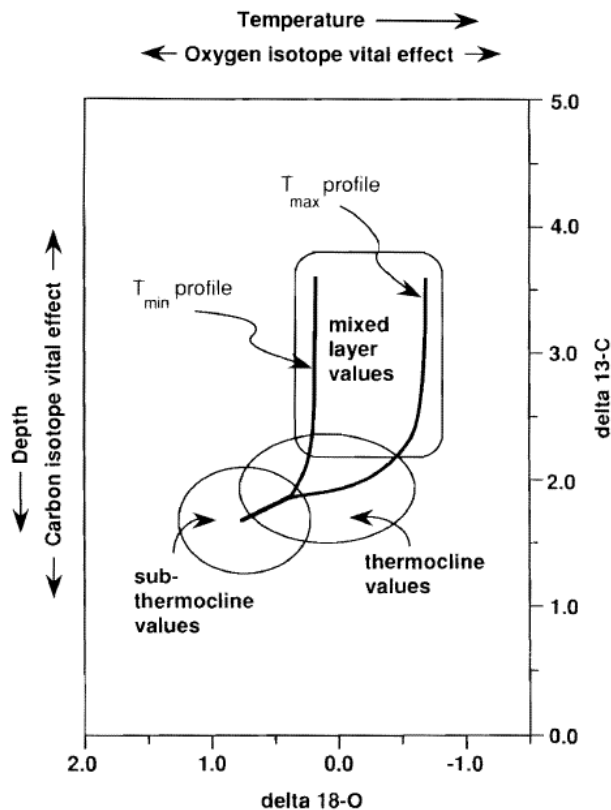
Figure 2.1: Model for the interpretation of the paleoecology of planktonic foraminifera from an open ocean site with year-round stable thermocline (Pearson et al.,1993).

Many planktonic foraminifera form symbiotic relationships with photosynthetic algae, especially diatoms and dinoflagellates (Hemleben et al., 1989), which release photosynthates and O_2 to the foraminiferal host, and benefit themselves from phosphorus (P), nitrogen (N), and respiratory CO_2 released by the foraminifer. The symbionts also display diurnal migration, by moving towards the ends of the spines during the day and retire for protection inside the test at night (Armstrong and Brasier, 2005).

2.2.2 The application of taxonomy in planktonic foraminifera

Both living and fossil foraminifera come in a wide variety of morphologies. It is the complexity and specific characteristics of the structure of foraminiferal tests as well as the evolution over deep time that form the basis of their geological usefulness. In fact, their evolution and taxonomic diversity throughout geological history provide continuous evidence of evolutionary changes, from which detailed phylogenetic relationships can be established (Aze et al., 2011; Ezard et al., 2015). Moreover, their continuous vital role in marine ecosystems means that foraminifera are of paramount importance and value in zonal stratigraphy, palaeoenvironmental, palaeobiological, palaeoceanographic, and palaeoclimatic interpretation and analysis (Armstrong and Brasier, 2005).

Thus, foraminiferal taxonomic research, despite the continuing revisions it is still undergoing, plays a pivotal role in maximising the usefulness of planktonic foraminifera in the research fields mentioned above. These microorganisms are classified taxonomically based on characteristics of their external calcite test: its general morphology which can be seen under the transmitted light microscope, as well as the ultrastructural and microstructural features of the test (Hemleben et al., 1989), which can be studied under the Scanning Electron Microscope (SEM) (Lipps, 1966; Scott, 1974; Cifelli, 1982). The main features that are used to differentiate planktonic foraminifera at species and genus level focus on the wall structure, apertures, the nature of sutures, chamber arrangement, and external ornamentation. At the family level, the details of wall structure and wall surface are usually prioritised (Armstrong and Brasier, 2005).

In this study, the species and genus recognition were carried out under a light transmitted microscope and based on the Pearson et al. (2006)'s Atlas of Eocene planktonic foraminifera, the Wade et al. (2018)'s Atlas of Oligocene planktonic foraminifera, and the Young et al. (2017)'s Mikrotax online database on planktonic foraminifera. Moreover, SEM observations were carried out to help further with foraminiferal species recognition and the assessment of test wall preservation. Full species lists are given in the assemblage studies in Chapter 4 (the Moogli mudstones of the early Eocene) and Chapter 6 (the late Eocene from Java).

2.3 Stable Isotopes

2.3.1 Oxygen isotopes ($\delta^{18}O$)

The stable oxygen isotope composition ($\delta^{18}O$) of marine calcite is the most extensively used of proxies available to reconstruct marine temperatures of the Cenozoic (Tindall et al., 2010). The $\delta^{18}O$ is defined as the ratio of ^{18}O to ^{16}O stable oxygen isotopes that are incorporated into the tests of foraminifera (Equation 2.1) and quantifiably depends on two main factors, namely the temperature and the $\delta^{18}O$ of the seawater (hereinafter $\delta^{18}O_{seawater}$ or $\delta^{18}O_{sw}$) in which the foraminifer secreted its calcite test. The $\delta^{18}O_{seawater}$ in turn depends on the salinity and the global seawater isotopic composition at a given time. The former mainly depends on the local regional variability (evaporation-precipitation balance), where the preferential removal of the lighter isotope ^{16}O during evaporation causes $\delta^{18}O_{sw}$ enrichment in the remaining surface waters, whilst the latter mainly depends on the global ice volume (Elderfield and Gassen, 2000), as ^{16}O is preferentially locked up in ice as a result of the latitudinally dependent Rayleigh fractionation, leaving the oceans enriched in ^{18}O. In fact, the $\delta^{18}O$ of precipitation and seawater tends to become progressively more depleted at high latitudes, as the ^{18}O gets progressively precipitated back into the oceans. The $\delta^{18}O$ of foraminiferal calcite is reported relative to a standard of known isotopic composition, the Vienna Pee Dee Belemnite (VPDB), while the $\delta^{18}O$ of seawater is reported relative to the Vienna Standard Mean Ocean Water (VSMOW) standard.

Other secondary effects influencing the variation of the global $\delta^{18}O_{sw}$ through geological time include the interaction of seafloor basalts and seawater, the chemical weathering of rocks, and meteoric waters, the latter to a smaller extent than the others (Pearson, 2012). Additional variability is brought about by river waters flowing into the ocean, iceberg melting, the local climate regime, and advection (Rohling and Cooke, 1999).

$$\delta^{18}O \text{ sample } (\text{‰}) = 1000 \times \frac{\left[\left(\frac{^{18}O}{^{16}O} \right) \text{sample} - \left(\frac{^{18}O}{^{16}O} \right) \text{standard} \right]}{\left(\frac{^{18}O}{^{16}O} \right) \text{standard}} \tag{2.1}$$

The idea of the $\delta^{18}O$ proxy was first put forward by Urey (1947) who proposed a palaeotemperature equation relating biogenic carbonate $\delta^{18}O$ to water temperature, and later tested by Epstein et al. (1951). Emiliani (1954) subsequently applied this technique

to planktonic foraminifera in deep sea cores and the study found that the foraminiferal tests were secreted in isotopic equilibrium with sea water and could therefore be used for palaeoclimatic reconstructions as long as the $\delta^{18}O_{seawater}$ was known.

The equilibrium isotopic fractionation between calcite and seawater is temperature dependent (Urey, 1947; Pearson, 2012), so that calcite secreted in warm seawater preferentially incorporates more of the lighter isotope (^{16}O) resulting in an isotopically lower signature, and vice versa when surrounded by colder waters (Pearson et al., 1993). The $\delta^{18}O$ of foraminiferal calcite is therefore inversely proportional to the temperature of ambient seawater, leading to a general increase in $\delta^{18}O$ values with water depth in accordance with the accompanying decrease in temperature relative to the surface waters (Emiliani, 1954; Pearson, 2012; John et al., 2013). Consequently, significant oxygen isotope differentials between the species are observed, which are also explained by their different ecologies (Emiliani, 1954; Pearson et al., 2001).

However, it is difficult to estimate an absolute value of $\delta^{18}O_{sw}$ in deep time, due to the absence of direct measurements, errors associated with the proxies the $\delta^{18}O_{sw}$ is derived from, and the fact that $\delta^{18}O_{sw}$ varies as a function of global ice volume alongside evaporation/precipitation and water mixing differences (Hollis et al., 2009, 2012; Tindall et al., 2010; Edgar et al., 2015). Thus, the direct interpretation of foraminiferal $\delta^{18}O$ is not straightforward. As the greenhouse climates of the Cretaceous and early Eocene are assumed to have been characterised by an ice-free world, attempts have been made at calculating a value for the $\delta^{18}O_{sw}$ in an ice-free world (Shackleton and Kennett, 1975; L'Homme et al., 2005; Cramer et al., 2011). In contrast, in intervals of time when ice sheets were present and quantifiably different from today, it is more challenging to infer how much ^{16}O was trapped in ice hence how much was present in the oceans in order to derive an estimated value for the $\delta^{18}O_{sw}$.

The so-called "vital effects" are biological processes that can cause foraminiferal tests to be calcified out of equilibrium with seawater (Ravelo and Hillaire-Marcel, 2007). These include the carbonate ion effect, whereby a higher ocean alkalinity reflects a higher concentration of carbonate ions $[CO_3^{2-}]$. As CO_3^{2-} favours the lighter oxygen and carbon isotopes during the dissociation of the carbonic acid (H_2CO_3) into bicarbonate (HCO_3^-) and CO_3^{2-} ions, the foraminiferal $\delta^{18}O$ and $\delta^{13}C$ decrease as a result of this exchange (Spero et al., 1997).

Some vital effects are also related to the photosynthetic activity of algal symbionts whereby species that contain algal symbionts seem to have higher calcification rates (through CO_2 consumption by algae), which induce a kinetic fractionation resulting in a more depleted $\delta^{18}O$ (Ravelo and Fairbanks, 1992; Spero, 1992; Spero and Lea, 1993). The $\delta^{18}O$ of foraminiferal shells may also change with size in some species which indicates that there are ontogenetic effects that probably reflect changes in the intensity of photosynthesis and/or changes in depth habitat, when the foraminifer matures from juvenile to adult (William et al., 1979; Spero and Lea, 1996). Many non-symbiont bearing species do not show size-dependent changes in $\delta^{18}O$, meaning that photosynthetic rates can drive some ontogenetic effects. In fact, in some cases, it is the addition of gametogenic calcite as the foraminifer sinks at the end of its life cycle that increases the $\delta^{18}O$ of non-symbiont bearing species (Lohmann, 1990; Spero and Lea, 1993).

Lastly, diagenetic alterations can also increase the foraminiferal $\delta^{18}O$ value, namely test dissolution, secondary recrystallisation, and the presence of overgrowths (Sexton et al., 2006a; Pearson and Burgess, 2008; Edgar et al., 2015) As a result of these processes, the tests acquires a "frosty", in contrast to "glassy", appearance and if geochemically analysed, they would produce inaccurate palaeotemperature estimates, in contrast to the "glassy" appearance of the typical well-preserved tests (Pearson et al., 2001; Wilson et al., 2002). Exceptionally preserved foraminiferal tests are usually found in clay-rich sediments, while recrystallised tests are more commonly found in carbonate and chalk-rich oozes (Pearson et al., 2001, 2015; Sexton et al., 2006a; Pearson and Burgess, 2008; Pearson, 2012). Because recrystallisation occurs below the seafloor, planktonic $\delta^{18}O$ is usually biased towards colder temperatures, especially in low latitude areas. In contrast, test infill generally causes a decrease in the foraminiferal $\delta^{18}O$ value, if the source of this inorganic calcite is derived from rainwater, which is isotopically lighter than seawater.

2.3.2 Carbon isotopes ($\delta^{13}C$)

The stable carbon isotopic composition ($\delta^{13}C$) of foraminiferal tests can be used to gain insight into the dissolved inorganic carbon (DIC) of the seawater ($\delta^{13}C_{DIC}$) in which the test was secreted (Ravelo and Hillaire-Marcel, 2007). The $\delta^{13}C$ is the ratio of ^{13}C to ^{12}C of the test and is reported relative to the VPDB standard (Equation 2.2).

$$\delta^{13}C \text{ sample } (\text{‰}) = 1000 \times \frac{\left[\left(\frac{^{13}C}{^{12}C}\right)\text{sample} - \left(\frac{^{13}C}{^{12}C}\right)\text{standard}\right]}{\left(\frac{^{13}C}{^{12}C}\right)\text{standard}} \qquad (2.2)$$

The biologically induced distribution of $\delta^{13}C_{DIC}$ in the marine water column is caused by photosynthesis and respiration. During photosynthesis, the preferential uptake of ^{12}C from the mixed layer reservoir of DIC causes an increase in the mixed layer $\delta^{13}C_{DIC}$. As organic matter descends through the water column, it undergoes oxidation, which causes the ^{12}C to be released back into the seawater, thus decreasing $\delta^{13}C_{DIC}$ of the deep ocean. This $\delta^{13}C_{DIC}$ gradient throughout the water column is recorded in the foraminiferal $\delta^{13}C$, according to the depth habitat the analysed species was living in. By analysing both surface-dwelling and thermocline-dwelling species, it is therefore possible to reconstruct the vertical $\delta^{13}C$ gradient of the water column at a given time interval (Ravelo and Hillaire-Marcel, 2007).

The $\delta^{13}C$ in foraminiferal shells can also be influenced by the carbonate ion effect (Spero et al., 1997), changing water masses, vital effects and air-sea gas exchanges. During the latter, the isotopically lighter atmospheric CO_2 lowers the $\delta^{13}C_{DIC}$, while any CO_2 outgassing into the atmosphere increases the $\delta^{13}C_{DIC}$ (Lynch-Stieglitz et al., 1995).

The vital effects controlling foraminiferal $\delta^{13}C$ in photosymbiont-bearing species include photosynthesis and ontogeny. During the former, the test becomes more enriched in ^{13}C as a result of the preferential uptake of ^{12}C by algal symbionts during photosynthesis, while during the latter, foraminiferal tests from the bigger size fractions record higher $\delta^{13}C$ signatures, as the test may have hosted a greater number of photosymbionts (Rohling and Cooke, 1999; Ravelo and Hillaire-Marcel, 2007).

2.3.2.1 Palaeotemperature equations for $\delta^{18}O$-based climatic reconstructions

After the first published and later revised oxygen-isotope palaeotemperature equations (McCrea, 1950; Epstein et al., 1951), several other equations have been proposed (Erez and Luz, 1983; Kim and O'Neil, 1997; Bemis et al., 1998), and they all have in common a quadratic form. Since the $\delta^{18}O$ is always measured on the VSMOW scale, they need to be converted to the VPDB scale in order to be used in a palaeotemperature equation. A conversion factor therefore needs to be added to the equation when calculating palaeotemperatures from calcite, and after several changes through time (Epstein et al., 1953; Friedman and O'Neil, 1977), the currently accepted value is 0.27‰ (Hut, 1987; Grossmann, 2012; Pearson, 2012).

In this study, the Kim and O'Neil (1997)'s palaeotemperature equation (Equation 2.3) will be used as it is calibrated over 30°C, and is therefore more suitable to reconstruct the greenhouse climate of the Eocene, where the ocean temperatures have been known to exceed 30°C (Aze et al., 2014; Frieling et al., 2017).

$$T(°C) = 16.1 - 4.64 \ (\delta^{18}O_{calcite} - \delta^{18}O_{seawater}) + 0.09 \ (\delta^{18}O_{calcite} - \delta^{18}O_{seawater})^2 \qquad (2.3)$$

2.3.2.1.1   Latitudinal correction

The value of $\delta^{18}O_{sw}$ is an essential variable in palaeotemperature equations, yet difficult to constrain. Since the study by Hollis et al. (2019), there are now two options to correct for latitudinal variation of surface waters relative to the mean oceanic $\delta^{18}O_{sw}$. One is the Zachos et al. (1994)'s correction (hereinafter referred to as the Zachos correction) and it has been a widely accepted method in the palaeoclimate community (Hollis et al., 2012; Pearson, 2012). The Zachos correction is based only on $\delta^{18}O_{sw}$ data from the Southern Hemisphere, and it can be calculated by inputting an absolute latitude value ranging 0-70° (the influence of ice is unknown hence the absence of the highest latitudes, Pearson, 2012) in the following polynomial equation (Equation 2.4):

$$\delta^{18}O_{SW} = 0.576 + 0.041x - 0.0017x^2 + 0.0000135x^3 \qquad (2.4)$$

The other method is the newly proposed Hollis et al. (2019)'s correction (hereinafter referred to as the Hollis correction). The script containing the global $\delta^{18}O_{sw}$ dataset from LeGrande and Schmidt (2006) can be opened on the Matlab® software, and by choosing a palaeolatitude, it is possible to compute a value for $\delta^{18}O_{sw}$ which can then be incorporated into the palaeotemperature equation. The $\delta^{18}O_{sw}$ value at the given palaeolatitude is the average value of the 10°x10° latitudinal bin the location falls in (see Figure 2.2). The script also gives the option to input the associated ice volume correction (discussed below), but in this study, this correction was directly applied in the palaeotemperature equation after retrieving the data from Matlab.
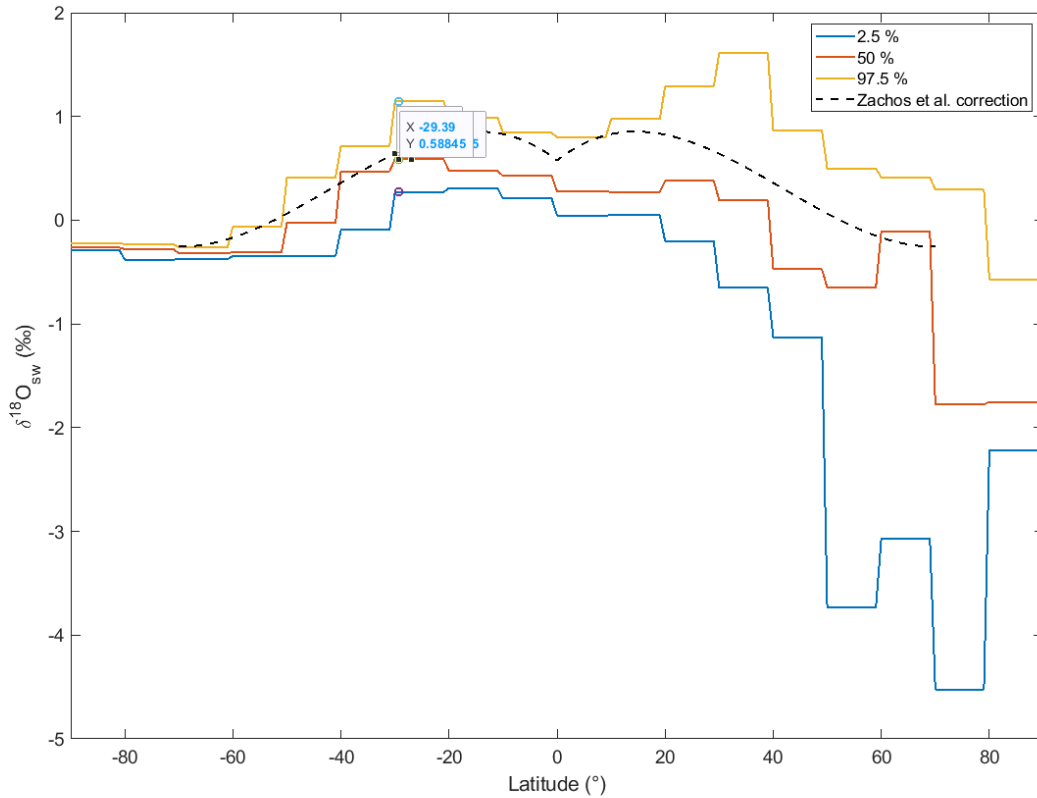
Figure 2.2: Matlab plot showing seawater δ^{18}O$_{sw}$ values against latitude. The black line represents the latitudinal correction based on Zachos et al. (1994). The other lines represent δ^{18}O$_{sw}$ values that were extracted on Matlab from the database of LeGrande and Schmidt (2006). The red line represents the 50th percentile of the data so the value considered when reconstructing temperatures with δ^{18}O. The blue line represents the 2.5th percentile, and the orange line represents the 97.5th percentile. The dot on each line indicates the inputted palaeolatitude so that when the mouse goes over the dot, a δ^{18}O$_{sw}$ value appears on the figure.

However, implicit in these corrections is the assumption that the latitudinal gradient and intensity of the hydrological cycle determining δ^{18}O$_{sw}$ values has remained constant through time (Pearson, 2012). A comparison of both methods alongside a discussion on the difference in the resulting data will be made in Chapter 4.

2.3.2.1.2   *Ice volume correction*

An ice volume correction also needs to be considered in palaeotemperature equations as the average δ^{18}O$_{sw}$ is influenced by the volume of global ice present on the planet at a specific time in geological history (Pearson, 2012). As this study includes samples from the early Eocene, late Eocene, and early Oligocene the ice-volume correction by Cramer et al. (2011) was used when reconstructing temperatures in order to remain consistent between chapters. This is because Cramer et al. (2011) is the only study that attempted at giving an ice correction value for all the three intervals on the same scale. A

comparison of Cramer et al. (2011) with other studies (Shackleton and Kennet, 1975; L'Homme et al., 2005) that estimated the ice volume correction for an ice-free world will be discussed in Chapter 4.

2.3.3 Mg/Ca in planktonic foraminifera

Mg/Ca thermometry has been widely applied to reconstruct the temperatures of the water column in the past (Elderfield and Ganssen, 2000; Pahnke et al., 2003; Rosenthal et al., 2003; Barker et al., 2005; Evans et al., 2018). It is based on the thermodynamically controlled incorporation of Mg into the calcite tests of foraminifera during growth, such that foraminiferal Mg/Ca ratios increase with increasing temperature (Rosenthal et al., 1997; Mashiotta et al., 1999; Lear et al., 2000, 2002, 2008; Tripati et al., 2003; Barker et al., 2005; Tripati and Elderfield, 2005; Pearson and Burgess, 2008; Creech et al., 2010). Absolute temperatures can be estimated by applying the empirical Mg/Ca-temperature calibrations to the Mg/Ca records (Lear et al., 2002; Anand et al., 2003; Tripati et al., 2003; Hollis et al., 2009, 2012; Creech et al., 2010). However, even if the oceanic residence times for Ca and Mg are relatively long (about 1 and 14 My respectively) (Evans and Müller 2012) concentrations of Mg and Ca in seawater may also be affected by hydrothermal alteration of basalt at mid-ocean ridges (Elderfield and Schultz, 1996), ion exchange reactions of Mg with clays (Gieskes and Lawrence, 1981), continental weathering rates (Berner et al., 1983; Wilkinson and Algeo, 1989), and carbonate deposition (Wilkinson and Algeo, 1989). Several models that have attempted to reconstruct Cenozoic Mg/Ca_{sw} suggest lower Mg/Ca_{sw} values than today's average value of ~5.2 mol/mol (Broecker et al., 1982; Wilkinson and Algeo, 1989; Dickson, 2002; Lear et al., 2002; Evans and Müller 2012), meaning that some of these parameters have varied over geological time, resulting in a broad increase in Mg/Ca_{sw} over the Cenozoic (Spero, 1998; Barker et al., 2005; Coggon et al., 2010; Evans and Müller 2012).

The Mg/Ca proxy can be used on both bulk and single test chamber analytical techniques. The former can also be viewed as a limitation, since the "whole-test" samples represent the integration of various depth habitats hence temperature profiles in which that particular species grew during calcification, leading to a deviation from the strict notion of sea surface temperatures, as many species of planktonic foraminifera live at depths greater than 50 meters (Anand et al., 2003). However, it is of fundamental importance to consider multiple species as this provides a powerful tool for reconstructing changes in upper water column thermal gradients and therefore reconstruct past oceanographic conditions of both the thermocline and mixed layer. For

instance, Elderfield and Ganssen (2000) analysed several different planktonic foraminifers in a site from the tropical Atlantic and observed that Mg/Ca temperature estimates yielded consistently warmer or colder temperatures as a result of the depth habitat preferences of each of the species considered.

The Mg/Ca ratio in the original calcite shell can also be altered by early stage dissolution post-mortem as the test sinks down through the water column hence through colder waters, where the Mg/Ca is lowered as Mg^{2+} is preferentially removed (Lea et al., 2000; Sexton et al., 2006a; Edgar et al., 2015). Moreover, the addition of secondary inorganic calcite may alter the primary foraminiferal Mg/Ca owing to the great difference in Mg^{2+} partition coefficients between biogenic and inorganic calcite (Mucci, 1987; Sexton et al., 2006a). However, Sexton et al. (2006a) found a smaller than expected increase in diagenetically altered foraminiferal Mg/Ca, and proposed that Mg/Ca is less sensitive to the secondary organic calcite than the $\delta^{18}O$ proxy. This suggests that the two proxies respond differently to diagenetic alteration, as well as that the Mg^{2+} partition coefficient for deep-sea precipitation of inorganic calcite is lower than the one derived from laboratory experiments, which was also found by Baker et al. (1982).

Lastly, foraminiferal Mg/Ca does not seem to conform to the theoretical calculations (Rosenthal et al., 1997) since its temperature sensitivity when incorporating Mg into their calcite tests is 2-3 times greater than that for inorganic calcite (Rosenthal et al., 1997; Hollis et al., 2019), suggesting that biological influences play an important role in the trace metal composition of foraminiferal calcite hence why empirical Mg/Ca-temperature calibrations are employed (Barker et al., 2005; Hollis et al., 2019).

More details about the palaeotemperature equation and estimate of Mg/Ca_{sw} used for the reconstruction in this study will be given in Chapter 4.

2.4   Sieving and picking planktonic foraminifera

All the samples processed in this study had already been previously washed, therefore no washing took take place unless there was evident presence of pyrite (visible under the light microscope), or clay (visible under SEM imaging). Moreover, as the samples were only available in small quantities, weighing the specimens was avoided as to reduce sample loss. Each sample was sieved into different size fractions ranging from 63 μm to 425 μm. A fine paintbrush dampened with 18.2 MΩ deionised water (DI H_2O) was used to turn around the foraminiferal tests in order to identify the species under all

its views: umbilical, lateral, and spiral. The aim was to recognise and pick as many species as possible in the sample so that a water column temperature profile with distinct depth habitats could be reconstructed for each site and time interval considered. Thus, both surface dwellers and thermocline dwellers, and different genera of each of the two categories were picked under a high-resolution binocular microscope (Nikon SMZ 745T, with Nikon lens G-AL 2x), as well as different species within the same genus, in order to study any intragenus variation and investigate whether a particular species had a consistently different depth habitat from the rest of the species within that genus. The number of specimens used for each species picked was mainly constrained by the quantity of sample available. However, the study by Birch et al. (2013) was used as a guidance for the minimum number of specimens that can be analysed for each size fraction.

The test preservation of the sample was also investigated under a Zeiss Sigma HD Field Emission Gun Analytical Scanning Electron Microscope (SEM) using the in the Electron Microbeam facility at Cardiff University. The instrument provides high-resolution imaging, and the samples were first coated in gold to render them conductive.

2.5   Crushing

Where planktonic foraminiferal tests were exceptionally well-preserved, the whole glassy shell was used. For any picked foraminiferal shells that contained some infill, they were gently broken open between glass plates and the infill was separated from the original fragments of the tests with a fine paint brush dampened in 18.2 MΩ DI H_2O in order to prevent the material on the glass slide from getting blown away. Only about 4-5 specimens were crushed each time to ensure a better control of the strength transferred to the glass slides as well as getting all the chambers to break open. The tests were placed on a glass slide, and the second glass slide was gently pressed against them in order to crack them open. Any visible contaminants were removed using the fine paintbrush. Between each crushing, the glass slides were cleaned with acetone followed by 18.2 MΩ DI H_2O, and finally dried with paper rolls, making sure that they were clear of any residual test fragments from the previous sample. Only species and size fractions with sufficient quantities of calcite were selected for geochemical analysis.

2.5.1 Foraminiferal oxygen and carbon isotopic analysis

2.5.1.1 Procedure for preparing samples for isotopic analyses

Following crushing, the test fragments and their associated infill (when analysed) were separately placed directly in the glass vials specific of the mass spectrometer, since the quantity of the sample was limited and transferring the sample from one test tube to the other may cause additional material loss.

2.5.1.2 Sample analysis

The samples were analysed on a Thermo Scientific KIEL IV Carbonate preparation device coupled to a Thermo MAT 253 isotope ratio mass spectrometer, which is calibrated against the international carbonate standard NBS-19. All the results are reported as a per mille deviation from the Vienna Pee Dee Belemnite scale (‰ VPDB), and the long-term uncertainty of the internal carbonate standard BT63 (Carrara marble) is ±0.03‰ for $\delta^{18}O$ (N=174, 1 standard deviation), and ± 0.03‰ for $\delta^{13}C$ (n=174, 1 standard deviation), while for the external standard NBS-19 it is ±0.10‰ for $\delta^{18}O$, and ±0.05‰ for $\delta^{13}C$ (n=469, 2 standard deviations).

2.5.2 Foraminiferal trace metal analysis

2.5.2.1 Sample cleaning

Following crushing, the test fragments and their associated infill (when analysed) were separately placed into individually labelled, acid cleaned (10% HCl, followed by 18.2 MΩ DI H_2O) microcentrifuge tubes.

Both the infill and test fragments were cleaned in the same manner in order to keep consistency. The procedure adopted aimed at removing any clays and organic matter from the samples, following the standard protocol (Boyle and Keigwin, 1985; Barker et al., 2003). As the SEM images of the specimens showed presence of clay on the test, the clay removal step was conducted four times. The reductive step which aims at removing any metal oxide coatings that can form on the foraminifer's test during diagenesis (Martin and Lea, 2002; Barker et al., 2003) was only conducted on some samples in order to verify whether this step was needed for this specific set of samples. This is because the planktonic foraminiferal tests are significantly thinner than benthic foraminiferal tests, therefore they tend to dissolve more easily. The reducing reagent

(hydrous hydrazine in a citric acid/ammonia buffer) is known to be corrosive to carbonate and thus causes partial dissolution of the test fragments (Barker et al., 2003, 2005), leading to a lowering of foraminiferal Mg/Ca ratios (Rosenthal et al., 2000). Because of this, reductively cleaned samples may contain lower Mg/Ca due to the partial dissolution of the sample during the reductive treatment. Carrying out the reductive step quickly in order to avoid the sample to be submerged in the reducing agent for too long is one way to avoid dissolution. An alternative approach to avoiding the reductive step and ensure the absence of Mn-oxide coating contamination is to check for any covariance between Mg/Ca and Mn/Ca, Fe/Ca, and Al/Ca. In this study, the latter approach was utilised as the sample was available in small amounts (see Chapter 4), and the reductive treatment would have likely caused a further reduction in the quantity, which in turn would have been too small to be detected by the ICP-MS.

2.5.2.2   Sample analysis

Prior to analysis, each cleaned sample was dissolved in 120 µl of 0.065 M Optima HNO_3, agitated using a vortex mixer to facilitate dissolution, and centrifuged to remove any remaining contaminant particles. Once dissolved, the resulting solution was split into two aliquots, one of 10 µl used to determine the Ca concentration, and the 100 µl was used to determine the trace metal concentration. Both aliquots were transferred to new acid cleaned tubes. On the same day as the Ca run analyses, 190 µl 0.5 M Optima HNO_3 was added to the 10 µl aliquot solutions, for a total sample volume of 200 µl, whilst on the same day as the trace metal analyses, 250 µl 0.5 M Optima HNO_3 was added to each 100 µl aliquot, for a total sample volume of 350 µl.

Both aliquot samples were analysed on a Thermo Scientific[TM] ELEMENT XR[TM] High-Resolution Inductively Coupled Plasma Mass Spectrometer (HR-ICP-MS) in combination with an Elemental Scientific SC-E2 Autosampler at Cardiff University. The Element XR[TM] is a double focusing mass analyser (magnetic sector and electrostatic sector) which benefits from high resolution, a large dynamic range and precise analysis at low concentrations (ppt-ppq). The Ca run was performed to minimise the matrix effects that occur during trace element analysis, and it produced the Ca intensity and concentration of each sample. This way, the standard could be appropriately diluted to "matrix -match" the foraminifer sample and ensure that the target element concentration was a function of variation of the element in the sample, rather than variations in Ca concentrations (Lear et al., 2002, 2010).

Replicate analyses of two internal consistency standards were performed to assess the long-term precision of the element ratio measurements on the ICP-MS used. One consistency standard was called CS1, with an accepted value of Mg/Ca = 1.24 mmol mol^{-1}, while the other was called CS2, with an accepted value of Mg/Ca = 7.15 mmol mol^{-1}. The long-term precision (% RSD) of Mg/Ca from both consistency standards was 0.7%.

Trace metal/calcium ratios were retrieved after applying blank correction to the isotope counts in order to correct for any background interferences and contamination from the sample introduction system.

2.6 Model-data comparison

2.6.1 Choosing the appropriate palaeoclimate models

A model-data comparison was carried out towards the end of the project by comparing the data produced from this study to modelled temperature reconstructions of both the early Eocene (Ypresian) and late Eocene (Priabonian) of the Indo-Pacific Warm Pool (IPWP) area. The modelling work was undertaken at the School of Geography at the University of Bristol, and it included coding and plotting model outputs. The coding program used is called IDL and was used on a Macbook Pro terminal. First, some maps of the IPWP during both intervals were downloaded from the model simulation database of the Bristol Research Initiative for the Dynamic Global Environment (BRIDGE) in order to gain insight on how the IPWP evolved throughout the Eocene in terms of both changing size and temperature throughout the water column. Secondly, IDL was used to extract and produce maps and plots of changing temperatures with increasing depth. This way, the plots displaying temperature against δ^{18}O produced from the geochemical analyses could be matched with the depth given by the models, and produce δ^{13}C as well as δ^{18}O plots against depth in order to gain insight into the structure of the water column of the IPWP area during the Ypresian and Priabonian intervals. The "TEU" model simulations were selected as they are the most updated model runs with the longest spin-up time, and they are the continuation of the "TDL" model simulations used in Lunt et al. (2016). Moreover, each Eocene interval is simulated under both 560 ppm CO_2 (2x CO_2 pre-industrial levels) and 1120 ppm (4x CO_2), thus it was also possible to compare scenarios under changing CO_2 concentrations. More details on the palaeoclimate models used will be given in the chapters involving the model-data comparison (Chapter 4, and Chapter 5).

- 36 -

Chapter 3

Biostratigraphy and foraminiferal test preservation: an evaluation of the South-East Asian section of the Former British Petroleum Collection, Natural History Museum, London

Chapter 3

3   Biostratigraphy and foraminiferal test preservation: an evaluation of the South-East Asian section of the Former British Petroleum Collection, Natural History Museum, London.

Abstract

The deeper in time palaeotemperature reconstructions are based, the harder the possibility to find well-preserved foraminiferal tests that are suitable for geochemical analyses. The enormous collections of Natural History Museums (NHMs) have been recently acquiring greater importance as the visibility of their microfossil archives is gradually improving thanks to the interest of scientists and international collaborations. Not only does searching for well-preserved foraminiferal tests from existing archives saves the efforts and additional costs of a newly planned fieldwork, but it also enhances the importance of re-visiting previous work and avoiding the duplication of field collection at similar sites. Moreover, studying NHM collections can better catalogue their databases and increase the likelihood of finding other useful study materials for future projects. In this study, the South-East Asian collection of planktonic foraminiferal picked slides of the Natural History Museum of London was investigated in order to look for well-preserved Eocene planktonic foraminifera as it would correspond to the region of the Indo-Pacific Warm Pool, which is currently the warmest region of the oceans and the associated geochemical analyses would help us understand if such a region maintained the highest temperatures in past greenhouse climates too. The investigation and identification of planktonic foraminifera with the aid of a light microscope resulted in finding species spanning between the late Cretaceous and recent times. Very few specimens from the early Eocene were found and only one picked slide contained some glassy foraminiferal tests filled with inorganic calcite. The sample, named "KRE83F", was donated to the Museum by the British Petroleum company and collected in the Moogli mudstones

outcrops of Papua New Guinea in the 1950's. Despite the infill and due to the early Eocene sample scarcity, the infilled foraminifera were used for palaeotemperature reconstructions. Moreover, while investigating the NHM collection, a method of cataloguing the South-East Asian picked slide archive was developed and will be made available to the wider community to enable and facilitate future scientific collaborations.

3.1   Introduction

The former British Petroleum (BP) Micropalaeontology Collection is located at the Natural History Museum (NHM) of London, and it contains micropalaeontological samples from over 3,800 wells and several hundred outcrop sequences from over 120 countries and oceans. The collection includes material that dates back to explorations undertaken in the late 1950's, it was acquired by the NHM in 1992, and since then it has been catalogued and databased by the staff at the Museum. This unique resource includes wet and dry residues, calcareous as well as siliceous microfossils, palynological preparations and nannofossil slides that derive from core, sidewall, and cutting samples, in addition to associated material from many outcrop localities. Initially, the access to the collection was restricted because of its commercial sensitivity.

There are three main sections to the collection:

- **The micropalaeontology type and reference collection** of about 60,000 named foraminifera and ostracod slides, and served at the reference library of microfossils used by BP to aid identification of specimens by their research scientists;

- **The micropalaeontology picked slide and residue collection** from BP well runs and outcrops; and

- **The palynological and calcareous nannofossil strew slide and residue collection** mainly comprising BP well runs and outcrops.

As an indication of the size of the collection, there are around 200,000 slides and residues. The quantity and quality of the microfossil assemblages could provide numerous potential research project spanning most micropalaeontological groups, geological periods, and geographical locations. Considering that it is now possible to obtain access to the resource and that the potential value of this collection to micropalaeontological research is very high, these are the main reasons why it was selected to investigate whether it contains well-preserved foraminiferal specimens from the South-Eastern region of Asia that dates back to the Eocene. In fact, a recent investigation of the "Ocean Bottom Deposits (OBD) collection" which is housed at the

NHM enabled the opportunity to investigate the effects of ocean acidification on planktonic calcifying organisms (Fox et al., 2020). This highlighted the importance of re-evaluating the often overlooked, invaluable information that historic ocean collections may contain (Marshall et al., 2018), including key answers to critical questions on climate change as they are often overlooked when considering investigating climate change (Fox et al., 2020).

In this study, the South-East Asian section of the micropalaeontology picked slide and residue collection that is part of the former British Petroleum (BP) collection located at the Natural History Museum in London, UK, was assessed in order to find well-preserved planktonic foraminiferal tests from the Eocene, on which to apply geochemical analyses and infer the SSTs of the IPWP during this time interval. The available samples were first assigned an age through the medium of biostratigraphy, and subsequently assessed on the basis of preservation of their planktonic foraminiferal content. Cataloguing the microfossil material will also help improve the usability of the collection for other studies, for instance involving taxonomy and other time intervals.

3.2   Materials and Methods

3.2.1 The former BP Micropalaeontology Collection from South-East Asia

This section of the former BP collection consists of the material from well runs in the form of picked slides and residues (Fig. 3.1). There is an available database on the NHM micropalaeontology website that allows search by country, basin, and well/outcrop keyword or name, and a summary of micropalaeontological material for that specific location can be obtained (Fig. 3.2). The main purpose of the database is to allow researchers to identify material of interest, based on its geographical location, and can be found on the NHM Data Portal (https://www.nhm.ac.uk/research-curation/scientific-resources/collections/palaeontological-collections/bp-microfossil/index.html).

Figure 3.1: An example of the micropalaeontology well sequence and outcrop slides and residues in the former BP collection cabinet, highlighting the variety in material contributing to this unique resource (Adapted from the poster of Hill et al., 2002).

The results and data obtained from this study will be added to the online database and thus made available to anyone wanting to access the NHM website.
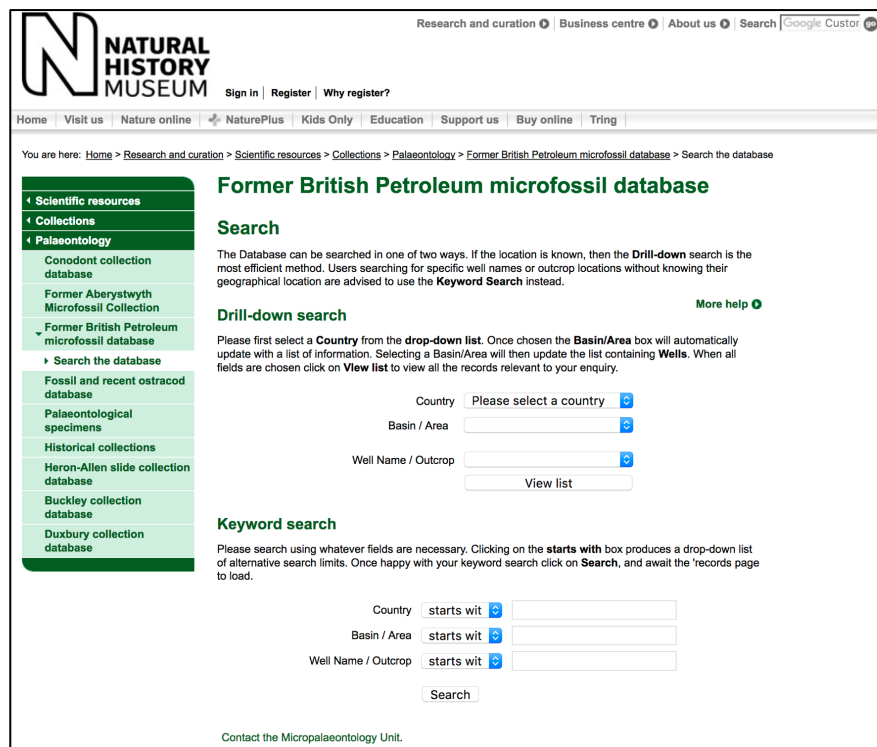
Figure 1.2: Example of the online collection database which summarises all well run and outcrop data available within the collection.

3.2.2 Location of the samples from South-East Asia

When donating the collection to the NHM, the BP provided scarce information on the wells explored and sequences given except for some information on the basin name, well number, and the type of material available (picked slide or residue). Thus, a thorough literature review was carried out in order to first locate the samples in the South-East Asian region, and to find as much detail as possible on the basins and wells.

Following this, the latitudes and longitude coordinates that were found for each well were plotted on a map (Fig. 3.3). Following this, the locations of the samples were investigated in order to assess whether they roughly overlapped the same region as the Eocene IPWP area, which was reconstructed in various different palaeomodelling studies (Kiehl and Shields, 2013; Alexander Farnsworth, *personal communication*). For instance, all the well locations from Australia do not overlap the Eocene IPWP region as they would have been located much more South relative to the Warm Pool back in the Eocene, but were assessed and catalogued regardless in order to fill the information gaps of the South-East Asian picked slides of this collection.
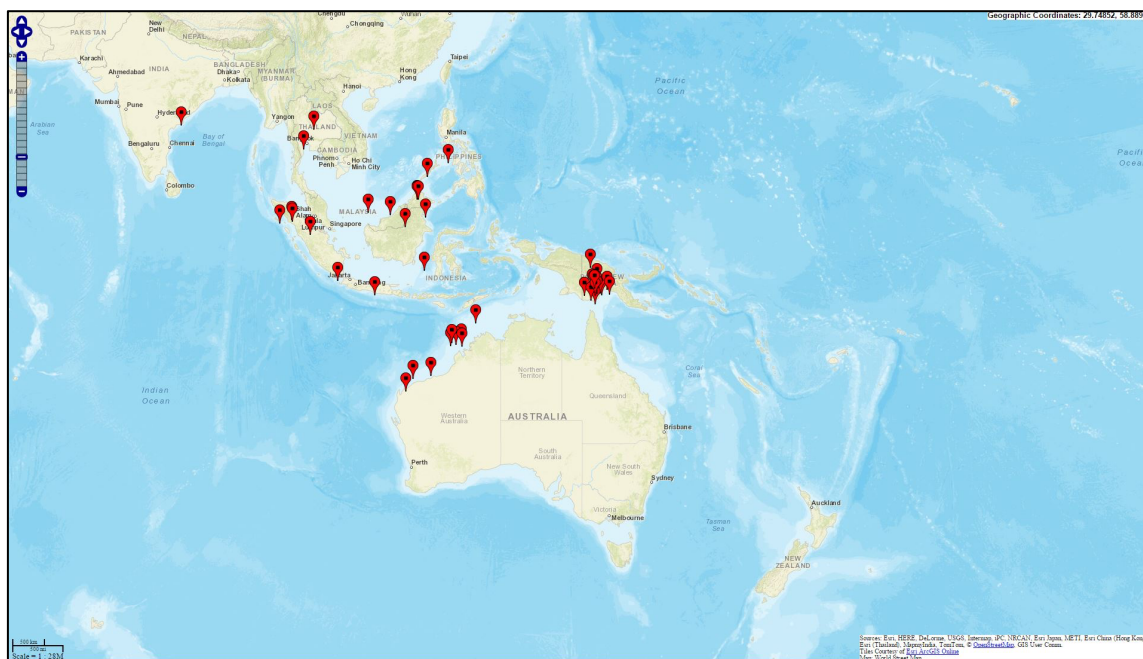
Figure 3.3: Map showing the location of the specimens found in the South-East Asian section of the former BP collection, Natural History Museum, London. Countries include India, Australia, Papua New Guinea, Indonesia, Borneo, Philippines, Vietnam, and Papua New Guinea.

3.2.3 *Approach for the age identification of the picked slides*

Updated biozone ranges and species-specific occurrence ranges by Wade et al. (2011) were used in order to assign an age to each picked slide. The authors provided a review and revision of the tropical planktonic foraminiferal biostratigraphy based on the lowest and highest occurrence of each species, as well as highlighting the marker species of each biozone (Fig. 3.4). Biochronology is an element of biostratigraphy where the absence and/or presence of specific microfossils is used to estimate the age of a stratigraphical unit or geological sample (Pearson, 1998), and was applied to the sample to determine its age. In order to constrain an age as narrowly as possible, a biozone was assigned to the age of the sample, which in turn is represented by a range of years. A biozone is a biostratigraphic unit that is characterised by the rocks containing specific types, or species of fossils (Armstrong and Brasier, 2005).
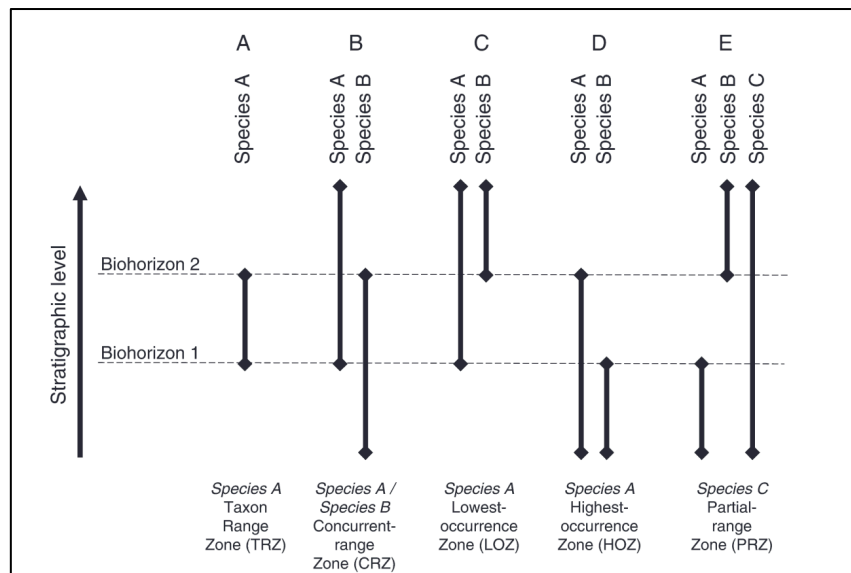
Figure 3.4: Nomenclature of biostratigraphic zones to illustrate the convention of Wade et al. 2011 (Image taken from Wade et al., 2011)

The definition of a biozone is based on the first appearance datum (FAD) and last appearance datum (LAD) of a species. There are five types of interval biozones (see Fig. Figure 3.4 from Wade et al., 2011), the most commonly used being the concurrent range zone, which is the interval anywhere below the LAD of one species, and anywhere above the FAD of the second species (Hedberg, 1976; Armstrong and Brasier, 2005), and the taxon range biozone, which is the interval that covers the total occurrence of a named species (Pearson, 1998). The level in the rock of a biostratigraphic event can be linked between sites via a biohorizon, which is any stratigraphic boundary, surface or interface

across which there is a significant change in biostratigraphic character (Hedberg, 1976; Pearson, 1998).

3.2.4 *Assessing the abundance and preservation of foraminifera in the picked slides*

The abundance scale was based on previous cataloguing techniques applied by the NHM on other sections of the BP microfossil collections. It is based on estimating the overall number of foraminiferal specimens present, including both benthic and planktonic foraminifera. The abundance scale is divided into 6 main ranges, as shown in Table 3.1.

Abundance of foraminifera in picked slides					
Excellent	Good	Average	Poor	Rare	Barren
>200	100-200	50-100	20-50	1-20	0

Table 3.1: Abundance scale used to quantify the number of both benthic and planktonic foraminifera in each picked slide.

The aim was to find and analyse the geochemistry of foraminifera that showed little evidence of micron-scale diagenetic alteration, and which appear translucent under the binocular light microscope, and contain near-pristine biogenic calcite (Norris and Wilson, 1999; Pearson et al., 2001, 2007; Wilson and Norris, 2001; Wilson et al., 2002; Sexton et al., 2006a; Burgess et al., 2008; Edgar et al., 2015).

During the investigation of the database, the details provided for each picked slide not only included the additional information on the inferred age of the sample, preservation and identified species present in the sample, but a cataloguing effort was also made in order to obtain an updated database on the details of the basin area and wells.

3.3 The development of the database: outcome of the investigation

A total of about 1260 picked slides were evaluated to determine the planktonic foraminiferal preservation, the species present, and the age by means of planktonic foraminiferal biostratigraphy (see Table 3.2, and see Appendix 1 for the whole database). The age ranged from the Upper Cretaceous (Mesozoic), to Recent and included all the Epochs in-between. All the specimens of each picked slide displayed some level of recrystallisation, and many were infilled too. Both factors, especially when present simultaneously, hampered the recognition of many foraminiferal genera and/or species

in the slide, leading to a large biostratigraphic range and the difficulty of their consideration for geochemical analyses and SST reconstructions. This was often aggravated by the evidence of pyritization in specimens from the Upper Cretaceous.

Table 3.2: Example of the Excel database showing the details provided for each picked slide. The whole database can be found in Appendix 1. The rows that are labelled in green indicate the range of depth covered by the specified well. The rows that are labelled in red indicate material that was found to date back to the Eocene. The information for each picked slide included: the country, basin area, well's name/number/depth, outcrop number, location within the museum, notes, and inferred age of sample. The "notes" tab contains information on the preservation of the planktonic species found, and the genera/species recognised. For some picked slides, the abbreviation "vrdi" was used, which stands for= very recrystallised, difficult to identify.

All the species that could be identified were assigned a geological interval (Stage) in which they occurred, using the most updated taxonomic sources (Kennett and Srinivasan, 1983; Pearson et al., 2006; Wade et al., 2011; Young et al., 2017) (Table 3.3).

Species/Genus Name	First appearance (Stage)	Last appearance (Stage)
Archaeoglobigerina genus	Turonian	Maastrichtian
Dentoglobigerina altispira	Aquitanian	Piacenzian
Dentoglobigerina tripartita	Priabonian	Serravallian
Dentoglobigerina venezuelana	Priabonian	Zanclean
Globigerinoides elongatus	Zanclean	Recent
Globigerinoides extremus	Tortonian	Gelasian
Fohsella lobata	Serravallian Stage (base of the Stage)	Serravallian (top of the Stage)
Fohsella peripheroacuta	Langhian	Serravallian
Fohsella perirorophonda	Chattian	Serravallian
Fohsella robusta	Serravallian (base of the Stage, Middle Miocene)	Serravallian (top of the Stage)
Fohsi lineage	Chattian	Messinian
Globorotalia arrcheomenardii	Burdigalian	Serravallian
Globigerina bulloides	Langhian	Recent
Globorotalia merotumida	Tortonian	Zanclean
Globigerinoides mitra	Burdigalian	Serravallian
Globorotalia plesiotumida	Tortonian	Piacenzian
Globigerina praebulloides	Late Oligocene	Middle Miocene
Globigerina praebulloides	Late Oligocene	Tortonian (Late Miocene)
Globorotalia praemenardii	Langhian	Serravallian

Globigerinoides rubber	Seravallian	Recent
Globorotalia tumida	Messinian	Recent
Globigerina bulloides	Langhian	Recent
Globigerina venezuelana	Lutetian	Zanclean
Globigerina woodi	Chattian	Piacenzian (Late Pliocene)
Globigerinelloides genus	Valanginian	Maastrichtian
Globigerinita	Rupelian	Recent
Globigerinoides obliquus	Aquitanian	Ionian
Globigerinoides parawoodi	Chattian	Burdigalian
Globigerinoides subquadratus	Chattian (Late Oligocene)	Messinian (Late Miocene)
Globoquadrina genus	Aquitanian (Early Miocene)	Recent
Globoquadrina praedehiscens	Chattian (Late Oligocene)	Burdigalian (Early Miocene)
Globoquadrina tripartita	Middle Miocene	
Globoquadrina genus	Aquitanian	Recent
Globorotalia genus	Serravallian	Recent
Globorotalia crassaformis	Zanclean	Recent
Globorotalia exilis	Messinian	Gelasian (Late Pliocene)
Globorotalia flexuosa	Chattian	Burdigalian
Globorotalia flexuosa	Ionian	Holocene
Globorotalia hirsuta	Ionian	Recent
Globorotalia hirsuta	Ionian	Recent
Globorotalia mayeri	Chattian	Tortonian
Globorotalia miocenica	Zanclean	Gelasian
Globorotalia multicamerata	Late Miocene	Late Pliocene
Globorotalia scitula	Langhian	Recent
Globorotalia siakensis	Chattian	Serravallian
Globorotalia truncatulinoides	Gelasian (Early Pleistocene)	Recent
Globorotalia	Chattian	Recent
Globotruncana	Coniacian	Maastrichtian
Globotrunicanita	Coniacian	Maastrichtian
Globoturborotalita bollii	Serravallian	Ionian
Glorotalia menardii	Burdigalian	Recent
Hastigerina pelagica	Tortonian	Recent
Hastigerina praesiphonifera	Chattian	Serravallian
Hastigerina siphonifera	Serravallian	Recent
Marginotruncana genus	Turonian	Campanian
Moroovella aragonensis	Ypresian	Lutetian
Morozovella subbotinae	Thanetian	Ypresian
Morozovella gracilis	Thanetian	Ypresian
Morozovella marginodentata	Thanetian	Ypresian
Globigerinoides obliquus	Aquitanian	Ionian
Orbulina bilobata	Langhian	Recent
Orbulina universa	Langhian	Recent
Parasubbotina inaequispira	Ypresian	Lutetian
Praeorbulina	Burdigalian	Langhian
Rotalipora genus	Cenomanian	Cenomanian
Tilobatus sacculifer	Chattian	Recent
Sphaeroidinellopsis paenedehiscens	Messinian	Piacenzian

Sphaeroidinellopsis disjuncta	Burdigalian (Early Miocene)	Serravallian (Middle Miocene)
Sphaeroidinellopsis seminulina	Burdigalian	Piacenzian
Globigerinoides subquadratus	Late Oligocene	Messinian
Trilobatus sicanus	Burdigalian	Langhian
Trilobatus trilobus	Chattian	Recent
Whiteinella archaeocretacea	Cenomanian	Santonian

Table 3.3: A summary of the planktonic foraminiferal species spanning from the late Cretaceous and recent times that were identified with the aid of various sources (Kennett and Srinivasan, 1983; Pearson et al., 2006; Wade et al., 2011; Young et al., 2017) across the whole South-East Asian NHM collection of planktonic foraminiferal picked slides. Moreover, the living temporal range of each species was also listed and was calculated with the aid of the mentioned different sources.

Among the total number of slides investigated, about 10 picked slides were identified to date back to the early Eocene (Table 3.4), even though they were all characterised by recrystallised and/or infilled specimens. One sample, in particular, had little level of recrystallisation, but the tests of the foraminifera it contained were infilled. The sample was collected by Walter Blow when he was working for BP, and it comes from the Moogli mudstones of the Kagua area, Papua New Guinea. Identification of the specimens at the species-level and the potential to carry out geochemical analyses on the sample will be further discussed in the next Chapter (see Chapter 4).

Country	Well	Outcrop number	Well depth	Picked Slides or Residues	Location NHM	Abundance of foraminifera	Notes	Inferred Age of Sample
India	Reiss	N/A		Picked slide	6.1(39G)	P	Reiss 5808; recrystallised. *Acarinina*, *Subbotina*	Eocene?
Indonesia	L40	1	7700	Picked slide	8.5(43G)	R	4 specimens, I think *Dentoglobigerina venezuelana*, vrdi.	Priabonian (Late Eocene) to Zanclean (Early Pliocene)
Indonesia	L40	1	8010	Picked slide	8.5(43G)	P	*Dentoglobigerina venezuelana*,some orange-	Priabonian (Late Eocene) to Zanclean (Early Pliocene)

							ish, and specimens vrdi.	
Indonesia	L49	1	4650	Picked slide	8.5(43G)	P	*Dentoglobigerina venezuelana*, some pyritised, vrdi.	Priabonian (Late Eocene) to Zanclean (Early Pliocene)
Papua New Guinea	D	107		Picked slide	11.3(88E)	G	*Tripartita Dentoglobigerina*, recrystallised.	Priabonian (Late Eocene) to Zanclean (Early Pliocene)
Papua New Guinea	D	108			11.3(88E)		Slide 2 of 2; *Globigerinoides*, *Dentoglobigerina venezuelana*, recrystallised.	Aquitanian (Early Miocene) to Zanclean (Early Pliocene)
Papua New Guinea	D	134			11.3(88E)	P	Eocene, *M. marginodentata*, pyritised and recrystallised	Thanetian (Late Paleocene) to Ypresian (Early Eocene)
Papua New Guinea		231				P	Slide 1 of 3, E.E., *Morozovella marginodentata*, *Acarinin*, *Parasubbotina inaequispira*, recrystallised	Ypresian (Early Eocene)
Papua New Guinea	DK5	19			13.5(74E)	P	Mainly benthics, maybe *Parasubbotina inaequispira*, Early Eocene /Middle Eocene	Thanetian (Late Paleocene) to Ypresian (Early Eocene)

						, but specimens pyritised, recrystallised, and little sample, so difficult to identify.	
Papua New Guinea	KRE		81F	8.4(45E)	R	*Morozovella subbotinae*, and maybe one foram glassy?! So Late Paleocene, Early Eocene	Thanetian (Late Paleocene) to Ypresian (Early Eocene)
Papua New Guinea	KRE		83F	8.4(45E)	R	We already know it's Moogli Mudstones, so Early Eocene. In fact *Morozovella* present like *formosa* and *marginodentata* present, infilled and recrystallised.	Thanetian (Late Paleocene) to Ypresian (Early Eocene)

Table 3.4: List of picked slides from the South-East Asian BP collection of the Natural History Museum (NHM) of London that contained specimens dating back to the early Eocene. The foraminiferal tests were recrystallised except the KRE83F sample which was infilled, meaning the outer foraminiferal test was still well-preserved. While cataloguing the collection and the investigated picked slides with the aid of a light microscope, additional information was added to each entry, including the location within the NHM, any notes including species found, the preservation and quantity of the foraminiferal tests, as well as an estimated age of the sample based on its biostratigraphy. More detailed information on the samples (including geographical coordinates), can be found in Appendix 1.

3.4   Conclusions and future directions of the database

The South-East Asian section of the former BP collection at the Natural History Museum, London, was extensively updated with new information on the wells and locations of the samples it contains. Moreover, each of the 1260 picked slides evaluated were given an inferred age based on the biostratigraphic range of the planktonic foraminiferal species present, as well as an assessment on the preservation of the foraminiferal tests. The updated and new pieces of information will be added to the NHM online database and its associated Google Earth Layer, which provide micropalaeontologists with the opportunity to undertake rapid evaluations of whether the collection may contain material beneficial to their research. Despite all the specimens being characterised by some level of recrystallisation and/or infilling that makes it challenging for them to be considered for geochemical analyses, there are numerous potential opportunities to develop based on these collections. This is due to the vast spatial and temporal relevance of the material present in the collection, but also due to the lack of published research associated with the well run and outcrops to date. In fact, it was quite challenging to find information on the locations of the BP's oil expeditions and explored wells. Thus, it would be beneficial to work closely with BP and improve the background context of the sequences so that any gaps in knowledge can complement the collections. Museum micropalaeontologists are currently already achieving so in other parts of the sections in order to ensure that the absence of sample specific data such as precise well locations and age-depth interpretations will not limit the collection's potential. Following this investigation, it is evident that micropalaeontologists could also use the collection for taxonomy purposes and evolutionary research of planktonic and benthic foraminifera rather than for palaeoceanographic and palaeoclimatic reconstructions. This way, the collection will be able to add value to existing projects or provide opportunities to develop new collaborative projects with the Museum.

Chapter 4

Sea surface temperatures and water column reconstruction from the early Eocene of the Moogli mudstones, Papua New Guinea

Chapter **4**

4 Sea surface temperatures and water column reconstruction from the early Eocene of the Moogli mudstones, Papua New Guinea.

Abstract

Sea surface temperatures approach but rarely exceed 30°C in the Western Pacific Warm Pool, the hottest part of the modern open ocean. Climate models with reconstructed continental configurations and elevated CO_2 concentrations suggest that a Western Pacific Warm Pool has existed since the Mesozoic but virtually no reliable paleotemperature proxy data from the region exist. Models suggest that temperatures in the Warm Pool may have become extremely hot, up to 40°C, during warm climate phases such as the early Eocene, potentially exceeding the tolerance limit of eukaryotic life, but foraminiferal species from the Warm Pool region are abundant and diverse. This chapter present carbon isotopes alongside oxygen isotope and Mg/Ca paleotemperature reconstructions from the early Eocene (55 to 54 Ma) planktonic foraminifera derived from a single sample of the Moogli mudstones, central Papua New Guinea, which was deposited in a deep-water continental slope setting on the southern edge of the paleo-Warm Pool (~29°S). The sample contains exceptionally well-preserved ('glassy') foraminifera but suffers from diagenetic infilling by late stage calcite. By crushing the samples and carefully separating foraminiferal test fragments from the infill we were able to obtain reliable geochemical data from a variety of surface and thermocline-dwelling species. We reconstruct sea surface temperatures (SSTs) of ~32-36°C, which is several degrees warmer than early Eocene data from a similar latitude in Tanzania. Thus, the data support the presence of a moderately hot Warm Pool in the early Eocene which supported an abundant and diverse eukaryotic plankton community. Moreover, the climate models underestimated SSTs by 2-4°C, so that intensified tropical activity as well as a higher CO_2 sensitivity back in the early Eocene were put forward as suggestions for this data-model mismatch.

4.1   Introduction

The conundrum of a significantly flattened thermal latitudinal gradient during the sustained, extreme warmth of the early Eocene relative to today has been a central debate between climate modellers and proxy scientists up to today (Pearson et al., 2001; Huber and Caballero, 2011; Lunt et al., 2017; Evans et al., 2018). Geological data suggest sea surface temperatures (SSTs) were considerably warmer than today (10-25°C) at high-latitudes, seafloor temperatures ~14°C compared to only 2-3°C today (Cramer et al., 2011), while tropical SSTs were only a few degrees Celsius warmer (Pearson et al., 2001). This considerably flatter SST gradient between the early Eocene and today poses a challenge for models in reproducing this past greenhouse climate and matching the simulations to the proxies. The models simulate either correct high-latitude SSTs and extremely warm tropics (polar amplification), or relatively low tropical SSTs similar to geological reconstructions, while keeping lower temperature at high-latitudes (tropical dampening). Recently, Cramwinckel et al. (2018) used organic proxy-based temperature reconstructions and suggested that the Atlantic Ocean during the early Eocene was indeed characterised by very warm tropical temperatures. However, more geological data from key areas such as the tropics are needed to better constrain SSTs and thermal gradients during extreme greenhouse intervals. However, the poor preservation of foraminiferal specimens in the tropics for the early Eocene renders this goal challenging, urging sample collection in areas where the impermeable mudstones may be present, and where maximum SST average trends may have been found in the past (hence excluding the SSTs during the short-lived hyperthermal events). Here, we present palaeotemperature estimates close to the Indo-Pacific Warm Pool (IPWP), which is currently the warmest ocean surface region of the world, with SSTs ranging 28-30°C (De Deckker, 2016). Being a major source of heat and water vapour, it plays a critical role in the redistribution of heat around the globe as well as regulation of global climate variability, via for instance, the Walker and Hadley circulations (Kim et al., 2012), and can therefore give insight into the potential thermo-regulation of the oceans in the past.

In this study, we reconstructed the temperatures of the water column around the waters of Papua New Guinea (also referred to as PNG throughout the text) during the early Eocene using different species of mixed layer and thermocline dwellers, as well as one species of benthic foraminifera. The aim was to understand the ocean palaeoecology of greenhouse climates which can give further insight into the biological pump of the ocean, as well as any disequilibrium effects to take into account when relying on geochemical proxies for palaeoclimate reconstructions. Temperatures were also reconstructed to

compare the results of geological data with climate model outputs in order to investigate the level of performance of palaeoclimate models during greenhouse climates and suggest possible feedback mechanisms that may have had a major role in controlling the heat distribution and transfer from the tropics to higher latitudes.

4.2   Materials and Methods

4.2.1 Sample collection and study site

The planktonic foraminiferal assemblage sample was found in the South-East Asian section of the Former British Petroleum (BP) collection at the Natural History Museum in London. The sample "K83F" (the field sample number given by the BP company, while the NHM's registration number is: NHMUK PM BP11927) was found in the subpart of the main collection, namely Blow's collection (Fig. 4.1) as a previously washed residue containing primarily planktonic foraminifera, and a few benthic foraminifera.

Figure 4.1: Cabinet room containing the former BP collection of the NHM containing micropalaeontological slides from all around the globe, including the Southeast Asian section. Subfigure 1 shows the size of the collection; subfigure 2 shows the content of the drawers, where samples are kept in varying types of containers; subfigure 3 shows a closer photo of the slides where the planktonic foraminifera can be found.

Because BP had solely donated the collection in the 1950's following their oil expedition, no information was given about the sample, except that it was collected from the outcrop called "Moogli Mudstones". From the sparse literature research on this precise outcrop,

it was found that the Moogli Mudstones (6°5'S, 143°42'E) are located in the Kagua Inlier, which is mainly characterised by Eocene siliceous and bioclastic limestones that occur on a discontinuous basis along approximately 1000 km of the eastern Papuan Basin from the Kagua area, to the southeast Papuan Peninsula, and offshore in the Coral Sea (Carman, 1990), as shown in Figure 4.2. Moreover, it sits on a fold and thrust belt called the Papuan Fold Belt formed as a result of compressional tectonics that led to the formation of a mountain chain extending longitudinally across Papua New Guinea, a process that started sometime between the Eocene and late Miocene (Pigram and Symonds, 1991).
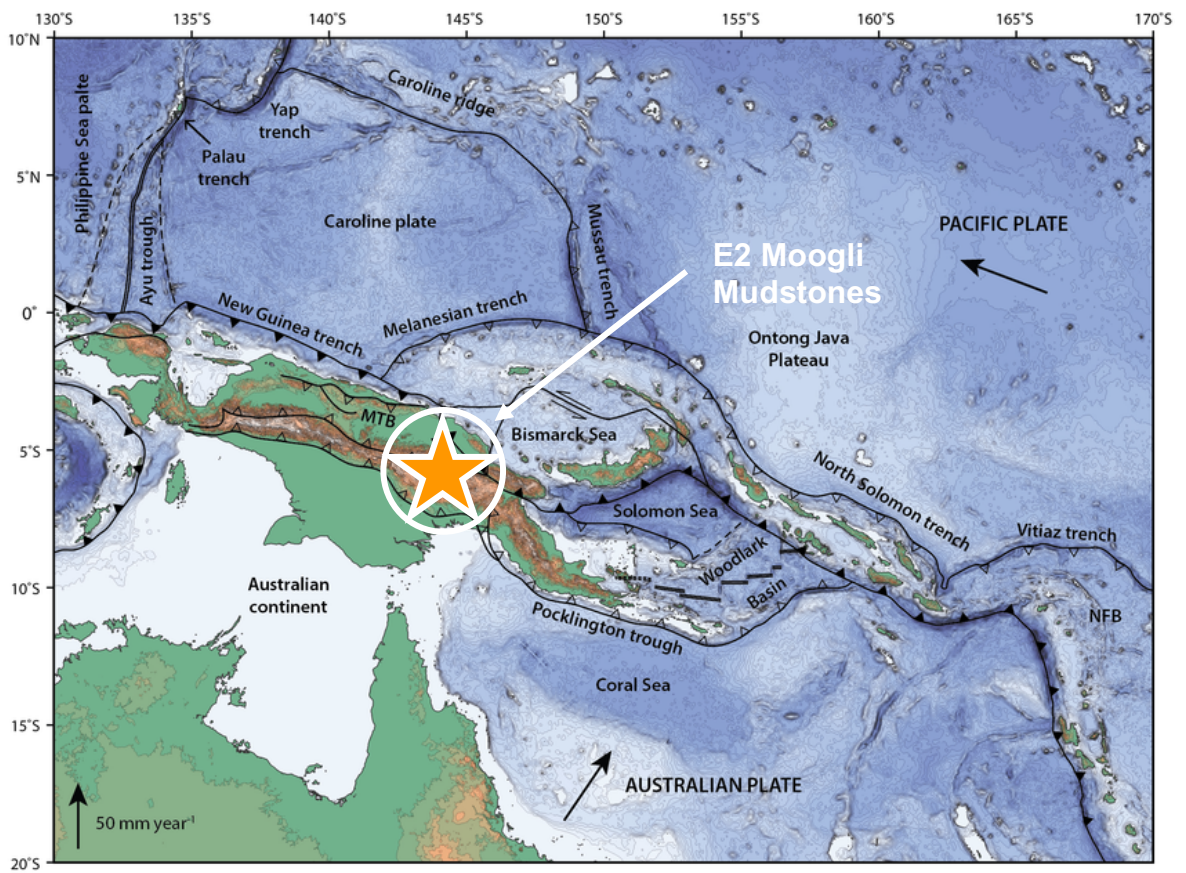
Figure 4.2: Location of the Moogli Mudstones outcrop in the Kagua Inlier where sample K83F was collected from, in the Eastern basin of Papua New Guinea. Topography, bathymetry and regional tectonic setting of New Guinea and Solomon Islands. Arrows indicate rate and direction of plate motion of the Australian and Pacific plates (MORVEL, DeMets et al., 2010); Mamberamo thrust belt, Indonesia (MTB); North Fiji Basin (NFB) (Figure adapted from Holm et al., 2016).

4.2.2 Preservation state of the foraminiferal tests and taxonomic identification

When studying the foraminiferal shells under a binocular light microscope, the state of preservation can be assessed. While the outer shells were exceptionally preserved and still retained the porous texture representative of original foraminiferal test wall, the test interior was filled with inorganic calcite which had a glassy, compact, and homogenous appearance, rather than a "frosty" appearance which is typical of recrystallised and diagenetically altered tests (Sexton et al., 2006a). Because the sample had the potential to come from the Eocene of a potentially broad Indo-Pacific Warm Pool at that time, it was decided to try and separate the infill from the test, so that the original part of the foraminiferal shells could still be analysed and used for paleoclimatic reconstructions. This is a very time-consuming and delicate task that is not ordinarily undertaken so a sound method needed to be developed. In order to ensure a successful separation, both the infill and test underwent SEM imaging and geochemical analyses. Moreover, because the sample contained a few benthic specimens, these were also analysed so that the study could be extended to represent the entire water column of the early Eocene around the area of Papua New Guinea. An assessment of the abundance of the benthic foraminifera relative to the planktonic foraminifera was also carried out in order to infer an estimated palaeodepth of the sample. The planktonic foraminiferal species were identified following the taxonomic criteria of Pearson et al. (2006), with the additional aid of the recently founded online taxonomic database called "Mikrotax" by Young et al. (2017). Lastly, with the aid of Dr. Tom Dunkley Jones at the University of Birmingham nannofossil biostratigraphic investigation was also performed on the sample in order to better constrain the age of the sample.

4.2.3 Sieving the sample and separating the original from the infill

The planktonic foraminiferal sample consisted of different species and genera representative of the early Eocene, and despite the sample being sieved under different size fractions, specifically 180-212 µm, 212-250 µm, 250-300 µm, 300-315 µm, 315-355 µm, 355-425 µm, and 425-500 µm, only the size fractions between 212 µm and 355 µm were considered for the temperature and carbon cycle reconstructions of the water column. This is the result of applying the criteria outlined by Birch et al. (2013), according to whom the size fractions outside of the mentioned interval can be particularly affected by foraminiferal vital effects, thus altering the primary foraminiferal $\delta^{13}C$ signatures and biasing palaeoclimatic reconstructions. Thus, the 180-212 µm and 425-500 µm size fractions will be still be analysed mainly to investigate different vital effects.

The sieved specimens were crushed under a light microscope, whereby the infill was manually separated from the test for all the specimens (Fig. 4.3). Both the infill and original test wall were subsequently analysed for both stable isotopes (δ^{18}O, δ^{13}C), and trace metals (Mg/Ca). Thus, each foraminiferal species of a specific size fraction had a data point for both its associated infill and its original outer part of the wall.
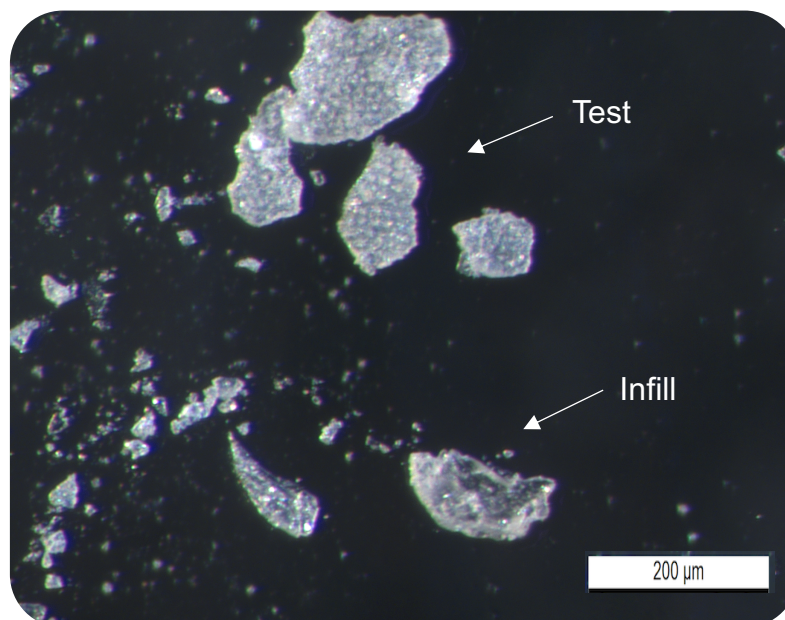
Figure 4.3: Evidence of distinct separation of the infilling from the porous test wall after crushing the planktonic foraminifera. Scale bar: 200 μm.

The planktonic foraminifera included mixed layer dwellers from the genera *Acarinina* and *Morozovella*, while for the thermocline and sub-thermocline genera *Globoturborotalita* and *Subbotina* were selected. A list of the species found for each genus is given in Appendix 2, and the study conducted by Birch et al. (2013) helped estimate the minimum number of specimens that should be used for each size fraction, especially when under sample scarcity circumstances which was the primary control in establishing the quantity used for the geochemical analyses. It was estimated that there should be a) ~100 specimens for size fraction 63-125 μm, b) 80 specimens for 125-150 μm, c) 40 for 150-180 μm, d) 20-25 specimens for 180-212 μm and 212-250 μm, e) 250-300 μm 12, f) ~10 specimens for 300-315 μm and 315-355 μm, and g) 3-4 for 425-500 μm and ≥500 μm size fractions. This way quantity consistency would be kept across different species and genera of the same size fraction.

In addition to this, images were taken with a Scanning Electron Microscope (SEM) to check on both the entire test and crushed fragments. The fragments were critical for investigating any contamination or recrystallization on the test, whilst the test served as

a measure of the extent of successful separation of the infill from the test. The SEM images of some of the species analysed are shown in the SEM plates of this chapter (Plates 4.1, 4.2, 4.3, 4.4, 4.5, and 4.6 placed at the end of this Chapter). For each specimen, the frontal, lateral, and spiral view is presented.

4.2.4 Oxygen and Carbon Stable Isotopes

The procedure used for measuring stable isotopes for $\delta^{18}O$ and $\delta^{13}C$ has been described in detail in Chapter 2. The original and associated infill fragments were analysed at Cardiff University (more details can be found in Chapter 2) for both $\delta^{18}O$ and $\delta^{13}C$ proxies. Given the little availability of the material, the sample was directly transferred from the glass slide to the mass spectrometer vial trays rather than in centrifuge tubes in order to minimise the number of steps that may have led to a greater loss of sample.

4.2.4.1 $\delta^{18}O$ conversion to water column palaeotemperatures

Temperatures from $\delta^{18}O$ were derived by inputting the values into the palaeotemperature equation published by Kim and O'Neil (1997) (Equation 4.1). This equation was chosen as its temperature calibration span ranges between 10°C and 40°C and thus makes it suitable for greenhouse climate reconstructions such as the early Eocene where the ocean temperatures have been known to exceed 30°C (Aze et al., 2014; Frieling et al., 2017), whereas for instance, the calibration for the palaeotemperature equation by Erez and Luz (1983) ranges between 14°C and 30°C. Kim and O'Neil (1997)'s equation is also more suitable for greenhouse climate reconstructions from benthic foraminifera, as seafloor temperatures may have reached 14°C in the early Eocene (Cramer et al., 2011). However, the calibration is based on the precipitation of inorganic calcite for a temperature range between 10°C and 40°C under controlled laboratory conditions, hence it does not take into consideration any vital effects, while it is known that the temperature dependence of the $\delta^{18}O$ of foraminifera is influenced by both thermodynamic and vital effects (Pearson, 2012; Hollis et al., 2019). Thus, it is important to take vital effects into account when reconstructing palaeotemperatures with the equation by Kim and O'Neil (1997), however using this equation derived from inorganic calcite helps to reduce biases by avoiding imposing the vital effects specific of foraminiferal groups, geographical regions, and shell size (Bemis et al., 1998). In fact, it is also unknown whether the vital effects may have changed through time as a result of species- or genus-level evolutionary processes (Vincent et al., 1985; Katz et al., 2003). This is important to consider particularly when reconstructing temperatures from symbiotic species. In fact, studies have found that the equation regression is very close

to the values of epibenthic and asymbiotic planktic foraminifera (Bemis et al., 1998; Costa et al., 2006).

$$T(°C) = 16.1 - 4.64 \, (\delta^{18}O_{calcite} - \delta^{18}O_{seawater}) + 0.09 \, (\delta^{18}O_{calcite} - \delta^{18}O_{seawater})^2 \qquad (4.1)$$

When using the palaeotemperature equations, three factors need to be taken into account. Firstly, the $\delta^{18}O_{sw}$ values are measured on the VSMOW scale, unlike the $\delta^{18}O_{calcite}$ values which are measured on the VPDB scale. Thus, the $\delta^{18}O_{sw}$ must be standardised to the VPDB scale hence a conversion factor needs to be applied to the $\delta^{18}O_{sw}$ value. As a result of the correction, both the 1) offset between the different absolute scales and 2) the experimental difference in the oxygen isotope fractionation occurring when reacting carbonate with phosphoric acid at 25°C versus that happening in equilibrium between water and CO_2 at 25.3°C would be corrected for. After several suggested values for the conversion factor (Epstein et al., 1953; Friedman and O'Neil, 1977), the value of 0.27‰ that was initially proposed by Hut (1987) is now currently accepted for the VSMOW to VPDB standard conversion. Lastly, because $\delta^{18}O_{sw}$ changes as a consequence of both interregional and temporal variability (the latter over geological time), these two next factors will be discussed next.

4.2.4.1.1   Correcting for regional variations in $\delta^{18}O_{sw}$: the "salinity effect"

The $\delta^{18}O_{sw}$ is affected by regional variability in the ocean as a consequence of the spatially varying balance in the evaporation-precipitation processes, as well as mixing and freshwater inputs, which all contribute to regional differences in salinity (Zachos et al., 1994; Rohling and Cooke, 1999; Pearson, 2012; Rohling, 2013). Today, the variability of $\delta^{18}O_{sw}$ ranges between -1.50‰ and +1.50‰, with most places being within ~0.50‰ of VSMOW, and the semi-enclosed basins such as the Red Sea and Mediterranean Sea recording the extreme values of the modern $\delta^{18}O_{sw}$ range (Schmidt et al., 1999; Bigg and Rohling, 2000; LeGrande and Schmidt, 2006).

As discussed in more detail in Chapter 2, initially the Zachos adjustment was adopted (Zachos et al., 1994) for this study, until a new method was proposed in 2019 (Hollis et al., 2019). The former is based on modern data collected solely from the Southern Hemisphere and it therefore assumes an identical variation in $\delta^{18}O_{sw}$ across latitudes in each hemisphere. The latter, in contrast, takes into consideration the modern global variability of $\delta^{18}O_{sw}$ with the data taken from the database of LeGrande and Schmidt (2006). Thus, the Hollis correction was chosen, also owing to its higher resolution (1° x 1° gridded data), and the database was processed on Matlab, in order to find the

corresponding value of the site's palaeolatitude. The Matlab script allows one to input the ice volume correction, but this was considered individually later, when using the equation to convert the $\delta^{18}O$ values to temperatures. It should be emphasised that a limitation of both the Zachos and Hollis approaches is that they apply the modern oxygen isotope variability to the past warm climate state which may not be strictly correct if the latitudinal patterns of evaporation, water vapour transport, condensation and precipitation were markedly different.

4.2.4.1.2   *Correcting for the temporal variations in $\delta^{18}O_{sw}$: the "the ice volume effect"*

There is still an existing debate on choosing an appropriate global $\delta^{18}O_{sw}$ value for the early Eocene, despite the commonly agreed assumption that the planet at the time was characterised by relative ice-free conditions (Lear et al., 2000; Bohaty and Zachos, 2003; Miller et al., 2005; Liu et al., 2009; Pearson, 2012; Hollis et al., 2019). The most sensible decision would be to use the value of -1‰ as it is the resulting compromise value from what the literature suggests for an ice-free world (Shackleton and Kennett, 1975; L'Homme et al., 2005; Cramer et al., 2011; Pearson, 2012; Hollis et al., 2019). However, this project focuses on both the early and late Eocene, so the value of -0.89‰ suggested by Cramer et al. (2011) for an ice-free world was selected in order to subsequently use the value they suggest for the late Eocene and therefore remain consistent with one record that includes both intervals. Nonetheless, a comparison will be made between palaeotemperatures derived from both an ice-free correction of -1‰ and -0.89‰.

4.2.4.1.3   *Accounting for the effect of pH on foraminiferal calcite*

The carbonate ion concentration ($[CO_3^{2-}]$) and the pH around the foraminifer at the time of calcification have been found to alter the primary foraminiferal $\delta^{18}O$ and $\delta^{13}C$ signatures (Spero, 1992; Spero and Lea, 1993; Spero et al., 1997; Russell and Spero, 2000; Zeebe, 2001), in a way that if both the pH and ($[CO_3^{2-}]$) are high in the seawater surrounding the test, the foraminifer will incorporate a higher proportion of ^{16}O and ^{12}C isotopes, which would lower its test $\delta^{18}O$ and $\delta^{13}C$ values. This is because there exists an isotopic fractionation between the different species of dissolved inorganic carbon (H_2CO_3, HCO_3^{-}, and CO_3^{2-}) and their proportion in the ocean vary as a function of pH (Zeebe, 1999). The ($[CO_3^{2-}]$) is the isotopically lightest form among those DIC species, while the H_2CO_3 is the isotopically heaviest form, leaving HCO_3^{-} as the intermediate. Thus, in greenhouse climates as well as during peak warming events such as PETM, where high atmospheric CO_2 levels were associated with a significantly lower pH than today, this effect may have resulted in higher foraminiferal $\delta^{18}O$ and underestimated sea surface temperature reconstructions (Zeebe, 2001; Aze et al., 2014). This pH effect can

be further enhanced in symbiont-bearing species whereby the presence of photosynthetic algae can lower the pH and increase concentration of carbonate ions around the foraminiferal test (Rink et al., 1998).

4.2.5 Trace metals

The procedure used for measuring trace metals has been described in detail in Chapter 2. The Mg/Ca data were retrieved from a Thermo Scientific™ ELEMENT XR™ HR-ICP-MS in combination with an Elemental Scientific SC-E2 Autosampler, after following the cleaning procedure protocol of Barker et al. (2003). As the sample was very scarce, a separate crushing procedure was performed for trace metal analyses, rather than splitting the initial sample and dedicating part of it for stable isotope analyses, and the rest to trace metals. The latter method would help reduce the bias of using new specimens for palaeotemperature reconstructions rather than the same specimens crushed into fragments which could be used for temperature reconstructions from both proxies. However, due to the low sample quantity, the decisions to carry out trace metal analyses was made at a later date, after ensuring the data from the stable isotopes had all been successfully processed by the mass spectrometer.

4.2.5.1   Converting foraminiferal Mg/Ca to ocean palaeotemperatures

Once the raw Mg/Ca values were obtained from the ICP-MS analyses, the approach by Evans et al. (2018) as adopted to convert the ratios to temperatures. Not only is the primary foraminiferal Mg/Ca signature mainly controlled by the temperature at the time of calcification, but it is also affected by non-thermal processes, such as salinity, changes in Mg/Ca$_{sw}$ through time, the carbonate ion concentration ($[CO_3^{2-}]$) at the time of calcification, and vital effects (Anand et al., 2003; Evans et al., 2016, 2018). Thus, it is important to acknowledge these processes when estimating palaeotemperatures. The approach of Evans et al. (2018) was adopted and values for both Mg/Ca$_{sw}$ and ocean pH during the Eocene were therefore estimated before inputting the resulting corrected Mg/Ca value into the palaeotemperature equation. There exists a non-linear relationship between Mg/Ca$_{sw}$ and the incorporation into foraminiferal calcite (Evans and Muller, 2012; Evans et al., 2016), and Evans et al. (2018) calculated a quadratic equation to estimate Mg/Ca$_{sw}$ by using the temperature measures from the shells of large benthic foraminifera (LBF) of the family Nummulitidae, which are known to be more sensitive to Mg/Ca$_{sw}$ than to temperature. Together with the fact that that are also no biases induced by changes in salinity and pH as for the case of planktonic foraminifera, this technique was chosen for Mg/Ca-derived temperature reconstructions of this study as it reduces

the uncertainties that can be associated with other methods (Dickson, 2002; Gothmann et al., 2015). The quadratic relationship that they found over the range that Mg/Ca$_{sw}$ has changed through the Phanerozoic (Mucci and Morse, 1983; De Choudens-Sanchez and Gonzalez, 2009) and is represented as follows (Equation 4.2):

$$Mg/Ca_{Calcite} = -1.96 \cdot Mg/Ca_{SW}^2 + Mg/Ca_{SW} \tag{4.2}$$

With a bootstrap approach and LOESS smoothing, Mg/Ca$_{sw}$ were reconstructed based on the 5th, 50th and 95th percentile of the dataset and spanned the period 30-55 Ma (for the values, please refer to S.I. of Evans et al., 2018). As the biostratigraphy of the sample under study revealed an estimated age of the sample, the 50th percentile value of Mg/Ca$_{sw}$ was chosen from composite Palaeogene Mg/Ca$_{sw}$ reconstruction relative to age, alongside the corresponding 5th and 95th percentiles to show the uncertainty of the results. Before the last step of conversion of Mg/Ca to temperatures, a pH-correction was applied to the raw Mg/Ca ratios by using the equation by Evans et al. (2018) that pH-normalises Mg/Ca and was constructed using the Cenozoic pH record modelled by Tyrrell and Zeebe (2004) (Equation 4.3):

$$Mg/Ca_{norm} = \frac{\frac{Mg/Ca_{measured}}{0.66}}{\frac{1}{1+\exp(6.9 \cdot (pH-8.0))} + 0.76} \tag{4.3}$$

As the pH record by Tyrrell and Zeebe (2004) was initially designed to reconstruct wide-scale shifts in pH, it does not record smaller climatic events that were characterised by carbon cycle perturbations, therefore a ±0.2 pH unit uncertainty is added to the Mg/Ca-pH normalised rations. An estimated value of ocean pH was chosen as a compromise value gathered from different studies after estimating the age of the sample (Pearson and Palmer, 2000; Tyrrell and Zeebe, 2004; Hönisch et al., 2012). Finally, these values were converted using the palaeotemperature exponential calibration of Evans et al. (2016) (Equation 4.4):

$$Mg/Ca_{foraminifera} = B\exp^{AT} \tag{4.4}$$

Where T is the temperature, and the *A* and *B* terms are the equation coefficients that both have a quadratic relationship with Mg/Ca$_{sw}$ (Equation 4.5; 4.6) as follows:

$$B = 0.019 \cdot \text{Mg/Ca}_{SW}{}^2 - 0.16 \cdot \text{Mg/Ca}_{SW} + 0.804 \qquad (4.5)$$

$$A = -0.0029 \cdot \text{Mg/Ca}_{SW}{}^2 + 0.032 \cdot \text{Mg/Ca}_{SW} \qquad (4.6)$$

It has been found that salinity can impact the Mg/Ca of planktonic foraminifera such that a 2-3 practical salinity unit difference (psu) corresponds to ~1°C bias (Hönisch et al., 2013; Gray et al., 2018). However, Hay et al. (2006) found that the mean Eocene ocean salinity was similar to today, within 1 psu. Moreover, this can be reinforced when looking at the ocean dataset by LeGrande and Schmidt (2006), where one can notice that there is, roughly, a net effect of precipitation and evaporation processes on the $\delta^{18}O_{sw}$ of the modern IPWP, meaning that the local salinity is similar to the mean ocean one rather than being heavily characterised by a local $\delta^{18}O_{sw}$.

4.2.6 The experimental design of the palaeoclimate model

The palaeoclimate model simulation used in this project is the most commonly used model simulation of the early Eocene (Lunt et al., 2010; Loptson et al., 2014), and it is a coupled ocean-atmosphere general circulation model HadCM3L VERSION 4.5 released by the UK Met Office. It is characterised by 19 vertical levels in the atmosphere and 20 ocean levels, which is important to take into account as the modelled water column was simulated in this study.

4.2.6.1 Palaeogeographies

The palaeogeographies used by the palaeoclimate models in this study were initially generated by the Getech Plc platform which in turn adopted an approach based on work performed by Markwick and Valdes (2004). The maps are based on the published data regarding depositional environments, lithology and tectonics specific of the geological Stage. Additionally, they were updated from the original maps of Markwick (2007) as they include essential information on bathymetry which is critical for atmosphere-ocean coupled models. The initial 0.5° x 0.5° resolution of the maps was further developed into a model resolution of 3.75° x 2.5° which included land-sea mask, topography, and bathymetry (Lunt et al., 2016). Even though it is still challenging to constrain the atmospheric CO_2 levels back in the Palaeogene, a reasonable range of 560-1120 ppm is used in the models as it was gathered from different published sources (Beerling and Royer, 2011; Hönisch et al., 2012; Royer et al., 2012; Anagnostou et al., 2016). Different feedbacks are considered in the simulations, including vegetation and emissivity and

planetary albedo feedbacks (Lunt et al., 2016). The emissivity feedbacks are represented by water vapour and the high-lying clouds that interact with emitted long-wave, radiation, whilst the planetary albedo feedbacks are composed of the low-lying clouds and the surface interacting with the incoming short-wave radiation (Lunt et al., 2016). In fact, the varying proportion of the different types of clouds is critical to better constrain the net feedback that they contribute to, which is also challenging to reconstruct in deep-time simulations.

4.2.6.2   Choosing the model experiment for the Ypresian Stage

Additional information of the palaeoclimate models used in this study is given in Chapter 2. The atmospheric CO_2 concentration chosen for the early Eocene simulations was the 4x pre-industrial level of 1120 ppm. This is also because the experiment called "teuyd" used only had simulations under 2x or 4x pre-industrial levels, and we know from the published literature that CO_2 may have been closer to 4x pre-industrial levels rather than 2x pre-industrial levels (Anagnostou et al., 2016). Moreover, because other greenhouse gases are even harder to reconstruct, such as methane (CH_4) and nitrous oxide (N_2O), the 1120 ppm concentration would also incorporate the contribution of such gases as they also may have been higher than today (Beerling et al., 2011). The teuyd experiment was selected because it is the updated model simulation of the previous tdlud, teugd, and teukd experiments for the Ypresian Stage, with a spin-up of 2249 years (Bridge, 2019), unlike previous versions that had shorter spin-ups which reflect lower resolution and are further from reaching equilibrium within the system (Lunt et al., 2016).

4.3   Results

4.3.1 Estimating the age of the sample

4.3.1.1   Foraminiferal biostratigraphy

The use of Biochronology (based on appearance and disappearances of species; more details found in Chapter 2) helped estimate the age of the sample. From the documentation found in Blow's collection at the Natural History Museum of London, the sample was described to belong to biozone P7, which is now part of the outdated biozonation system introduced by Blow (1969). In this study, together with the knowledge of the P7 biozone, the updated Eocene biozonation scheme of Wade et al. (2011) was used to assign a biozone to the sample based on the presence of planktonic foraminiferal species (Fig. 4.4). The oldest age limit was constrained by the presence of planktonic foraminifer *Acarinina wilcoxensis* and the absence of foraminifer *Acarinina sibaiyaensis* at an age of ~55 Myr, while the youngest age limit was constrained by the presence of

foraminifer *Morozovella velascoensis*, and the absence of foraminifer *Morozovella formosa*, at an age of ~54.5 Myr.
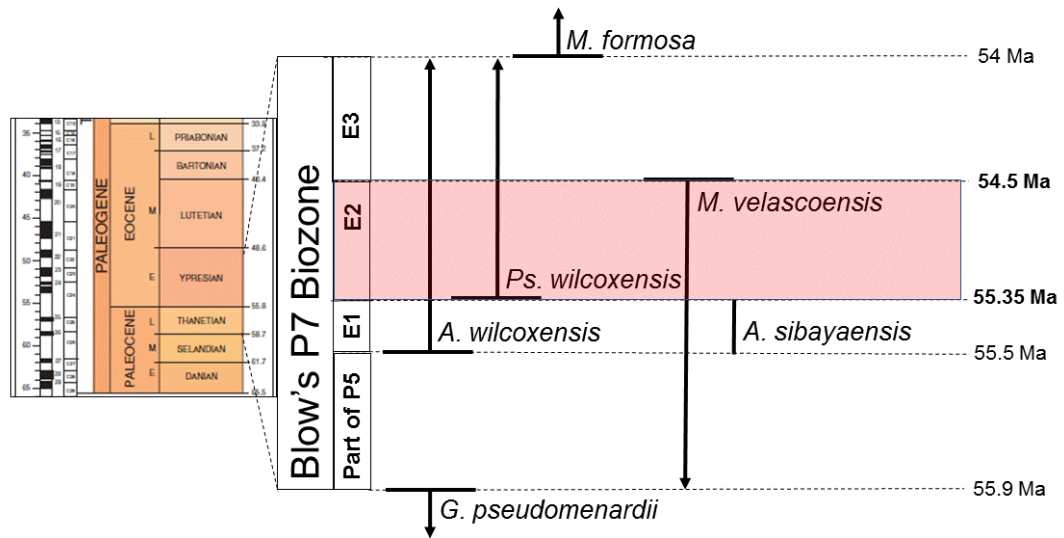
Figure 4.4: Estimated biozone and resulting age range of KR83F sample (E2 biozone, from ~55.35 to ~54.5 Ma, marked by the red shaded area), using biostratigraphy and the interval ranges of planktonic foraminifera in the Eocene. The arrow lines that cross the red shaded area represent the species of this schematic present in the E2 biozone, namely *Pseudohastigerina wilcoxensis*, *Morozovella velascoensis*, and *Acarinina wilcoxensis*. The orange scheme was taken from the Internal Stratigraphic Chart (ISC, 2013-2019) to put the biozones into the geological context. The biozonation scheme of Blow (1969) which the sample was initially described with, is also shown in relation to the updated Eocene biozonation scheme of Wade et al. (2011).

4.3.1.2   Nannofossil biostratigraphy

Calcareous nannoplankton includes coccolithophores which are unicellular planktonic protozoa with chrysophyte-like photosynthetic pigments, therefore providing a major nutritional source for the herbivorous plankton in the ocean (Armstrong and Brasier, 2005). Their generally spherical shape derives from the secretion by the organism of calcareous disc-like plates called coccoliths, held together by an organic coating to form the coccosphere (UCL, 2002). Their ubiquitous presence in marine sediments makes calcareous nannoplankton an ideal tool for biostratigraphic correlation with other microfossils. In fact, the assemblage composition of coccolithophores was investigated (personal communication with Dr Tom Dunkley Jones) with the aim of constraining even further the age of the samples that was previously estimated by foraminiferal biostratigraphy. Because the sample had initially been donated to the Natural History Museum of London as a foraminiferal residue, the nannofossils were low in abundance hence there was little fine matrix left. Despite most coccoliths being fragmented, their

preservation was considered good as they were neither affected by overgrowth nor dissolution (Fig. 4.5).
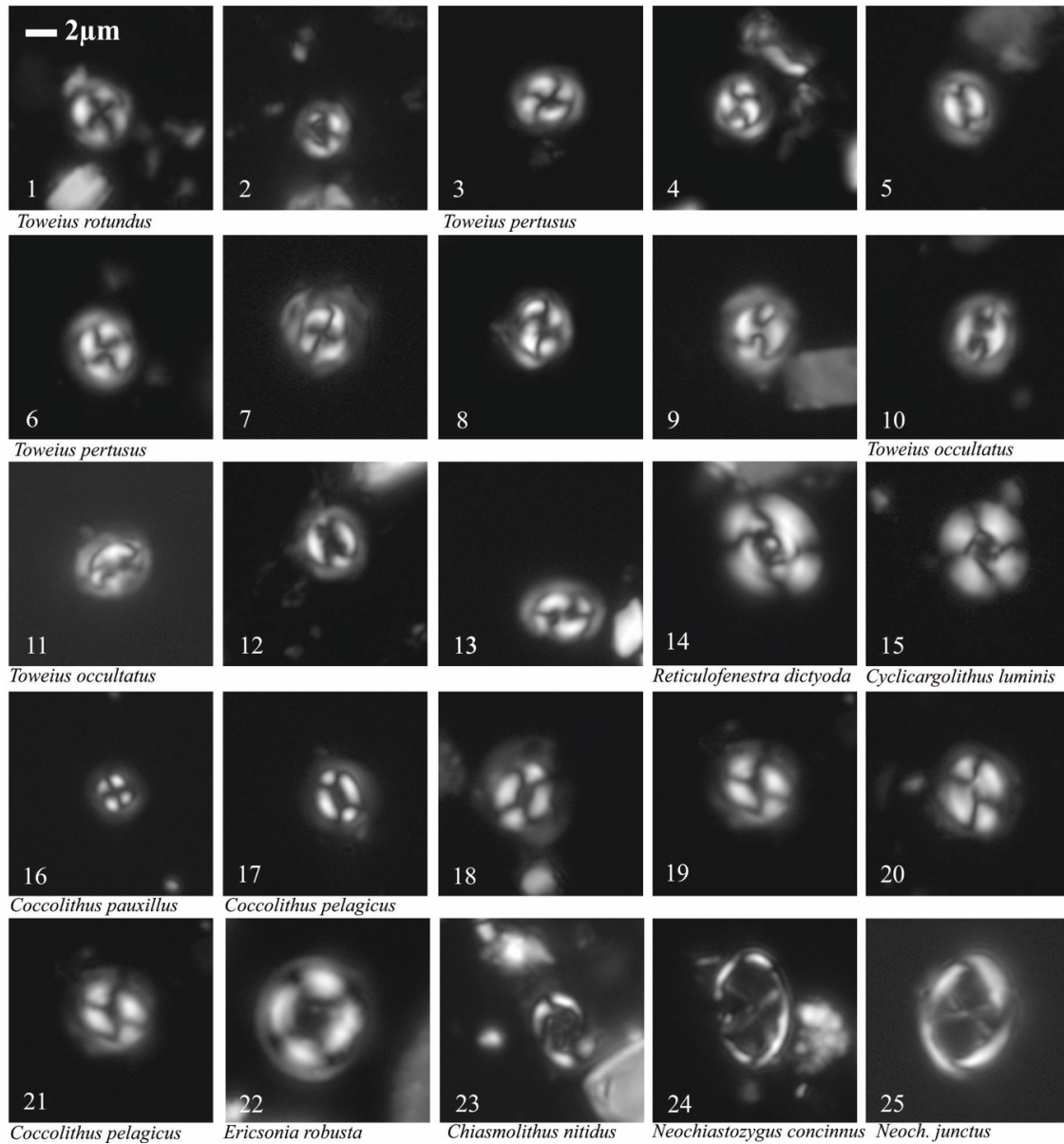
Figure 4.5: Coccolith plates of coccolithophores found in the K83F sample and used to further constrain the estimate age of the sample. Scale bar: 2 µm (Images were taken by Dr Tom Dunkley Jones).

The fragmented coccospheres recovered from the washed foraminiferal residue are dominated by simple placolith coccoliths (when the rim of the coccolith has two or more well developed shields), mostly species belonging to the genera *Toweius* and *Coccolithus*, but rare reticulofenestrids (*Reticulofenestra dictyoda* and *Cyclicargolithus luminis*). Following the nannofossil biozonation scheme of Agnini et al. (2014), the simultaneous presence of genera *Toweius* and *Reticulofinestra* would place the sample

in the CNE4 biozone (from ~52.7 Ma to ~50.6 Ma), therefore indicating an early Eocene age pelagic assemblage, which is further reinforced by the placolith assemblage, and rare specimens of *Neochiastozygus muroliths*. However, it is important to specify that only two specimens from the genus *Reticulofinestra* were found, whilst it is known that the *Toweius/Reticulofinestra* overlap started with an immediate equal abundance of both genera. Moreover, this is in disagreement with the evidence given by the foraminiferal biostratigraphy of the sample which places the sample in the CNE2 biozone with the presence of *Pseudohastigerina wilcoxensis*. Considering the fact that this particular nannofossil evidence is solely based on the presence of secondary biomarkers, while the foraminiferal evidence is using primary biomarkers too, the CNE2 was chosen to be the most sensible and logical biozone estimate to assign the sample to.

4.3.2 Estimating the depth of deposition of the sample

The equation of Van der Zwann et al. (1990) represents the relationship between bathymetric depth and the ratio between planktonic and benthic foraminifera, where %P is the percentage number of planktonic foraminifera relative to benthic foraminifera (P/B ratio) in the sample (Equation 4.7). Particularly, the abundance of planktonic foraminifera relative to benthic foraminifera increases with the distance from the coast, primarily due to lower turbidity offshore and therefore greater primary production and nutrient-low areas (Berger and Diester-Haass, 1988). In contrast, benthic foraminifera thrive better in shelf seas and at the continental edge, where the amount of organic carbon in the sediment is highest, therefore following a pattern based on food availability (Berger and Diester-Haass, 1988; Van der Zwann, 1990).

$$\text{Depth} = e^{(3.58718 + (0.03534 \times \% P))} \tag{4.7}$$

However, the equation can only be used on samples with an estimated paleodepth between 36 m and 1250 m. Because the sample in this study had 98% planktonic foraminifera relative to benthics, the equation would result in an underestimated depth. The high percentage of planktic foraminifera suggests that the foraminifera from the sample were most likely living further away from the shore hence at greater depths.

As an alternative solution, the diagrams reported by Armstrong and Brasier (2005) were used to estimate a palaeodepth for the sample. Figure 4.6 shows that at present, benthic

Bulimina species tend to live between 100 m and 3000 m depth at tropical/sub-tropical latitudes in the Pacific Ocean, while Figure 4.7 shows that a sample percentage of 98% planktonic foraminifera corresponds to living between 2500 m and 3000 m depth, which narrows down the estimated depth range from Figure 4.6.
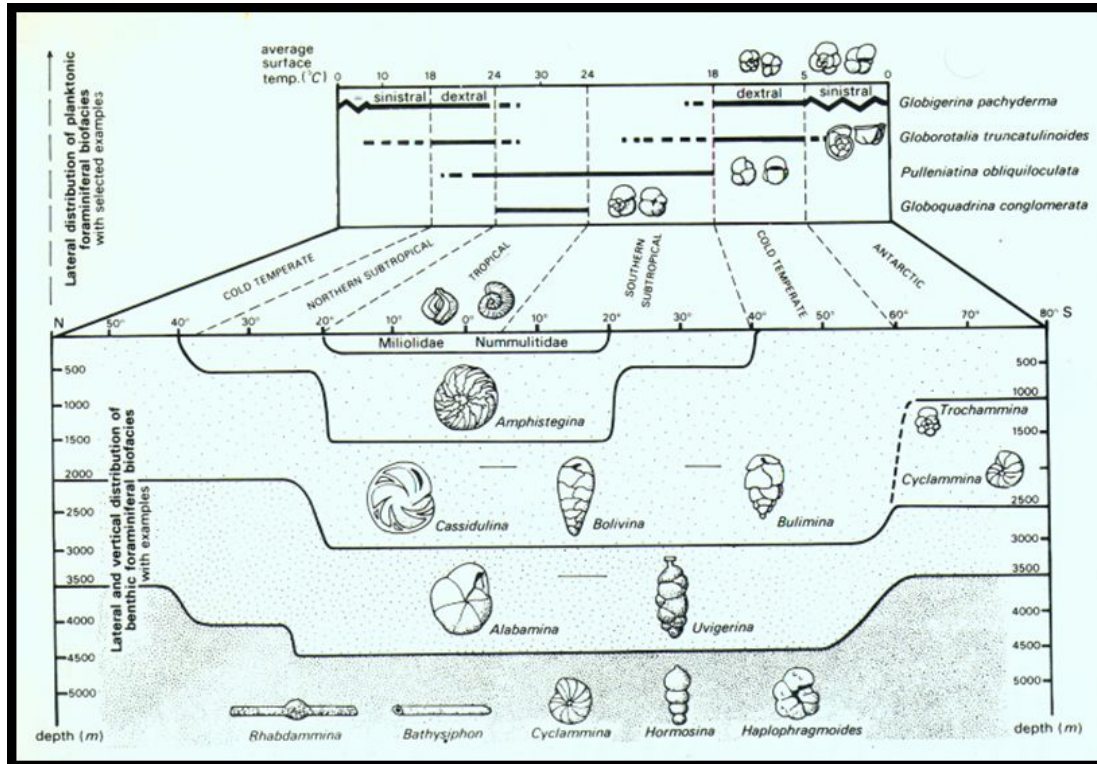
Figure 4.6: Distribution of planktonic and benthic foraminiferal assemblages with temperature, latitude, and depth. In the current study, the key part of this figure is the presence of Bulimina genus between 1000 m and 3000 m at tropical/subtropical latitudes, which helps estimate the palaeodepth of the sample (taken from Armstrong and Brasier, 2005).

If one was to assume that the living depth of *Bulimina* in the early Eocene was similar to today, the sample was likely to be located in a semi-pelagic setting, probably on a continental slope between 2500 m and 3000 m depth.
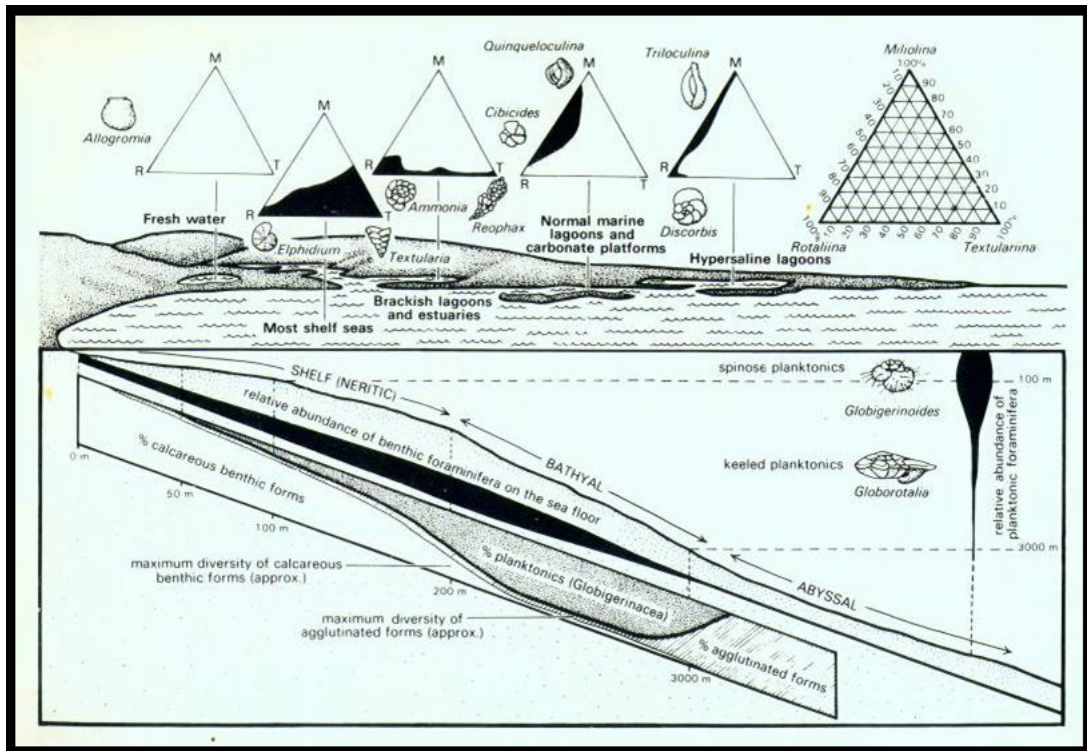
Figure 4.7: Distribution of benthic and planktonic foraminifera in the water column taken from Armstrong and Brasier, 2005).

4.3.3 Stable isotopes

4.3.3.1   Oxygen isotopes from planktonic tests and their infill

The results (Fig. 4.8) show the $\delta^{18}O$ values that were retrieved from different species (hereinafter spp.) of the genera *Acarinina*, *Morozovella*, *Subbotina* and species *Globoturborotalita bassriverensis,* along with the associated infill found inside their tests in order to test the reliability of the separation method of the infill from the original part of the foraminiferal test. The size fractions shown on Figure 4.8 range between 212 μm and 355μm as it is considered the most suitable size fraction range for $\delta^{13}C_{DIC}$ reconstructions when trying to minimise the biases caused by vital effects (Birch et al., 2013). Even though it has been found that some species of foraminifera can incorporate a fraction of isotopically light metabolic oxygen into their shells as a result of respiration (Erez, 1978; Pearson, 2012), to date there is no clear evidence that this metabolic oxygen affects the $\delta^{18}O$ of a specific foraminiferal species consistently across test size unlike for $\delta^{13}C$. Thus, we commonly assumed the $\delta^{18}O$-based palaeotemperature reconstructions were not greatly affected by metabolic fractionation, unlike $\delta^{13}C$, and the size fractions outside of 212-355 μm (hereinafter referred to as Birch range), namely 180-212 μm and >355-425 μm were only shown when investigating the effect of size fraction on $\delta^{18}O$ and $\delta^{13}C$ (see

Section 4.3.3.5), whereby individual $\delta^{18}O$ and $\delta^{13}C$ plots were produced. Moreover, when explaining the $\delta^{18}O$ ranges of each genus (see this Section below) as well as reconstructing the temperatures of the water column from $\delta^{18}O$, all the size fractions (Birch range and outside Birch range) were taken into consideration (the whole range for each genus is therefore only plotted in Section 4.3.3.5 where individual $\delta^{18}O$ plots were produced).

The $\delta^{18}O$ values agree with the conventional palaeoecology model of the ecology groups the analysed species belong to, whereby *Acarinina* and *Morozovella* species are classified as mixed layer dwellers, occupying the uppermost part of the water column as they possess symbiont algae, with $\delta^{18}O$ ranging between -3.94‰ and -4.22‰ and between -3.57‰ and -4.29‰, respectively. In contrast, *Subbotina* spp. and *Globoturborotalita bassriverensis* preferentially inhabited the thermocline and sub-thermocline of the water column (Shackleton et al., 1985; Pearson et al., 1993; D'Hondt et al., 1994; Birch et al., 2012; Si and Aubry, 2018) with their tests recording relatively higher $\delta^{18}O$ values, ranging between -2.20‰ and -3.78‰ and between -2.16‰ and -3.36‰, respectively. There is a slight overlap between the two ecology groups of ~0.50‰, specifically between subbotinids and morozovellids. In contrast, the associated infill of all the species analysed is distinctly separated from all the measured $\delta^{18}O$ values of the tests, being characterised by a relatively lower $\delta^{18}O$ signature, ranging between -4.80‰ and -5.30‰, unlike the whole range of test $\delta^{18}O$ contained within the range of -4.60‰ and -2.20‰. This low $\delta^{18}O$ signature further confirms the hypothesis that the test was affected by infilling rather than recrystallisation, as the latter would be characterised by a $\delta^{18}O$ higher than the test $\delta^{18}O$, while the former is characterised by a lower $\delta^{18}O$ signature as a result of its source, which is most likely meteoric water that when percolating through the outcrop led to the formation of diagenetic cement (Corfield et al., 1990). The infill $\delta^{18}O$ of the thermocline dwellers gives more depleted values compared to the $\delta^{18}O$ infill of the mixed layer dwellers, so that there is a smaller difference between the test $\delta^{18}O$ and the infill $\delta^{18}O$ of mixed layer dwellers than there is between the test $\delta^{18}O$ and the infill $\delta^{18}O$ of the thermocline dwellers.
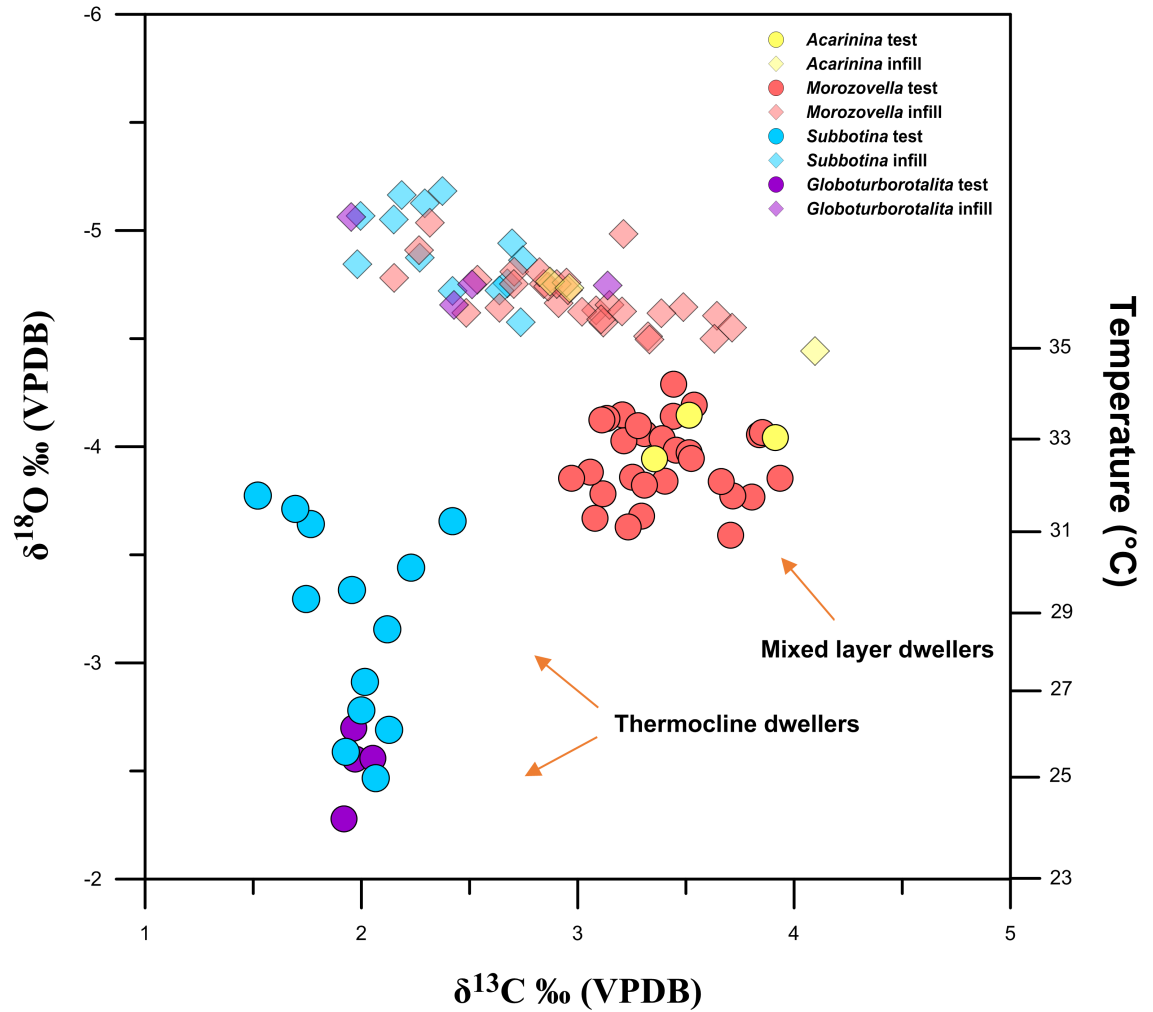
Figure 4.8: Temperature and depth habitat reconstructions of the water column around Papua New Guinea during the early Eocene (~55-54 Ma) from the geochemical proxies $\delta^{18}O$ and $\delta^{13}C$ which were derived from planktonic foraminiferal tests (circles). Since the samples were infilled, the associated infill was also analysed (opaque diamonds). The $\delta^{18}O$ scale is reversed such that the lower values indicating mixed layer waters are found at the top, while the higher values at the bottom, intercepting with the $\delta^{13}C$ axis. The different colours represent different genera: yellow is for *Acarinina* spp.; tropical pink is for *Morozovella* spp.; sky blue is for *Subbotina* spp.; purple is for *Globoturborotalita bassriverensis*. Acarininids and morozovellids are labelled as mixed layer dwellers, while subbotinids and *Globoturborotalita bassriverensis* are labelled as thermocline dwellers. The temperature on the second y-axis were derived from inserting the test $\delta^{18}O$ values into the palaeotemperature equation of Kim and O'Neil (1997). A latitudinal correction of +0.59‰ was applied after Hollis et al. (2019), as well as an ice-free volume correction of -0.89‰ after Cramer et al. (2011). Only the size fraction within the 212-355 μm range are shown (Birch et al., 2013).

4.3.3.2   Carbon isotopes from planktonic tests and their infill

The test $\delta^{13}C$ values show a similar trend as the $\delta^{18}O$ values regarding the differentiation in depth habitats with morozovellids and acarininids living in the mixed layer, while subbotinids and *Globoturborotalita bassriverensis* living relatively deeper in the water column. In fact, the test $\delta^{13}C$ ranges between 2.95‰ and 3.90‰ for morozovellids, and

between 3.35‰ and 3.50‰ for acarininids. In contrast, the test of thermocline dwellers possessed more depleted $\delta^{13}C$ values, ranging between 1.50‰ and 2.42‰ for subbotinids, and between 1.90‰ and 2.18‰ for *Globoturborotalita bassriverensis*. This pattern between the mixed layer and thermocline reflects the conventional biological pump structure of the water column, whereby the mixed layer becomes depleted in ^{12}C as this isotope is preferentially utilised by photosynthesis, and is returned back to the water column with a progressive, increasing $\delta^{13}C_{sw}$ trend down through the water column, as a result of remineralisation and respiration processes at greater depths (Ravelo and Hillaire-Marcel, 2007).

4.3.3.3   Oxygen and carbon isotopes from benthic tests and their infill

Initially, the study was going to focus solely on the water column temperature measurements and depth habitat reconstructions derived from planktonic foraminifera. However, a few benthic specimens were found in the sample and were therefore sieved and analysed as well. Only stable isotopes were retrieved from the benthics due their scarcity in the sample. By adopting the same size fraction criteria as for the planktonics (212-355 µm), both the test and associated infill were analysed (Fig. 4.9). The only species that was present in sufficient amounts hence the most dominant benthic specimen present was identified as *Bulimina tuxpamensis*, which is a benthic infaunal species from the upper Paleocene and lower Eocene (Corliss, 1985). It is characterised by a particularly thick test; an upper depth limit at the middle-upper bathyal boundary (500–700 m) (Van Morkhoven et al., 1986; Alegret et al., 2009) and preference for high-nutrient conditions (Thomas, 1990; Gibson et al., 1993). The results show that the test $\delta^{18}O$ values range between -1.10‰ and -2.20‰, which indicates a higher $\delta^{18}O$ signature relative to the planktonics, hence a colder and deeper habitat in the water column. The test $\delta^{13}C$ signature also supports the idea of a deeper habitat, by showing $\delta^{13}C$ values lower than for the planktonics, ranging between 0.20‰ and 0.95‰.

However, the behaviour of the infill $\delta^{18}O$ and $\delta^{13}C$ is the reason why the benthics were discussed separately from the infill of the planktonics. In fact, they give anomalous values with respect to the rest of the data. The infill should generally have a lower $\delta^{18}O$ than $\delta^{18}O_{sw}$, as it would be derived from either rainwater, or water reservoirs flowing from land through the sediment.
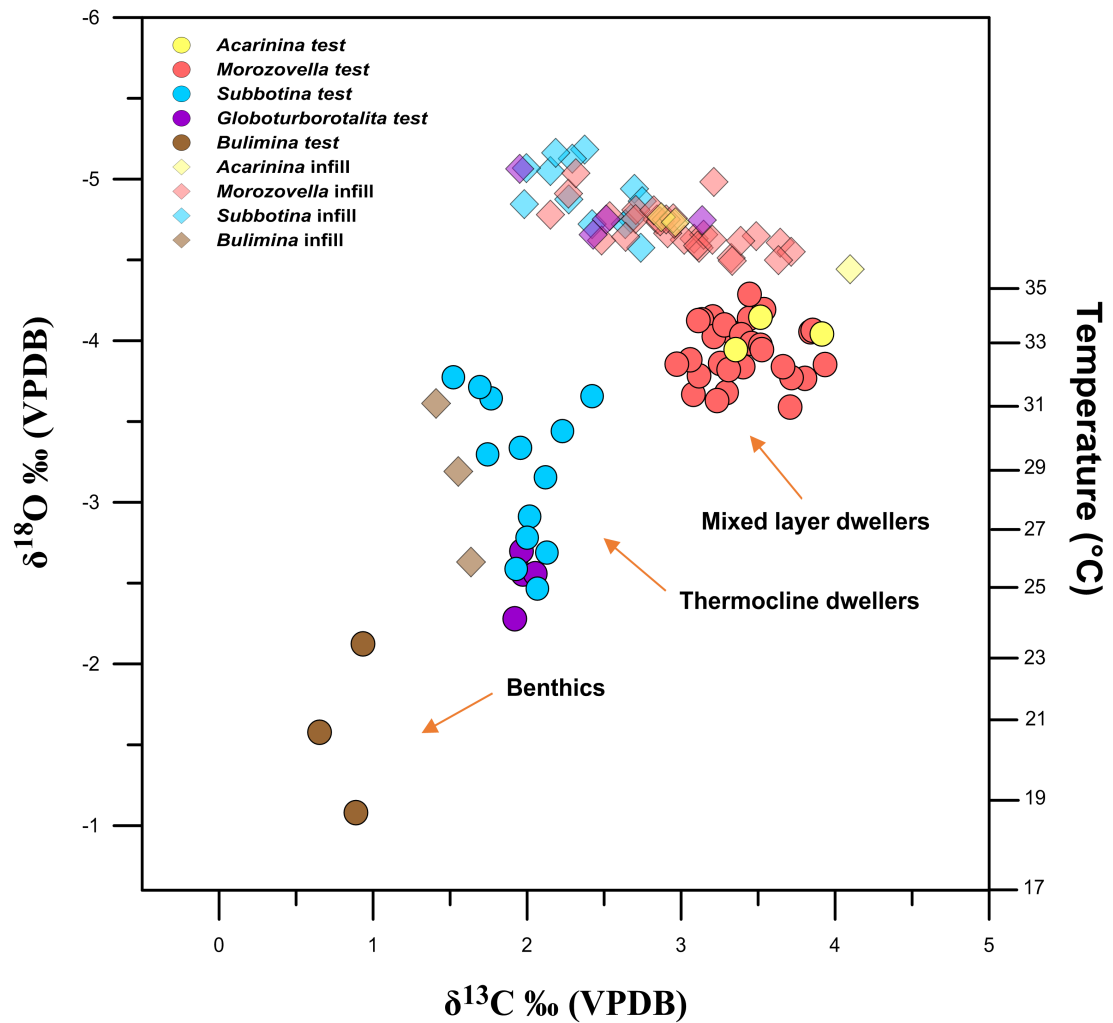
Figure 4.9: Temperature and depth habitat reconstructions of the water column around Papua New Guinea during the early Eocene (~55-54 Ma) from the geochemical proxies $\delta^{18}O$ and $\delta^{13}C$ which were derived from both planktonic and benthic foraminiferal tests (circles). Since the samples were infilled, the associated infill was also analysed (opaque diamonds). The $\delta^{18}O$ scale is reversed such that the lower values indicating mixed layer waters are found at the top, while the higher values at the bottom, intercepting with the $\delta^{13}C$ axis. The different colours represent different genera: yellow is for *Acarinina* spp.; tropical pink is for *Morozovella* spp.; sky blue is for *Subbotina* spp.; purple is for *Globoturborotalita bassriverensis*; brown is for *Bulimina tuxpamensis*. Acarininids and morozovellids are labelled as mixed layer dwellers, subbotinids and *Globoturborotalita bassriverensis* are labelled as thermocline dwellers, and *Bulimina tuxpamensis* is a benthic infaunal species from the upper Paleocene and lower Eocene. The temperature on the second y-axis were derived from inserting the test $\delta^{18}O$ values into the palaeotemperature equation of Kim and O'Neil (1997). A latitudinal correction of +0.59‰ was applied after Hollis et al. (2019), as well as an ice-free volume correction of -0.89‰ after Cramer et al. (2011). Only the size fraction within the 212-355 µm range are shown (Birch et al., 2013).

However, even if the infill $\delta^{18}O$ of the *Bulimina tuxpamensis* is more depleted than its associated test, with values ranging between -2.60‰ and -3.60‰, it is still higher than the test $\delta^{18}O$ of morozovellids and acarininids. Interestingly, the test $\delta^{18}O$ of subbotinids and *Globoturborotalita bassriverensis* lies within the same range as the infill $\delta^{18}O$ of

Bulimina tuxpamensis, suggesting that the infill of the latter may have either been derived from either cement formed out of calcium carbonate precipitated in seawater, or meteoric waters with a large contribution of $\delta^{18}O_{sw}$.

4.3.3.4 $\delta^{18}O$-based temperature reconstruction of the water column

The test $\delta^{18}O$ values of the mixed layer and thermocline dwellers as well as of the benthic foraminifera were converted to temperatures according to the approach outlined in Section 4.2.4.1. The modern $\delta^{18}O_{sw}$ value that corresponds to a latitude of ~29°S (the resulting palaeolatitude of Papua New Guinea from the models, see Section 4.3.5 below) was +0.59‰, and the ice volume correction used was that of an ice-free world, equivalent to -0.89‰ according to the Cenozoic reconstruction of Cramer et al. (2011). The sea surface temperatures resulting from the measurements on mixed layer dwellers, namely *Morozovella* spp. and *Acarinina* spp., vary from 31°C to 34.6°C, while the thermocline/sub-thermocline temperatures vary from 25.6°C to 32°C. Lastly, bottom water temperatures reconstructed from *Bulimina tuxpamensis* recorded temperatures ranging between 18.5°C and 23.5°C.

In comparison, an ice volume correction of -1‰ was applied, which is the compromise value among different studies for an ice-free world (see Section 4.2.4.1.2), SSTs would be ~0.5°C lower than with the ice volume correction of -0.89‰. Moreover, if Zachos' latitudinal correction of +0.66‰ was applied (see Section 4.2.4.1.1), SSTs would be ~0.40°C higher than with Hollis' latitudinal correction of +0.59‰. Due to the proxy uncertainty, a pH correction was not directly applied to the temperature reconstructions. As an estimate, according to the "pH" effect of Spero et al. (1997), when considering the reconstructed Eocene surface ocean pH of 7.7 as a compromise value among different studies (Pearson and Palmer, 2000; Tyrrell and Zeebe, 2004; Hönisch et al., 2012), as well as the estimated change in foraminiferal $\delta^{18}O$ per unit of pH (Uchikawa and Zeebe, 2010), $\delta^{18}O$-derived temperatures would be up to 2°C warmer.

4.3.3.5 The relationship between size fraction and stable isotopes in foraminifera

The foraminiferal life ecology, as well as the vertical column structure (e.g. thermal stratification and $\delta^{13}C_{DIC}$) can be reconstructed by analysing the foraminiferal $\delta^{13}C$ and $\delta^{18}O$ signatures (Kroon and Ganssen, 1989; Mulitza et al., 1997; Rohling and Cooke, 1999; Spero et al., 2003; Rohling et al., 2004; Friedrich et al., 2012). However, contrary to the assumption, there are chemical and physiological processes that cause the foraminiferal $\delta^{13}C$ and $\delta^{18}O$ values to deviate from the $\delta^{13}C$ and $\delta^{18}O$ of seawater (Berger et al., 1978; Spero and Williams, 1988, 1989; Kroon and Ganssen, 1989;

McConnaughey, 1989; Spero et al., 1991; Spero and Lea, 1993; Bijma et al., 1999; Bemis et al., 2000; Schiebel and Hemleben, 2005). Nonetheless, it has been found that by carefully analysing different size fractions with their size-related ontogenetic effects, these vital effects can be reduced when interpreting palaeoclimates (Kroon and Ganssen, 1989; Kroon and Darling, 1995; Faul et al., 2000; Spero et al., 2003; Lončarić et al., 2006). For extinct species, the test $\delta^{18}O$ and $\delta^{13}C$ signatures are the only way to reconstruct growth-related vital effects and depth migration throughout the water column (Pearson et al., 1993; D'Hondt et al., 1994; Norris, 1996; Coxall et al., 2000; Bornemann and Norris, 2007; Birch et al., 2012). A study by Birch et al. (2013) identified 212-355 µm to be the optimal range of size fractions where vital effects are minimum and thus can best represent the $\delta^{13}C$ of the seawater surrounding the foraminifer at the time of calcification. Therefore, we only used this range when reconstructing the palaeoecology from $\delta^{13}C$, but we also analysed the 180-212 µm and 355-425 µm size fractions to investigate the magnitude of the vital effects the early Eocene tropical foraminifera may have been affected by and to reconstruct temperatures from $\delta^{18}O$.

4.3.3.5.1 *Carbon isotopes, size fraction and interspecies variability*

The $\delta^{13}C$ of both mixed layer dwellers and thermocline dwellers was further investigated against changing size fraction in order to study the vital effects associated with planktonic foraminifera. *Morozovella* spp. and *Acarinina* spp. host symbiotic algae which preferentially utilise the ^{12}C pool of the water column for their photosynthetic reactions, leaving the mixed layer more depleted in ^{12}C hence higher in the $\delta^{13}C$ signature. This is reflected on the foraminiferal shells, as when calcification occurs the foraminifer absorbs the enriched $\delta^{13}C$ signature of the mixed layer, when assuming this is occurring close to equilibrium with $\delta^{13}C_{DIC}$. As a result, the bigger the test, the more symbionts it may be able to host, and the larger the effect on the $\delta^{13}C$ enrichment of the shell such that the bigger size fractions will possess a higher $\delta^{13}C$. The results obtained from the mixed layer dwellers show a very clear evidence of this $\delta^{13}C$ effect with increasing size fraction (Fig. 4.10). Even if the effect may not necessarily be constant throughout each size fraction, there is a general, positive trend between $\delta^{13}C$ enrichment and increasing size fraction.
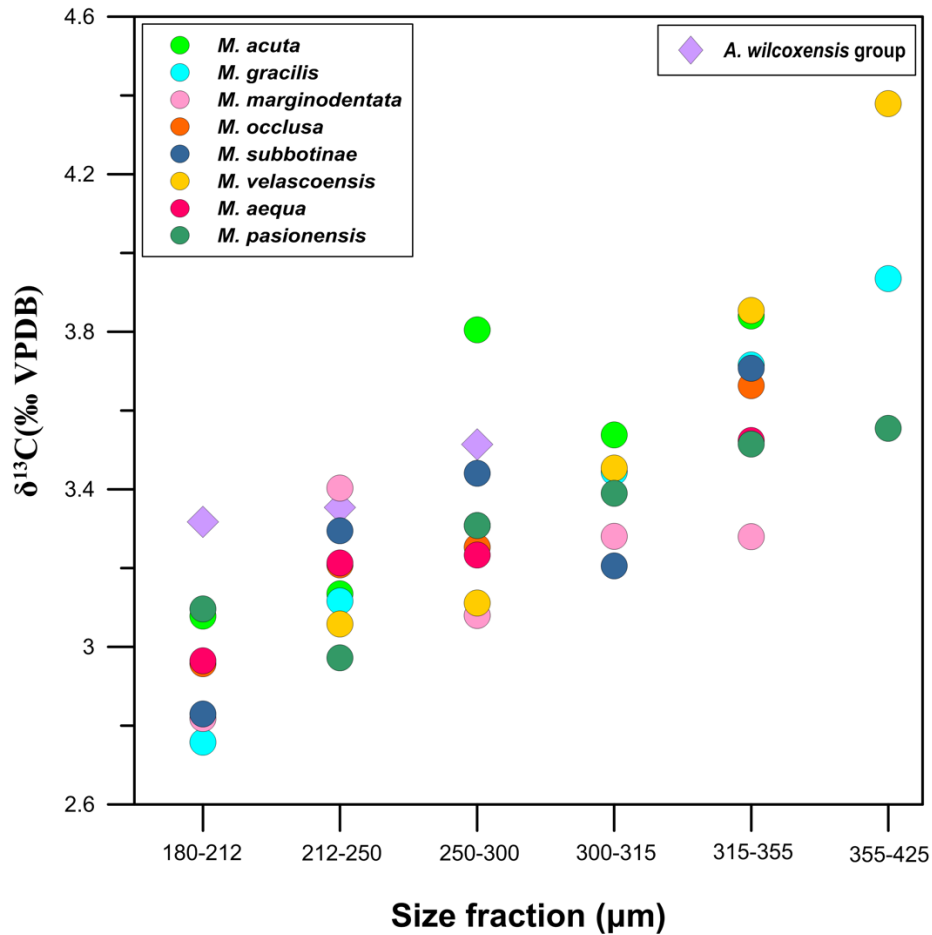
Figure 4.10: Relationship between foraminiferal $\delta^{13}C$ (‰) of mixed layer dwellers and increasing size fraction (µm). The different colours of the circles represent a different species of the *Morozovella* genus. The diamonds represent *Acarinina* species. As many size fractions as possible were used for each species, but not all of them were available for each species because of sample scarcity.

Here, 180-212 µm and 355-425 µm size fractions were also included to investigate other vital effects that will be further discussed (see Section 4.4.3.2). Evidently, these two size fractions seem to have a less consistent behaviour than the others, with 180-212 µm being significantly more depleted in ^{12}C than its neighbouring bigger size fraction, and differing from the other size fractions to a greater extent than how these differ in ^{12}C between each other. Additionally, the 355-425 µm also exposed a range of $\delta^{13}C$ values that is larger than the other size fractions, despite only three specimens being investigated.

Conversely, the thermocline dweller *Subbotina* spp. do not display a distinct trend, being asymbiotic (Fig. 4.11). Interestingly, *Globoturborotalita bassriverensis*, which on the main depth habitat plot (Fig. 4.11) revealed $\delta^{13}C$ and $\delta^{18}O$ values similar to thermocline dwellers subbotinids, experiences a gradual $\delta^{13}C$ enrichment with increasing size

fraction. If it hosted symbiotic algae too, this may mean that it may have indeed lived within the euphotic zone, hence within or very close to the mixed layer, or it may have migrated seasonally. This controversy will be discussed in Section 4.4.3.3. where the $\delta^{18}O$ of *Globoturborotalita bassriverensis* will also be taken into account.
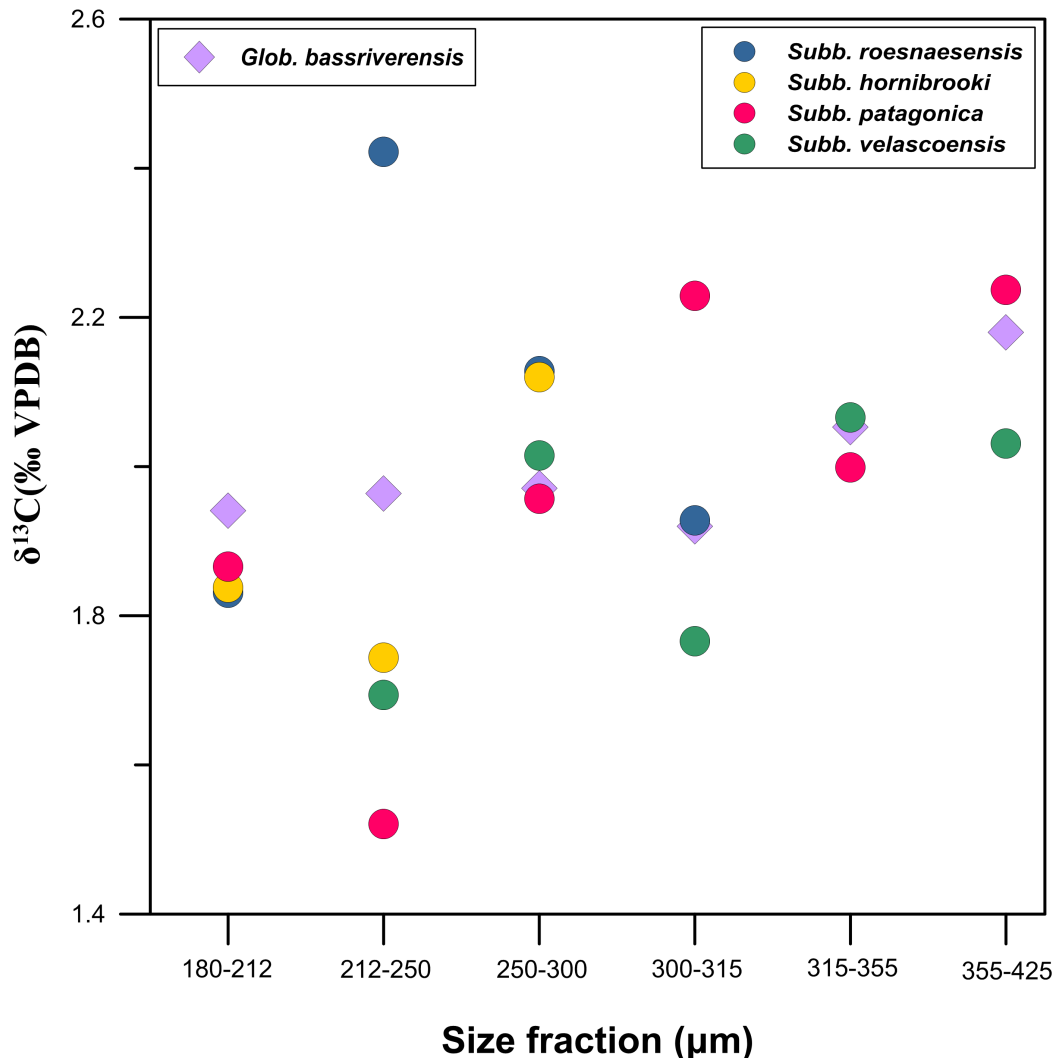
Figure 4.11: Relationship between the foraminiferal $\delta^{13}C$ (‰) of thermocline dwellers and increasing size fraction (μm). The different colours of the circles represent a specific species of the *Subbotina* genus. The diamonds represent *Globoturborotalita bassriverensis*. As many size fractions as possible were used for each species, but not all of them were available for each species because of sample scarcity.

4.3.3.5.2   Oxygen isotopes, size fraction and interspecies variability

The $\delta^{18}O$ of both mixed layer dwellers and thermocline dwellers was also investigated against changing size fraction in order to study the vital effects associated with planktonic foraminifera that may affect the original $\delta^{18}O$ signal. When looking at the $\delta^{18}O$ of the mixed layer dwellers morozovellids and acarininids against changing size fraction, there is no clear trend at neither species- nor genus-level for most size fractions (Fig. 4.12).

There seems to be a shift towards lower $\delta^{18}O$ values for *M. pasionensis* and *M. marginodentata*, which continues in the 315-255 μm and 355-425 μm size fractions. Furthermore, at species-level, the $\delta^{18}O$ of *M. occlusa* increases with size fraction. In other species such as *M. gracilis* and *M. subbotinae*, the $\delta^{18}O$ decreases in 250-300 μm, 300-315 μm, to then increase again in the last two biggest size fractions, which could be an indication of either depth migration or ontogenetic effects.
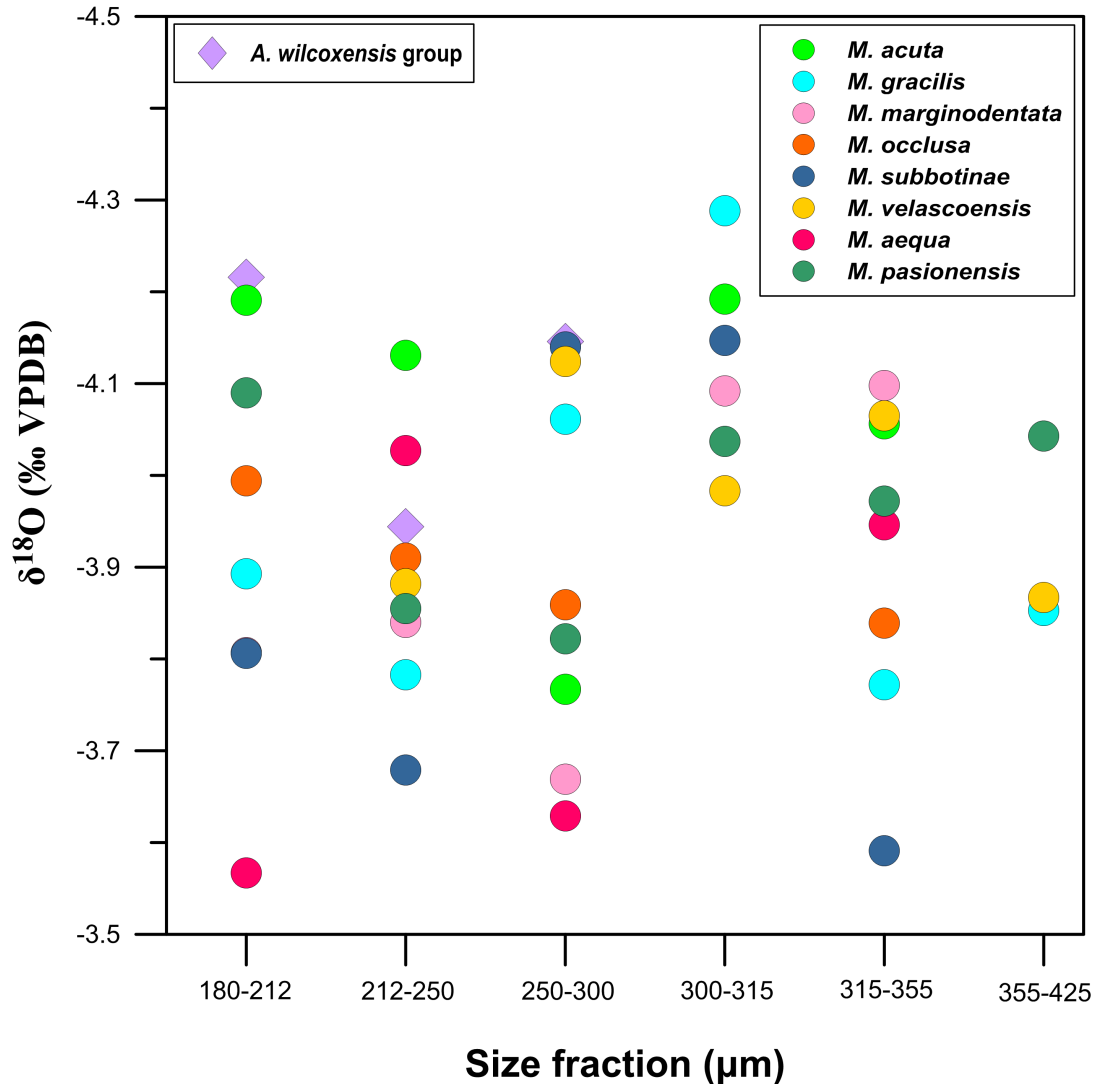
Figure 4.12: Relationship between foraminiferal $\delta^{18}O$ (‰) of mixed layer dwellers and increasing size fraction (μm). Each circle colour represents a different species of the *Morozovella* genus. The diamonds represent *Acarinina* species. As many size fractions as possible were used for each species, but not all of them were available for each species because of sample scarcity.

In contrast, there is a clearer pattern for the thermocline dwellers between their $\delta^{18}O$ signature and increasing size fraction (Fig. 4.13). Here, there is a general trend at both species- and genus-level that the $\delta^{18}O$ becomes higher as size fraction increases, at least certainly between the smallest and the biggest size fractions, less so during the

intermediate size fractions, where the δ¹⁸O of specific species may alternate between lower and higher δ¹⁸O values, especially in the case of *Subbotina velascoensis* and *Subbotina patagonica*.

The pattern is slightly more consistent for *Globoturborotalita bassriverensis*, where the δ¹⁸O becomes higher with increasing size fraction, except at size fraction 315-355 μm where it gets lower by almost 0.80‰.
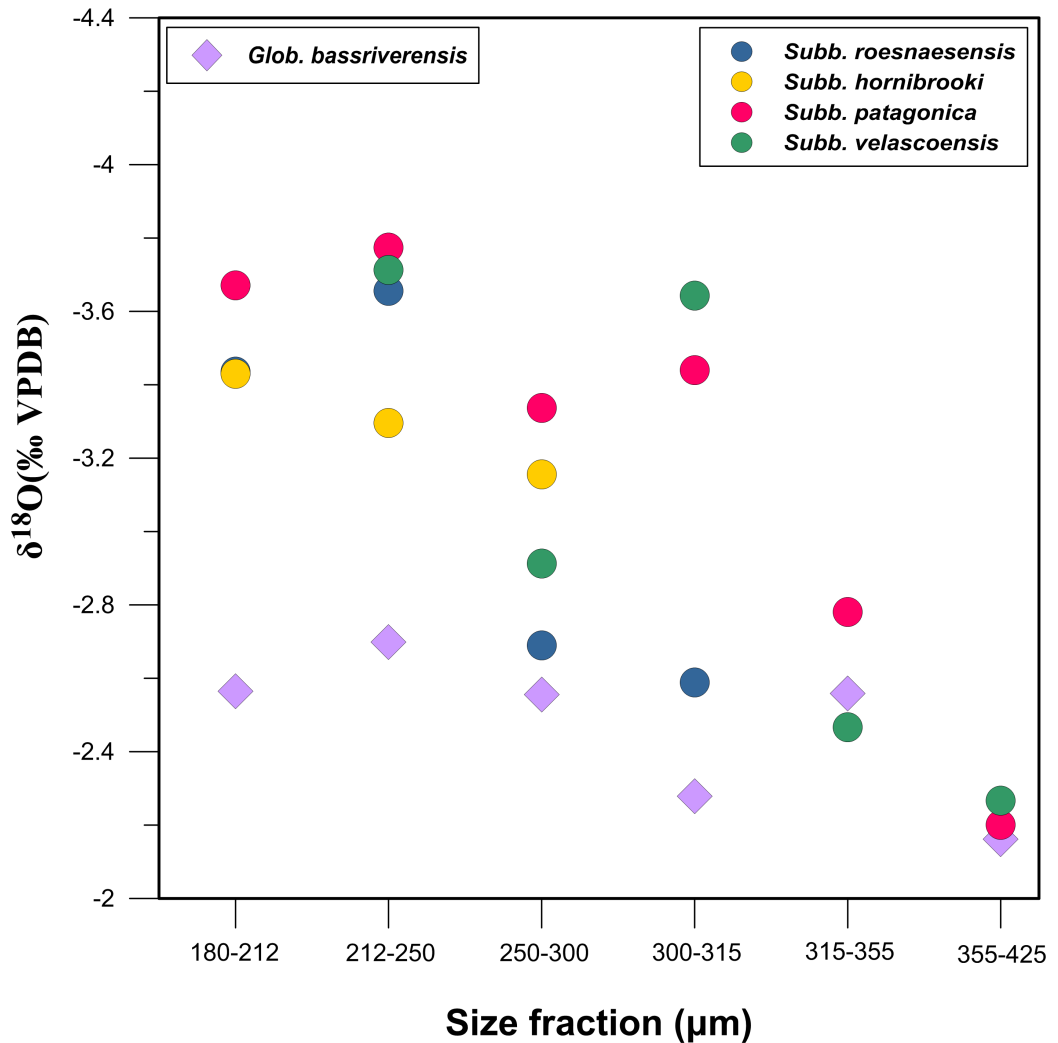
Figure 4.13: Relationship between foraminiferal δ¹⁸O (‰) of thermocline dwellers and increasing size fraction (μm). The different colours of the circles represent a different species of the *Morozovella* genus. The diamonds represent *Acarinina* species. As many size fractions as possible were used for each species, but not all of them were available for each species because of sample scarcity.

4.3.4 Trace metals from planktonic tests and their infill

The Mg/Ca of planktonic foraminiferal tests and their associated infill was also analysed for temperature reconstructions and multi-proxy comparison purposes. The Mg/Ca of benthic foraminiferal tests was not analysed due to the scarcity of the sample. The measurements were derived from mixed layer *Acarinina* spp. and *Morozovella* spp., alongside thermocline dweller *Subbotina* spp. *and Globoturborotalita bassriverensis*. Only one size fraction was used, 212-250 μm, in order to reduce additional biases (Elderfield et al., 2002), but where sample quantity allowed, specimens from the 250-300μm size fraction were also analysed to investigate the effect of size fraction on foraminiferal Mg/Ca. The results (Fig. 4.14) were shown in a way that the two different ecology groups could be distinguished. Only one Mg/Ca data point was retrieved from the *Acarinina wilcoxensis* group, giving a value of 5.10 mmol/mol. The measured Mg/Ca for morozovellids ranges between 4.18 mmol/mol and 5.98 mmol/mol, while the Mg/Ca for subbotinids ranges between 3.76 mmol and 4.79 mmol/mol. Lastly, only two Mg/Ca data points were measured for *Globoturborotalita bassriverensis*, giving values of 4.60 mmol/mol and 4.75 mmol/mol. When looking at the foraminiferal Mg/Ca measurements, one can say the highest Mg/Ca value came from the mixed layer dwellers morozovellids, while the lowest Mg/Ca value was derived from the thermocline dwellers subbotinids. However, there is an evident overlap between the two depth habitats that cannot be ignored.

Interestingly, the infill seems to have a preferential Mg/Ca range that agrees reasonably well with both ecology groups. In fact, the infill from the thermocline dwellers ranges between 5.10 mmol/mol and 5.60 mmol/mol for subbotinids and between 5.38 mmol/mol and 5.60 mmol/mol for *Globoturborotalita bassriverensis*, while the infill from the mixed layer dwellers ranges between 5 mmol/mol and 5.54 mmol/mol for the morozovellids, with a single infill Mg/Ca data point at 5 mmol/mol for the acarininids. While the infill Mg/Ca from the thermocline dwellers is distinctly separated from the test Mg/Ca, with a difference of ~0.25 mmol/mol between the two, the infill Mg/Ca of the mixed layer dwellers tends to be higher than the test Mg/Ca except for two test Mg/Ca values derived from morozovellids, yet still lying in the same range as the infill Mg/Ca of subbotinids. Inorganic calcite tends to have higher Mg/Ca than foraminiferal calcite (Baker et al., 1982), which is in agreement with our results, as the infill Mg/Ca does not go any lower than 3.50 mmol/mol unlike the test Mg/Ca. This may mean that either the Mg/Ca of the infill is not necessarily higher or lower than the foraminiferal Mg/Ca, rather it contains a specific Mg/Ca ratio that is typical of the meteoric waters when the infill was formed, or

that the test Mg/Ca of the specimens that is higher than its associated infill may have been contaminated with the infill itself as a result of an unsuccessful crushing attempt.
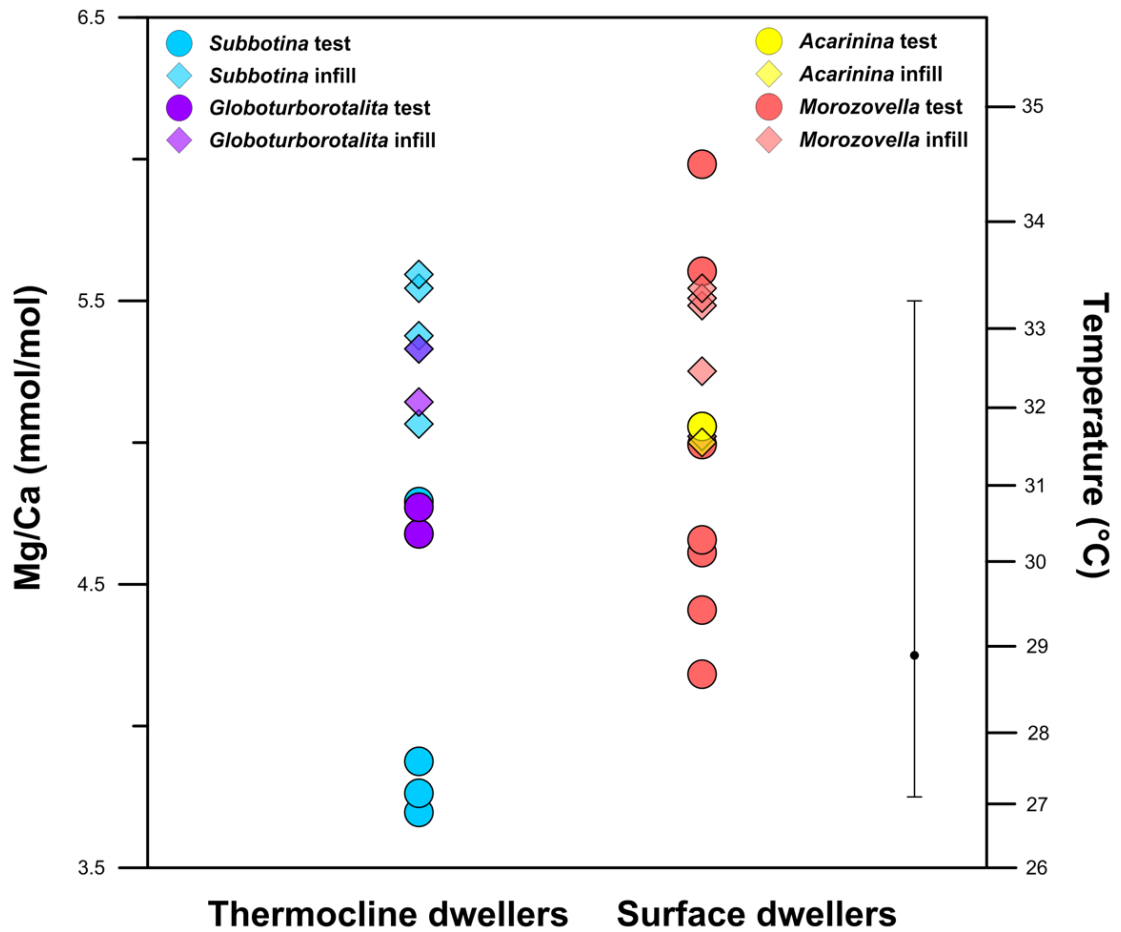
Figure 4.14: Temperature and depth habitat reconstructions of the water column around Papua New Guinea during the early Eocene (~55-54 Ma) from Mg/Ca which were derived from both planktonic and benthic foraminiferal tests (circles). Since the samples were infilled, the associated infill was also analysed (opaque diamonds). The Mg/Ca scale is reversed such that the higher values indicating the warmer mixed layer waters are found at the top, while the lower values are found at the bottom. The different colours represent different genera: yellow is for *Acarinina* spp.; tropical pink is for *Morozovella* spp.; sky blue is for *Subbotina* spp.; and purple is for *Globoturborotalita bassriverensis*. Acarininids and morozovellids are labelled as mixed layer dwellers, subbotinids and *Globoturborotalita bassriverensis* are labelled as thermocline dwellers. The temperatures on the second y-axis were derived from inserting the pH-corrected Mg/Ca values into the palaeotemperature equation of Evans et al. (2018). A pH correction was therefore applied to the raw Mg/Ca values, as well as a reconstructed Mg/Ca$_{sw}$ correction for the early Eocene following the technique and values suggested by Evans et al. (2018). The error bar includes both the analytical and calibration uncertainty, amounting to +5°C for the upper temperature limit, and -2°C for the lower temperature limit.

4.3.4.1   The effects of size fraction and interspecies variability

Only four species were sufficiently abundant to be analysed for both 212-250 µm and 250-300 µm size fractions so that the effect of size fraction on foraminiferal Mg/Ca could

be investigated (Fig. 4.15). There is no definite trend in changes in Mg/Ca between the two size fractions, as both *Morozovella acuta* and *Globoturborotalita bassriverensis* increase with size fraction, while both *Morozovella subbotinae* and *Morozovella marginodentata* decrease with increasing size fraction. Moreover, their change in Mg/Ca with size fraction lies within the analytical uncertainty of ±0.02 mmol/mol as well as the likelihood of the restricted number of samples being insufficient to make a sound judgement on the effect of size fraction.
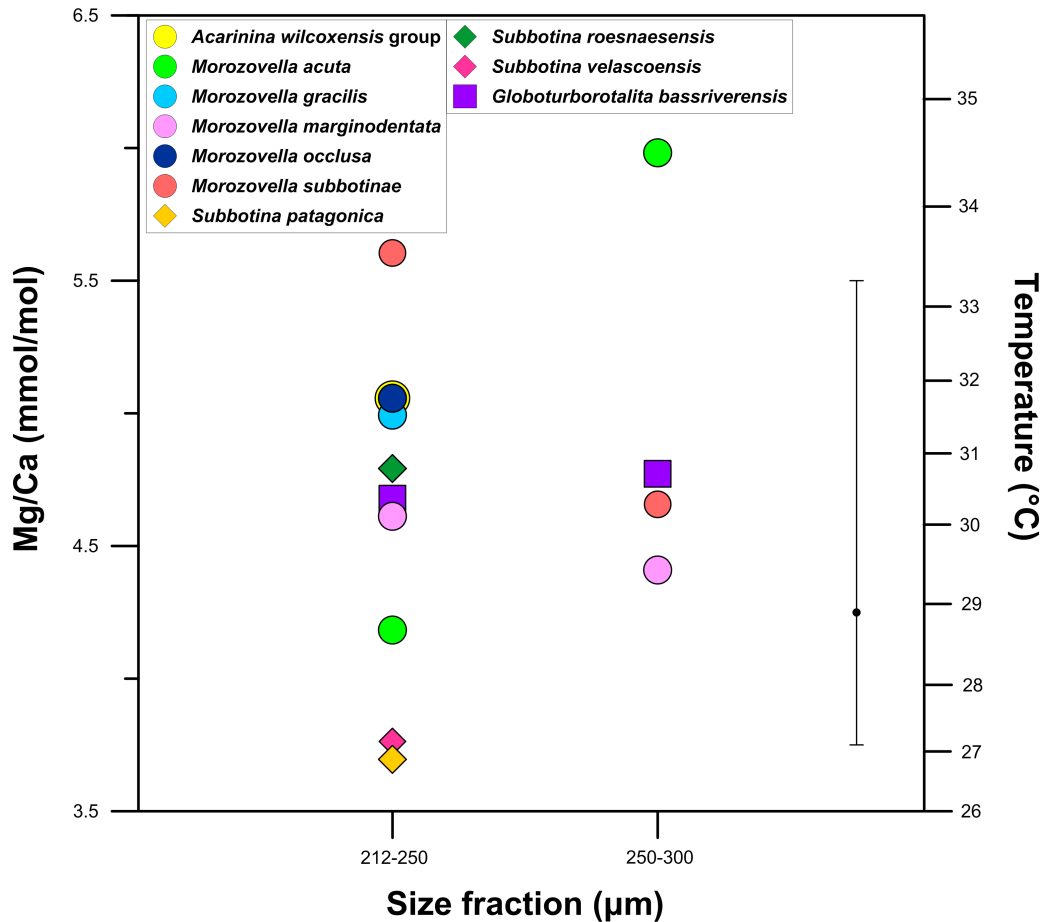
Figure 4.15: Relationship between foraminiferal Mg/Ca and size fraction. Different colours represent different species. The squares represent *Globoturborotalita bassriverensis*; circles are morozovellids; and diamonds are subbotinids. The error bar includes both the analytical and calibration uncertainty, amounting to +5°C for the upper temperature limit, and -2°C for the lower temperature limit.

Even though experimental studies show that the primary Mg/Ca ratio in planktonic foraminiferal calcite is significantly most sensitive to temperature changes than any other variable (Lea et al., 1999; Russell et al., 2004), it can still be prone to alteration from both pre- and post-mortem processes. The former include salinity (Lea et al., 1999; Evans et al., 2018; Gray, 2018) dissolution in the water column (Lea et al., 1999; Fehrenbacher and Martin, 2014), vital effects (Elderfield et al., 2002; Sadekov et al., 2005), while the

latter include contaminant overgrowth (Barker et al., 2003, 2005), diagenesis (Edgar et al., 2015), and post-depositional dissolution at or beneath the sea floor (Pena et al., 2005). Dissolution, under both circumstances, can lower Mg/Ca values in many species, and at the seafloor its extent is mainly governed by the saturation carbonate ion concentration state of bottom waters (ΔCO_3^{2-}), which in turn depends on temperature and depth (Fehrenbacher and Martin, 2014; Regenberg et al., 2014; Rongstad et al., 2017). Foraminiferal vital effects include change in Mg/Ca values as a result of increasing size fraction, and production of gametogenic calcite following the release of gametes during the reproduction stage. As a result, these processes need to be investigated and assessed when using both oxygen isotopes and Mg/Ca as temperature proxies (see Section 4.4.4).

4.3.4.2   Mg/Ca-based temperature reconstruction of the water column

The Mg/Ca values that were converted to temperatures using the approach of Evans et al. (2018), were first pH- and Mg/Ca_{sw}- corrected (see more details in Section 4.2.5.1). A pH value of 7.7 was chosen for the estimated age of ~55 Myr from both nannofossil and foraminiferal biostratigraphy (Pearson and Palmer, 2000; Tyrrell and Zeebe, 2004; Hönisch et al., 2013). After obtaining the pH-corrected Mg/Ca values, a Mg/Ca_{sw} value of 2.50 mol/mol as the 50th percentile was chosen from Evans et al. (2018), according to the same age criteria, alongside a value of 2.09 and 2.82 mol/mol for its 5th and 95th percentile, respectively, which served to calculate the calibration uncertainty. The resulting temperatures range between 28.5°C and 34.5°C for the mixed layer dwellers, and between 26.8°C and 31°C for the thermocline dwellers (Fig. 4.14). When calculating absolute temperatures, both the analytical and calibration uncertainties must be taken into consideration. When solely considering the analytical uncertainty, a very low representative value of ±0.02 mmol/mol can be attributed to this uncertainty, after averaging the RSD (%) values of each sample, which ranged between 0.01 mmol/mol and 0.06 mmol/mol. However, when applying the calibration uncertainty, which accounts for pH as well as Mg/Ca_{sw} correction, the two uncertainties combined result in an averaged representative temperature uncertainty of -2°C and +5°C (as a result of 1000 bootstrap runs). Generally, there is a slight trend of surface dwellers showing warmer temperatures relative to the thermocline dwellers. However, when considering the large calibration uncertainty, this differentiation may also be due to natural variability. Thus, these trends must be handled with caution, and perhaps one can at least rely on the key message from the results that confirm that SSTs may have almost reached 35°C around the area of Papua New Guinea during the early Eocene.

4.3.4.3   Checking for contamination phases

Diagenetic overgrowth and contaminant phases such as silicates, ferro-manganese and oxide/oxyhydroxides coatings can contaminate the foraminiferal test and change the primary Mg/Ca signature during diagenetic processes or post-depositional reactions (Boyle, 1983; Lea et al., 2005; Pena et al., 2005; Hasenfratz et al., 2017), resulting in biased palaeotemperature reconstructions. This is a consequence of remobilised Mn^{2+} and Fe^{2+} (both in aqueous forms, aq) diffusing upwards through pore waters, and precipitating in oxic conditions as Mn-Fe- oxide and -oxyhydroxide coatings on different surfaces including foraminiferal tests (Pedersen and Price, 1982; Boyle, 1983; Lear et al., 2015). As a result, the covariance of Mg/Ca with such contaminants is checked before confirming its validity. The presence of silicate contaminants is indicated by a covariance between Mg/Ca and Al/Ca ratios which need to be higher than 80 µmol/mol (Mawbey and Lear, 2013), as aluminium is indicative of the presence of silicate grains (Lea et al., 2005). Above the same value, Mn/Ca and Fe/Ca may also become contaminants for the foraminiferal Mg/Ca ratios (Boyle, 1983; Barker et al., 2003), which means the test may contain high levels of Mn-carbonates, Mn-Fe-oxides, or Mn-Fe-oxyhydroxides which in turn have incorporated in them magnesium derived from sources other than the foraminiferal calcite (Barker et al., 2003).

Adding the reductive step during the cleaning procedure of the foraminiferal tests is meant to remove most of these metal oxide coatings (Barker et al., 2003), but it comes with its associated disadvantages. In fact, the buffered solution of hydrous hydrazine that is used as a reducing agent (Boyle and Keigwin, 1985) is corrosive and would therefore partially dissolve the test fragments, and dissolution is known to reduce Mg/Ca ratios (Brown and Elderfield, 1996; Rosenthal et al., 2000; Rosenthal and Lohmann, 2002), by up to 10-15% (Barker et al., 2003). Because of the risk of losing sample, the reductive step was not carried out, but instead the clay removal step was repeated twice so that any silicates could be removed thoroughly. Following this, the co-variance was checked between Mg/Ca and the potential contaminants, namely Al/Ca, Mn/Ca, and Fe/Ca, for both the test and the infill (Fig. 4.16). The results show that Mn/Ca, Fe/Ca and Al/Ca all exceed 100 µmol/mol for both the test and infill. However, they all have a weak covariance with Mg/Ca, with the highest for the test being $R^2=0.33$ between Mg/Ca and Mn/Ca, and for the infill $R^2=0.46$ between Mg/Ca and Fe/Ca. Furthermore, this may indeed indicate the presence of contaminant phases and redox conditions, but the weak covariance with Mg/Ca may also mean that the contaminant coatings have not affected the Mg/Ca ratios (Lear et al., 2015).
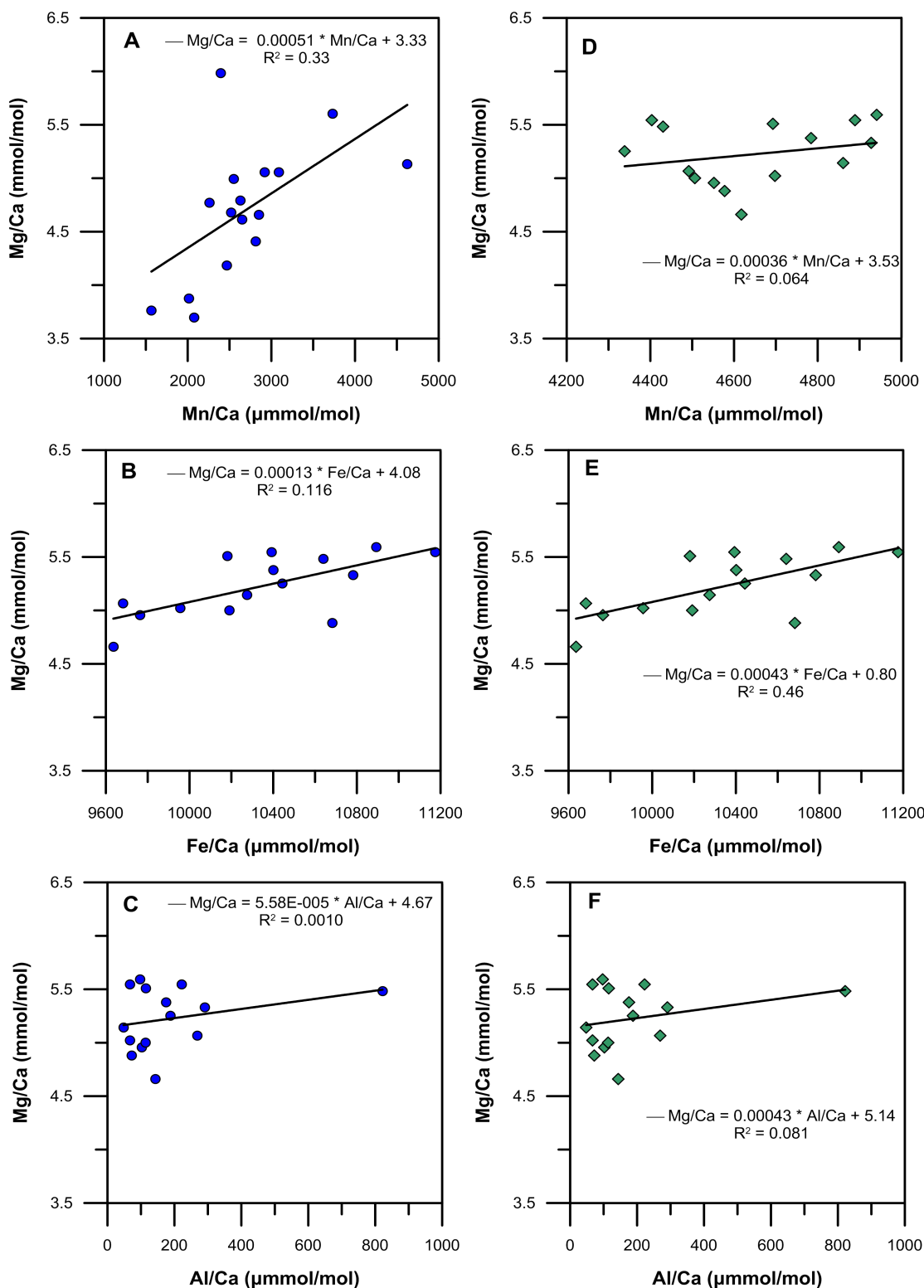
Figure 4.16: Covariance plots between Mg/Ca and contaminant phases, namely Mn/Ca, Fe/Ca, and Al/Ca. The relationship between the foraminiferal test and Mg/Ca is shown by the blue circles, whilst the infill Mg/Ca is represented by the green diamonds. (A-C) plots show the covariance (R^2) between test Mg/Ca and Mn/Ca (A); Fe/Ca (B), and Al/Ca (C); (D-F) plots show the covariance infill Mg/Ca and Mn/Ca (D); Fe/Ca (E), and Al/Ca (F).

4.3.5 Modelled ocean temperatures of early Eocene Papua New Guinea

A map of the early Eocene displaying global mean annual sea surface temperatures was produced using the teuyd simulation experiment under atmospheric CO_2 concentrations of 1120 ppm (4x pre-industrial levels) (Fig. 4.17).
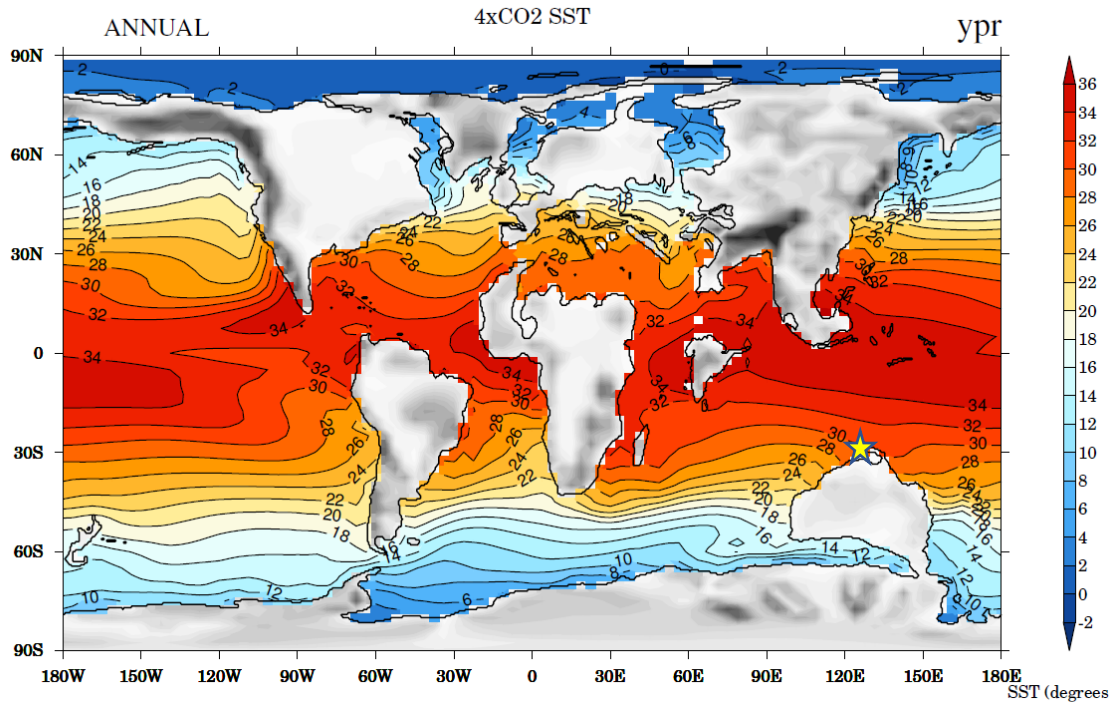
Figure 4.17: Model simulation of global early Eocene (Ypresian Stage) sea surface temperatures from teuyd experiment (4x pre-industrial levels of CO_2, 1120 ppm). The colours represent temperatures, with red being the hottest, and blue the coldest. The isotherms are 2°C apart from each other. The star symbol shows where Java was located according to the palaeogeographic data. The palaeogeographies were derived from the Getech Plc platform which in turn adopted an approach based on work performed by Markwick and Valdes (2004).

The incorporated tectonic plate rotations (see details for the palaeogeographies in Section 4.2.6.1) located early Eocene Papua New Guinea at 29.39°S, which means the island moved ~23°N in order to acquire the modern geographical position. India had yet to collide with the Asian plate and the South-East Asian islands had not fully developed yet, meaning that the IPWP had a larger open space to expand and its hottest core could almost bathe the Tanzanian coasts. The climate model simulated the core of the IPWP to reach 34°C, and Papua New Guinea to be surrounded by water temperatures ranging between 28 and 32°C. It may be likely that PNG was not located right in the hottest core of the IPWP, rather on its edges, hence it may represent a lower temperature limit of the early Eocene IPWP, meaning that the centre of the pool was even higher than 34.5°C.

Modelling the water column of Papua New Guinea was not a straightforward task. This is because, when inputting the modern location of the Moogli mudstones outcrop, the model gave a palaeolatitude showing the Site was located on a continental shelf, with a maximum depth of ~50 m. However, we know from the benthic foraminiferal assemblage, the P/B ratio of 98% and the great diversity of planktonic foraminifera that the sample may have most likely come from a more semi-open ocean, continental slope setting. Because the area is characterised by a highly complex tectonic history and a current position in a fold-and-thrust belt, it was assumed that the model may have miscalculated the early Eocene position of the Site by a few hundred kilometres. Under this scenario, a location on the continental slope of ~2000 m depth was selected to represent the water column site. This selection was performed by shifting the palaeolongitude to the next available grid in an eastward direction (each grid is ~2.5° x 2.5°), without changing the palaeolatitude because this may have introduced the bias of having a different insolation constant over the location. The water column is divided into 20 depth levels, which differ in size from each other.

Each depth level is represented by the average temperature of the specific depth block such that, for instance, the sea surface temperature of the water column was derived from the average temperature of the upper 5 meters. This would be more in line with the temperatures represented by the mixed layer dwellers as realistically, they do not occupy the very first centimetres of the sea surface, and they may migrate within the mixed layer throughout their life cycle. According to the model reconstruction (Fig. 4.18), the sea surface temperatures of the water column for early Eocene Papua New Guinea reached ~30°C, followed by a thermocline with temperatures ranging between 29°C and 16°C, extending down to 400 meters.
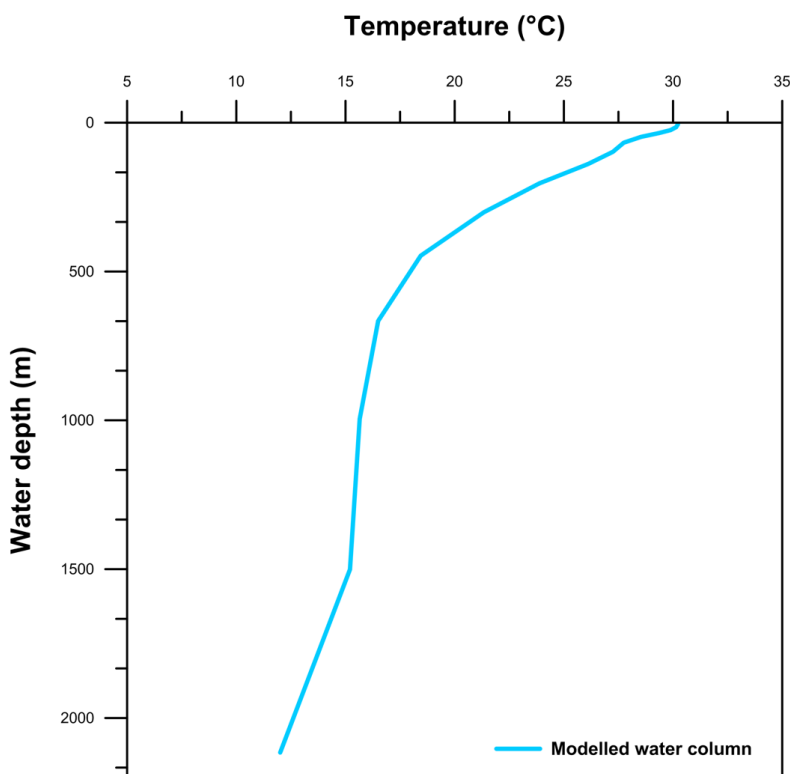
Figure 4.18: Modelled plot of the water column structure around the waters of early Eocene Papua New Guinea. The experiment used was called teuyd, at 4x CO_2 atmospheric levels (1120 ppm), and representing the Ypresian Stage.

4.4   Discussion

4.4.1 The original test vs. the infill

The associated infill fragments of the planktonic foraminiferal tests (opaque diamonds, Fig. 4.19) consistently showed lower $\delta^{18}O$ values relative to their test (circles, Fig. 4.19), which is indicative of the influence of meteoric waters. Unlike the $\delta^{18}O$ infill cloud which has a narrow range of values, the $\delta^{13}C$ infill cloud covers a broader range of values, with the lower $\delta^{13}C$ signature mainly coming from the infill inside thermocline dwellers, and the highest values coming from the infill inside mixed layer dwellers. It may be that, during the percolation of freshwater down through the mudstone outcrop, *Subbotina* and *Globoturborotalita* tests were filled with inorganic calcite first as they are characterized by a wider aperture than *Morozovella* and *Acarinina*, as well as possessing more space to fill owing to their globular-shaped chambers, thus making it easier for the initial stage of precipitation to occur inside their tests. As the process of inorganic calcite precipitation preferentially utilizes the heavier isotopes, the infill inside the thermocline dwellers may have had greater portions of ^{13}C as they were easier to fill, and with time, the tests of the

surface dwellers may have been filled with the remaining, more ^{12}C-depleted meteoric waters. In addition to this, the lines connecting the tests to their associated infill show that they would eventually converge, along a mixing line, at a mixing point (outside the graph, in this case), which would be characterised by the pure, lower δ^{18}O isotopic signature characterising the local meteoric waters, as well as a unique δ^{13}C signature.
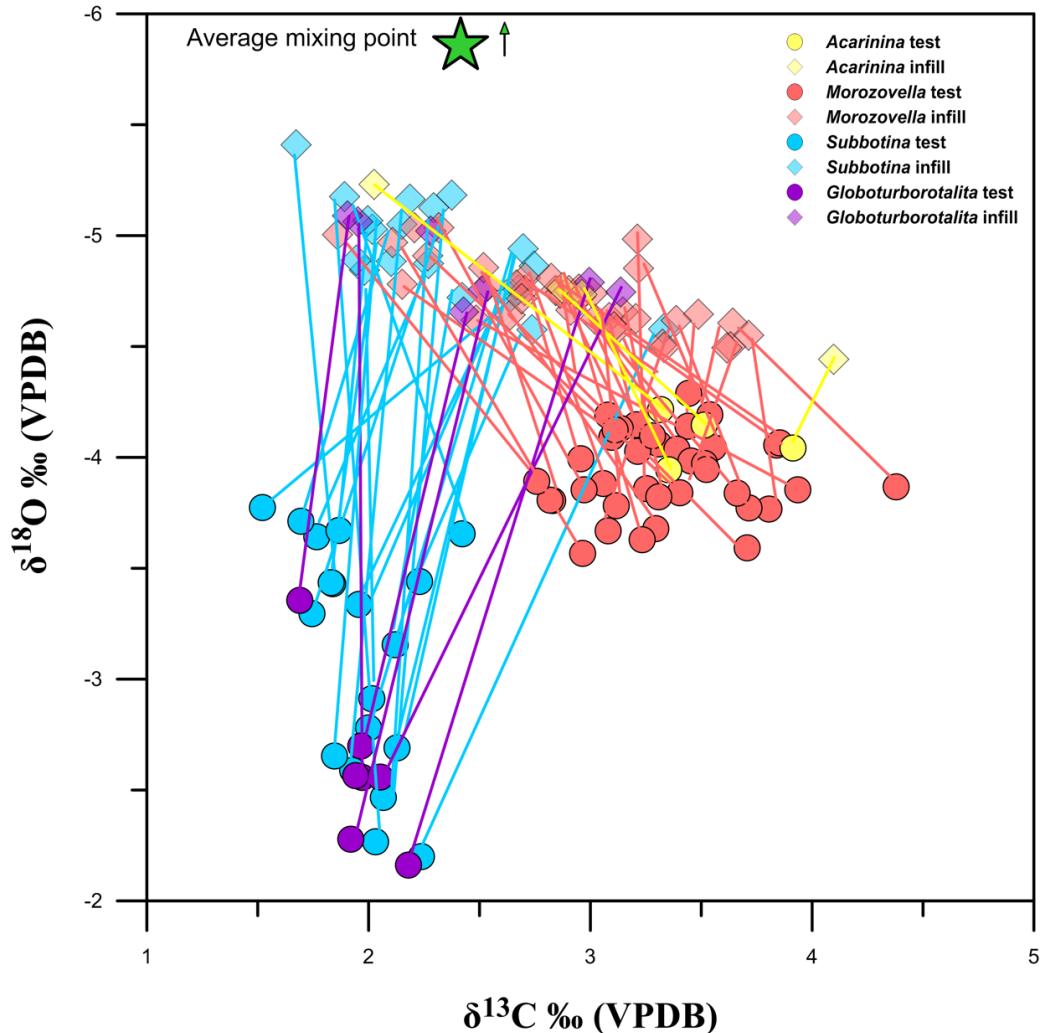
Figure 4.19: Depth habitat reconstructions of the water column around Papua New Guinea during the early Eocene (~55-54 Ma) from the geochemical proxies δ^{18}O and δ^{13}C which were derived from both planktonic and benthic foraminiferal tests (circles). Since the samples were infilled, the associated infill was also analysed (opaque diamonds). The δ^{18}O scale is reversed such that the lower values indicating mixed layer waters are found at the top, while the higher values are found at the bottom, intercepting with the δ^{13}C axis. The different colours represent different genera: yellow is for *Acarinina* spp.; tropical pink is for *Morozovella* spp.; sky blue is for *Subbotina* spp.; and purple is for *Globoturborotalita bassriverensis*. Acarininids and morozovellids are labelled as mixed layer dwellers, while subbotinids and *Globoturborotalita bassriverensis* are labelled as thermocline dwellers. The lines were introduced to connect the foraminiferal tests (circles) to their associated infill (opaque diamonds) to show the mixing lines that eventually converge to an average mixing point (the green star symbol).

In addition to this, the lines connecting the tests of morozovellids and acarininids with their infill are more inclined than the lines of subbotinids and *Globoturborotalita bassriverensis*, suggesting that the infill of the mixed layer dwellers lies further away from the hypothetical average mixing compared to the infill of the thermocline dwellers, where the connecting lines are almost vertical relative to the mixing point. This may be explained by the fact that as subbotinids and *Globoturborotalita bassriverensis* possess a globular-shaped test, this may have been easier to handle when separating the infill from the test, leading to a more effective separation of the two different types of fragment. Moreover, because acarininids and morozovellids both possess a muricate-walled test, they have a larger-to-volume ratio as well as a less compact structure than the thermocline dwellers, suggesting that during possible dilution events, the contribution of the test towards the $\delta^{13}C$ and $\delta^{18}O$ values may have been greater than for the thermocline dwellers. Overall, the clear distinction in $\delta^{18}O$ signature between the infill and the original portion of the test wall suggests a successful separation of the infill fragments from the outer shell during the crushing procedure.

4.4.2 Assessing the extent of separation of the test from the infill

During the crushing procedure, some specimens were dedicated to SEM imagining so that they could be examined under high resolution as well as investigating the effect of crushing on the separation of the test from the infill (Fig. 4.20). The fragments shown in Figure 4.20 were not derived from the same whole specimen shown, rather the best images that could convey the message were selected. The infill fragment (Fig. 4.20, box c) predictably appears as a homogenous, block of inorganic calcite. Conversely, the test fragments show a preserved original wall texture, with visible pores around the test (Fig. 4.20, box b,d). However, the internal pores are less visible, probably owing to the presence of some inorganic cement that adhered to the internal walls upon infilling the test. When looking at the contribution, there is a gap (Fig. 4.20, box a) between the original wall of the foraminifer and the infill, which may have helped the distinct separation of the infill from the test. When assessing the SEM images, an estimated 5-10% of inorganic cement relative to the whole test is attached to the internal walls of the test. As the difference between the $\delta^{18}O$ of the infill and the $\delta^{18}O$ of the test is of ~1‰, one can say that it is likely that the presence of this cement contributed ~0.05-0.10‰ to the test. When converting this to temperature estimates, the contribution is equivalent to less than 0.5°C. Lastly, from specimens analysed under the SEM, no gametogenic calcite was detected on the outer walls of the test. However, the production of gametogenic calcite is also known to depend on the size fraction and the species. Because not all size fractions of all species were investigated under the SEM, one cannot

exclude that some specimens in specific size fractions or belonging to a particular genus may have developed gametogenic calcite towards the end of their life cycle. The initial aim of this SEM investigation was to solely assess the extent of success in the separation of the infill from the test, which seems to have worked in a way that does not significantly alter the primary, foraminiferal $\delta^{18}O$ signal.
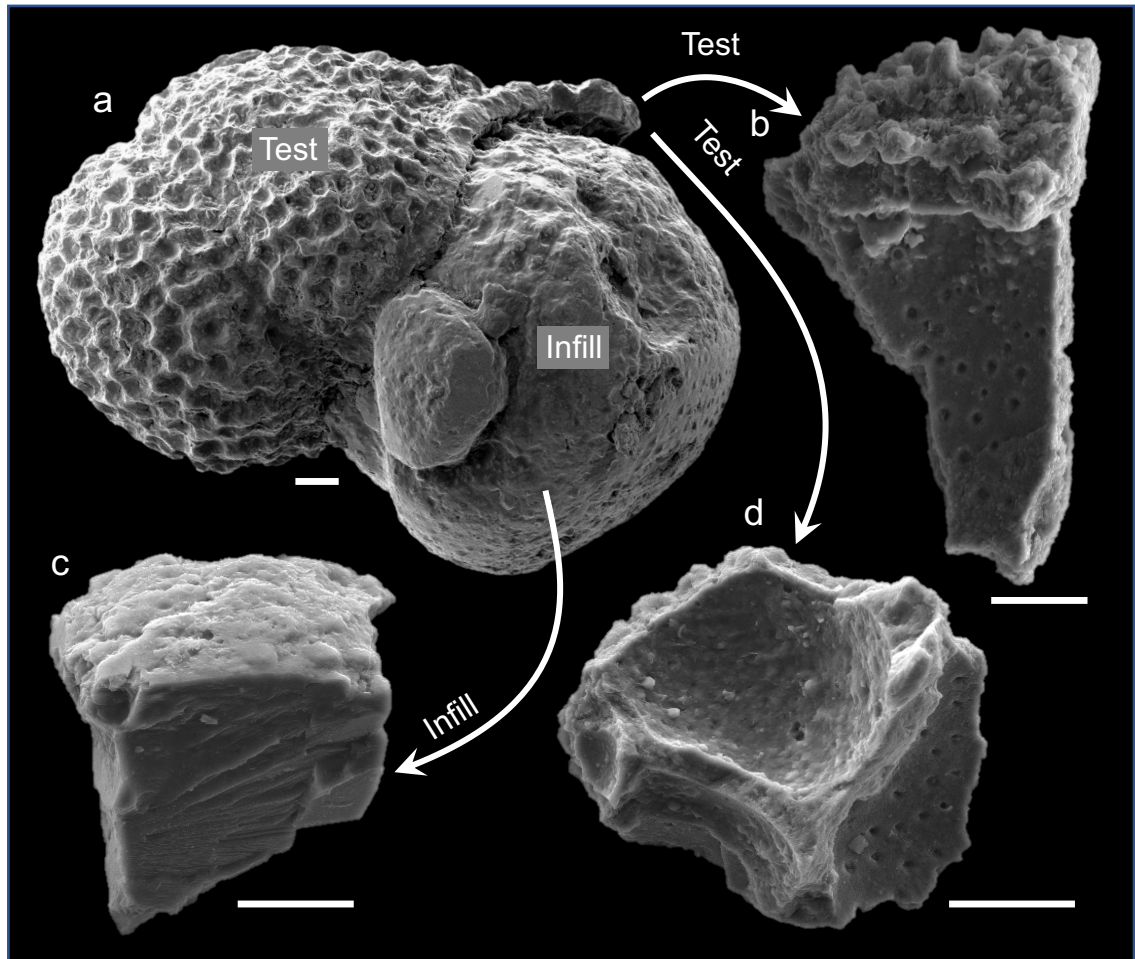
Figure 4.20: SEM images of an infilled planktonic foraminiferal test *(*subbotinid sp.) The SEM images show the entire infilled test before crushing and the result of the separation of the test from the infill: a) Infilled test of a specimen belonging to the *Subbotina* genus*;* b) Test fragment of a morozovellid sp.; c) Infill fragment; d) test fragment of a morozovellid sp. The b) and d) test fragments did not come from a foraminiferal test but they were the best images able to show the outcome of the crushing. Specimen a) was selected as the best representation because of the visible gap between the infill and test which likely aided the successful separation. All scale bars: 20 μm.

4.4.3 Interpreting the effect of size fraction on the foraminiferal geochemical proxies

4.4.3.1   Mg/Ca

There are contrasting views about the effect of size fraction on foraminiferal Mg/Ca, whereby some argue that there is a positive correlation between the two (Elderfield et al., 2002), whilst others assert that Mg/Ca decreases with increasing size fraction as this reflects a change in depth habitat during the life cycle of the foraminifer (Friedrich et al., 2012). According to the latter theory, the 150 µm and >250 µm size fractions record the lowest Mg/Ca values as they represent juveniles and reproductive stages, respectively, which preferentially inhabit thermocline depths (Hemleben et al., 1989), compared to the size fractions within the 150-250 µm range which preferentially inhabit supra-thermocline depths. It is therefore advised to use a narrow size fractions to reduce such biases, as narrow as 50 µm according to Friedrich et al. (2012). However, the specimens of this study were infilled, and it would have been difficult to successfully separate the infill from the original test in such small size fractions. Thus, as an alternative option, just one size fraction (212-250 µm) was chosen where possible, as the sample quantity was scarce and at times it was necessary to resort to the next available bigger size fraction to investigate different species. From the results, it is hard to judge whether there was any effect on size fraction as there is no defined pattern of increase or decrease in Mg/Ca between 212-250 µm and 250-300 µm size fractions. Moreover, specific foraminiferal species produce an additional layer of calcite (gametogenic crust) on top of their primary calcite test (ontogenetic calcite) as they sink down to deeper waters to release their gametes during reproduction (Sadekov et al., 2005). This process would result in a signature bias of the Mg/Ca towards lower values relative to the inner layers of the ontogenetic test, as the gametogenic calcite crust would precipitate in colder waters during this life-cycle related migration down through the water column (Brown and Elderfield, 1996; Elderfield and Ganssen, 2000).

4.4.3.2 $\delta^{18}O$ and $\delta^{13}C$

There is a variety of vital effects that can alter the primary foraminiferal $\delta^{13}C$ and $\delta^{18}O$ signatures and cause a disequilibrium between the signal the foraminifers records and the real signal of $\delta^{18}O$ and $\delta^{13}C$ from seawater. It is therefore critical to assess, where possible, the different size fractions to investigate if any of these disequilibrium effects are present, despite the task being challenging due to the unknown extent of each vital effect for deep-time species such as the Eocene foraminifera. If overlooked, they might

under- or overestimate the temperature reconstructions. Because of this, the 180-212 µm and 355-425 µm size fractions were also analysed, in order to investigate these vital effects, after Birch et al. (2013) asserted that the disequilibrium effects within the 212-355 µm size fraction range are at minimum relative to any size fraction outside of this range.

Interestingly, studies (Ezard et al., 2015; Edgar et al., 2017) suggested that metabolic processes influenced by both evolutionary and environmental factors dominate the modern foraminiferal $\delta^{13}C$. For instance, the $\delta^{13}C$ offset is similar among closely related taxa, while foraminiferal $\delta^{18}O$ offsets showed no significant evolutionary influence. This means that vital effects may have varied to a different extent through the geological record with the evolutionary processes and newly emerging taxa. Thus, size-specific $\delta^{13}C$ offsets may well differ across time (environmental control) and genera (evolutionary control) in foraminifera, therefore comparisons between modern and deep-time size-specific $\delta^{13}C$ gradients in the water column are not directly comparable but are instead the product of biological and environmental controls specific of their taxon group and geological time they lived in.

4.4.3.2.1   Photosymbiotic algae

The symbiont-bearing *Morozovella* and *Acarinina* spp. clearly show a strong positive correlation between $\delta^{13}C$ and increasing size fraction, but lack any significant size related $\delta^{18}O$ correlation, which is in accordance with the findings of Birch et al. (2013). This is because the larger the foraminiferal test, the larger the cloud of symbionts it can host, therefore the more ^{13}C- and ^{18}O-enriched its calcification pool will be as a consequence of the preferential removal of ^{12}C by the photosymbionts (Spero and DeNiro, 1987; Spero and Williams, 1988, 1989; Spero et al., 1991; Spero, 1992; Spero and Lea, 1993; Norris, 1996). Under this scenario, a small slope of this correlation may reflect a weak or absent photosynthetic activity, while a steeper slope may indicate a very active photosynthetic activity (Si and Aubry, 2018). This effect becomes incredibly marked at size fractions >355 µm whereas it is small in size fractions <212 µm (Birch et al., 2013; John et al., 2013). Moreover, the study by Norris (1996) found that this vital effect can leave the test $\delta^{13}C$ being enriched by 0.50-1‰.

Moreover, symbionts influence the ambient carbonate ion concentration as their photosynthetic activity lowers the local pH, leading to a decrease of carbonate ions (CO_3^{2-}), which is the species among the dissolved inorganic carbon species with the highest proportion of lighter carbon and oxygen isotopes (Spero et al., 1997; Bijma et al., 1999; Uchikawa and Zeebe, 2010). However, this effect is not considered to have as

much of an impact on the stable isotopes as the photosynthetic activity itself described above (Birch et al., 2013).

In this study, the particularly enriched $\delta^{13}C$ of surface dwellers is evident especially for *M. gracilis*, *M. pasionensis*, and *M. velascoensis*, which are also the only species analysed in size fraction 355-425 μm, where these effects are thought to be acting the most. In fact, these three species at this size fraction display a broader range of values in foraminiferal $\delta^{13}C$ than the other species from the remaining size fractions (Fig. 4.10), suggesting these largest individuals may carry secondary signals different from and in addition to the seawater $\delta^{13}C$ (hence in greater isotopic disequilibrium from seawater $\delta^{13}C$). The positive $\delta^{13}C$-size fraction trend may be less obvious at species level, and the biggest size fraction for some species may actually display less enriched $\delta^{13}C$ than expected. This is the case for *M. pasionensis*, whereby the $\delta^{13}C$ value at 355-425 μm size fraction is almost identical as at 315-355 μm. It may be caused by the ingestion of its own symbionts (Bé et al., 1985), which would deplete $\delta^{13}C$, and this is supported by the $\delta^{18}O$ values too for the same size fraction, where $\delta^{18}O$ also becomes slightly more depleted. Conversely, the $\delta^{13}C$ of the thermocline dwellers does not display a similarly evident positive correlation with increasing size fraction being asymbiotic species, and nor does the largest size fraction possess a higher $\delta^{13}C$ signature than the other size fractions below 355 μm, meaning that they may be in closer isotopic equilibrium with the seawater $\delta^{13}C$ (Spero and Williams, 1988; Bolton et al., 2012). However, despite the range of values of both $\delta^{13}C$ and $\delta^{18}O$ being more similar to subbotinids than the surface dwellers, *Globoturborotalita bassriverensis* displays a similar pattern as the surface dwellers whereby each size fraction progressively becomes more enriched in $\delta^{13}C$, and particularly at test sizes >355 μm. For this reason, the case of this species will be discussed further in a separate paragraph. Nonetheless, on average, *Globoturborotalita bassriverensis* does display some of the heaviest $\delta^{13}C$ signatures among the different thermocline dwellers species.

In conclusion, these findings suggest that even back in the early Eocene and under extreme warmth, symbiont-bearing species displayed a clear relationship between size fraction and the size of their photosymbiotic cloud, hence they seemed to have thrived and adapted to the extremely warm temperatures of the mixed layer at that time, whereby there was a high diversity and abundance of species of different genera.

4.4.3.2.2   *The metabolic and kinetic fractionation effect*

Previous laboratory experiments (Bé, 1982) have shown that larger foraminifera (adults) tend to grow more slowly and display a lower metabolic activity and kinetic fractionation,

the latter probably attributed to the slower CO_2 hydration and hydroxylation reactions by the molecules enriched in the heavier ^{13}C and ^{18}O isotopes. In contrast, small foraminifera (juveniles or small individuals) tend to grow more rapidly and have a higher metabolic activity and kinetic fractionation (Berger et al., 1978; Kahn, 1979; Vincent and Berger, 1981; Wefer and Berger, 1991; Ravelo and Fairbanks, 1995; Ortiz et al., 1996; Spero et al., 1997). As a result of this, the smaller individuals will incorporate a higher proportion of respired CO_2 (which is enriched in ^{16}O and ^{12}C isotopes) (Barras et al., 2010; Filipsson et al., 2010; Pearson, 2012), leading to a negative offset of the $\delta^{18}O$ and $\delta^{13}C$ from seawater $\delta^{18}O$ and $\delta^{13}C$ values, respectively. Moreover, the reduced food availability and colder waters the thermocline dwellers inhabited may also contribute to the lower metabolic rates in larger individuals and this will result in $\delta^{13}C$ values closer to equilibrium with $\delta^{13}C_{DIC}$ values (Berger et al., 1978; Vincent and Berger, 1981; Birch et al., 2013). Thus, at smaller size stages, Birch et al. (2013) found that the metabolic fractionation plays a bigger role than photosymbiosis for size fractions below 150 μm, and Bornemann and Norris (2007) found it can shift $\delta^{13}C$ values from equilibrium with $\delta^{13}C$ seawater by 0.30-0.50‰, causing disequilibrium overprints on the originally recorded water column DIC gradient. In contrast, the fact that there is a clear trend in $\delta^{13}C$ enrichment with increasing size fractions proves that the photosymbiotic effect is the dominant vital effect at bigger size fractions, compared to the metabolic fractionation.

Interestingly, the results showed that there is a larger difference between the lower $\delta^{13}C$ value from 180-212 μm size fraction than between the other size fractions, suggesting that the smallest individuals may have been affected by the metabolic fractionation to a greater extent, causing this visible, larger "jump" between 180-212 μm and 212-250 μm size fractions (Fig. 4.10). A similar pattern is shown by the $\delta^{18}O$ of the surface dwellers, whereby the 180-212 μm size fraction shows a broader range of $\delta^{18}O$ values hence higher variability compared to the other test sizes, suggesting there may be a disequilibrium effect among the specimens of the 180-212 μm size fraction, even though they do not show particularly depleted $\delta^{18}O$ values relative to the other test sizes.

In contrast, neither the $\delta^{13}C$ nor $\delta^{18}O$ values from the smallest size fraction for the thermocline dwellers were particularly more depleted relative to the other size fractions. As Bijma and Hemleben (1994) argue, some small species tend to live deeper in the water column and combined with the low metabolic activity caused by the lower temperatures of the thermocline (Birch et al., 2013) this could explain why this metabolic effect seemed less accentuated in thermocline dwellers.

4.4.3.2.3 *Life-cycle-related depth migration and gametogenesis*

During their life cycle, many species migrate upwards during ontogeny and sink deeper in the water column during reproduction, producing an additional layer of calcite known as the gametogenic crust. This depth migration is reflected in the $\delta^{18}O$ which would register a range of different temperatures across size fractions. However, none of the morozovellids display this clear trend. Either none of the *Morozovella* species had a preference for a deeper habitat during the release of their gametes, or it may be that they ingested or lost their own symbionts, which would cause a depletion in $\delta^{18}O$ and $\delta^{13}C$ values and therefore cancel out any potential depth-related $\delta^{18}O$ shift towards higher values at the end of their life cycle (Bé et al., 1985; Houston and Huber, 1998; Ni et al., 2007). Moreover, Bé et al. (1985) suggested gamete release occurs before the test sinks below the euphotic zone, in which case the gametogenic calcification would take place in shallow, warmer waters. At species-level, Si and Aubry (2018) suggested that during the PETM, *M. velascoensis* and *M. acuta* (MAV lineage) displayed lower $\delta^{18}O$ values than *M. subbotinae* and *M. aequa* (MAS lineage), suggesting that the latter two species inhabited the lower part of the mixed layer. In this study, *M. acuta* does display the most depleted $\delta^{18}O$ values among all the *Morozovella* spp., except for size fraction 250-300 µm, but this is not the case for *M. velascoensis* where its $\delta^{18}O$ value does vary in relation to the other morozovellids. Furthermore, neither *M. acuta* nor *M. subbotinae* display a particularly higher $\delta^{18}O$ value with respect to the other species, suggesting that perhaps this difference in depth habitat preference between the two lineages had disappeared or reduced in significance by the early Eocene.

However, for the thermocline dwellers, there seems to be a shift towards higher $\delta^{18}O$ values from the 250-300 µm size fraction, which may indicate the addiction of a gametogenic crust at greater depths hence incorporating higher $\delta^{18}O$ values. Previous studied suggested a lack of strong correlation between test size and $\delta^{18}O$ in subbotinids because they probably maintained a relatively constant depth habitat (Pearson et al., 1993; D'Hondt et al., 1994; Norris, 1996; Quillévéré et al., 2001; Coxall et al., 2007). By lacking symbionts, the thermocline dwellers did not need to migrate great lengths from the mixed layer to deeper layers to reproduce. Nonetheless, the $\delta^{18}O$ for subbotinids in this study results seem to suggest a gradual migration for both globoturborotalids and subbotinids towards the colder deep waters, perhaps dictated by the particularly warm temperatures the early Eocene was characterised by.

4.4.3.2.4 Benthics

The species *Bulimina tuxpamensis* was an infaunal species, thus living in the sediment and in contact with pore waters (Corliss, 1985). It is therefore important to consider the potential impact of pore waters on the $\delta^{13}C$ and $\delta^{18}O$ signatures of the species. The difference between epifaunal and infaunal living foraminifera has been suggested to be sensible to changes in organic matter remineralisation rates, which in turn are dependent on the oxygen availability (Zahn et al., 1986; Loubere, 1987; McCorkle and Keigwin, 1990; Mackensen et al., 2000; Schilman et al., 2003, Holsten et al., 2004; Fontanier, 2006; Schmiedl and Mackensen, 2006). It has been suggested that species adapted to low oxygen conditions on the sea floor may have special adaptations enabling oxygen exchange with their environment, and so tend to precipitate their tests closer to equilibrium compared to other species (Grossman, 1987). Different studies have reported the results of growing deep-sea benthic foraminifera in culture and found that the temperature relationships of the cultured species are significantly close to the published inorganic paleotemperature relationship (Wilson-Finelli et al., 1998; McCorkle et al., 2008; Barras et al., 2010; Filipsson et al., 2010). Considering that the infaunal buliminid group is characterised by detrital feeders that tolerate reduced oxygen concentrations (Sen Gupta and Machain-Castillo, 1993; Arreguín-Rodríguez et al., 2016), one can assume that *Bulimina tuxpamensis* may have been able to calcify closer to equilibrium with seawater $\delta^{13}C$ and $\delta^{18}O$.

It is important to note that there are other factors that may impact the benthic isotopic signature. The profile of $\delta^{13}C$ pore waters commonly displays a rapid $\delta^{13}C$ depletion with depth in the sediment as a result of the decomposition of sedimentary organic matter (Grossman, 1984, 1987; McCorkle et al., 1985). Moreover, benthic foraminifera are affected by vital effects too, mainly caused by kinetic isotope fractionation during calcification and the incorporation of light metabolic CO_2 into their test, alongside the carbonate ion effect similar to the planktonic foraminifera (Brückner and Mackensen, 2008; Rathmann and Kuhnert, 2008; Rollion-Bard et al., 2008). However, *Bulimina tuxpamensis* did not display a depletion of $\delta^{13}C$ and $\delta^{18}O$ with size, suggesting the effect may be negligible or reduced by the low metabolic rates caused by low water temperatures. Thus, it is challenging, especially in deep time, to quantify the vital effects as well as the extent of disequilibrium of the $\delta^{13}C$ of pore waters from seawater $\delta^{13}C$.

4.4.3.3 The interesting case of thermocline dweller *Globoturborotalita bassriverensis*

Globoturborotalita bassriverensis displays $\delta^{18}O$ and $\delta^{13}C$ values similar to subbotinids, suggesting a thermocline depth habitat for the species (Fig. 4.8). However, up to today, there are contrasting views on its habitat preference. *Globoturborotalita bassriverensis* is the first species of its genus that evolved from *Subbotina* (species *Subbotina hornibrooki*) (Pearson et al., 2006), which occurred in the Ypresian stage. Sexton et al. (2006b) classified the species as a Winter mixed layer species in the middle Eocene as it was characterised by relatively higher $\delta^{18}O$ and $\delta^{13}C$ values. In contrast, Aze et al. (2011) classified the species as an asymbiotic mixed layer dweller, as characterised by low $\delta^{13}C$ and $\delta^{18}O$ values. This choice of a shallow water habitat was supported by Pearson et al. (2001). However, in the case of the early Eocene of this study, *Globoturborotalita bassriverensis* strongly match the depth habitat of subbotinids, as well as having a higher $\delta^{18}O$ signature, indicating deeper habitat then the subbotinids. Interestingly, the results showed a gradual $\delta^{13}C$ enrichment with size fraction, but overall the values did remain relatively constant as well as its $\delta^{18}O$ values, when compared to the other species analysed. This may also support the findings of Elderfield et al. (2002) and Friedrich et al. (2012), whereby some living asymbiotic planktonic foraminifera display a positive $\delta^{13}C$-test size correlation, possibly caused by the incorporation of metabolic CO_2, even at intermediate size fractions (~300 μm). Moreover, if we were to suggest that *Globoturborotalita bassriverensis* was indeed an asymbiotic species, the gradual enrichment of both $\delta^{13}C$ and $\delta^{18}O$ with increasing size fraction may indicate the production of gametogenic calcite at bigger size fractions, when the species may have probably sunk towards greater depth to reproduce. In fact, this suggestion cannot be excluded from the Mg/Ca values, whereby the 250-300 μm size fraction contains, even if slightly, a higher Mg/Ca ratio than the 212-250 μm size fraction, which would imply agreeing with the school of thought that gametogenic crust may indeed increase, rather than reduce, the Mg/Ca of the foraminiferal test owing to the very rapid calcification process involved (Caroline Lear, *personal communication*).

4.4.4 A multi-proxy comparison of the early Eocene ocean temperatures around Papua New Guinea

When estimating ocean temperatures in deep time, a multi-proxy approach is ideal in order to reduce the degrees of freedom. Every proxy has its limitations, so the combined application of multiple proxies is essential if important variables, such as SSTs, are to be

determined (Pearson, 2012). Besides, using proxies together can help highlight when one or another is compromised.

The sea surface temperatures retrieved from the $\delta^{18}O$ of morozovellids and acarininids ranged between ~31°C and ~34.5°C, while the Mg/Ca values from species of both genera converted into a sea surface temperature range between 28°C and 34.5°C, with a calibration uncertainty of +7°C for the upper temperature limit, and –2°C for the lower temperature limit. This calibration uncertainty is the sum of the different pH and Mg/Ca$_{sw}$ from today that had to be acknowledged, and which are still represented by large uncertainties as they are very difficult to reconstruct at a higher resolution (Sexton et al., 2006b). Both proxies greatly agree with a high SST up to ~34.5°C, with the highest SSTs derived from *M. acuta* and *M. gracilis* for the $\delta^{18}O$, and *M. acuta* and *M. subbotinae* for Mg/Ca. When compared to the SSTs observed at different sites around modern Papua New Guinea (ranging between ~13°N and ~6°S), the SSTs from the $\delta^{18}O$ of this study were up to 4°C warmer than today's core of the IPWP (Hollstein et al., 2017). In fact, according to Hollstein et al. (2017) who show mean annual SST from the main surface sub-and surface currents in the IPWP area, SSTs range between 27°C and 30°C.

However, it is rather controversial to compare the modern PNG with early Eocene PNG. This is because PNG is placed on a fast-moving tectonic plate, meaning that its latitudinal position has changed dramatically between the early Eocene and today, shifting from a position of ~29.39°S to a modern location of ~6°S, implying a significance difference in the latitudinally-induced insolation rates that PNG would have received back in the early Eocene compared to today. Nonetheless, we cannot compare early Eocene PNG with the current latitude of 29.39°S. This is because back in the early Eocene, the IPWP was located in an open space, allowing the pool to expand to higher latitudes, hence beyond the tropical line of ~23°N/S. Today, a latitude of 29.39°S has a completely different ocean and surface temperature setting, and it is not even bathed by the edge of the IPWP. Thus, the comparison of early Eocene PNG with the modern IPWP must be taken with caution. Nevertheless, we can argue that the SSTs of this study suggest that, because the edges of early Eocene IPWP (or just outside the IPWP) peaked in temperature at ~34.5°C, the core may have likely been even higher.

When looking at the water column structure, the Mg/Ca values suggest a temperature range between 27°C and 31°C, and the range in temperatures of the thermocline given by subbotinids and globoturborotalids similarly range between 24°C and 32°C, thus slightly overlapping the depth habitats of the surface dwellers in the mixed layer. This may suggest either a downward shift of depth habitats by the morozovellids, or an

expansion of the depth habitat range by the subbotinids. Under both scenarios, both genera would have adapted to the high temperatures, since morozovellids still record an enriched $\delta^{13}C$ typical of mixed layer waters, while some subbotinids record stable isotopic signatures very similar to the measured mixed layer. Today, Hollstein al. (2017) show a thermocline of the IPWP reaching temperatures down to 10°C, suggesting the early Eocene thermocline around the area of PNG may have been less steep than the modern thermocline, which is an observation also found by John et al. (2013) from the Eocene waters of Tanzania. Interestingly, the Mg/Ca values suggest a depth habitat for globoturborotalids in the upper temperature range of the thermocline, while subbotinids were placed in the lower part of the range. Conversely, $\delta^{18}O$ values show the opposite, with globoturborotalids occupying the lower section of the temperature range from the measured thermocline temperatures. This may have to do with $\delta^{18}O$-associated disequilibrium effects that may have altered the primary foraminiferal $\delta^{18}O$ signature, such as the production of gametogenic calcite, which would cause a reduced $\delta^{18}O$ signature (more details discussed in Section 4.4.3.2.3).

Finally, the temperatures reconstructed by analysing the benthic foraminiferal tests of *Bulimina tuxpamensis* recorded BWTs ranging between ~18°C and ~23.5°C, which is just 0.5°C colder than the lower range of temperatures from the thermocline reconstruction from thermocline dwellers. This may suggest that either the subbotinids were able to expand their depth habitat through a relatively more homogeneous water column in terms of temperatures (John et al., 2013), just like the mixed layer dwellers in order to escape from the overlying warm temperatures (Si and Aubry, 2018), or that the sub-thermocline temperatures were quite similar to the BTWs. In fact, while the SSTs have been considered rather stable through the Eocene epoch despite the high latitudes being up to 20°C warmer than today, the BWTs may have also exceeded 10-12°C in the early Eocene (John et al., 2013). Moreover, Makarova et al. (2017) reached a conclusion that suggested there was greater warming in the thermocline relative to the mixed layer so that the gradient the during the PETM would have been more reduced between the thermocline and benthic dwellers, than between the thermocline and surface dwellers. We do not exclude either of the two scenarios, as there seemed to be an overlap between the depth habitat of surface and thermocline dwellers, yet the difference between the depth habitat of the thermocline and benthic foraminifera was reduced too. This much more reduced surface-to-deep temperature gradient is in line with previous studies (Huber and Caballero, 2011, and references therein). Despite this, it is worth noting that as *Bulimina tuxpamensis* was an infaunal benthic foraminifer, it may have been affected by the depleted $\delta^{18}O$ of pore waters, although the magnitude of this effect on this particular species is currently absent from the literature.

4.4.4.1   Heat tolerance

Modern warm water-species such as *Trilobatus sacculifer*, *Glogiberinoides ruber* (Bijma et al., 1990), *and Globigerinella siphonifera* (Žarić et al., 2005) exhibit the widest SST tolerance range with an upper tolerance limit of ~31-32°C, which is in good agreement with the ~33°C upper limit found by Hemleben et al. (1989), the enzyme inactivation theory for symbiont-bearing foraminifera above 32°C by Lombard et al. (2009), as well as the theory postulated by Somero (1995) of such temperatures being uninhabitable by most marine eukaryotic organisms today. Furthermore, Aze et al. (2014) found a reduction in planktonic foraminiferal abundance in Tanzania during the PETM, where SSTs may have exceeded 40°C, while Frieling et al. (2017) found a decline in dinoflagellate assemblages during the PETM off the coasts of Nigeria under SSTs >36°C, even though specific dinoflagellate species such as heterotrophic dinoflagellate *Apectodinium* actually increased in abundance during the PETM as a consequence of enhanced nutrient levels in close proximity to continents (Bujak and Brinkhuis 1998; Crouch et al., 2001; Sluijs et al., 2006; Sluijs et al., 2007a, 2007b).

However, in our early Eocene record, the planktonic foraminifer assemblages of both mixed layer and thermocline dwellers are diverse and abundant, suggesting an SST tolerance for the mixed layer dwellers of at least ~35°C. This may be the result of two possible scenarios. Firstly, the early Eocene species may have been more tolerant to heat than modern mixed layer species; secondly, unlike the short-lived extreme warmth of the PETM, the prolonged period of extreme warmth of the early Eocene may have given species the necessary time to adapt to high SSTs by, for instance, developing vital effects specific to their location (Si and Aubry, 2018) or migrating slightly deeper within the euphotic zone of the mixed layer. Comparably, during the prolonged warm interval of the late Cretaceous, no decline in planktonic foraminiferal species was found (Forster et al., 2007; Si and Aubry, 2018), suggesting the ability of warm-water mixed layer species to increase their thermal tolerances and adapt to sustained, extreme warmth (Hönisch et al., 2012; Penman et al., 2014), despite the interactions between biotic adaptation and environmental pressure over thousands or tens of thousands of years being yet poorly constrained (Si and Aubry, 2018). The overlap in depth habitat between subbotinids and morozovellids may indeed suggest that some *Morozovella* spp. may have migrated slightly deeper in the water column to escape a potential thermal stress imposed by the warm mixed layer temperatures. The record of Si and Aubry (2018) suggests that during the PETM at temperatures above 32°C, *M. velascoensis* temporarily disappeared as it was considered to live in the uppermost part of the water column. In contrast, the *M. velascoensis* of this study recorded SSTs >33.5°C. Thus, the

results suggest that the mixed layer dwellers were able to adapt to the extreme warmth of the early Eocene provided that the interval was prolonged enough to allow this adaptation, and that heat tolerance was at least as high as 35°C.

4.4.5 Model-data comparison of tropical ocean temperatures in the early Eocene

The water column around the waters of early Eocene PNG was simulated on a "teuyd" climate model experiment, under atmospheric CO_2 concentrations of 1120 ppm (4 x CO_2 pre-industrial levels). Following this, the temperatures retrieved from the $\delta^{18}O$ values of the foraminifera were superimposed on the modelled line representing the water column, so that a depth for each depth habitat could be estimated (Fig. 4.21). At present, there are no depth habitat reconstructions for tropical early Eocene foraminiferal species, so a comparison between proxy-derived and model-derived depth habitats was not carried out. The model calculated SSTs of ~31°C, which is almost 4°C colder than the measured SSTs from foraminiferal $\delta^{18}O$ of ~34.5°C. The $\delta^{18}O$ of the thermocline dwellers suggested a thermocline temperature range of 24-32°C, while the modelled water column suggests a thermocline down to a depth of ~460 meters at a temperature of 17°C. Lastly, the BWTs of the models displayed temperatures of around 12.5°C, while the $\delta^{18}O$ of benthic foraminifera suggested temperatures ranging between 18°C and 24°C. When assigning a modelled depth to the proxy-calculated depth habitats, the thermocline dwellers would occupy the mixed layer as well as the first upper 150 meters of the water column, which also represent the upper thermocline. The benthic foraminifera, instead, would be assigned a depth between 250 m and 300 m. However, the modelled water column recognises this area as a pelagic environment, leading to deduce that the $\delta^{18}O$-estimated temperatures of the benthics were either derived temperature overestimates, or the water column of the models has been underestimated in terms of temperatures and there may have actually existed a more temperature-homogenous water column, with a reduced gradient between the depth habitats of the thermocline dwellers and the benthics.
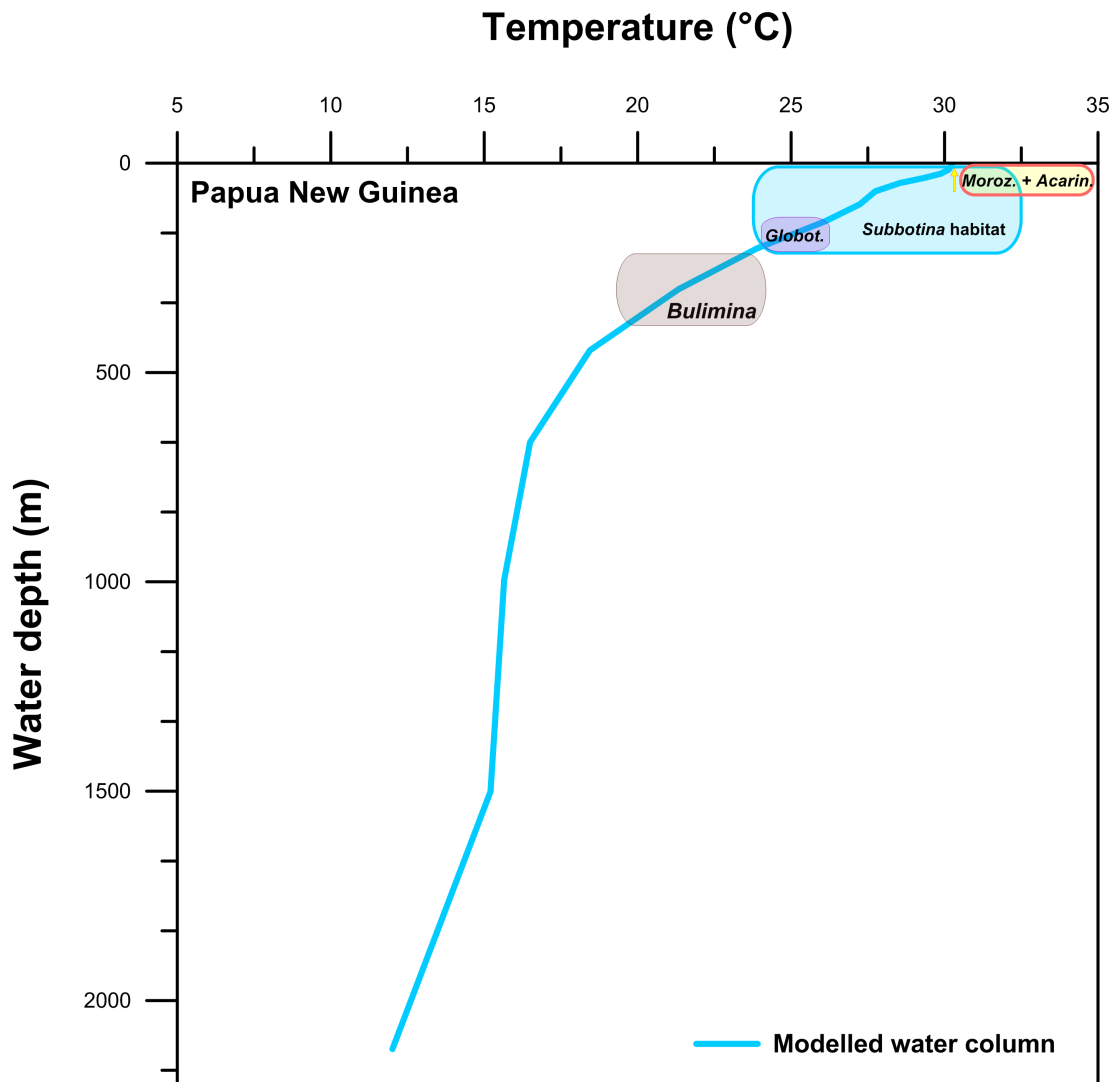
Figure 4.21: Modelled plot of the water column structure around the waters of early Eocene Papua New Guinea. The experiment used was called teuyd, at 4x CO_2 atmospheric levels (1120 ppm), from the Ypresian Stage. Depth habitat of acarininids + morozovellids (yellow box, with tropical pink border); subbotinids (sky blue box); globoturborotalids (purple box); and benthics (brown box) were superimposed on the modelled line by matching the proxy-generated temperatures with the model-generated water column temperatures.

As explained in detail in Section 4.3.5, the initial palaeodepth of the Moogli mudstones was estimated at 50 meters, which seemed incompatible with the 98% P/B ratio as planktonic foraminifera preferentially inhabit semi-open/open ocean settings. It may have been different in the past, but clearly the models are also underestimating the sea surface temperatures, suggesting a steeper thermocline for the early Eocene and a narrower range of temperatures throughout the water column. This model-data mismatch may be explained by the inability of the models to represent the potential existence of a feedback whereby heat is transferred to the high latitudes but is not necessarily significantly lost at the tropics. Instead, there may have been a mechanism that rapidly

replenished the "lost" heat, perhaps through an increased hydrological cycle (Bice and Marotzke, 2002; Lunt et al., 2010), as well as a greater heat transfer through the water column, rendering it more homogenous as suggested by the geochemical proxies. Thus, a broader range of temperatures of the water column combined with a more homogenous water column as suggested by the geological data cannot exclude the idea of a semi-tropical thermostat that may have existed at the tropics compared to the mid-latitudes, rather than an absolute one (Pierrehumbert, 1995), or none (Frieling et al., 2017; Cramwinckel et al., 2018).

4.4.5.1   Tropical cyclones

One explanation behind this efficient transport of heat from the tropics to the poles may be explained by the enhanced frequency and intensity of tropical cyclones in warm climates.

Tropical cyclone intensity is strongly sensitive to tropical ocean temperatures, meaning that the net poleward heat flux is highly dependent on tropical ocean temperatures (Emanuel, 2001). Consequently, rising SSTs would reduce tropical climate sensitivity and increase climate sensitivity at higher latitudes (Emanuel, 2001). In fact, a substantial portion of poleward heat flux is carried by wind-driven lateral gyres in the principal ocean basins (Hall and Bryden, 1982; Wang et al., 1995). Tropical cyclones cause a substantial disturbance to the water column, and at the tropics this could imply decreasing mixed layer temperatures by a few degrees Celsius (Leipper, 1967).

Thus, this induced upper ocean mixing can constitute a strong negative feedback on changes in tropical upper ocean temperatures, implying that a poleward heat flux by the ocean would be strongly affected by net global tropical cyclone activity. Although the times of recovery following the induced disturbance to the water column are relatively fast, it may be that in the early Eocene, tropical cyclone activity was intensified by significant evaporation and increased high water vapour content in the atmosphere, leaving the tropics slightly cooler than what they would be, while substantially warming the higher latitudes.

4.4.6 Comparing the early Eocene between sites with well-preserved foraminiferal tests

The depth habitats as well as the temperature of the water column were compared with the early Eocene Tanzania (~19°S), whereby exceptionally preserved foraminifera were found (Pearson et al., 2001, 2007). Initially, it was thought that both Early Eocene (E.E.) E.E. PNG and Tanzania were located at the same latitude, making the latitudinal comparison more reliable. However, the models suggested PNG sat at 29.39°S, and it is therefore important to take a cautionary measure when comparing the two sites, as Tanzania was exposed to a greater insolation constant than E.E. PNG, therefore biasing the temperature comparison between the two sites.

4.4.6.1 Temperatures of the water column

A clear distinction in depth habitat between the mixed layer dwellers and the thermocline dwellers exists for Tanzania too (Fig. 4.22). The geological data-retrieved SSTs for Tanzania were also warmer by ~4°C compared to the modern average SST of 29°C (John et al., 2013). Thus, the SSTs of E.E. PNG were ~2°C warmer than Tanzania, and this temperature offset between the two sites continued down the water column (Fig. 4.22). This suggests the existence of a Warm Pool back in the early Eocene. It may be argued that this difference could be solely due to proxy uncertainty. Alternatively, considering the different tectonic configuration back in the early Eocene that may have led to the influence of the IPWP in Tanzanian waters too, the SST values that we retrieved for the two locations may both sit at the edge of the E.E. IPWP and therefore represent a lower temperature limit of the IPWP. The thermocline structure of the early Eocene Tanzania suggests the presence of a thermocline that decreased in temperature less rapidly than in the modern-day Tanzanian waters (John et al., 2013), which we also found for the E.E. PNG.
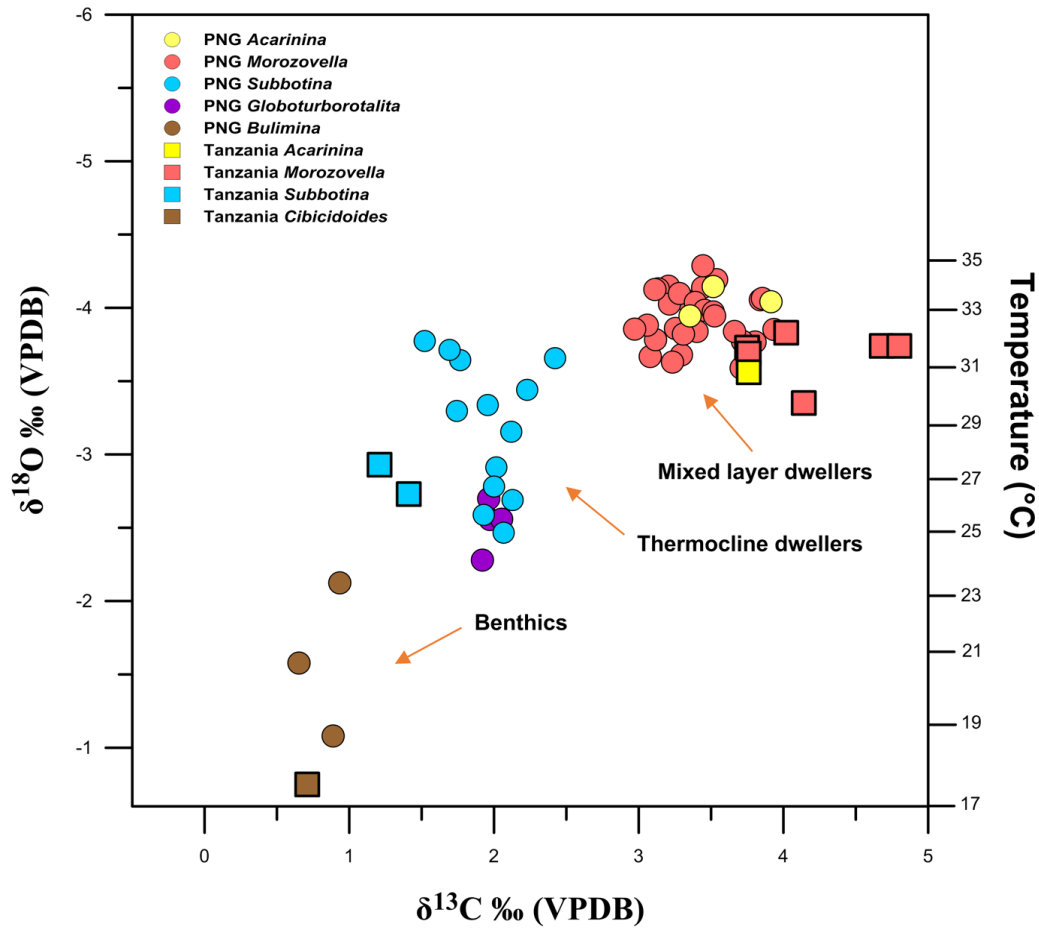
Figure 4.22: Temperature and depth habitat reconstructions of the water column around Papua New Guinea (circles) and Tanzania (squares) during the early Eocene (~55-54 Ma) from the geochemical proxies $\delta^{18}O$ and $\delta^{13}C$ which were derived from both planktonic and benthic foraminiferal tests. Since the samples were infilled, the associated infill was also analysed for PNG (opaque diamonds). The $\delta^{18}O$ scale is reversed such that the lower values indicating mixed layer waters are found at the top, while the higher values are found at the bottom, intercepting with the $\delta^{13}C$ axis. The different colours represent different genera: yellow is for *Acarinina* spp.; tropical pink is for *Morozovella* spp.; sky blue is for *Subbotina* spp.; purple is for *Globoturborotalita bassriverensis*; brown is for *Bulimina tuxpamensis* (circle) and *Cibicidoides* sp. (square). Acarininids and morozovellids are labelled as mixed layer dwellers, subbotinids and *Globoturborotalita bassriverensis* are labelled as thermocline dwellers, *Bulimina tuxpamensis* as an infaunal species, and *Cibicidoides* sp. as an epifaunal benthic foraminifer. The temperature on the second y-axis were derived from inserting the test $\delta^{18}O$ values into the palaeotemperature equation of Kim and O'Neil (1997). A latitudinal correction of +0.59‰ for PNG and +0.48‰ for Tanzania was applied after Hollis et al. (2019), as well as an ice-free volume correction of -0.89‰ after Cramer et al. (2011). Only the size fraction within the 212-355 μm range are shown (Birch et al., 2013).

4.4.6.2   The depth habitats compared to the modelled water column

A modelled water column was produced for both E.E. Tanzania and E.E. Papua New Guinea (Fig. 4.23), using the teuyd climate experiment which was used throughout this chapter, at 1120 ppm of CO_2. The modelled SSTs for Tanzania reached 33°C, therefore matching the values obtained by the oxygen isotope proxy. The modelled water column

for Tanzania displays a steeper thermocline ranging in temperatures between 33°C and 21°C and extending down to 300 meters, unlike the 31°C – 17°C range of the thermocline for PNG which extended down to 450 meters, indicating less uniform water column temperatures for Tanzania. This suggests that the models were able to better match the SSTs from the geological data of Tanzania, while they underestimated the SSTs of PNG by ~4°C (see Section 4.4.5). It may be that the complex tectonic setting of PNG may have led to biases in its palaeolatitudinal reconstruction which in turn may have led to a different insolation constant than what the actual geological data suggested. Indeed, it may be that PNG site actually sat more North than 29.39°S, as the Site currently sits on the edge of two tectonic plates in the central mountain ranges of PNG that are part of a thrust-belt system. If the Site were located on the northern tectonic plate, PNG may have been located a few degrees latitude North and may have progressively moved southwards to eventually converge with the southern tectonic plate and form the mountain range. It is worth noting that the benthic *Cibicidoides* spp. from Tanzania are epifaunal species, unlike the infaunal *Bulimina* species found in the PNG samples. While the epifaunal benthics almost match the BWT of the modelled water column, *Bulimina* according to the temperature vs depth plot, would sit in a pelagic environment between 250 and 350 meters. The $\delta^{18}O$ of the infaunal benthics may have been altered through the incorporation of pore water depleted $\delta^{18}O$ surrounding the test during its lifecycle.
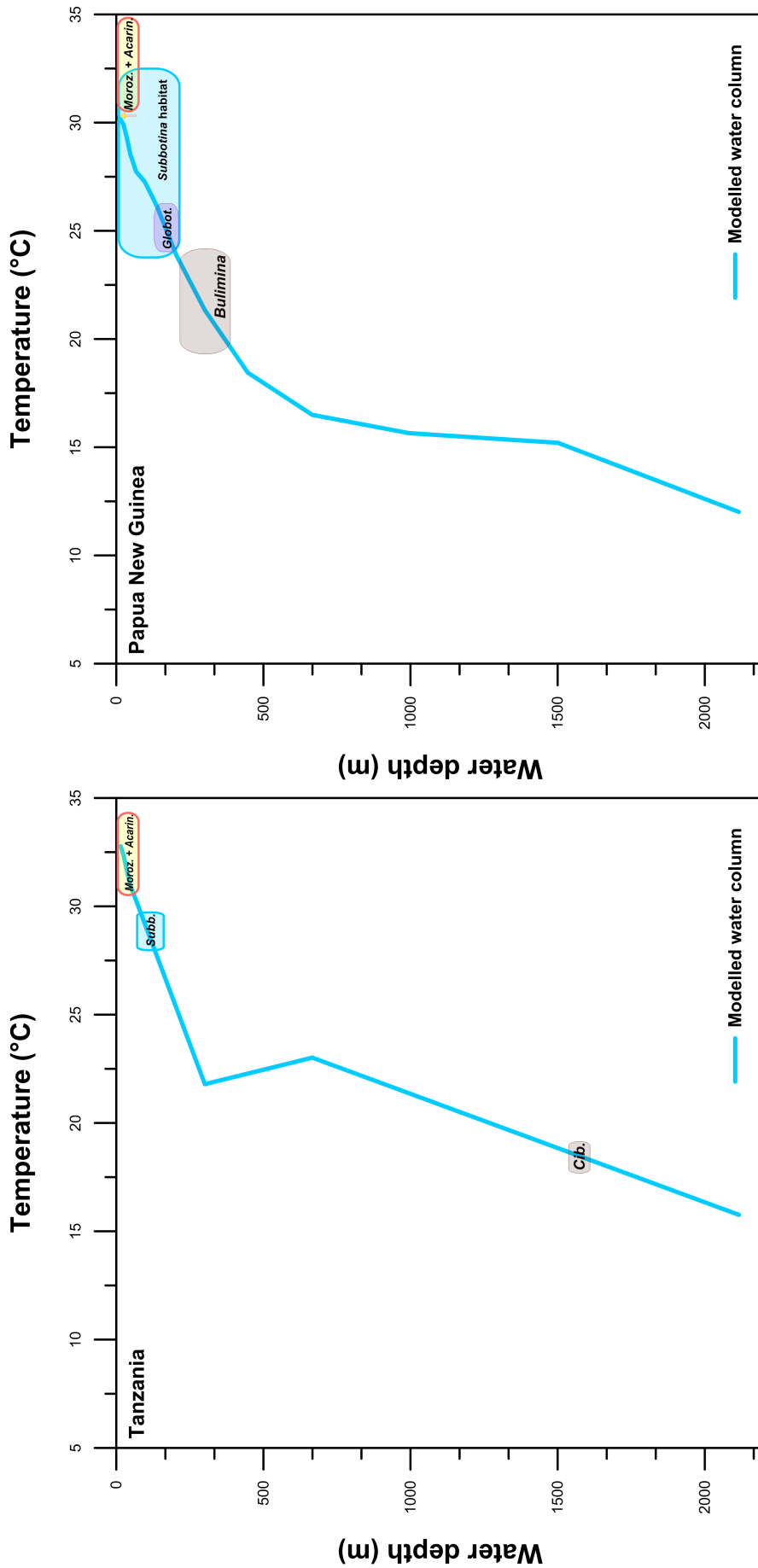
Figure 4.23: Modelled plot of the water column structure and temperatures around the waters of early Eocene Papua New Guinea (right-hand side) and Tanzania (left hand-side). The experiment used was called teuyd, at 4 x CO_2 atmospheric levels (1120 ppm), from the Ypresian Stage. Depth habitat of acarininids + morozovellids (yellow box, with tropical pink border); subbotinids (sky blue box); globoturborotalids (purple box); and benthics (brown box) were superimposed on the modelled line by matching the proxy-generated temperatures with the model-generated water column temperatures. The two water columns were compared as they were both derived from well-preserved, original foraminiferal test.

4.4.6.3   Interpretation of the carbon cycle

A modelled water column profile of $\delta^{13}C$ changing with depth was not produced for PNG as the models involved in this study were unable to reproduce $\delta^{13}C$ water column profiles. Moreover, a comparison with the modern $\delta^{13}C$ profile would be controversial due to the significant latitudinal difference between the E. E. PNG and its current location. However, John et al. (2013) produced Eocene models as well modern plots of $\delta^{13}C$ vs depth for Tanzania, and since the results of this study revealed both sites to be characterised by a weakened surface-to-deep temperature gradient, a comparison of their changing $\delta^{13}C$ with depth was performed to test whether the conclusions drawn by John et al. (2013) from the Tanzania case on the carbon cycle can be applied to E.E. PNG too. In fact, in the study by John et al. (2013), faster temperature-induced remineralisation rates were suggested for the E.E. water column of Tanzania, owing to the sharp $\delta^{13}C_{DIC}$ gradients found in the upper water column as derived from thermocline and surface dwellers. Several studies had already found that the Eocene oceans were characterised by a steeper surface-to-deep $\delta^{13}C_{DIC}$ gradient (Sexton et al., 2006b; Hilting et al., 2008; Huber and Caballero, 2011). Being the temperature higher back in the early Eocene as well as the major control on bacterial respiration rates (Gillooly et al., 2001, 2002), bacterial metabolic rates may have sped up, leading to a shallower remineralisation of organic matter and release of ^{12}C isotopes back into the water column, causing a sharp $\delta^{13}C$ gradient when combined with the $\delta^{13}C$-enriched mixed layer. Moreover, as the temperature sensitivity of respiration is higher than for photosynthesis, (Brown et al., 2004; Allen et al., 2005; Chen et al., 2012), the $\delta^{13}C$-enrichment caused by photosymbiotic algae in the mixed layer would not be affected as much by the high temperatures as the metabolic rates of bacteria (Allen et al., 2005; Lopez-Urrutia et al., 2006; Chen et al., 2012; Regaudie-de-Gioux and Duarte, 2012). This would lead to a reduced efficiency of the biological pump, as most of the particulate organic matter (POC) would be recycled back into a shallower layer of the water column and cause a reduced transfer of POC to the ocean interior rates alongside a reduced carbon burial. Unlike the steeper surface-to-deep gradient of Tanzania represented by the $\delta^{13}C$ difference between surface and thermocline dwellers, which amounted to ~2.50‰, the E.E. PNG record shows a difference of ~1.20‰ (refer back to Fig. 4.22), which is almost half as much of the Tanzania $\delta^{13}C_{DIC}$ gradient and is similar to the modern surface-to-deep gradients, which rarely exceed 2‰ (Kroopnik, 1985).

The Q_{10} term (or Arrhenius equation) has been used to describe the sensitivity of biological processes to temperature (Cossins and Bowler, 1987; Moyes and Schulte, 2008; Boscolo-Galazzo et al., 2018). According to the equation, the rate of any biological

process doubles at every increase in Temperature (T) of 10°C (Moyes and Schulte, 2008). This means that as T increases by 10°C, double the number of molecules reach a level of energy greater than the activation energy that is required to start a chemical reaction (Kremer et al., 2017). Because temperatures were ~10°C higher than today in the thermocline of the waters off the Tanzanian coast hence twice the temperatures of today, an equivalent value of Q_{10} equal to 2 would mean that the remineralisation rates were twice as high as today. Thus, despite sharing a similar shallow surface-to-deep temperature gradient, we cannot firmly assert that PNG had higher bacterial metabolic rates than today hence a shallower remineralisation depth.

4.5   Conclusions

The study reconstructed the temperatures and water column structure waters around early Eocene Papua New Guinea from both geological data and climate model simulations. The former was retrieved from geochemical analyses of planktonic and benthic foraminiferal $\delta^{18}O$ and Mg/Ca, while the latter used a combination of $\delta^{13}C$ and $\delta^{18}O$ of different species inhabiting distinct habitats in the water column. Planktonic and benthic foraminifera were found to be infilled but possessed a well-preserved outer test wall. The test was manually separated from the infill in the attempt to retrieve the primary foraminiferal signal of the geochemical proxies. The distinct values between the $\delta^{18}O$ of the infill and the $\delta^{18}O$ of the test indicated a successful separation of the two different parts of the infilled foraminifera.

Sea surface temperatures from geochemical proxies almost reached 35°C during the early Eocene at 29.39°S, compared to the modern average annual values of 29°C which are found right at the core of the modern IPWP (~6°S), meaning that the tropics were indeed able to maintain their warmth contrary to a previously stated existence of an absolute thermostat, or the modelled representation of cooler tropics relative to higher latitudes. It is likely that the early Eocene Papua New Guinea was not located in the highest temperature part of the IPWP, but we can at least constrain a minimum temperature of its edges, adding that the IPWP core may have been higher by a few degrees Celsius. Moreover, we found a highly abundant and diverse plankton community which therefore thrived in such warm temperatures and was not stressed by temperatures higher than 33°C, as was suggested by previous studies. This is likely due to the fact that following the onset of the PETM, species had sufficient time to adapt to the prolonged periods of extreme warmth that characterised the early Eocene, and may have adapted life strategies such as depth migration through the water column, which is reflected in similar yet distinct $\delta^{18}O$ and $\delta^{13}C$ signatures between the surface and

thermocline dwellers, as well as between the benthic foraminifera, also indicating a less steep thermocline. When compared to the early Eocene of Tanzania, where also well-preserved foraminifera were found, the weak surface-to-deep temperature gradient agreed with the data from PNG, however the increased temperature-induced remineralisation rates were only reflected in the $\delta^{13}C_{DIC}$ of the water column structure of Tanzania, while the $\delta^{13}C_{DIC}$ of the waters around Papua New Guinea had a similar gradient to today.

The climate model simulations underestimated the weak temperature gradient throughout the water column, as well as underestimating sea surface temperatures by ~5°C, further underlying the need to better constrain the possible feedbacks controlling the prolonged, extreme warmth of the tropics during the early Eocene. The possibility of an intensified hydrological cycle whereby an increased intensification of tropical cyclones enabled a more efficient heat transfer to the higher latitudes is likely, but it yet unknown what mechanisms may have helped the tropics develop and preserve such extreme warmth.

SEM Plates of early Eocene (E2 Biozone) Planktonic Foraminifera from the Moogli Mudstones, Papua New Guinea (all scale bars: 20 μm)
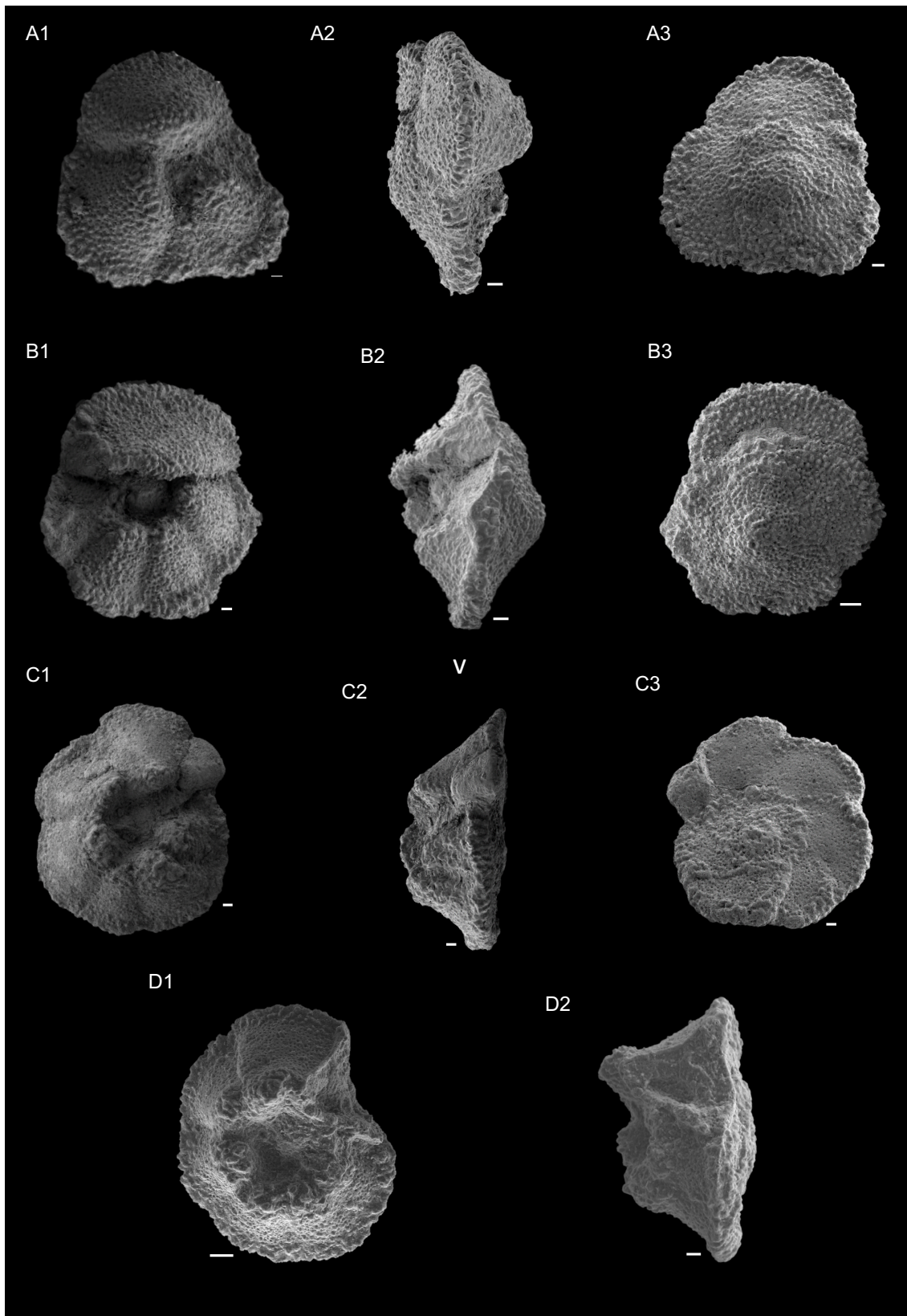
Plate 4.1

A1, A2, A3 = *Morozovella aequa*
B1,B2,B3 = Morozovella sp.
C1,C2,C3 = *Morozovella pasionensis*
D1,D2 = *Morozovella velascoensis*

Plate 4.2
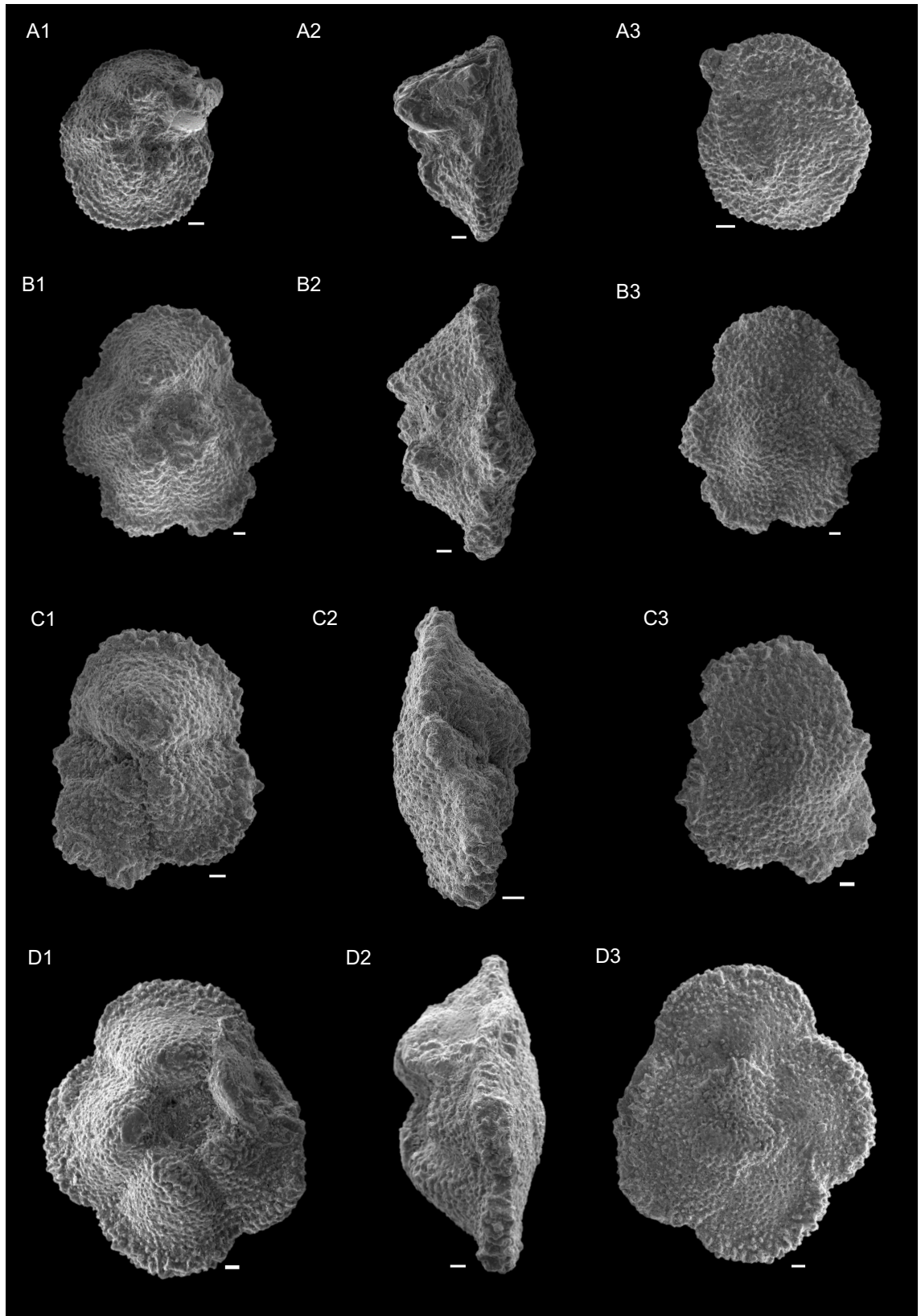
A1, A2, A3 = *Morozovella acuta*
B1,B2,B3 = *Morozovella gracilis*
C1,C2,C3 = *Morozovella aequa*
D1,D2,D3 = *Morozovella acuta*

Plate 4.3
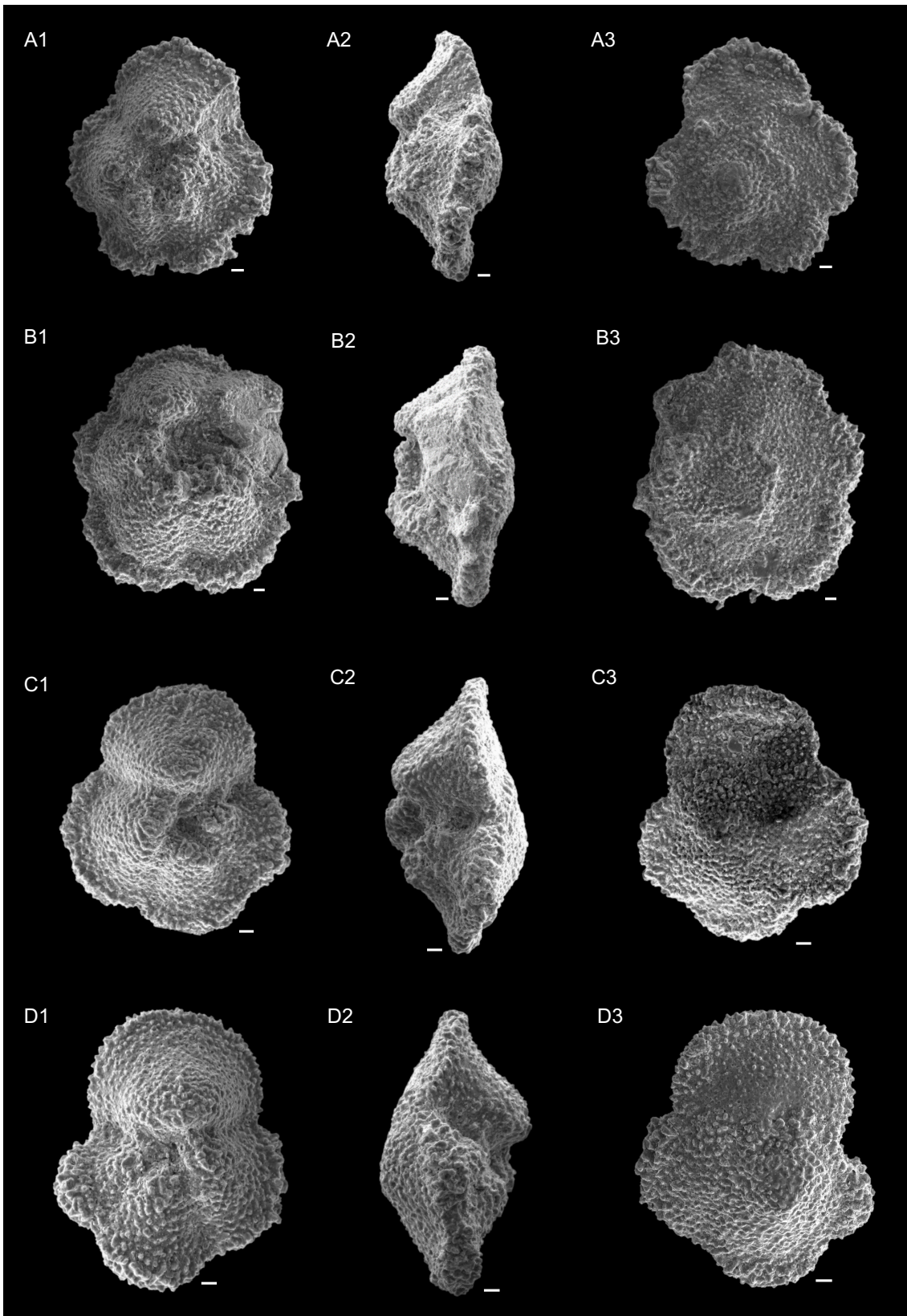
A1, A2, A3 = *Morozovella marginodentata*
B1,B2,B3 = *Morozovella gracilis*
C1,C2,C3 = *Morozovella subbotinae*
D1,D2,D3 = *Morozovella subbotinae*

Plate 4.4
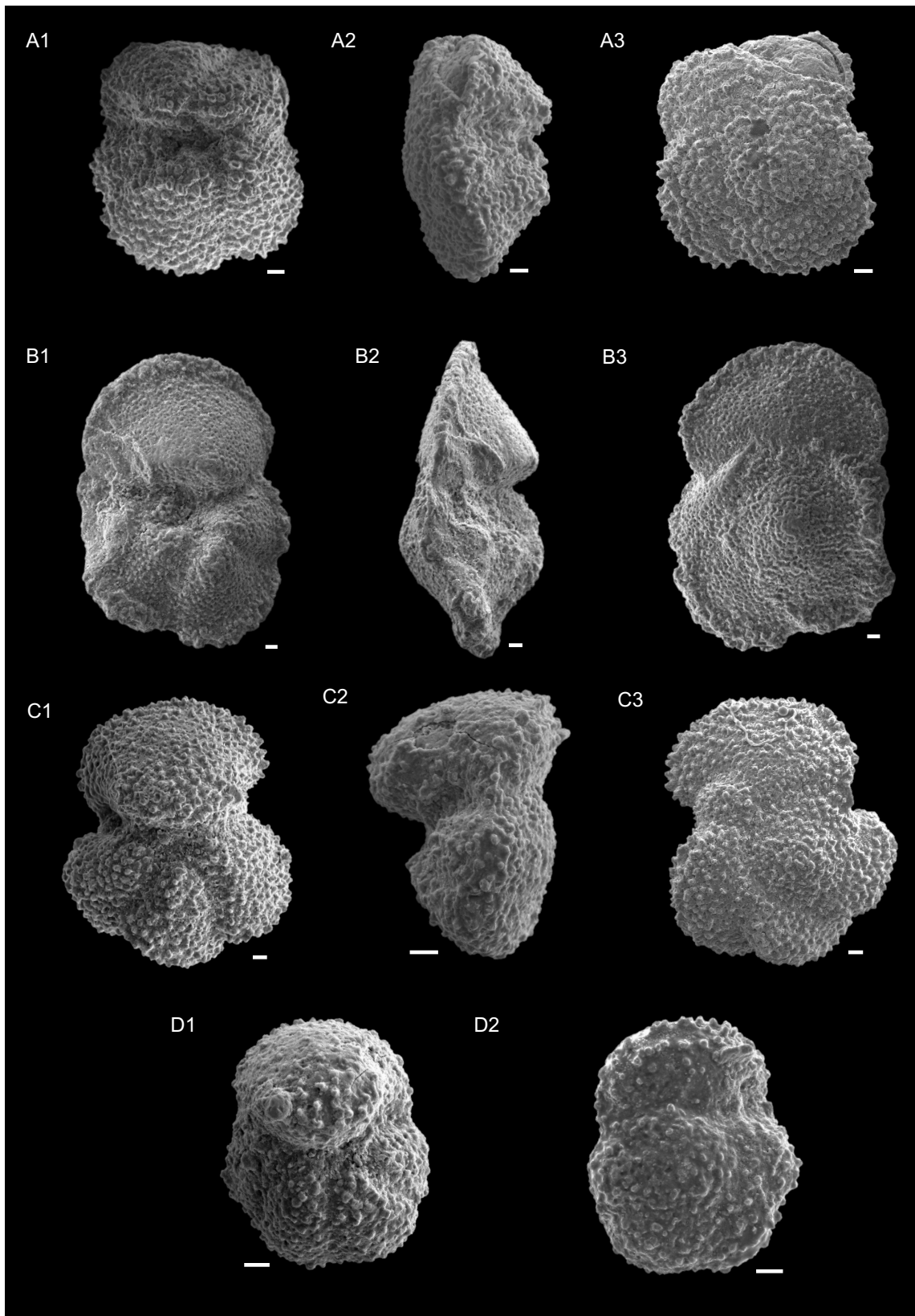
A1, A2, A3 = *Acarinina* sp.
B1,B2,B3 = *Morozovella* sp.
C1,C2,C3 = *Acarinina* sp.
D1,D2 = *Acarinina* sp.

Plate 4.5
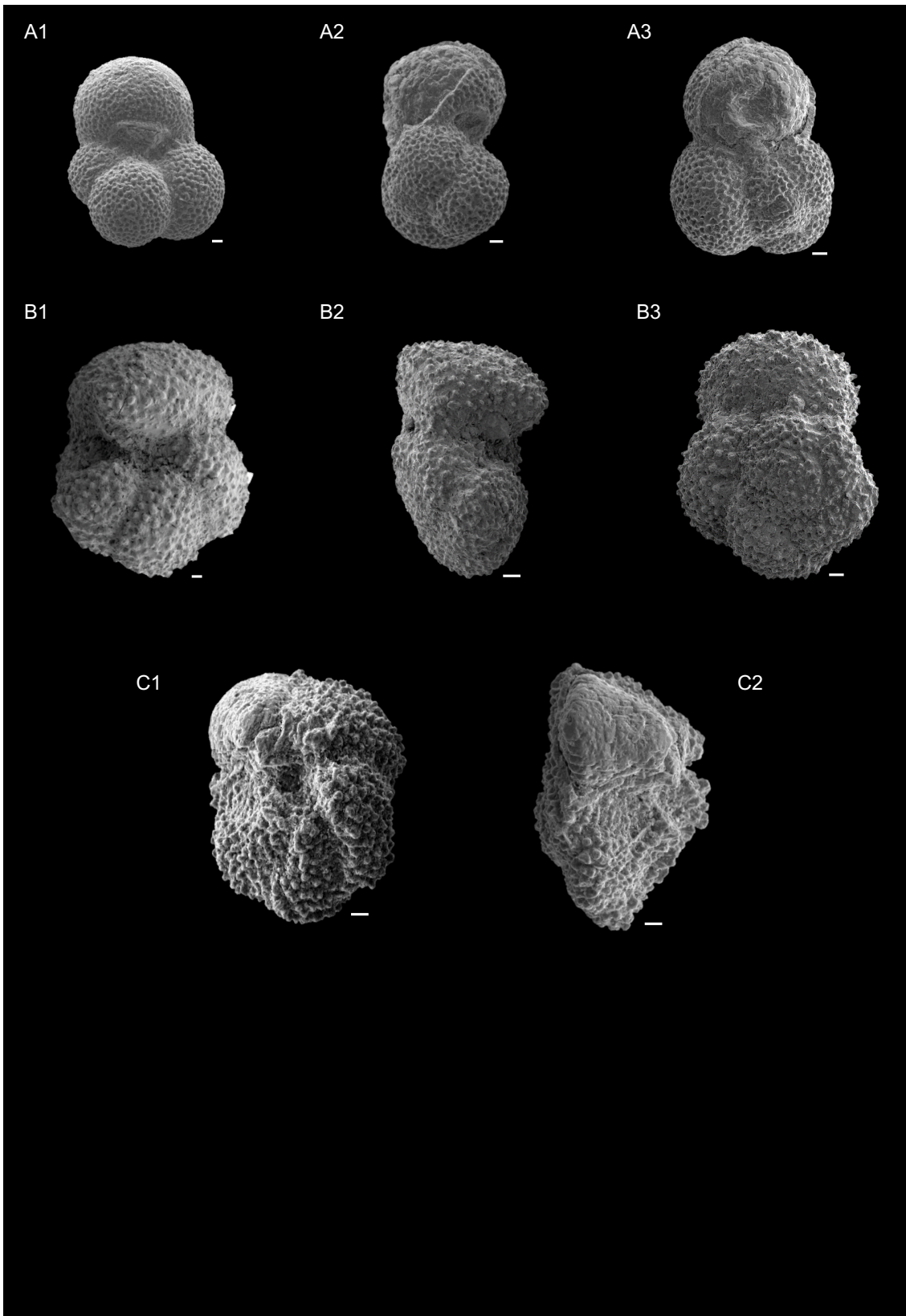
A1, A2, A3 = *Globoturborotalita bassriverensis*
B1,B2,B3 = *Acarinina* sp.
C1,C2 = *Acarinina* sp.

Plate 4.6
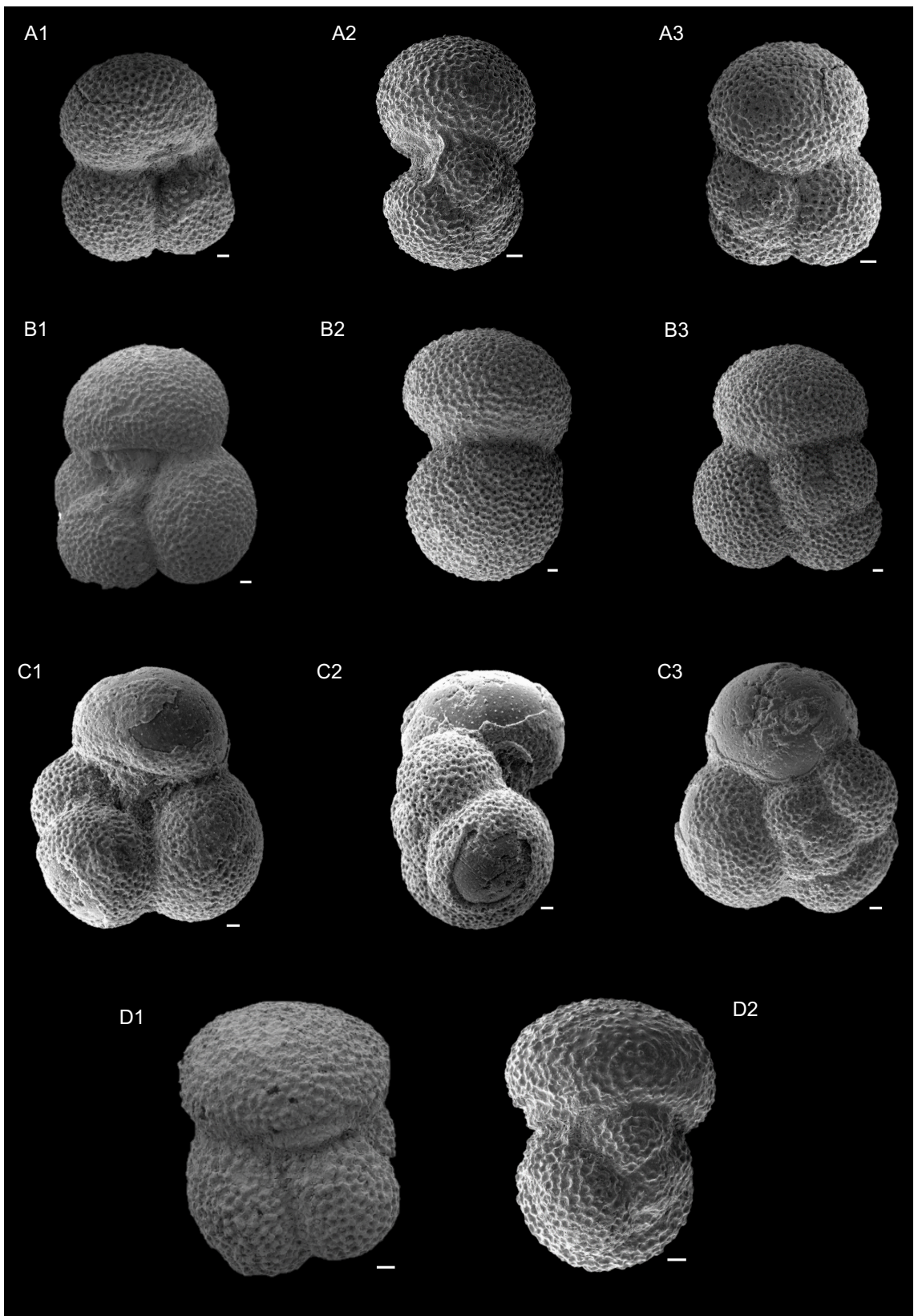
A1, A2, A3 = *Subbotina patagonica*
B1,B2,B3 = *Subbotina roesnaesensis*
C1,C2,C3 = *Subbotina hornibrooki*
D1,D2 = *Subbotina velascoensis*

Chapter 5

Late Eocene tropical temperatures from Java

Chapter **5**

5 Late Eocene tropical temperatures from Java

Abstract

The Eocene is such a critical geological interval to study to better understand the ocean-atmosphere dynamics of greenhouse climates as well as improving climate model performance. During the challenging search for well-preserved tropical foraminiferal tests of the Eocene, an academic-based coring operation based in Java found exceptionally preserved foraminiferal tests dating back to the late Eocene. This chapter reconstructed sea surface and water column temperatures as well as the planktonic foraminiferal palaeoecology of the tropical waters around Java (0.54°N) during the late Eocene (34.3 to 33.7 Ma), using both geological data and climate model simulations. The $\delta^{18}O$ and $\delta^{13}C$ proxies were used for temperature and depth habitat reconstructions, and they were derived from exceptionally preserved planktonic foraminiferal species known to occupy a diverse range of depth habitats in the water column. The $\delta^{18}O$-derived sea surface temperatures reached ~37°C around the tropical waters of late Eocene Java, compared to the modern average annual values of 29°C which are found right at the core of the modern IPWP (~6°S). This large difference in temperature suggests that the tropical areas were indeed able to remain extremely warmth almost as much as higher latitudes during greenhouse climates, unlike previously thought. Moreover, previous studies on the thermal stress of living species indicated an upper tolerance limit below 34°C, while we found a diverse and abundant range of species occupying different depths of the water column. The climate model simulations greatly matched the geological data, with only an SST underestimation of ~2°C. It may be that a combination of a potentially less intensified hydrological cycle just before entering an icehouse state, and the choice of a 1120 ppm CO_2 scenario instead of 560 ppm, contributed to the improved agreement between geological data and climate models for the Eocene Epoch.

5.1   Introduction

The so called "background climates" refer to those long geological intervals wherein the Earth is in a relatively constant climate state between transient climate events (e.g. PETM and EECO) major extinction events (e.g. K/Pg boundary), and transitions from a greenhouse to an icehouse state. It is just as critical to explore background climates because they give insight into the recovery times of the climate following a perturbation to the Earth system, as well as manifesting specific signals within the system before the perturbation itself. Many investigations focus on the major climate perturbations such as the Eocene-Oligocene Transition (EOT) and PETM because it is important to investigate how the climate reacts to extreme disturbances. In fact, when excluding these major events, there are sparse data available for individual intervals such as the late Eocene which just preceded the transition of the Earth from a greenhouse to an icehouse state. For instance, prior research suggests that precursor signals to the EOT in proxies such as $\delta^{13}C$ showed an increase in productivity and eutrophication in the Southern Ocean (Wright and Miller, 1993; Coxall and Pearson, 2007; Lazarus et al., 2008; Pascher et al., 2015), which would have significantly affected the tropical areas at a later time as the Southern Ocean was believed to be the main source of deep water during the late Eocene (Bohaty et al., 2012; Huck et al., 2017). Moreover, many low latitude planktonic foraminiferal species after following a peak in diversity during the early middle Eocene, had undergone extinction by the early late Eocene, indicating an association with the global cooling trend which culminated at the end of the late Eocene (Keller, 1983; Boersma and Premoli Silva, 1991; Keller et al., 1992; Pearson, 1996; Coxall and Pearson, 2007), and enabled cold-tolerant species to thrive in great abundance and diversity (Keller et al., 1992).

In this study, we reconstructed the sea surface and water column temperatures around the waters of Java during the late Eocene using a diverse range of planktonic foraminiferal species that occupied different depth habitats, namely the mixed layer, the upper thermocline, and the lower thermocline. The aim was to understand the ocean palaeoecology and carbon cycle in the Warm Pool just ahead of a transition from a greenhouse to an icehouse state, as well as disentangling any disequilibrium effects that need consideration when relying on geochemical proxies for palaeoclimate reconstructions. Temperatures were also simulated with climate models to compare the results of geological data with model outputs in order to investigate the level of performance of palaeoclimate models during greenhouse climates and suggest possible feedback mechanisms that may have caused any existing model-data mismatches.

Lastly, a global compilation of planktonic foraminiferal $\delta^{18}O$ was produced for both the late Eocene and early Oligocene. The database included $\delta^{18}O$ data from both recrystallised and well-preserved planktonic foraminifera in order to emphasise the bias that diagenetic alterations can cause on temperature reconstructions, as well as reviewing and highlighting the urge to target sites with a greater potential of containing exceptionally preserved tests, such as the tropical areas as they play a pivotal role in the redistribution of heat around the globe and for which only a handful of data exists today.

5.2   Materials and Methods

5.2.1 Study Site

The Nanggulan formation (7.79°S, 110.21°E) is located on the eastern slope of the Menoreh Hills northwest of the village of Kenteng on the island of Java (Coxall et al., *in preparation*). The sample "NKK-1/47, 45-55 cm" was collected from an Academic-based drilling operation in the formation in January and February 2006, more specifically on a slope above the Kali Kunir Stream. The name of the sample breaks down as follows: "NKK" stands for Nanggulan Kali Kunir, "1" is the Site number, "47" is the Core number, and "47-55" cm is the specific position of the sample from the top of the core. This sample was selected for detailed study because of its excellent "glassy" preservation of diverse planktonic foraminifera, and it was also the best preserved among other well-preserved sections of the same core. A sample from the lower Oligocene had already been studied by H.K. Coxall and the aim was to provide and Eocene comparison to understand changes across the EOT in the Warm Pool. The cores are stored at the Indonesian Geological Research and Development Centre, and more information on the coring operation can be found in Coxall et al. (*in preparation)*.

Java is currently an active volcanic island that sits on the Eurasian plate margin in the Indonesian archipelago (Fig. 5.1), above the subducting oceanic crust of the Indian Ocean/Australian plate which has been moving northwards since its separation from Antarctica ~100 Ma.
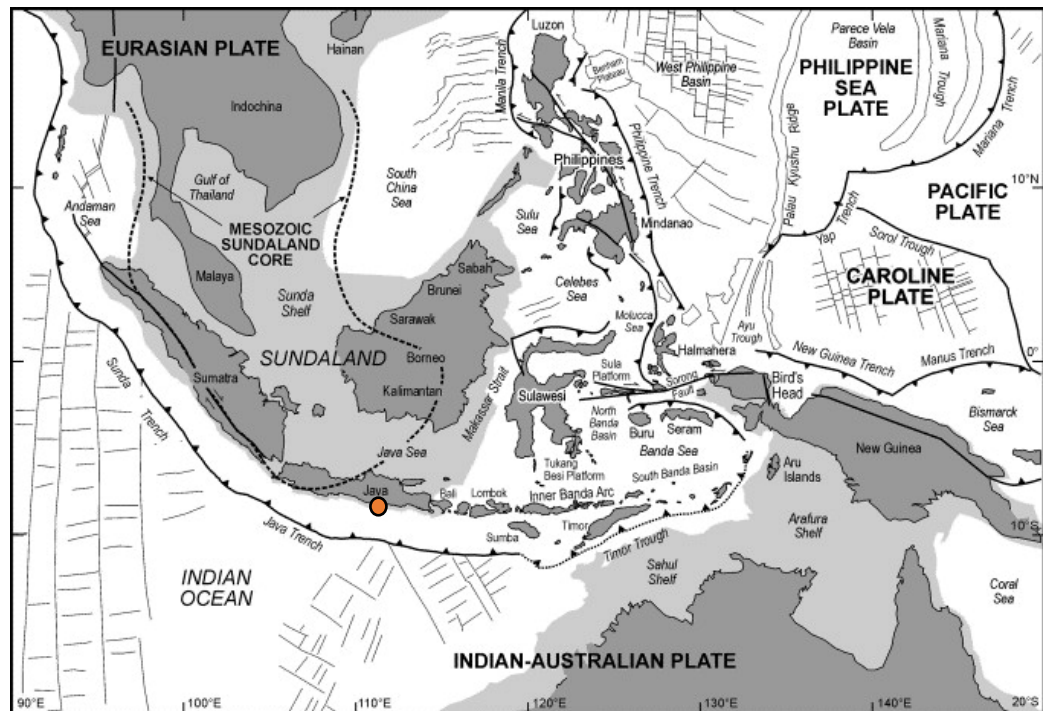
Figure 5.1: Map of South-East Asia highlighting the main geographical features of the region, including the regional tectonics and basins. The position of the Nanggulan Formation is indicated by an orange circle located on the southern edge of Java. The light shaded areas indicate the continental shelves of Eurasia and Australia (adapted from Hall, 2002).

From an oceanographic point of view, late Eocene paleogeographic reconstructions place the Nanggulan Formation in the core of the Indo-Pacific Warm Pool (IPWP), and together with the fact that is one of the few sites that contains very well-preserved late Eocene and early Oligocene microfossils, the NKK1 borehole plays therefore a critical role in understanding tropical ocean palaeotemperatures during greenhouse climates. Today, islands and basins restrict the expansion of the IPWP into the Indian Ocean, whilst during the Eocene Epoch, the area was yet free of such barriers hence the IPWP extended over a greater area in both the Pacific and Indian Ocean (von der Heydt and Dijkstra, 2011). Under this paleogeographic setting, the Indonesian seas would have recorded among the warmest sea surface temperatures, being very close to, or even right, at the heart of the Warm Pool.

5.2.2 Lithostratigraphy and biostratigraphy of the NKK1 borehole

The preservation of microfossils varied between the sections, from infilled foraminifera to exceptionally preserved, glassy looking calcareous nannofossil and foraminiferal assemblages which makes them ideal candidates for geochemical analyses and palaeoclimatic reconstructions. The best quality of the recovered foraminiferal shells was

derived from the clay sections, where it is thought that the impermeable clay protected the calcite from diagenetic alteration such as dissolution and recrystallisation.
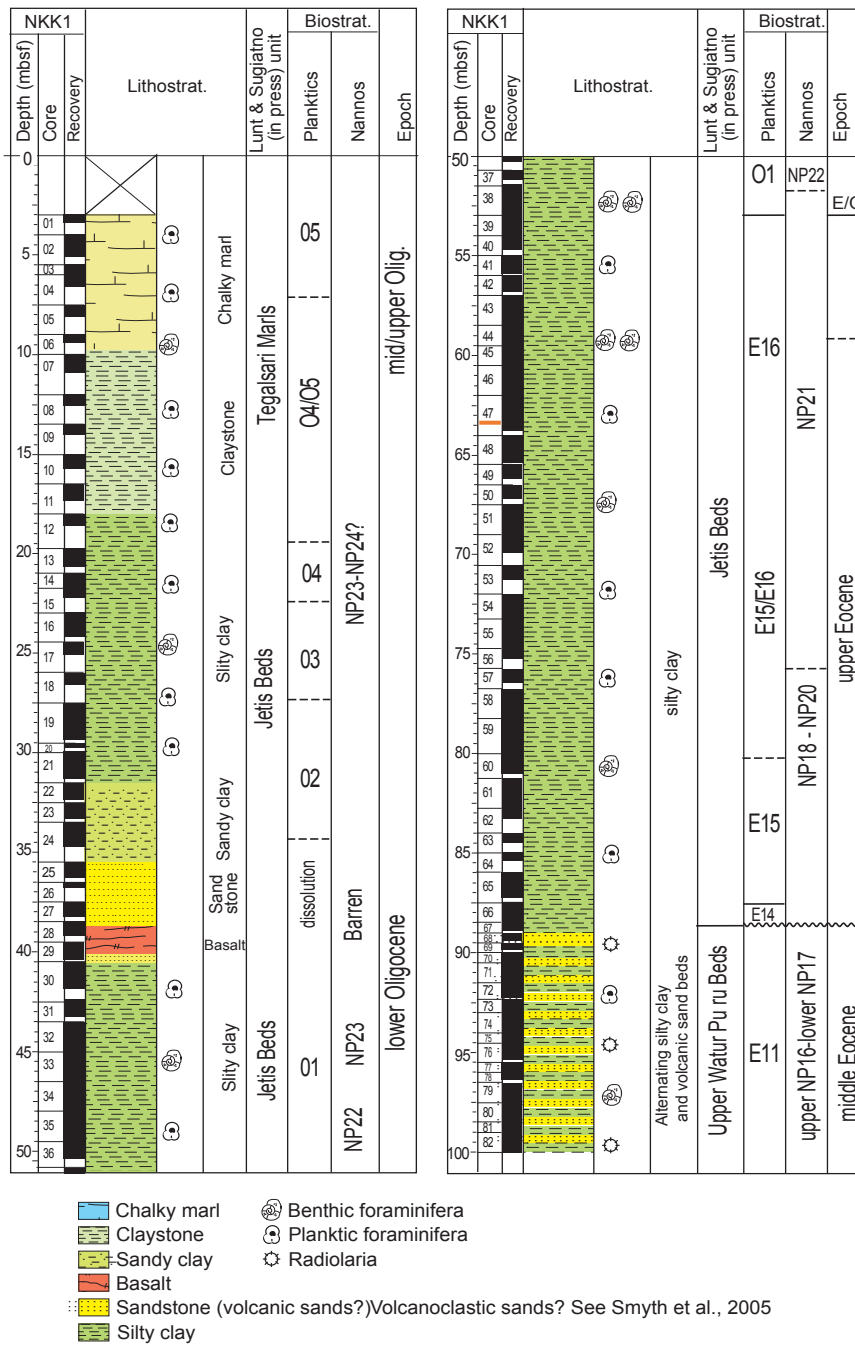
Figure 5.2: Coring summary NKK1 borehole, Kali Kunir, Nanggulan Formation, Java. The geographical coordinates are as follows: 7.79°S, 110.21°E. Both the lithostratigraphy and the biostratigraphy are shown, and they were both used to assign a geological interval to each section of the core. The sample used in this study is called NKK1-47, 45-55 cm, and its position is indicated by an orange bar. The abbreviation mbs stands for "meters below surface" (Taken from: Coxall et al., *in preparation*).

According to the composition of calcareous nannofossil and foraminiferal assemblages, the sample of this study was placed into the late Eocene E16 biozone (Wade et al., 2011), which ranges in age between 34.3 Ma and 33.7 Ma according to the timescale provided by Cande and Kent (1995).

Initially, the calcareous nannofossil evidence constrained the age of the sample as it placed it into the NP21 calcareous nannofossil zone, whereby its base is defined by the extinction of *Discoaster saipanensis*, and its top is found in the early Oligocene. The planktonic foraminiferal biozones further constrained the age of the sample by placing it into the E16 biozone (34.3 to 33.7 Ma). The base of the E16 is defined by the highest occurrence of *Globigerinatheka index*, while the top is defined by the highest occurrence of *Hantkenina alabamensis*. The secondary biomarker for this zone, which also defines the start of the EOT, is defined by the highest common occurrence of *Pseudohastigerina micra* (Wade et al., 2011). The clearest evidence of the sample belonging to the E16 biozone is the presence of *Turborotalia cocoaensis*, which only occurred in the E16 biozone. Both the lithostratigraphy (e.g. the proportion of the different strata) and biostratigraphy (e.g. P/B ratio), suggest that the Nanggulan Formation was deposited in a deep-water (>800 m) depositional environment (Lunt and Sugiatno, 2003).

5.2.3 Cleaning the foraminiferal sample prior to stable isotope analyses

The NKK1 sample had already been washed in deionised water a Cardiff University for preservation assessments so it was already known to contain well-preserved foraminiferal tests. However, further investigation under the binocular light microscope revealed the presence of clay in the matrix as well as some clay adhering to the test walls, urging further cleaning. First, the sample was divided into three size fractions with the following mesh sieve sizes: 63-125 µm, 125-250 µm, and ≥355 µm. These ranges were specifically chosen because previous studies on the core had been carried out under these test sizes, hence a comparison between the data would be easier and consistent when identifying the different vital effects dominating at specific size fractions (Birch et al., 2013). Despite being outside of the 212-355 µm size fraction range advised by Birch et al. (2013) (hereinafter referred to as the Birch range), the 63-125 µm and 125-250 µm size fractions were chosen because some genera, such as *Pseudohastigerina* and *Chiloguembelina*, were characterised by individuals with small test sizes. A list of the species found for each genus is given in Appendix 4, and the study conducted by Birch et al. (2013) helped estimate the minimum number of specimens that should be used for each size fraction, especially when under sample

scarcity circumstances which was the primary control in establishing the quantity used for the geochemical analyses (please refer to Section 4.2.3, Chapter 4).

After this, the samples were placed on a 63 µm mesh sieve in an ultrasound bath filled with deionised water only for 5-10 seconds in order to reduce the risk of damaging the shells. Visible clay particles were subsequently removed with a paintbrush under the light microscope, before drying the sample overnight in the oven at 40°C. Following this, the specimens were identified at both species and genus level.

5.2.4 Taxonomic identification of planktonic foraminifera

Following the sieving and cleaning procedures, all the sieved specimens from the different size fractions were investigated under a light microscope and identified at genus and species level, where possible. The species were identified following the taxonomic criteria of Pearson et al. (2006), Wade et al. (2018), and the additional aid of the online taxonomic database called "Mikrotax" developed by Young et al. (2017). Based on the foraminiferal genera present in the sample, three main ecology groups were selected to represent the depth habitats of each species present in the sample. The first ecology group (Ecology group 1) referred to the foraminifera that mostly inhabited the mixed layer during their life cycle (mixed layer dwellers), namely *Pseudohastigerina* and *Chiloguembelina* spp. The second group (Ecology group 2) included upper thermocline dwellers from the *Turborotalia*, *Hantkenina*, *Paragloborotalia*, and *Globigerina* genera. Lastly, the third group (Ecology group 3) was composed of those species that mainly inhabited the lower part of the thermocline and intermediate waters just below it, namely *Dentoglobigerina*, *Subbotina*, and *Catapsydrax* spp. We are aware that there are more detailed sub-divisions of depth habitats within the water column but to simplify the structure of the community as well as explaining possible depth habitat migrations, these three main sections were taken into account. The genus *Globoturborotalita* was also analysed but the sample, which was mainly derived from the smaller size fractions 63-125 µm, and 125-250 µm, was too small to be detected by the mass spectrometer, therefore no data could be shown for this genus.

5.2.5 Geochemical analyses on planktonic foraminiferal oxygen and carbon stable isotopes

After performing the procedures outlined above, the specimens, 4-5 at a time, were placed on a glass slide under a binocular microscope and a second glass slide was gently pressed against the specimens in order to extract the original test wall and

subsequently manually separate it from the infill with a fine paint brush. The original test wall fragments were directly transferred to the mass spectrometer vials to avoid any potential sample loss. Isotopic analyses were performed at Cardiff University on a MAT253 gas source mass spectrometer with an automated KIEL carbonate preparation unit (more details can be found in Chapter 2, including the analytical precision) for both the $\delta^{18}O$ and $\delta^{13}C$ proxies. Unlike for the early Eocene (see Chapter 4), the infill was not analysed as the aim of assessing the extent of separation of the primary calcite shell from the infill was already investigated in Chapter 4, with a successful outcome.

5.2.6 Palaeoclimate modelling for model-data comparisons

The climate model experiment used for the late Eocene is called "teuya" and was available under both 560 ppm (2x pre-industrial levels) and 1120 ppm (4x pre-industrial levels) CO_2 scenarios. The teuya experiment was selected because it is the updated model simulation of the tdlua, teuga, and teuka experiments for the Priabonian Stage (late Eocene), with a spin-up of 2249 years (Bridge, 2019), unlike previous versions that had shorter spin-ups which reflect lower resolution and are further from reaching equilibrium within the system (Lunt et al., 2016). Additional information on the palaeoclimate models used in this study is given in Chapter 2. Thus, both CO_2 simulations were used to model the sea surface and water column temperatures of the waters around Java during the late Eocene, and a model-data comparison was subsequently performed where the most appropriate CO_2 climate model simulation was also selected.

5.2.7 Developing late Eocene and early Oligocene global databases from planktonic foraminiferal $\delta^{18}O$

As well as reconstructing the carbon cycle and the sea surface as well as water column temperatures of tropical Java during the late Eocene, a part of this Chapter also focused on developing a global compilation comprising all the available planktonic foraminiferal $\delta^{18}O$ data from the existing literature (see Appendix 6 for the late Eocene database, and Appendix 7 for the early Oligocene database). The time intervals chosen were the late Eocene and early Oligocene, thus avoiding the EOT and EOGM, as the aim was to reconstruct the background climates before and after the Earth's transition from a greenhouse to an icehouse state. Exceptionally preserved (glassy looking) foraminifera are commonly found in clay-rich hemipelagic marine sequences and they can provide the closest estimate of the $\delta^{18}O_{seawater}$ at the time of calcification, hence

palaeotemperatures as well. In contrast, poorly preserved foraminifera (frosty looking) can bias the signal following post-mortem diagenetic alteration (Pearson et al., 2001; Sexton et al., 2006a). Both types of preservation were recorded in the database, firstly to remark the dominance of frosty foraminiferal shells in the wider literature over well-preserved ones, and secondly to reassess the preservation state of the study materials that were once thought to contain well-preserved microfossils by several studies. The occurrence of glassy foraminiferal shells is gradually increasing, and this database also aims to highlight the urge to look for potential sites containing glassy material, as well as remark the bias that frosty material can cause among different sites at a specific palaeolatitude. Specific pieces of information had to be found for each site in order to be considered suitable for the database. The precise geographical coordinates were needed for the palaeolatitude reconstructions, while the $\delta^{18}O$ values, species names, and the preservation state of the sample were necessary to divide the well-preserved material from the poorly preserved material as well as reconstructing sea surface and water column temperatures.

5.2.7.1   Selecting the late Eocene $\delta^{18}O$ values from each study

There is a multitude of ways that the $\delta^{18}O$ values of planktonic foraminifera are displayed in the different research studies. Often, in the older investigations, the $\delta^{18}O$ values were either directly listed within the article, or clearly plotted on graphs showing both $\delta^{18}O$ and $\delta^{13}C$ signatures. If the latter was the case, a ruler was manually used to precisely retrieve the $\delta^{18}O$ values from the graphs of the study. The values were selected according to the following criteria in priority order: the geomagnetic reversals (Chrons), the foraminiferal biozonation system after matching it with the revised version by Wade et al. (2011), the calcareous nannonofossil zonation system after matching it with the revised version by Agnini et al. (2014), and lastly the authors' definition of late Eocene when the magnetostratigraphy and microfossil zonation systems were unavailable for a particular site. The EOT was avoided by omitting the clearly higher $\delta^{18}O$ values in the assemblage, especially easier to detect on $\delta^{18}O$ graphs when plotted as a function of time. One may think that this may lead to a time interval bias as different authors used different time scales. However, time scales such as the ones provided by Cande and Kent (1995) and Gradstein et al. (2012) only differ from each other by about one to two hundred thousand years, and the resolution of our age estimates are at the million-year level, therefore they would not cause such a significant uncertainty towards our interpretation. The Cande and Kent (1995) time scale was used as it is accurately matched with the foraminiferal biozonation in Wade et al. (2011), and this resulted in the late Eocene, which is represented by the Priabonian Epoch and foraminiferal biozones E16, E15, and part of

E14, to range between 33.7 Ma and 37.2 Ma, hence with a mid-point of ~35.5 Ma, which is needed when reconstructing the palaeolatitude of each site.

5.2.7.2   Selecting the early Oligocene δ^{18}O values from each study

The same criteria adopted for the late Eocene were also applied to the early Oligocene when selecting the δ^{18}O data in each research study (see Section 5.2.7.1). According to the time scale of Cande and Kent (1995), the early Oligocene, represented by the Rupelian, ranged between 33.9 Ma and 28.1 Ma. However, this study aimed to only represent the background climate of both the late Eocene and early Oligocene, hence without the EOT and the EOGM. It is known the EOGM covers most of Chron 13n (Coxall and Pearson, 2007; Wade et al., 2011). The Rupelian is composed of biozones O1, O2, O3 and O4, and the EOGM sets the base of biozone O1 and the end of the EOT, with a δ^{18}O peak derived from benthic foraminifera species belonging to the *Stilostomella* genus. The top of the last biozone called O4 representing the Rupelian is defined by the extinction of *Chiloguembelina cubensis*, at ~28.4 Ma (Wade et al., 2011). Thus, by excluding the EOT and the EOGM hence the initial phase of the foraminiferal biozone O1, the early Oligocene of the database ranged between 33.2 Ma and 28.4 Ma, therefore with a mid-point of ~30.8 Ma, which is needed when reconstructing the palaeolatitude of each site.

5.2.7.3   Ecology groups, updated species names, and site preservation

The different species found in the literature were divided into the three ecological groups that were also used for this study (see Section 5.2.4), thus mixed layer dwellers were placed in ecological group 1, while the upper and lower thermocline dwellers were placed in ecological group 2 and group 3, respectively. Some species and genera, especially from older studies, have either changed name or been discovered to belong to other genera with time, therefore, species names were updated in accordance with the existing taxonomic information available (Olsson et al., 1999; Pearson et al., 2006; Young et al., 2017; Paul Pearson, *personal communication*). Moreover, the foraminiferal test preservation of each site was investigated by assessing any available SEM images, description of the samples within the study, alongside previous knowledge of the sedimentary and microfossil history of the site (Paul Pearson, *personal communication*).

5.2.7.4   Palaeolatitude and temperature reconstructions

The geographical coordinates were retrieved from the research studies or associated DSDP/IODP reports. Both latitudes and longitudes were recorded as they were both

necessary for palaeolatitude reconstructions. The palaeolatitude calculator developed by van Hinsbergen et al. (2015) was used to reconstruct the palaeolatitude of each site after converting the modern geographical coordinates into decimal places and inputting them into the calculator which is available online (van Hinsbergen et al., 2015). The Nanggulan formation was found to sit on an unconstrained plate and therefore the palaeolatitude calculator was unable to assign the site a palaeolatitude. Because this study also involved modelled palaeogeographic reconstructions, the palaeolatitude of Java could be retrieved from the model simulations instead of the palaeolatitude calculator.

The $\delta^{18}O$ values of each site and both intervals were converted to temperature estimates using the palaeotemperature equation of Kim and O'Neil (1997). Before the temperature conversion, a latitudinal correction was applied to each site by inputting its palaeolatitude during the late Eocene and early Oligocene (although not every site had $\delta^{18}O$ available for both intervals) following the criteria of Hollis et al. (2019), hence using a script on Matlab (see Chapter 2 for more details). After this, an ice-volume correction was also applied to the $\delta^{18}O$ values before their temperature conversion following the criteria of Cramer et al. (2011). Thus, an ice-volume correction of -0.75‰ and -0.25‰ was applied to the $\delta^{18}O$ values of the late Eocene and early Oligocene, respectively. A salinity correction was not applied to the oxygen isotope-derived results because Hay et al. (2006) found that the mean Eocene ocean salinity was similar to today, within 1 psu. Moreover, this can be reinforced when looking at the ocean dataset by LeGrande and Schmidt (2006), where one can notice that there is, roughly, a net effect of precipitation and evaporation processes on the $\delta^{18}O_{sw}$ of the modern IPWP, meaning that the local salinity is similar to the mean ocean one rather than being heavily characterised by a local $\delta^{18}O_{sw}$.

5.3   Results

5.3.1 Stable Isotopes

Even though it has been found that some species of foraminifera can incorporate a fraction of isotopically light metabolic oxygen into their shells as a result of respiration (Erez, 1978; Pearson, 2012), to date there is no clear evidence that this metabolic oxygen affects the $\delta^{18}O$ of a specific foraminiferal species consistently across test size unlike for $\delta^{13}C$. Thus, we commonly assumed that the $\delta^{18}O$-based palaeotemperature reconstructions were not greatly affected by metabolic fractionation, unlike $\delta^{13}C$. However, as the results (Fig. 5.3) are displayed as a function of both $\delta^{18}O$ and $\delta^{13}C$, the

size fractions outside of Birch et al. (2013)'s range were highlighted so that caution in interpreting the δ^{13}C of those data can be made clearly. The 63-125 μm size fraction only applied to the mixed layer dwellers *Pseudohastigerina* and *Chiloguembelina* as they were the only glassy whole shells present in the sample. Moreover, at such a small size fraction, it becomes harder to successfully separate the infill from the original test wall, therefore reducing the reliability of the crushing procedure when retrieving geochemical data.

5.3.1.1 Oxygen isotopes from planktonic tests

The results (Fig. 5.3) show the δ^{18}O values that were retrieved from different species (hereinafter spp.) of the three ecology groups: ecology group 1 includes genera *Pseudohastigerina*, and *Chiloguembelina*, ecology group 2 includes genera *Globigerina*, *Hantkenina*, *Paragloborotalia*, and *Turborotalia*, while ecology group 3 includes genera *Dentoglobigerina*, *Subbotina*, and *Catapsydrax*.

Initially the ecology groups were established according to prior knowledge (Paul Pearson, *personal communication*) and published literature where the same species were investigated and assigned a specific ecology group (or depth habitat) (Poore and Matthews, 1984; Coxall et al., 2000; Pearson et al., 2007; Wade and Pearson, 2008; Aze et al., 2011) However, from the results of this study, the depth habitats very clearly overlap with each other, particularly with regards to the lower thermocline and upper thermocline dwellers. As expected, the mixed layer dwellers from the genera *Pseudohastigerina* and *Chiloguembelina* recorded the lowest δ^{18}O, indicating a shallower depth habitat which is characterised by warmer temperatures with respect to the deeper layers of the water column. Both genera range in δ^{18}O between ~4.75‰ and ~4.90‰.

With the regards to the upper thermocline dwellers, the lowest δ^{18}O values were recorded by *Hantkenina*, with values ranging between -4.70‰ and -3.80‰, whereby the biggest analysed size fraction ≥355 μm yielded the intermediate δ^{18}O values of this range, and the 125-250 μm size fraction yielded the highest, leaving the 212-250 μm size fraction range to record the lowest δ^{18}O values of this range. Only size fraction 125-250 μm contained enough material for *Globigerina officinalis* to be analysed, therefore only one data point is shown for this species, and it records a δ^{18}O value of -4.80‰. The same situation occurred for *Paragloborotalia nana*, for which size fraction 125-250 μm yielded a δ^{18}O value of -4.30‰. The genus *Turborotalia* does show δ^{18}O values similar to the other upper thermocline dwellers, with most values ranging between -3.80‰ and

-4.30‰. However, two *Turborotalia* spp. recorded δ^{18}O values of -2.60‰ and -1.90‰, the latter coming from the biggest size fraction ≥355 µm, and both indicating a deeper thermocline habitat, and more in line with the lower thermocline dwellers. The ecology group 3, composed of the lower thermocline dwellers, showed mixed δ^{18}O values that reflected both upper and lower thermocline depth habitats. The genus *Catapsydrax* recorded the highest δ^{18}O of the whole assemblage of this study, with a narrower range of values with respect to the other lower thermocline dwellers, specifically varying between -1.80‰ and -2‰. In fact, the genera *Subbotina* and *Dentoglobigerina* extend over a much larger δ^{18}O range, varying between -4‰ and -3.60‰ and between -4.10‰ and -2.45‰, respectively, meaning that they overlap the δ^{18}O-induced depth habitat of the upper thermocline dwellers. For all the three lower thermocline dwellers, the highest δ^{18}O value was derived from the largest size fraction ≥355 µm.
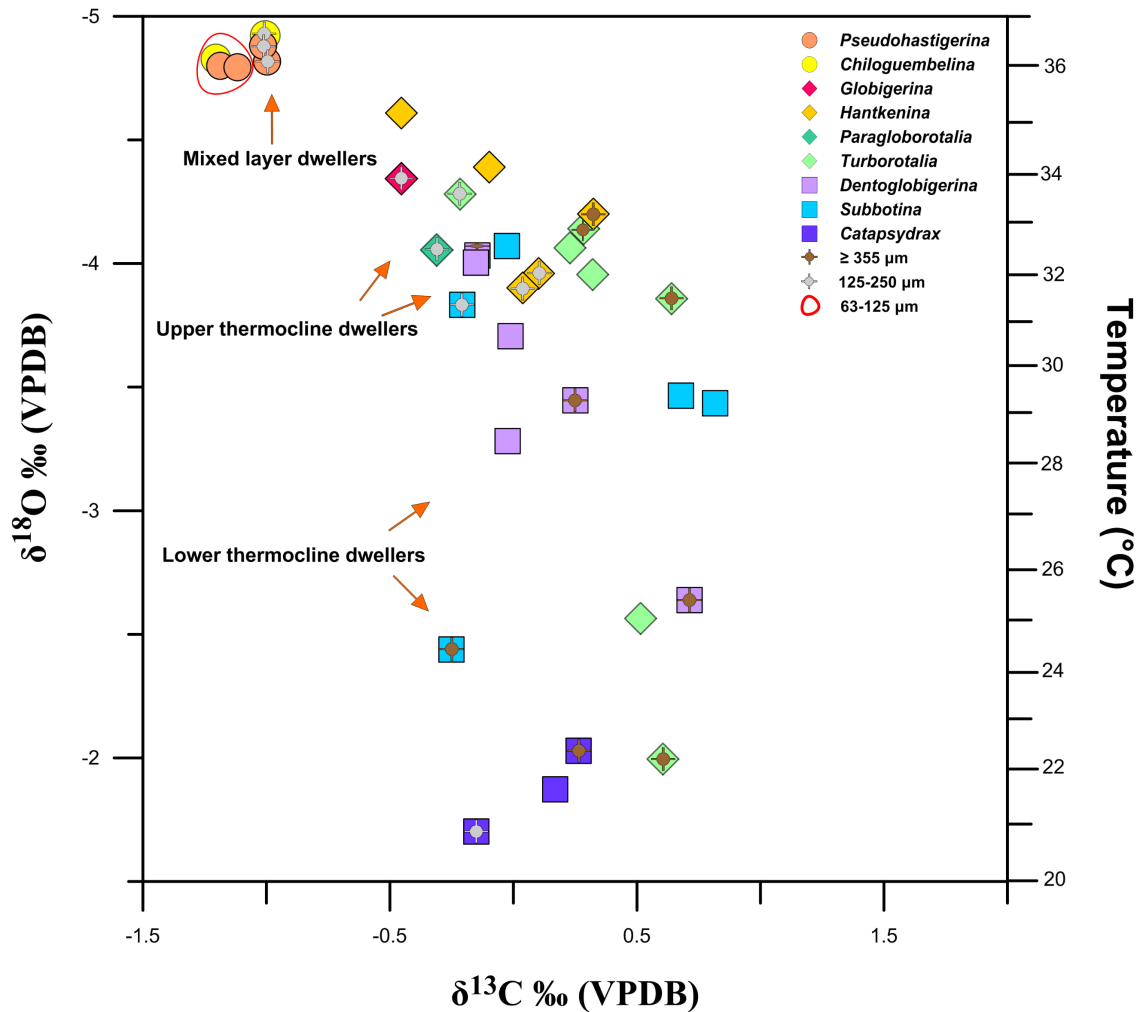
Figure 5.3: Temperature and depth habitat reconstructions of the water column off the coast of southern Java (Nanggulan Formation) during the late Eocene (the estimated age ranges between 34.4 and 33.7 Ma) from the geochemical proxies $\delta^{18}O$ and $\delta^{13}C$ which were derived from the planktonic foraminiferal tests of sample NKK-1/47, 45-55 cm. The different symbols represent the three different ecology groups which reflect different depth habitats: ecology group 1 is composed of mixed layer dwellers (circles); ecology group 2 is upper thermocline dwellers (diamonds); ecology group 3 is lower thermocline dwellers (squares). The different colours represent the different genera (shown in the legend). Each genus may contain different species. The grey cross inside the symbol indicates size fraction 125-250 µm; the brown cross indicates size fraction ≥355 µm; and lastly, the red polygon indicates size fraction 63-125 µm. These size fractions were highlighted following the criteria of Birch et al. (2013), whereby stable isotopes can be affected by vital effects to a greater extent in the size fractions outside of the 212-355 µm range. The temperatures on the second y-axis were derived from inserting the test $\delta^{18}O$ values into the palaeotemperature equation of Kim and O'Neil (1997). A latitudinal correction of +0.28‰ was applied after Hollis et al. (2019), as well as an ice-free volume correction of -0.75‰ after Cramer et al. (2011).

5.3.1.2   Carbon isotopes from planktonic tests

The $\delta^{13}C$ signatures of the mixed layer dwellers were all derived from size fractions 63-125 µm and 125-250 µm, as both genera are characterised by small individuals and are therefore scarce above these test sizes. It is known that test sizes smaller than the ideal

range of 212-355 µm (Birch et al., 2013) can be significantly affected by metabolic fractionation, whereby a major fraction of metabolic CO_2 is incorporated into the calcite shell as a result of faster metabolic rates, shifting the foraminiferal $\delta^{13}C$ towards lower values relative to $\delta^{13}C_{DIC}$. Conversely, test sizes bigger than the ideal range of 250-355 µm are known to be significantly affected by symbiont-induced $\delta^{13}C$ enrichment in symbiotic planktonic foraminifera, slower metabolic rates, and gametogenesis which causes a disequilibrium of the foraminiferal $\delta^{13}C$ from ambient seawater as an additional layer of calcite crust is added to the shell during the late-stage sinking of the foraminifer through the water column during reproduction. By taking all this into account, the size fractions outside of the Birch range were highlighted with symbols in the results to try and investigate any potential trend or evidence of these different vital effects which would result in a possible bias on the foraminiferal $\delta^{13}C$ signatures.

Both mixed layer dwellers *Pseudohastigerina* and *Chiloguembelina* recorded the lowest $\delta^{13}C$ values of the assemblage and a similar, narrow $\delta^{13}C$ range for both genera, with values ranging between -1.25‰ and -1‰. In contrast, all the upper thermocline dwellers recorded higher $\delta^{13}C$ values by at least ~0.50‰, with values ranging between -0.50‰ and 1.25‰ for *Hantkenina* spp., and between -0.25‰ and 0.60‰ for *Turborotalia*. For both genera, the largest size fraction ≥355 µm yielded the highest $\delta^{13}C$ values within the range, whilst upper thermocline dwellers *Paragloborotalia nana* and *Globigerina officinalis* recorded the lowest $\delta^{13}C$ values among the upper thermocline dwellers, with values of -0.60‰ and -0.50‰, respectively. Lastly, the lower thermocline dwellers registered a similar range of values to the upper thermocline dwellers, with values ranging between -0.55‰ and 0.75‰ for *Dentoglobigerina*, and between -0.25‰ and 0.75‰ for *Subbotina*. In contrast, *Catapsydrax* registered a narrower range of $\delta^{13}C$ relative to the other lower thermocline dwellers, with values ranging between -0.15‰ and 0.26‰.

5.3.1.3   Intragenus and interspecies variability across different test sizes

5.3.1.3.1   Ecology group 1: Mixed layer dwellers

According to the conventional palaeoecology model (Shackleton et al., 1985; Pearson et al., 1993; D'Hondt et al., 1994; Birch et al., 2012; Si and Aubry, 2018), the mixed layer dwellers register the lowest $\delta^{18}O$ values as a consequence of occupying the upper part of the water column, and they also register the highest $\delta^{13}C$ values as a result of calcifying in the ^{13}C-enriched mixed layer where photosynthesis occurs and preferentially utilises ^{12}C. However, in this study, although *Pseudohastigerina* spp. and

Chiloguembelina cubensis registered the most depleted $\delta^{18}O$ values, they also registered the lowest $\delta^{13}C$ values, which is in disagreement with the theory (Fig. 5.4).
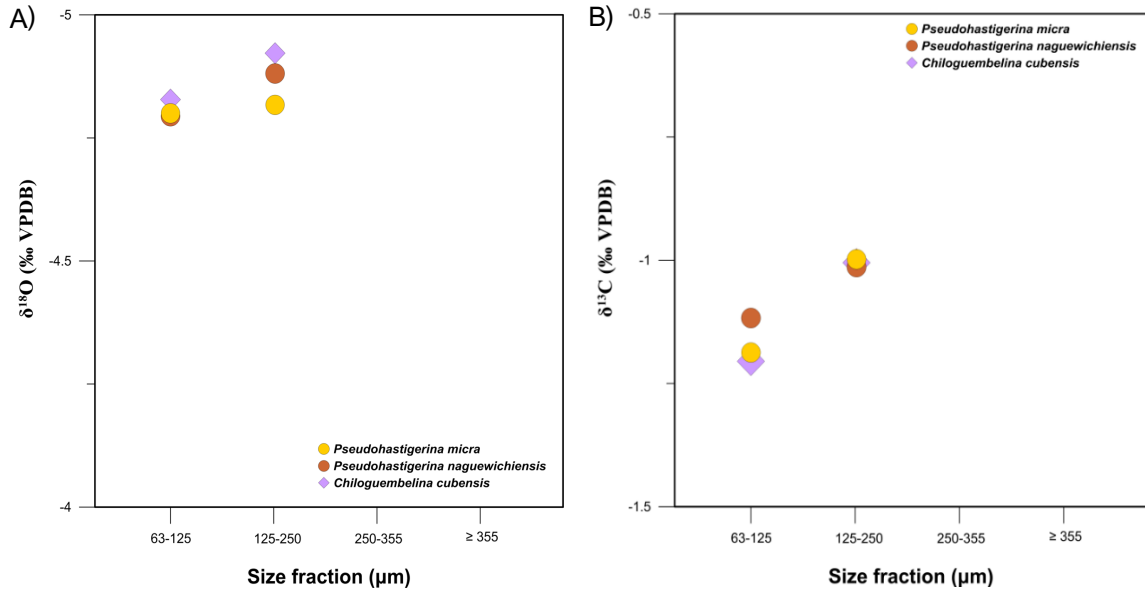
Figure 5.4: Relationship between both foraminiferal $\delta^{18}O$ (panel A) and $\delta^{13}C$ (panel B) of the mixed layer dwellers and increasing size fraction (μm). The circles represent the different *Pseudohastigerina* species found in the sample, while the diamonds represent the species *Chiloguembelina cubensis*. The different colours of the circles represent specific species within the genus *Pseudohastigerina*. Both genera are characterised by small individuals, hence only the smallest size fractions were analysed, specifically the 63-125 μm and 125-250 μm size fractions.

Both *Pseudohastigerina micra* and *Pseudohastigerina naguewichiensis* have the highest $\delta^{18}O$ values compared to *Chiloguembelina cubensis*, especially at 125-250 μm size fraction whereby the three different species differ in $\delta^{18}O$ the most compared to the 63-125 μm size fraction. In contrast, the $\delta^{13}C$ of *Chiloguembelina cubensis* registered the lowest values at 63-125 μm size fraction, while all three species registered almost an identical $\delta^{13}C$ value of ~-1‰ at size fraction 125-250 μm. Only these two size fractions were analysed as both genera mostly occur in small size, including during their adult stage. Overall, for all the three species, a similar pattern can be seen, whereby the $\delta^{18}O$ signature becomes lower and the $\delta^{13}C$ higher with increasing size fraction.

5.3.1.3.2   Ecology group 2: Upper thermocline dwellers

The ecology group 2 is composed of the upper thermocline dwellers which, in this study, are represented by different species within the genera *Turborotalia* and *Hantkenina.* Although both genera registered higher $\delta^{18}O$ values relative to the mixed layers, indicative of a deeper depth habitat, *Hantkenina* spp. recorded lower $\delta^{18}O$ values than *Turborotalia* species, except for the 125-250 μm size fraction (Fig. 5.5). For the

turborotalids, there is a trend of higher $\delta^{18}O$ with increasing size fraction, except for *Turborotalia increbescens*. *Turborotalia cocoaensis* recorded significantly higher $\delta^{18}O$ values relative to the whole assemblage of upper thermocline dwellers, and the largest difference in $\delta^{18}O$ between size fractions, suggesting a clearer change of depth habitat with increasing size fraction with respect to the other species of both genera. In fact, *Hantkenina nanggulanensis* also records as a large difference in $\delta^{18}O$ between size fractions as *Turborotalia cocoaensis*, but in the opposite direction between 125-250 μm and 250-355 μm where $\delta^{18}O$ becomes lower, whereas the $\delta^{18}O$ becomes higher between 250-255 μm but still not as high as at 125-250 μm. Species *Hantkenina primitiva* also shows a lower $\delta^{18}O$ signature with increasing size fraction. Overall, except for *Turborotalia cocoaensis* which ranges in $\delta^{18}O$ between -2‰ and -2.50‰, all the remaining species fall in the $\delta^{18}O$ range between -3.80‰ and -4.65‰, which equals to a temperature difference of almost 8°C and suggests a thermocline habitat whereby temperatures decrease rapidly with increasing depth.
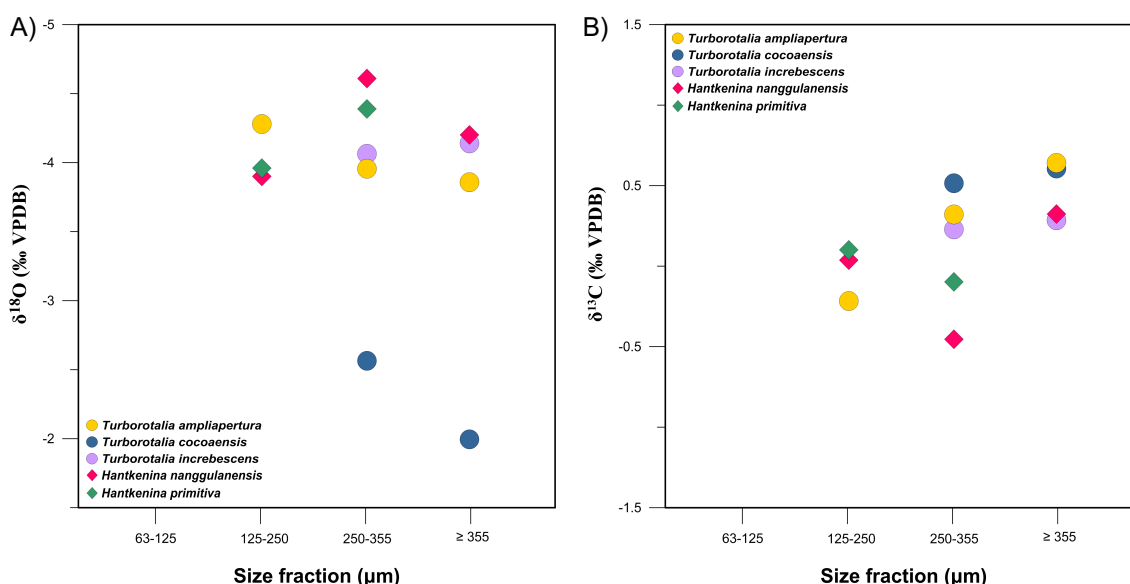
Figure 5.5: Relationship between both foraminiferal $\delta^{18}O$ (panel A) and $\delta^{13}C$ (panel B) of the upper thermocline dwellers and increasing size fraction (μm). The circles represent the different *Turborotalia* species found in the sample, while the diamonds represent different *Hantkenina* species. The different colours of the circles represent specific species within the genus *Turborotalia*, while the different colours of the diamonds represent specific species within the genus *Hantkenina*. Both genera were found in all the size fractions under investigation, except for the 63-125 μm size fraction.

Regarding the $\delta^{13}C$ signature, there is a clear pattern of increasing $\delta^{13}C$ values with increasing size fraction, except for hantkeninids at 250-355 μm size fraction, where both *Hantkenina nanggulanensis* and *Hantkenina primitiva* register $\delta^{13}C$ values lower than the preceding 125-250 μm size fraction. Just like for $\delta^{18}O$, *Turborotalia increbescens* is the species that shows the smallest change in $\delta^{13}C$ the species that shows the smallest

change in δ^{13}C across the different size fractions, suggesting a consistent depth habitat through its lifecycle.

5.3.1.3.3   Ecology group 3: Lower thermocline dwellers

There is a mixed pattern of δ^{18}O signatures with changing size fractions for the lower thermocline dwellers (Fig. 5.6). Both *Dentoglobigerina tripartita* and *Dentoglobigerina galavisi* decrease in δ^{18}O value with increasing size fraction, unlike *Dentoglobigerina pseudovenezuelana*. In contrast, the δ^{18}O of both *Subbotina angiporoides* and *Subbotina corpulenta* decrease with increasing size fraction, while the same cannot be said for *Subbotina linaperta* as enough sample of this species was found only in the 250-255 µm size fraction. The difference in δ^{18}O between size fractions is quite consistent for the genus *Dentoglobigerina* with a difference in δ^{18}O on average of ~0.50‰. Conversely, the largest difference in δ^{18}O between size fractions was derived from *Subbotina corpulenta*, which changed from -4.10‰ to -2.45‰ between size fractions 250-355 µm and ≥355 µm, suggesting the species was characterised by the largest change in depth habitats among the other thermocline dwellers. Interestingly, the δ^{18}O of species *Catapsydrax unicavus* decreases linearly with size fraction, suggesting an upward migration throughout its lifecycle.
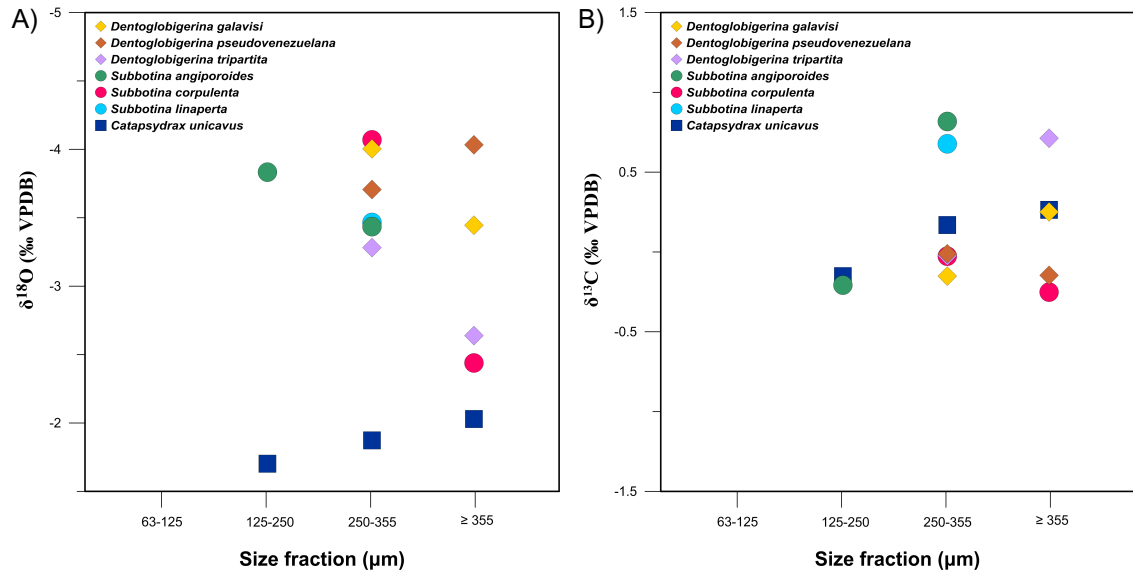
Figure 5.6: Relationship between both foraminiferal δ^{18}O (panel A) and δ^{13}C (panel B) of the lower thermocline dwellers and increasing size fraction (µm). The circles represent the different *Subbotina* species found in the sample, while the diamonds represent the different *Dentoglobigerina* species, and the squares the species *Catapsydrax unicavus*. The different colours of the circles represent specific species within the genus *Subbotina*. Both genera were found in all the size fractions under investigation, except for the 63-125 µm size fraction.

The δ^{13}C signature also registered mixed trends at both species and genus levels. Just like for δ^{18}O, the δ^{13}C of *Catapsydrax unicavus* increases linearly with increasing test size. In contrast, subbotinids and dentoglobigerinids registered both an increase in δ^{13}C with increasing size fraction for *Subbotina angiporoides* and *Dentoglobigerina galavisi*, and a decrease in δ^{13}C with increasing size fraction for *Subbotina corpulenta* and *Dentoglobigerina pseudovenezuelana*. Moreover, both subbotinids and dentoglobigerinids displayed an overall range in δ^{13}C values of ~1‰, while *Catapsydrax unicavus* was characterised by a smaller range and no larger than ~0.40‰, just like for its associated δ^{18}O signature.

5.3.2 *Modelled sea surface and water column temperatures*

A map of the late Eocene displaying global mean annual sea surface temperatures was produced using the teuya simulation experiment under both atmospheric CO_2 concentrations of 560 ppm (2x pre-industrial levels) and 1120 ppm (4x pre-industrial levels) (Fig. 5.7) in order to investigate the extent of the temperature response of the oceans to varying atmospheric CO_2 levels.

The incorporated tectonic plate rotations (see details for palaeogeographies in Chapter 4, section 4.2.6.1) located late Eocene Java at 0.54°N, which means the island moved about 7 degrees South in order to acquire the modern geographical position (~7.79°S). From the modelled tectonic configuration, it is clear that the IPWP, just like in the early Eocene, had a larger surface area relative to today which allowed the core of the IPWP (warmest part of the Warm Pool) to extend beyond Australia, and almost bathing the coasts of Tanzania. Under 560 ppm of atmospheric CO_2, the climate model simulated the core of the IPWP to reach 32°C and to be positioned around the Philippines, hence around the waters bathing Java back in the late Eocene, covering the longitudinal area between 75°E and 130°E, and the latitudinal area between 10°N and 10°S. In contrast, under 1120 ppm of CO_2, the core of the IPWP was simulated to reach SSTs up to 34°C and the core to expand over a larger surface area, both eastward and westward, bathing the eastern coasts of India, occupying the longitudinal area between 75°E and 165°E, and the latitudinal area between 10°N and 15°S. Thus, the model simulations suggest that Java may have well been located in the warmest part hence at the core of the late Eocene IPWP, under both CO_2 simulations, and the temperature reconstructions from the exceptionally preserved foraminiferal tests of the mixed layer dwellers should therefore provide the peak temperatures that the IPWP reached during this interval. The modelled palaeolocation of Java (more precisely, the Nanggulan Formation) is in disagreement with previous palaeolocation estimates, specifically the 6.5°S estimate

suggested by Jones et al. (2019) and Hall (2012) as they assumed the position to be similar to today, as well as the 2°S estimate put forward by Coxall et al. (*in preparation).*
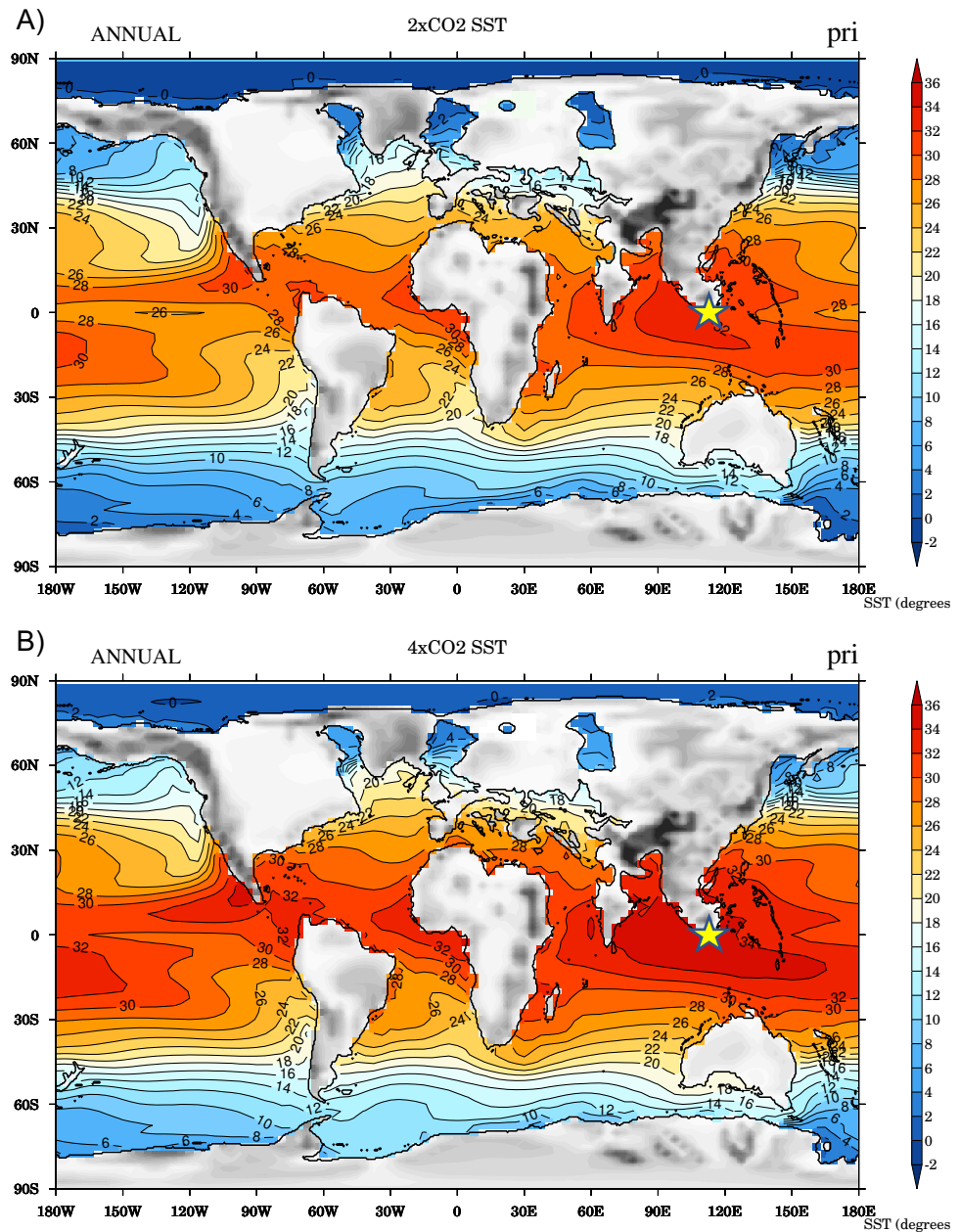
Figure 5.7: Model simulation of global late Eocene (Priabonian Stage) sea surface temperatures from the teuya experiment under A) 560 ppm of atmospheric CO_2 (2x pre-industrial levels), and B) under 1120 ppm of atmospheric CO_2 (4x pre-industrial levels). The colours represent temperatures, with red being the hottest, and blue the coldest. The isotherms are 2°C apart from each other. The star symbol shows where Java was located according to the palaeogeographic data. The palaeogeographies were derived from the Getech Plc platform which in turn adopted an approach based on work performed by Markwick and Valdes (2004).

The water column structure was reconstructed by retrieving values from the teuya model experiment for the Priabonian interval at latitude 0.54°N. The climate model divides the water column into 20 depth levels, and the results (Fig. 5.8) show that it may have been as deep as about ~3200 meters, which is supported by the rare presence of benthic foraminifera relative to planktonic foraminifera. Just like for the early Eocene (Chapter 4), each of these depth levels is represented by the average temperatures of the specific depth block such that, for instance, the sea surface temperature of the water column was derived from the average temperature of the upper 5 meters. This would be more in line with the temperatures represented by the mixed layer dwellers as realistically, they do not occupy the very first centimetres of the sea surface, and they may migrate within the mixed layer throughout their life cycle. According to the model reconstruction, under 1120 ppm of atmospheric CO_2 (Fig. 5.8, sky blue line), the sea surface temperatures of the water column for late Eocene Java reached ~35°C, but actually peaked in the subsurface by slightly more than (yet within the same degree) 35°C.
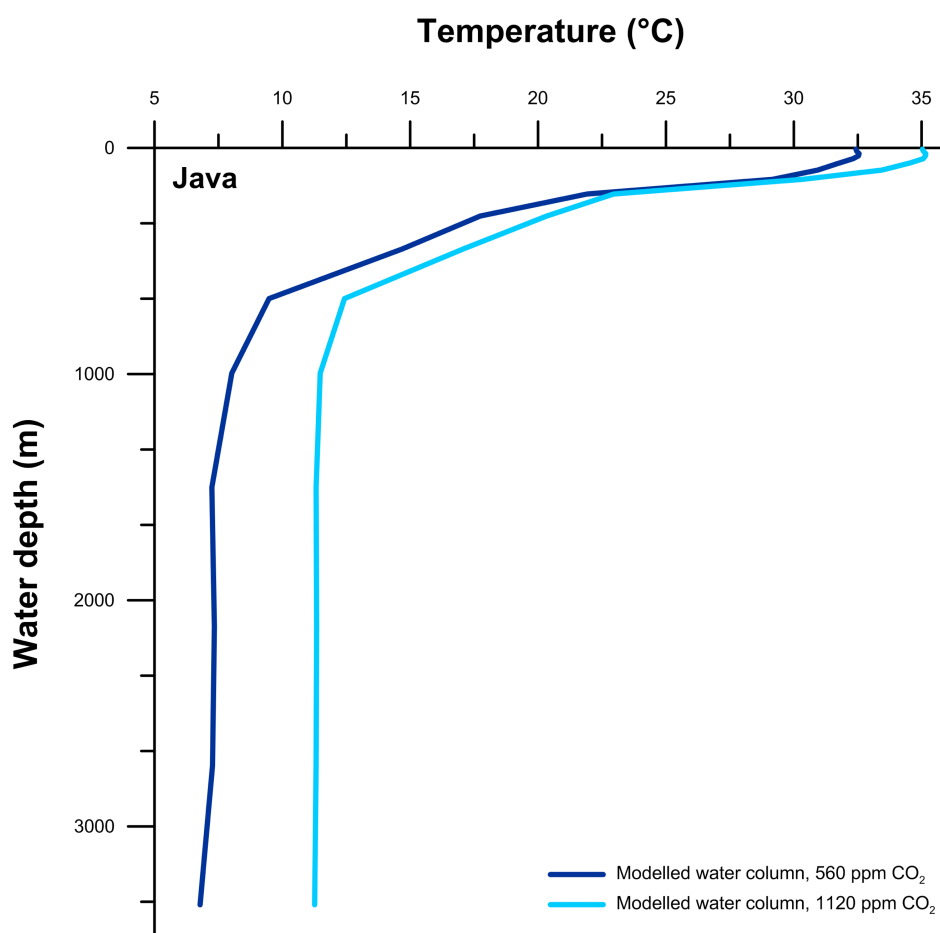
Figure 5.8: Modelled temperature plot of the water column off the coasts of late Eocene Java. The climate model experiment used was called teuya, and for comparison purposes both CO_2 simulations available, 560 ppm (dark blue line), and 1120 ppm (sky blue line) were plotted on the same graph.

This feature was followed down the water column by a thermocline with temperatures ranging between ~35°C and 12.5°C, extending down to ~666 meters, and characterised by a two-step gradient that is steepest between 15 m and 320 m, and less steep between 320 and 666 m depth. This specific trend of the thermocline induces one to think there may be two different water masses occupying the thermocline and underlying a subsurface that tends to become warmer than its overlying surface. The water column below the thermocline remained constant, reaching bottom water temperatures of ~12°C. In contrast, the model reconstruction of the water column under 560 ppm of atmospheric CO_2 (Figure 5.8, dark blue line) simulates lower SSTs that reached ~32°C, and were followed downwards by subsurface waters slightly warmer than (yet within the same degree) 32°C, which is the same pattern as the 1120 ppm simulation (Figure 5.8, sky blue line). The thermocline ranging between ~32°C and 9°C is also characterised mainly by a two-step temperature gradient, with the steepest part between 15 m and 333 m depth, and the less steep section between 333 m and 666 m depth. Below the thermocline, temperatures decrease from ~9°C to bottom water temperatures of ~6°C. Thus, the water column under 560 ppm of CO_2 is similar in structure with the 1120 ppm of CO_2 simulation but shifted towards cooler temperatures by 3°C, almost throughout all depths.

5.4   Discussion

5.4.1 Investigating disequilibrium effects and depth migrations

Although all the species under this study were assigned a specific depth habitat, there were overlaps in depth habitats between the established ecological groups (see Section 5.3.1; Fig.5.3). This may arise from biases brought about by the somehow strict ecological group assignment, whereby the species within a genus may have actually changed their depth habitat throughout their lifecycle or specific species may have had a different depth habitat than the rest of the species from the same genus. Moreover, disequilibrium effects such as vital effects and gametogenesis-induced depth migration can also play a major role in deviating the original foraminiferal $\delta^{18}O$ and $\delta^{13}C$ signatures from the seawater values. It is therefore important to consider all these possible biases in order to better constrain the palaeoecology of the water column as well as its reconstructed ocean temperatures.

5.4.1.1   Mixed layer dwellers
The palaeoecology and temperatures inferred from the mixed layer dwellers of this study were derived from size fractions outside of the ideal Birch range, precisely from 63-125

µm and 125-250 µm. According to Birch et al. (2013), test size smaller than 212-355 µm can be significantly affected by metabolic fractionation effects, whereby the higher metabolic rates of smaller adults or juveniles incorporate a higher dose of metabolic CO_2, which is highly enriched in ^{12}C as a result of respiration processes. This effect can shift the foraminiferal $\delta^{13}C$ signature from equilibrium with seawater $\delta^{13}C$, towards more negative values by as much as 0.30-0.50‰ according to Bornemann and Norris (2007), and by up to 0.20-2‰ as suggested by John et al. (2013). In contrast, with increasing test size, the metabolic rate of the foraminifer decreases leading to an improved exchange of carbon with ambient seawater (Berger et al., 1978; Wefer and Berger, 1991; Ortiz et al., 1996; Spero et al., 1997; Schmidt et al., 2008; Pearson and Wade, 2009).

It would be logical to think that if higher metabolic rates lead to a higher uptake of metabolic CO_2 hence ^{12}C, then the same should apply to a higher uptake of ^{16}O. However, up to now, no evidence has been found for this hypothesis regarding $\delta^{18}O$, so one can assume that the metabolic fractionation effect does not apply to $\delta^{18}O$, or at least not significantly enough to cause major disequilibrium effects, unlike for $\delta^{13}C$. In fact, when looking at the $\delta^{18}O$ values, they do not deviate largely from the $\delta^{18}O$ of upper thermocline dwellers which were derived from size fractions within the Birch range, thus palaeotemperature reconstructions from the mixed layer dwellers from this study can be considered valid. There is indeed a trend towards higher $\delta^{18}O$ values from 63-125 µm to 125-250 µm size fractions for both *Pseudohastigerina naguewichiensis* and *Chiloguembelina cubensis* and a very slight, almost negligible, increase for *Pseudohastigerina micra*. However, this trend is defined by less than 0.25‰, so even if the $\delta^{18}O$ was to be affected by metabolic rates which are higher in the smallest individuals, this would only be translated to less than 1°C.

In contrast, when considering the carbon isotopes, all the species displayed a clear enrichment in $\delta^{13}C$ with increasing size fraction, from 0.5‰ to 1‰. Normally, one would expect the $\delta^{13}C$ to be higher than species living below the mixed layer, as a result of the photosynthetic processes occurring in the mixed layer which preferentially utilise ^{12}C, even though the genera *Pseudohastigerina* and *Chiloguembelina* are considered to be asymbiotic so their $\delta^{13}C$ signature would be more depleted with respect to the mixed layer symbiotic species (Aze et al., 2011). In the case of the mixed layers of this study, as the size fractions used were outside of the Birch range, the $\delta^{13}C$ enrichment of ~1‰ relative to the $\delta^{13}C$ of the upper thermocline dwellers can be justified by the metabolic fractionation effect, as it is contained within the range suggested by previous studies and mentioned earlier (Bornemann and Norris, 2007; John et al., 2013). Moreover, various studies have found *Pseudohastigerina micra* to register strongly depleted $\delta^{13}C$ values

that suggest a carbon metabolism different from other surface dwellers (Poore and Matthews, 1984; Boersma et al., 1987; Pearson et al., 2001), which would further explain this strong δ^{13}C depletion relative to deeper habitats. In addition to this, the temperature difference between the lower δ^{18}O of the upper thermocline and the mixed layer dwellers is less than 0.25‰ which corresponds to less than 1°C, therefore it may also be that the asymbiotic mixed layer dwellers, perhaps slightly stressed by the higher temperatures of the mixed layer (Si and Aubry, 2018), migrated downwards in the lower part of the mixed layer, thus approaching δ^{18}O and δ^{13}C values similar to the upper thermocline dwellers. The lowest δ^{18}O values were retrieved from *Chiloguembelina cubensis* which is in line with the results of Poore and Matthews (1984), even though Zachos et al. (1992) found the δ^{13}C to be relatively enriched for this species rather than depleted like this study found. Finally, both *Pseudohastigerina micra* and *Chiloguembelina cubensis* display a δ^{18}O enrichment with increasing size fraction, suggesting a downward migration throughout the water column during gametogenesis and the resultant addition of a gametogenic crust on top of their original tests.

5.4.1.2   Upper thermocline dwellers

The genus *Hantkenina* registered the lowest δ^{18}O values among all the thermocline dwellers. In addition to this, even if most of the hantkeninids registered δ^{18}O values similar to the other upper thermocline dwellers that is within the range -3.80‰ and -4.4‰, the δ^{18}O of *Hantkenina primitiva* and *Hantkenina nanggulanensis* from the 250-355 µm size fraction almost overlapped the δ^{18}O of the mixed layer dwellers. Different studies have indeed suggested a mixed layer habitat for specific *Hantkenina* spp. in the late Eocene (Poore and Matthews, 1984; Boersma et al., 1987; Coxall et al., 2000; Pearson et al., 2001; Wade and Kroon, 2002; Coxall and Pearson, 2006) as they were characterised by negative δ^{18}O and positive δ^{13}C values relative to the rest of the assemblage, despite still possessing a lower δ^{13}C signature than symbiotic species (Aze et al., 2011). This individual preference in depth habitat between species of the same genus is well represented by the species of this study too. In fact, *Hantkenina nanggulanensis* has been categorised as a mixed layer dweller before (Coxall et al., 2000; Coxall and Pearson, 2006), and *Hantkenina primitiva* as a thermocline dweller (Aze et al., 2011). However, *Hantkenina primitiva* also registered among the lowest δ^{18}O values in this study, specifically at 250-355 µm size fraction, therefore its depth habitat preference may also be dictated by its test size so that during its mid-life cycle it may have migrated upwards and then downwards again for reproduction at the end of its lifecycle.

Only one data point was available for both *Globigerina officinalis* and *Paragloborotalia nana*, therefore it was not possible to investigate their stable isotope signatures against size fraction (see Fig. 5.3). Both generally fall within the $\delta^{18}O$ of most upper thermocline dwellers, with *Globigerina officinalis* positioned in the lowest part of this range, perhaps as a consequence of living very close to the lower base of the mixed layer, as also found by Pearson et al. (2001) and Spezzaferri et al. (2018). Conversely, *Paragloborotalia nana* registered a rather intermediate value within the $\delta^{18}O$ range of ecology group 2, which may act as a compromise depth habitat after the contrasting views of studies that suggest different calcification depth preferences for this species, namely an upper thermocline habitat (Wade et al., 2007; Pearson and Wade, 2009; Matsui et al., 2016), a deeper thermocline habitat (Douglas and Savin, 1978; Poore and Matthews, 1984), or even a mixed layer habitat (Leckie et al., 2018). Interestingly, both genera registered among the lowest $\delta^{13}C$ values of the ecological group 2, which may have been caused by the fact that they were both retrieved from a smaller size fraction outside of the Birch range, therefore metabolic fractionation effects may have contributed to the depleted $\delta^{13}C$ signatures.

The genus from ecological group 2 with the largest range of $\delta^{18}O$ is *Turborotalia*. Most of the values fell within the $\delta^{18}O$ cloud where most upper thermocline dwellers were found, but two data points registered significantly higher $\delta^{18}O$ values of -2.50‰ and -2‰ and were both derived from *Turborotalia cocoaensis*. In fact, while *Turborotalia increbescens* and *Turborotalia ampliapertura* were found to occupy shallow-water habitats in the late Eocene by different studies (Poore and Matthews, 1984; Boersma et al., 1987; Coxall et al., 2000; Pearson et al., 2006), *Turborotalia cocoaensis* has recorded higher $\delta^{18}O$ signatures relative to *Turborotalia ampliapertura* in other studies as well (Pearson et al., 2001; Wade and Kroon, 2002; Pearson et al., 2006), therefore suggesting, on average, a deeper depth habitat. Moreover, the offset in $\delta^{18}O$ of ~0.50‰ between *Turborotalia ampliapertura* and *Pseudohastigerina micra* was also found by Wade and Pearson (2008), further confirming the successful separation of the glassy, original test from the infill for the analysed specimens. Moreover, *Turborotalia ampliapertura* and *Turborotalia cocoaensis* as well as *Hantkenina nanggulanensis* display a $\delta^{18}O$ enrichment with increasing size fraction, suggesting a downward depth migration during their lifecycle and a component of gametogenic calcite added at depth, which is in agreement with the findings of Poore and Matthews (1984) and Wade and Pearson (2008).

In conclusion, as the $\delta^{18}O$ values of the upper thermocline dwellers are very similar to the $\delta^{18}O$ of the mixed layer dwellers, it may be that *Turborotalia* spp. and *Hantkenina*

spp., which were regarded as thermocline dwellers throughout the Eocene, may have shifted towards shallower depth habitats during the late Eocene, as also shown by the data in Coxall et al. (2000).

5.4.1.3   Lower thermocline dwellers

Catapsydrax unicavus registered a significantly higher $\delta^{18}O$ signature relative to the other species of ecological group 3, indicating a sub-thermocline calcification depth rather than a lower thermocline habitat. This clear distinction in depth habitat between *Catapsydrax unicavus* and the lower thermocline dwellers is also found in other species of the genus as they often register the highest $\delta^{18}O$ signatures of an assemblage (Poore and Matthews, 1984; Arthur et al., 1989; van Eijden and Ganssen, 1995; Sexton et al., 2006b; Wade et al., 2007; Spezzaferri and Pearson, 2009). The highest $\delta^{18}O$ value for *Catapsydrax unicavus* was actually registered by the ≥355 μm size fraction hence outside of the Birch range, suggesting a possible addition of gametogenic calcite during the later stages of the lifecycle. This feature was also identified in the highest $\delta^{18}O$ value of subbotinids, which was indeed derived from the ≥355 μm test size of *Subbotina corpulenta*, and it is the closest $\delta^{18}O$ signature to *Catapsydrax unicavus* among the lower thermocline dwellers. In fact, *Subbotina corpulenta* has been often mistaken for *Catapsydrax unicavus* as it is quite a rare species (Wade et al., 2018) and it was characterised by the highest $\delta^{18}O$ among planktonic species (Poore and Matthews, 1984; Boersma et al., 1987). Overall, despite other studies assigning a mixed layer habitat to late Eocene subbotinids owing to their depleted $\delta^{18}O$ values of ~-3‰ (Douglas and Savin, 1978; Boersma et al., 1987) the $\delta^{18}O$ signature of most subbotinids in this study suggests their depth habitat to be indeed in the lower thermocline as they were mostly found just below the main $\delta^{18}O$ cloud of the upper thermocline dwellers, and their $\delta^{18}O$ signature differs from the mixed layer dwellers by almost 1‰.

Together with the dentoglobigerinids, the subbotinids cover a large range of $\delta^{18}O$, suggesting a migration throughout their lifecycle rather than just during gametogenesis. In fact, *Dentoglobigerina* spp. were found both in the cloud of the upper thermocline dwellers and just below it with most subbotinids. The highest $\delta^{18}O$ value for *Dentoglobigerina* was derived from the ≥355 μm test size of *Dentoglobigerina tripartita*, suggesting the influence of a gametogenic crust on the foraminiferal $\delta^{18}O$, which is a trend that was found by Wade and Pearson (2008) in Tanzania too, when considering the biggest size fractions of dentoglobigerinids. It may be that both subbotinids and dentoglobigerinids adapted to a broader range of temperatures during the late Eocene, allowing them to migrate upwards and downwards in the water column, while still

preferring a thermocline habitat as also suggested by other proxies applied to dentoglobigerinids, such as δ^{11}B (Pearson and Palmer, 1999), and Mg/Ca (Wade et al., 2012). However, it cannot be excluded that genera may have gradually settled in the shallower depth habitats hence changed their palaeoecology through the Oligocene and Miocene, as proposed by Douglas and Savin (1978), van Eijden and Gassen (1995), and Wade et al. (2007), as they found relative depleted δ^{18}O values for the dentoglobigerinids.

5.4.2 Late Eocene temperatures from Java vs modern temperatures of the IPWP

The sea surface temperatures derived from the δ^{18}O of *Pseudohastigerina* spp. and *Chiloguembelina* spp. ranged between 36.3°C and 37°C which is a quite a narrow range suggesting almost identical depth habitats for *Pseudohastigerina micra*, *Pseudohastigerina naguewichiensis*, and *Chiloguembelina cubensis*. All these small species may have bloomed in the surface mixed layer when food was available. Hollstein et al. (2017) measured modern sea surface as well as water column temperatures around the area of Papua New Guinea. Although located at different longitudes, Java and PNG are situated at similar latitudes, therefore we can assume a valid comparison between modern PNG and our site from Java. The results from this study indicate that SST were up to 7°C warmer than the modern SST range of 27-30°C found by Hollstein et al. (2017). It an interesting finding as PNG is currently situated closer to the core of the IPWP compared to Java, which makes this comparison even more significant. The palaeoclimate reconstructions did simulate Java to be located right in the core of the late Eocene IPWP (see Section 5.3.2, Fig. 5.7), further confirming the validity between the modern data of Hollstein et al. (2017) and our study. However, it is important to consider that the model outputs locate late Eocene Java at 0.54°N, while modern PNG is located at 6°N, therefore late Eocene Java, being much closer to the equator, would have been exposed to a higher insolation constant than modern PNG, contributing to the extremely warm temperatures found in our record. Evans et al. (2018) calculated SSTs from middle Eocene Java (~39 Ma) using the clumped isotope temperature proxy (Δ_{47}), and their highest values reached 36.3°C, suggesting that the IPWP might have been warmer in the late Eocene. This possible trend of a progressively warmer IPWP throughout the Eocene is also in line with the clumped isotope results from the early Eocene (~54.9 Ma) Kutch formation in India, which registered peak SSTs of ~35.1°C within 5° of the equator at the time thus highly likely situated in the core of the early Eocene IPWP. The waters around early Eocene India may have actually been cooler than the ocean around middle

Eocene Java as the Kutch formation is located on the western coast of India compared to the West Pacific position of middle Eocene Java, suggesting a position slightly outside or only slightly bathed by the IPWP. Thus, early Eocene equatorial SSTs may have actually been higher since as shown in Chapter 4 even SSTs 29.39°S reached ~35°C.

When shifting away from the surface and investigating the water column, the $\delta^{18}O$ signatures derived from the upper and lower thermocline dwellers registered temperatures ranging between 35°C and ~20°C. In the modern water column of the IPWP, Hollstein et al. (2017) found a thermocline of the IPWP reaching temperatures down to 10°C and extending over a depth range between 100 m and 200 m, therefore covering a larger temperature range than the late Eocene thermocline. This feature of a less steep thermocline in the Eocene relative today was also found in the early Eocene water column structure (see Chapter 4) and in the Eocene waters of Tanzania (John et al., 2013).

Finally, at the time of the geochemical analysis carried out for this study, no benthic foraminifera were present in the sample. However, Coxall et al. (*in preparation*) produced one data point from benthic foraminifer *Cibicidoides havanensis* prior to receiving the samples of this study, and it registered a $\delta^{18}O$ value of -1.21‰ and a $\delta^{13}C$ value of -1.70‰. *Cibicidoides havanensis* is an abyssal, epifaunal species and has been used in different studies involving stable isotopes and the Eocene/Oligocene transition (Coxall and Pearson, 2007). After applying an ice-volume correction of -0.75‰ and a latitudinal correction of 0.28‰, converting the $\delta^{18}O$ to temperature with the Kim and O'Neil (1997) palaeotemperature equation yielded bottom water temperatures of 18.3°C. This value is about ~2.5°C lower than the highest $\delta^{18}O$-inferred temperatures from the planktonic foraminifera, that is *Catapsydrax unicavus*, which yielded a sub-thermocline temperature of just below 21°C. No comparison could be made with $\delta^{18}O$-inferred BWT from the modern IPWP as Hollstein et al. (2017) focused on investigating planktonic foraminifera, but it is clear that there was a small difference between the sub-thermocline dwellers and the benthic foraminifera, in the same way as between the upper thermocline and mixed layer dwellers (~0.50‰, corresponding to ~2°C). This reduced temperature gradient between the different depth habitats may be attributed to the persistent warming of the Eocene which may have likely caused heat diffusion into the deeper layers of the water column below the mixed layer, and consequently contributing to a more uniform water column characterised by a less step thermocline, as also found by Makarova et al. (2017) for the PETM, as well as Huber and Caballero (2011).

In conclusion, the extreme temperatures found in the mixed layer from the $\delta^{18}O$ of ecological group 1 strengthens the hypothesis postulated in Chapter 4 (see Section 4.4.4.1), whereby foraminifera, under prolonged periods of extreme warmth, may have indeed adapted to the new challenging climatic conditions and their thermal tolerance was higher than previously found, that is clearly higher than 33°C. It may be likely that the mixed layer dwellers may have migrated downward (Makarova et al., 2017; Si and Aubry, 2018) to avoid any potential heat-related stress, but they still registered temperatures far beyond the previously proposed temperature limit and seem to have thrived considering both their high abundance and diversity.

5.4.3 Model-data comparison under two different CO_2 scenarios

The water column around the waters of late Eocene Java was modelled on a "teuya" climate model experiment, under both atmospheric CO_2 concentrations of 560 ppm (2 x pre-industrial levels), and 1120 ppm (4 x CO_2 pre-industrial levels). Under a 560 ppm CO_2 scenario, the model calculated SSTs of ~32°C, which is almost 5°C cooler than the measured SSTs from the foraminiferal $\delta^{18}O$ of ~37°C. The $\delta^{18}O$ from the thermocline dwellers suggested a thermocline temperature range between 35°C and 20°C, while the modelled water column suggests a thermocline down to a depth of ~666 meters that reached temperatures as low as 9°C. Lastly, the BWTs of the models displayed temperatures of around 6°C, while the $\delta^{18}O$ of benthic foraminifera from Coxall et al. (*in preparation*) suggested a BWT of 18.3°C, suggesting a temperature underestimation by the model of ~12°C.

In contrast, under a 1120 ppm CO_2 scenario, the modelled SSTs reached ~35°C, hence an underestimation of 2°C relative to the late Eocene SSTs reconstructed from the proxies. Furthermore, the modelled thermocline reached a depth of 666 meters with a temperature of ~12.5°C. Below this, the temperature kept decreasing very slightly until BWTs were simulated to measure ~12°C, which represents an underestimation of ~6°C relative to the $\delta^{18}O$-inferred BWT. Thus, the scenario under 1120 ppm seems to best match the geological data at all levels, namely sea surface, thermocline, and seafloor. When comparing these results to the early Eocene model-data comparison (see Chapter 4, Section 4.4.5), there was a modelled temperature underestimation of ~4°C at the surface, of ~7°C at the base of the thermocline, and of 5°C at the seafloor. Thus, under 1120 ppm, the model performed largely better for the late Eocene at the surface, but matched less with the proxy-derived temperatures at the thermocline and seafloor. Even though the ideas related to the model-data mismatch and modelled temperature

underestimations discussed in Chapter 4 (see Section 4.4.5) are also valid for late Eocene Java including a potential underestimation of atmospheric CO_2 concentrations, these findings of a different magnitude in mismatch between the two sites and intervals should be explored. It may be that the SSTs recorded for Java were actually derived from mixed layer dwellers that inhabited the lower part of the mixed layer, as discussed earlier and suggested by the proximity in $\delta^{18}O$ values between the ecological group 1 and ecological group 2. This would have lowered the SST estimates and would have therefore improved the model-data mismatch. At the thermocline and seafloor levels, it may be that the late Eocene may have been underestimated to a greater extent than the early Eocene as a result of enhanced mixing typical of the late Eocene (Scher et al., 2014; Houben et al., 2019) which would propagate the heat from the upper layers into the thermocline and close to the seafloor. Even though the best model-data comparison was derived from a 1120 ppm CO_2 scenario, it is important to evaluate the CO_2 reconstructions that are currently available in the literature in order to reinforce this assertion.

According to the boron isotope proxy ($\delta^{11}B$), atmospheric concentrations of CO_2 reached 1400 ppm in the early Eocene (Anagnostou et al., 2016), decreased by several hundred ppm throughout the Epoch (Pagani et al., 2005), declined even more rapidly at the EOT (Pearson et al., 2009; Pagani et al., 2011; Zhang et al., 2013), and declined by at least a factor of two by the Miocene (Pearson and Palmer, 2000). Alternatively, after collecting $\delta^{11}B$ data from Tanzania, Pearson et al. (2009) proposed that the $pCO2$ may have declined very rapidly from 1500 ppm to 760 ppm during the extended $\delta^{18}O$ shift (hence including both $\delta^{18}O$ steps), increased to ~1150 ppm during the second $\delta^{18}O$ step, and declined again even further to ~625 ppm which would have triggered widespread Antarctic glaciation (DeConto and Pollard, 2003, 2008; Pearson et al., 2009; Pagani et al., 2011). This finding of a relatively rapid decline in pCO_2 was also supported by Bohaty et al. (2012). Conversely, Pearson and Palmer (1999) argued that CO_2 concentrations in the middle Eocene were similar or slightly higher than today, postulating that either the Earth may have indeed been more sensitive to slight changes in pCO_2 or that the global cooling that occurred at the end of the Eocene was primarily driven by other factors, such as the opening of ocean gateways which resulted in an ocean re-organisation. In fact, there are contrasting views on the climate sensitivity back in the Eocene. Anagnostou et al. (2016) found that climate sensitivity was relatively constant throughout the Eocene, while model outputs from Keery et al. (2018) suggested that the climate sensitivity is state dependent such that it is higher in a low CO_2 state owing to the positive feedback mechanism of a reducing albedo effect as vegetation increases up to its maximum value when 1000 ppm of CO_2 are reached. Thus, as a result of all the

above, the climate model experiment of the water column under 1120 ppm of CO_2 was selected to be the most appropriately representative simulation for the late Eocene, also owing to the fact that it better agrees with our geological data. It is true that a 1120 ppm of CO_2 simulation was also used in Chapter 4 for the early Eocene, despite acknowledging that CO_2 levels during the early Eocene may have been significantly higher relative to the late Eocene. However, it may be that either the levels were higher but as of now only 560 ppm and 1120 ppm simulations were available, or that other GHGs may have played a more significant role in the early Eocene compared to the late Eocene. The warmer temperatures may have increased the moisture content of the atmosphere, increasing the concentration of atmospheric water vapour. Moreover, there is a scarce availability of data on the levels of methane (CH_4) during this period and therefore it is unknown how much it may have contributed to the GHG effect, even though CH_4 can rapidly convert into CO_2 once released back into the atmosphere which is a factor that climate models take into account (Alexander Farnsworth, *personal communication*).

5.4.4 Comparison of late Eocene Java with late Eocene Tanzania

Exceptionally preserved planktonic foraminifera from the late Eocene were also found in Tanzania prior to this study (~18°S) (Pearson et al., 2007). Thus, the depth habitats, as well as the sea surface and water column temperature were compared with the results of this study. The data for late Eocene Tanzania were retrieved from the supplementary information of Pearson et al. (2007). The sample called TDP12/20-3 (74-83 cm) was chosen as it was assigned an age of 33.75 Ma and was found just below the extinction of the genus *Hantkenina*, hence representative of the late Eocene Epoch and unaffected by the EOT transition, just like the sample from Java.

Java and Tanzania were located at different latitudes in the late Eocene, but according to the modelled maps (Fig. 5.9), the IPWP bathed the coasts of Java and reached, or almost, the coasts of Tanzania too, making this comparison ideal to understand how the temperatures of the Warm Pool were zonally stretched over such a much larger area than today.

5.4.4.1 Comparison of ocean temperatures and depth habitats between Java and Tanzania

5.4.4.1.1 Depth Habitats

The data for late Eocene Tanzania were retrieved from Pearson et al. (2007, *supplementary information*), and show $\delta^{18}O$, $\delta^{13}C$ as well as reconstructed temperatures from planktonic foraminiferal tests (Fig. 5.9, panel B). The same ecological groups for Java were assigned to the species found in Tanzania, therefore *Pseudohastigerina* was placed in group 1 (mixed layer dwellers), *Hantkenina* and *Turborotalia* in group 2 (upper thermocline dwellers), and lastly *Subbotina* and *Dentoglobigerina* in group 3 (lower thermocline dwellers). Moreover, two genera were found in the Tanzanian record that were absent in the sample from Java, namely *Globoturborotalita* and *Cibrohantkenina* and they were assigned to group 1 and group 2, respectively. After considering the fact that the Tanzanian record is composed of fewer data points, as well as *Catapsydrax unicavus* being absent which is the species that appeared to occupy the deepest depth habitat within group 3 in our assemblage, the record is characterised by a smaller $\delta^{18}O$ range, especially when looking at ecological group 2. Interestingly, the $\delta^{13}C$ for both sites is characterised by a similar change in $\delta^{13}C$ across all the investigated species of ~2‰, even though the mid-point for the $\delta^{13}C$ of Tanzania is found at 0.50‰, while at -0.50‰ for Java. Thus, the water column of Tanzania was more enriched in $\delta^{13}C$, suggesting either a higher productivity or a more efficient biological pump, whereby the ^{12}C-enriched organic matter was transported into the deeper layers of the water column and buried into the sediments. Alternatively, the higher $\delta^{13}C$ value found throughout the Tanzanian water column may reflect the influence of a $\delta^{13}C$-enriched local deep-water mass. *Pseudohastigerina* and *Globoturborotalita* registered among the lowest $\delta^{18}O$ as expected, indicating a shallower water habitat relative to the other species. Moreover, as both genera were only retrieved from the 63-125 μm and 125-212 μm size fractions hence outside the Birch range, they registered more depleted $\delta^{13}C$ values relative to the average of the assemblage, by up to ~1.50‰.

Thus, the metabolic fractionation effect observed in Java was also registered in the mentioned size fractions of the mixed layer dwellers in Tanzania. Regarding ecological group 2, *Turborotalia* spp. display higher $\delta^{18}O$ value at ≥355 μm size fraction at both sites, suggesting addition gametogenic calcite towards the end of their lifecycle, and together with *Cibrohantkenina* and *Hantkenina,* are positioned just below the mixed layer dwellers, suggesting an overlap in depth habitat between ecological group 1 and 2 either caused by a downward migration of the mixed layer dwellers towards the base of this

layer, or an upward migration of the upper thermocline dwellers. Interestingly, ecological group 3 in Tanzania exhibited a slightly different behaviour from Java. The *Dentoglobigerina* spp. do overlap with turborotalids and hantkeninids like in Java (Fig. 5.9, panel A), but display an opposite trend of $\delta^{18}O$ with increasing size fraction, whereby the specimens from the ≥355 μm size fraction actually registered among the lowest $\delta^{18}O$ values of the genus, unlike for Java. Furthermore, it cannot even be suggested that gametogenic calcite may be species dependent in this case, as the species with the highest $\delta^{18}O$ within the Birch range are the ones with the lowest $\delta^{18}O$ at ≥355 μm size fraction. Conversely, in agreement with Java, the highest $\delta^{18}O$ value among the subbotinids was indeed registered by the ≥355 μm size fraction in Tanzania, as well as the lowest $\delta^{13}C$ signature coming from the size fraction below the Birch range, specifically size fraction 125-212 μm.
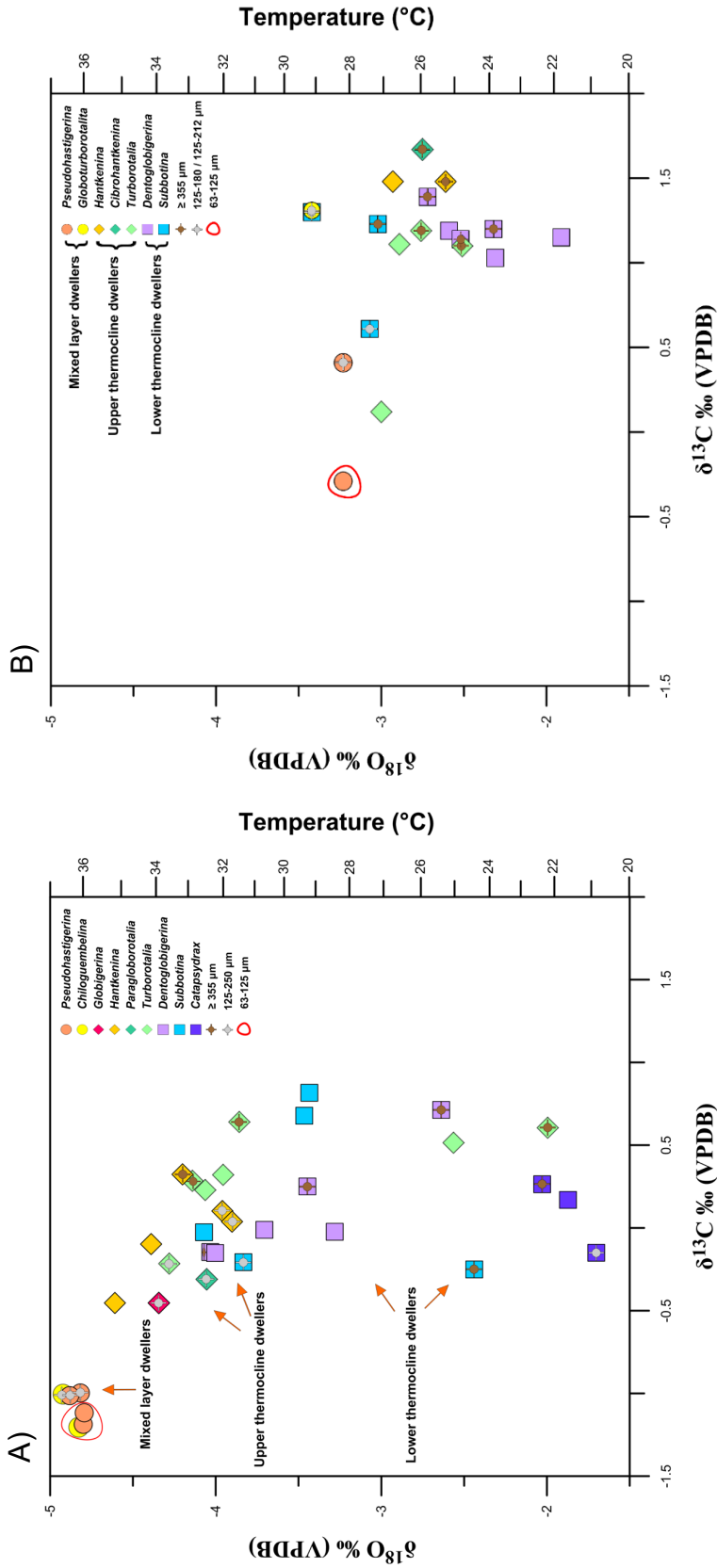
Figure 5.9: Temperature and depth habitat reconstructions of the water column off the coast of southern Java (panel A) and Tanzania (panel B), during the late Eocene (34.3-33.7 Ma), from the geochemical proxies $\delta^{18}O$ and $\delta^{13}C$ which were derived from planktonic (this study) and benthic (Coxall et al., *in preparation*) foraminiferal tests. The different symbols represent the three different ecology groups which reflect different depth habitats: ecology group 1 is composed of mixed layer dwellers (circles); ecology group 2 is upper thermocline dwellers (diamonds); ecology group 3 is lower thermocline dwellers (squares). The different colours represent the different genera (shown in the legend). Each genus may contain different species. The grey cross inside the symbol indicates size fraction 125-250 µm; the brown cross indicates the size fraction ≥355 µm, and lastly, the red polygon indicates size fraction 63-125 µm. The size fractions were highlighted following the criteria by Birch et al. (2013), whereby stable isotopes can be affected by vital effects to a greater extent in size fractions outside of the 212-355 µm range. The $\delta^{18}O$ scale is reserved such that the lower value indicating mixed layer waters are found at the top, while the higher values are at bottom, intercepting with the $\delta^{13}C$ axis. The temperature on the second y-axis were derived from inserting the test $\delta^{18}O$ values into the palaeotemperature equation of Kim and O'Neil (1997). A latitudinal correction of +0.28‰ was applied after Hollis et al. (2019) for Java and of +0.48‰ for Tanzania, as well as an ice-free volume correction of -0.75‰ after Cramer et al. (2011).

Interestingly, the subbotinids in Tanzania exhibited a lower δ^{18}O than the lower thermocline dwellers, and species *Subbotina gortanii* even registered the same δ^{18}O signature as *Globoturborotalita ouachitaensis* hence even lower than *Pseudohastigerina* from the Tanzanian assemblage, suggesting a shallow mixed layer habitat rather than a lower thermocline one. Even though Pearson et al. (2001) recorded this species as a deep dweller in the late Eocene, Douglas and Savin (1978) as well as Boersma et al. (1987) reported relatively depleted δ^{18}O values for *Subbotina gortanii* (previously identified as *Globoquadrina gortanii*) in the late Oligocene tropical Pacific Ocean, suggesting an upward migration and change of depth habitat. This study suggests that, at least in the tropical late Eocene IPWP*, Subbotina gortanii* may have already migrated upward in the water column, perhaps aided by the very warm temperatures it would have been surrounded by which may have helped outcompete less heat-tolerant species.

5.4.4.1.2   Tropical sea surface and water column palaeotemperatures

The temperatures for Tanzania were retrieved from the δ^{18}O of planktonic foraminiferal tests (Fig. 5.9, panel B). An ice-volume correction of -0.75‰ as well as a latitudinal correction of +0.48‰ were applied to the δ^{18}O before converting the values to temperatures with the palaeotemperature equation provided by Kim and O'Neil (1997) (for more information on the conversion of δ^{18}O to tempearature including latitudinal and ice-volume corrections, see Chapter 2 and the Methodology Section in Chapter 4). The SSTs retrieved from late Eocene Tanzania were actually similar to the modern average SSTs of ~29°C (John et al., 2013). While it may be likely that in the early Eocene SSTs were ~2°C warmer than modern as a result of the IPWP bathing the waters just off the coast of Tanzania, and further supported by the modelled palaeogeographies and temperatures (see Chapter 4), the results from late Eocene Tanzania suggest no influence of the IPWP on this site. In fact, the modelled palaeogeographies and temperatures (Fig. 5.7) showed that in the late Eocene both Madagascar and India (merged together as an island at the time) may have acted as a barrier that may have impeded the super warm waters of the IPWP from reaching the waters just off the coast of Tanzania. The thermocline in late Eocene Tanzania was characterised by a narrower range of temperatures between ~27.8°C and ~22°C with respect to Java and consisted of a 12°C change in temperature. Both thermoclines reached down to at least 20°C with the Tanzanian one perhaps reaching even further down if the lower thermocline dweller *Catapsydrax unicavus* had been analysed. Thus, not only do these data confirm that there was indeed a Warm Pool back in the late Eocene reaching at least ~37°C where, up to now, has not be found anywhere in the late Eocene tropics, but there also still existed a zonal temperature gradient of about ~7°C between Tanzania and Java, which

is ~4°C larger than the modern gradient between the two sites. The IPWP may have well been more contained zonally during the late Eocene than in the early Eocene as islands and future peninsulas were moving northwards hence acting as a barrier for the Warm Pool waters to reach any further East in the late Eocene than it may have been possible during the early Eocene.

5.4.4.2   The depth habitats compared to the modelled water column

A modelled water column was simulated for the late Eocene of both Tanzania and Java, using the teuya climate experiment at 1120 ppm of CO_2 (Fig. 5.10). The modelled SSTs for Tanzania reached ~31.6°C, therefore ~1°C warmer than the foraminiferal data. The modelled water column for Tanzania is characterised by a similar thermocline to the one modelled for Java, ranging between 31.6°C and 12.5°C, and extending down to a water depth of ~625 meters. This suggests that the models were able to match the SSTs of both sites to a greater extent than for the early Eocene (see Chapter 4), and only underestimated SSTs by 1.5°C for Java, while they overestimated SSTs by ~1°C for Tanzania. For both sites, the depth habitat of the mixed layer dwellers overlaps the depth habitat of the upper thermocline dwellers, suggesting either an upward migration of ecological group 2, or a downward migration of ecological group 1, or a combination of both. The lower thermocline dwellers in Tanzania lived at depths both below and above the upper thermocline dwellers, perhaps gradually changing depth habitat as temperatures decreased towards the EOT. Moreover, they also overlapped the depth habitat of the mixed layer dwellers, suggesting an occupation of all three depth habitats, namely mixed layer, and upper and lower thermocline. In contrast, the depth habitat of the lower thermocline dwellers in Java is more consistent with its definition, even though there also is an overlap between ecological group 2 and group 3, whereby a similar upward migration for dentoglobigerinids and subbotinids may have happened at both sites. Lastly, benthic foraminiferal data from the genus *Cibicidoides* were only available for Java and retrieved from Coxall et al. (*in preparation*). The temperature derived from *Cibicidoides havanensis* positioned the species at a water depth of ~300 meters, and well below the overlying three depth habitats, by ~3°C. However, the modelled water column suggests a seafloor temperature of ~12.5°C, rather than ~18.3°C, indicating an underestimation of BWTs by the model of ~6.5°C.

Thus, the model was unable to simulate a relatively uniform and less stratified water column whereby the proxy results suggest there is only a difference of ~18°C between the mixed layer dwellers and the benthic foraminifera, unlike the ~22.5°C suggested by the model. The smaller difference suggested by the proxies may be due to the nature of

the Warm Pool, whereby the high temperatures of the upper layer may have been transferred more efficiently into the lower layers of the water column, and possibly reaching the seafloor which would have been as warm as 18°C.
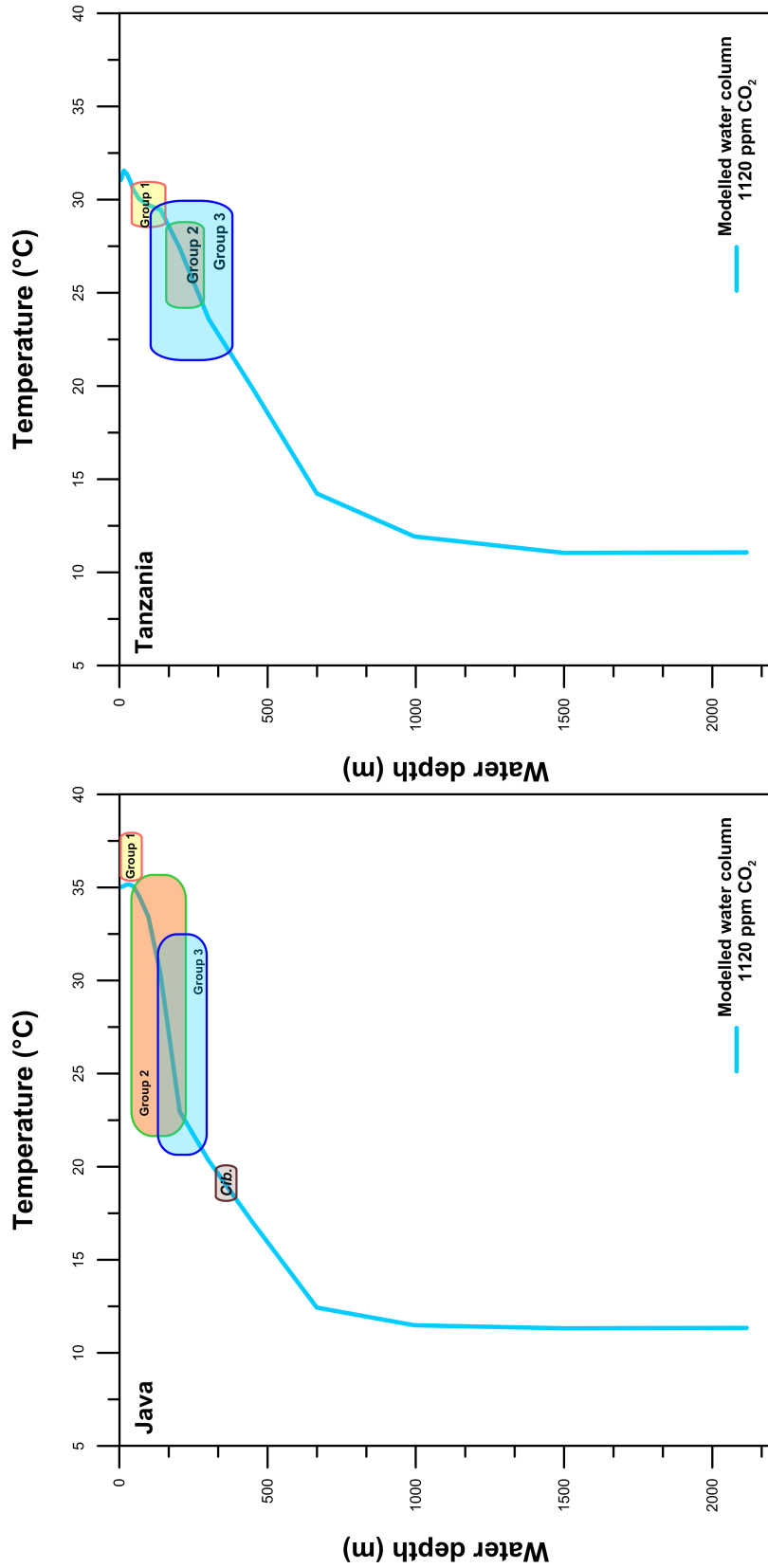
Figure 5.10: Modelled plot of the water column structure and temperatures off the coast of late Eocene Tanzania (right-hand side) and Java (left hand-side). The experiment used was called teuya, at 4 x CO_2 atmospheric levels (1120 ppm), from the Priabonian Stage. The depth habitats of the mixed layer dwellers, Ecological Group 1 (yellow box, with tropical pink border); upper thermocline dwellers, Ecological group 2 (orange box, with green border); lower thermocline dwellers, Ecological Group 3 (sky blue box); and benthics (brown box) were superimposed on the modelled line by matching the proxy-generated temperatures with the model-generated water column temperatures. The two water columns were compared as they were both derived from tropical, well-preserved, original foraminiferal tests.

5.4.5 Interpretation of the global carbon cycle during the late Eocene

The gradual opening of the Tasman Gateway and Drake Passage in the middle to late Eocene (Goldner et al., 2014) led to the enhanced circulation and cooling of the Southern Ocean, which was probably the dominant deep-water source from at least the late Eocene (Wright and Miller, 1993; Coxall and Pearson, 2007; Huck et al., 2017). This in turn increased ocean mixing, surface ocean productivity, leading to a drawdown of atmospheric CO_2 and accelerated global cooling (Zachos and Kump, 2005; Scher and Martin, 2006; Coxall and Pearson, 2007; Egan et al., 2013; Goldner et al., 2014). The increased nutrient leakage (with waters rich in ^{13}C) from the Southern Ocean reached the lower latitudes (Egan et al., 2013) similar to the modern setting (Sarmiento et al., 2004; Jones et al., 2019), and would have only become part of a substantial nutrient supply to the tropical oceans at the very start of the EOT (McKay et al., 2016).

However, in our record which was derived just before the EOT, the $\delta^{13}C$ is depleted throughout the water column relative to records from the early and middle Eocene (John et al., 2013) and is fairly uniform throughout the water column, contrasting with the previous point of nutrient waters reaching the tropics at the start of the EOT. This global $\delta^{13}C$ depletion just before the EOT is noticeable in other records as well including at mid- and high latitudes (Coxall et al., 2005; Coxall and Pearson, 2007; McKay et al., 2016), further suggesting this $\delta^{13}C$ depletion was a global signature rather than a tropical one. In fact, the $\delta^{13}C$ record has been found to respond more to global changes in the carbon system such as ocean circulation and upwelling intensity changes (Cramer et al., 2009; Pusz et al., 2011). Boersma and Premoli Silva, (1989) as well as Pearson et al. (2001) also found a uniform $\delta^{13}C$ throughout the water column in their Eocene foraminiferal assemblages.

Usually, a large near-surface to bottom carbon isotope contrast indicates high oceanic productivity, while a reduced surface to bottom carbon isotopic has been attributed to a decrease in oceanic primary productivity (Boersma and Premoli Silva, 1986, 1989). As nutrient supply to the tropical oceans increased in the late Eocene, this would have led to more eutrophic waters. Planktonic foraminifera commonly thrive in oligotrophic waters, therefore this increase in oceanic productivity would have led to a diminished, tropical plankton community. Jones et al. (2019) found the nannofossil community to decrease in diversity as a consequence of the eutrophication of the IPWP surface waters, as warm water, oligotrophic species went extinct.

However, the IPWP in our record shows a highly diverse plankton assemblage, especially when considering the extremely warm temperature, which further suggests the foraminifera were not affected by neither thermal stresses nor by the globally enhanced nutrient leakage from the Southern Ocean to the low latitudes. It may be that, as the IPWP may have acted as an isolated system, characterised by its own, strong thermal and nutricline gradients, as well as by a thick, super warm, mixed layer, had less interaction with the surrounding waters than the rest of the oceans. Additionally, the mixed layer dwellers may have been able to adopt a migration strategy and migrate down to the subsurface waters, as also shown by the overlap in depth habitat between the mixed layer and upper thermocline dwellers.

The uniform $\delta^{13}C$ gradient throughout the water column may have also been attributed to a shallower remineralisation depth caused by the warm temperatures (John et al., 2013, 2014, more details on this principle and the Q_{10} temperature coefficient are found in Chapter 4). John et al. (2013) argued that a shallower $\delta^{13}C$ minimum may be caused by an enhanced stratification relating to warmer climate. Moreover, temperature-induced faster rates of remineralisation of sinking organic matter could also explain the shallower presence of a depleted $\delta^{13}C$, which extended down to below the thermocline as registered by both the lower thermocline and benthic foraminifera. This process would have in turn caused a shallowing of the Oxygen Minimum Zone (OMZ). The depth of the OMZ is uncertain but foraminiferal genera such as *Chiloguembelina* and *Pseudohastigerina* were able to live in oxygen-deprived waters (Boersma et al., 1979; Resig and Kroopnick, 1983; Boersma and Premoli Silva, 1989). The depleted $\delta^{13}C$ signature of both the upper and lower thermocline dwellers may be explained by a shallower and faster remineralisation of ^{12}C in the water column, as well as the overlap in $\delta^{18}O$ between the two ecological groups, suggesting a similar depth habitat as the lower thermocline dwellers may have migrated upwards towards more oxygenated water layers. The organic matter remineralisation would have continued down in the deeper layers of the water column, reaching the seafloor whereby the benthic foraminifer *Cibicidoides havanensis* registered slightly more negative $\delta^{13}C$ values relative to the planktonic foraminifera.

These adaptative strategies caused by the eutrophication of the waters and reflected in depth migration, as well as a thriving plankton community despite the high temperatures may strengthen the hypothesis of Jones et al. (2018), whereby progressive eutrophication had a larger impact on the plankton communities than the gradual cooling of the oceans.

5.4.6 The late Eocene and early Oligocene planktonic foraminiferal $\delta^{18}O$ compilation: a comparison

The $\delta^{18}O$-reconstructed temperatures showed and emphasized how many recrystallised foraminiferal samples are available for the late Eocene and early Oligocene with respect to the glassy material that was only found in the past two decades including the Java material from this study, which was added to the results (Fig. 5.11). All the sites shown in the results and recorded in the databases (Appendix 6 for the late Eocene, and Appendix 7 for the early Oligocene) are IODP and DSDP sites except for site E-67-128 which was collected from Eureka (Shell) borehole expedition. The glassy foraminiferal shells were seldom and were found in Brown's Creek (BC, southern Victoria, Australia), Glen Aire (GA, southern Victoria, Australia); Tanzania (TDP Site 12; PP98-L11; and NAM99-01), Saint Stephens Quarry (SSQ, Alabama), Cocoa Sands Formation (CS, Alabama), and the site of this study, Java (NKK1 borehole) for the late Eocene, while for the early Oligocene they were found in Java (NKK1 borehole) (data from Coxall et al., *in preparation*), Glen Aire (southern Victoria, Australia), Saint Stephens Quarry (SSQ, Alabama). The recrystallised material, regardless of the palaeolatitude, registered consistently colder temperatures with respect to the glassy material as a result of recrystallisation whereby the $\delta^{18}O$ foraminiferal shell incorporated a fraction of the ^{18}O-enriched $\delta^{18}O_{seawater}$ when in contact with the deeper, colder waters. The recrystallised $\delta^{18}O$ from the low-latitude sites was lower than at higher latitudes. This may be a result of different processes, including the $\delta^{18}O$ being affected by both recrystallised $\delta^{18}O$ and the original lower $\delta^{18}O$ signal typical of warmer waters, as well as bottom water temperatures being warmer at lower latitudes hence carrying a lower $\delta^{18}O$ signal than the BWTs at higher latitudes. In fact, for some sites, such as 690C, 689b,d, and U1411, the original foraminiferal depth habitat differentiation is still visible and represented by a progressive decrease in temperature from the mixed layer dwellers, to the upper thermocline and lastly lower thermocline dwellers, suggesting that part of the original $\delta^{18}O$ from the foraminiferal tests was preserved.
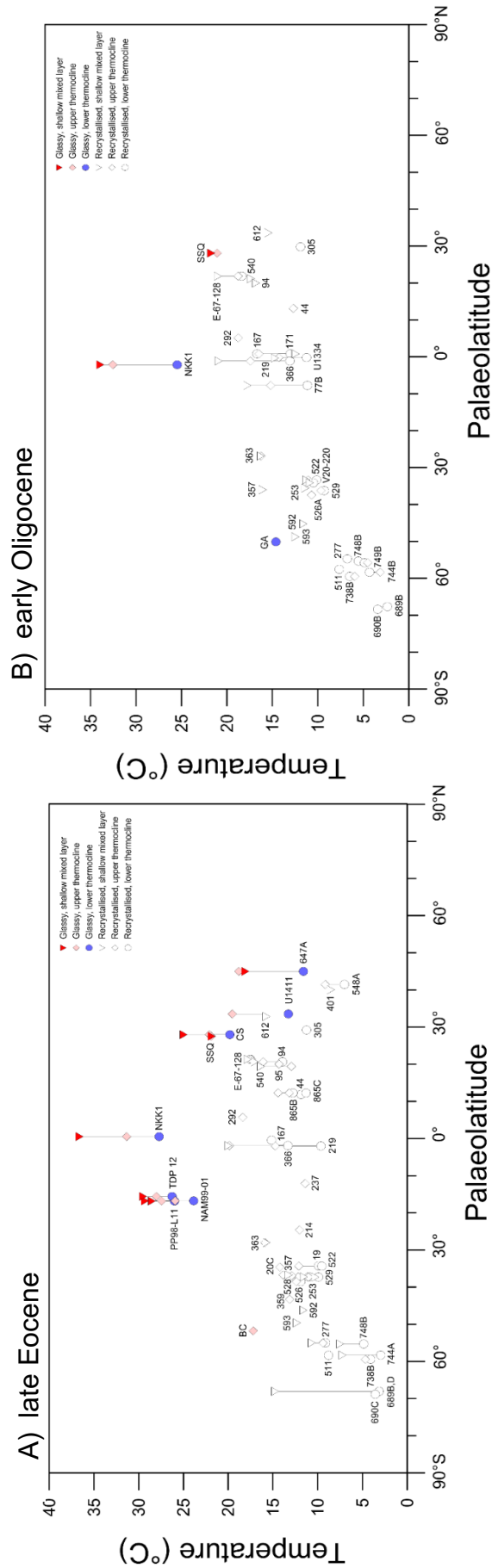
Figure 5.11: Compilation of sea surface and water column temperatures derived from the $\delta^{18}O$ of planktonic foraminifera of the late Eocene (panel A), and early Oligocene (panel B), as a function of palaeolatitude. The colour-filled symbols represent the $\delta^{18}O$ signatures retrieved from well-preserved foraminiferal tests, while the empty symbols represent the $\delta^{18}O$ signatures derived from recrystallised foraminifera which can further bias the true signal of seawater $\delta^{18}O$. The planktonic foraminifera were divided into three ecological groups according to the depth habitat they occupied: ecological group 1 is composed of the mixed layer dwellers (reversed triangles), ecological group 2 is composed of the upper thermocline dwellers (diamonds); and ecological group 3 is composed of the lower thermocline dwellers (circles). All the sites shown on the graph are IODP and DSDP sites, except for site E-67-128, which comes from Eureka (Shell) borehole expedition. Name abbreviations for some of the sites: BC= Brown's Creek, southern Victoria, Australia; GA= Glen Aire (Clays), southern Victoria, Australia; SSQ= St. Stephens Quarry, Alabama; CS= Cocoa Sands Formation, Alabama; NKK-1= borehole, Java. The data for the late Eocene of NKK1 were obtained from this study, while the data for the early Oligocene of NKK1 were taken from Coxall et al. (2015). Each $\delta^{18}O$ value was converted to temperature using the palaeotemperature equation of Kim and O'Neil (1997). A latitudinal correction from Hollis et al. (2019) was applied, as well as an ice-volume correction of -0.75‰ for the late Eocene and -0.25 ‰ for the early Oligocene, as suggested by Cramer et al (2011). The $\delta^{18}O$ retrieved from recrystallised foraminiferal tests registered much colder temperatures than the $\delta^{18}O$ derived from the glassy foraminiferal tests, reflecting the influence of deep waters on biasing the temperature towards colder values.

5.4.6.1 δ¹⁸O-reconstructed temperatures of the water column during the late Eocene and early Oligocene

All the sites comprising well-preserved foraminiferal tests registered consistently warmer temperatures relative to the recrystallised sites at the same latitude hence under similar palaeoclimatic conditions. In the late Eocene, this temperature difference was smaller at higher latitudes and corresponded to ~5°C between the lower thermocline dwellers and ~10°C between both the mixed layer dwellers and upper thermocline dwellers. In contrast, at sub-tropical and tropical sites, the difference amounted to ~10°C between the lower thermocline dwellers and peaked at ~15°C between the mixed layer dwellers. Moreover, there is a clear pattern of temperatures becoming gradually warmer with decreasing latitude in the glassy material, unlike for the frosty material whereby there is an up-and-down pattern. The tropical sea surface temperatures peaked at around 37°C (NKK1, this study), and were still as high as 30°C at 16.5°S (Tanzania), and 26°C at ~27.6°N (Alabama, Gulf of Mexico). Conversely, only three sites containing well-preserved planktonic foraminifera were found for the early Oligocene, namely Glen Aire (southern Victoria, Australia), Saint Stephens Quarry (SSQ, Alabama), and Java (NKK1, Coxall et al., *in preparation*). The results show that the sea surface temperatures peaked at ~34°C around Java at 2°S (Fig. 5.11, panel B), and were still as high as 22°C in the Gulf of Mexico at 29°N. Interestingly, for both intervals the temperatures derived from glassy upper thermocline dwellers mostly registered temperatures very similar to the mixed layer dwellers, indeed suggesting either an upward depth habitat migration by the upper thermocline dwellers, or a downward migration of the mixed layer dwellers, or a mixture of the two changes in depth habitat.

5.4.6.2 Ocean temperature changes between the late Eocene and early Oligocene

When looking at the temperature shift from the late Eocene to the early Oligocene at the tropical sites (from glassy material) such as Java (NKK1 borehole, this study for the late Eocene data and Coxall et al., *in preparation* for the early Oligocene data), the sea surface and lower thermocline temperatures decreased by ~3°C and ~2°C respectively, while the upper thermocline temperatures increased by ~2°C. The only other site comprising glassy material and that registered δ¹⁸O values for both the late Eocene and early Oligocene was the Saint Stephens Quarry in the Gulf of Mexico (Wade et al., 2012), whereby SSTs actually stayed the same at ~22°C. Interestingly, when Wade et al. (2012) measured the change in SSTs across the EOT, they found a consistent reduction in SST of ~3-4°C across different proxies, namely δ¹⁸O, Mg/Ca, and TEX$_{86}$. In contrast, our databases recorded no change in background climate between the late Eocene and

early Oligocene, suggesting a return to the initial conditions of the late Eocene following the EOT and EOGM at this subtropical northern site. Moreover, because the same magnitude of reduction in temperature was recorded in $\delta^{18}O$ as well as the other proxies, Wade et al. (2012) agreed with the previous schools of thought that suggest that the first $\delta^{18}O$ increase was mainly driven by a temperature decrease, rather than an expansion of Antarctic ice (Katz et al., 2008; Lear et al., 2008; Pusz et al., 2011). It is important to note, though, that the $\delta^{18}O_{sw}$ values for each site during both the late Eocene and early Oligocene were estimated using the methodology by Hollis et al. (2019) rather than back-calculating $\delta^{18}O_{sw}$ from a multi-proxy approach, the latter being more approximate than the former when estimating what the local $\delta^{18}O_{sw}$ may have been at the time.

5.5   Conclusions

The study reconstructed sea surface and water column temperatures as well as the planktonic foraminiferal palaeoecology of the tropical waters around Java (0.54°N) during the late Eocene (34.3-33.7 Ma), using both geological data and climate model simulations. The $\delta^{18}O$ and $\delta^{13}C$ proxies were used for temperature and depth habitat reconstructions, and they were derived from exceptionally preserved planktonic foraminiferal species known to occupy a diverse range of depth habitats in the water column.

The $\delta^{18}O$-derived sea surface temperatures reached ~37°C around the tropical waters of late Eocene Java, compared to the modern average annual values of 29°C which are found right at the core of the modern IPWP (~6°S). This large difference in temperature suggests that the tropical areas were indeed able to remain extremely warm almost as effectively as higher latitudes during greenhouse climates, unlike previously thought. Moreover, previous studies on thermal stress of living species indicated an upper temperature tolerance limit below 34°C, while we found a diverse and abundant range of species occupying different depths of the water columns above this value. Nonetheless, previously defined foraminiferal depth habitats such as the upper thermocline and the lower thermocline displayed overlaps, as well as the mixed layer and the upper thermocline. It may be that the species, under prolonged periods of extreme warmth, developed downward migration strategies to escape the probably even warmer upper part of the mixed layer, as well as migrating upwards to escape the spreading of the OMZs as a result of temperature-induced faster metabolic rates.

The climate model simulations greatly matched with the geological data, with only an SST underestimation of ~2°C, which is a small error compared to other intervals (see early Eocene, Chapter 4), and considering the fact that climate model generally struggle to simulate high tropical SSTs. It may be that a combination of a potentially less intensified hydrological cycle just before entering an icehouse state, and the choice of a 1120 ppm CO_2 scenario instead of 560 ppm of CO_2, contributed to the improved agreement between geological data and climate models for the late Eocene.

Lastly, a $\delta^{18}O$ compilation from planktonic foraminiferal tests collected all around the world was produced by gathering all the data available from the existing scientific literature and spanning the late Eocene and early Oligocene intervals. Many sites were reassessed on the preservation of the microfossils they contained, which resulted in the realisation of an exceptionally scarce availability of glassy material for palaeoclimatic reconstructions of the late Eocene and early Oligocene. This further emphasises the importance of targeting sites containing hemipelagic clays where glassy foraminifera can be commonly found, as well as shifting the focus to the tropical areas as they represent the heat engine and heat redistribution system of the global climate, as well as surprisingly being able to conserve as much as heat as 37°C and yet host a diverse range of thriving plankton communities.

Chapter 6

Conclusions

Chapter 6

6 Conclusions

6.1 Synthesis

As an excellent window into the global carbon cycle and ocean temperatures during greenhouse climates, the early and late Eocene Epochs were investigated by looking at the tropical areas of the oceans as they have the critical role of redistributing heat around the globe and can be tested against climate models to assess the performance of the latter.

Due to the scarcity of exceptionally preserved foraminiferal microfossils from deep geological times such as the Eocene, a thorough investigation was carried out in the South-East Asian microfossil collection of the Natural History Museum in London where infilled planktonic foraminifera that had been previously collected from Papua New Guinea were selected for geochemical analyses. The original test wall was carefully and successfully separated from the infill as it displayed consistently lower $\delta^{18}O$ values relative to its associated test fragments. This search and experiment highlighted the importance of reviewing old archives and the useful resort to infilled specimens for palaeoclimate reconstructions of geological intervals where it is challenging to find whole well-preserved foraminiferal tests. A similar screening procedure was performed for the late Eocene and early Oligocene from the existing literature, whereby when plotted together with established glassy tests, many previously studied samples proved to have been characterised by recrystallised foraminifera, which can highly alter the $\delta^{18}O$ of the test and result in falsely colder ocean palaeotemperatures. Even though the tropical ocean temperature reconstructions are pivotal to test climate models and understand how the Earth's climate behaves under extreme warmth, we found that fewer than previously assumed samples available are actually suitable for geochemical analyses, further urging targeted fieldwork in those areas.

Early Eocene (E.E) sea surface temperatures around Papua New Guinea peaked at ~35 °C, while bottom water temperatures were as warm as ~18°C. Palaeogeographic reconstructions indicated a palaeolatitude of ~29.39°S for early Eocene Papua New

Guinea, which means that even tropical/sub-tropical areas were ~6°C warmer than the annual average of modern sea surface temperatures in the core of the Indo-Pacific Warm Pool (IPWP), and that the core of the E.E. IPWP may have been several degrees higher. This means that a super Warm Pool may have also existed back in deep climate and such high temperatures partially disagree with previously postulated ideas that the Earth's tropics acted as a thermostat owing to the continuous model-data mismatches present in early Eocene data. In fact, an extensive diversity and abundance across various size fractions of foraminiferal tests was found at such temperatures and occupying different depth habitats, indicating an absence of thermal stress even on the species living in the mixed layer, unlike previously suggested upper temperature limits of >33°C. Nonetheless, it is very likely that during this interval of prolonged warmth, species had also developed adaptation mechanisms via downward depth habitat migration owing to the extra hot SSTs, and upward migration owing to the temperature-induced faster rates of bacterial respiration which would have brought oxygen minimum zones at shallower depths in the water column.

The depth migration as an adaptation technique was visible through overlaps between previously known species-specific depth habitats, and this pattern was also encountered in late Eocene data, whereby tropical sea surface temperatures from Java (palaeolatitude at 0.54°N) reached 37°C but may have been even higher if mixed layer dwellers in our study actually recorded sub-surface temperatures. Here, too, we found a highly diverse foraminiferal assemblage which seemed to perfectly withstand extreme temperatures and the initial eutrophication of the oceans just before the Eocene-Oligocene transition. The IPWP may have indeed been a unique system with its own thermocline and nutricline systems and hence a specialised plankton community that managed to resist the surrounding super warm and extreme climatic changes of the Eocene Epoch.

The model-data comparison greatly matched the tropical late Eocene at Java under 1120 ppm CO_2, indicating this scenario would have been more realistic for the interval than a 560 ppm CO_2 simulation. However, the 1120 ppm simulation underestimated the temperatures and thermocline of our early Eocene data, either suggesting that the CO_2 may have been significantly higher in the early Eocene than in the late Eocene, or that the Earth's climate sensitivity was considerably higher in the early Eocene, perhaps due to the higher moisture content alongside the effects of the PETM-related perturbations in the atmosphere, which would both contribute further to the greenhouse gas effect.

In conclusion, not only were Eocene tropical temperatures significantly higher than today supporting the existence of a deep time IPWP, but also completely different plankton communities inhabited the Eocene waters as they possessed thermal tolerances that are thought to be unbearable by modern species and theoretical biology. Thus, palaeoecology helped us discover the outstanding capacity of marine plankton to adapt to extreme climatic conditions, but the rate of climate change they can withstand is another, associated issue that should be considered in light of the global accelerated warming and the approaching uncertain future of Earth's climate.

6.2   Future Directions

There are currently a multitude of unexplored microfossil archives in museums that would be highly worth re-assessing, especially after our investigation showed valuable material can be found and even if infilled, it can still be assessed geochemically by carefully separating the original test from the infill. This would also help target areas that have not been explored before or have not been re-considered to contain recrystallised foraminifera so that the focus can be shifted to new areas with the potential presence of hemipelagic clays where most exceptionally preserved foraminiferal shells can be found.

In our study, early Eocene Papua New Guinea was simulated to be positioned at 29.39°S, hence likely outside the core of the early Eocene Indo-Pacific Warm Pool, which was the initial target area of this study. Thus, proposing new fieldwork in countries such as India and Philippines may be more suitable for sea surface reconstructions of the Warm Pool. Moreover, South-East Asia is characterised by a highly complex and dynamic geological system, therefore both the tectonic activity history and the sedimentary history of these places should be carefully assessed beforehand to maximise the success of finding exceptionally preserved foraminiferal tests that may reveal the peak SSTs located in the core of the early Eocene Warm Pool.

Lastly, we used the solution ICP-MS approach for trace metal analyses when reconstructing temperature from the Mg/Ca proxy, which means that the different temperatures recorded by the whole foraminiferal test during its lifecycle were averaged out. However, a significant advantage of the Mg/Ca-palaeothermometer over δ^{18}O-derived results is that trace element data may also be obtained by plasma-based analytical techniques including the laser ablation inductively coupled plasma mass spectrometry (LA-ICP-MS), which is faster and enables intra-specimen spatial resolution up to a few tens of microns (Eggins et al., 2003; Barker et al., 2005; Evans and Müller,

2012). This type of analysis allows multiple analysis to be made on a single specimen or within a single test chamber, which can give valuable information on inter- and intra-individual trace element heterogeneity, itself related to factors such as ecological or vital effects (Eggins et al., 2003) which are yet undefined for deep time such as the Eocene Epoch. Moreover, it is possible to derive a trace element depth profile through the foraminiferal test wall which can be used to detect and exclude zones of both external and internal contamination caused by diagenetic coatings (oxide coatings and oxy-hydroxides), mineralisation and presence of detrital sediment (Eggins et al., 2003; Creech et al., 2010).

6.3   Concluding remarks

This study demonstrates that the temperatures of the Indo-Pacific Warm Pool, which is currently the warmest sea surface regions in the World (~28-30°C), are not controlled by an absolute thermostat-like system, as they reached 37°C under higher CO_2 concentrations during the greenhouse climates of the geological past such as the Eocene (~66-33.7 Ma). Initially, it was thought that the tropics were able to avoid overheating through an efficient heat distribution system, but considering that our study found the IPWP to peak at ~37°C during the late Eocene, sea surface temperatures may have reached even higher temperatures in the core of the Warm Pool during the early Eocene, which is the warmest interval of the Eocene Epoch as characterised by higher levels of greenhouse gases. This evident link between high atmospheric CO_2 concentrations and a super warm IPWP lead us to suggest that at the current rate of fossil fuel burning and consequential increase in atmospheric CO_2, the IPWP will unceasingly become warmer unless the continuous increase in CO_2 is tamed and greater efforts are made at reducing the burning of fossil fuels. At temperatures higher than 31.5°C it was found that convective clouds overlying the Warm Pool will disappear and allow long wave radiation to escape (De Deckker, 2016), causing a sharp reduction in nocturnal temperatures and thus affecting the human populations living in nearby islands such as Papua New Guinea, West Papua, and Sulawesi. Moreover, the IPWP is governed by a highly dynamic and complex atmosphere-ocean system, and rainfall patterns may drastically change and affect crops hence the local economy and food availability of the populations nearby. As we know, the Warm Pool controls the global heat distribution, as well as being connected through both the atmosphere and the ocean with the rest of the World, and a continuous warming of the area may surpass a climate threshold beyond which we will be challenged to adapt to and will require significant governmental action and policy implementations to develop more ambitious greenhouse

gas emissions reductions targets. The success of such actions can be facilitated by continuing to improve our knowledge of the Earth system's response to a rapidly warming climate.

Chapter 7

References

Chapter **7**

7. References

Abram, N., Mcgregor, H. V., Gagan, M., Hantoro, W. and Suwargadi, B. 2009. 'Oscillations in the southern extent of the Indo- Pacific Warm Pool during the mid-Holocene'. *Quaternary Science Reviews*, 28(25-26), pp. 2794-2803.

Agnini, C., Fornaciari, E., Raffi, I., Catanzariti, R., Pälike, H., Backman, J. And Rio, D. 2014. 'A New Low-to Middle-Latitude Biozonation and Revised Biochronology of Palaeogene Calcareous Nannofossils Biozonation and biochronology of Paleogene calcareous nannofossils from low and middle latitudes'. *Newsletters on Stratigraphy*, 47(2), pp. 131–181. doi: 10.1007/978-3-319-04364-7_28.

Alegret, L., Ortiz, S., Orue-Etxebarria, X., Bernaola, G., Baceta, J. I., Monechi, S., Apellaniz, E. And Pujalte, V. 2009. 'The Paleocene-Eocene thermal maximum: New data on microfossil turnover at the Zumaia Section, Spain'. *PALAIOS*, 24(5), pp. 318–328.

Allen, A. P., Gillooly, J. F. and Brown, J. H. 2005. 'Linking the global carbon cycle to individual metabolism'. *Functional Ecology*, 19, pp. 202–213. doi: 10.1111/j.1365-2435.2005.00952

Anagnostou, E., John, E. H., Edgar, K. M., Foster, G. L., Ridgwell, A., Inglis, G. N., Pancost, R. D., Lunt, J.D., and Pearson, P. N. 2016. 'Changing atmospheric CO_2 concentration was the primary driver of early Cenozoic climate'. *Nature*, 533(7603), pp. 380-384.

Anand, P., Elderfield, H. and Conte, M. H. 2003. 'Calibration of Mg/Ca thermometry in planktonic foraminifera from a sediment trap time series'. *Paleoceanography*. American Geophysical Union (AGU), 18(2), doi: 10.1029/2002pa000846.

Anderson, D. 2007. *Global environments through the Quaternary: exploring environmental change*. Goudie, A. and Parker, A. Oxford: Oxford University Press.

Armstrong McKay, D. I., Tyrrell, T. and Wilson, P. A. 2016. 'Global carbon cycle perturbation across the Eocene-Oligocene climate transition'. *Paleoceanography*, 31(2), pp. 311–329. doi: 10.1002/2015PA002818.

Armstrong, H. and Brasier, M. D. 2005. *Microfossils*. Malden [etc.]: Blackwell Publishing.

Arreguín-Rodríguez, G. J., Alegret, L. and Thomas, E. 2016. 'Late Paleocene-middle Eocene benthic foraminifera on a Pacific seamount (Allison Guyot, ODP Site 865): Greenhouse climate and superimposed hyperthermal events'. *Paleoceanography*, 31(3), pp. 346–364. doi: 10.1002/2015PA002837.

Arthur, M. A., Dean, W. E., Zachos, J. C., Kaminski, M., Rieg, S. H. & Elmstrom, K. 1989. 'Geochemical expression of early diagenesis in middle Eocene-lower Oligocene pelagic sediments in the southern Labrador Sea'. Site 647, ODP Leg 10. *Proceedings of the Ocean Drilling Program, Scientific Results*. 105, pp. 111-135.

Aze, T., Ezard, T.H.G., Purvis, A., Coxall, H.K., Stewart, D.R.M., Wade, B.S., Pearson, P.N. 2011. 'A phylogeny of Cenozoic macroperforate planktonic foraminifera from fossil data'. *Biological Reviews,* 86(4), pp. 900-927. doi: 10.1111/j.1469-185X.2011.00178.x.

Aze, T., Pearson, P. N., Dickson, A.J., Badger, M.P.S., Bown, P. R., Pancost, R. D., Gibbs, S. J., Huber, B. T., Leng, M. J., Coe, A.L., Cohen, A.S., and Foster, G. L. 2014. 'Extreme warming of tropical waters during the Paleocene-Eocene Thermal Maximum'. *Geology*, 4(9): pp. 739–742

Baker, P. A., Gieskes, J. and Elderfield, H. 1982. 'Diagenesis of carbonates in deep-sea sediments-Evidence from Sr/Ca ratios and interstitial dissolved Sr^{2+} data'. *Journal of Sedimentary Petrology*, 52(1), pp. 71-82.

Barker, S., Cacho, I., Benway, H. and Tachikawa, K. 2005. 'Planktonic foraminiferal Mg/Ca as a proxy for past oceanic temperatures: A methodological overview and data compilation for the Last Glacial Maximum'. *Quaternary Science Reviews*, 24(7-9), pp. 821-834.

Barker, S., Greaves, M. and Elderfield, H. 2003. 'A study of cleaning procedures used for foraminiferal Mg/Ca paleothermometry'. *Geochemistry, Geophysics, Geosystems*, 4(9). doi: 10.1029/2003GC000559.

Barras, C., Duplessy, J.C., Geslin, E., Michel, E., Jorissen, F.J. 2010. 'Calibration of $\delta^{18}O$ of cultured benthic foraminiferal calcite as a function of temperature'. *Biogeosciences,* 7, pp. 1349–1356. doi: 10.5194/bg-7-1349-2010.

Barron, E. J. 1987. 'Eocene equator-to- pole surface ocean temperatures: A significant climate problem?' *Paleoceanography*, 2(6), pp. 729-739.

Barron, E. J. and Peterson, W. H. 1991. 'The Cenozoic ocean circulation based on ocean General Circulation Model results'. *Palaeogeography, Palaeoclimatology, Palaeoecology*, 83(1), pp. 1-28.

Bé, A. W. H. 1982. 'Biology of Planktonic Foraminifera'. *Notes for a Short Course: Studies in Geology*. Cambridge University Press (CUP), 6, pp. 51–89. doi: 10.1017/s0271164800000506.

Bé, A. W. H., James, K.B., Bishop, M. S, Sverdlove, Gardner, W.D. 1985, 'Standing stock, vertical distribution and flux of planktonic foraminifera in the Panama Basin'. *Marine Micropaleontology*. Elsevier, 9(4), pp. 307–333. doi: 10.1016/0377-8398(85)90002-7.

Beerling, D. J. and Royer, D. L. 2011. 'Convergent Cenozoic CO_2 history'. *Nature Geoscience*, 4(7), pp. 418-420.

Beerling, D. J., Fox, A., Stevenson, D.S., Valdes, P.J. 2011. 'Enhanced chemistry-climate feedbacks in past greenhouse worlds'. *Proceedings of the National Academy of Sciences of the Unites States of America*, 108(24). doi: 10.1073/pnas.1102409108/-/DCSupplemental.

Bemis, B. E., Spero, H.J., Bijma, J., Lea, D.W. 1998. 'Reevaluation of the oxygen isotopic composition of planktonic foraminifera: Experimental results and revised paleotemperature equations'. *Paleoceanography*, 13(2), pp. 150–160. doi: 10.1029/98PA00070.

Bemis, B. E., Spero, H.J., Lea, D.W., Bijma, J. 2000. 'Temperature influence on the carbon isotopic composition of *Globigerina bulloides* and *Orbulina universa* (planktonic foraminifera)'. *Marine Micropaleontology*, 38(3-4), pp. 213-228

Berger, W. H. and Diester-Haass, L. 1988 'Paleoproductivity: The benthic/planktonic ratio in foraminifera as a productivity index'. *Marine Geology*, 81(1–4), pp. 15–25. doi: 10.1016/0025-3227(88)90014-X.

Berger, W. H. and Wefer, G. 1991. 'Productivity of the glacial ocean: Discussion of the iron hypothesis'. *Limnology and Oceanography*, 36(8), pp. 1899-1918.

Berger, W. H., Killingley, J.S., Vincent, E.R. 1978. 'Stable isotopes in deep-sea carbonates: Box Core ERDC-92, West Equatorial Pacific'. *Oceanologica Acta*, 1(2). Available at: http://archimer.ifremer.fr/doc/00123/23381/21208.pdf (Accessed: 17 September 2018).

Berner, R. A. 1994. 'GEOCARB II; a revised model of atmospheric CO_2 over Phanerozoic time'. *American Journal of Science*, 294 (1), pp. 56-91.

Berner, R. A., Lasaga, A. C. and Garrels, R. M. 1983. 'The carbonate-silicate geochemical cycle and its effect on atmospheric carbon dioxide over the past 100 million years'. *American Journal of Science*, 283(7), pp. 641–683. doi: 10.2475/ajs.283.7.641.

Bice, K. L. and Marotzke, J. 2002. 'Could changing ocean circulation have destabilized methane hydrate at the Paleocene/Eocene boundary?'. *Paleoceanography*, American Geophysical Union (AGU), 17(2), pp. 8-1-8–12. doi: 10.1029/2001pa000678.

Bigg, G. R. and Rohling, E. J. 2000. 'An oxygen isotope data set for marine waters'. *Journal of Geophysical Research: Oceans*. American Geophysical Union (AGU), 105(C4), pp. 8527–8535. doi: 10.1029/2000jc900005.

Bijl, P. K., Schouten, S., Sluijs, A., Reichart, G.-J., Zachos, J. C. and Brinkhuis, H. 2009. 'Early Palaeogene temperature evolution of the southwest Pacific Ocean'. *Nature*, 461(7265), pp. 776-779.

Bijma, J. and Hemleben, C. 1994. 'Population dynamics of the planktic foraminifer *Globigerinoides sacculifer* (Brady) from the central Red Sea'. *Deep-Sea Research Part I*, 41(3), pp. 485–510. doi: 10.1016/0967-0637(94)90092-2.

Bijma, J., Faber, W. W. and Hemleben, C. 1990. 'Temperature and salinity limits for growth and survival of some planktonic foraminifers in laboratory cultures'. *The Journal of Foraminiferal Research*, 20(2), pp. 95–116. doi: 10.2113/gsjfr.20.2.95.

Bijma, J., Spero, H. J. and Lea, D. W. 1999. 'Reassessing Foraminiferal Stable Isotope Geochemistry: Impact of the Oceanic Carbonate System (Experimental Results)'.

in *Use of Proxies in Paleoceanography*. Berlin, Heidelberg: Springer Berlin Heidelberg, pp. 489–512. doi: 10.1007/978-3-642-58646-0_20.

Birch, H. S., Coxall, H. K. and Pearson, P. N. 2012. 'Evolutionary ecology of Early Paleocene planktonic foraminifera: size, depth habitat and symbiosis'. *Paleobiology*, 38(3), pp. 374-390. doi: 10.1666/11027.1.

Birch, H., Coxall, H. K., Pearson, P. N., Kroon, D. and O'Regan, M., 2013. 'Planktonic foraminifera stable isotopes and water column structure: Disentangling ecological signals'. *Marine Micropaleontology*, 101, pp. 127-145.

Bjerknes, J. 1969. 'Atmospheric teleconnections from the Equatorial Pacific'. *Journal of Physical Oceanography*, 97(3), pp. 163-172.

Blow, W. H. 1969. 'Late middle Eocene to Recent planktonic foraminiferal biostratigraphy'. In Brönnimann, P., and Renz, H. H. (ed.) *Planktonic Microfossils, Geneva, 1967: Leiden (E.J. Brill), :1*. Geneva, pp. 99-422.

Boersma, A, Shackleton, N.J., Hall, M., Given, Q. 1979. 'Carbon and oxygen isotope records at DSDP Site 384 (North Atlantic) and some Paleocene paleotemperatures and carbon isotope variations in the Atlantic Ocean'. *In: Tucholke, B.E., Vogt, P.R., et al. (eds.), Initial Reports of the Deep Sea Drilling Project, Washington (U.S. Government Print Office)*, 43, pp. 695-717

Boersma, A. and Premoli Silva, I. 1986. 'Terminal Eocene events: Planktonic foraminifera and isotopic evidence'. *Developments in Palaeontology and Stratigraphy*, 9(C), pp. 213–223. doi: 10.1016/S0920-5446(08)70124-9.

Boersma, A. and Premoli Silva, I. 1991 'Distribution of Paleogene planktonic foraminifera - analogies with the Recent?' *Palaeogeography, Palaeoclimatology, Palaeoecology*, Elsevier, 83(1–3), pp. 29–47. doi: 10.1016/0031-0182(91)90074-2.

Boersma, A. and Silva, I. P. 1989 'Atlantic Paleogene biserial heterohelicid foraminifera and oxygen minima'. *Paleoceanography*, 4(3), pp. 271–286. doi: 10.1029/PA004i003p00271.

Boersma, A., Shackleton, N. J., Hall, M. A. and Given, Q. 1979. 'Stable carbon and oxygen isotope ratios of foraminifera from Cretaceous and Paleocene sediments. Supplement to: Boersma, Anne; Shackleton, Nicholas J; Hall, Michael A; Given, Quentin (1979): Carbon and oxygen isotope records at DSDP Site 384 (North

Atlantic) and some Paleocene paleotemperatures and carbon isotope variations in the Atlantic Ocean'. In: Tucholke, B.E. et al. eds. *Initial Reports of the Deep Sea Drilling Project*, Washington (U.S. Government Print Office) 43, pp. 695-717, PANGAEA.

Boersma, A., Silva, I. P. and Shackleton, N. J. 1987. 'Atlantic Eocene planktonic foraminiferal paleohydrographic indicators and stable isotope paleoceanography'. *Paleoceanography*, 2(3), pp. 287–331. doi: 10.1029/PA002i003p00287.

Bohaty, S. M. and Zachos, J. C. 2003. 'Significant Southern Ocean warming event in the late middle Eocene'. *Geology*, 31(11), pp. 1017–1020. doi: 10.1130/G19800.1.

Bohaty, S. M., Zachos, J. C. and Delaney, M. L. 2012. 'Foraminiferal Mg/Ca evidence for Southern Ocean cooling across the Eocene-Oligocene transition'. *Earth and Planetary Science Letters*, 317–318, pp. 251–261. doi: 10.1016/j.epsl.2011.11.037.

Bolton, C. T., Stoll, H. M. and Mendez-Vicente, A. 2012. 'Vital effects in coccolith calcite: Cenozoic climate-pCO$_2$ drove the diversity of carbon acquisition strategies in coccolithophores?'. *Paleoceanography*, Blackwell Publishing Ltd, 27(4). doi: 10.1029/2012PA002339.

Bornemann, A. and Norris, R. D. 2007. 'Size-related stable isotope changes in Late Cretaceous planktic foraminifera: Implications for paleoecology and photosymbiosis'. *Marine Micropaleontology*, 65(1–2), pp. 32–42. doi: 10.1016/j.marmicro.2007.05.005.

Boscolo-Galazzo, F., Chrichton, K.A., Barker, S., Pearson, P.N. 2018. 'Temperature dependency of metabolic rates in the upper ocean: A positive feedback to global climate change?'. *Global and Planetary Change*, Elsevier, 170 (September), pp. 201–212. doi: 10.1016/j.gloplacha.2018.08.017.

Boyle, E. A. 1983. 'Manganese carbonate overgrowths on foraminifera tests'. *Geochimica et Cosmochimica Acta*, Pergamon, 47(10), pp. 1815–1819. doi: 10.1016/0016-7037(83)90029-7.

Boyle, E. A. and Keigwin, L. D. 1985. 'Comparison of Atlantic and Pacific paleochemical records for the last 215,000 years: changes in deep ocean circulation and chemical inventories'. *Earth and Planetary Science Letters*, 76(1–2), pp. 135–150. doi: 10.1016/0012-821X(85)90154-2.

Bradley, R., S. 2014. *Paleoclimatology: Reconstructing Climates of the Quaternary*. San Diego, Cali: London, Academic Press.

Bralower, T. J., Zachos, J. C., Thomas, E., Parrow, M., Paull, C. K., Kelly, D. C., Silva, I. P., Sliter, W. V. and Lohmann, K. C. 1995. 'Late Paleocene to Eocene paleoceanography of the equatorial Pacific Ocean: Stable isotopes recorded at Ocean Drilling Program Site 865, Allison Guyot'. *Paleoceanography*, 10(4), pp. 841-865.

BRIDGE (2019) *Bristol Research Initiative for the Dynamic Global Environment | School of Geographical Sciences | University of Bristol*. Available at: http://www.bristol.ac.uk/geography/research/bridge/ (Accessed: 15 February 2020).

Broecker, W. S. and Peng, T.-H. 1982. *Tracers In The Sea*. A Publication of The Lamont-Doherty Geological Observatory, Columbia University, Palisades, New York, New York.

Broecker, W., Kennett, J. P., Flower, B., Teller, J., Trumbore, S., Bonani, G. and Wolfli, W. 1989. 'Routing of Meltwater from The Laurentide Ice- Sheet During The Younger Dryas Cold Episode'. *Nature*, 341(6240), pp. 318-321.

Brown, J. H., Gillooly, J. F., Allen, A. P., Savage, V. M. And West, G. B. 2004. 'Toward A Metabolic Theory of Ecology'. *Ecology*, 85(7), pp. 1771–1789. Ecological Society of America. doi: 10.1890/03-9000.

Brown, S. J. and Elderfield, H. 1996. 'Variations in Mg/Ca and Sr/Ca ratios of planktonic foraminifera caused by postdepositional dissolution: Evidence of shallow Mg-dependent dissolution'. *Paleoceanography*, 11(5), pp. 543–551. doi: 10.1029/96PA01491.

Brückner, S. and Mackensen, A. 2008. 'Organic matter rain rates, oxygen availability, and vital effects from benthic foraminiferal $\delta^{13}C$ in the historic Skagerrak, North Sea'. *Marine Micropaleontology*, 66(3–4), pp. 192–207. doi: 10.1016/j.marmicro.2007.09.002.

Brummer, G. J. A., Hemleben, C. and Spindler, M. 1986. 'Planktonic foraminiferal ontogeny and new perspectives for micropalaeontology'. *Nature*, 319(6048), pp. 50–52. doi: 10.1038/319050a0.

Bujak, J. and Brinkhuis, H. 1998. 'Global warming and dinocyst changes across the Paleocene/Eocene Epoch boundary'. *Columbia University Press New York*.

Burgess, C. E., Pearson, P. N., Lear, C. H., Morgans, H. E., Handley, L., Pancost, R. D. And Schouten, S. 2008 'Middle Eocene climate cyclicity in the southern Pacific: Implications for global ice volume'. *Geology*, 36(8), pp. 651–654. doi: 10.1130/G24762A.1.

Caballero, R. and Huber, M. 2013. 'State-dependent climate sensitivity in past warm climates and its implications for future climate projections'. *Proceedings of the National Academy of Sciences*, 110 (35), pp. 14162-14167.

Caballero, R. and Langen, P. 2005. 'The dynamic range of poleward energy transport in an atmospheric general circulation model'. *Geophysical Research Letters*, 32(2).

Cande, S. C. and Kent, D. V. 1995. 'Revised calibration of the geomagnetic polarity timescale for the late Cretaceous and Cenozoic'. *Journal of Geophysical Research*, 100(B4), pp. 6093–6095. doi: 10.1029/94JB03098.

Cane, M. A. 1983. 'Oceanographic events during El Niño'. *Science*, 222(4629), pp. 1189-1195.

Cane, M. A. 1998. 'A Role for the Tropical Pacific'. *Science*, 282(5386), pp. 59-61.

Carman, G. J. 1990. 'Occurrence and nature of Eocene Strata in the eastern Papuan Basin'. *Petroleum Exploration in Papua New Guinea. Proceedings of the First PNG Petroleum Convention, Port Moresby*, (March), pp. 169–183.

Castañeda, I. S. and Schouten, S. 2011. 'A review of molecular organic proxies for examining modern and ancient lacustrine environments'. *Quaternary Science Reviews*, doi: 10.1016/j.quascirev.2011.07.009.

Chen, B., Landry, M.R., Huang, B., and Liu, H., 2012. 'Does warming enhance the effect of microzooplankton grazing on marine phytoplankton in the ocean?'. *Limnology and Oceanography*, John Wiley & Sons, Ltd, 57(2), pp. 519–526. doi: 10.4319/lo.2012.57.2.0519.

Cifelli, R. L. 1982. 'Early occurrences and some phylogenetic implications of spiny, honeycomb textured planktonic foraminifera'. *The Journal of Foraminiferal Research*, 12(2), pp. 105–115. doi: 10.2113/gsjfr.12.2.105.

Coggon, R. M., Teagle, D.A.H., Smith-Duque, C.E., Alt, J.C., Cooper, M.J. 2010. 'Reconstructing past seawater Mg/Ca and Sr/Ca from mid-ocean ridge flank calcium carbonate veins'. *Science*, 327(5969), pp. 1114–1117. doi: 10.1126/science.1182252.

Collinson, M. E. and Hooker, J. 2003. Paleogene vegetation of Eurasia: framework for mammalian faunas. In: Reumer, J. et al. eds. *Distribution and migration of tertiary mammals in Eurasia: DEINSEA*, 10, pp. 41–83.

Conway, D., Hanson, C. E., Doherty, R. and Persechino, A. 2007. 'GCM simulations of the Indian Ocean dipole influence on East African rainfall: Present and future'. *Geophysical Research Letters*, 34(3), pp. 1-6.

Corfield, R. M., Hall, M. A. and Brasier, M. D. 1990. 'Stable isotope evidence for foraminiferal habitats during the during of the Cenomanian/Turonian ocean anoxic event'. *Geology*. Geological Society of America, 18(2), pp. 175–178.

Corliss, B. H. 1985. 'Microhabitats of benthic foraminifera within deep-sea sediments'. *Nature*, 314(6010), pp. 435–438. doi: 10.1038/314435a0.

Cossins, A. R. and Bowler, K. 1987. *Temperature biology of animals*. London: Chapman and Hall.

Coxall, H. K. and Pearson, P. 2007. 'The Eocene-Oligocene Transition: The Eocene – Oligocene Transition' in *Deep Time Perspectives on Climate Change: Marrying the Signal from Computer Models and Biological Proxies*, edited by M. Williams et al., pp. 351– 387, Geol. Soc., London.

Coxall, H. K., Pearson, P.N., Shackleton, N. J., Hall, M. H. 2000. 'Hantkeninid depth adaptation: An evolving life strategy in a changing ocean'. *Geology*, Geological Society of America, 28(1), p. 87.

Coxall, H. K., Wilson, P.A., Pälike, H., Lear, C.H., Backman, J. 2005. 'Rapid stepwise onset of Antarctic glaciation and deeper calcite compensation in the Pacific Ocean'. *Nature*, 433(7021), pp. 53–57. doi: 10.1038/nature03135.

Coxall, H. K., Wilson, P.A., Pearson, P.N., Sexton, P.F. 2007. 'Iterative evolution of digitate planktonic foraminifera'. *Paleobiology*, Cambridge University Press (CUP), 33(4), pp. 495–516. doi: 10.1666/06034.1.

Coxall, H.K. and Pearson, P.N., 2006. Taxonomy, biostratigraphy and phylogeny of Hantkeninidae (*Clavigerinella*, *Hantkenina* and *Cribrohantkenina*). In Pearson,

P.N., Olsson, R.K., Hemleben, C., Huber, B.T. and Berggren, W.A. (Eds.), *Atlas of Eocene planktonic foraminifera*. Cushman Foundation of Foraminiferal Research, Special Publication 41: 213-252

Cramer, B. S., Miller, K. G., Barrett, P. J. and Wright, J. D. 2011. 'Late Cretaceous–Neogene trends in deep ocean temperature and continental ice volume: Reconciling records of benthic foraminiferal geochemistry (δ^{18}O and Mg/Ca) with sea level history'. *Journal of Geophysical Research: Oceans*, 116(C12).

Cramer, B. S., Toggweiler, J.R., Wright, J.D., Katz, M.E., Miller, K.G. 2009. 'Ocean overturning since the late cretaceous: Inferences from a new benthic foraminiferal isotope compilation'. *Paleoceanography*, John Wiley & Sons, Ltd, 24(4). doi: 10.1029/2008PA001683.

Cramwinckel, M. J., Huber, M., Kocken, I. J., Agnini, C., Bijl, P.K., Bohaty, S. M., Frieling J., Goldner A., Hilgen F.J., Kip, E.L., Peterse, F., van der Ploeg, R., Röhl, U., Schouten, S., Sluijs, A. 2018. 'Synchronous tropical and polar temperature evolution in the Eocene'. *Nature*, 559, pp. 382-386. doi: 10.1038/s41586-018-0272-2.

Cravatte, S., Delcroix, T., Zhang, D., Mcphaden, M. and Leloup, J. 2009. 'Observed freshening and warming of the western Pacific Warm Pool'. *Climate Dynamics*, 33(4), pp. 565-589.

Creber, G. T. and Chaloner, W. G. 1985. 'Three growth in the Mesozoic and Early Tertiary and the reconstruction of palaeoclimates'. *Palaeogeography, Palaeoclimatology, Palaeoecology*, 52(1), pp. 35-59.

Creech, J., Baker, J., Hollis, C. J., Morgans, H. and Smith, E. 2010. 'Eocene sea temperatures for the mid- latitude southwest Pacific from Mg/Ca ratios in planktonic and benthic foraminifera'. *Earth and Planetary Science Letters*, 299(3-4), pp. 483-495.

Crouch, E. M., Heilmann-Clause, C., Brinkhuis, H., Morgans, H.E.G. 2001. 'Global dinoflagellate event associated with the late Paleocene thermal maximum'. *Geology*, 29(4), pp. 315–318.

Crowley, T.J. and Zachos, J.C., 2000. Comparison of zonal temperature profiles for past warm time periods, in Huber, B.T. et al., eds. *Warm Climates in Earth History*. Cambridge: Cambridge University Press, pp. 50–76.

D'Hondt, S. and Arthur, M. A. 1996. 'Late cretaceous oceans and the cool tropic paradox'. *Science*, 271(5257), pp. 1838-1841.

D'Hondt, S., Zachos, J. C. and Schultz, G. 1994. 'Stable Isotopic Signals and Photosymbiosis in Late Paleocene Planktic Foraminifera'. *Paleobiology*, 20(3), pp. 391–406.

De Choudens-Sanchez, V. and Gonzalez, L. A. 2009. 'Calcite and Aragonite Precipitation Under Controlled Instantaneous Supersaturation: Elucidating the Role of CaCO3 Saturation State and Mg/Ca Ratio on Calcium Carbonate Polymorphism'. *Journal of Sedimentary Research*. 79(6), pp. 363–376. doi: 10.2110/jsr.2009.043.

De Deckker, P. 2016. 'The Indo-Pacific Warm Pool: critical to world oceanography and world climate'. *Geoscience Letters*, 3(1), p. 20. doi: 10.1186/s40562-016-0054-3.

DeConto, R. M. and Pollard, D. 2003. 'Rapid Cenozoic glaciation of Antarctica induced by declining atmospheric CO_2'. *Nature*, 421(6920), pp. 245–249. doi: 10.1038/nature01290.

DeConto, R. M., Hay, W., Thompson, S. and Bergengren, J. 1999. 'Late Cretaceous climate and vegetation interactions: Cold continental interior paradox. In: Barrera, E. et al. eds. *Evolution of the Cretaceous ocean-climate system*. Boulder, Colorado: Geological Society of America Special Paper, 332.

DeConto, R. M., Pollard, D., Wilson, P.A., Pälike, H., Lear, C.H., Pagani, M. 2008. 'Thresholds for Cenozoic bipolar glaciation'. *Nature*, Nature Publishing Group, 455(7213), pp. 652–656. doi: 10.1038/nature07337.

DeMets, C., Gordon, R. G. and Argus, D. F. 2010. 'Geologically current plate motions'. *Geophysical Journal International*, 181(1), pp. 1–80.

Dickens, G. R., O'Neil, J. R., Rea, D. K. and Owen, R. M. 1995. 'Dissociation of oceanic methane hydrate as a cause of the carbon isotope excursion at the end of the Paleocene'. *Paleoceanography*, 10(6), pp. 965-971.

Dickson, J. 2002. 'Fossil echinoderms as monitor of the Mg/ Ca ratio of phanerozoic oceans'. *Science*, 298(5596), pp. 1222-1224.

Dijkstra, H. A. and Neelin, J. D. 1995. 'Ocean-Atmosphere Interaction and the Tropical Climatology. Part II: Why the Pacific Cold Tongue Is in the East'. *Journal of Climate*, 8(5), pp. 1343-1359.

Doria, G., Royer, D. L., Wolfe, A. P., Fox, A., Westgate, J. A. and Beerling, D. J. 2011. 'Declining atmospheric CO_2 during the late middle Eocene climate transition'. *American Journal of Science*, 311, pp. 63–75.

Douglas, R. G. and Savin, S. M. 1978. 'Oxygen isotopic evidence for the depth stratification of tertiary and cretaceous planktic foraminifera'. *Marine Micropaleontology*, 3(2), pp. 175–196.

Dunkley Jones, T., Lunt, D., Schmidt, D., Ridgwell, A., Sluijs, A., Valdes, P. and Maslin, M. 2013. 'Climate model and proxy data constraints on ocean warming across the Paleocene- Eocene Thermal Maximum'. *Earth-Science Reviews*, 125, pp. 123-145.

Dutton, A., Lohmann, K. C. and Leckie, R. M. 2005. 'Insights from the Paleogene tropical Pacific: Foraminiferal stable isotope and elemental results from Site 1209, Shatsky Rise'. *Paleoceanography*, 20(3).

Edgar, K. M., Wilson, P. A., Sexton, P. F., Gibbs, S. J., Roberts, A. P. and Norris, R. D. 2010. 'New biostratigraphic, magnetostratigraphic and isotopic insights into the Middle Eocene Climatic Optimum in low latitudes'. *Palaeogeography, Palaeoclimatology, Palaeoecology*, 297(3–4), pp. 670-682.

Edgar, K. M., Anagnostou, E., Pearson, P. N. and Foster, G. L. 2015. 'Assessing the impact of diagenesis on $\delta^{11}B$, $\delta^{13}C$, $\delta^{18}O$, Sr/Ca and B/Ca values in fossil planktic foraminiferal calcite'. *Geochimica et Cosmochimica Acta*, 166, pp. 189-209.

Edgar, K.M., Hull, P.M., and Ezard, T.H.G., 2017.' Evolutionary history biases inferences of ecology and environment from $\delta^{13}C$ but not $\delta^{18}O$ values'. *Nature Communications*, 8, 1106. doi: 10.1038/s41467-017-01154-7

Egan, K. E., Rosalind, E.M., Rickaby, K.R., Hendry, A., Halliday, N. 2013. 'Opening the gateways for diatoms primes Earth for Antarctic glaciation'. *Earth and Planetary Science Letters*, 375, pp. 34–43. doi: 10.1016/j.epsl.2013.04.030.

Eggins, S., De Deckker, P. and Marshall, J. 2003. 'Mg/Ca variation in planktonic foraminifera tests: implications for reconstructing palaeo-seawater temperature

and habitat migration'. *Earth and Planetary Science Letters*, 212(3–4), pp. 291-306.

Eglinton, T. and Eglinton, G. 2008. 'Molecular proxies for paleoclimatology'. *Earth and Planetary Science Letters,* 275(1-2), pp. 1-16.

Elderfield, H. and Ganssen, G. 2000. 'Past temperature and δ^{18}O of surface ocean waters inferred from foraminiferal Mg/Ca ratios'. *Nature*, 405(6785), pp. 442–445. doi: 10.1038/35013033.

Elderfield, H. and Schultz, A. 1996. 'Mid-ocean ridge hydrothermal fluxes and the chemical composition of the ocean'. *Annual Review of Earth & Planetary Sciences*, 24, pp. 191–224. doi: 10.1146/annurev.earth.24.1.191.

Elderfield, H., Vautravers, M. and Cooper, M. 2002. 'The relationship between shell size and Mg/Ca, Sr/Ca, δ^{18}O, and δ^{13}C of species of planktonic foraminifera'. *Geochemistry, Geophysics, Geosystems*, Wiley-Blackwell, 3(8), pp. 1–13. doi: 10.1029/2001GC000194.

Eldrett, J. S., Greenwood, D. R., Harding, I. C. and Huber, M. 2009. 'Increased seasonality through the Eocene to Oligocene transition in northern high latitudes'. *Nature*, 459, pp. 969–973.

Elling, F. J., Könneke, M., Greve, A., Hinrichs, K.-U. and Mußmann, M. 2015. 'Influence of temperature, pH, and salinity on membrane lipid composition and TEX$_{86}$ of marine planktonic thaumarchaeal isolates'. *Geochimica et Cosmochimica Acta*, 171, pp. 238-255.

Emanuel, K. 2001. 'Contribution of tropical cyclones to meridional heat transport by the oceans'. *Journal of Geophysical Research: Atmospheres*, Wiley-Blackwell, 106(D14), pp. 14771–14781. doi: 10.1029/2000JD900641.

Emanuel, K. 2002. 'A simple model of multiple climate regimes'. *Journal of Geophysical Research D: Atmospheres*, 107(9-10), pp. 4-1.

Emiliani, C. 1954. 'Depth habitats of some species of pelagic Foraminifera as indicated by oxygen isotope ratios'. *American Journal of Science*, 252(3), pp. 149–158. doi: 10.2475/ajs.252.3.149.

Epstein, S., Buchsbaum, R., Lowenstam, H., Urey, H.C. 1951 'Carbonate-Water Isotopic Temperature Scale'. *Bulletin of the Geological Society of America*, 62(4), pp. 417-426.

Epstein, S., R. Buchsbaum, H. A. Lowen- Stam, and Urey, H. C. 1953. 'Revised carbonate-water isotopic temperature scale'. *Geological Society of America Bulletin*, 64(11), pp. 1315– 1325.

Erez, J. 1978. 'Vital effect on stable-isotope composition seen in foraminifera and coral skeletons'. *Nature*, 273(5659), pp. 199–202. doi: 10.1038/273199a0.

Erez, J. and Luz, B. 1983. 'Experimental paleotemperature equation for planktonic foraminifera'. *Geochimica et Cosmochimica Acta*, 47(6), pp. 1025–1031. doi: 10.1016/0016-7037(83)90232-6.

Evans, D. and Müller, W. 2012. 'Deep time foraminifera Mg/Ca paleothermometry: Nonlinear correction for secular change in seawater Mg/Ca'. *Paleoceanography*, 27(4), pp. 1–11. doi: 10.1029/2012PA002315.

Evans, D., Brierley, C., Raymo, M.E., Erez, J., Mueller, W. 2016. 'Planktic foraminifera shell chemistry response to seawater chemistry: Pliocene–Pleistocene seawater Mg/Ca, temperature and sea level change'. *Earth and Planetary Science Letters*, Elsevier, 438, pp. 139–148. doi: 10.1016/J.EPSL.2016.01.013.

Evans, D., Sagoo, N, Renema, W., Cotton, L.J., Müller, W., Todd, J.A., Saraswati, P.K., Stassen, P., Ziegler, M., Pearson, P.N., Valdes, P.J., Affek, H.P. W. 2018. 'Eocene greenhouse climate revealed by coupled clumped isotope-Mg/Ca thermometry'. *Proceedings of the National Academy of Sciences of the United States of America*, p. 201714744. doi: 10.1073/pnas.1714744115.

Ezard, H.G., Edgar, K.M., and Hull, P.M., 2015. Environmental and biological controls on size-specific $\delta^{13}C$ and $\delta^{18}O$ in recent planktonic foraminifera. *Paleoceanography*, 30, pp. 151-173. doi: 10.1002/2014PA002735.

Fansworth, A., *personal communication*, University of Bristol, 2017-2019.

Faul, K. L., Ravelo, A. C. and Delaney, M. L. 2000. 'Reconstructions of Upwelling, Productivity, And Photic Zone Depth In The Eastern Equatorial Pacific Ocean Using Planktonic Foraminiferal Stable Isotopes And Abundances'. *Journal of Foraminiferal Research*, 30(2), pp. 110–125

Fedorov, A. V. and Philander, S. G. 2000. 'Is El Niño changing?' *Science* 288(5473), pp. 1997-2002.

Fehrenbacher, J. S. and Martin, P. A. 2014. 'Exploring the dissolution effect on the intrashell Mg/Ca variability of the planktic foraminifer *Globigerinoides ruber*'. *Paleoceanography*, Blackwell Publishing Ltd, 29(9), pp. 854–868. doi: 10.1002/2013PA002571.

Filipsson, H. L., Bernhard, J.M., Lincoln, S.A., McCorkle, D.C. 2010. 'A culture-based calibration of benthic foraminiferal paleotemperature proxies: $\delta^{18}O$ and Mg/Ca results'. *Biogeosciences*, 7(1), pp. 351–385. doi: 10.5194/bgd-7-351-2010.

Fletcher, B. J., Brentnall, S. J., Anderson, C. W., Berner, R. A. and Beerling, D. J. 2008. 'Atmospheric carbon dioxide linked with Mesozoic and early Cenozoic climate change'. *Nature Geoscience*, 1, pp. 43-48.

Foster, G., Royer, D. & Lunt, D., 2017. Future climate forcing potentially without precedent in the last 420 million years. *Nature Communications*, 8(14845), p. n/a-n/a. doi: 10.1038/ncomms14845

Forster, A., Schouten, S., Moriya, K., Wilson, P.A., Sinninghe Damsté, J.S. 2007. 'Tropical warming and intermittent cooling during the Cenomanian/Turonian oceanic anoxic event 2: Sea surface temperature records from the equatorial Atlantic'. *Paleoceanography*, 22(1), p. n/a-n/a. doi: 10.1029/2006PA001349.

Fox, L., Stukins, S., Hill, T., Miller, C.G. 2020. 'Quantifying the Effect of Anthropogenic Climate Change on Calcifying Plankton'. *Scientific reports*, 10(1), p. 1620. doi: 10.1038/s41598-020-58501-w.

Friedman, I., and O'Neil, J. R. 1977. Compilation of stable isotope fractionation factors of geochemical interest. In M. Fleischer (Ed.), Data of Geochemistry, 6th edition. Geochemical Survey Professional Paper, 440, KK1–KK12. https://doi.org/10.3133/pp440KK.

Friedrich, O., Schiebel, R., Wilson, P.A., Weldeab, S. 2012. 'Influence of test size, water depth, and ecology on Mg/Ca, Sr/Ca, $\delta^{18}O$ and $\delta^{13}C$ in nine modern species of planktic foraminifers'. *Earth and Planetary Science Letters*, 319–320, pp. 133–145. doi: 10.1016/j.epsl.2011.12.002.

Frieling, J., Gebhardt, H., Huber, M., Adekeye, O.A., Adande, S.O., Reichart, Gert-Jan, Middleburg, J.J., Schouten, S., Sluijs, A. 2017. 'Extreme warmth and heat-

stressed plankton in the tropics during the Paleocene-Eocene Thermal Maximum'. *Science Advances*, 3(3), p. e1600891. doi: 10.1126/sciadv.1600891.

Gagan, M. K., Hendy, E. J., Haberle, S. G. and Hantoro, W. S. 2004. 'Post-glacial evolution of the Indo-Pacific Warm Pool and El Niño-Southern oscillation'. *Quaternary International*, 118–119, pp. 127-143.

Ghil, M., Ide, M. R., Kondrashov, M. D., Robertson, K., Saunders, D., Tian, M. E., Varadi, A. W., Ghil, A., Allen, Y., Dettinger, F., Mann, P., Robertson, P., Tian, P. and Yiou, P. 2002. 'Advanced spectral methods for climatic time series'. *Reviews of Geophysics*, 40(1), pp. 3-41.

Gibson, T. G., Bybell, L. M. and Owens, J. P. 1993. 'Latest Paleocene lithologic and biotic events in neritic deposits of southwestern New Jersey'. *Paleoceanography*, 8(4), pp. 495–514. doi: 10.1029/93PA01367.

Gieskes, J. M. and Lawrence, J. R. 1981. 'Alteration of volcanic matter in deep sea sediments: evidence from the chemical composition of interstitial waters from deep sea drilling cores'. *Geochimica et Cosmochimica Acta*, 45(10), pp. 1687–1703. doi: 10.1016/0016-7037(81)90004-1.

Gillooly, J. F., Brown, J.H., West, G.B., Savage, V.M., Charnov, E.L. 2001. 'Effects of size and temperature on metabolic rate'. *Science*, 293(5538), pp. 2248–2251. doi: 10.1126/science.1061967.

Gillooly, J. F., Charnov, E.L., West, G.B., Savage, V.M., Brown, J.H. 2002. 'Effects of size and termperature on development time'. *Nature*, 417, pp. 70–73. doi: 10.1002/lary.25455.

Gothmann, A. M., Stolarski, J., Adkins, J. F., Schoene, B., Dennis, K. J., Schrag, D. P., Mazur, M., Bender, M. L. 2015. 'Fossil corals as an archive of secular variations in seawater chemistry since the Mesozoic'. *Geochimica et Cosmochimica Acta*, Elsevier Ltd, 160, pp. 188–208. doi: 10.1016/j.gca.2015.03.018.

Gradstein, F. M., Ogg, J. G. and Hilgen, F. J. 2012. 'On the geologic time scale'. *Newsletters on Stratigraphy*, 45(2), pp. 171–188. doi: 10.1127/0078-0421/2012/0020.

Gray, W. R., Weldeab, S., Lea, D.W., Rosenthal, Y., Gruber, N., Donner, B., Fischer, G. 2018. 'The effects of temperature, salinity, and the carbonate system on Mg/Ca

in *Globigerinoides ruber* (white): A global sediment trap calibration'. *Earth and Planetary Science Letters*, 482, pp. 607-620. doi: 10.1016/j.epsl.2017.11.026.

Greenwood, D. R. and Wing, S. L. 1995. 'Eocene continental climates and latitudinal temperature gradients'. *Geology*, 23, pp. 1044–1048.

Grossman, E. L. 1984 'Stable isotope fractionation in live benthic foraminifera from the southern California Borderland'. *Palaeogeography, Palaeoclimatology, Palaeoecology*, Elsevier, 47(3–4), pp. 301–327. doi: 10.1016/0031-0182(84)90100-7.

Grossman, E.L., 1987. 'Stable isotopes in modern benthic foraminifera: a study of vital effect'. *Journal of Foraminiferal Research*, 17(1), pp. 48-61.

Hall, M. M. and Bryden, H. L. 1982. 'Direct estimates and mechanisms of ocean heat transport'. *Deep Sea Research Part A. Oceanographic Research Papers*. Elsevier, 29(3), pp. 339–359. doi: 10.1016/0198-0149(82)90099-1.

Hall, R. 2002. 'Cenozoic geological and plate tectonic evolution of SE Asia and the SW Pacific: Computer-based reconstructions, model and animations'. *Journal of Asian Earth Sciences*, 20(4), pp. 353–431. doi: 10.1016/S1367-9120(01)00069-4.

Hall, R. 2012. 'Late Jurassic-Cenozoic reconstructions of the Indonesian region and the Indian Ocean'. *Tectonophysics*, doi: 10.1016/j.tecto.2012.04.021.

Hallegraeff, G.M., Valentine, J.P., Marshall, J., and Bolch, C.J., 1997. 'Temperature tolerances of toxic dinoflagellate cysts: application to the treatment of ships' ballast water'. *Aquatic Ecology,* 31, pp. 47–52. doi: https://doi.org/10.1023/A:1009972931195

Harrington, G. J. and Jaramillo, C. A. 2007. 'Paratropical floral extinction in the Late Palaeocene–Early Eocene'. *Journal of the Geological Society*, 164(2), pp. 323-332.

Hasenfratz, A. P., Martínez-García, A., Jaccard, S., Vance, D., Wälle, M., Greaves, M., and Haug, G. 2017. 'Determination of the Mg/Mn ratio in foraminiferal coatings: An approach to correct Mg/Ca temperatures for Mn-rich contaminant phases'. *Earth and Planetary Science Letters*, Elsevier B.V., 457, pp. 335–347. doi: 10.1016/j.epsl.2016.10.004.

Hay, W. W., Middisov, A., Balukhovsky, A.N., Wold, C.N., Flögel, S., Söding, E. 2006. 'Evaporites and the salinity of the ocean during the Phanerozoic: Implications for climate, ocean circulation and life'. *Palaeogeography, Palaeoclimatology, Palaeoecology*, doi: 10.1016/j.palaeo.2006.03.044.

Hedberg, H. D. 1976. 'International stratigraphic guide: a guide to stratigraphic classification, terminology, and procedure'. *International Stratigraphic Guide*, John Wiley, New York.

Heinemann, M., Jungclaus, J. H. and Marotzke, J. 2009. 'Warm Paleocene/Eocene climate as simulated in ECHAM5/MPI-OM.' *Climate of the Past*, 5(4), pp. 785-802.

Hemleben, C., Spindler, M. and Anderson, O. R. 1989. 'Modern Planktonic Foraminifera'. . New York: Springer-Verlag New York. doi: 10.1007/978-1-4612-3544-6.

Herfort, L., Schouten, S., Boon, J. P. and Sinninghe Damsté, J. S. 2006. 'Application of the TEX_{86} temperature proxy to the southern North Sea'. Orga*nic* Geochemistry, 37, pp. 1715–1726

Hilting, A. K., Kump, L. R. and Bralower, T. J. 2008. 'Variations in the oceanic vertical carbon isotope gradient and their implications for the Paleocene-Eocene biological pump'. *Paleoceanography*, John Wiley & Sons, Ltd, 23(3), p. n/a-n/a. doi: 10.1029/2007PA001458.

Hollis, C. J., Dunkley Jones, T., Anagnostou, E., Bijl, P. K., Cramwinckel, M. J., Cui, Y., Dickens, G. R., Edgar, K. M., Eley, Y., Evans, D., Foster, G. L., Frieling, J., Inglis, G. N., Kennedy, E. M., Kozdon, R., Lauretano, V., Lear, C. H., Littler, K., Lourens, L., Meckler, A. N., Naafs, B. D. A., Pälike, H., Pancost, R. D., Pearson, P. N., Röhl, U., Royer, D. L., Salzmann, U., Schubert, B. A., Seebeck, H., Sluijs, A., Speijer, R. P., Stassen, P., Tierney, J., Tripati, A., Wade, B., Westerhold, T., Witkowski, C., Zachos, J. C., Zhang, Y. G., Huber, M. And Lunt, D. J. 2019. 'The DeepMIP contribution to PMIP4: methodologies for selection, compilation and analysis of latest Paleocene and early Eocene climate proxy data, incorporating version 0.1 of the DeepMIP database'. *Geoscientific Model Development*, 12, pp. 3149–3206. doi: 10.5194/gmd-12-3149-2019.

Hollis, C. J., Handley, L., Crouch, E. M., Morgans, H. E., Baker, J. A., Creech, J., Collins, K. S., Gibbs, S. J., Huber, M., Schouten, S., Zachos, J. C. And Pancost, R. D.

2009. 'Tropical sea temperatures in the high-latitude South Pacific during the Eocene'. *Geology*, 37(2), pp. 99–102. doi: 10.1130/G25200A.1.

Hollis, C. J., Taylor, K. W., Handley, L., Pancost, R. D., Huber, M., Creech, J. B., Hines, B. R., Crouch, E. M., Morgans, H. E., Crampton, J. S., Gibbs, S., Pearson, P. N. And Zachos, J. C. 2012. 'Early Paleogene Temperature History of The Southwest Pacific Ocean: Reconciling Proxies And models'. *Earth and Planetary Science Letters*, 349–350, pp. 53–66. doi: 10.1016/j.epsl.2012.06.024.

Hollstein, M., Mohtadi, M., Rosenthal, Y., Moffa Sanchez, P., Oppo, D., Martínez Méndez, G., Steinke, S. And Hebbeln, D. 2017. 'Stable Oxygen Isotopes and Mg/Ca in Planktic Foraminifera from Modern Surface Sediments of the Western Pacific Warm Pool: Implications for Thermocline Reconstructions'. *Paleoceanography*, 32(11), pp. 1174–1194. doi: 10.1002/2017PA003122.

Holm, R. J., Rosenbaum, G. and Richards, S. W. 2016. 'Post 8 Ma reconstruction of Papua New Guinea and Solomon Islands: Microplate tectonics in a convergent plate boundary setting'. *Earth-Science Reviews*, Elsevier B.V., pp. 66–81. doi: 10.1016/j.earscirev.2016.03.005.

Holsten, J., Stott, L. and Berelson, W. 2004. 'Reconstructing benthic carbon oxidation rates using d 13 C of benthic foraminifers'. *Marine Micropaleontology*, 53(1–2), pp. 117–132. doi: 10.1016/j.marmicro.2004.05.006.

Hönisch, B., Allen, K. A., Lea, D. W., Spero, H. J., Eggins, S. M., Arbuszewski, J., deMenocal, P., Rosenthal, Y., Russell, A. D. And Elderfield, H. 2013. 'The influence of salinity on Mg/Ca in planktic foraminifers - Evidence from cultures, core-top sediments and complementary $\delta^{18}O$'. *Geochimica et Cosmochimica Acta*, 121, pp. 196-213. doi: 10.1016/j.gca.2013.07.028.

Hönisch, B., Ridgwell, A., Schmidt, D. N., Thomas, E., Gibbs, S. J., Sluijs, A., Zeebe, R., Kump, L., Martindale, R. C., Greene, S. E., Kiessling, W., Ries, J., Zachos, J. C., Royer, D. L., Barker, S., Marchitto, T. M., Moyer, R., Pelejero, C., Ziveri, P., Foster, G. L. And Williams, B. 2012. 'The geological record of ocean acidification'. *Science,* 335(6072), pp. 1058–1063. doi: 10.1126/science.1208277.

Horrell, M. A. 1990. 'Energy balance constraints on $\delta^{18}O$ based paleo-sea surface temperature estimates'. *Paleoceanography*, 5, pp. 339–348.

Houben, A. J. P., Bijl, P. K., Sluijs, A., Schouten, S. And Brinkhuis, H. 2019. 'Late Eocene Southern Ocean Cooling and Invigoration of Circulation Preconditioned

Antarctica For Full-Scale Glaciation'. *Geochemistry, Geophysics, Geosystems*, Blackwell Publishing Ltd, 20(5), p. 2019GC008182. doi: 10.1029/2019GC008182.

Huber, M. 2008. 'A hotter greenhouse?'. *Science*, 321 (5887), pp. 353-354.

Huber, M. 2012. 'Progress in greenhouse climate modelling'. In: Linda Ivany, B. H. eds. Reconstructing Earth's Deep-Time Climate – The State of the Art in 2012. *Paleontological Society Papers: The Palaeontological Society*, pp. 213-262.

Huber, M. and Caballero, R. 2003. 'Eocene El Niño: Evidence for robust tropical dynamics in the "hothouse"'. *Science*, 299 (5608), pp. 877-881.

Huber, M. and Caballero, R. 2011. 'The early Eocene equable climate problem revisited'. *Climate of the Past*, 7 (2), pp. 603-633.

Huber, M. and Sloan, L. C. 2000. 'Climatic responses to tropical sea surface temperature changes on a "greenhouse" Earth'. *Paleoceanography*, 15 (4), pp. 443-450.

Huber, M. and Sloan, L. C. 2001. 'Heat transport, deep waters, and thermal gradients: Coupled simulation of an Eocene Greenhouse Climate'. *Geophysical Research Letters*, 28 (18), pp. 3481-3484.

Huck, C. E., Flierdt, T. van de, Bohaty, S. M., and Hammond, S.J., 2017. 'Antarctic climate, Southern Ocean circulation patterns, and deep water formation during the Eocene'. *Palaeoceanography*, 32, pp. 674-691. doi: 10.1002/2017PA003135.

Hut, G. 1987. 'Consultants' group meeting on stable isotope reference samples for geochemical and hydrological investigations'. *Report to the Director General*, (September 1985), pp. 16–18. doi: 18075746.

Inglis, G., Farnsworth, A., Lunt, D., Foster, G., Hollis, C. J., Pagani, M., Jardine, P., Pearson, P., Markwick, P., Galsworthy, A., Raynham, L., Taylor, K. and Pancost, R. D. 2015. 'Descent toward the Icehouse: Eocene sea surface cooling inferred from GDGT distributions'. *Paleoceanography*, 30 (7), pp. 1000-1020.

Jagniecki, E. A., Lowenstein, T. K., Jenkins, D. M. and Demicco, R. V. 2015. 'Eocene atmospheric CO_2 from the nahcolite proxy'. *Geology*, 43, pp. 1075–1078.

Jaramillo, C., Rueda, M. J. and Mora, G. 2006. 'Cenozoic Plant Diversity in the Neotropics'. *Science*, 311 (5769), pp. 1893-1896.

Jin, F. 1996. 'Tropical ocean- atmosphere interaction, the Pacific cold tongue, and the El Niño Southern Oscillation'. *Science* 274 (5284), pp. 76-78.

John, E. H., Pearson, P. N., Coxall, H. K., Birch, H., Wade, B. S. and Foster, G. L. 2013. 'Warm ocean processes and carbon cycling in the Eocene'. *Philosophical Transactions of the Royal Society of London A: Mathematical, Physical and Engineering Sciences*, 371 (2001).

John, E. H., Wilson, J. D., Pearson, P. N. And Ridgwell, A. 2014. 'Temperature-dependent remineralization and carbon cycling in the warm Eocene oceans'. *Palaeogeography, Palaeoclimatology, Palaeoecology*, Elsevier, 413, pp. 158–166. doi: 10.1016/j.palaeo.2014.05.019.

Jones, A. P., Dunkley Jones, T., Coxall, H., Pearson, P. N., Nala, D. And Hoggett, M. 2019. 'Low-Latitude Calcareous Nannofossil Response in the Indo-Pacific Warm Pool Across the Eocene-Oligocene Transition of Java, Indonesia'. *Paleoceanography and Paleoclimatology*, 34(11), pp. 1833–1847. doi: 10.1029/2019PA003597.

Kahn, M. I. 1979. 'Non-equilibrium oxygen and carbon isotopic fractionation in tests of living planktonic foraminifera'. *Oceanologica Acta*, 2(2), pp. 195–208.

Katz, M. E, Katz, D. R., Wright, J. D., Miller, K. G., Pak, D. K., Shackleton, N. J. And Thomas, E. 2003. 'Early Cenozoic benthic foraminiferal isotopes: Species reliability and interspecies correction factors'. *Paleoceanography*, 18(2). doi: 10.1029/2002PA000798.

Katz, M. E., Miller, K. G., Wright, J. D., Wade, B. S., Browning, J. V., Cramer, B. S. And Rosenthal, Y. 2008. 'Stepwise transition from the Eocene greenhouse to the Oligocene icehouse'. *Nature Geoscience*, 1(5), pp.329-334. doi: 10.1038/ngeo179.

Keery, J. S., Holden, P. B. and Edwards, N. R. 2018. 'Sensitivity of the Eocene climate to CO2 and orbital variability'. *Climate of the Past*, 14(2), pp. 215–238. doi: 10.5194/cp-14-215-2018.

Keller, G. 1983. 'Paleoclimatic Analyses of Middle Eocene through Oligocene Planktic Foraminiferal Faunas'. *Palaeoecology*, 43(1-2), pp. 73-94.

Keller, G., Macleod, N., and Barrera, E. 1992. 'Eocene-Oligocene Faunal Turnover and Antarctic Glaciation'. in. Princeton: Princeton University Press, pp. 218–244.

Kennett, J. P. and Shackleton, N. J. 1976. 'Oxygen isotopic evidence for the development of the psychrosphere 38 Myr ago'. *Nature*, 260 (5551), pp. 513-515.

Kennett, J. P. and Srinivasan, M. S. 1983. *Neogene planktonic foraminifera: a phylogenetic atlas*. Stroudsburg, Pa.; New York, NY: Hutchinson Ross; Distributed by worldwide by Van Nostrand Reinhold.

Kerrick, D. M. and Caldeira, K. 1998. 'Metamorphic CO_2 degassing from orogenic belts'. *Chemical Geology*, 145 (3–4), pp. 213-232.

Kiehl, J. 2011. 'Lessons from Earth's Past'. *Science*, 331 (6014), pp. 158-159.

Kiehl, J. and Shields, C. 2013. Sensitivity of the Palaeocene- Eocene Thermal Maximum climate to cloud properties. *Philosophical Transactions of The Royal Society A-Mathematical Physical and Engineering Sciences*, 371 (2001).

Kim, J., Schouten, S., Hopmans, E. C., Donner, B. and Damste, J. 2008. 'Global sediment core- top calibration of the TEX_{86} paleothermometer in the ocean'. *Geochimica et Cosmochimica Acta*, 72 (4), pp. 1154-1173.

Kim, J., Van Der Meer, J., Schouten, S., Helmke, P., Willmott, V., Sangiorgi, F., Koc, N., Hopmans, E. C. and Damste, J. 2010. 'New indices and calibrations derived from the distribution of crenarchaeal isoprenoid tetraether lipids: Implications for past sea surface temperature reconstructions'. *Geochimica et Cosmochimica Acta*, 74(16), pp. 4639-4654.

Kim, S. T., Yu, J.Y. and Lu, M.M. 2012. 'The distinct behaviors of Pacific and Indian Ocean warm pool properties on seasonal and interannual time scales distinct behaviors of Pacific and Indian Ocean warm pool properties on seasonal and interannual time scales'. *Journal of Geophysical Research*, 117, p. 5128. doi: 10.1029/2011JD016557.

Kim, S.T. and O'Neil, J. R. 1997. 'Equilibrium and nonequilibrium oxygen isotope effects in synthetic carbonates'. *Geochimica et Cosmochimica Acta*, Pergamon, 61(16), pp. 3461–3475. doi: 10.1016/S0016-7037(97)00169-5.

Kremer, C. T., Thomas, M. K. and Litchman, E. 2017. 'Temperature- and size-scaling of phytoplankton population growth rates: Reconciling the Eppley curve and the metabolic theory of ecology'. *Limnology and Oceanography*, Wiley Blackwell, 62(4), pp. 1658–1670. doi: 10.1002/lno.10523.

Kroon, D. and Darling, K. 1995. 'Size and upwelling control of the stable isotope composition of Neogloboquadrina dutertrei (d'Orbigny), Globigerinoides ruber (d'Orbigny) and Globigerina bulloides d'Orbigny: examples from the Panama Basin and Arabian Sea'. *Journal of Foraminiferal Research*, 25(1), pp. 39–52. doi: 10.2113/gsjfr.25.1.39.

Kroon, D. and Ganssen, G. 1989. 'Northern Indian Ocean upwelling cells and the stable isotope composition of living planktonic foraminifers'. *Deep Sea Research Part A. Oceanographic Research Papers Deep Sea Research Part A. Oceanographic Research Papers*, 36(8), pp. 1219–1236.

Kroopnick, P. M. 1985. 'The distribution of ^{13}C of ΣCO_2 in the world oceans'. *Deep Sea Research Part A, Oceanographic Research Papers*, Elsevier, 32(1), pp. 57–84. doi: 10.1016/0198-0149(85)90017-2.

Krumhardt, K. M., Lovenduski, N. S., Iglesias-Rodriguez, M. D. And Kleypas, J. A. 2017. 'Coccolithophore growth and calcification in a changing ocean'. *Progress in Oceanography*, Elsevier Ltd, pp. 276–295. doi: 10.1016/j.pocean.2017.10.007.

Kump, L. R. and Pollard, D. 2008. 'Amplification of cretaceous warmth by biological cloud feedbacks'. *Science*, 320, p. 195.

Kvacek, Z. 2010. 'Forest flora and vegetation of the European early Palaeogene - a review'. *Bulletin of Geoscience*s, 85(1), pp. 63-76.

L'Homme, N., Clarke, G. K. C. and Ritz, C. 2005. 'Global budget of water isotopes inferred from polar ice sheets'. *Geophysical Research Letters*, 32(20). doi: 10.1029/2005GL023774.

Lazarus, D., Hollis, C., and Apel, M. 2008. 'Patterns of opal and radiolarian change in the Antarctic mid-Paleogene: Clues to the origin of the Southern Ocean'. *Micropaleontology*, 54, pp. 41–48.

Lea, D. W., Mashiotta, T. A. and Spero, H. J. 1999. 'Controls on magnesium and strontium uptake in planktonic foraminifera determined by live culturing'. *Geochimica et Cosmochimica Acta*, 63(16), pp. 2369–2379. doi: 10.1016/S0016-7037(99)00197-0.

Lea, D. W., Pak, D. K. and Paradis, G. 2005. 'Influence of volcanic shards on foraminiferal Mg/Ca in a core from the Galápagos region'. *Geochemistry,*

Geophysics, Geosystems, John Wiley & Sons, Ltd, 6(11), p. n/a-n/a. doi: 10.1029/2005GC000970.

Lea, D. W., Pak, D. K. and Spero, H. J. 2000, 'Climate impact of late quaternary equatorial Pacific sea surface temperature variations'. *Science*, 289(5485), pp. 1719–1724. doi: 10.1126/science.289.5485.1719.

Lear, C. H., Bailey, T. R., Pearson, P. N., Coxall, H. K. And Rosenthal, Y. 2008. 'Cooling and ice growth across the Eocene-Oligocene transition'. *Geology*, 36(3), pp. 251–254. doi: 10.1130/G24584A.1.

Lear, C. H., Coxall, H. K., Foster, G. L., Lunt, D. J., Mawbey, E. M., Rosenthal, Y., Sosdian, S. M., Thomas, E. And Wilson, P. A. 2015. 'Neogene ice volume and ocean temperatures: Insights from infaunal foraminiferal Mg/Ca paleothermometry'. *Paleoceanography*, doi: 10.1002/2015PA002833.

Lear, C. H., Elderfield, H. and Wilson, P. A. 2000. 'Cenozoic deep-sea temperatures and global ice volumes from Mg/Ca in benthic foraminiferal calcite'. *Science*, 287(5451), pp. 269–272. doi: 10.1126/science.287.5451.269.

Lear, C. H., Mawbey, E. M. and Rosenthal, Y. 2010. 'Cenozoic benthic foraminiferal Mg/Ca and Li/Ca records: Toward unlocking temperatures and saturation states'. *Paleoceanography*, Blackwell Publishing Ltd, 25(4), p. n/a-n/a. doi: 10.1029/2009PA001880.

Lear, C. H., Rosenthal, Y. and Slowey, N. 2002. 'Benthic foraminiferal Mg/Ca-paleothermometry: A revised core-top calibration'. *Geochimica et Cosmochimica Acta*, 66(19), pp. 3375–3387. doi: 10.1016/S0016-7037(02)00941-9.

Leckie, R., Wade, B.S. Pearson, P.N., Fraass, A.J., King, D.J. Olsson, R.K. Premoli Silva, I. Spezzaferri, S., Berggren, W.A. 2018. 'Taxonomy, biostratigraphy, and phylogeny of Oligocene and early Miocene *Paragloborotalia* and *Parasubbotina'*. In: Wade, BS and Olsson, RK and Pearson, PN and Huber, BT and Berggren, WA, (eds.) *Atlas of Oligocene Planktonic Foraminifera. (pp. 125-178). Cushman Foundation for Foraminiferal Research: Lawrence, KS, USA.*

LeGrande, A. N. and Schmidt, G. A. 2006. 'Global gridded data set of the oxygen isotopic composition in seawater'. *Geophysical Research Letters* 33(12), doi: 10.1029/2006GL026011.

Leipper, D. F. 1967. 'Observed Ocean Conditions and Hurricane Hilda, 1964'. *Journal of the Atmospheric Sciences*, 24(2), pp. 182–186. doi: 10.1175/1520-0469(1967)024<0182:OOCAHH>2.0.CO;2.

Lin, C., Ho, C. R., Lee, Y., Kuo, N. and Liang, S. J. 2013. 'Thermal variability of the Indo-Pacific warm pool'. *Global and Planetary Change*, 100, pp. 234-244.

Lipps, J. H. 1966. 'Wall Structure, Systematics, and Phylogeny Studies of Cenozoic Planktonic, Source'. *Journal of Paleontology,* 40(6), pp. 1257-1274.

Liu, Z. and B. Huang, 1997. A coupled theory of tropical climatology: Warm pool, cold tongue and Walker Circulation. *Journal of Climate,* 10, pp. 1662-1679.

Liu, Z., Pagani, M., Zinniker, D., Deconto, R., Huber, M., Brinkhuis, H., Shah, Sr., Leckie, R. M. and Pearson, A. 2009. 'Global Cooling During the Eocene- Oligocene Climate Transition'. *Science,* 323(5918), pp. 1187-1190.

Lohmann, G. P. and Schweitzer, P. N. 1990. '*Globorotalia truncatulinoides*'' Growth and chemistry as probes of the past thermocline: 1. Shell size'. *Paleoceanography and Paleoclimatology*, 5(1), pp. 55–75. doi: 10.1029/PA005i001p00055.

Lombard, F., Labeyrie, L., Michel, E., Spero, H. J. And Lea, D. W. 2009. 'Modelling the temperature dependent growth rates of planktic foraminifera'. *Marine Micropaleontology*, 70(1–2), pp. 1–7. doi: 10.1016/j.marmicro.2008.09.004.

Lončarić, N., Peeters, F. J. C., Kroon, D. And Brummer, G. A. 2006. 'Oxygen isotope ecology of recent planktic foraminifera at the central Walvis Ridge (SE Atlantic)'. *Paleoceanography and Paleoclimatology*, 21(3). doi: 10.1029/2005PA001207.

López-Urrutia, Á., San Martin, E., Harris, R. P. And Irigoien, X. 2006. 'Scaling the metabolic balance of the oceans'. *Proceedings of the National Academy of Sciences of the United States of America*, National Academy of Sciences, 103(23), pp. 8739–8744. doi: 10.1073/pnas.0601137103.

Loptson, C. A., Lunt, D. J. and Francis, J. E. 2014. 'Investigating vegetation-climate feedbacks during the early Eocene'. *Climate of the Past*, 10(2), pp. 419–436. doi: 10.5194/cp-10-419-2014.

Loubere, P. 1987. 'Changes in mid-depth North Atlantic and Mediterranean circulation during the Late Pliocene - Isotopic and sedimentological evidence'. *Marine Geology*, 77(1–2), pp. 15–38. doi: 10.1016/0025-3227(87)90081-8.

Lunt, D. J. *et al.* (2010) 'Haywood, A. M., Schmidt, G. A., Salzmann, U., Valdes, P. J. And Dowsett, H. J., *Nature Geoscience*, 3(1), pp. 60–64. Doi: 10.1038/Ngeo706.

Lunt, D.J., Haywood, A.M., Schmidt, G.A., Salzmann, U., Valdes, P.J., and Dowsett, H.J. 2010. 'Earth system sensitivity inferred from Pliocene modelling and data'. *Nature Geosciences*, 3, pp. 60-64. doi:10.1038/NGEO706.

Lunt, D. J., Dunkley Jones, T., Heinemann, M., Huber, M., Legrande, A., Winguth, A., Loptson, C., Marotzke, J., Roberts, C. D., Tindall, J., Valdes, P. and Winguth, C. 2012. 'A model-data comparison for a multi-model ensemble of Early Eocene atmosphere-ocean simulations: EoMIP'. *Climate of the Past*, 8(5), pp. 1717-1736.

Lunt, D. J., Elderfield, H., Pancost, R., Ridgwell, A., Foster, G., Haywood, A., Kiehl, J., Sagoo, N., Shields, C., Stone, E. and Valdes, P. 2013. 'Warm climates of the past - a lesson for the future? '*Philosophical Transactions of The Royal Society A-Mathematical Physical and Engineering Sciences*, 371(2001).

Lunt, D. J., Farnsworth, A., Loptson, C., Foster, G. L., Markwick, P., O'brien, C. L., Pancost, R. D., Robinson, S. A. and Wrobel, N. 2015. 'Palaeogeographic controls on climate and proxy interpretation'. *Climate of the Past Discussions*, 11(6), pp. 5683-5725.

Lunt, D. J., Farnsworth, A., Loptson, C., Foster, G. L., Markwick, P., O'Brien, C. L., Pancost, R. D., Robinson, S. A. And Wrobel, N. 2016. 'Palaeogeographic controls on climate and proxy interpretation'. *Climate of the Past*, 12(5), pp. 1181–1198. doi: 10.5194/cp-12-1181-2016.

Lunt, D. J., Huber, M., Anagnostou, E., Baatsen, M. L. J., Caballero, R., Deconto, R., Dijkstra, H. A., Donnadieu, Y., Evans, D., Feng, R., Foster, G. L., Gasson, E., Von Der Heydt, A. S., Hollis, C. J., Inglis, G. N., Jones, S. M., Kiehl, J., Kirtland Turner, S., Korty, R. L., Kozdon, R., Krishnan, S., Ladant, J., Langebroek, P., Lear, C. H., Legrande, A. N., Littler, K., Markwick, P., Otto-Bliesner, B., Pearson, P., Poulsen, C. J., Salzmann, U., Shields, C., Snell, K., Stärz, M., Super, J., Tabor, C., Tierney, J. E., Tourte, G. J. L., Tripati, A., Upchurch, G. R., Wade, B. S., Wing, S. L., Winguth, A. M. E., Wright, N. M., Zachos, J. C. And Zeebe, R. E. 2017. 'The DeepMIP contribution to PMIP4: experimental design for model simulations of the EECO, PETM, and pre-PETM (version 1.0)'. *Geoscientific Model Development*, 10, pp. 889–901. doi: 10.5194/gmd-10-889-2017.

Lunt, P., and Sugiatno, H. in press. 'A review of the Eocene and Oligocene in the Nanggulan area, south central Java'. GRDC Report.

Lynch-Stieglitz, J., Stocker, T. F., Broecker, W. S. and Fairbanks, R. G. 1995. 'The influence of air-sea exchange on the isotopic composition of oceanic carbon: Observations and modeling'. *Global Biogeochemical Cycles*, John Wiley & Sons, Ltd, 9(4), pp. 653–665. doi: 10.1029/95GB02574.

Mackensen, A., Schumacher, S., Radke, J. And Schmidt, D. 2000. 'Microhabitat Preferences and Stable Carbon Isotopes of Endobenthic Foraminifera: Clue to quantitative reconstruction of oceanic new production?'. *Marine Micropaleontology*, Elsevier, 40(3), pp. 233–258. doi: 10.1016/S0377-8398(00)00040-2.

Makarova, M., Wright, J. D., Miller, K. G., Babila, T. L., Rosenthal, Y. And Park, J. I. 2017. 'Hydrographic And ecologic implications of foraminiferal stable isotopic response across the U.S. mid-Atlantic continental shelf during the Paleocene-Eocene Thermal Maximum'. *Paleoceanography*, 32(1), pp. 56–73. doi: 10.1002/2016PA002985.

Markwick, P. J. (2007) 'The palaeogeographic and palaeoclimatic significance of climate proxies for data-model comparisons'. *Geological Society Special Publication*, pp. 251–312. doi: 10.1144/tms002.13.

Markwick, P. J. 1998. 'Fossil crocodilians as indicators of Late Cretaceous and Cenozoic climates: Implications for using palaeontological data in reconstructing palaeoclimate'. *Palaeogeography, Palaeoclimatology, Palaeoecology*, 137(3-4), pp. 205-271.

Markwick, P. J. and Valdes, P. J. 2004. 'Palaeo-digital elevation models for use as boundary conditions in coupled ocean–atmosphere GCM experiments: a Maastrichtian (late Cretaceous) example'. *Palaeogeography, Palaeoclimatology, Palaeoecology*, 213, pp. 37–63. doi: 10.1016/j.palaeo.2004.06.015.

Martin, P. A. and Lea, D. W. 2002. 'A simple evaluation of cleaning procedures on fossil benthic foraminiferal Mg/Ca'. *Geochemistry, Geophysics, Geosystems*, Blackwell Publishing Ltd, 3(10). doi: 10.1029/2001GC000280.

Mashiotta, T. A., Lea, D. W. and Spero, H. J. 1999. 'Glacial-interglacial changes in Subantarctic sea surface temperature and δ^{18}O-water using foraminiferal Mg'.

Earth and Planetary Science Letters, Elsevier, 170(4), pp. 417–432. doi: 10.1016/S0012-821X(99)00116-8.

Matsui, H., Nishi, H., Takashima, R., Kuroyanagi, A., Ikehara, M., Takayanagi, H. And Iryu, Y. 2016. 'Changes in The Depth Habitat of The Oligocene Planktic Foraminifera (*Dentoglobigerina venezuelana*) induced by thermocline deepening in the eastern equatorial Pacific'. *Paleoceanography*, Blackwell Publishing Ltd, 31(6), pp. 715–731. doi: 10.1002/2016PA002950.

Mawbey, E. M. and Lear, C. H. 2013. 'Carbon cycle feedbacks during the oligocene-miocene transient glaciation'. *Geology*, 41(9), pp. 963–966. doi: 10.1130/G34422.1.

McConnaughey, T. 1989. '^{13}C and ^{18}O isotopic disequilibrium in biological carbonates: I. Patterns'. *Geochimica et Cosmochimica Acta*, 53(1), pp. 151–162. doi: 10.1016/0016-7037(89)902822.

McCorkle, D. C. Keigwin, L. D., Corliss, B. H. And Emerson, S. R. 1990. 'The influence of microhabitats on the carbon isotopic composition of deep-sea benthic foraminifera'. *Paleoceanography*, John Wiley & Sons, Ltd, 5(2), pp. 161–185. doi: 10.1029/PA005i002p00161.

McCorkle, D. C., Bernhard, J. M., Hintz, C. J., Blanks, J. K., Chandler, G. T. And Shaw, T. J. 2008. 'The carbon and oxygen stable isotopic composition of cultured benthic foraminifera'. *Geological Society Special Publication*, Geological Society of London, 303(1), pp. 135–154. doi: 10.1144/SP303.10.

McCorkle, D. C., Emerson, S. R. and Quay, P. D. 1985. 'Stable carbon isotopes in marine porewaters'. *Earth and Planetary Science Letters*, Elsevier, 74(1), pp. 13–26. doi: 10.1016/0012-821X(85)90162-1.

Mccrea, J. M. 1950. 'On the Isotopic Chemistry of Carbonates and a Paleotemperature Scale'. *The Journal of Chemical Physics*, 18, p. 391. doi: 10.1063/1.1747785.

McInerney, F. A. and Wing, S. L. 2011. 'The Paleocene-Eocene Thermal Maximum: A Perturbation of Carbon Cycle, Climate, and Biosphere with Implications for the Future'. *Annual Review of Earth and Planetary Sciences*, 39(1), pp. 489-516.

Mcphaden, M. and Picaut, J. 1990. 'El-Niño Southern Oscillation Displacements Of The Western Equatorial Pacific Warm Pool'. *Science*, 250(4986), pp. 1385-1388.

Mikolajewicz, U. and Crowley, T. J. 1997. Response of a coupled ocean/energy balance model to restricted flow through the Central American Isthmus. *Paleoceanography*, 12(3), pp. 429-441.

Miller, K. G., Wright, J. D. and Browning, J. V. 2005. 'Visions of ice sheets in a greenhouse world'. *Marine Geology*, 217(3–4), pp. 215–231. doi: 10.1016/j.margeo.2005.02.007.

Moyes, C. D. and Schulte, P. M. 2008. *Principles of animal physiology.* San Francisco; London: Pearson/Benjamin Cummings.

Mucci, A. 1987. 'Influence of temperature on the composition of magnesian calcite overgrowths precipitated from seawater'. *Geochimica et Cosmochimica Acta*, Pergamon, 51(7), pp. 1977–1984. doi: 10.1016/0016-7037(87)90186-4.

Mucci, A. and Morse, J. W. 1983. 'The incorporation of Mg2+ and Sr2+ into calcite overgrowths: influences of growth rate and solution composition'. *Geochimica et Cosmochimica Acta*, 47(2), pp. 217–233. doi: 10.1016/0016-7037(83)90135-7.

Mulitza, S., Dürkoop, A., Hale, W., Wefer, G. And Stefan Niebler, H. 1997. 'Planktonic foraminifera as recorders of past surface-water stratification'. *Geology*. Geological Society of America, 25(4), pp. 335–338. doi: 10.1130/0091-7613(1997)025<0335:PFAROP>2.3.CO;2.

Neelin, J. D., Battisti, D. S., Hirst, A. C., Jin, F.F., Wakata, Y., Yamagata, T. and Zebiak, S. E. 1998. 'ENSO theory'. *Journal of Geophysical Research: Oceans*, 103(C7), pp. 14261-14290.

Nieto-Moreno, V., Martínez-Ruiz, F., Gallego-Torres, D., Ortega-Huertas, S., Giralt, J., García-Orellana, P., Masqué, P., Masqué, J. S. and Sinninghe Damsté, M. 2015. 'Palaeoclimate and palaeoceanographic conditions in the westernmost mediterranean over the last millennium: An integrated organic and inorganic approach'. Jo*urnal of the Geological Society*, 172(2), pp. 264-271.

Norris, R. D. 1996. 'Symbiosis as an Evolutionary Innovation in the Radiation of Paleocene Planktic Foraminifera'. *Paleobiology*, 22(4), pp. 461–480.

Norris, R. D. and Wilson, P. A. 1998. 'Low- latitude sea- surface temperatures for the mid- Cretaceous and the evolution of planktic foraminifera'. *Geology*, 26(9), pp. 823-826.

Norris, R. D. and Wilson, P. A. 1999. 'Low-latitude sea-surface temperatures for the mid-Cretaceous and the evolution of planktic foraminifera: Reply'. *Geology*, 27(9), pp. 857-858.

Olsson, R. K, Berggren, W. A., Hemleben, C. And Huber, B. T. 1999. 'Atlas of Paleocene Planktonic Foraminifera'. *Smithsonian Contributions to Paleobiology*, (85), pp. 1–252. doi: 10.5479/si.00810266.85.1.

Ortiz, J. D., Mix, A., Rugh, W., Watkins, J. And Collier, R. 1996. 'Deep-dwelling planktonic foraminifera of the northeastern Pacific Ocean reveal environmental control of oxygen and carbon isotopic disequilibria'. *Geochimica et Cosmochimica Acta*, 60(22), pp. 4509–4523. doi: 10.1016/S0016-7037(96)00256-6.

Pagani, M., Huber, M., Liu, Z., Bohaty, S. M., Henderiks, J., Sijp, W., Krishnan, S. And Deconto, R. M. 2011. 'The role of carbon dioxide during the onset of antarctic glaciation'. *Science*, American Association for the Advancement of Science, 334(6060), pp. 1261–1264. doi: 10.1126/science.1203909.

Pagani, M., Zachos, J. C., Freeman, K. H., Tipple, B. and Bohaty, S. 2005. 'Marked Decline in Atmospheric Carbon Dioxide Concentrations During the Paleogene'. *Science*, 309(5734), pp. 600-603.

Pahnke, K., Zahn, R., Elderfield, H. and Schulz, M. 2003. '340,000- year centennial-scale marine record of Southern Hemisphere climatic oscillation'. *Science*, 301(5635), pp. 948-952.

Pascher, K. M., Hollis, C. J., Bohaty, S. M., Cortese, G., McKay, R. M., Seebeck, H., Suzuki, N., and Chiba, K., 2015. Expansion and diversification of high-latitude radiolarian assemblages in the late Eocene linked to a cooling event in the southwest Pacific, *Climate of the. Past*, 11, pp. 1599–1620. doi: 10.5194/cp-11-1599-2015, 2015.

Pearson, P. and Palmer, M. 2000. 'Atmospheric carbon dioxide concentrations over the past 60 million years'. *Nature*, 406(6797), pp. 695-699.

Pearson, P. N. 1996. 'Cladogenetic, Extinction and Survivorship Patterns from a Lineage Phylogeny: The Paleogene Planktonic Foraminifera'. *Micropaleontology*, 42(2), pp. 179-188. doi: 10.2307/1485869.

Pearson, P. N. 1998. 'Speciation and Extinction Asymmetries in Paleontological Phylogenies: Evidence for evolutionary progress?'. *Paleobiology*, 24(3), pp. 305-335.

Pearson, P. N. 2012. 'Oxygen isotopes in foraminifera: Overview and historical review'. *Paleontological Society Papers*, 18, pp. 1-38.

Pearson, P. N. and Burgess, C. E. 2008. 'Foraminifer test preservation and diagenesis: comparison of high latitude Eocene sites'. In: Austin, W. E. N. et al. eds. Biogeochemical Controls on Palaeoceanographic Proxies. *The Geological Society, London, Special Publications*, 303(1), pp.59-72. pp. 59–72.

Pearson, P. N. and Palmer, M. R. 1999. 'Middle Eocene seawater pH and atmospheric carbon dioxide concentrations'. *Science*, 284(5421), pp. 1824–1826. doi: 10.1126/science.284.5421.1824.

Pearson, P. N. and Wade, B. S. 2009. 'Taxonomy and stable isotope paleoecology of well-preserved planktonic foraminifera from the uppermost Oligocene of Trinidad'. *Journal of Foraminiferal Research*, 39(3), pp. 191–217. doi: 10.2113/gsjfr.39.3.191.

Pearson, P. N., Ditchfield, P. W., Singano, J., Harcourt-Brown, K. G., Nicholas, C. J., Olsson, R. K., Shackleton, N. J. and Hall, M. A. 2001. 'Warm tropical sea surface temperatures in the Late Cretaceous and Eocene epochs'. *Nature*, 413(6855), pp. 481-487.

Pearson, P. N., Evans, S. L. and Evans, J. 2015. 'Effect of diagenetic recrystallization on the strength of planktonic foraminifer tests under compression'. *Journal of Micropalaeontology*, 34(1), pp. 59-64. doi: 10.1144/jmpaleo2013-032.

Pearson, P. N., Foster, G. and Wade, B. S. 2009. 'Atmospheric carbon dioxide through the Eocene- Oligocene climate transition'. *Nature*, 461(7267), pp. 1110-1204.

Pearson, P. N., Mcmillan, I. K., Wade, B. S., Jones, T. D., Coxall, H. K., Bown, P. R. And Lear, C. H. 2008. 'Extinction and environmental change across the Eocene-Oligocene boundary in Tanzania'. *Geology*, 36(2), pp. 179–182. doi: 10.1130/G24308A.1.

Pearson, P. N., Olsson, Richard K., Huber, Brian T., Hemleben, C. and Berggren, W. A. 2006. *Atlas of Eocene planktonic foraminifera*. Fredericksburg: Cushman Foundation for Foraminiferal Research.

Pearson, P. N., Shackleton, N. J. and Hall, M. A. 1993. 'Stable isotope paleoecology of Middle Eocene planktonic foraminifera and multi-species isotope stratigraphy, DSDP Site 523, South Atlantic'. *Journal of Foraminiferal Research*, 23(2), pp. 123–146. doi: 10.2113/gsjfr.23.2.123.

Pearson, P. N., Van Dongen, B. E., Nicholas, C. J., Pancost, R. D., Schouten, S., Singano, J. M. and Wade, B. S. 2007. 'Stable warm tropical climate through the Eocene Epoch'. *Geology*, 35(3), pp. 211-214.

Pedersen, T. F. and Price, N. B. 1982. 'The geochemistry of manganese carbonate in Panama Basin sediments'. *Geochimica et Cosmochimica Acta*, Pergamon, 46(1), pp. 59–68. doi: 10.1016/0016-7037(82)90290-3.

Pena, L. D., Calvo, E., Cacho, I., Eggins, S. And Pelejero, C. 2005. 'Identification and removal of Mn-Mg-rich contaminant phases on foraminiferal tests: Implications for Mg/Ca past temperature reconstructions'. *Geochemistry, Geophysics, Geosystems*, 6(9). doi: 10.1029/2005GC000930.

Penman, D. E., Hönisch, B., Zeebe, R. E., Thomas, E. And Zachos, J. C. 2014. 'Rapid and sustained surface ocean acidification during the Paleocene-Eocene Thermal Maximum'. *Paleoceanography*, 29(5), pp.357-369. doi: 10.1002/2014PA002621.

Pierrehumbert, R. T. 1995. 'Thermostats, Radiator Fins, and the Local Runaway Greenhouse'. *Journal of the Atmospheric Sciences*, 52(10), pp. 1784–1806. doi: 10.1175/1520-0469(1995)052<1784:TRFATL>2.0.CO;2.

Pierrehumbert, R. T. 2000. 'Climate change and the tropical Pacific: The sleeping dragon wakes'. *Proceedings of the National Academy of Sciences*, 97(4), pp. 1355-1358.

Pierrehumbert, R. T. 2002. 'The hydrologic cycle in deep- time climate problems'. *Nature*, 419(6903), p. 191.

Pigram, C. J. and Symonds, P. A. 1991. 'A review of the timing of the major tectonic events in the New Guinea Orogen'. *Journal of Southeast Asian Earth Sciences*, doi: 10.1016/0743-9547(91)90076-A.

Poore, R. Z. and Matthews, R. K. 1984. 'Oxygen isotope ranking of late Eocene and Oligocene planktonic foraminifers: Implications for Oligocene sea-surface temperatures and global ice-volume'. *Marine Micropaleontology*, 9(2), pp. 111–134. doi: 10.1016/0377-8398(84)90007-0.

Port, U. and Claussen, M. 2015. 'Transitivity of the climate–vegetation system in a warm climate'. *Climate of the Past*, 11, pp. 1563-1574.

Pusz, A. E., Thunell, R. C. and Miller, K. G. 2011. 'Deep water temperature, carbonate ion, and ice volume changes across the Eocene-Oligocene climate transition'. Paleoceanography 2(26). doi: 10.1029/2010PA001950.

Quillévéré, F., Norris, R. D., Moussa, I. And Berggren, W. A 2001. 'Role of photosymbiosis and biogeography in the diversification of early Paleogene acarininids (planktonic foraminifera)'. *Paleobiology*, Cambridge University Press (CUP), 27(2), pp. 311–326. doi: 10.1666/0094-8373(2001)027<0311:ropabi>2.0.co;2.

Ramstein, G., Fluteau, F., Besse, J. and Joussaume, S. 1997. 'Effect of orogeny, plate motion and land sea distribution on Eurasian climate change over the past 30 million years'. *Nature*, 386(6627), pp. 788-795.

Rasmusson, E. M. and Wallace, J. M. 1983. 'Meteorological aspects of the El Niño/ Southern Oscillation'. *Science*, 222(4629), pp. 1195-1202.

Rasmusson, E. M. and Wallace, J. M. 1983. Meteorological aspects of the El Niño/ Southern Oscillation. *Science*, 222(4629), pp. 1195-1202.

Rathmann, S. and Kuhnert, H. 2008. 'Carbonate ion effect on Mg/Ca, Sr/Ca and stable isotopes on the benthic foraminifera *Oridorsalis umbonatus* off Namibia'. *Marine Micropaleontology*, 66(2), pp. 120–133. doi: 10.1016/j.marmicro.2007.08.001.

Ravelo, A. C. and Fairbanks, R. G. 1992. 'Oxygen Isotopic Composition of Multiple Species of Planktonic Foramtnifera: Recorders of The Modern Photic Zone Temperature Gradient'. *Paleoceanography*, 6(7), pp. 815-831.

Ravelo, A. C. and Fairbanks, R. G. 1995. 'Carbon isotopic fractionation in multiple species of planktonic foraminifera from core-tops in the tropical Atlantic'. *Journal of Foraminiferal Research*, 25(1), pp. 53–74. doi: 10.2113/gsjfr.25.1.53.

Ravelo, A. C. and Hillaire-Marcel, C. 2007. *Proxies in Late Cenozoic Paleoceanography*, *Developments in Marine Geology*. doi: 10.1016/S1572-5480(07)01023-8.

Raymo, M. E. and Ruddiman, W. F. 1992. 'Tectonic forcing of late Cenozoic climate'. *Nature*, 359(6391), pp. 117-122.

Regaudie-de-Gioux, A. and Duarte, C. M. 2012, 'Temperature dependence of planktonic metabolism in the ocean'. *Global Biogeochemical Cycles*, John Wiley & Sons, Ltd, 26(1), p. n/a-n/a. doi: 10.1029/2010GB003907.

Regenberg, M., Regenberg, A., Garbe-Schönberg, D. And Lea, D. W. 2014, 'Global dissolution effects on planktonic foraminiferal Mg/Ca ratios controlled by the calcite-saturation state of bottom waters'. *Paleoceanography*, American Geophysical Union, 29(3), pp. 127–142. doi: 10.1002/2013PA002492.

Resig, J. M. and Kroopnick, P. M. 1983, 'Isotopic and distributional evidence of a planktonic habit for the foraminiferal genus *Streptochilus* Brönnimann and Resig, 1971'. *Marine Micropaleontology*, Elsevier, 8(3), pp. 235–248. doi: 10.1016/0377-8398(83)90026-9.

Rind, D. 1998. 'Latitudinal temperature gradients and climate change'. *Journal of Geophysical Research: Atmospheres*, 103(D6), pp. 5943-5971.

Rink, S., Ühl, M., Bijma, J. And Spero, H. J. 1998, 'Microsensor studies of photosynthesis and respiration in the symbiotic foraminifer *Orbulina universa'. Marine Biology*, Springer-Verlag, 131(4), pp. 583–595. doi: 10.1007/s002270050350.

Roberts, C. D., Legrande, A. N. and Tripati, A. K. 2009. 'Climate sensitivity to Arctic seaway restriction during the early Paleogene'. *Earth and Planetary Science Letters*, 286(3), pp. 576-585.

Roberts, C. D., Legrande, A. N. and Tripati, A. K. 2011. 'Sensitivity of seawater oxygen isotopes to climatic and tectonic boundary conditions in an early Paleogene simulation with GISS ModelE-R'. *Paleoceanography*, 26(4).

Rohling, E. J. 2013, Oxygen Isotope Composition of Seawater. In: Elias S.A. (ed.) The *Encyclopedia of Quaternary Science*, 2, pp. 915-922. Amsterdam: Elsevier.

Rohling, E. J. and Cooke, S. 1999. 'Stable oxygen and carbon isotope ratios in foraminiferal carbonate'. In: Sen Gupta, B. K. eds. *Modern Foraminifera*. Dordrecht, The Netherlands: Kluwer Academic, pp. 239-258.

Rohling, E. J., Sprovieri, M., Cane, T., Casford, J., Cooke, S., Bouloubassi, I., Emeis, K., Schiebel, R., Rogerson, M., Hayes, A., Jorissen, F. And Kroon, D. 2004. 'Reconstructing past planktic foraminiferal habitats using stable isotope data: a case history for Mediterranean sapropel S5'. *Marine Micropaleontology*, 50(1–2), pp. 89–123. doi: 10.1016/S0377-8398(03)00068-9.

Rollion-Bard, C., Erez, J. and Zilberman, T. 2008. 'Intra-shell oxygen isotope ratios in the benthic foraminifera genus *Amphistegina* and the influence of seawater carbonate chemistry and temperature on this ratio'. *Geochimica et Cosmochimica* Acta, 72(24), pp. 6006-6014doi: 10.1016/j.gca.2008.09.013.

Rongstad, B. L., Marchitto, T. M. and Herguera, J. C. 2017. 'Understanding the Effects of Dissolution on the Mg/Ca Paleothermometer in Planktic Foraminifera: Evidence from a Novel Individual Foraminifera Method'. *Paleoceanography*, Blackwell Publishing Ltd, 32(12), pp. 1386–1402. doi: 10.1002/2017PA003179.

Rosenthal, Y. and Lohmann, G. P. 2002. 'Accurate estimation of sea surface temperatures using dissolution-corrected calibrations for Mg/Ca paleothermometry'. *Paleoceanography*, American Geophysical Union (AGU), 17(3), pp. 16-1-16–6. doi: 10.1029/2001pa000749.

Rosenthal, Y., Boyle, E. A. and Slowey, N. 1997. 'Temperature control on the incorporation of magnesium, strontium, fluorine, and cadmium into benthic foraminiferal shells from Little Bahama Bank: Prospects for thermocline paleoceanography'. *Geochimica et Cosmochimica Acta*, Elsevier Ltd, 61(17), pp. 3633–3643. doi: 10.1016/S0016-7037(97)00181-6.

Rosenthal, Y., Lohmann, G. P., Lohmann, K. C. And Sherrell, R. M. 2000. 'Incorporation and preservation of Mg in *Globigerinoides sacculifer*: Implications for reconstructing the temperature and $^{18}O/^{16}O$ of seawater'. *Paleoceanography*, Blackwell Publishing Ltd, 15(1), pp. 135–145. doi: 10.1029/1999PA000415.

Rosenthal, Y., Oppo, D. and Linsley, B. 2003. 'The amplitude and phasing of climate change during the last deglaciation in the Sulu Sea, western equatorial Pacific'. *Geophysical Research Letters*, 30(8).

Royer, D. L., Ani, M. P. and Beerling, D. J. 2012. 'Geobiological constraints on Earth system sensitivity to CO2 during the Cretaceous and Cenozoic'. *Geobiology*, 10, pp. 298–310. doi: 10.1111/j.1472-4669.2012.00320.x.

Royer, D. L., Wing, S. L., Beerling, D. J., Jolley, D. W., Koch, P. L., Hickey, L. J. and Berner, R. A. 2001. 'Paleobotanical Evidence for Near Present-Day Levels of Atmospheric CO_2 during Part of the Tertiary'. *Science*, 292(5525), pp. 2310-2313.

Russell, A. D. and Spero, H. J. 2000. 'Field examination of the oceanic carbonate ion effect on stable isotopes in planktonic foraminifera'. *Paleoceanography*, Blackwell Publishing Ltd, 15(1), pp. 43–52. doi: 10.1029/1998PA000312.

Russell, A. D., Hönisch, B., Spero, H. J. And Lea, D. W. 2004. 'Effects of seawater carbonate ion concentration and temperature on shell U, Mg, and Sr in cultured planktonic foraminifera'. *Geochimica et Cosmochimica Acta*, Pergamon, 68(21), pp. 4347–4361. doi: 10.1016/j.gca.2004.03.013.

Sadekov, A. Y., Eggins, S. M. and De Deckker, P. 2005. 'Characterization of Mg/Ca distributions in planktonic foraminifera species by electron microprobe mapping'. *Geochemistry, Geophysics, Geosystems*, 6(12). doi: 10.1029/2005GC000973.

Sagoo, N., Valdes, P., Flecker, R. and Gregoire, L. J. 2013. 'The Early Eocene equable climate problem: can perturbations of climate model parameters identify possible solutions?'. *Philosophical Transactions of the Royal Society of London A: Mathematical, Physical and Engineering Sciences*, 371(2001).

Sarmiento, J. L., Slater, R., Barber, R., Bopp, L., Doney, S.C., Hirst,A.C., Klevpas, J., Matear, R., Mikolajewicz, U., Monfray, P., Soldatovc, V., Spall, S.A.,Stouffer, R. 2004. 'Response of ocean ecosystems to climate warming'. *Global Biogeochemical Cycles*, John Wiley & Sons, Ltd, 18(3). doi: 10.1029/2003GB002134.

Scher, H. D. and Martin, E. E. 2006. 'Timing and climatic consequences of the opening of drake passage'. *Science*, 312(5772), pp. 428–430. doi: 10.1126/science.1120044.

Scher, H. D., Bohaty, S. M., Smith, B. W. And Munn, G. H. 2014. 'Isotopic interrogation of a suspected late Eocene glaciation'. *Paleoceanography*, Blackwell Publishing Ltd, 29(6), pp. 628–644. doi: 10.1002/2014PA002648.

Schiebel, R. 2002. 'Planktic foraminiferal sedimentation and the marine calcite budget'. *Global Biogeochemical Cycles*, doi: 10.1029/2001gb001459.

Schiebel, R. and Hemleben, C. 2005. 'Modern planktic foraminifera'. *Paläontologische Zeitschrift*, Springer Science and Business Media LLC, 79(1), pp. 135–148. doi: 10.1007/bf03021758.

Schilman, B., Almogi-Labin, A., Bar-Matthews, M. And Luz, B. 2003. 'Late Holocene productivity and hydrographic variability in the eastern Mediterranean inferred from benthic foraminiferal stable isotopes'. *Paleoceanography*, American Geophysical Union (AGU), 18(3), p. n/a-n/a. doi: 10.1029/2002pa000813.

Schmidt, D., Elliott, T. and Kasemann, S. 2008. 'The influences of growth on planktic foraminifers as proxies for palaeostudies'. *Geological Society of London*, pp. 73–85.

Schmidt, G. A., Bigg, G. R. and Rohling., E. J. 1999. *Global Seawater Oxygen-18 Database - v1.22*. Available at: https://data.giss.nasa.gov/o18data/

Schmidt, G., A. 1999. 'Forward modelling of carbonate proxy data from planktonic foraminifera using oxygen isotope tracers in a global ocean model.' *Paleoceanography*, 14(4), pp. 482-497.

Schmidt, M. W., Vautravers, M. J. and Spero, H. J. 2006. 'Western Caribbean sea surface temperatures during the late Quaternary'. *Geochemistry, Geophysics, Geosystems*, 7(2), p. n/a-n/a. doi: 10.1029/2005GC000957.

Schneider, E. K., Lindzen, R. S. and Kirtman, B. P. 1997. 'A Tropical Influence on Global Climate'. *Journal of the Atmospheric Sciences*, 54(10), pp. 1349-1358.

Schouten, S., Forster, A., Panoto, F. and Damste, J. 2007. 'Towards calibration of the TEX$_{86}$ palaeothermometer for tropical sea surface temperatures in ancient greenhouse worlds'. *Organic Geochemistry*, 38(9), pp. 1537-1546.

Schouten, S., Hopmans, E. C. and Sinninghe Damsté, J. S. 2013. 'The organic geochemistry of glycerol dialkyl glycerol tetraether lipids: A review'. *Organic Geochemistry*, 54, pp. 19-61.

Schouten, S., Hopmans, E. C., Schefuß, E. and Sinninghe Damsté, J. S. 2002. 'Distributional variations in marine crenarchaeotal membrane lipids: a new tool for reconstructing ancient sea water temperatures?'. *Earth and Planetary Science Letters*, 204(1–2), pp. 265-274.

Schrag, D. 1999. 'Effects of diagenesis on the isotopic record of late Paleogene tropical sea surface temperatures'. *Chemical Geology*, 161(1-3), pp. 215-224.

Scotese, C. R. 2013. Atlas of Earth History, Volume 1, Paleogeography, PALEOMAP Project, Arlington, Texas [Online]. Available at: http://www.scotese.com

Scott, G. 1974. 'Biometry of the foraminiferal shell: in *Foraminifera*, vol. 1 (Hedley, RH and Adams, CG, Eds.)'.

Sewall, J., Sloan, L. C., Huber, M. and Wing, S. 2000. 'Climate sensitivity to changes in land surface characteristics'. *Global and Planetary Change*, 26(4), pp. 445-465.

Sexton, P. F., Wilson, P. A. and Pearson, P. N. 2006a. 'Microstructural and geochemical perspectives on planktic foraminiferal preservation: "glassy" versus "frosty"'. *Geochemistry, Geophysics, Geosystems,* 7(12). doi: 10.1029/2006GC001291.

Sexton, P. F., Wilson, P. A. and Pearson, P. N. 2006b. 'Palaeoecology of late middle Eocene planktic foraminifera and evolutionary implications'. *Marine Micropaleontology*, 60(1), pp. 1–16. doi: 10.1016/j.marmicro.2006.02.006.

Shackleton, N. J. and Kennett, J. P. 1975. Paleotemperature History of the Cenozoic and the Initiation of Antarctic Glaciation: Oxygen and Carbon Isotope Analyses in DSDP Sites 277, 279 and 281. *Initial Reports of the Deep Sea Drilling Project, 29*, pp. 743–755. doi: 10.2973/dsdp.proc.29.117.1975.

Shackleton, N. J., Corfield, R. M. and Hall, M. A. 1985. 'Stable isotope data and the ontogeny of Paleocene planktonic foraminifera'. *Journal of Foraminiferal Research*, 15(4), pp. 321–336. doi: 10.2113/gsjfr.15.4.321.

Shellito, C. J., Sloan, L. C. and Huber, M. 2003. 'Climate model sensitivity to atmospheric CO_2 levels in the Early-Middle Paleogene'. *Palaeogeography, Palaeoclimatology, Palaeoecology*, 193, pp. 113–123.

Si, W. and Aubry, M. P. 2018. 'Vital Effects and Ecologic Adaptation of Photosymbiont-Bearing Planktonic Foraminifera During the Paleocene-Eocene Thermal Maximum, Implications for Paleoclimate'. *Paleoceanography and Paleoclimatology*, 33(1), pp. 112–125. doi: 10.1002/2017PA003219.

Sloan, L. C. and Barron, E. 1990. 'Equable" climates during Earth history'. *Geology*, 18, pp. 489–492.'

Sloan, L. C., Walker, J., Moore, T. C., Rea, D. and Zachos, J. 1992. 'Possible Methane-Induced Polar Warming in The Early Eocene'. *Nature*, 357(6376), pp. 320-322.

Sluijs, A. Brinkhuis, H., Schouten, S., Bohaty, S. M., John, C. M., Zachos, J. C., Reichart, G., Sinninghe Damsté, J. S., Crouch, E. M. And Dickens, G. R. 2007a. 'Environmental precursors to rapid light carbon injection at the Palaeocene/Eocene boundary'. *Nature*, 450(7173), pp. 1218–1221. doi: 10.1038/nature06400.

Sluijs, A., Bowen, G.J., Brinkhuis, H., Lourens, L. 2007b. 'The Palaeocene-Eocene Thermal Maximum super greenhouse: Biotic and geochemical signatures, age models and mechanisms of global change'. *Geological Society Special Publication*, pp. 323–349. doi: 10.1144/tms002.15.

Sluijs, A., Schouten, S., Pagani, M., Woltering, M., Brinkhuis, H., Damsté, J. S. S., Dickens, G. R., Huber, M., Reichart, G.-J., Stein, R., Matthiessen, J., Lourens, L. J., Pedentchouk, N., Backman, J., Moran, K. and The Expedition, S. 2006. 'Subtropical Arctic Ocean temperatures during the Palaeocene/Eocene thermal maximum'. *Nature*, 441(7093), pp. 610-613.

Solomon, S., Qin, D., Manning, M., Chen, Z., Marquis, M., Averyt, K.M., Tignor, M. and Millier, H.L. 2007. Contributions of Working Group 1 to the Fourth Assessment Report of the Intergovernmental Panel on Climate Change. Cambridge, UK: Cambridge University Press.

Somero, G. N. 1995. 'Proteins and Temperature'. *Annual Review of Physiology*, 57(1), pp. 43–68. doi: 10.1146/annurev.ph.57.030195.000355.

Spero, H. J. 1992. 'Do planktic foraminifera accurately record shifts in the carbon isotopic composition of sea water ΣCO_2?'. *Marine Micropaleontology*, 19, pp. 275–285.

Spero, H. J. 1998. 'Life History and Stable Isotope Geochemistry of Planktonic Foraminifera'. *The Paleontological Society Papers*, Cambridge University Press (CUP), 4, pp. 7–36. doi: 10.1017/s1089332600000383.

Spero, H. J. and Lea, D. W. 1993. 'Intraspecific stable isotope variability in the planktic foraminifera *Globigerinoides sacculifer*: Results from laboratory experiments'. *Marine Micropaleontology*, 22(3), pp. 221–234. doi: 10.1016/0377-8398(93)90045-Y.

Spero, H. J. and Williams, D. F. 1989. 'Opening the carbon isotope "vital effect" black box 1. Seasonal temperatures in the euphotic zone'. *Paleoceanography*, John Wiley & Sons, Ltd, 4(6), pp. 593–601. doi: 10.1029/PA004i006p00593.

Spero, H. J., Bijma, J., Lea, D. W., Bemis, B. E.1997. 'Effect of seawater carbonate concentration on foraminiferal carbon and oxygen isotopes'. *Nature*, 390(6659), pp. 497-500.

Spero, H. J., Lerche, I. and Williams, D. F. 1991. 'Opening the carbon isotope "vital effect" black box, 2, Quantitative model for interpreting foraminiferal carbon

isotope data'. *Paleoceanography*, John Wiley & Sons, Ltd, 6(6), pp. 639–655. doi: 10.1029/91PA02022.

Spero, H. J., Mielke, K. M., Kalve, E. M., Lea, D. W. And Pak, D. K. 2003. 'Multispecies approach to reconstructing eastern equatorial Pacific thermocline hydrography during the past 360 kyr'. *Paleoceanography*, American Geophysical Union, 18(1). doi: 10.1029/2002PA000814.

Spero, H.J., DeNiro, M. J. 1987. 'The Influence of Symbiont Photosynthesis on the δ^{18}O and δ^{13}C Values of Plantkonic Foraminiferal Shell Calcite'. *Symbiosis*, 4, pp. 213–228.

Spero, H.J., Williams, D. F. 1988. 'Extracting environmental information from planktonic foraminiferal δ^{13}C data'. *Nature*, 335, pp. 717–719.

Spezzaferri, S. and Pearson, P. N. 2009. 'Distribution and ecology of *Catapsydrax Indianus*, a new planktonic foraminifer index species for the late Oligocene-early Miocene'. *Journal of Foraminiferal Research*, 39(2), pp. 112–119. doi: 10.2113/gsjfr.39.2.112.

Spezzaferri, S., Coxall, H. K., Olsson, R. K. & Hemleben, C. (2018). Taxonomy, biostratigraphy, and phylogeny of Oligocene *Globigerina*, *Globigerinella*, and *Quiltyella* n. gen. *In*, Wade, B. S., Olsson, R. K., Pearson, P. N., Huber, B. T. & Berggren, W. A. (eds) Atlas of Oligocene Planktonic Foraminifera. *Cushman Foundation for Foraminiferal Research, Special Publication*, 46(Chap 6): 179-214

Sriver, R. and Huber, M. 2007. 'Observational evidence for an ocean heat pump induced by tropical cyclones'. *Nature*, 447(7144), pp. 577-580.

Stott, L., Cannariato, K., Thunell, R., Haug, G. H., Koutavas, A. and Lund, S. 2004. 'Decline of surface temperature and salinity in the western tropical Pacific Ocean in the Holocene epoch'. *Nature*, 431(7004), pp. 56-59.

Sun, D. and Trenberth, K. 1998. 'Coordinated heat removal from the equatorial Pacific during the 1986-87 El Niño'. *Geophysical Research Letters*, 25(14), pp. 2659-2662.

Tewksbury, J. J., Huey, R. B. and Deutsch, C. A. 2008. 'Putting the Heat on Tropical Animals'. *Science*, 320(5881), pp. 1296-1297.

Thomas, D., Korty, R., Huber, M., Schubert, J. and Haines, B. 2014. 'Nd isotopic structure of the Pacific Ocean 70- 30 Ma and numerical evidence for vigorous ocean circulation and ocean heat transport in a greenhouse world.' *Paleoceanography*, 29(5), pp. 454-469.

Thomas, E. 1990. 'Late Cretaceous through Neogene Deep-Sea Benthic Foraminifers (Maud Rise|Weddell Sea|Antarctica)'. *Proceedings of the Ocean Drilling Program, Scientific Results (113)*.

Tindall, J., Flecker, R., Valdes, P., Schmidt, D., Markwick, P. and Harris, J. 2010. 'Modelling the oxygen isotope distribution of ancient seawater using a coupled ocean-atmosphere GCM: Implications for reconstructing Early Eocene climate'. *Earth and Planetary Science Letters*, 292(3-4), pp. 265-273.

Trenberth, K. E. and Shea, D. J. 1987. 'On the Evolution of the Southern Oscillation'. *Monthly Weather Review*, 115(12), pp. 3078-3096.

Trenbeth, K. E., Caron, J. M., Stepaniak, D. P. and Worley, S. 2002. 'Evolution of El Niño-Southern Oscillation and global atmospheric surface temperatures'. *Journal of Geophysical Research D: Atmospheres*, 107(7-8), p. 4066.

Tripati, A. and Elderfield, H. 2005. 'Deep- sea temperature and circulation changes at the Paleocene- Eocene thermal maximum.' *Science*, 308(5730), pp. 1894-1898.

Tripati, A. K., Delaney, M. L., Zachos, J. C., Anderson, L. D., Kelly, D. C. and Elderfield, H. 2003. 'Tropical sea-surface temperature reconstruction for the early Paleogene using Mg/Ca ratios of planktonic foraminifera'. *Paleoceanography*, 18(4).

Tyrrell, T. and Zeebe, R. E. 2004, 'History of carbonate ion concentration over the last 100 million years'. *Geochimica et Cosmochimica Acta*, 68(17), pp. 3521–3530. doi: 10.1016/j.gca.2004.02.018.

Uchikawa, J. and Zeebe, R. E. 2010. 'Examining possible effects of seawater pH decline on foraminiferal stable isotopes during the Paleocene-Eocene Thermal Maximum'. *Paleoceanography*, Wiley-Blackwell, 25(2). doi: 10.1029/2009PA001864.

University College London (2002) 'An insight into micropalaeontology'. Postgraduate Unit of Micropalaeontology, Department of Earth Sciences, University College London, Gower Street, London, WC1E 6BT.

Urey, H. C. 1947. 'The thermodynamic properties of isotopic substances'. *Journal of the Chemical Society (Resumed)*, Royal Society of Chemistry (RSC), (0), pp. 562-581. doi: 10.1039/jr9470000562.

Urey, H. C., Lowenstam, H. A., Epstein, S. and Mckinney, C. R. 1951. 'Measurement of paleotemperatures and temperatures of the upper cretaceous of England, Denmark, and the southeastern United States'. *Bulletin of the Geological Society of America*, 62(4), pp. 399-416.

Valdes, P. 2011. 'Built for stability'. *Nature Geoscience*, 4(7), pp. 414-416.

van der Zwaan, G. J., Jorissen, F. J. and de Stigter, H. C. 1990. 'The depth dependency of planktonic/benthic foraminiferal ratios: Constraints and applications'. *Marine Geology*, 95(1), pp. 1–16. doi: 10.1016/0025-3227(90)90016-D.

van Eijden, A. J. M. and Ganssen, G. M. 1995, 'An Oligocene multi-species foraminiferal oxygen and carbon isotope record from ODP Hole 758A (Indian Ocean): paleoceanographic and paleo-ecologic implications'. *Marine Micropaleontology*, 25(1), pp. 47–65. doi: 10.1016/0377-8398(94)00028-L.

van Hinsbergen, D. J. J., de Groot, L.V., van Schaik, S.J., Spakman, W., Bijl, P.K., Sluijs, A., Langereis, C.G., Brinkhuis, H. 2015, 'A Paleolatitude Calculator for Paleoclimate Studies'. *PLoS ONE*, Edited by D. L. Royer. Public Library of Science, 10(6), p. e0126946. doi: 10.1371/journal.pone.0126946.

Van Morkhoven, F. P. C. M., Berggren, W. A. and Edwards, A. S. 1986. 'Cenozoic cosmopolitan deep-water benthic Foraminifera.'. *Bulletin - Centres de Recherches Exploration-Production Elf- Aquitaine, Memoire*, 11. doi: 10.2113/gsjfr.18.1.90.

Vecchi, G. A. and Soden, B. J. 2007. 'Global Warming and the Weakening of the Tropical Circulation'. *Journal of Climate*, 20(17), pp. 4316-4340.

Vincent, E., & Berger W. H. 1981. Planktonic foraminifera and their use in Paleoceanography. In: C. Emiliani (Ed.), *The oceanic lithosphere*. The sea (Vol. 7, pp. 1025–1119). Hoboken, N. J.: Wiley-Interscience.

Vincent, E., Killingley, J. S. and Berger, W. H. 1985. 'Oxygen and carbon isotope record for the early and middle Miocene in the central equatorial Pacific (Leg 85) and paleoceanographic implications.'. *Initial reports DSDP, Leg 85, Los Angeles to*

Honolulu. US Govt. Printing Office; UK distributors, IPOD Committee, NERC, Swindon, pp. 749–769. doi: 10.2973/dsdp.proc.85.122.1985.

von der Heydt, A. S., Nnafie, A. and Dijkstra, H. A. 2011. 'Cold tongue/Warm pool and ENSO dynamics in the Pliocene'. *Climate of the Past*, 7(3), pp. 903–915. doi: 10.5194/cp-7-903-2011.

Wade, B. S. and Kroon, D. 2002. 'Middle Eocene regional climate instability: Evidence from the western North Atlantic'. *Geology*, 30(11), pp. 1011–1014.

Wade, B. S. and Pearson, P. N. 2008. 'Planktonic foraminiferal turnover, diversity fluctuations and geochemical signals across the Eocene/Oligocene boundary in Tanzania'. Marine Micropaleontology, 68(3-4), pp.244-242. doi: 10.1016/j.marmicro.2008.04.002.

Wade, B. S., Berggren, W. A. and Olsson, R. K. 2007. 'The biostratigraphy and paleobiology of Oligocene planktonic foraminifera from the equatorial Pacific Ocean (ODP Site 1218)'. *Marine Micropaleontology*, 62(3), pp. 167–179. doi: 10.1016/j.marmicro.2006.08.005.

Wade, B. S., Houben, A. J., Quaijtaal, W., Schouten, S., Rosenthal, Y., Miller, K. G., Katz, M. E., Wright, J. D. And Brinkhuis, H. 2012. 'Multiproxy record of abrupt sea-surface cooling across the Eocene-Oligocene transition in the Gulf of Mexico'. *Geology*, 40(2), pp. 159–162. doi: 10.1130/G32577.1.

Wade, B. S., Pearson, P. N., Berggren, W. A. And Pälike, H. 2011. 'Review and revision of Cenozoic tropical planktonic foraminiferal biostratigraphy and calibration to the geomagnetic polarity and astronomical time scale'. *Earth-Scale Reviews*, 104(1-3), pp. 111-142. doi: 10.1016/j.earscirev.2010.09.003.

Wade, B.S., Olsson, R.K., Pearson, P.N., Huber, B.T. and Berggren, W. A. 2018. 'Atlas of Oligocene Planktonic Foraminifera'. Cushman Foundation for Foraminiferal Research.

Wang, H. and Mehta, V. M. 2008. 'Decadal Variability of the Indo-Pacific Warm Pool and Its Association with Atmospheric and Oceanic Variability in the NCEP–NCAR and SODA Reanalyses'. *Journal of Climate*, 21 (21), pp. 5545-5565..

Wang, X., Stone, P., and Marotzke, J. 1995. 'Poleward Heat Transport in a Barotropic Ocean Model'. *Journal of Physical Oceanography*, 25(2), pp. 256–265. doi: 10.1175/1520-0485(1995)025<0256:PHTIAB>2.0.CO;2.

Webster, P., Magana, V., Palmer, T., Shukla, J., Tomas, R., Yanai, M. and Yasunari, T. 1998. 'Monsoons: Processes, predictability, and the prospects for prediction'. *Journal of Geophysical Research: Oceans*, 103 (C7), pp. 14451-14510.

Wefer, G. and Berger, W. H. 1991. 'Isotope paleontology: growth and composition of extant calcareous species'. *Marine Geology*, 100(1–4), pp. 207–248. doi: 10.1016/0025-3227(91)90234-U.

Weijers, J. W. H., Schouten, S., Spaargaren, O. and Sinninghe Damsté, J. S. 2006. 'Occurrence and distribution of tetraether membrane lipids in soils: Implications for the use of the TEX$_{86}$ proxy and the BIT index'. *Organic Geochemistry*, 37, pp. 1680-1693.

Wetmore, D. K. 1988. 'Burrowing and sediment movement by benthic foraminifera, as shown by time-lapse cinematography'. *Revue de Paleobiologie*, 2(9), pp. 21–927.

Wilkinson, B. H. and Algeo, T. J. 1989. 'Sedimentary carbonate record of calcium-magnesium cycling'. *American Journal of Science*, 289(10), pp. 1158–1194. doi: 10.2475/ajs.289.10.1158.

Wilson-Finelli, A., Chandler, G. T. and Spero, H. J. 1998. 'Stable isotope behavior in paleoceanographically important benthic Foraminifera; results from microcosm culture experiments'. *Journal of Foraminiferal Research*, 28 (4), pp. 312–320.

Wilson, P. A. and Norris, R. D. 2001 'Warm tropical ocean surface and global anoxia during the mid-Cretaceous period'. *Nature*, 412(6845), pp. 425–429. doi: 10.1038/35086553.

Wilson, P. A., Norris, R. D. and Cooper, M. 2002. 'Testing the Cretaceous greenhouse hypothesis using glassy foraminiferal calcite from the core of the Turonian tropics on Demerara Rise'. *Geology*, 30(7), pp. 607-610.

Wing, S. L. and Greenwood, D. R. 1993. 'Fossils and fossil climate: The case for equable continental interiors in the Eocene'. *Philosophical Transactions of the Royal Society B*, 341, pp. 243–252.

Wright, J. D. and Miller, K. G. 1993. 'Southern Ocean Influences on Late Eocene to Miocene Deepwater Circulation'. *American Geophysical Union (AGU),* pp. 1–25. doi: 10.1002/9781118668061.CH1.

Wuchter, C., Schouten, S., Wakeham, S. G. and Damste, J. 2006. 'Archaeal tetraether membrane lipid fluxes in the northeastern Pacific and the Arabian Sea: Implications for TEX_{86} paleothermometry'. *Paleoceanography*, 21(4).

Yan, X., Ho, C. R., Zheng, Q. and Klemas, V. 1992. 'Temperature and Size Variabilities of The Western Pacific Warm Pool'. *Science*, 258(5088), pp. 1643-1645.

Yapp, C. J. 2004. $Fe(CO_3)OH$ in goethite from a mid-latitude North American Oxisol: estimate of atmospheric CO_2 concentration in the Early Eocene "climatic optimum". *Geochimica et Cosmochimica Acta*, 68(5), pp. 935-947.

Young, J.R., Wade, B.S., & Huber B.T. (eds) pforams@mikrotax website. 21 Apr. 2017. URL: http://www.mikrotax.org/pforams

Zachos, J. C. and Kump, L. R. 2005 'Carbon cycle feedbacks and the initiation of Antarctic glaciation in the earliest Oligocene'. *Global and Planetary Change*, 47(1), pp. 51–66. doi: 10.1016/j.gloplacha.2005.01.001.

Zachos, J. C., Berggren, W. A., Aubry, M. P., and Mackensen, A. 1992. 'Isotope and trace element geochemistry of Eocene and Oligocene foraminifers from Site 748, Kerguelen Plateau'. *Proceedings of the Ocean Drilling Program, Scientific Results.*

Zachos, J. C., Lohmann, K. C., Walker, J. C. and Wise, S. W. 1993. 'Abrupt climate change and transient climates during the Paleogene: a marine perspective'. *The Journal of Geology*, 101(2), pp. 191-213.

Zachos, J. C., Schouten, S., Bohaty, S., Quattlebaum, T., Sluijs, A., Brinkhuis, H., Gibbs, S. J. and Bralower, T. J. 2006. 'Extreme warming of mid-latitude coastal ocean during the Paleocene-Eocene Thermal Maximum: Inferences from TEX_{86} and isotope data'. *Geology*, 34(9), pp. 737-740. doi:10.1130/G22522.1.

Zachos, J. C., Stott, L. D. and Lohmann, K. C. 1994. 'Evolution of Early Cenozoic marine temperatures'. *Paleoceanography*, 9(2), pp. 353-387. doi: 10.1029/93PA03266.

Zachos, J., Dickens, G. and Zeebe, R. 2008. 'An early Cenozoic perspective on greenhouse warming and carbon-cycle dynamics'. *Nature*, 451(7176), pp. 279-283.

Zachos, J., Pagani, H., Sloan, L., Thomas, E. and Billups, K. 2001. 'Trends, rhythms, and aberrations in global climate 65 Ma to present'. *Science*, 292(5517), pp. 686-693.

Zachos, J., Wara, M., Bohaty, S., Delaney, M., Petrizzo, M., Brill, A., Bralower, T. and Premoli-Silva, I. 2003. 'A transient rise in tropical sea surface temperature during the Paleocene- Eocene Thermal Maximum'. *Science*, 302(5650), pp. 1551-1554.

Zahn, R., Winn, K. and Sarnthein, M. 1986. 'Benthic foraminiferal $\delta13C$ and accumulation rates of organic carbon: *Uvigerina Peregrina* group and *Cibicidoides Wuellerstorfi*'. *Paleoceanography*, 1(1), pp. 27–42. doi: 10.1029/PA001i001p00027.

Žarić, S., Donner, B., Fischer, G., Mulitza, S. And Wefer, G. 2005. 'Sensitivity of planktic foraminifera to sea surface temperature and export production as derived from sediment trap data'. *Marine Micropaleontology*, 55(1–2), pp. 75–105. doi: 10.1016/j.marmicro.2005.01.002.

Zeebe, R. E. 1999. 'An explanation of the effect of seawater carbonate concentration on foraminiferal oxygen isotopes'. *Geochimica et Cosmochimica Acta*, 63(13–14), pp. 2001–2007. doi: 10.1016/S0016-7037(99)00091-5.

Zeebe, R. E. 2001. 'Seawater pH and isotopic paleotemperatures of Cretaceous oceans'. *Palaeogeography, Palaeoclimatology, Palaeoecology*, 170(1–2), pp. 49–57. doi: 10.1016/S0031-0182(01)00226-7.

Zeebe, R. E., Bijma, J., Hönisch, B., Sanyal, A., Spero, H. J. And Wolf-Gladrow, D. A. 2008. 'Vital effects and beyond: A modelling perspective on developing palaeoceanographical proxy relationships in foraminifera'. *Geological Society Special Publication*, Geological Society of London, 303(1), pp. 45–58. doi: 10.1144/SP303.4.

Zhang, Y. G., Pagani, M., Liu, Z., Bohaty, S. M. And Deconto, R. 2013. 'A 40-million-year history of atmospheric CO_2'. *Philosophical Transactions of the Royal Society A: Mathematical, Physical and Engineering Sciences*, 371(2001). doi: 10.1098/rsta.2013.0096.

- 220 -

Chapter 8

Appendices

Appendix **1**

Foraminiferal Database from the South-East Asian Section of the British Petroleum Collection at the Natural History Museum, London

Foraminiferal database from the South-East Asian section of the microfossil British Petroleum Collection located at the Natural History Museum, London. The database includes the location and the name of the site, the abundance and the foraminiferal species found in the sample, and the resulting inferred age. The green labels represent the beginning of each well/section, while the red labels represent samples from the Eocene after dating them with the biostratigraphic method (see details in Chapter 3).

The abundance of the specimens present in each picked slide is represented as follows: "E" stands for excellent (>200 specimens); "G" for good (100-200); "A" for average (50-100); "P" for poor (20-50); "R" for rare (1-20); and "B" for barren (0 specimens). The notes include the species that could be identified (either at species or genus level), and which helped towards the inferred estimated age of the sample where possible, presented as a geological interval rather than an age in million years. Some abbreviations present in the notes, such as "vrdi" which stands for a sample that was categorised as "very recrystallised, difficult to identify". The species identification was performed using the Atlas of the Eocene on planktonic foraminifera written by Pearson et al., 2006, and the Neogene book on planktonic foraminifera written by Kennett and Srinivasan (1983).

Country	Basin Area	Well				Outcrop number	Picked Slides or Residues	Location NHM	Abundance of foraminifera	Notes	Inferred Age of Sample
		Name	Number	Depth from (m)	Depth to (m)						
Australia	NW Shelf	Brolga	1	170 - 3090		N/A	Picked Slides	9.1(94D)	N/A	N/A	N/A
Australia	NW Shelf	Brolga	1	170		N/A	Picked Slides	9.1(94D)	P	Sacculifer, orb. Univ., trilobus, glob. ruber, H. pelagica, elongatus	Zanclean (Early Pliocene) to Recent
Australia	NW Shelf	Brolga	1	200		N/A	Picked Slides	9.1(94D)	P	Mainly benthics;	
Australia	NW Shelf	Brolga	1	3075		N/A	Picked Slides	9.1(94D)	P	Ss. Semilunina seminulina, extremus, trilob.,	Tortonian (Late Miocene) to Piacenzian (Late Pliocene)
Australia	NW Shelf	Brolga	1	3090		N/A	Picked Slides	9.1(94D)	R	SS. Praedehiscens, plesiotumida, maybe tumida tumida, elongatus, extremus, trilob., orb. Univ.,	Messinian (Late Miocene) to Piacenzian (Late Pliocene)
Australia	SW Shelf	Brolga	1	1897.9		N/A	Picked Slides	9.1(94D)	P	orb. Univ., elongatrus, obliquus, trilob.,	Middle Miocene to Late Pliocene
Australia	SW Shelf	Brolga	1	2108.3		N/A	Picked Slides	9.1(94D)	R	I think some tumida forms,	Middle Miocene to Late Pliocene
Australia	SW Shelf	Brolga	1	2350.1		N/A	Picked Slides	9.1(94D)	P	paenedehiscens or semilunina semilunina?, trilob., woodi?, obliquus, merotumida?	Burdigalian (Early Miocene)
Australia	unspecified	Scott Reef	1	3630 - 4140		N/A	Picked Slides	9.1(94D)	N/A	N/A	
Australia	unspecified	Scott Reef	1	3630		N/A	Picked Slides	9.1(94D)	A	Slide 1; Cretaceous because of Globotruncana and Rotalipora,	Coaniacian to Maastrichtian (Upper Cretaceous)

Australia	unspecified	Scott Reef	1	3631	N/A	Picked Slides	9.1(94D)	P	Slide 2; Cretaceous because of Globotruncana and Rotalipora,	Coaniacian to Maastrichtian (Upper Cretaceous)
Australia	unspecified	Scott Reef	1	4110	N/A	Picked Slides	9.1(94D)	P	Cretaceous because of Rotalipora	Cenomanian (Upper Cretaceous)
Australia	unspecified	Scott Reef	1	4170	N/A	Picked Slides	9.1(94D)	P	Some pritised, some orange-ish,	
Australia	unspecified	Brecknock	1	3505-3805	N/A	Picked Slides	9.1(94D)	N/A	N/A	
Australia	unspecified	Brecknock	1	3505	N/A	Picked Slides	9.1(94D)	A	Cretaceous because of Rotalipora genus forms present,	Cenomanian (Upper Cretaceous)
Australia	unspecified	Brecknock	1	3805	N/A	Picked Slides	9.1(94D)	P	Most pyritised and recryst. Diff. to identify.	
Australia	unspecified	Caswell	1	3330-3920	N/A	Picked Slides	9.1(94D)	N/A	N/A	
Australia	unspecified	Caswell	1	3330	N/A	Picked Slides	9.1(94D)	P	Cretaceous because of Marginotruncana genus forms present,	Turonian (Upper Cretaceous) to Campanian (Upper Cretaceous)
Australia	unspecified	Caswell	1	3920	N/A	Picked Slides	9.1(94D)	P	Most pyritised and recryst. Diff. to identify.	
Australia	unspecified	Yamp	1	1430-2030	N/A	Picked Slides	9.1(94D)	N/A	N/A	
Australia	unspecified	Yamp	1	1430	N/A	Picked Slides	9.1(94D)	P	Slide 1; Cretaceous because of Marginotruncana genus forms present,	Turonian (Upper Cretaceous) to Campanian (Upper Cretaceous)
Australia	unspecified	Yamp	1	1430	N/A	Picked Slides	9.1(94D)	P	Slide 2; smaller size fraction, some pyritised, and sp. Recryst., difficult to identify.	

Australia	unspecified	Yamp	1	1970	N/A	Picked Slides	9.1(94D)	P	Some pyritised, and sp. Recryst., difficult to identify.	
Australia	unspecified	Yamp	1	2030	N/A	Picked Slides	9.1(94D)	P	Sp. Look liken Cretaceous forms, vrdi.	
Australia	unspecified	Brewster	1A	2230 - 3420	N/A	Picked Slides	9.1(94D)	N/A	N/A	
Australia	unspecified	Brewster	1A	2230	N/A	Picked Slides	9.1(94D)	A	Cretaceous because of and Rotalipora genus forms present, some pyritised, vrdi.	Cenomanian (Upper Cretaceous)
Australia	unspecified	Brewster	1A	3420	N/A	Picked Slides	9.1(94D)	P	Most pyritised and recryst. Diff. to identify.	
Australia	unspecified	Barracouta I	N/A	2340 - 8692	N/A	Picked Slides	6.4(57D)	N/A	N/A	
Australia	unspecified	Barracouta I	N/A	2340	N/A	Picked Slides	6.4(57D)	P	Misc. Microfossils including ostracods, Orb. Univ., maybe praebulloides, vrdi.	Middle Miocene to Recent
Australia	unspecified	Barracouta I	N/A	8692	N/A	Picked Slides	6.4(57D)	R	About 3 specimens, not even sure they are forams, one pyritised, vrdi.	
Australia	unspecified	Voltaire	1	1450 - 2450	N/A	Picked Slides	10.3(103E)	N/A	N/A	
Australia	unspecified	Voltaire	1	1450	N/A	Picked Slides	10.3(103E)	P	benthics only, recryst.	
Australia	unspecified	Voltaire	1	1550	N/A	Picked Slides	10.3(103E)	P	benthics only, recryst.	
Australia	unspecified	Voltaire	1	1650	N/A	Picked Slides	10.3(103E)	P	bulloides and trilobus, recryst.	Langhian (Middle Miocene) to Recent
Australia	unspecified	Voltaire	1	2409	N/A	Picked Slides	10.3(103E)	P	Some pyritised, vrdi.	

Australia	unspecified	Voltaire	1	2428	N/A	Picked Slides	10.3(103E)	P	Most pyritised, not even sure they are planktic forams, vrdi.	
Australia	unspecified	Voltaire	1	2438	N/A	Picked Slides	10.3(103E)	R	under 10 specimens, most pyritised, vrdi.	
Australia	unspecified	Voltaire	1	2350	N/A	Picked Slides	10.3(103E)	P	marginotruncana present, some pyritised, vrdi.	Turonian - Campanian (Upper Cretaceous)
Australia	unspecified	Voltaire	1	2450	N/A	Picked Slides	10.3(103E)	P	marginotruncana present, some pyritised, vrdi.	Turonian - Campanian (Upper Cretaceous)
Australia	unspecified	Voltaire	1	240 - 2440	N/A	Picked Slides	10.3(103F)	N/A	N/A	
Australia	unspecified	Voltaire	1	240	N/A	Picked Slides	10.3(103F)	P	Mainly benthics, orb. Univ., veruy recryst.	
Australia	unspecified	Voltaire	1	610	N/A	Picked Slides	10.3(103F)	P	only benthics.	
Australia	unspecified	Voltaire	1	2080	N/A	Picked Slides	10.3(103F)	P	Globotruncanita, some pyritised, vrdi.	Turonian - Campanian (Upper Cretaceous)
Australia	unspecified	Voltaire	1	2020	N/A	Picked Slides	10.3(103F)	R	benthics only.	
Australia	unspecified	Voltaire	1	1840	N/A	Picked Slides	10.3(103F)	R	benthics only.	
Australia	unspecified	Voltaire	1	2260	N/A	Picked Slides	10.3(103F)	A	Cretaceous because of Globotruncanita, some pyritised, recryst.	Turonian - Campanian (Upper Cretaceous)
Australia	unspecified	Voltaire	1	2380	N/A	Picked Slides	10.3(103F)	R	Under 10 specimens, some pyritised, recryst.	
Australia	unspecified	Voltaire	1	2440	N/A	Picked Slides	10.3(103F)	R	Under 10 specimens, most pyritised, vrdi.	

India	Bay of Bengal	Investigator			N/A	Picked Slides	10.3(103F)	A	recryst.;trilobus, ruber, globoquadrina; Pleistocene	Langhian (Middle Miocene) to Recent
India	unspecified	Reiss	N/A	N/A	N/A	Picked Slides	14.1(37B)	A	Recryst.; Reiss 2979.	
India	unspecified	Reiss	N/A	N/A	N/A	Picked Slides	6.1(39G)	P	Reiss 5808; recryst.Acarinina, Subbotina	Eocene?
India	unspecified	Reiss	N/A	N/A	N/A	Picked Slides	6.1(39G)	P	5808, mainly benthics, recryst.	
India	unspecified	Reiss	N/A	N/A	N/A	Picked Slides	6.1(39G)	P	8139; mainly benthics, recryst.	
Indian Ocean	nr Mauritius	Rodrigues Is.	N/A	N/A	N/A	Picked Slides	6.1(39D)	Slides not found in the collection	Slides not found in the collection	
Indonesia	Balambangam	1	N/A	200 - 1999.3	N/A	Picked Slides	15.4(61A)	N/A	N/A	
Indonesia	Balambangam	1	N/A	200	N/A	Picked Slides	15.4(61A)	R	Diff. To identify.	
Indonesia	Balambangam	1	N/A	300	N/A	Picked Slides	15.4(61A)	P	mainly benthics, diff. To identify.	
Indonesia	Balambangam	1	N/A	400	N/A	Picked Slides	15.4(61A)	P	Mainly benthics, trilob.,	
Indonesia	Balambangam	1	N/A	1920	N/A	Picked Slides	15.4(61A)	P	mainly benthics, diff. To identify, recryst.	
Indonesia	Balambangam	1	N/A	1931	N/A	Picked Slides	15.4(61A)	P	vrdi.	
Indonesia	Balambangam	1	N/A	1999.3	N/A	Picked Slides	15.4(61A)	P	some pyritised, trilob. Praebulloides, vrdi.	Late Oligocene - Middle Miocene
Indonesia	Bangau	1	N/A	4600 - 7500	N/A	Picked Slides	16.4(105C)	N/A	N/A	
Indonesia	Bangau	1	N/A	4600	N/A	Picked Slides	16.4(105C)	R	Mainly benthics, some orange-ish, recryst.	
Indonesia	Bangau	1	N/A	4660	N/A	Picked Slides	16.4(105C)	R	obliquus, most pyritised,	Langhian (Early Miocene) to Ionian (Late Pleistocene).

Indonesia	Bangau	1	N/A	7460	N/A	Picked Slides	16.4(105C)	P	woodi, orb. Univ., maybe rubver, soe pyritised, vrdi.	Burdigalian (Early Miocene)
Indonesia	Bangau	1	N/A	7500	N/A	Picked Slides	16.4(105C)	R	mitra, some blue dyed, recryst.	Burdigalian (Early Miocene)
Indonesia	Balambangam	1	N/A	2000 - 2163.2	N/A	Picked Slides	9.2(100G)	N/A	N/A	
Indonesia	Balambangam	1	N/A	2000	N/A	Picked Slides	9.2(100G)	P	extremuus, trilob., merotumida I think, some pyritised, vrdi.	From Tortonian (Late Miocene) to Zanclean (Early Pliocene)
Indonesia	Balambangam	1	N/A	2044	N/A	Picked Slides	9.2(100G)	P	very recreyst., some broken, diff. To identify.	
Indonesia	Balambangam	1	N/A	2163.2	N/A	Picked Slides	9.2(100G)	P	maybe praebulloides,	
Indonesia	Balambangam	1	N/A	2164.5	N/A	Picked Slides	9.2(100G)	P	venez., obesa or siphonifera, some pyritised, vrdi.	
Indonesia	Sumatra	Unjung Tanjun	N/A	N/A	N/A	Picked Slides	9.1(94D)	P	miscellaneous microfossils, including ostracods; not even sure they are forams, but if so, benthics mainly, vrdi.	
Indonesia	Unspecified	Kindu	1	490-6210	N/A	Picked Slides	8(50D)			
Indonesia	Unspecified	Kindu	N/A	5609-5612	N/A	Picked Slides	8(50D)	P	very recrystallise,d some orange-ish, some bright red-ish, vrdi.	
Indonesia	Unspecified	Kindu	N/A	5609-5612 rewash	N/A	Picked Slides	8(50D)	R	Trilob., most orange ish, vrdi.	Chattian (Late Oligocene) to Recent
Indonesia	Unspecified	Kindu	N/A	5624-5628	N/A	Picked Slides	8(50D)	P	trilob., some blue dyed, some orange-ish, vrdi.	Chattian (Late Oligocene) to Recent
Indonesia	Unspecified	Kindu	s	6160-6170	N/A	Picked Slides	8(50D)	P	venez., trilob., siphoniph., merotumida I think.	

Indonesia	Unspecified	L40	1	7700-12010	N/A	Picked Slides	8.5(43G)	R	Maybe globoquadrina dehiscens in one of the slidres (David King)	
Indonesia	Unspecified	L40	1	7700	N/A	Picked Slides	8.5(43G)	R	4 specimens, I think venez., vrdi.	Priabonian (Late Eocene) to Zanclean (Early Pliocene)
Indonesia	Unspecified	L40	1	8010	N/A	Picked Slides	8.5(43G)	P	venez.,some orange-ish, and specimens vrdi.	Priabonian (Late Eocene) to Zanclean (Early Pliocene)
Indonesia	Unspecified	L40	1	8500	N/A	Picked Slides	8.5(43G)	P	some pyritised, orange-ish, recrystr., diff. To identify.	Chattian (Late Oligocene)
Indonesia	Unspecified	L40	1	9100	N/A	Picked Slides	8.5(43G)	P	Some orange-ish, sime pyritised, sp. Small and very recryst., diffi. To identify.	
Indonesia	Unspecified	L40	1	9700	N/A	Picked Slides	8.5(43G)	P	trilob., venez., some pyritised, sp. Very recryst., some orange-.ish, vrdi.	Chattian (Late Oligocene)
Indonesia	Unspecified	L40	1	10200	N/A	Picked Slides	8.5(43G)	P	Maybe morozovella (muricate wall outline) on quadrant number 11.	
Indonesia	Unspecified	L40	1	10600	N/A	Picked Slides	8.5(43G)	P	Some pyritised, some orange-ish, small specimens and recryst., diff. To identify.	
Indonesia	Unspecified	L40	1	11000	N/A	Picked Slides	8.5(43G)	R	2 specimens, not even sure they are forams, one seems benthic, one is pyritised and vrdi.	

Indonesia	Unspecified	L40	1	11600	N/A	Picked Slides	8.5(43G)	B	no forams, nothing.	
Indonesia	Unspecified	L40	1	12010	N/A	Picked Slides	8.5(43G)	P	Some pyritised, maybe g. ciperoensis, vrdi.	
Indonesia	Unspecified	L46	1	7480-7620	N/A	Picked Slides	8.5(43G)	N/A	Only three slides	
Indonesia	Unspecified	L46	1	7480	N/A	Picked Slides	8.5(43G)	P	Slide 1; venez., trilob.,	Chattian (Late Oligocene)
Indonesia	Unspecified	L46	1	7480	N/A	Picked Slides	8.5(43G)	P	Slide 2; smaller size fractions, very small and vrdi.	
Indonesia	Unspecified	L46	1	7620	N/A	Picked Slides	8.5(43G)	P	trilob., venez., orb. Univ.,	Chattian (Late Oligocene)
Indonesia	Unspecified	L49	1	4560-6650	N/A	Picked Slides	8.5(43G)	N/A	Only three slides	
Indonesia	Unspecified	L49	1	4650	N/A	Picked Slides	8.5(43G)	P	venez., some pyritised, vrdi.	Priabonian (Late Eocene) to Zanclean (Early Pliocene)
Indonesia	Unspecified	L49	1	5760	N/A	Picked Slides	8.5(43G)	B	no forams, nothing.	
Indonesia	Unspecified	L49	1	6650	N/A	Picked Slides	8.5(43G)	R	Very small size fractions, not even sure they are forams, most pyritised, some bright orange-ish, vrdi.	
Indonesia	Unspecified	LORO	1	190-1890	N/A	Picked Slides	16.4(105H)	N/A		
Indonesia	Unspecified	LORO	1	190	N/A	Picked Slides	16.4(105H)	P	Mainly Benthics, trilob., orb. Univ., recryst.	Langhian (Middle Miocene) to Recent
Indonesia	Unspecified	LORO	1	230	N/A	Picked Slides	16.4(105H)	P	Benthics only.	
Indonesia	Unspecified	LORO	1	1830	N/A	Picked Slides	16.4(105H)	P	venez., orb. Univ., extremuus, bulloides,	
Indonesia	Unspecified	LORO	1	1890	N/A	Picked Slides	16.4(105H)	P	orb. Univ., some pyritsed, very recryst.	Langhian (Middle Miocene) to Recent

Papua New Guinea	unspecified	Andabare Island	N/A	**69.5-349**	N/A	Picked Slides	13.5 (74E)	N/A	N/A	
Papua New Guinea	unspecified	Andabare Island	N/A	69.5	N/A	Picked Slides	13.5 (74E)	P	glob. Trilobus, but specimens very small, and very recryst., difficult to identify.	Langhian (Late Oligocene) to Recent
Papua New Guinea	unspecified	Andabare Island	N/A	75.6	N/A	Picked Slides	13.5 (74E)	G	Middle or Late Miocene, because of the simultaneous presence of glob. Praebulloides and glob. Bulloides, specimens very small and recryst., difficult to identify.	Chattian (Late Oligocene) to Middle Miocene
Papua New Guinea	unspecified	Andabare Island	N/A	84.5	N/A	Picked Slides	13.5 (74E)	A	recryst.	
Papua New Guinea	unspecified	Andabare Island	N/A	93.5	N/A	Picked Slides	13.5 (74E)	A	recryst.	
Papua New Guinea	unspecified	Andabare Island	N/A	102.5	N/A	Picked Slides	13.5 (74E)	P	recryst.	
Papua New Guinea	unspecified	Andabare Island	N/A	111.5	N/A	Picked Slides	13.5 (74E)	R	recryst., 2 benthics and 2 plantiks, sediments.	
Papua New Guinea	unspecified	Andabare Island	N/A	126.5	N/A	Picked Slides	13.5 (74E)	P	recryst.	
Papua New Guinea	unspecified	Andabare Island	N/A	135.5	N/A	Picked Slides	13.5 (74E)	B	No forams	
Papua New Guinea	unspecified	Andabare Island	N/A	150.5	N/A	Picked Slides	13.5 (74E)	A	recryst.	
Papua New Guinea	unspecified	Andabare Island	N/A	162.5	N/A	Picked Slides	13.5 (74E)	A	recryst.	

Papua New Guinea	unspecified	Andabare Island	N/A	174.5	N/A	Picked Slides	13.5 (74E)	R	recryst.	
Papua New Guinea	unspecified	Andabare Island	N/A	186.5	N/A	Picked Slides	13.5 (74E)	R	recryst.	
Papua New Guinea	unspecified	Andabare Island	N/A	231.4	N/A	Picked Slides	13.5 (74E)	P	recryst.	
Papua New Guinea	unspecified	Andabare Island	N/A	240.5	N/A	Picked Slides	13.5 (74E)	P	recryst.	
Papua New Guinea	unspecified	Andabare Island	N/A	300.4	N/A	Picked Slides	13.5 (74E)	B	No forams	
Papua New Guinea	unspecified	Andabare Island	N/A	310	N/A	Picked Slides	13.5 (74E)	A	recryst.	
Papua New Guinea	unspecified	Andabare Island	N/A	337	N/A	Picked Slides	13.5 (74E)	R	recryst.	
Papua New Guinea	unspecified	Andabare Island	N/A	349	N/A	Picked Slides	13.5 (74E)	B	No forams	
Papua New Guinea	unspecified	Aramia	N/A	N/A	N/A	Picked Slides	18.0 (44D)	B	No forams	
Papua New Guinea	unspecified	Baia	1	9310- 9830	N/A	Picked Slides	9.4(97A)	N/A	General: Benthics, little forams (around 4-5 forams in slides number: 9480, 9530, 9580, 9630,9670,9690), black-coloured. Benthics decreasing with depth, more biserial at the top.	
Papua New Guinea	unspecified	Baia	1	9310	N/A	Picked Slides	9.4(97A)	G	recrystallised; pyritised, no Eocene, orbulina, biserial forams,	Langhian (Middle Miocene) to Recent

									different sizes of planktics.	
Papua New Guinea	unspecified	Baia	1	9330	N/A	Picked Slides	9.4(97A)	G	recrystallised; pyritised, no Eocene, orbulina, biserial foram, different sizes of planktics.	Langhian (Middle Miocene) to Recent
Papua New Guinea	unspecified	Baia	1	9380	N/A	Picked Slides	9.4(97A)	A	pyritised; no sign of Eocene foraminifera; recrystallised	
Papua New Guinea	unspecified	Baia	1	9430	N/A	Picked Slides	9.4(97A)	P	recrystallised; pyritised, no Eocene	
Papua New Guinea	unspecified	Baia	1	9480	N/A	Picked Slides	9.4(97A)	A	pyritised; no sign of Eocene foraminifera; recrystallised	
Papua New Guinea	unspecified	Baia	1	9530	N/A	Picked Slides	9.4(97A)	P	recrystallised; pyritised, no Eocene	
Papua New Guinea	unspecified	Baia	1	9580	N/A	Picked Slides	9.4(97A)	P	recrystallised; pyritised, no Eocene, orbulina	
Papua New Guinea	unspecified	Baia	1	9630	N/A	Picked Slides	9.4(97A)	P	recrystallised; pyritised, no Eocene	
Papua New Guinea	unspecified	Baia	1	9670	N/A	Picked Slides	9.4(97A)	P	under 20 foram specimens; recrystallised; pyritised, no Eocene,	
Papua New Guinea	unspecified	Baia	1	9690	N/A	Picked Slides	9.4(97A)	P	under 20 foram specimens; recrystallised; pyritised, no Eocene, biserial foram	

Papua New Guinea	unspecified	Baia	1	9710	N/A	Picked Slides	9.4(97A)	A	pyritised; no sign of Eocene foraminifera; recrystallised	
Papua New Guinea	unspecified	Baia	1	9730	N/A	Picked Slides	9.4(97A)	P	pyritised; no sign of Eocene foraminifera; recrystallised, a few glassy.	
Papua New Guinea	unspecified	Baia	1	9750	N/A	Picked Slides	9.4(97A)	P	pyritised; no sign of Eocene foraminifera; recrystallised.	
Papua New Guinea	unspecified	Baia	1	9770	N/A	Picked Slides	9.4(97A)	A	pyritised; no sign of Eocene foraminifera; recrystallised, serial foram	
Papua New Guinea	unspecified	Baia	1	9790	N/A	Picked Slides	9.4(97A)	R	under 20 foram specimens; recrystallised; pyritised, no Eocene	
Papua New Guinea	unspecified	Baia	1	9810	N/A	Picked Slides	9.4(97A)	P	recrystallised; pyritised, no Eocene	
Papua New Guinea	unspecified	Baia	1	9830	N/A	Picked Slides	9.4(97A)	P	pyritised; no sign of Eocene foraminifera; recrystallised.	
Papua New Guinea	unspecified	Barakewa	2	80- 1744.5	N/A	Picked Slides	15.4(61F)	N/A	As Barakiva,	
Papua New Guinea	unspecified	Barakewa	2	80	N/A	Picked Slides	15.4(61F)	B	no sign of forams, one rock?	
Papua New Guinea	unspecified	Barakewa	2	100	N/A	Picked Slides	15.4(61F)	B	no sign of forams	
Papua New Guinea	unspecified	Barakewa	2	100	N/A	Picked Slides	15.4(61F)	B	100 mw, no sign of forams, 1 rock?	

Papua New Guinea	unspecified	Barakewa	2	120	N/A	Picked Slides	15.4(61F)	R	1 benthic? And 1 rock?	
Papua New Guinea	unspecified	Barakewa	2	150	N/A	Picked Slides	15.4(61F)	R	150 m by mw; < or = 5 forams present, frosty	
Papua New Guinea	unspecified	Barakewa	2	150	N/A	Picked Slides	15.4(61F)	R	150 m by mw; < or = 10 forams present, frosty, perhaps one orbulina?	
Papua New Guinea	unspecified	Barakewa	2	150	N/A	Picked Slides	15.4(61F)	B	empy slide, one rock fragment	
Papua New Guinea	unspecified	Barakewa	2	150	N/A	Picked Slides	15.4(61F)	P	150 m by c, frosty	
Papua New Guinea	unspecified	Barakewa	2	210	N/A	Picked Slides	15.4(61F)	R	Mainly benthics, 2 planktonics.	
Papua New Guinea	unspecified	Barakewa	2	250	N/A	Picked Slides	15.4(61F)	R	< or = 5 forams present, frosty	
Papua New Guinea	unspecified	Barakewa	2	300	N/A	Picked Slides	15.4(61F)	B	no sign of forams, loads of rock fragments, perhaps forams in there?	
Papua New Guinea	unspecified	Barakewa	2	350	N/A	Picked Slides	15.4(61F)	P	under 20 benthic and planktonic specimens (planktics, really?	
Papua New Guinea	unspecified	Barakewa	2	400	N/A	Picked Slides	15.4(61F)	R	under 20 benthic and planktonic specimens (planktics, really?	
Papua New Guinea	unspecified	Barakewa	2	410	N/A	Picked Slides	15.4(61F)	P	only benthics	
Papua New Guinea	unspecified	Barakewa	2	450	N/A	Picked Slides	15.4(61F)	R	only benthic, rock fragments, and fragments of about 2 planktics	

Papua New Guinea	unspecified	Barakewa	2	500	N/A	Picked Slides	15.4(61F)	P	500 m by vc, < or = 5 planktics present, frosty	
Papua New Guinea	unspecified	Barakewa	2	500	N/A	Picked Slides	15.4(61F)	B	500 m, empy slide	
Papua New Guinea	unspecified	Barakewa	2	550	N/A	Picked Slides	15.4(61F)	R	550 m by cr, no sign of planktics	
Papua New Guinea	unspecified	Barakewa	2	550	N/A	Picked Slides	15.4(61F)	P	550 m by mw, no sign of planktics	
Papua New Guinea	unspecified	Barakewa	2	600	N/A	Picked Slides	15.4(61F)	P	no sign of planktics	
Papua New Guinea	unspecified	Barakewa	2	650	N/A	Picked Slides	15.4(61F)	P	no sign of planktics	
Papua New Guinea	unspecified	Barakewa	2	670	N/A	Picked Slides	15.4(61F)	R	no sign of planktics	
Papua New Guinea	unspecified	Barakewa	2	700	N/A	Picked Slides	15.4(61F)	A	Benthics	
Papua New Guinea	unspecified	Barakewa	2	750	N/A	Picked Slides	15.4(61F)	P	750 m by p.c.,	
Papua New Guinea	unspecified	Barakewa	2	750	N/A	Picked Slides	15.4(61F)	R	750 m	
Papua New Guinea	unspecified	Barakewa	2	770	N/A	Picked Slides	15.4(61F)	R	benthics	
Papua New Guinea	unspecified	Barakewa	2	790	N/A	Picked Slides	15.4(61F)	P	Trilobatus; only 2 planktonics.	Langhian (Late Oligocene) to Recent
Papua New Guinea	unspecified	Barakewa	2	800	N/A	Picked Slides	15.4(61F)	P	1 orbulina, only 1 planktonic, benthics	Middle Miocene to Recent
Papua New Guinea	unspecified	Barakewa	2	820	N/A	Picked Slides	15.4(61F)	P	1 broken trilobatus (I think), only 1	Langhian (Late Oligocene) to Recent

									planktonic, benthics.	
Papua New Guinea	unspecified	Barakewa	2	840	N/A	Picked Slides	15.4(61F)	P	Frosty forams	
Papua New Guinea	unspecified	Barakewa	2	860	N/A	Picked Slides	15.4(61F)	P	Frosty forams	
Papua New Guinea	unspecified	Barakewa	2	880	N/A	Picked Slides	15.4(61F)	P	Frosty forams	
Papua New Guinea	unspecified	Barakewa	2	900	N/A	Picked Slides	15.4(61F)	P	Frosty forams	
Papua New Guinea	unspecified	Barakewa	2	920	N/A	Picked Slides	15.4(61F)	P	Benthics	
Papua New Guinea	unspecified	Barakewa	2	940	N/A	Picked Slides	15.4(61F)	R	Frosty forams	
Papua New Guinea	unspecified	Barakewa	2	970	N/A	Picked Slides	15.4(61F)	A	Frosty forams	
Papua New Guinea	unspecified	Barakewa	2	980	N/A	Picked Slides	15.4(61F)	R	Frosty forams, one caramel-coloured orbulina?	
Papua New Guinea	unspecified	Barakewa	2	983.5	N/A	Picked Slides	15.4(61F)	P	no sign of planktics	
Papua New Guinea	unspecified	Barakewa	2	989.5	N/A	Picked Slides	15.4(61F)	P	no sign of planktics	
Papua New Guinea	unspecified	Barakewa	2	1017.5	N/A	Picked Slides	15.4(61F)	A	mainly benthics, recryst.; some pyritised	
Papua New Guinea	unspecified	Barakewa	2	1242.5	N/A	Picked Slides	15.4(61F)	R	2 planktics = 2 orbulina? One of them was green-ish and the other had like a small protuberance from	

									the globe-like shape.	
Papua New Guinea	unspecified	Barakewa	2	1414.5	N/A	Picked Slides	15.4(61F)	A	only benthics	
Papua New Guinea	unspecified	Barakewa	2	1553	N/A	Picked Slides	15.4(61F)	B	N/A	
Papua New Guinea	unspecified	Barakewa	2	1595	N/A	Picked Slides	15.4(61F)	B	N/A	
Papua New Guinea	unspecified	Barakewa	2	1638	N/A	Picked Slides	15.4(61F)	R	2 benthics only present in slide. 1 brown, 1 black (pyritised?), recrystallised.	
Papua New Guinea	unspecified	Barakewa	2	1695	N/A	Picked Slides	15.4(61F)	P	only benthics, and pyritised, recryst.	
Papua New Guinea	unspecified	Barakewa	2	1744.5	N/A	Picked Slides	15.4(61F)	B	N/A	
Papua New Guinea	unspecified	D	N/A	N/A	106-385	Picked Slides	11.3(88E)	N/A		
Papua New Guinea	unspecified	D	N/A	N/A	106	Picked Slides	11.3(88E)	G	Fohsella periheroacuta, recryst.	Langhian (Late Oligocene) to Serravallian (Middle Miocene)
Papua New Guinea	unspecified	D	N/A	N/A	107	Picked Slides	11.3(88E)	G	Dentoglobigerina tripartita, recryst.	Priabonian (Late Eocene) to Serravallian (Middle Miocene))
Papua New Guinea	unspecified	D	N/A	N/A	108	Picked Slides	11.3(88E)	A	Slide 1 of 2; Middle Miocene, recryst.	

Papua New Guinea	unspecified	D	N/A	N/A	108	Picked Slides	11.3(88E)	E	Slide 2 of 2;Globigerinoides venezuelana, recryst.	Aquitanian ((Early Miocene) Zanclean (Early Pliocene)
Papua New Guinea	unspecified	D	N/A	N/A	109	Picked Slides	11.3(88E)	A	fohsella peripheroacuta, recryst.	Langhian (Middle Miocene) to Serravallian (Middle Miocene)
Papua New Guinea	unspecified	D	N/A	N/A	110	Picked Slides	11.3(88E)	A	primarily benthics	
Papua New Guinea	unspecified	D	N/A	N/A	111	Picked Slides	11.3(88E)	R	primarily benthics	
Papua New Guinea	unspecified	D	N/A	N/A	112	Picked Slides	11.3(88E)	A	recryst.	
Papua New Guinea	unspecified	D	N/A	N/A	122	Picked Slides	11.3(88E)	R	primarily benthics	
Papua New Guinea	unspecified	D	N/A	N/A	130	Picked Slides	11.3(88E)	P	M. M., Fohsella Peripheronda, recryst.	Chattian (Late Oligocene) to Serravallian (Middle Miocene)
Papua New Guinea	unspecified	D	N/A	N/A	133	Picked Slides	11.3(88E)	P	primarily benthics, pyritised planktics, recryst.	
Papua New Guinea	unspecified	D	N/A	N/A	134	Picked Slides	11.3(88E)	P	Eocene, M. marginodentata, pyritised and recryst.	Thanetian (Late Paleocene) to Ypresian (Early Eocene)
Papua New Guinea	unspecified	D	N/A	N/A	138	Picked Slides	11.3(88E)	P	primarily benthics, recryst.	
Papua New Guinea	unspecified	D	N/A	N/A	200	Picked Slides	11.3(88E)	P	Globigerinoides bollii, fohsella, recryst., broken forams	Serravallian (Middle Miocene)
Papua New Guinea	unspecified	D	N/A	N/A	210	Picked Slides	11.3(88E)	P	lots of orbulina universa, no praerobulina, recryst.	Langhian (Middle Miocene) to Recent

Papua New Guinea	unspecified	D	N/A	N/A	213	Picked Slides	11.3(88E)	P	Slide 1 of 2; preorbulina, orbulina bilobata (surface not very smooth though) ruber, recryst.	(Middle Miocene)
Papua New Guinea	unspecified	D	N/A	N/A	213	Picked Slides	11.3(88E)	P	Slide 2 of 2;	(Middle Miocene)
Papua New Guinea	unspecified	D	N/A	N/A	214	Picked Slides	11.3(88E)	P	M. M. ? recryst., difficult to read	
Papua New Guinea	unspecified	D	N/A	N/A	215	Picked Slides	11.3(88E)	A	Middle M., recryst.	
Papua New Guinea	unspecified	D	N/A	N/A	216	Picked Slides	11.3(88E)	B	N/A	
Papua New Guinea	unspecified	D	N/A	N/A	217	Picked Slides	11.3(88E)	R	Dentoglobigerina tripartita pyritised, recryst.	Priabonian (Late Eocene) to Serravallian (Middle Miocene)
Papua New Guinea	unspecified	D	N/A	N/A	229	Picked Slides	11.3(88E)	B	N/A	
Papua New Guinea	unspecified	D	N/A	N/A	230	Picked Slides	11.3(88E)	R	M.M., recryst.	
Papua New Guinea	unspecified	D	N/A	N/A	231	Picked Slides	11.3(88E)	A	Slide 1 of 3, E.E., morozovella marginodentata, acarinina formosa formosa, Parasubbotina inaequispira, recryst.	Ypresian (Early Eocene)
Papua New Guinea	unspecified	D	N/A	N/A	231	Picked Slides	11.3(88E)	A	Slide 2 of 3, E.E., recryst.	
Papua New Guinea	unspecified	D	N/A	N/A	231	Picked Slides	11.3(88E)	A	Slide 3 of 3, E.E., recryst.	

Papua New Guinea	unspecified	D	N/A	N/A	232	Picked Slides	11.3(88E)	R	mainly benthics, recryst.	
Papua New Guinea	unspecified	D	N/A	N/A	233	Picked Slides	11.3(88E)	A	Slide 1 of 2, recryst., broken forams.	
Papua New Guinea	unspecified	D	N/A	N/A	233	Picked Slides	11.3(88E)	P	Slide 2 of 2, recryst., broken forams.	
Papua New Guinea	unspecified	D	N/A	N/A	234	Picked Slides	11.3(88E)	P	marginotruncana, pyritised, recryst.	Turonian - Campanian (Upper Cretaceous)
Papua New Guinea	unspecified	D	N/A	N/A	250	Picked Slides	11.3(88E)	R	unidentifiable because recryst.	
Papua New Guinea	unspecified	DB1	N/A	N/A	26-34	Picked Slides	13.5(74E)	N/A	N/A	
Papua New Guinea	unspecified	DB1	N/A	N/A	26	Picked Slides	13.5(74E)	R	mainly bentics, pyritised and recryst., unidentifiable	
Papua New Guinea	unspecified	DB1	N/A	N/A	27	Picked Slides	13.5(74E)	A	orbulina universa, pyritised and recryst., difficult to identify.	Langhian (Middle Miocene)
Papua New Guinea	unspecified	DB1	N/A	N/A	30	Picked Slides	13.5(74E)	P	mainly benthics, recryst., difficult to identify	
Papua New Guinea	unspecified	DB1	N/A	N/A	31	Picked Slides	13.5(74E)	P	recryst. Difficult to identify	
Papua New Guinea	unspecified	DB1	N/A	N/A	32	Picked Slides	13.5(74E)	R	benthics only, recryst.	
Papua New Guinea	unspecified	DB1	N/A	N/A	33	Picked Slides	13.5(74E)	P	benthics only, recryst.	
Papua New Guinea	unspecified	DB1	N/A	N/A	34	Picked Slides	13.5(74E)	P	benthics only, recryst.	

Papua New Guinea	unspecified	DK2	N/A	N/A	2A-10	Picked Slides	13.5(74E)	N/A	N/A	
Papua New Guinea	unspecified	DK2	N/A	N/A	2A	Picked Slides	13.5(74E)	R	mainly benthics, pyritised and recryst. Difficult to identify	
Papua New Guinea	unspecified	DK2	N/A	N/A	2B	Picked Slides	13.5(74E)	R	pyritised and recryst. Difficult to identify, too little sample	
Papua New Guinea	unspecified	DK2	N/A	N/A	3	Picked Slides	13.5(74E)	R	pyritised and recryst. Difficult to identify, too little sample.	
Papua New Guinea	unspecified	DK2	N/A	N/A	6	Picked Slides	13.5(74E)	R	pyritised and recryst. Difficult to identify, too little sample	
Papua New Guinea	unspecified	DK2	N/A	N/A	7	Picked Slides	13.5(74E)	P	pyritised and recryst. Difficult to identify, too little sample	
Papua New Guinea	unspecified	DK2	N/A	N/A	7G	Picked Slides	13.5(74E)	P	pyritised and recryst. Difficult to identify, too little sample	
Papua New Guinea	unspecified	DK2	N/A	N/A	8	Picked Slides	13.5(74E)	R	mainly benthics, pyritised and recryst. Difficult to identify	
Papua New Guinea	unspecified	DK2	N/A	N/A	9	Picked Slides	13.5(74E)	B	N/A	
Papua New Guinea	unspecified	DK2	N/A	N/A	10	Picked Slides	13.5(74E)	P	mainly benthics, from benthics (reticulina), Late Cretaceous from benthonic foraminifera, pyritised and recryst. Difficult to identify.	

Papua New Guinea	unspecified	DK5	N/A	N/A	1-30	Picked Slides	13.5(74E)	N/A	N/A	
Papua New Guinea	unspecified	DK5	N/A	N/A	1	Picked Slides	13.5(74E)	P	Late Cretaceous from benthics, mainly benthics, pyritised and recryst. Difficult to identify	
Papua New Guinea	unspecified	DK5	N/A	N/A	2	Picked Slides	13.5(74E)	R	mainly benthics, Late Cretaceous, with Marginotruncana sigali and Whiteinella archeocretacea	Turonian - Santonian (Upper Cretaceous)
Papua New Guinea	unspecified	DK5	N/A	N/A	3	Picked Slides	13.5(74E)	R	mainly benthics, recryst and too little sample, difficult to identify.	
Papua New Guinea	unspecified	DK5	N/A	N/A	4	Picked Slides	13.5(74E)	P	benthics= Palaeocene or older, planktonic= Late Cretaceous.	
Papua New Guinea	unspecified	DK5	N/A	N/A	5	Picked Slides	13.5(74E)	R	mainly benthics, pyritised and recryst. Difficult to identify	
Papua New Guinea	unspecified	DK5	N/A	N/A	6	Picked Slides	13.5(74E)	R	mainly benthics, pyritised and recryst. Difficult to identify	
Papua New Guinea	unspecified	DK5	N/A	N/A	7	Picked Slides	13.5(74E)	P	only benthics	
Papua New Guinea	unspecified	DK5	N/A	N/A	8	Picked Slides	13.5(74E)	B	no forams, black fish tooth and black scale	
Papua New Guinea	unspecified	DK5	N/A	N/A	9	Picked Slides	13.5(74E)	B	no forams, black fish scale.	

Papua New Guinea	unspecified	DK5	N/A	N/A	11	Picked Slides	13.5(74E)	P	mainly benthics, pyritised and recryst. Difficult to identify	
Papua New Guinea	unspecified	DK5	N/A	N/A	12	Picked Slides	13.5(74E)	R	mainly benthics, pyritised and recryst., difficult to identify other forams, too little sample. Round little balls but not orbulina universa.	
Papua New Guinea	unspecified	DK5	N/A	N/A	13	Picked Slides	13.5(74E)	R	mainly benthics, very recryst. and too little sample, difficult to identiy.	
Papua New Guinea	unspecified	DK5	N/A	N/A	14	Picked Slides	13.5(74E)	P	Mainly benthics, Planktonic Globotruncana present so Late Cretaceous, pyritised and recryst.	Coniacian - Maastrichtian (Upper Cretaceous)
Papua New Guinea	unspecified	DK5	N/A	N/A	16	Picked Slides	13.5(74E)	B	No forams	
Papua New Guinea	unspecified	DK5	N/A	N/A	17	Picked Slides	13.5(74E)	B	No forams	
Papua New Guinea	unspecified	DK5	N/A	N/A	18	Picked Slides	13.5(74E)	P	Mainly benthics, Morozovella marginodentata so Late Palaeocene or Early Eocene, but specimens infilled and recryst. So hard to tell, for example marginasnt very dentate; some pyritised; some brown-ish.	Thanetian (Late Paleocene) to Ypresian (Early Eocene)

Papua New Guinea	unspecified	DK5	N/A	N/A	19	Picked Slides	13.5(74E)	P	Mainly benthics, maybe Parasubbotina inaequispira, Early Eocene/Middle Eocene, but specimens pyritised, recrystall., and little sample, so difficult to identify.	Ypresian (Early Eocene) to Lutetian (Middle Eocene)
Papua New Guinea	unspecified	DK5	N/A	N/A	20	Picked Slides	13.5(74E)	P	probably sieved at small size, very small spcimens (all of them), recryst., infilled and loads of broken forams so no many intact ones, therefore difficult to identify. Maybe ruber present but apertures infilled so only outline deduced (then sample would be corresponding to or younger than the Miocene.	
Papua New Guinea	unspecified	DK5	N/A	N/A	23	Picked Slides	13.5(74E)	P	mainly benthics, pyritised and recyst., difficult to identify, too little sample	
Papua New Guinea	unspecified	DK5	N/A	N/A	24	Picked Slides	13.5(74E)	P	Globorotalia multicamerata, Orb. Universa, pyritised and recryst.	Late Miocene to Late Pliocene
Papua New Guinea	unspecified	DK5	N/A	N/A	27	Picked Slides	13.5(74E)	R	very recryst. And too litle sample, difficult to identify.	

Papua New Guinea	unspecified	DK5	N/A	N/A	27g	Picked Slides	13.5(74E)	A	globotruncana, recryst.	Coniacian - Maastrichtian (Upper Cretaceous)
Papua New Guinea	unspecified	DK5	N/A	N/A	29, slide 1	Picked Slides	13.5(74E)	P	Maybe Cretaceous, recryst. And pyritised, difficult to identify.	
Papua New Guinea	unspecified	DK5	N/A	N/A	29, slide 2	Picked Slides	13.5(74E)	R	recryst. And too little sample, difficult to identify	
Papua New Guinea	unspecified	DK5	N/A	N/A	30, slide 1	Picked Slides	13.5(74E)	P	globotruncana, recryst.	Coniacian - Maastrichtian (Upper Cretaceous)
Papua New Guinea	unspecified	DK5	N/A	N/A	30, slide 2	Picked Slides	13.5(74E)	P	Juveniles (sieved at smaller fractons), recryst.	
Papua New Guinea	unspecified	DK5	N/A	N/A	36	Picked Slides	13.5(74E)	B	no forams	
Papua New Guinea	unspecified	DP1	N/A	N/A	2-16	Picked Slides	13.5(74E)	N/A	N/A	
Papua New Guinea	unspecified	DP1	N/A	N/A	2	Picked Slides	13.5(74E)	B	N/A	
Papua New Guinea	unspecified	DP1	N/A	N/A	4	Picked Slides	13.5(74E)	B	N/A	
Papua New Guinea	unspecified	DP1	N/A	N/A	6	Picked Slides	13.5(74E)	B	N/A	
Papua New Guinea	unspecified	DP1	N/A	N/A	10	Picked Slides	13.5(74E)	R	pyritised, recryst. Forams, unidentifiable	
Papua New Guinea	unspecified	DP1	N/A	N/A	11	Picked Slides	13.5(74E)	P	mainly benthics, maybe Chiloguembelina?	
Papua New Guinea	unspecified	DP1	N/A	N/A	12	Picked Slides	13.5(74E)	R	mainly benthics, pyritised and	

									recyst. Difficult to identify	
Papua New Guinea	unspecified	DP1	N/A	N/A	13	Picked Slides	13.5(74E)	B	N/A	
Papua New Guinea	unspecified	DP1	N/A	N/A	16	Picked Slides	13.5(74E)	P	pyritised and recryst., unidentifiable	
Papua New Guinea	unspecified	DP2	N/A	N/A	1-3	Picked Slides	13.5(74E)	N/A	N/A	
Papua New Guinea	unspecified	DP2	N/A	N/A	1	Picked Slides	13.5(74E)	R	Slide 1 of 2, pyritised and recryst., unidentifiable	
Papua New Guinea	unspecified	DP2	N/A	N/A	1	Picked Slides	13.5(74E)	P	Slide 2 of 2, pyritised and recryst., unidentifiable	
Papua New Guinea	unspecified	DP2	N/A	N/A	3	Picked Slides	13.5(74E)	P	Lower Cretaceous, e.g. Albian with Rotalipora apenninica, recryst,	Albian (Lower Cretaceous) to Cenomanian (Upper Cretaceous)
Papua New Guinea	unspecified	MD1	N/A	N/A	1-11	Picked Slides	13.5(74E)	N/A	N/A	
Papua New Guinea	unspecified	MD1	N/A	N/A	1	Picked Slides	13.5(74E)	R	benthics, recryst.	
Papua New Guinea	unspecified	MD1	N/A	N/A	2	Picked Slides	13.5(74E)	R	benthics, recryst.	
Papua New Guinea	unspecified	MD1	N/A	N/A	3	Picked Slides	13.5(74E)	R	benthics, recryst.	
Papua New Guinea	unspecified	MD1	N/A	N/A	4	Picked Slides	13.5(74E)	R	Miocene or younger, globorotalia present, little sample, difficult to	Chattian (Late Oligocene) to Recent

									identify at the species level.	
Papua New Guinea	unspecified	MD1	N/A	N/A	8	Picked Slides	13.5(74E)	R	Only one planktonic foram present, very pyritised and recryst., difficult to identify so obviously too little sample too.	
Papua New Guinea	unspecified	MD1	N/A	N/A	9	Picked Slides	13.5(74E)	B	no forams	
Papua New Guinea	unspecified	MD1	N/A	N/A	10	Picked Slides	13.5(74E)	R	benthics, maybe some planktonics but broken mostly, difficult to identify, too little sample	
Papua New Guinea	unspecified	MD1	N/A	N/A	11	Picked Slides	13.5(74E)	R	Very pyritised, difficult to identify, and too little sample.	
Papua New Guinea	unspecified	MD2	N/A	N/A	1-6	Picked Slides	13.5(74E)	N/A	N/A	
Papua New Guinea	unspecified	MD2	N/A	N/A	1	Picked Slides	13.5(74E)	R	very recryst. And too litle sample, difficult to identify.	
Papua New Guinea	unspecified	MD2	N/A	N/A	2	Picked Slides	13.5(74E)	P	Globorotalia Menardii present, and then also identified trilobus, bullloides, and maybe ruber, recryst.	Serravallian (Middle Miocene) to Recent

Papua New Guinea	unspecified	MD2	N/A	N/A	4	Picked Slides	13.5(74E)	P	broken and recryst., difficult to identify, also, very small specimens, perhaps sieved at smaller fractipons (hence juveniles).	
Papua New Guinea	unspecified	MD2	N/A	N/A	5	Picked Slides	13.5(74E)	R	broken and recryst., difficult to identify	
Papua New Guinea	unspecified	MD2	N/A	N/A	6	Picked Slides	13.5(74E)	B	no forams	
Papua New Guinea	unspecified	PPL86	N/A	N/A	A3-40 - A3-55; A4-29A; A5-85 - A5-91	Picked Slides	13.5(74E)	N/A	N/A	
Papua New Guinea	unspecified	PPL86	N/A	N/A	A1- SB or 5B?	Picked Slides	13.5(74E)	E	trilob. Trilobatus; orb. Univ., middle miocene or recent; vrdi;	Langhian (Middle Miocene) to Recent
Papua New Guinea	unspecified	PPL86	N/A	N/A	A3-40	Picked Slides	13.5(74E)	P	Middle Miocene or younger, orbulina universa, ver recryst., difficult to identify.	Langhian (Middle Miocene) to Recent
Papua New Guinea	unspecified	PPL86	N/A	N/A	A3-41	Picked Slides	13.5(74E)	P	Middle Miocene or younger, orbulina universa, ver recryst., difficult to identify.	Langhian (Middle Miocene) to Recent
Papua New Guinea	unspecified	PPL86	N/A	N/A	A3-43	Picked Slides	13.5(74E)	R	very recryst. And too litle sample, difficult to identify.	

Papua New Guinea	unspecified	PPL86	N/A	N/A	A3-49	Picked Slides	13.5(74E)	E	because praeorbulina glomerosa curva and praeorbulina transitoria but no orbulina universa, trilobus present too, recryst.	Chattian (Late Oligocene) to Langhian (Middle Miocene)
Papua New Guinea	unspecified	PPL86	N/A	N/A	A3-55	Picked Slides	13.5(74E)	A	Middle Miocene or younger, orbulina universa and globorotalia genus present, recryst., some pyritised.	Langhian (Middle Miocene) to Recent
Papua New Guinea	unspecified	PPL86	N/A	N/A	A4-29A	Picked Slides	13.5(74E)	R	very recryst. And some pyritised, too little sample to even identify if they are forams.	
Papua New Guinea	unspecified	PPL86	N/A	N/A	A5-85	Picked Slides	13.5(74E)	E	Middle Miocene because of Globigerina Quadrilobata, then also present trilobatus, dentoglobigerina venezuelana, Paragloborotalia siakensis, fohsella peripheronda, infilled and recryst.	
Papua New Guinea	unspecified	PPL86	N/A	N/A	A5-87	Picked Slides	13.5(74E)	E	Middle to Late Miocene because of dentglobigerina tripatita, then MAYBE also present neogloboquadrina acostaensis which would be Late Miocene onwards.	

Papua New Guinea	unspecified	PPL86	N/A	N/A	A5-91	Picked Slides	13.5(74E)	P	Late Cretaceous because of genus Globotruncana present, pyritised and recryst.	Coniacian - Maastrichtian (Upper Cretaceous)
Papua New Guinea	unspecified	PPL86	N/A	N/A	A10-2	Picked Slides	13.5(74E)	P	pyritised and very recryst., difficult to identify.	
Papua New Guinea	unspecified	PPL86	N/A	N/A	A10-3	Picked Slides	13.5(74E)	P	Very pyritised and recryst., difficult to identify, maybe genus morozovella	Early Eocene
Papua New Guinea	unspecified	PPL86	N/A	N/A	A10-4	Picked Slides	13.5(74E)	P	Late Cretaceous because of genus Globotruncana present, pyritised and recryst.	Coniacian - Maastrichtian (Upper Cretaceous)
Papua New Guinea	unspecified	PPL86	N/A	N/A	A10-5	Picked Slides	13.5(74E)	R	Very pyritised and recryst., difficult to identify.	
Papua New Guinea	unspecified	PPL86	N/A	N/A	A10-7	Picked Slides	13.5(74E)	R	very pyritised and recryst., difficult to identify, also little sample.	
Papua New Guinea	unspecified	PPL86	N/A	N/A	A10-8	Picked Slides	13.5(74E)	R	very pyritised and recryst., difficult to identify, also little sample.	
Papua New Guinea	unspecified	PPL86	N/A	N/A	A10-9	Picked Slides	13.5(74E)	R	one foram present, very pyritised and recryst., difficult to identify.	
Papua New Guinea	unspecified	PPL86	N/A	N/A	A10-10	Picked Slides	13.5(74E)	R	Maybe Late Cretaceous lookgn at the benthic assemblage (the spherical benthic with a small "protuberanza"), but very pyritised, recryst. and too	

									little sample, difficult to identify.	
Papua New Guinea	unspecified	PPL86	N/A	N/A	A10-11	Picked Slides	13.5(74E)	R	Very pyritised, recryst., and too little sample, difficult to identify.	
Papua New Guinea	unspecified	PPL86	N/A	N/A	A10-12	Picked Slides	13.5(74E)	R	Very pyritised, recryst., and too little sample, difficult to identify, maybe orbulina universa (1 speciment of maybe orbulina universa present), but cannot be sure due to the surface being pyritised and recryst.	
Papua New Guinea	unspecified	PPL86	N/A	N/A	A10-13	Picked Slides	13.5(74E)	B	no forams.	
Papua New Guinea	unspecified	PPL86	N/A	N/A	A10-14	Picked Slides	13.5(74E)	B	no forams but other bits (things) present.	
Papua New Guinea	unspecified	PPL86	N/A	N/A	A10-15	Picked Slides	13.5(74E)	B	no forams.	
Papua New Guinea	unspecified	Unspecified	N/A	N/A	A2-12	Picked Slides	13.5(74E)	B	no forams	
Papua New Guinea	unspecified	Unspecified	N/A	N/A	A2-15	Picked Slides	13.5(74E)	R	Middle Miocene or younger, recryst.	

Papua New Guinea	unspecified	Unspecified	N/A	N/A	A3-1B	Picked Slides	13.5(74E)	P	Very recryst. And infilled, difficult to identify	
Papua New Guinea	unspecified	Unspecified	N/A	N/A	A3-13	Picked Slides	13.5(74E)	P	Very recryst. And infilled, difficult to identify.	
Papua New Guinea	unspecified	Unspecified	N/A	N/A	A3-21	Picked Slides	13.5(74E)	R	Very recryst. And infilled, difficult to identify.	
Papua New Guinea	unspecified	Unspecified	N/A	N/A	A3-22	Picked Slides	13.5(74E)	R	Very recryst. And infilled, difficulty to identify	
Papua New Guinea	unspecified	Unspecified	N/A	N/A	A3-27	Picked Slides	13.5(74E)	P	simultaneous presence of Orbulina Universa, Praeorbulina Transitoria	Langhian (Middle Miocene)
Papua New Guinea	unspecified	Unspecified	N/A	N/A	A3-28	Picked Slides	13.5(74E)	R	Only three pieces, not even sure it's forams, very recryst., difficult to identify	
Papua New Guinea	unspecified	Unspecified	N/A	N/A	A5-3	Picked Slides	13.5(74E)	P	Globorotalia hirsuta, recryst. A	Ionian (Late Pleistocene) to Recent
Papua New Guinea	unspecified	PPL86	N/A	N/A	A8-34	Picked Slides	13.5(74E)	P	Mainly benthics, recryst. And some pyritised.	
Papua New Guinea	unspecified	PPL86	N/A	N/A	A8-36	Picked Slides	13.5(74E)	R	mainly benthics, too little sample and recryst., difficult to identify.	
Papua New Guinea	unspecified	PPL86	N/A	N/A	A8-37	Picked Slides	13.5(74E)	G	Orb. Universa then Middle Miocene or younger, specimens very small and very recryst., difficult to identify.	Langhian (Middle Miocene) to Recent

Papua New Guinea	unspecified	PPL86	N/A	N/A	AIA-5	Picked Slides	13.5(74E)	P	Mainly benthic, recryst. And too little (or no) sample (of planktics) to be able to identify.	
Papua New Guinea	unspecified	PPL86	N/A	N/A	A9-3	Picked Slides	13.5(74E)	R	Too recryst. And too little sample to identify.	
Papua New Guinea	unspecified	PPL86	N/A	N/A	A9-10	Picked Slides	13.5(74E)	P	Praeorbulina, orb. Universa and orb. Bilobata so M6, Early Middle Miocene for their simultaneous presence, recryst.	Early Miocene
Papua New Guinea	unspecified	PPL86	N/A	N/A	A9-14	Picked Slides	13.5(74E)	P	(A); only benthics (if any), other things present.	
Papua New Guinea	unspecified	PPL86	N/A	N/A	A9-14	Picked Slides	13.5(74E)	R	(B), only benthics (if any), other things present.	
Papua New Guinea	unspecified	PPL86	N/A	N/A	A9-15	Picked Slides	13.5(74E)	R	Very recryst. And too little sample, difficult to identify.	
Papua New Guinea	unspecified	PPL86	N/A	N/A	A9 - 22	Picked Slides	13.5(74E)	P	Slide 1; Ruber, globorotalia scitula and another one with the last chamber quite thick on one side? Maybe trilob. Too. Some pyritised, vrdi.	Ionian (Late Pleistocene) to Recent
Papua New Guinea	unspecified	PPL86	N/A	N/A	A9 - 23	Picked Slides	13.5(74E)	P	Slide 2; evidently smaller size fraction; trilob., vrdi.	Chattian (Late Oligocene) to Recent
Papua New Guinea	unspecified	PPL86	N/A	N/A	A9 - 23	Picked Slides	13.5(74E)	P	vrdi, some pyritised, trilob., glob. Scitula.	Ionian (Late Pleistocene) to Recent

Papua New Guinea	unspecified	PPL86; Wylie Creek, 9.9 m	N/A	N/A	N/A	Picked Slides	13.5(74E)	E	Eocene, M. subbotinae vrdi., M. aragonensis Vrdi.	Ypresian (Early Eocene)
Papua New Guinea	unspecified	Unspecified	N/A	N/A	A4-21	Picked Slides	13.5(74E)	P	Mainly benthics, recryst. And too little sample, difficult to identify.	
Papua New Guinea	unspecified	Unspecified	N/A	N/A	A4-22	Picked Slides	13.5(74E)	R	Mainly benthics and too little sample, difficult to identify.	
Papua New Guinea	unspecified	Unspecified	N/A	N/A	A4-24	Picked Slides	13.5(74E)	E	Loads of different praorbulina including praeorb. Transitoria., but no orbulina universa or orb. Suturalis, so should be at the transition, recryst.	Burdigalian (Early Miocene)
Papua New Guinea	unspecified	Unspecified	N/A	N/A	A4-25	Picked Slides	13.5(74E)	R	Very recryst. And too little sample, difficult to identify.	
Papua New Guinea	unspecified	Unspecified	N/A	N/A	A4-27	Picked Slides	13.5(74E)	P	mainly benthics, too little sample and recryst., difficult to identify.	
Papua New Guinea	unspecified	Unspecified	N/A	N/A	A5-7	Picked Slides	13.5(74E)	P	Slide 1 of 2; Orbulina Universa, globorotalia archeomenardii which narrows it down to Early Micoene - Early Middle Miocene only.	Serravallian (Middle Miocene

Papua New Guinea	unspecified	Unspecified	N/A	N/A	A5-7	Picked Slides	13.5(74E)	P	Slide 2 of 2; more orb. Universa than slide 1 and bigger specimens (mainly benthics ones the larger ones), Early Miocene - Early Middle Miocene, as deduced from Slide 1.	Serravallian (Middle Miocene
Papua New Guinea	unspecified	Unspecified	N/A	N/A	A5-12	Picked Slides	13.5(74E)	P	orb. Universa; too little sample and very recryst., difficult to identify.	Langhian (Middle Miocene)
Papua New Guinea	unspecified	Unspecified	N/A	N/A	A5-13	Picked Slides	13.5(74E)	R	mainly benthics, too little sample and recryst., difficult to identify.	
Papua New Guinea	unspecified	Unspecified	N/A	N/A	A5-14	Picked Slides	13.5(74E)	R	Too recryst., pyritised, and too little sample, difficult to identify.	
Papua New Guinea	unspecified	Unspecified	N/A	N/A	A5-15	Picked Slides	13.5(74E)	P	orb. Universa, some specimens very recryst. And pyritised , difficult to identify to narrow down range.	Langhian (Middle Miocene) to Recent
Papua New Guinea	unspecified	Unspecified	N/A	N/A	A5-32	Picked Slides	13.5(74E)	R	4-5 specimens, not even sure if benthic forams? "Long sticks", recryst.	
Papua New Guinea	unspecified	Unspecified	N/A	N/A	A5-36	Picked Slides	13.5(74E)	P	Early Miocene or younger because of Globigerinoides trilobus, mainly benthics, recryst., and too little sample, difficult to identify	Chattian (Late Oligocene) to Recent

Papua New Guinea	unspecified	Unspecified	N/A	N/A	A6-1	Picked Slides	13.5(74E)	R	4-5 specimens, recryst., very small, and too little sample, difficult to recrystallise	
Papua New Guinea	unspecified	Unspecified	N/A	N/A	A6-4	Picked Slides	13.5(74E)	P	Slide 1 of 2; Early Miocene or younger because of Globigerinoides trilobus, mainly benthics, recryst., and too little sample, difficult to identify	Chattian (Late Oligocene) to Recent
Papua New Guinea	unspecified	Unspecified	N/A	N/A	A6-4	Picked Slides	13.5(74E)	P	Slide 2 of 2; Early Miocene because of Slide 1; specimens smaller than slide 1, very recryst., and too little sample, difficult to identify.	Chattian (Late Oligocene) to Recent
Papua New Guinea	unspecified	Unspecified	N/A	N/A	A6-22	Picked Slides	13.5(74E)	R	Slide 1 of 2?; Few specimens and recryst., difficult to identify.	
Papua New Guinea	unspecified	Unspecified	N/A	N/A	A6-22	Picked Slides	13.5(74E)	P	Slide 2 of 2?; Late Early Miocene or younger because of Orbulina Universa (loads of them), rest of specimens very small, very recryst., and too little sample, difficult to identify.	Langhian (Middle Miocene) to Recent

Papua New Guinea	unspecified	PPL86	N/A	N/A	A7-42	Picked Slides	13.5(74E)	P	Late Early Miocene or younger because of Orbulina Universa, rest of specimens very small, very recryst., and too little sample, difficult to identify.	Langhian (Middle Miocene) to Recent
Papua New Guinea	unspecified	PPL86	N/A	N/A	A8-35	Picked Slides	13.5(74E)	E	Early Middle Miocene because of Orbulina Universa, globorotal. Archeomenardii, glob. Praemenardii, only a few spcimens very big, the rest very small and very recryst., difficult to identify.	Langhian (Early Miocene) to Serravallian (Middle Miocene)
Papua New Guinea	unspecified	PPL86	N/A	N/A	A8-22	Picked Slides	13.5(74E)	A	Late Early Miocene because of narrower with Praeorbulina transitoria, then also Hastigerina praesiphonifera, and globigerinoides Sicarus, recryst., a few big samples like globigerinoides and praorb. and then a lot of small samples difficult to identify because very small and recryst.	Burdigalian (Early Miocene) to Langhian (Middle Miocene)
Papua New Guinea	unspecified	PPL86	N/A	N/A	A8-23	Picked Slides	13.5(74E)	P	Late Early Miocene - Middle Miocene because of Hastigerina	Chattian (Late Oligocene) to Serravallian (Middle Miocene)

									praeisphonifera, etc…	
Papua New Guinea	unspecified	PPL86	N/A	N/A	A8-25	Picked Slides	13.5(74E)	G	simultaneous presenceof hastigerina praeisphonifera and Hastigerina siphonifera, a few big specimens and rest quite small, recryst., and infilled.	Serravallian (Middle Miocene)
Papua New Guinea	unspecified	PPL86	N/A	N/A	A8-26	Picked Slides	13.5(74E)	R	Not even sure if all benthics, too recrystallised, and too little sample, difficult to identify.	
Papua New Guinea	unspecified	PPL86	N/A	N/A	A8-31	Picked Slides	13.5(74E)	P	Late Early Miocene - Early Middle Miocene because of Praeorb. Transitoria, recryst.	Burdigalian (Early Miocene) to Langhian (Middle Miocene)
Papua New Guinea	unspecified	PPL86	N/A	N/A	A8-32	Picked Slides	13.5(74E)	G	Late Early Miocene - Early Middle Miocene because of Praeorb. Transitoria, Praeorb. Glomerosa curva, recryst.	Burdigalian (Early Miocene) to Langhian (Middle Miocene)
Papua New Guinea	unspecified	PPL86	N/A	N/A	A8-33	Picked Slides	13.5(74E)	P	Late Early Miocene - Early Middle Miocene because of Globorotalia Archeomenardii, and Praeorbulina glomerosa curva, recryst. And some pyritised.	Burdigalian (Early Miocene) to Langhian (Middle Miocene)

Papua New Guinea	unspecified	PPL86	N/A	N/A	A6-57	Picked Slides	13.5(74E)	P	Specimens too small, very recryst., too little sample, difficult to identify	
Papua New Guinea	unspecified	PPL86	N/A	N/A	A7-7	Picked Slides	13.5(74E)	E	Late Early Miocene - Early Middle Miocene because of praeorb. Glomerosa curva, few big specimens, reecryst.	Burdigalian (Early Miocene) to Langhian (Middle Miocene)
Papua New Guinea	unspecified	PPL86	N/A	N/A	A7-8	Picked Slides	13.5(74E)	P	Late Early Miocene - Early Middle Miocene because of Hastigerina praesiphonifera, Globigerinoides Trilobus, recryst. And infilled	Chattian (Late Oligocene) to Serravallian (Middle Miocene)
Papua New Guinea	unspecified	PPL86	N/A	N/A	A7-18	Picked Slides	13.5(74E)	P	Erly Miocene or younger because of glob. Trilobus, specimens very recryst., difficult to identify.	Chattian (Late Oligocene) to Recent
Papua New Guinea	unspecified	PPL86	N/A	N/A	A7-19	Picked Slides	13.5(74E)	P	Middle Miocene because of Globorotalia siakensis, recryst.	Chattian (Late Oligocene) to Serravallian (Middle Miocene)
Papua New Guinea	unspecified	PPL86	N/A	N/A	A7-20	Picked Slides	13.5(74E)	P	Middle Miocene or younger because of orb. Bilobata, very small specimens and very recryst., difficult to identify.	Langhian (Middle Miocene) to Recent
Papua New Guinea	unspecified	PPL86	N/A	N/A	A7-22	Picked Slides	13.5(74E)	R	Mainly benthics, specimens very small and recrystallised, difficult to identify	

Papua New Guinea	unspecified	PPL86	N/A	N/A	A7-23	Picked Slides	13.5(74E)	P	Early Miocene or younger because of orb. Universa, specimens very small and very recryst., difficult to identify.	Langhian (Middle Miocene) to Recent
Papua New Guinea	unspecified	PPL86	N/A	N/A	A7-41	Picked Slides	13.5(74E)	P	Early Middle Miocene because of simultaneous presence of praeorb. Transitoria and orb. Universa, recryst.	Burdigalian (Early Miocene) to Langhian (Middle Miocene)
Papua New Guinea	unspecified	PPL86	N/A	N/A	A3-38	Picked Slides	13.5(74E)	P	Early Miocene or younger because of globig. Trilobus, very recryst., difficult to identify.	Chattian (Late Oligocene) to recent
Papua New Guinea	unspecified	PPL86	N/A	N/A	A7-43	Picked Slides	13.5(74E)	R	Very recryst. And few specimens, difficult to identify.	
Papua New Guinea	unspecified	PPL86	N/A	N/A	A8-9	Picked Slides	13.5(74E)	E	End of Early Eocene because of praoerb. Transitoria, then also present are Hastigerina praesiphonifera, Globoquadrina dehiscens, globigerinoides subquadratus, no orbulina, recryst.	Burdigalian (Early Miocene)
Papua New Guinea	unspecified	PPL86	N/A	N/A	A8-11	Picked Slides	13.5(74E)	P	Specimens pyritised and recryst, and few spcimens, difficult to identify.	

Papua New Guinea	unspecified	PPL86	N/A	N/A	A8-16	Picked Slides	13.5(74E)	G	Late Middle Miocene or younger because of globigerinoides ruber, recryst.	Serravallian (Middle Miocene) to Recent
Papua New Guinea	unspecified	PPL86	N/A	N/A	A8-170	Picked Slides	13.5(74E)	P	Slide 1 of 2; Early Miocene or younger, little sample and mainl trilob. And orb. Universa present.	Langhian (Middle Miocene) to Recent
Papua New Guinea	unspecified	PPL86	N/A	N/A	A8-170	Picked Slides	13.5(74E)	G	Slide 2 of 2; Early Miocene or younger because of Globigerinoides trilobus.	Langhian (Middle Miocene) to Recent
Papua New Guinea	unspecified	PPL86	N/A	N/A	A8-18	Picked Slides	13.5(74E)	E	Early Middle Miocene because of Fohsella genus present, and then also present Globorotalia scitula scitula, recryst.	Langhian (Middle Miocene) to Messinian (Late Miocene)
Papua New Guinea	unspecified	PPL86	N/A	N/A	A8-20	Picked Slides	13.5(74E)	P	Late Early Miocene - Early Middle Miocene because of Hastigerina praesiphonifera, recryst.	Chattian (Late Oligocene) to Serravallian (Middle Miocene)
Papua New Guinea	unspecified	PPL86	N/A	N/A	A6-24	Picked Slides	13.5(74E)	B	no forams	
Papua New Guinea	unspecified	PPL86	N/A	N/A	A6-36	Picked Slides	13.5(74E)	B	no forams	
Papua New Guinea	unspecified	PPL86	N/A	N/A	A6-37	Picked Slides	13.5(74E)	P	Early Miocene or younger because of glob. Trilobus, few specimens and very recryst., difficult to identigy.	Chattian (Late Oligocene) to Recent

Papua New Guinea	unspecified	PPL86	N/A	N/A	A6-38	Picked Slides	13.5(74E)	P	Very recryst., difficult to identify.	
Papua New Guinea	unspecified	PPL86	N/A	N/A	A6-39	Picked Slides	13.5(74E)	R	Very recryst., and few specimens, difficult to identify.	
Papua New Guinea	unspecified	PPL86	N/A	N/A	A6-54	Picked Slides	13.5(74E)	P	Mainly benthics, few specimens and recryst., difficult to identify.	
Papua New Guinea	unspecified	PPL86	N/A	N/A	A6-55	Picked Slides	13.5(74E)	R	Mainly benthics, a few spcimens and very recryst., some broken, difficult to identify.	
Papua New Guinea	unspecified	PPL86	N/A	N/A	A6-56	Picked Slides	13.5(74E)	R	Mainly benthics, few specimens and very recryst. And some broken, difficult to identify.	
Papua New Guinea	unspecified	PPL86	N/A	N/A	A7-52	Picked Slides	13.5(74E)	P	orb. Universa, specimens recryst., difficult to identify.	Langhian (Middle Miocene) to Recent
Papua New Guinea	unspecified	Unspecified	N/A	N/A	A6-23	Picked Slides	13.5(74E)	P	Mainly benthics, specimens recryst., and few specimens, and some specimens broken, difficult to identify.	
Papua New Guinea	unspecified	Unspecified	N/A	N/A	A6-25	Picked Slides	13.5(74E)	P	Mainly benthics, specimens broken, very recryst. And some broken, difficult to identify.	
Papua New Guinea	unspecified	Unspecified	N/A	N/A	A6-26	Picked Slides	13.5(74E)	R	Not even sure if all benthics, too recrystallised, and too little sample, difficult to identify.	

Papua New Guinea	unspecified	Komewu	2	1926	7040	N/A	Picked Slides	13.5(74E)	N/A	N/A	
Papua New Guinea	unspecified	Komewu	2	1926		N/A	Picked Slides	13.5(74E)	B	no forams	
Papua New Guinea	unspecified	Komewu	2	6630		N/A	Picked Slides	13.5(74E)	R	Only 1-5 specimens, some pyritised, difficult to identify.	
Papua New Guinea	unspecified	Komewu	2	6845		N/A	Picked Slides	13.5(74E)	R	Some agglutinated forams, no planktics	
Papua New Guinea	unspecified	Komewu	2	7040		N/A	Picked Slides	13.5(74E)	R	One element, orange-ish, not even sure it's a foram., vrdi.	
Papua New Guinea	unspecified	Orie	1	1865	2330	N/A	Picked Slides	13.5(74E)	N/A	N/A	
Papua New Guinea	unspecified	Orie	1	1865		N/A	Picked Slides	13.5(74E)	B	no forams, some echinoids spines	
Papua New Guinea	unspecified	Orie	1	1950		N/A	Picked Slides	13.5(74E)	B	no forams	
Papua New Guinea	unspecified	Orie	1	2090		N/A	Picked Slides	13.5(74E)	R	only benthics (1-2 specimens).	
Papua New Guinea	unspecified	Orie	1	2210		N/A	Picked Slides	13.5(74E)	B	no forams	
Papua New Guinea	unspecified	Orie	1	2330		N/A	Picked Slides	13.5(74E)	R	only betnhics (one specimen).	
Papua New Guinea	unspecified	unspecified	unspecified	unspecified		N/A	Picked Slides	13.5(74E)	B	Only notes on the slide: 90/MJ-03-11); miscellaneous microfossils, no forams	

Papua New Guinea	unspecified	Iamara	1	3510	4013	N/A	Picked Slides	13.5(74E)	N/A	N/A	
Papua New Guinea	unspecified	Iamara	1	3510		N/A	Picked Slides	13.5(74E)	B	little rocks/sediments	
Papua New Guinea	unspecified	Iamara	1	3629		N/A	Picked Slides	13.5(74E)	B	little rocks/sediments	
Papua New Guinea	unspecified	Iamara	1	3773		N/A	Picked Slides	13.5(74E)	B	little rocks/sediments	
Papua New Guinea	unspecified	Iamara	1	3883		N/A	Picked Slides	13.5(74E)	B	miscellaneous microfossils, no forams	
Papua New Guinea	unspecified	Iamara	1	4013		N/A	Picked Slides	13.5(74E)	B	no forams	
Papua New Guinea	unspecified	Hides	1	2598-2969		N/A	Picked Slides	13.5(74E)	R	miscellaneous microfossils, maybe a few forams but very recrystallised.	
Papua New Guinea	unspecified	Hides	1	2988-2991		N/A	Picked Slides	13.5(74E)	R	miscellaneous microfossils, maybe a few forams but very recrystallised.	
Papua New Guinea	unspecified	Hides	1	3069-3072		N/A	Picked Slides	13.5(74E)	B	miscellaneous microfossils, no forams	
Papua New Guinea	unspecified	Hides	1	3216-3219		N/A	Picked Slides	13.5(74E)	B	little rocks/sediments	
Papua New Guinea	unspecified	Hides	1	3288-3291		N/A	Picked Slides	13.5(74E)	B	echinoids spines?	
Papua New Guinea	unspecified	Iagifu	4x	8040 - 10170		N/A	Picked Slides	13.5(74E)	N/A	N/A	

Papua New Guinea	unspecified	lagifu	4x	8040	N/A	Picked Slides	13.5(74E)	R	1 element, not even sure it's a foram.	
Papua New Guinea	unspecified	lagifu	4x	8270	N/A	Picked Slides	13.5(74E)	R	Specimens pyritised and recryst, and few specimens, difficult to identify.	
Papua New Guinea	unspecified	lagifu	4x	8450	N/A	Picked Slides	13.5(74E)	R	Only 1 speciment present, maybe a foram? Very pyritised and recryst., difficult to identify.	
Papua New Guinea	unspecified	lagifu	4x	8610	N/A	Picked Slides	13.5(74E)	B	miscellaneous microfossils, no forams	
Papua New Guinea	unspecified	lagifu	4x	8760	N/A	Picked Slides	13.5(74E)	R	Specimens pyritised and recryst, and few specimens, and very small, difficult to identify.	
Papua New Guinea	unspecified	lagifu	4x	8960	N/A	Picked Slides	13.5(74E)	B	no forams	
Papua New Guinea	unspecified	lagifu	4x	9100	N/A	Picked Slides	13.5(74E)	B	miscellaneous microfossils	
Papua New Guinea	unspecified	lagifu	4x	9450	N/A	Picked Slides	13.5(74E)	B	miscellaneous microfossils	
Papua New Guinea	unspecified	lagifu	4x	9760	N/A	Picked Slides	13.5(74E)	R	Benthics only, very recryst., miscellaneous microfossils	
Papua New Guinea	unspecified	lagifu	4x	10170	N/A	Picked Slides	13.5(74E)	R	miscellanneous microfossils, maybe one foram, seems benthics, very recryst.	

Papua New Guinea	unspecified	Elevala	1	20 - 1090	N/A	Picked Slides	13.5(74E)	N/A	N/A; lagoonal shallow environment due to main presence of benthics, very few planktics, probably been reworked or transported there.	
Papua New Guinea	unspecified	Elevala	1	20	N/A	Picked Slides	13.5(74E)	B	Miscellaneous microfossils, no forams.	
Papua New Guinea	unspecified	Elevala	1	30	N/A	Picked Slides	13.5(74E)	R	Miscellaneous microfosisls, maybe a few benthics but recryst., orange colour.	
Papua New Guinea	unspecified	Elevala	1	60	N/A	Picked Slides	13.5(74E)	R	Benthics only, recryst.	
Papua New Guinea	unspecified	Elevala	1	75	N/A	Picked Slides	13.5(74E)	R	Miscellaneous microfossils, 1-2 planktics ut vey recryst. And pyritised, difficult to identify	
Papua New Guinea	unspecified	Elevala	1	90	N/A	Picked Slides	13.5(74E)	R	Miscellaneous microfossils, maybe some benthics, very recryst., and some pyritised, difficult to identify.	
Papua New Guinea	unspecified	Elevala	1	105	N/A	Picked Slides	13.5(74E)	R	Early Miocene or younger because of glob. Trilobus, then also Orb. Universa, orb. Bilobata, but few specimens and mostly these species, very recryst., And	Langhian (Middle Miocene) to Recent

									pyritised, difficult to identify.
Papua New Guinea	unspecified	Elevala	1	120	N/A	Picked Slides	13.5(74E)	R	Maybe forams, 1-2 planktics but very recryst. And pyritised, difficult to identify.
Papua New Guinea	unspecified	Elevala	1	135	N/A	Picked Slides	13.5(74E)	R	Literally 2 specimens, one benthic and one planktic, but very recryst., difficult to identify.
Papua New Guinea	unspecified	Elevala	1	150	N/A	Picked Slides	13.5(74E)	R	Few planktics, very recryst., difficult to identify, seem like recent forams though (glob. Species and maybe orb.)
Papua New Guinea	unspecified	Elevala	1	165	N/A	Picked Slides	13.5(74E)	R	Miscellaneous microfossils, maybe 1-2 planktics but very recryst. And some pyritised, difficult to identify.
Papua New Guinea	unspecified	Elevala	1	210	N/A	Picked Slides	13.5(74E)	R	1-2 benthics, 1-5 planktics but very recryst. And some pyritised, difficult to identify. Maybe one orb. Universa

Papua New Guinea	unspecified	Elevala	1	230	N/A	Picked Slides	13.5(74E)	B	Miscellaneous microfossils, no sign of forams.	
Papua New Guinea	unspecified	Elevala	1	260	N/A	Picked Slides	13.5(74E)	R	Middle Miocene or younger, because there are 3 specimens, of which 2 are orb. Universa.	Langhian (Middle Miocene) to Recent
Papua New Guinea	unspecified	Elevala	1	280	N/A	Picked Slides	13.5(74E)	R	Benthics and 1-5 specimens of planktics, bt very recryst., and infilled, difficult to identify.	
Papua New Guinea	unspecified	Elevala	1	300	N/A	Picked Slides	13.5(74E)	R	Middle Miocene or younger because there are 1-3 planktics, maybe one bilobata (very pyritised, recryst. And infilled), and one Orb. Univesa, benthics also present,recryst.	Langhian (Middle Miocene) to Recent
Papua New Guinea	unspecified	Elevala	1	320	N/A	Picked Slides	13.5(74E)	R	Miscellaneous microfossils, specimens very recryst., infilled, and some pyritised, difficult to identify.	
Papua New Guinea	unspecified	Elevala	1	340	N/A	Picked Slides	13.5(74E)	R	Few specimens and very recryst., maybe one orb. Universa.	
Papua New Guinea	unspecified	Elevala	1	360	N/A	Picked Slides	13.5(74E)	R	Few specimens and red-ish, maybe one bilobata and maybe one praeorb. (bottom seem too small compared to the	

									"ball" above), recryst. And infilled.	
Papua New Guinea	unspecified	Elevala	1	380	N/A	Picked Slides	13.5(74E)	R	Few specimens, maybe one belongs to Globotruncana genus (especially, the back is similar), but difficult to identify, ver recryst., and infilled.	
Papua New Guinea	unspecified	Elevala	1	410	N/A	Picked Slides	13.5(74E)	R	1-3 specimens, maybe one ob. Bilobata, red-ish and recryst., recryst.	
Papua New Guinea	unspecified	Elevala	1	430	N/A	Picked Slides	13.5(74E)	R	Few specimens, very recryst., difficult to identify.	
Papua New Guinea	unspecified	Elevala	1	460	N/A	Picked Slides	13.5(74E)	R	Few specimens, maybe 1-2 glob. Trilobus, very red-ish/black red-ish, and very recryst., difficult to identify.	Chattian (Late Oligocene) to Recent
Papua New Guinea	unspecified	Elevala	1	480	N/A	Picked Slides	13.5(74E)	R	Few specimens, very recryst., difficult to identify.	
Papua New Guinea	unspecified	Elevala	1	500	N/A	Picked Slides	13.5(74E)	R	Miscellaneous microfossils, maybe a few benthics.	
Papua New Guinea	unspecified	Elevala	1	520	N/A	Picked Slides	13.5(74E)	R	Benthics only	

Papua New Guinea	unspecified	Elevala	1	540	N/A	Picked Slides	13.5(74E)	R	Few specimens and red-ish/dark red-ish and very rcryst., maybe one orb. Bilobata, 1 orb. Universa, and 1 praeorb. Glomerosa curva, thus it would be about Early Middle Miocene or younger.	
Papua New Guinea	unspecified	Elevala	1	560	N/A	Picked Slides	13.5(74E)	R	Few specimens, planktics all red-ish/dark red-ish and very recryst., maybe one praeorb. (bottom seem too small compared to the "ball" above, maybe one orb. Universa, in that case it would be Early Miocene or younger.	
Papua New Guinea	unspecified	Elevala	1	580	N/A	Picked Slides	13.5(74E)	R	Few specimens, red-ish/dark red-ish and very recryst., maybe some orb. Universa, orb. Bilobata, one praoerb. Transitoria, maybe one praeorb. (bottom seem too small compared to the "ball" above), thus it would be Early Miocene or younger.	

Papua New Guinea	unspecified	Elevala	1	600	N/A	Picked Slides	13.5(74E)	R	Few specimens, red-ish/dark red-ish and very recryst., maybe some orb. Bilobata, orb. Universa and maybe one praeorb. (bottom seem too small compared to the "ball" above) in that case Middle Miocene or younger.	
Papua New Guinea	unspecified	Elevala	1	640	N/A	Picked Slides	13.5(74E)	P	Few specimens, red-ish/dark red-ish and very recryst., maybe some orb. Bilobata, and one orb. Universa, difficult to identify.	
Papua New Guinea	unspecified	Elevala	1	660	N/A	Picked Slides	13.5(74E)	P	Few specimens,some red-ish/dark red-ish, and some pyritised, and very recryst., maybe some orb. Bilobata, in that case Early Miocene or younger.	
Papua New Guinea	unspecified	Elevala	1	680	N/A	Picked Slides	13.5(74E)	R	Few specimens, very recryst., some, red-ish/dark red-ish, difficult to identify.	
Papua New Guinea	unspecified	Elevala	1	700	N/A	Picked Slides	13.5(74E)	R	Few specimens, red-ish and very recryst., difficult to identify.	
Papua New Guinea	unspecified	Elevala	1	720	N/A	Picked Slides	13.5(74E)	R	Miscellaneous, maybe 1-2 forams, maybe benthics.	

Papua New Guinea	unspecified	Elevala	1	740	N/A	Picked Slides	13.5(74E)	R	Few specimens, maybe one orb. Universa, very recryst. And red-ish/dark red-ish, in that case Middle Miocene or younger.	
Papua New Guinea	unspecified	Elevala	1	760	N/A	Picked Slides	13.5(74E)	R	Few specimens, maybe orb. Universa, very recryst., in that case Middle Miocene or younger.	
Papua New Guinea	unspecified	Elevala	1	780	N/A	Picked Slides	13.5(74E)	R	Middle Miocene or younger beacause of orb. Bilobata, specimens mainly that species so few specimens, pirytised, redd-ish, and recryst., difficult to identify.	Langhian (Middle Miocene) to Recent
Papua New Guinea	unspecified	Elevala	1	800	N/A	Picked Slides	13.5(74E)	P	Middle Miocene or younger beacause of orb. Bilobata, pyritised, redd-ish, and recryst., difficult to identify.	Langhian (Middle Miocene) to Recent
Papua New Guinea	unspecified	Elevala	1	820	N/A	Picked Slides	13.5(74E)	R	Middle Miocene or younger beacause of orb. Bilobata, few specimens, pyritised, redd-ish, and recryst., difficult to identify.	Langhian (Middle Miocene) to Recent
Papua New Guinea	unspecified	Elevala	1	840	N/A	Picked Slides	13.5(74E)	R	1-5 specimens, pyritised, red-ish, and recryst., difficult to identify	

Papua New Guinea	unspecified	Elevala	1	880	N/A	Picked Slides	13.5(74E)	R	Few specimens, pyritised, redd-ish, and recryst., difficult to identify.	
Papua New Guinea	unspecified	Elevala	1	900	N/A	Picked Slides	13.5(74E)	R	Few specimens, pyritised, redd-ish, and recryst., difficult to identify.	
Papua New Guinea	unspecified	Elevala	1	920	N/A	Picked Slides	13.5(74E)	P	Early Miocene or younger because of Globigerinoides trilobus, mainly benthics, recryst., and too little planktonic sample, difficult to identify	Chattian (Late Oligocene) to Recent
Papua New Guinea	unspecified	Elevala	1	940	N/A	Picked Slides	13.5(74E)	R	1-5 planktonic specimens, mainly benthics, and red-ish, very recryst., difficult to identify.	
Papua New Guinea	unspecified	Elevala	1	960	N/A	Picked Slides	13.5(74E)	P	Slide 1 of 2; benthics only, different colours and some seem recryst.	
Papua New Guinea	unspecified	Elevala	1	960	N/A	Picked Slides	13.5(74E)	R	Slide 2 of 2; Few specimens, very small, pyritised, and recryst., difficult to identify. Probably the smaller fraction after sieving.	
Papua New Guinea	unspecified	Elevala	1	980	N/A	Picked Slides	13.5(74E)	P	Slide 1 of 2; benthics only, different colours and some seem recryst.	

Papua New Guinea	unspecified	Elevala	1	980	N/A	Picked Slides	13.5(74E)	P	Slide 2 of 2; Few specimens, very small, pyritised, and recryst., difficult to identify, probably the smaller fraction after sieving.	
Papua New Guinea	unspecified	Elevala	1	1000	N/A	Picked Slides	13.5(74E)	P	Benthics only, different colour and some sem recryst.	
Papua New Guinea	unspecified	Elevala	1	1020	N/A	Picked Slides	13.5(74E)	P	Early Miocene or younger because of globigerinoides trilobus, few specimens, mainly benthics 9different colours, some seem recryst.), and red-ish, very recryst., difficult to identify.	Chattian (Late Oligocene) to Recent
Papua New Guinea	unspecified	Elevala	1	1040	N/A	Picked Slides	13.5(74E)	R	Miscellaneous microfossils, only a few benthics, seem recryst.	
Papua New Guinea	unspecified	Elevala	1	1060	N/A	Picked Slides	13.5(74E)	P	Benthics only, different colour and some seem recryst.	
Papua New Guinea	unspecified	Elevala	1	1060	N/A	Picked Slides	13.5(74E)	P	Early Miocene or younger because of globigerinoides trilobus, few specimens, 1-6, mainly benthics (different colours, some seem recryst.), and red-ish, and very recryst., difficult to identify.	Chattian (Late Oligocene) to Recent

Papua New Guinea	unspecified	Elevala	1	1080	N/A	Picked Slides	13.5(74E)	P	Middle Miocene because of one globorot. Merotumida I think!! Only planktonic foram found. Mainly benthics (different colours, some recryst.),	Tortonian (Late Miocene) to Zanclean (Early Pliocene)
Papua New Guinea	unspecified	Elevala	1	1090	N/A	Picked Slides	13.5(74E)	P	Benthics only, different colours, some seem recryst.	
Papua New Guinea	unspecified	Elevala	1	2885 - 2330	N/A	Picked Slides	13.5(74E)	N/A	N/A	
Papua New Guinea	unspecified	Elevala	1	2885	N/A	Picked Slides	13.5(74E)	P	Middle Miocene because of Fohsella robusta, recryst.	Serravallian (Middle Miocene)
Papua New Guinea	unspecified	Elevala	1	2300	N/A	Picked Slides	13.5(74E)	P	Middle Eocene or up to Middle Miocene (not younger because previous one is Middle Miocene) because of genus globoquadrina, recryst.	Aquitanian (Early Miocene) to Serravallian (Middle Miocene)
Papua New Guinea	unspecified	Elevala	1	2315	N/A	Picked Slides	13.5(74E)	P	Only benthics it seems, majority recrystallised.	
Papua New Guinea	unspecified	Elevala	1	2330	N/A	Picked Slides	13.5(74E)	R	Early Miocene or Middle Miocene (because previous slide is Middle Miocene) because of globigerinoides trilobus, recryst.	Chattian (Late Oligocene) to Serravallian (Middle Miocene)

Papua New Guinea	unspecified	Elevala	1	1085.1	N/A	Picked Slides	13.5(74E)	P	Middle Miocene or Late Miocene because of globigerina praebulloides and globigerina bulloides, recryst., and some pyritised.	Langhian (Early Miocene) to Tortonian (Late Miocene)
Papua New Guinea	unspecified	Elevala	1	1013.1	N/A	Picked Slides	13.5(74E)	P	Mainly benthics, only 1-5 planktic specimens, globoquadrina venezuelana so Middle Eocene up to Early Pliocene, very recryst. And some broken, difficult to identify.	Priabonian (Late Eocene) to Zanclean (Early Pliocene)
Papua New Guinea	unspecified	Elevala	1	985.9	N/A	Picked Slides	13.5(74E)	R	1-5 specimens, maybe one orb. Univesa bt ver small and yellow-ish, other specimens very small and rcryst., difficult to identify.	
Papua New Guinea	unspecified	Elevala	1	837.3	N/A	Picked Slides	13.5(74E)	R	Few spcimens, very recryst. And some pyritised, difficult to identify.	
Papua New Guinea	unspecified	Elevala	1	798.5	N/A	Picked Slides	13.5(74E)	R	Under five specimens and very recryst., very small, difficult to identify.	
Papua New Guinea	unspecified	Elevala	1	753.6	N/A	Picked Slides	13.5(74E)	R	Under five specimens and very recryst., difficult to identify.	

Papua New Guinea	unspecified	Elevala	1	721.9	N/A	Picked Slides	13.5(74E)	R	Specimens very small and pyritised (black) so not even sure they are forams, maybe some orb. Universa but very small.	
Papua New Guinea	unspecified	Elevala	1	653.5	N/A	Picked Slides	13.5(74E)	R	Literally two specimens, very recryst, one of which is yellow-ish and could be orb. Universa, but very small.	
Papua New Guinea	unspecified	Elevala	1	614.8	N/A	Picked Slides	13.5(74E)	R	Spcimens very small and under 10, not sure they're even forams, recryst., difficult to identify.	
		Elevala	1	366.9	N/A	Picked Slides	13.5(74E)	R	Some specimens very small and pyritised, and maybe 4 porb. Universa but very small, and yellow-ish, so both types of specimens difficult to identify, recryst.	
Papua New Guinea	unspecified	Elevala	1	530.4	N/A	Picked Slides	13.5(74E)	R	Under 10 specimens, some seem pyritised, not even sur ethey are forams, recryst., difficult to identify.	
Papua New Guinea	unspecified	Elevala	1	493.9	N/A	Picked Slides	13.5(74E)	P	Specimens very recryst. And infileld, and brown-ish, difficult to identify.	

Papua New Guinea	unspecified	Elevala	1	468.3	N/A	Picked Slides	13.5(74E)	R	Literally 1-4 specimens, very recryst., and very small, one brown-ish, one pyritised, difficult to identify.	
Papua New Guinea	unspecified	Elevala	1	435.5	N/A	Picked Slides	13.5(74E)	R	Literally 1 specimen, it seems planktic but brown-ish and difficult to identify chambers and the foram.	
Papua New Guinea	unspecified	Elevala	1	402.3	N/A	Picked Slides	13.5(74E)	R	Literally 2 specimens, very small and pyritised, difficult to identify.	
Papua New Guinea	unspecified	Elevala	1	369.4	N/A	Picked Slides	13.5(74E)	P	Specimens brown-ish and very recryst., maybe orb. Bilobata, difficult to identify	
Papua New Guinea	unspecified	Elevala	1	344.4	N/A	Picked Slides	13.5(74E)	R	Under 10 specimens, maybe three orb. Universa but very small, one yellow-ish and the other two orange-ish, difficult to identify.	
Papua New Guinea	unspecified	Elevala	1	310.9	N/A	Picked Slides	13.5(74E)	B	Some bits of rocks, no forams.	
Papua New Guinea	unspecified	Elevala	1	240.7	N/A	Picked Slides	13.5(74E)	R	Middle up to Early Pliocene because of simultaneous presence of Globigerinoides Obliquus Obliquus and Orbulina Universa, recryst., and infilled.	Aquitanian (Early Miocene) to Ionian (Late Pleistocene)

Papua New Guinea	unspecified	Elevala	1	153.6	N/A	Picked Slides	13.5(74E)	P	Specimens very small and recryst., maybe one orb. Universa but very small, recryst.	
Papua New Guinea	unspecified	88K	1	310 - 369	N/A	Picked Slides	13.5(74E)	N/A	N/A	
Papua New Guinea	unspecified	88K	1	310	N/A	Picked Slides	13.5(74E)	B	little rocks/sediments (three fractions), no forams	
Papua New Guinea	unspecified	88K	1	311	N/A	Picked Slides	13.5(74E)	R	Only benthics.	
Papua New Guinea	unspecified	88K	1	312	N/A	Picked Slides	13.5(74E)	P	glob. Praebulloides, recryst., some ostracods present too.	Serravallian (Middle Miocene)
Papua New Guinea	unspecified	88K	1	334	N/A	Picked Slides	13.5(74E)	B	Miscellaneous microfossils, no forams.	
Papua New Guinea	unspecified	88K	1	335	N/A	Picked Slides	13.5(74E)	P	fohsella genus present, including fohsella robusta, recryst.	Serravallian (Middle Miocene)
Papua New Guinea	unspecified	88K	1	336	N/A	Picked Slides	13.5(74E)	P	Few specimens, very small, and very recryst., difficult to identify.	
Papua New Guinea	unspecified	88K	1	355	N/A	Picked Slides	13.5(74E)	R	Miscellaneous microfossils, maybe a few benthics.	
Papua New Guinea	unspecified	88K	1	358	N/A	Picked Slides	13.5(74E)	R	Miscellaneous microfossils, maybe 1-2 planktics and 1-2 benthics, but very recryst., difficult to	

									identify, if even forams!!	
Papua New Guinea	unspecified	88K	1	366	N/A	Picked Slides	13.5(74E)	R	Miscellaneous microfossils, maybe a few forams but not even sure if benthics or planktics since they are very recryst., and in different colors, difficult to identify.	
Papua New Guinea	unspecified	88K	1	368	N/A	Picked Slides	13.5(74E)	P	Specimens very small and recryst., difficult to identify.	
Papua New Guinea	unspecified	88K	1	369	N/A	Picked Slides	13.5(74E)	P	Slide 1 of 2; Middle Miocene and Late Miocene together because of the simultaneous presence of Fohsella genus (including fohsella robusta), sacculifer (sac-like final chamber, evolved form), then also present orb. universa, recryst.	Serravallian (Middle Miocene)
Papua New Guinea	unspecified	88K	1	369	N/A	Picked Slides	13.5(74E)	P	Slide 2 of 2; specimens very small, probably a smaller fraction of slide 1 of 2., recryst.	Serravallian (Middle Miocene)

Papua New Guinea	unspecified	Ketu	1	20 1260	N/A	Picked Slides	13.5(74F)	N/A	N/A, when 4 slides usually 1 very small fractions, one large, 1 mainly benthic, and 1 intermediate.
Papua New Guinea	unspecified	Ketu	1	20	N/A	Picked Slides	13.5(74F)	R	4 specimens, 2 of which not even sure they are forams, very recryst.
Papua New Guinea	unspecified	Ketu	1	50	N/A	Picked Slides	13.5(74F)	R	Under specimens, of which 1 benthic and 2-3 planktics, but very recryst., difficult to identify.
Papua New Guinea	unspecified	Ketu	1	80	N/A	Picked Slides	13.5(74F)	R	Maybe one praoerb. In that case Late Early Miocene/Early Middle Miocene, other specimens black-red-ish, some pyritised, infilled and very recryst., difficult to identify.
Papua New Guinea	unspecified	Ketu	1	100	N/A	Picked Slides	13.5(74F)	R	specimens black-red-ish, some pyritised, infilled and very recryst., difficult to identify.
Papua New Guinea	unspecified	Ketu	1	130	N/A	Picked Slides	13.5(74F)	B	miscellaneous microfossils, including ostracods, no sign of forams.
Papua New Guinea	unspecified	Ketu	1	150	N/A	Picked Slides	13.5(74F)	R	specimens black-red-ish, some pyritised, infilled and very recryst., difficult to identify.

Papua New Guinea	unspecified	Ketu	1	180	N/A	Picked Slides	13.5(74F)	R	Miscellaneous microfossils (including ostracods?), too few specimens, maybe 2 orb. Univ. but very recryst. And one red-ish, difficult to identify.	
Papua New Guinea	unspecified	Ketu	1	200	N/A	Picked Slides	13.5(74F)	R	Very recryst., and few specimens., difficult to identify.	
Papua New Guinea	unspecified	Ketu	1	230	N/A	Picked Slides	13.5(74F)	R	Under 10 specimens, very recryst. Some black red-ish amd very small, maybe one orb. Bilobata but infilled, pyritised and recryst., difficult to identify.	
Papua New Guinea	unspecified	Ketu	1	250	N/A	Picked Slides	13.5(74F)	R	Maybe some orb. Universa and a recent glob. Specis, but specimens very small, infilled blac red-ish, and very recryst., difficult to identify.	
Papua New Guinea	unspecified	Ketu	1	280	N/A	Picked Slides	13.5(74F)	B	Miscellaneous microfossils, no sign of forams.	
Papua New Guinea	unspecified	Ketu	1	300	N/A	Picked Slides	13.5(74F)	R	Specimens very small, some black red-ish, infilled, and very recryst., maybe one orb. Bilobata, but red black-ish, difficult to identify.	

Papua New Guinea	unspecified	Ketu	1	330	N/A	Picked Slides	13.5(74F)	R	Miscellaneous microfossils mainly, specimens very infilled, some red black-ish, some very small, recryst., maybe one orb. Universda but very small, difficult to identify.	
Papua New Guinea	unspecified	Ketu	1	350	N/A	Picked Slides	13.5(74F)	R	Specimens infileld and recryst., some black red-ish, difficult to identify.	
Papua New Guinea	unspecified	Ketu	1	380	N/A	Picked Slides	13.5(74F)	R	Under 5 specimens, not even sure thye are forams, very small and recryst., difficult to identify.	
Papua New Guinea	unspecified	Ketu	1	400	N/A	Picked Slides	13.5(74F)	P	Specimens infilled and recryst., most of them either black red-ish or recrystallised, maybe orb. Universa and orb. bilobata, some very small, difficult to identify.	
Papua New Guinea	unspecified	Ketu	1	430	N/A	Picked Slides	13.5(74F)	R	Most specimens red-black ish, infilled and recryst., maybe one orb. Universa but very small and recryst., difficult to identify.	

Papua New Guinea	unspecified	Ketu	1	450	N/A	Picked Slides	13.5(74F)	R	Specimens infilled and recryst., some black red-ish, maybe some glob. Trilobus, and one orb. bilobata but very recryst. And glob. Bilobata black red-ish, difficult to identify.	
Papua New Guinea	unspecified	Ketu	1	480	N/A	Picked Slides	13.5(74F)	R	7 specimens, mainly orb. Universa, and orb. Bilobata, some black red-ish, recryst.	Langhian (Middle Miocene) to Recent
Papua New Guinea	unspecified	Ketu	1	500	N/A	Picked Slides	13.5(74F)	R	Miscellaneous microfossils, specimens mostly black red-ish, maybe some orb. Bilobata, recryst., difficult to identify.	
Papua New Guinea	unspecified	Ketu	1	530	N/A	Picked Slides	13.5(74F)	R	Miscellaneous microfossils, specimens mostly black red-ish, maybe one orb. universa, recryst., difficult to identify.	
Papua New Guinea	unspecified	Ketu	1	550	N/A	Picked Slides	13.5(74F)	R	3 specimens, very recryst., difficult to identify.	
Papua New Guinea	unspecified	Ketu	1	580	N/A	Picked Slides	13.5(74F)	R	Miscellaneous microfossils, specimens very small, infilled, and recryst., difficult to identify.	
Papua New Guinea	unspecified	Ketu	1	600	N/A	Picked Slides	13.5(74F)	R	a conglomerate of forams perhaps? Infilled, and black red-ish.	

Papua New Guinea	unspecified	Ketu	1	630	N/A	Picked Slides	13.5(74F)	R	Specimens very recryst. And specimens small, some pyritised, difficult to identify.	
Papua New Guinea	unspecified	Ketu	1	650	N/A	Picked Slides	13.5(74F)	R	Under 5 specimens, recryst., some pyritised, maybe some light red-ish, difficult to identify.	
Papua New Guinea	unspecified	Ketu	1	680	N/A	Picked Slides	13.5(74F)	R	About 5 specimens (including conglomerate of forams), maybe two orb. Bilobata but red light-ish and recryst., difficult to identify.	
Papua New Guinea	unspecified	Ketu	1	700	N/A	Picked Slides	13.5(74F)	R	Specimens black red-ish, maybe some orb. Bilobata and orb. Universa, recryst., difficult to identify.	
Papua New Guinea	unspecified	Ketu	1	730	N/A	Picked Slides	13.5(74F)	R	Under 10 specimens, maybe one orb. Universa but black red-ish and recryst., difficult to identify.	
Papua New Guinea	unspecified	Ketu	1	750	N/A	Picked Slides	13.5(74F)	R	Mainly conglomerates of forams, maybe some orb. Universa but in different sizes, blac red-ish, recryst., difficult to identify.	

Papua New Guinea	unspecified	Ketu	1	780	N/A	Picked Slides	13.5(74F)	R	Few specimens, maybe one orb. Bilobata, and one orb. Universa (dark red-ish), infilled and recryst., difficult to identify.	
Papua New Guinea	unspecified	Ketu	1	800	N/A	Picked Slides	13.5(74F)	R	Miscellaneous microfossils, conglomerate and one butdark red-ish,infilled and recryst., difficult to identify.	
Papua New Guinea	unspecified	Ketu	1	830	N/A	Picked Slides	13.5(74F)	R	Miscellaneous microfossils, maybe one orb. Universa and one orb. Bilobata, but very infilled and recryst., difficult to identify.	
Papua New Guinea	unspecified	Ketu	1	850	N/A	Picked Slides	13.5(74F)	R	Few specimens, maybe one orb. Bilobata and one praeorb. Glomerosa (but bottom rounded part is very small compared to above rounded part) and it is dark red-ish, recryst., difficult to identify.	
Papua New Guinea	unspecified	Ketu	1	880	N/A	Picked Slides	13.5(74F)	P	Specimens are dark brown-ish, infilled and recryst., maybe some ob. Bilobata, and orb. Universa, difficult to identify.	

Papua New Guinea	unspecified	Ketu	1	900	N/A	Picked Slides	13.5(74F)	R	Specimens are dark brown-ish, infilled and recryst., maybe some ob. Bilobata, and orb. Universa and one praeorb. Glomerosa (but bottom rounded part is very small compared to above rounded part) and it is dark-red ish, difficult to identify.	
Papua New Guinea	unspecified	Ketu	1	930	N/A	Picked Slides	13.5(74F)	R	Some specimens are very recryst., some conglomerates and dark red-ish, maybe some orb. Universa but very small and dark red-ish, difficult to identify.	
Papua New Guinea	unspecified	Ketu	1	950	N/A	Picked Slides	13.5(74F)	R	Some specimens dark-redi-ish and mainly conglomerates of foramsn, some others very recryst., maybe one orb. Universa but very small and dark red-ish, difficult to identify.	

Papua New Guinea	unspecified	Ketu	2	980	N/A	Picked Slides	13.5(74F)	R	Some specimens dark red-ish, some pyritised, and some very recryst., maybe some orb. Bilobata (dark red-ish and infileld), maybe some orb. Universa but quite small and very recryst., difficult to identify.	
Papua New Guinea	unspecified	Ketu	3	1000	N/A	Picked Slides	13.5(74F)	R	Quite a few orb. Universa butvery small, very recryst. And light brown-ish	
Papua New Guinea	unspecified	Ketu	4	1030	N/A	Picked Slides	13.5(74F)	R	Some very recryst., some pyritised, difficult to identify.	
Papua New Guinea	unspecified	Ketu	5	1050	N/A	Picked Slides	13.5(74F)	R	Miscellaneous microfossils, maybe one orb. Universa but very small, recryst., difficult toidentify.	
Papua New Guinea	unspecified	Ketu	6	1080	N/A	Picked Slides	13.5(74F)	R	Specimens very recryst., some black red-ish, maybe some orb. Universa, but black red-ish and some small, difficult to identify.	
Papua New Guinea	unspecified	Ketu	7	1100	N/A	Picked Slides	13.5(74F)	P	Specimens very recryst., some black red-ish, maybe some orb. Universa, but black red-ish and some small, maybe orb. Bilobata but very	

										infilled and recryst., difficult to identify.
Papua New Guinea	unspecified	Ketu	8	1130	N/A	Picked Slides	13.5(74F)	P		Mainly benthics, maybe some orb. Universa and glob. Trilobus, but very recryst., difficult to identify.
Papua New Guinea	unspecified	Ketu	9	1150	N/A	Picked Slides	13.5(74F)	P		Slide 1 of 2; benthics only, maybe one planktic, but very recryst. And light red-ish colour, difficultt o identify.
Papua New Guinea	unspecified	Ketu	10	1150	N/A	Picked Slides	13.5(74F)	P		Slide 2 of 2; predominantly benthics, maybe a few planktics but very recryst., maybe one orb. Universa but quite small and red-ish, difficult to identify.
Papua New Guinea	unspecified	Ketu	11	1180	N/A	Picked Slides	13.5(74F)	P		Slide 1 of 2; Predominantly benthics, maybe under 5 planktics, and maybe one glob. Trilobus, but very pyritised, difficult to identify.

Papua New Guinea	unspecified	Ketu	12	1180	N/A	Picked Slides	13.5(74F)	P	Slide 2 of 2; mainly benthics, a few planktic but very small and some pyritised, maybe one glob. Trilobus, but pyritised, difficult to identify.	
Papua New Guinea	unspecified	Ketu	13	1200	N/A	Picked Slides	13.5(74F)	P	Slide 1 of 2; miscellaneous microfossils; predominantly benthics, maybe under 5 planktics, and maybe one glob. Trilobus or glob. Trilobus immaturus (Early Miocene), but very recryst., difficult to identify. Quinqueloculina and elphidium (planktics) typical of shallow environments; coral fragments and gastropod shells. Maybe reticulina.	
Papua New Guinea	unspecified	Ketu	14	1200	N/A	Picked Slides	13.5(74F)	P	Slide 2 of 2; Late Miocene- Early Pliocene because of globigerina woodi; spheronidella semilunina; globigerinita macroperforate (very smal - not globigerinoides Diminutus because the latter has a	Burdigalian (Early Miocene)

Papua New Guinea	unspecified	Ketu							supplementary aperture).	
Papua New Guinea	unspecified	Ketu	15	1230	N/A	Picked Slides	13.5(74F)	P	Late Miocene - Early Miocene; Globigrinella?; spheroidella semilulina; globigerina Woodi (not globigerinoides woodi as the latter has supplementary apertures), globigerinita glutinata;	Burdigalian (Early Miocene) to Piacenzian (Late Pliocene)
Papua New Guinea	unspecified	Ketu	16	1230	N/A	Picked Slides	13.5(74F)	P	Mainly benthics, pterapod shells, ostracoda, gastropods, fragments of corals,. Quinqueloculina; elphidium, amolegina typical of shallow enviornment lagoons.	
Papua New Guinea	unspecified	Ketu	17	1240	N/A	Picked Slides	13.5(74F)	P	Late Miocene; Mainly benthics? Echinoids spines; glob. Obliquus, spheroinidella disjuncta, glob. Trilobus-	Burdigalian (Early Miocene) to Serravallian (Middle Miocene)

Papua New Guinea	unspecified	Ketu	18	1250	N/A	Picked Slides	13.5(74F)	P	Mainly benthics, pterapod shells, ostracoda, gastropods, fragments of corals,. Quinqueloculina; elphidium, amolegina typical of shallow enviornment lagoons., glob. Ruber; Miocene because of pyrgo benthic foram, maybe Late Miocene to Early Pliocene because of globorotalia exilis?	Messinian (Late Miocene) to Gelasian (Late Pliocene)
Papua New Guinea	unspecified	Ketu	19	1260	N/A	Picked Slides	13.5(74F)	P	Mainly benthics, pterapod shells, ostracoda, gastropods, fragments of corals, elphidium, amolegina typical of shallow enviornment lagoons., under 10 specimens, globorotalia (menardella), so Miocene.	Maybe Miocene
Papua New Guinea	unspecified	unspecified	Slide number 134	N/A	N/A	Picked Slides	13.5(74F)	P	pyritised, vrdi; maybe M. maerginodentata, Eocaena.	Ypresian (Early Eocene)
Papua New Guinea	unspecified	unspecified	Slide number 231	N/A	N/A	Picked Slides	13.5(74F)	A	Slide 1; eocaena; M. marginodentata; M. subbotinae; M. gracilis; infilled.	Ypresian (Early Eocene)

Papua New Guinea	unspecified	unspecified	Slide number 231	N/A	N/A	Picked Slides	13.5(74F)	A	Slide 2; Eocaena; subbotinae, infilled.	Ypresian (Early Eocene)
Papua New Guinea	unspecified	unspecified	Slide number 231	N/A	N/A	Picked Slides	13.5(74F)	A	Slide 3; smallest size fraction; maybe M. subbotinae, small forams and infilled, difficult to identify!	Thanetian (Late Paleocene) to Ypresian (Early Eocene)
Papua New Guinea	unspecified	KRE	N/A	N/A	5-399	Picked Slides	8.4(45E)	N/A	Difficulty emphasied by the structure the slide, whereby glass is glued to carton slide, so quite dusty and view is blurred. Furthermore, cannot really revert and move specimens to look at the different angles.	
Papua New Guinea	unspecified	KRE	N/A	N/A	5	Picked Slides	8.4(45E)	P	4 slides, of which 1 R; recent, including orb. Universa, vrdi.	Langhian (Middle Miocene) to Recent
Papua New Guinea	unspecified	KRE	N/A	N/A	11	Picked Slides	8.4(45E)	P	4 slides of which 1 P, orb. Universa and orb. Bilobata present, vrdi.	Langhian (Middle Miocene) to Recent
Papua New Guinea	unspecified	KRE	N/A	N/A	14	Picked Slides	8.4(45E)	P	4 slides of which 1 R and mainly benthics; orb. Universa, Middle Miocene or younger, specimens vrdi.	Langhian (Middle Miocene) to Recent
Papua New Guinea	unspecified	KRE	N/A	N/A	81F	Picked Slides	8.4(45E)	R	Moroz. Subbotinae, and maybe one foram glassy?! So Late Palaeocene, Early Eocene	Thanetian (Late Paleocene) to Ypresian (Early Eocene)

Papua New Guinea	unspecified	KRE	N/A	N/A	83F	Picked Slides	8.4(45E)	R	We already know it's Moogli Mudstone, so Early Eocene. In fact morozovella present like formosa formosa and marginodentata present, infilled and recryst.	
Papua New Guinea	unspecified	KRE	N/A	N/A	105 L	Picked Slides	8.4(45E)	P	Specimens very recryst., and some broken, difficult to identify	
Papua New Guinea	unspecified	KRE	N/A	N/A	149	Picked Slides	8.4(45E)	A	4 slides of which 1 R (mainly benthcs), orb. Universa and bilobata, spec. very recryst., diff. to identify.	Langhian (Middle Miocene) to Recent
Papua New Guinea	unspecified	KRE	N/A	N/A	150	Picked Slides	8.4(45E)	P	4 slides of which 2 R (1 mainly benthics and 1 smaller size fractions), orb. Universa and bil. Middle Miocene or younger, other specimens very recryst., diff. to identify.	Langhian (Middle Miocene) to Recent
Papua New Guinea	unspecified	KRE	N/A	N/A	166	Picked Slides	8.4(45E)	P	4 slides of which 1 R and mainly benthics; globig. Venezuelana; trilob., and bulloides, so Early Miocene to Early Pliocene both inclusive.	Langhian (Middle Miocene) to Zanclean (Early Pliocene)

Papua New Guinea	unspecified	KRE	N/A	N/A	167	Picked Slides	8.4(45E)	P	4 slides of which one is R with benthics only; orb. Universa Middle Miocene or younger, spec. very recryst., diff. to identify.	Langhian (Middle Miocene) to Recent
Papua New Guinea	unspecified	KRE	N/A	N/A	170	Picked Slides	8.4(45E)	P	3 slides of which 1 R with benthics only; trilob. But maybe also praesiph. (2 but broken ones) so maybe Early Miocene, spec. very recryst., diff. to identify.	
Papua New Guinea	unspecified	KRE	N/A	N/A	210	Picked Slides	8.4(45E)	P	4 slides of which 1 R and benthics only; trilo. So Ealy Miocene or younger, spe. Very recryst., diff. to identify.	Chattian (Late Oligocene) to Recent
Papua New Guinea	unspecified	KRE	N/A	N/A	214	Picked Slides	8.4(45E)	R	Under 5 specimens, very small and ery recryst., difficult to identify.	
Papua New Guinea	unspecified	KRE	N/A	N/A	215	Picked Slides	8.4(45E)	R	Under 5 specimens, very small and ery recryst., difficult to identify.	
Papua New Guinea	unspecified	KRE	N/A	N/A	217	Picked Slides	8.4(45E)	P	4 slides of which 1 is R and mainy benthics; maybe orb. Univ. then Middle Miocene or younger, otherwise trilob. So Early Miocene or	Chattian (Late Oligocene) to Recent

									younger, very recryst., diff. id.	
Papua New Guinea	unspecified	KRE	N/A	N/A	218	Picked Slides	8.4(45E)	P	4 slides of which 1 R and mainly benthics; Praoerb. Glomerosa so Late Early Miocene, recryst., vrdi	Burdigalian (Early Miocene) to Langhian (Middle Miocene)
Papua New Guinea	unspecified	KRE	N/A	N/A	225	Picked Slides	8.4(45E)	P	4 slides of which 1 R mainly benthics; orb. Univ. Middle Miocene or younger., vrdi.	Langhian (Middle Miocene) to Recent
Papua New Guinea	unspecified	KRE	N/A	N/A	227	Picked Slides	8.4(45E)	P	4 slides of which 1 R mainly benthics; orb. Univ. M. M or younger; vrdi.	Langhian (Middle Miocene) to Recent
Papua New Guinea	unspecified	KRE	N/A	N/A	230	Picked Slides	8.4(45E)	P	3 slides; orb. Universa so M. M. or younger, recryst., vrdi.	Langhian (Middle Miocene) to Recent
Papua New Guinea	unspecified	KRE	N/A	N/A	232	Picked Slides	8.4(45E)	P	3 slides; orb. Universa so M. M. or younger, maybe one praemenardii or archeomenardii form so in that case M. M. but can't move the speciment to check it from the different angles, recryst., vrdi.	Langhian (Middle Miocene) to Recent

Papua New Guinea	unspecified	KRE	N/A	N/A	236	Picked Slides	8.4(45E)	P	4 slides of which 1 R and only benthics; 1 A; orb. Universa and venezuelana so Middle Miocene - Early Pliocene, vrdi.	Langhian (Middle Miocene) to Zanclean (Early Pliocene)
Papua New Guinea	unspecified	KRE	N/A	N/A	239	Picked Slides	8.4(45E)	P	4 slides of which 1 R; orb. Universa and maybe 1 archeomenardii or praemenardii form, M.M., otherwise M.M. or younger, recryst, vrdi; one slide for ostracods.	Langhian (Middle Miocene) to Recent
Papua New Guinea	unspecified	KRE	N/A	N/A	240	Picked Slides	8.4(45E)	P	4 slides of which 2 R; orb. Universa so M. M. or younger, vrdi.	Langhian (Middle Miocene) to Recent
Papua New Guinea	unspecified	KRE	N/A	N/A	243	Picked Slides	8.4(45E)	A	4 slides of which 1 R and mainly benthics; orb. Universa and veneuelana, so M. M. - Early Pliocene, vrdi.	Langhian (Middle Miocene) to Zanclean (Early Pliocene)
Papua New Guinea	unspecified	KRE	N/A	N/A	244	Picked Slides	8.4(45E)	P	4 slides of which 1 R and mainly benthincs; orb. Univ. so M. M. or younger, vrdi.	Langhian (Middle Miocene) to Recent
Papua New Guinea	unspecified	KRE	N/A	N/A	248	Picked Slides	8.4(45E)	P	4 slides; praeorb. Forms so Late Early Miocene; vrdi; one slide for ostracods.	Burdigalian (Early Miocene) to Langhian (Middle Miocene)
Papua New Guinea	unspecified	KRE	N/A	N/A	250	Picked Slides	8.4(45E)	A	4 slides of which 1 R andmainly benthics and 1 P;	Chattian (Late Oligocene) to Recent

									trilob. So E. M. or younger, vrdi.	
Papua New Guinea	unspecified	KRE	N/A	N/A	252	Picked Slides	8.4(45E)	G	4 slides of which 1 R and mainly benthics, 1 P; vrdi.	
Papua New Guinea	unspecified	KRE	N/A	N/A	260	Picked Slides	8.4(45E)	P	4 slides of which 1 R and mainly benthics; orb. Univ. so M. M., vrdi.	Langhian (Middle Miocene) to Recent
Papua New Guinea	unspecified	KRE	N/A	N/A	261	Picked Slides	8.4(45E)	P	Orb. Universa then Middle Miocene or younger, specimens very recryst., difficult to identify; ostracods present (F).	Langhian (Middle Miocene) to Recent
Papua New Guinea	unspecified	KRE	N/A	N/A	262	Picked Slides	8.4(45E)	P	Maybe trilob. And orb. Univ. but vrdi.	
Papua New Guinea	unspecified	KRE	N/A	N/A	263	Picked Slides	8.4(45E)	A	3 slides of which 2 P; orb. Univ. so M. M. or younger, vrdi.	
Papua New Guinea	unspecified	KRE	N/A	N/A	264	Picked Slides	8.4(45E)	P	orb. Univ.; venez. So M. M. - Early Pliocene, vrdi.	Langhian (Middle Miocene) to Zanclean (Early Pliocene)
Papua New Guinea	unspecified	KRE	N/A	N/A	266	Picked Slides	8.4(45E)	P	orb. Univ.; venez. So M. M. - Early Pliocene, vrdi.	Langhian (Middle Miocene) to Zanclean (Early Pliocene)
Papua New Guinea	unspecified	KRE	N/A	N/A	267	Picked Slides	8.4(45E)	P	orb. Univ. So M. M. or younger, vrdi.	Langhian (Middle Miocene) to Recent
Papua New Guinea	unspecified	KRE	N/A	N/A	269	Picked Slides	8.4(45E)	R	vrdi	
Papua New Guinea	unspecified	KRE	N/A	N/A	270	Picked Slides	8.4(45E)	P	orb. Univ. M. M., vrdi.	Langhian (Middle Miocene) to Recent

Papua New Guinea	unspecified	KRE	N/A	N/A	271	Picked Slides	8.4(45E)	P	univ. and bilob., vrdi.	Langhian (Middle Miocene) to Recent
Papua New Guinea	unspecified	KRE	N/A	N/A	272	Picked Slides	8.4(45E)	P	orb. Univ. M. M., vrdi.	Langhian (Middle Miocene) to Recent
Papua New Guinea	unspecified	KRE	N/A	N/A	273	Picked Slides	8.4(45E)	A	Early M. M. because of Orb. Universa and praeisph., vrdi.	Langhian (Middle Miocene) to Serravallian (Middle Miocene)
Papua New Guinea	unspecified	KRE	N/A	N/A	274	Picked Slides	8.4(45E)	P	M. M. because of orb. Univ., vrdi.	Langhian (Middle Miocene) to Recent
Papua New Guinea	unspecified	KRE	N/A	N/A	275	Picked Slides	8.4(45E)	P	M. M. - Early Pliocene bc of orb. Univ. and venez., vrdi.	Langhian (Middle Miocene) to Zanclean (Early Pliocene)
Papua New Guinea	unspecified	KRE	N/A	N/A	276	Picked Slides	8.4(45E)	P	M. M. - Early Pliocene bc of orb. Univ. and venez., vrdi.	Langhian (Middle Miocene) to Zanclean (Early Pliocene)
Papua New Guinea	unspecified	KRE	N/A	N/A	277	Picked Slides	8.4(45E)	P	M. M. - Early Pliocene bc of orb. Univ. and venez., vrdi.	Langhian (Middle Miocene) to Zanclean (Early Pliocene)
Papua New Guinea	unspecified	KRE	N/A	N/A	279	Picked Slides	8.4(45E)	P	M. M. - Early Pliocene bc of orb. Univ. and venez., maybe one Glob. Scitula, vrdi.	Langhian (Middle Miocene) to Zanclean (Early Pliocene)
Papua New Guinea	unspecified	KRE	N/A	N/A	280	Picked Slides	8.4(45E)	P	M. M. - Early Pliocene bc of orb. Univ. and venez., vrdi.	Langhian (Middle Miocene) to Zanclean (Early Pliocene)
Papua New Guinea	unspecified	KRE	N/A	N/A	281	Picked Slides	8.4(45E)	P	M. M. - Early Pliocene bc of orb. Univ. and venez., maybe one Glob. Margaritae margaritae and in that case Early Pliocene, vrdi.	Langhian (Middle Miocene) to Zanclean (Early Pliocene)

Papua New Guinea	unspecified	KRE	N/A	N/A	282	Picked Slides	8.4(45E)	P	M. M. - Early Pliocene bc of orb. Univ. and venez., vrdi.	Langhian (Middle Miocene) to Zanclean (Early Pliocene)
Papua New Guinea	unspecified	KRE	N/A	N/A	283	Picked Slides	8.4(45E)	P	M. M. - Early Pliocene bc of orb. Univ. and venez., vrdi.	Langhian (Middle Miocene) to Zanclean (Early Pliocene)
Papua New Guinea	unspecified	KRE	N/A	N/A	284	Picked Slides	8.4(45E)	P	M. M. - Early Pliocene bc of orb. Univ. and venez., vrdi.	Langhian (Middle Miocene) to Zanclean (Early Pliocene)
Papua New Guinea	unspecified	KRE	N/A	N/A	285	Picked Slides	8.4(45E)	P	Early M. M. because of sim. Pres. Of praesip. And Orb. Univ., and bilob. Vrdi.	Langhian (Early Miocene) to Serravallian (Middle Miocene)
Papua New Guinea	unspecified	KRE	N/A	N/A	286	Picked Slides	8.4(45E)	P	M. M. - Early Pliocene bc of orb. Univ. and venez., vrdi.	Langhian (Middle Miocene) to Zanclean (Early Pliocene)
Papua New Guinea	unspecified	KRE	N/A	N/A	287	Picked Slides	8.4(45E)	P	M. M. - Early Pliocene bc of orb. Univ. and venez., vrdi.	Langhian (Middle Miocene) to Zanclean (Early Pliocene)
Papua New Guinea	unspecified	KRE	N/A	N/A	288	Picked Slides	8.4(45E)	P	M. M. - Early Pliocene bc of orb. Univ. and venez., vrdi.	Langhian (Middle Miocene) to Zanclean (Early Pliocene)
Papua New Guinea	unspecified	KRE	N/A	N/A	289	Picked Slides	8.4(45E)	P	M. M. - Early Pliocene bc of orb. Univ. and venez., vrdi.	Langhian (Middle Miocene) to Zanclean (Early Pliocene)
Papua New Guinea	unspecified	KRE	N/A	N/A	290	Picked Slides	8.4(45E)	P	M. M. - Early Pliocene bc of orb. Univ. and venez., vrdi.	Langhian (Middle Miocene) to Zanclean (Early Pliocene)
Papua New Guinea	unspecified	KRE	N/A	N/A	291	Picked Slides	8.4(45E)	P	M. M. - Early Pliocene bc of orb. Univ. and venez., vrdi.	Langhian (Middle Miocene) to Zanclean (Early Pliocene)

Papua New Guinea	unspecified	KRE	N/A	N/A	292	Picked Slides	8.4(45E)	P	M. M. - Early Pliocene bc of orb. Univ. and venez., vrdi.	Langhian (Middle Miocene) to Zanclean (Early Pliocene)
Papua New Guinea	unspecified	KRE	N/A	N/A	293	Picked Slides	8.4(45E)	P	M. M. - Early Pliocene bc of orb. Univ. and venez., vrdi.	Langhian (Middle Miocene) to Zanclean (Early Pliocene)
Papua New Guinea	unspecified	KRE	N/A	N/A	294	Picked Slides	8.4(45E)	P	M. M. or younger because of orb. Univ., vrdi.	Langhian (Middle Miocene) to Recent
Papua New Guinea	unspecified	KRE	N/A	N/A	295	Picked Slides	8.4(45E)	P	3 slides of which 1 is R and mainly benthics, orb. Univ. so M. M., vrdi.	Langhian (Middle Miocene) to Recent
Papua New Guinea	unspecified	KRE	N/A	N/A	299	Picked Slides	8.4(45E)	P	4 slides of which one is R and mainly benthics, orb. Univ. so M. M., vrdi.	Langhian (Middle Miocene) to Recent
Papua New Guinea	unspecified	KRE	N/A	N/A	300	Picked Slides	8.4(45E)	P	M. M. - Early Pliocene because of sim. Pres. Of orb. Univ. and venez. , vrdi.	Langhian (Middle Miocene) to Zanclean (Early Pliocene)
Papua New Guinea	unspecified	KRE	N/A	N/A	301	Picked Slides	8.4(45E)	P	4 slides of which 1 is R and mainly benthics; M. M. or younger because of orb. Univ., vrdi.	Langhian (Middle Miocene) to Recent
Papua New Guinea	unspecified	KRE	N/A	N/A	302	Picked Slides	8.4(45E)	P	M. M. - Early Pliocene because of sim. Pres. Of orb. Univ. and venez. , vrdi.	Langhian (Middle Miocene) to Zanclean (Early Pliocene)
Papua New Guinea	unspecified	KRE	N/A	N/A	303	Picked Slides	8.4(45E)	A	M. M. - Early Pliocene because of sim. Pres. Of orb. Univ. and venez. , vrdi.	Langhian (Middle Miocene) to Zanclean (Early Pliocene)

Papua New Guinea	unspecified	KRE	N/A	N/A	305	Picked Slides	8.4(45E)	P	4 slides of which one is R and mainly benthics, orb. Univ. so M. M., vrdi.	Langhian (Middle Miocene) to Recent
Papua New Guinea	unspecified	KRE	N/A	N/A	306	Picked Slides	8.4(45E)	P	M. M. - Early Pliocene because of sim/ pres. Of orb. Univ. and venez., vrdi.	Langhian (Middle Miocene) to Zanclean (Early Pliocene)
Papua New Guinea	unspecified	KRE	N/A	N/A	307	Picked Slides	8.4(45E)	P	4 slides of which one is R and mainly benthics, orb. Univ. so M. M., vrdi.	Langhian (Middle Miocene) to Recent
Papua New Guinea	unspecified	KRE	N/A	N/A	308	Picked Slides	8.4(45E)	P	4 slides of which one is R and mainly benthics, orb. Univ. and venez. so M. M. - Early Plioc., vrdi.	Langhian (Middle Miocene) to Zanclean (Early Pliocene)
Papua New Guinea	unspecified	KRE	N/A	N/A	309	Picked Slides	8.4(45E)	P	4 slides of which one is R and mainly benthics, orb. Univ. and venez. so M. M. - Early Plioc., vrdi.	Langhian (Middle Miocene) to Zanclean (Early Pliocene)
Papua New Guinea	unspecified	KRE	N/A	N/A	310	Picked Slides	8.4(45E)	P	M. M. because of sim. Pres. Of orb. Univ. and hastig. Praesiphon., then also present venez., vrdi.	Langhian (Early Miocene) to Serravallian (Middle Miocene)
Papua New Guinea	unspecified	KRE	N/A	N/A	311	Picked Slides	8.4(45E)	P	4 slides of which 2 is R; very small forams, but in one orb. Univ. so M. M. or younger, vrdi.	Langhian (Middle Miocene) to Recent
Papua New Guinea	unspecified	KRE	N/A	N/A	312	Picked Slides	8.4(45E)	R	Early M. M. because of sim. Pres. Of orb. Bilob., then also	Langhian (Middle Miocene) to Zanclean (Early Pliocene)

							present venez., vrdi.			
Papua New Guinea	unspecified	KRE	N/A	N/A	313	Picked Slides	8.4(45E)	R	Specimens very few and very small, vrdi.	
Papua New Guinea	unspecified	KRE	N/A	N/A	314	Picked Slides	8.4(45E)	P	5 slides of which 1 R and 2 mainly benthics (1 is the R); orb. Univ. M. M. or younger, vrdi.	Langhian (Middle Miocene) to Recent
Papua New Guinea	unspecified	KRE	N/A	N/A	315	Picked Slides	8.4(45E)	P	Early M. M. because of sim. Pres. Of orb. Bilob., vrdi.	Langhian (Middle Miocene) to Recent
Papua New Guinea	unspecified	KRE	N/A	N/A	316	Picked Slides	8.4(45E)	P	M. M. - Early Pliocene because of orb. Univ. and venez., vrdi.	Langhian (Middle Miocene) to Zanclean (Early Pliocene)
Papua New Guinea	unspecified	KRE	N/A	N/A	317	Picked Slides	8.4(45E)	R	4 slides, orb. Univ., M. M. or younger, very small specimens in 2 size fractions/picked slides, vrdi.	Langhian (Middle Miocene) to Recent
Papua New Guinea	unspecified	KRE	N/A	N/A	318	Picked Slides	8.4(45E)	P	3 slides of which 1 R; orb. Univ. so M. M. or younger; one more slide for ostracods.	Langhian (Middle Miocene) to Recent
Papua New Guinea	unspecified	KRE	N/A	N/A	323	Picked Slides	8.4(45E)	P	4 slides of which 1 is R and mainly benthics; M. M. - Early Pliocene because of sim. Presence of orb. Univ. and venez., vrdi.	Langhian (Middle Miocene) to Zanclean (Early Pliocene)

Papua New Guinea	unspecified	KRE	N/A	N/A	324	Picked Slides	8.4(45E)	P	4 slides of which 1 R and mainly benthics, orb. Univ. so M. M. or younger.	Langhian (Middle Miocene) to Recent
Papua New Guinea	unspecified	KRE	N/A	N/A	326	Picked Slides	8.4(45E)	P	4 slides of which 1 R is mainly benthics; orb. Univ. and venez. So M. M. - Early Pliocene, vrdi.	Langhian (Middle Miocene) to Zanclean (Early Pliocene)
Papua New Guinea	unspecified	KRE	N/A	N/A	327	Picked Slides	8.4(45E)	P	3 slides of which 1 is R and mainly benthics; orb. Univ. so M. M. or younger.	Langhian (Middle Miocene) to Recent
Papua New Guinea	unspecified	KRE	N/A	N/A	328	Picked Slides	8.4(45E)	P	4 slides of which 1 is R and mainly benthics; M. M. or younger because of orb. Univ., vrdi.	Langhian (Middle Miocene) to Recent
Papua New Guinea	unspecified	KRE	N/A	N/A	329	Picked Slides	8.4(45E)	P	4 slides of which 2 R of which 1 is mainly benthics; orb. Univ. so M. M. or younger, vrdi.	Langhian (Middle Miocene) to Recent
Papua New Guinea	unspecified	KRE	N/A	N/A	330	Picked Slides	8.4(45E)	P	M. M. - Early Pliocene because of sim. Pres. Of orb. Univ. and venez. , vrdi.	Langhian (Middle Miocene) to Zanclean (Early Pliocene)
Papua New Guinea	unspecified	KRE	N/A	N/A	331	Picked Slides	8.4(45E)	P	2 slides of which 1 is R; orb. Univ. so M. M. or younger, but few specimens and specimens vrdi.	Langhian (Middle Miocene) to Recent
Papua New Guinea	unspecified	KRE	N/A	N/A	333	Picked Slides	8.4(45E)	P	M. M. because of orb. Univ., vrdi.	Langhian (Middle Miocene) to Recent

Papua New Guinea	unspecified	KRE	N/A	N/A	334	Picked Slides	8.4(45E)	P	3 slides; orb. Univ. so M. M. or younger, vrdi; 1 more slide for ostracods.	Langhian (Middle Miocene) to Recent
Papua New Guinea	unspecified	KRE	N/A	N/A	335	Picked Slides	8.4(45E)	P	3 slides of which 1 is R and mainly benthics; orb. Univ. so M. M. or younger, vrdi; 1 more slide for ostracods.	Langhian (Middle Miocene) to Recent
Papua New Guinea	unspecified	KRE	N/A	N/A	336	Picked Slides	8.4(45E)	P	4 slides of which 1 is mainly benthics; glob. Univ. so M. M. or younger, but vrdi.	Langhian (Middle Miocene) to Recent
Papua New Guinea	unspecified	KRE	N/A	N/A	337	Picked Slides	8.4(45E)	P	3 slides; orb. Univ. so M. M. or younger, vrdi; 1 more slide for ostracods.	Langhian (Middle Miocene) to Recent
Papua New Guinea	unspecified	KRE	N/A	N/A	338	Picked Slides	8.4(45E)	P	4 slides of which one is R and mainly benthics; orb. Univ. so M. M. or younger, vrdi;	Langhian (Middle Miocene) to Recent
Papua New Guinea	unspecified	KRE	N/A	N/A	339	Picked Slides	8.4(45E)	P	4 slides of which 1 is R and mainly benthics; orb. Univ. so M. M., vrdi.	Langhian (Middle Miocene) to Recent
Papua New Guinea	unspecified	KRE	N/A	N/A	340	Picked Slides	8.4(45E)	P	4 slides of which 2 is R (one R is mainly benthics and the other R seems the smallest size fraction of outcrop 340); orb. Univ. so M. M. or younger vrdi.	Langhian (Middle Miocene) to Recent

Papua New Guinea	unspecified	KRE	N/A	N/A	341	Picked Slides	8.4(45E)	P	4 slides of which 1 is R and mainly benthics; M. M. or younger because of orb. Univ., vrdi.	Langhian (Middle Miocene) to Recent
Papua New Guinea	unspecified	KRE	N/A	N/A	342	Picked Slides	8.4(45E)	P	4 slides of which 1 is mainly benthics; glob. Univ. so M. M. or younger, but vrdi.	Langhian (Middle Miocene) to Recent
Papua New Guinea	unspecified	KRE	N/A	N/A	343	Picked Slides	8.4(45E)	A	4 slides of which 1 is R and mainly benthics, and 1 is P; M. M. because of fohsella lobata, vrdi.	Serravallian (Middle Miocene)
Papua New Guinea	unspecified	KRE	N/A	N/A	344	Picked Slides	8.4(45E)	P	4 slides of which 1 is mainly benthics; praeorb. Forms so Late E. M., vrdi.	Burdigalian (Early Miocene) to Langhian (Middle Miocene)
Papua New Guinea	unspecified	KRE	N/A	N/A	345	Picked Slides	8.4(45E)	P	E. M.or younger because of glob. Trilobus, vrdi.	Chattian (Late Oligocene) to Recent
Papua New Guinea	unspecified	KRE	N/A	N/A	347	Picked Slides	8.4(45E)	P	3 slides; glob. Trilob. So E. M. or younger, vrdi.	Chattian (Late Oligocene) to Recent
Papua New Guinea	unspecified	KRE	N/A	N/A	348	Picked Slides	8.4(45E)	P	4 slides of which 1 is R and mainly benthics; orb. Univ. so M. M., vrdi.	Langhian (Middle Miocene) to Recent
Papua New Guinea	unspecified	KRE	N/A	N/A	349	Picked Slides	8.4(45E)	P	4 slides of which 1 is mainly benthics; glob. Trilob., so E. M. or younger, vrdi; one more slide with ostracods.	Chattian (Late Oligocene) to Recent
Papua New Guinea	unspecified	KRE	N/A	N/A	350	Picked Slides	8.4(45E)	P	4 slides of which 1 R is mainly benthics; glob. Trilob. So E. M. or younger, but vrdi.	Chattian (Late Oligocene) to Recent

Papua New Guinea	unspecified	KRE	N/A	N/A	351	Picked Slides	8.4(45E)	P	4 slides of which 1 R is mainly benthics; sim. Pres. Of glob. Trilobus, maybe praoerb. Forams, and then also venez. So E. M. - Early Pliocene, vrdi.	Chattian (Late Oligocene) to Zanclean (Early Pliocene)
Papua New Guinea	unspecified	KRE	N/A	N/A	352	Picked Slides	8.4(45E)	A	4 slides of which 2 P and one of P contains mainly benthics; glob. Trilobus so E.M. or younger, vrdi.	Chattian (Late Oligocene) to Recent
Papua New Guinea	unspecified	KRE	N/A	N/A	353	Picked Slides	8.4(45E)	P	4 slides; hastig. Praesiph. And venez. Present, so E.M. - Early M. M., vrdi.	Chattian (Late Oligocene) to Serravallian (Middle Miocene)
Papua New Guinea	unspecified	KRE	N/A	N/A	354	Picked Slides	8.4(45E)	A	4 slides of which 1 R is mainly benthics and 3 P; glob. Trilob. So E. M. or younger, vrdi.	Chattian (Late Oligocene) to Recent
Papua New Guinea	unspecified	KRE	N/A	N/A	355	Picked Slides	8.4(45E)	A	4 slides of which 1 P and 1 R with mainly benthics; glob. Trilob. And venez. So E. M. - Early Pliocene, vrdi.	Chattian (Late Oligocene) to Zanclean (Early Pliocene)
Papua New Guinea	unspecified	KRE	N/A	N/A	356	Picked Slides	8.4(45E)	P	4 slides of which 1 R is mainly benthics; glob. Trilob. And venez. So E. M. - Early Pliocene, vrdi	Chattian (Late Oligocene) to Zanclean (Early Pliocene)

Papua New Guinea	unspecified	KRE	N/A	N/A	357	Picked Slides	8.4(45E)	P	4 slides of which 1 R is mainly benthics; diff. praeorb. Forms including praeorb. Transitoria, so Late E. M., vrdi.	Burdigalian (Early Miocene) to Langhian (Middle Miocene)
Papua New Guinea	unspecified	KRE	N/A	N/A	358	Picked Slides	8.4(45E)	P	4 slides of which 1 is mainly benthics; glob. Trilobus so E. M. or younger, vrdi.	Chattian (Late Oligocene) to Recent
Papua New Guinea	unspecified	KRE	N/A	N/A	359	Picked Slides	8.4(45E)	P	4 slides; glob. Trilob. And venez., so E. M. - Early Pliocene, vrdi; one more slide with ostracods.	Chattian (Late Oligocene) to Zanclean (Early Pliocene)
Papua New Guinea	unspecified	KRE	N/A	N/A	360	Picked Slides	8.4(45E)	P	3 slides; glob. Trilob. So E. M. or younger, vrdi; one more slide with ostracods.	Chattian (Late Oligocene) to Recent
Papua New Guinea	unspecified	KRE	N/A	N/A	361	Picked Slides	8.4(45E)	P	5 slides of which 1 R is mainly benthics; glob. Trilob. And venez. So E. M. - Early Pliocene, vrdi.	Chattian (Late Oligocene) to Zanclean (Early Pliocene)
Papua New Guinea	unspecified	KRE	N/A	N/A	362	Picked Slides	8.4(45E)	P	5 slides; glob. Trilob. So E. M. or younger, vrdi; one more slide for ostracods.	Chattian (Late Oligocene) to Recent
Papua New Guinea	unspecified	KRE	N/A	N/A	363	Picked Slides	8.4(45E)	A	5 slides of which 3 P and 1 R which contains mainly benthics; glob. Trilob. And venez. So E. M. - Early Pliocene, vrdi.	Chattian (Late Oligocene) to Zanclean (Early Pliocene)

Papua New Guinea	unspecified	KRE	N/A	N/A	354	Picked Slides	8.4(45E)	P	5 slides of which one is R and mainly contains benthics; glob. Trilob. so E. M. or younger, vrdi.	Chattian (Late Oligocene) to Recent
Papua New Guinea	unspecified	KRE	N/A	N/A	365	Picked Slides	8.4(45E)	P	4 slides of which one is R and mainly benthics; glob. Trilob. So E. M. or younger, vrdi.	Chattian (Late Oligocene) to Recent
Papua New Guinea	unspecified	KRE	N/A	N/A	366	Picked Slides	8.4(45E)	P	4 slides; trilob. So E M. or younger, vrdi; one more slide for ostracods.	Chattian (Late Oligocene) to Recent
Papua New Guinea	unspecified	KRE	N/A	N/A	367	Picked Slides	8.4(45E)	P	5 slides of which 1 is mainly benthics; trilob. So E. M. or younger, vrdi.	Chattian (Late Oligocene) to Recent
Papua New Guinea	unspecified	KRE	N/A	N/A	368	Picked Slides	8.4(45E)	P	5 slides; glob. Trilob. So E. M. or younger, vrdi; one more slide for ostracods.	Chattian (Late Oligocene) to Recent
Papua New Guinea	unspecified	KRE	N/A	N/A	369	Picked Slides	8.4(45E)	P	5 slides of which 1 is R and mainly benthics; orb. Univ. so M. M. or younger, vrdi; one more slide for ostracods.	Langhian (Middle Miocene) to Recent
Papua New Guinea	unspecified	KRE	N/A	N/A	370	Picked Slides	8.4(45E)	P	4 slides; trilob. And venez. So E. M. - Early Pliocene, vrdi; one more slide for ostracods.	Chattian (Late Oligocene) to Zanclean (Early Pliocene)
Papua New Guinea	unspecified	KRE	N/A	N/A	371	Picked Slides	8.4(45E)	P	2 slides; trilob. And venez. So E. M. - Early Pliocene, but vrdi.	Chattian (Late Oligocene) to Zanclean (Early Pliocene)

Papua New Guinea	unspecified	KRE	N/A	N/A	372	Picked Slides	8.4(45E)	P	4 slides of which 1 is R; trilob. And venez., E. M. - E. Pl., vrdi.	
Papua New Guinea	unspecified	KRE	N/A	N/A	373	Picked Slides	8.4(45E)	A	5 slides of which 1 R is mainly benthics, 3 P; trilob. E. M. or younger, but vrdi.	Chattian (Late Oligocene) to Recent
Papua New Guinea	unspecified	KRE	N/A	N/A	374	Picked Slides	8.4(45E)	P	5 slides; trilob. And venez. E. M. - E. pl., but vrdi; one more slide with "Lamelli and ostracods".	Chattian (Late Oligocene) to Zanclean (Early Pliocene)
Papua New Guinea	unspecified	KRE	N/A	N/A	375	Picked Slides	8.4(45E)	P	5 slides of which 1 R is mainly benthics; glob. Trilob. so E. M., but vrdi.	Chattian (Late Oligocene) to Recent
Papua New Guinea	unspecified	KRE	N/A	N/A	376	Picked Slides	8.4(45E)	P	4 slides; trilob. So E M. or younger, vrdi; one more slide for ostracods.	Chattian (Late Oligocene) to Recent
Papua New Guinea	unspecified	KRE	N/A	N/A	377	Picked Slides	8.4(45E)	A	5 slides of which 1 P is mainly benthics, 3 P; trilob. And venez. So E. M - Early Pl., vrdi.	Chattian (Late Oligocene) to Zanclean (Early Pliocene)
Papua New Guinea	unspecified	KRE	N/A	N/A	379	Picked Slides	8.4(45E)	P	5 slides of which 1 is mainly benthics; trilob. And venez., so E.M. - E. Pl., vrdi.	Chattian (Late Oligocene) to Zanclean (Early Pliocene)
Papua New Guinea	unspecified	KRE	N/A	N/A	380	Picked Slides	8.4(45E)	P	3 slides of which R is mainly benthics; glob. Trilob. And venez. E. M. - E. Pl., vrdi.	Chattian (Late Oligocene) to Zanclean (Early Pliocene)
Papua New Guinea	unspecified	KRE	N/A	N/A	381	Picked Slides	8.4(45E)	P	3 slides of which 1 R; trilob. And	Chattian (Late Oligocene) to

									venez. So E. M. - E. Pl., vrdi.	Zanclean (Early Pliocene)
Papua New Guinea	unspecified	KRE	N/A	N/A	382	Picked Slides	8.4(45E)	P	5 slides of which 1 R with mainly benthics; trilob. And venez. So E. M. - E. Pl., vrdi; one more slide for ostracods.	Chattian (Late Oligocene) to Zanclean (Early Pliocene)
Papua New Guinea	unspecified	KRE	N/A	N/A	383	Picked Slides	8.4(45E)	P	4 slides of which 1 R; glob. Trilob. So E. M. or younger; one more slide with Ostracods.	Chattian (Late Oligocene) to Recent
Papua New Guinea	unspecified	KRE	N/A	N/A	384	Picked Slides	8.4(45E)	P	5 slides of which 1 R is mainly benthics; trilob. And venez. So E. M. - E. Pl., vrdi.	Chattian (Late Oligocene) to Zanclean (Early Pliocene)
Papua New Guinea	unspecified	KRE	N/A	N/A	385	Picked Slides	8.4(45E)	P	4 slides; trilob. So E M. or younger, vrdi.	Chattian (Late Oligocene) to Recent
Papua New Guinea	unspecified	KRE	N/A	N/A	386	Picked Slides	8.4(45E)	P	5 slides of which 1 is mainly benthics; trilob. And venez., so E.M. - E. Pl., vrdi.	Chattian (Late Oligocene) to Zanclean (Early Pliocene)
Papua New Guinea	unspecified	KRE	N/A	N/A	387	Picked Slides	8.4(45E)	P	5 slides of which 1 R is mainly benthics; trilob. And venez. So E. M. - E. Pl., vrdi.	Chattian (Late Oligocene) to Zanclean (Early Pliocene)
Papua New Guinea	unspecified	KRE	N/A	N/A	388	Picked Slides	8.4(45E)	P	5 slides of which 1 R is mainly benthics; glob. Trilob. so E. M., but vrdi.	Chattian (Late Oligocene) to Recent
Papua New Guinea	unspecified	KRE	N/A	N/A	389	Picked Slides	8.4(45E)	P	4 slides of which one is R; glob. Trilob. So E. M. but vrdi; one more	Chattian (Late Oligocene) to Recent

								slide with ostracods.	
Papua New Guinea	unspecified	KRE	N/A	N/A	390	Picked Slides	8.4(45E)	P	2 slides; few specimens, and vrdi.	
Papua New Guinea	unspecified	KRE	N/A	N/A	391	Picked Slides	8.4(45E)	P	5 slides of 1 P with mainly benthics; glob. Trilob., and venez., so E. M. - E. Pl., but vrdi.	Chattian (Late Oligocene) to Zanclean (Early Pliocene)
Papua New Guinea	unspecified	KRE	N/A	N/A	394	Picked Slides	8.4(45E)	R	3 slides; glob. Trilob. So E. M. or younger. Under 10 specimens in 2 of the slides, and vrdi.	Chattian (Late Oligocene) to Recent
Papua New Guinea	unspecified	KRE	N/A	N/A	398	Picked Slides	8.4(45E)	P	5 slides of which 1 R is mainly benthics; glob. Trilob. And venez. So E. M. - Early Pliocene, vrdi.	Chattian (Late Oligocene) to Zanclean (Early Pliocene)
Papua New Guinea	unspecified	KRE	N/A	N/A	399	Picked Slides	8.4(45E)	P	5 slides; glob. Trilob., and venez. So E. M. - Early Pliocene, vrdi, one more slide with ostracods.	Chattian (Late Oligocene) to Zanclean (Early Pliocene)
Papua New Guinea	unspecified	KRE	N/A	N/A	400-1478	Picked Slides	8.4(45G)	N/A	N/A	
Papua New Guinea	unspecified	KRE	N/A	N/A	400	Picked Slides	8.4(45G)	A	5 slides of wqhich 1 P is mainly benthics; 3 P; trilob. And venez., so E. M. - E. Pl., vrdi.	Chattian (Late Oligocene) to Zanclean (Early Pliocene)

Papua New Guinea	unspecified	KRE	N/A	N/A	401	Picked Slides	8.4(45G)	P	5 slides of which 1 R is mainly benthics; trilob. And venez. So E. M. - E. Pl., vrdi; one more slide with ostracods.	Chattian (Late Oligocene) to Zanclean (Early Pliocene)
Papua New Guinea	unspecified	KRE	N/A	N/A	402	Picked Slides	8.4(45G)	P	5 slides of which 1 R is mainly benthics; 1 R; trilob. And venez., E. M. - E. P., vrdi.	Chattian (Late Oligocene) to Zanclean (Early Pliocene)
Papua New Guinea	unspecified	KRE	N/A	N/A	403	Picked Slides	8.4(45G)	P	5 slides of which 1 R is mainly benthics, 1 R; trilob. And venez., E. M. - E. Pl., vrdi; one more slide with ostracods.	Chattian (Late Oligocene) to Zanclean (Early Pliocene)
Papua New Guinea	unspecified	KRE	N/A	N/A	404	Picked Slides	8.4(45G)	P	4 slides of which 1 R is mainly bentics; trilob. And venez., so E. M. - E. Pl., vrdi.	Chattian (Late Oligocene) to Zanclean (Early Pliocene)
Papua New Guinea	unspecified	KRE	N/A	N/A	405	Picked Slides	8.4(45G)	P	6 slides of which 1 is R; trilob. And venez., so E. M. - E. Pl., vrdi.	Chattian (Late Oligocene) to Zanclean (Early Pliocene)
Papua New Guinea	unspecified	KRE	N/A	N/A	406	Picked Slides	8.4(45G)	P	4 slides of which 3 R; few specimens and some are red-ish, specimens are very recrystallised, difficult to identify.	
Papua New Guinea	unspecified	KRE	N/A	N/A	407	Picked Slides	8.4(45G)	P	4 slides of which 1 is mainly benthics; E. M. - M. M. because of hastig. Praeisphonif., then also trilob. And venez., vrdi.	Chattian (Late Oligocene) to Serravallian (Middle Miocene)

Papua New Guinea	unspecified	KRE	N/A	N/A	408	Picked Slides	8.4(45G)	A	4 slides of which 2 P and one of which is mainly benthics; sim. Pres. of praesiph. And siphonif. So M. M., then also trilob. And venez., vrdi.	Serravallian (Middle Miocene)
Papua New Guinea	unspecified	KRE	N/A	N/A	409	Picked Slides	8.4(45G)	P	4 slides of which 1 R is mainly benthics; trilob. So E. M. or younger, vrdi.	Chattian (Late Oligocene) to Recent
Papua New Guinea	unspecified	KRE	N/A	N/A	410	Picked Slides	8.4(45G)	A	4 slides of which 1 P is mainly benthics; 2 P; trilob. And venez., E. M. - E. Pl., vrdi.	Chattian (Late Oligocene) to Zanclean (Early Pliocene)
Papua New Guinea	unspecified	KRE	N/A	N/A	415	Picked Slides	8.4(45G)	P	3 slides; bilob. Univ. and venez., so M. M. - E. Pl., vrdi.	Langhian (Middle Miocene) to Zanclean (Early Pliocene)
Papua New Guinea	unspecified	KRE	N/A	N/A	417	Picked Slides	8.4(45G)	P	3 slides; orb. Univ. and venez., so M. M. - E. Pl., vrdi.	Langhian (Middle Miocene) to Zanclean (Early Pliocene)
Papua New Guinea	unspecified	KRE	N/A	N/A	423	Picked Slides	8.4(45G)	P	4 slides ; univ. and venez., so M. M. - E. Pl., vrdi.	Langhian (Middle Miocene) to Zanclean (Early Pliocene)
Papua New Guinea	unspecified	KRE	N/A	N/A	427	Picked Slides	8.4(45G)	P	4 slides; univ. and venez., so M. M. - E. Pl., vrdi.	Langhian (Middle Miocene) to Zanclean (Early Pliocene)
Papua New Guinea	unspecified	KRE	N/A	N/A	432	Picked Slides	8.4(45G)	A	3 slides of which 2 P (the bigger size fraction and Median are P); orb. Univ., but vrdi.	Langhian (Middle Miocene) to Recent
Papua New Guinea	unspecified	KRE	N/A	N/A	435	Picked Slides	8.4(45G)	A	3 slides of which 1 is P; orb. Univ. and venez., so M. M. - E. Pl., vrdi.	Langhian (Middle Miocene) to Zanclean (Early Pliocene)

Papua New Guinea	unspecified	KRE	N/A	N/A	436	Picked Slides	8.4(45G)	A	3 slides of which 1 is P; orb. Univ. and venez., so M. M. - E. Pl., vrdi	Langhian (Middle Miocene) to Zanclean (Early Pliocene)
Papua New Guinea	unspecified	KRE	N/A	N/A	438	Picked Slides	8.4(45G)	P	4 slides; of which 1 is mainly benthics; simult. Pres. Of praeisphon. And orb. Univ. so Early M. M., vrdi.	Langhian (Early Miocene) to Serravallian (Middle Miocene)
Papua New Guinea	unspecified	KRE	N/A	N/A	439	Picked Slides	8.4(45G)	P	4 slides; some praoerb. Forms including trans. And glomerosa, so Late E. M., vrdi; one more slide with ostracods.	Burdigalian (Early Miocene) to Langhian (Middle Miocene)
Papua New Guinea	unspecified	KRE	N/A	N/A	441	Picked Slides	8.4(45G)	P	4 slides; trilob. So E. M. or younger, vrdi; one more slide with ostracods.	Chattian (Late Oligocene) to Recent
Papua New Guinea	unspecified	KRE	N/A	N/A	452	Picked Slides	8.4(45G)	P	5 slides; orb. Univ. and venez., so M. M. - E. pl., vrdi.	Langhian (Middle Miocene) to Zanclean (Early Pliocene)
Papua New Guinea	unspecified	KRE	N/A	N/A	453	Picked Slides	8.4(45G)	P	4 slides of which 1 R is mainly benthics; trilob. So E. M. or younger, vrdi.	Chattian (Late Oligocene) to Recent
Papua New Guinea	unspecified	KRE	N/A	N/A	455	Picked Slides	8.4(45G)	A	3 slides; hastig. Praeisph., trilob., E. M. - M. M., vrdi.	Chattian (Late Oligocene) to Serravallian (Middle Miocene)
Papua New Guinea	unspecified	KRE	N/A	N/A	456	Picked Slides	8.4(45G)	A	3 slides of which 1 is P; orb. Univ. and venez., M. M. - E. Pl., vrdi.	Langhian (Middle Miocene) to Zanclean (Early Pliocene)

Papua New Guinea	unspecified	KRE	N/A	N/A	459	Picked Slides	8.4(45G)	P	4 slides of which 1 is mainly benthics; trilob. And venez., so E. M. - E. Pl., vrdi.	Chattian (Late Oligocene) to Zanclean (Early Pliocene)
Papua New Guinea	unspecified	KRE	N/A	N/A	460	Picked Slides	8.4(45G)	A	3 slides of which 2 are P; trilob. And venez., so E. M. - E. Pl., vrdi.	Chattian (Late Oligocene) to Zanclean (Early Pliocene)
Papua New Guinea	unspecified	KRE	N/A	N/A	463	Picked Slides	8.4(45G)	P	4 slides of which 1 is mainly benthics; praesiphon. So E. M. - M. M., vrdi.	Chattian (Late Oligocene) to Serravallian (Middle Miocene)
Papua New Guinea	unspecified	KRE	N/A	N/A	464	Picked Slides	8.4(45G)	P	4 slides of which 1 is R and 1 is mainly benthics; praeisphonif. So E. M. - M. M., vrdi; one more slide with ostracods.	Chattian (Late Oligocene) to Serravallian (Middle Miocene)
Papua New Guinea	unspecified	KRE	N/A	N/A	465	Picked Slides	8.4(45G)	P	2 slides; sim. Pres. Of praeisphonif. And siphoni., so M. M., vrdi; one more slide with ostracods.	Serravallian (Middle Miocene)
Papua New Guinea	unspecified	KRE	N/A	N/A	467	Picked Slides	8.4(45G)	P	3 slides; trilob. So E. M. or younger, vrdi; one more slide with ostracods.	Chattian (Late Oligocene) to Recent
Papua New Guinea	unspecified	KRE	N/A	N/A	469	Picked Slides	8.4(45G)	P	4 slides of which 1 R is mainly benthics; sim. Pres. Of praeisphon., glob. Archeomenardii, and orb. Univ., so Early M. M., vrdi.	Langhian (Early Miocene) to Serravallian (Middle Miocene)

Papua New Guinea	unspecified	KRE	N/A	N/A	471	Picked Slides	8.4(45G)	P	4 slides; sim. Presence of praeisph., glob. Archeomenardii, and orb. Univ., so E. M. M., vrdi; one more slide with ostracods.	Langhian (Early Miocene) to Serravallian (Middle Miocene)
Papua New Guinea	unspecified	KRE	N/A	N/A	473	Picked Slides	8.4(45G)	A	4 slides of which 1 P is mainly benthics, and 1 P; sim. Pres. or praes. And orb. Univ. so M. M., vrdi.	Langhian (Early Miocene) to Serravallian (Middle Miocene)
Papua New Guinea	unspecified	KRE	N/A	N/A	475	Picked Slides	8.4(45G)	A	4 slides of which 1 R is mainly benthics, 1 P; orb. Univ. and venez., M. M. - E. Pl., vrdi.	Langhian (Middle Miocene) to Zanclean (Early Pliocene)
Papua New Guinea	unspecified	KRE	N/A	N/A	476	Picked Slides	8.4(45G)	A	3 slides of which 1 P; orb. Univ. and venez., so M. M. - e. Pl., vrdi.	Langhian (Middle Miocene) to Zanclean (Early Pliocene)
Papua New Guinea	unspecified	KRE	N/A	N/A	479	Picked Slides	8.4(45G)	P	3 slides of which 1 A; orb. Univ. and venez., so M. M. - E. Pl., vrdi.	Langhian (Middle Miocene) to Zanclean (Early Pliocene)
Papua New Guinea	unspecified	KRE	N/A	N/A	526	Picked Slides	8.4(45G)	P	Cretaceous because of Marginotruncana and Globigerinelloides genus forms present,; mainly benthics; specimens pyritised and recryst., difficult to identify.	Turonian (Late Cretaceous) to Campanian (Late Cretaceous)
Papua New Guinea	unspecified	KRE	N/A	N/A	666	Picked Slides	8.4(45G)	P	3 slides; orb. Univ. (mainly), M. M. or younger, vrdi.	Langhian (Middle Miocene) to Recent

Papua New Guinea	unspecified	KRE	N/A	N/A	668	Picked Slides	8.4(45G)	P	4 slides; sim. Pres. or praeisp., venez., and orb. Univ., so M. M., vrdi.	Serravallian (Middle Miocene)
Papua New Guinea	unspecified	KRE	N/A	N/A	670	Picked Slides	8.4(45G)	P	4 slides; sim. Pres. Of glob. Archeomenardii and orb. Univ., vrdi; one more slide with ostracods.	Serravallian (Middle Miocene)
Papua New Guinea	unspecified	KRE	N/A	N/A	672	Picked Slides	8.4(45G)	P	4 slides; glob. Archeomen., orb. Univ. and venez., so E. M. M., vrdi.	Langhian (Early Miocene) to Serravallian (Middle Miocene)
Papua New Guinea	unspecified	KRE	N/A	N/A	673	Picked Slides	8.4(45G)	A	3 slides; orb. Univ., so M. M. or younger, vrdi.	Langhian (Middle Miocene) to Recent
Papua New Guinea	unspecified	KRE	N/A	N/A	692	Picked Slides	8.4(45G)	A	4 slides of which 1 is P and larger size fractions; orb. Univ., so M. M. or younger, but vrdi.	Langhian (Middle Miocene) to Recent
Papua New Guinea	unspecified	KRE	N/A	N/A	730	Picked Slides	8.4(45G)	P	Few specimens and very recryst., difficult to identify.	
Papua New Guinea	unspecified	KRE	N/A	N/A	731	Picked Slides	8.4(45G)	A	Cretaceous because of marginotruncana and globigerinelloides genus forms present; specimens seem pyritised and specimens are recryst., difficult to identify.	Turonian (Late Cretaceous) to Campanian (Late Cretaceous)
Papua New Guinea	unspecified	KRE	N/A	N/A	738	Picked Slides	8.4(45G)	A	5 slides of which 3 P; orb. Univ. and venez., so M. M. - Early Pl., vrdi; one more slide with ostracods.	Langhian (Middle Miocene) to Recent

Papua New Guinea	unspecified	KRE	N/A	N/A	740	Picked Slides	8.4(45G)	A	2 slides of which 1 is P; Cretaceous because of marginotruncana genus forms present; vrdi.	Turonian (Late Cretaceous) to Campanian (Late Cretaceous)
Papua New Guinea	unspecified	KRE	N/A	N/A	743	Picked Slides	8.4(45G)	P	Specimens light red-ish, pyritised, infilled and recrystallised, difficult to identify.	
Papua New Guinea	unspecified	KRE	N/A	N/A	744	Picked Slides	8.4(45G)	A	4 slides of which 1 R is mainly benthics, 2 P; orb. Univ. and venez., so M. M. - Early Pl., vrdi.	Langhian (Middle Miocene) to Zanclean (Early Pliocene)
Papua New Guinea	unspecified	KRE	N/A	N/A	748	Picked Slides	8.4(45G)	P	2 slides in which 1 is mainly benthics; specimens very recryst., some pyritised, difficult to identify; maybe from the spiral side marginotruncana, so in that case it would be Cretaceous.	Turonian (Late Cretaceous) to Campanian (Late Cretaceous)
Papua New Guinea	unspecified	KRE	N/A	N/A	751	Picked Slides	8.4(45G)	P	2 slides; maybe Cretaceous as spiral side of 1 looks like globigerinelloides, but specimens very recryst., difficult to identify.	Valanginian (Early Cretaceous) to Maastrichtian (Late Cretaceous)
Papua New Guinea	unspecified	KRE	N/A	N/A	799	Picked Slides	8.4(45G)	A	2 slides of which 1 is P; Cretaceous because of globotruncana genus forms, vrdi.	Coniacian (Late Cretaceous) - Maastrichtian (Late Cretaceous)

Papua New Guinea	unspecified	KRE	N/A	N/A	1021	Picked Slides	8.4(45G)	A	3 slides of which 1 is P (larger size fractions); trilob. And venez., so E. M. - E. Pl., vrdi.	Chattian (Late Oligocene) to Zanclean (Early Pliocene)
Papua New Guinea	unspecified	KRE	N/A	N/A	1022	Picked Slides	8.4(45G)	A	3 slides of which 1 is P; trilob. And venez., so E. M. - E. Pl., vrdi.	Chattian (Late Oligocene) to Recent
Papua New Guinea	unspecified	KRE	N/A	N/A	1052	Picked Slides	8.4(45G)	A	3 slides; trilob., so E. M. or younger, vrdi.	Chattian (Late Oligocene) to Recent
Papua New Guinea	unspecified	KRE	N/A	N/A	1053	Picked Slides	8.4(45G)	A	4 slides of which 1 is P; trilob. And praeisphonif., so E. M., vrdi.	Chattian (Late Oligocene) to Serravallian (Middle Miocene)
Papua New Guinea	unspecified	KRE	N/A	N/A	1056	Picked Slides	8.4(45G)	P	Specimens very recryst., and specimens small, difficult to identify.	
Papua New Guinea	unspecified	KRE	N/A	N/A	1057	Picked Slides	8.4(45G)	A	3 slides; E. M. because of trilo., vrdi.	Chattian (Late Oligocene) to Recent
Papua New Guinea	unspecified	KRE	N/A	N/A	1058	Picked Slides	8.4(45G)	P	4 slides of which 1 is mainly benthics; praesiphon. And trilob., so E. M. - M. M., vrdi.	Chattian (Late Oligocene) to Serravallian (Middle Miocene)
Papua New Guinea	unspecified	KRE	N/A	N/A	1059	Picked Slides	8.4(45G)	P	3 slides; some specimens pyritsed, trilob. And praeisphonif. But vrdi.	Chattian (Late Oligocene) to Serravallian (Middle Miocene)
Papua New Guinea	unspecified	KRE	N/A	N/A	1060	Picked Slides	8.4(45G)	P	2 slides; trilob. So E. M. or younger, but vrdi, some pyritised.	Chattian (Late Oligocene) to Recent
Papua New Guinea	unspecified	KRE	N/A	N/A	1066	Picked Slides	8.4(45G)	A	4 slides of which 1 R is mainly benthics, 1 P; maybe trilob., but	Chattian (Late Oligocene) to Recent

									vrdi, some pyritised.	
Papua New Guinea	unspecified	KRE	N/A	N/A	1058	Picked Slides	8.4(45G)	P	3 slides; trilob., but vrdi.	Chattian (Late Oligocene) to Recent
Papua New Guinea	unspecified	KRE	N/A	N/A	1076	Picked Slides	8.4(45G)	A	3 slides and 1 is P; trilob. But most specimens light-brown-ish and very infilled and recrystallised, difficult to identify.	Chattian (Late Oligocene) to Recent
Papua New Guinea	unspecified	KRE	N/A	N/A	1077	Picked Slides	8.4(45G)	R	4 slides and under 10 specimens in each, in one pyritised and very recrystallised specimens, maybe trilob., in that case E. M. or younger, vrdi.	
Papua New Guinea	unspecified	KRE	N/A	N/A	1078	Picked Slides	8.4(45G)	R	Few specimens and recryst., difficult to identify	
Papua New Guinea	unspecified	KRE	N/A	N/A	1079	Picked Slides	8.4(45G)	P	2 slides; trilob., but vrdi.	Chattian (Late Oligocene) to Recent
Papua New Guinea	unspecified	KRE	N/A	N/A	1087	Picked Slides	8.4(45G)	R	Few specimens and specimens are very small, maybe one trilob., but very recryst., difficult to identify	
Papua New Guinea	unspecified	KRE	N/A	N/A	1089	Picked Slides	8.4(45G)	P	2 slides; very recryst., difficult to identify.	

Papua New Guinea	unspecified	KRE	N/A	N/A	1107	Picked Slides	8.4(45G)	P	4 slides and in 1 mainly benthics; trilob. And venez. So E. M. - Early Pliocene, vrdi.	Chattian (Late Oligocene) to Zanclean (Early Pliocene)
Papua New Guinea	unspecified	KRE	N/A	N/A	1109	Picked Slides	8.4(45G)	P	Trilob., so E. M. or younger, vrdi.	Chattian (Late Oligocene) to Recent
Papua New Guinea	unspecified	KRE	N/A	N/A	1113	Picked Slides	8.4(45G)	P	3 slides, some specimens are light brown-ish; trilob., so E. M. or younger, but vrdi.	Chattian (Late Oligocene) to Recent
Papua New Guinea	unspecified	KRE	N/A	N/A	1115	Picked Slides	8.4(45G)	P	4 slides in which 1 is R and benthics only; trilob., most specimens are light brown-ish so E. M., but vrdi.	Chattian (Late Oligocene) to Recent
Papua New Guinea	unspecified	KRE	N/A	N/A	1129	Picked Slides	8.4(45G)	R	M. M. or younger because of orb. Univ., but only under 10 specimens big enough and mostly orb. Univ., other very small and difficult to identify, recrystallised.	Langhian (Middle Miocene) to Recent
Papua New Guinea	unspecified	KRE	N/A	N/A	1130	Picked Slides	8.4(45G)	A	4 slides in which 1 R is benthics only, 2 P; orb. Univ. and venez., so M. M. - E. Pl., vrdi.	Langhian (Middle Miocene) to Zanclean (Early Pliocene)
Papua New Guinea	unspecified	KRE	N/A	N/A	1143	Picked Slides	8.4(45G)	P	4 slides in which 1 R is benthics only; orb. Univ. and venez., so M. M. - E. pl, vrdi.	Langhian (Middle Miocene) to Zanclean (Early Pliocene)

Papua New Guinea	unspecified	KRE	N/A	N/A	1144	Picked Slides	8.4(45G)	P	4 slides in which 1 R is mainly benthics; orb. Univ. and praeisph. So E. M. M., vrdi.	Langhian (Early Miocene) to Serravallian (Middle Miocene)
Papua New Guinea	unspecified	KRE	N/A	N/A	1177	Picked Slides	8.4(45G)	P	4 slides in which 1 R is mainly benthics; orb. Univ. and praeisph. So E. M. M., vrdi.	Langhian (Early Miocene) to Serravallian (Middle Miocene)
Papua New Guinea	unspecified	KRE	N/A	N/A	1178	Picked Slides	8.4(45G)	P	4 slides in which 1 R is mainly benthics; orb. Univ., so M. M. or younger, vrdi.	Langhian (Middle Miocene) to Recent
Papua New Guinea	unspecified	KRE	N/A	N/A	1179	Picked Slides	8.4(45G)	A	3 slides in which 1 R is benthics only, 1 P; sim. Presence of praeisphon., archeomen., and trilob., so E. M. M., then also venez., vrdi.	Burdigalian (Early Miocene) to Langhian (Middle Miocene)
Papua New Guinea	unspecified	KRE	N/A	N/A	1190	Picked Slides	8.4(45G)	P	4 slides in which 1 R is benthics only; orb. Univ. and venez., so M. M. - E. pl, vrdi.	Langhian (Middle Miocene) to Zanclean (Early Pliocene)
Papua New Guinea	unspecified	KRE	N/A	N/A	1192	Picked Slides	8.4(45G)	P	4 slides in which 1 R is benthics only; orb. Univ., venez., praeisphon., so E. M. M., vrdi.	Langhian (Early Miocene) to Serravallian (Middle Miocene)
Papua New Guinea	unspecified	KRE	N/A	N/A	1193	Picked Slides	8.4(45G)	P	4 slides in which 1 R is benthics only; Orb. Univ., and praeisphon., so E. M. M., vrdi.	Langhian (Middle Miocene) to Recent
Papua New Guinea	unspecified	KRE	N/A	N/A	1194	Picked Slides	8.4(45G)	P	3 slides in which 1 R is mainly benthics; trilob., so E. M. or younger, vrdi.	Chattian (Late Oligocene) to Recent

Papua New Guinea	unspecified	KRE	N/A	N/A	1196	Picked Slides	8.4(45G)	P	4 slides; orb. Univ. and venez., so M. M. - E. Pl., vrdi.	Langhian (Middle Miocene) to Zanclean (Early Pliocene)
Papua New Guinea	unspecified	KRE	N/A	N/A	1197	Picked Slides	8.4(45G)	P	4 slides in which 1 R is benthics only; specimens light brown-ish; orb. Univ. and venez., so M. M. - E. Pl., vrdi.	Langhian (Middle Miocene) to Zanclean (Early Pliocene)
Papua New Guinea	unspecified	KRE	N/A	N/A	1199	Picked Slides	8.4(45G)	P	3 slides; trilob., so E.M. or younger, but vrdi.	Chattian (Late Oligocene) to Recent
Papua New Guinea	unspecified	KRE	N/A	N/A	1201	Picked Slides	8.4(45G)	P	4 slides; trilob., praeisphonif., and venez., so E. M. M., but vrdi.	Langhian (Early Miocene) to Serravallian (Middle Miocene)
Papua New Guinea	unspecified	KRE	N/A	N/A	1202	Picked Slides	8.4(45G)	P	4 slides in which 1 R is mainly benthics; trilob., globigerinoides parawoodi, and venez., so E. M. - E. Pl., vrdi.	Chattian (Late Oligocene) to Burdigalian (Early Miocene)
Papua New Guinea	unspecified	KRE	N/A	N/A	1205	Picked Slides	8.4(45G)	P	4 slides in which 1 is mainly benthics; trilob. And praeisphon., so E. M. - E. M. M., vrdi.	Chattian (Late Oligocene) to Serravallian (Middle Miocene)
Papua New Guinea	unspecified	KRE	N/A	N/A	1238	Picked Slides	8.4(45G)	A	2 slides; Cretaceous because of rotalipora genus forms, pyritised, vrdi.	Turonian (Late Cretaceous) to Campanian (Late Cretaceous)
Papua New Guinea	unspecified	KRE	N/A	N/A	1242	Picked Slides	8.4(45G)	A	2 slides; Cretaceous because of marginotruncana genus forms, pyritised, vrdi.	Turonian (Late Cretaceous) to Campanian (Late Cretaceous)

Papua New Guinea	unspecified	KRE	N/A	N/A		1471	Picked Slides	8.4(45G)	A	3 slides; Cretaceous because of marginotruncana genus forms, pyritised, vrdi.	Turonian (Late Cretaceous) to Campanian (Late Cretaceous)
Papua New Guinea	unspecified	KRE	N/A	N/A		1472	Picked Slides	8.4(45G)	A	Mainly benthics, very recrystallised, difficult to identify.	
Papua New Guinea	unspecified	KRE	N/A	N/A		1473	Picked Slides	8.4(45G)	P	2 slides; Cretaceous because of Rotalipora genus forms, some specimens red-ish, vrdi.	Cenomanian (Late Cretaceous)
Papua New Guinea	unspecified	KRE	N/A	N/A		1475	Picked Slides	8.4(45G)	A	Cretaceous because of Rotalipora genus forms, specimens pyritised, vrdi.	Cenomanian (Late Cretaceous)
Papua New Guinea	unspecified	KRE	N/A	N/A		1478	Picked Slides	8.4(45G)	P	2 slides in which 1 is benthics only; Cretaceous because of Rotalipora genus forms, some pyritised	Cenomanian (Late Cretaceous)
Papua New Guinea	unspecified	Muabu	1	0	11600	N/A	Picked Slides	5.4(38C)	N/A	N/A	
Papua New Guinea	unspecified	Muabu	1	0-30		N/A	Picked Slides	5.4(38C)	R	Miscellaneous microfossils, 2 specimens, maybe benthics.	
Papua New Guinea	unspecified	Muabu	1	100-130		N/A	Picked Slides	5.4(38C)	P	Very recryst. Diff. to identify, maybe some orb. Univ., but quite small, some light-brown ish specimens, vrdi.	Langhian (Middle Miocene) to Recent

Papua New Guinea	unspecified	Muabu	1	190-220	N/A	Picked Slides	5.4(38C)	R	Maybe trilob., vrdi and few specimens.	Chattian (Late Oligocene) to Recent
Papua New Guinea	unspecified	Muabu	1	280-310	N/A	Picked Slides	5.4(38C)	P	trilob. And orb. Univ., so M. M. or younger, vrdi.	Langhian (Middle Miocene) to Recent
Papua New Guinea	unspecified	Muabu	1	400-430	N/A	Picked Slides	5.4(38C)	P	E. M. - Late Pliocene because of globigerinoides obliquus, vrdi.	Aquitanian (Early Miocene) to Ionian (Late Pleistocene)
Papua New Guinea	unspecified	Muabu	1	490-520	N/A	Picked Slides	5.4(38C)	R	Under 5 specimens, mainly benthics, vrdi.	
Papua New Guinea	unspecified	Muabu	1	580-610	N/A	Picked Slides	5.4(38C)	P	Slide number 1; E. M. - late Pl. because of glob. Obliquus; mainly benthics; recryst.	Aquitanian (Early Miocene) to Ionian (Late Pleistocene)
Papua New Guinea	unspecified	Muabu	1	580-610	N/A	Picked Slides	5.4(38C)	P	Benthics only, recryst.	
Papua New Guinea	unspecified	Muabu	1	700-730	N/A	Picked Slides	5.4(38C)	P	Trilob. So E. M. or younger; some sp. Are light brown-ish, vrdi.	Chattian (Late Oligocene) to Recent
Papua New Guinea	unspecified	Muabu	1	790-820	N/A	Picked Slides	5.4(38C)	P	Benthics only.	
Papua New Guinea	unspecified	Muabu	1	910-940	N/A	Picked Slides	5.4(38C)	P	Specimens orange-ish; maybe trilob. Vrdi.	
Papua New Guinea	unspecified	Muabu	1	1000-1030	N/A	Picked Slides	5.4(38C)	P	Specimens light orange-ish; maybe trilob. Vrdi.	Chattian (Late Oligocene) to Recent
Papua New Guinea	unspecified	Muabu	1	Circ:1122	N/A	Picked Slides	5.4(38C)	P	M. M. because of sim. Pres. Of glob. Mayeri and orb. Univ., some sp. Are light orange-ish, recryst.	Chattian (Late Oligocene) to Tortonian (Late Miocene)

Papua New Guinea	unspecified	Muabu	1	1190-1200	N/A	Picked Slides	5.4(38C)	P	Slide number 1; Mainly benthics, under 10 pl. spec. and very recryst., some pyrt. And some light orange-ish, diff. to identify.	
Papua New Guinea	unspecified	Muabu	1	1190-1200	N/A	Picked Slides	5.4(38C)	R	Miscellaneous microfossils, maybe benthics; recryst.	
Papua New Guinea	unspecified	Muabu	1	1290-1300	N/A	Picked Slides	5.4(38C)	P	E. M. - M. M. because of maybe praeisph. Then also pres. Trilob. And venez., vrdi, some sp. Light orange-ish.	Chattian (Late Oligocene) to Serravallian (Middle Miocene)
Papua New Guinea	unspecified	Muabu	1	1390-1400	N/A	Picked Slides	5.4(38C)	P	E. M. or younger because of trilob.	Chattian (Late Oligocene) to Recent
Papua New Guinea	unspecified	Muabu	1	1490-1500	N/A	Picked Slides	5.4(38C)	P	Slide number 1; Sp. Recryst., some light orange-ish, diff. to identify.	
Papua New Guinea	unspecified	Muabu	1	1490-1500	N/A	Picked Slides	5.4(38C)	R	Slide number 2; Miscellaneous microfossils, including gastropods (as written on the slide itself), maybe some benthics, recryst.	
Papua New Guinea	unspecified	Muabu	1	1590-1600	N/A	Picked Slides	5.4(38C)	P	Sp. Very recryst., some light oange-ish, diff. to identify.	
Papua New Guinea	unspecified	Muabu	1	1690-1700	N/A	Picked Slides	5.4(38C)	P	Slide number 1; Miscellaneous microfossils (maybe some conodonts? Some teeth present on a	

									"stick"0, benthics only.	
Papua New Guinea	unspecified	Muabu	1	1690-1700	N/A	Picked Slides	5.4(38C)	P	Slide number 2; Miscellaneous microfossils, benthics only.	
Papua New Guinea	unspecified	Muabu	1	1790-1800	N/A	Picked Slides	5.4(38C)	R	Slide number 1; Benthics only, some orange-ish.	
Papua New Guinea	unspecified	Muabu	1	1790-1800	N/A	Picked Slides	5.4(38C)	P	Slide number 2; some pyrits., some orange-ish, very recryst., difficult to identify.	
Papua New Guinea	unspecified	Muabu	1	1890-1900	N/A	Picked Slides	5.4(38C)	P	trilob. And maybe praebulloid., E. M. - M. M.?? When is praeob.?, vrdi.	Chattian (Late Oligocene) to Recent
Papua New Guinea	unspecified	Muabu	1	1990-2000	N/A	Picked Slides	5.4(38C)	P	Benthics only.	
Papua New Guinea	unspecified	Muabu	1	2090-2100	N/A	Picked Slides	5.4(38C)	P	Slide number 1; some pyrit., some orange-ish; trilob., vrdi.	
Papua New Guinea	unspecified	Muabu	1	2090-2100	N/A	Picked Slides	5.4(38C)	R	Slide number 2; miscellaneous microfossils, including gastropods (as written on the slide itself), maybe some benthics.	
Papua New Guinea	unspecified	Muabu	1	2190-2200	N/A	Picked Slides	5.4(38C)	A	Slide number 1; trilob. So E. M. or younger, some sp. orange-ish, vrdi.	Chattian (Late Oligocene) to Recent

Papua New Guinea	unspecified	Muabu	1	2190-2200	N/A	Picked Slides	5.4(38C)	R	Slide number 2; miscellaneous microfossils; benthics too.	
Papua New Guinea	unspecified	Muabu	1	2290-2300	N/A	Picked Slides	5.4(38C)	A	Slide number 1; Trilob. And maybe orb., in that case M. M. or younger, some pyrits. (include. Orb.), some orange-ish; vrdi.	Chattian (Late Oligocene) to Recent
Papua New Guinea	unspecified	Muabu	1	2290-2300	N/A	Picked Slides	5.4(38C)	R	Slide number 2; miscell. Microfos., benthics too.	
Papua New Guinea	unspecified	Muabu	1	2305	N/A	Picked Slides	5.4(38C)	P	Only around 10 pl. specimens; some orange-ish, vrdi.	
Papua New Guinea	unspecified	Muabu	1	2390-2400	N/A	Picked Slides	5.4(38C)	P	Mainly benthics, only one pl. sp. Spotted and found!! Trilob.	
Papua New Guinea	unspecified	Muabu	1	2490-2500	N/A	Picked Slides	5.4(38C)	P	Maybe glob. Obliquus; Sp. Very recryst., some light orange-ish, some pyritis., diff. to identify.	Aquitanian (Early Miocene) to Ionian (Late Pleistocene)
Papua New Guinea	unspecified	Muabu	1	2590-2600	N/A	Picked Slides	5.4(38C)	P	Slide number 2, trilob., sp. Very recryst., and some orange-ish, vrdi.	Chattian (Late Oligocene) to Recent
Papua New Guinea	unspecified	Muabu	1	2590-2600	N/A	Picked Slides	5.4(38C)	P	Slide number 2; mainly benthics, only one pl. sp. Spotted and found! Maybe glob. Woodi.	Chattian (Late Oligocene) to Burdigalian (Early Miocene)
Papua New Guinea	unspecified	Muabu	1	2690-2700	N/A	Picked Slides	5.4(38C)	P	Slide number 1; maybe glob. Obliquus, glob.	Aquitanian (Early Miocene) to Ionian (Late Pleistocene)

									Extremus, trilob., vrdi.	
Papua New Guinea	unspecified	Muabu	1	2690-2700	N/A	Picked Slides	5.4(38C)	P	Slide number 2; benthics only.	
Papua New Guinea	unspecified	Muabu	1	2700-2800	N/A	Picked Slides	5.4(38C)	P	Slide number 1; benthics only.	
Papua New Guinea	unspecified	Muabu	1	2700-2800	N/A	Picked Slides	5.4(38C)	P	Slide number 2; Glob. Obliquus, trilob., recryst.	Aquitanian (Early Miocene) to Ionian (Late Pleistocene)
Papua New Guinea	unspecified	Muabu	1	2890-2900	N/A	Picked Slides	5.4(38C)	A	Mainly benthics; Trilob., orb. Univ., and maybe praebull. Form., recryst.	Langhian (Middle Miocene) to Recent
Papua New Guinea	unspecified	Muabu	1	2990-3000	N/A	Picked Slides	5.4(38C)	P	Glob. Obliquus, orb. Univ., trilob., recryst.	Langhian (Middle Miocene) to Ionian (Late Pleistocene)
Papua New Guinea	unspecified	Muabu	1	3090-3100	N/A	Picked Slides	5.4(38C)	P	trilob., some orange-ish, soe pyritis., vrdi.	Chattian (Late Oligocene) to Recent
Papua New Guinea	unspecified	Muabu	1	3190-3200	N/A	Picked Slides	5.4(38C)	A	Trilob., maybe one praemenardii, some sp. Orange-is, some pyrit. Vrdi.	Langhian (Early Miocene) to Serravallian (Middle Miocene)
Papua New Guinea	unspecified	Muabu	1	3290-3300	N/A	Picked Slides	5.4(38C)	A	Glob. Obliquus extremus, maybe metotumida withan extra chamber (last chamber seems "shifted" by the extra chamber)?, orb. Univ., trilob., some orange-ish; recryst.	Langhian (Middle Miocene) to Ionian (Late Pleistocene)

Papua New Guinea	unspecified	Muabu	1	3390-3400	N/A	Picked Slides	5.4(38C)	P	Slide number 1; Trilob., venez., maybe obliquus, vrdi.	Aquitanian (Early Miocene) to Ionian (Late Pleistocene)
Papua New Guinea	unspecified	Muabu	1	3390-3400	N/A	Picked Slides	5.4(38C)	A	Mainly benthics; under 10 specimens, 1-2 glob. Tumida flexuosa, recryst.	Chattian (Late Oligocene) to Burdigalian (Early Miocene)
Papua New Guinea	unspecified	Muabu	1	3490-3500	N/A	Picked Slides	5.4(38C)	P	Orb. Univ., trilob., venez., glob. Obliquus, recryst.	Langhian (Middle Miocene) to Ionian (Late Pleistocene)
Papua New Guinea	unspecified	Muabu	1	3590-3600	N/A	Picked Slides	5.4(38C)	A	Orb. Univ., praesiphoni., Recryst.	Langhian (Early Miocene) to Serravallian (Middle Miocene)
Papua New Guinea	unspecified	Muabu	1	3690-3700	N/A	Picked Slides	5.4(38C)	R	Slide number 1; misc. microfossils, benthics too.	
Papua New Guinea	unspecified	Muabu	1	3690-3700	N/A	Picked Slides	5.4(38C)	A	Slide number 2; orb. Univ., trilob. Venez., so M. M. - E. Pl., recryst.	Langhian (Middle Miocene) to Zanclean (Early Pliocene)
Papua New Guinea	unspecified	Muabu	1	3790-3800	N/A	Picked Slides	5.4(38C)	P	Slide 1; Menardii, orb. Univ. trilob., venez., recryst.	Serravallian (Middle Miocene) to Zanclean (Early Pliocene)
Papua New Guinea	unspecified	Muabu	1	3790-3800	N/A	Picked Slides	5.4(38C)	P	Slide 2; globigerina woodi; ruber, recryst.	Serravallian (Middle Miocene) to Piacenzian (Late Pliocene)
Papua New Guinea	unspecified	Muabu	1	3890-3900	N/A	Picked Slides	5.4(38C)	P	orb. Univ., trilob., venez., archeomenardii, recryst.	Langhian (Early Miocene) to Serravallian (Middle Miocene)
Papua New Guinea	unspecified	Muabu	1	3990-4000	N/A	Picked Slides	5.4(38C)	P	Orb. Univ., trilob., plesiotumida, venez., recryst.	Tortonian (Middle Miocene) to Zanclean (Early Pliocene)

Papua New Guinea	unspecified	Muabu	1	4090-4100	N/A	Picked Slides	5.4(38C)	A	plesiotumida (the hard one!), dentoglobigerina altispira; Orb. Univ., trilob., venez., recryst. Late Miocene-Early Pliocene.	Tortonian (Middle Miocene) to Zanclean (Early Pliocene)
Papua New Guinea	unspecified	Muabu	1	4190-4200	N/A	Picked Slides	5.4(38C)	A	Laste Miocene because of glob. Merotumida, then also present orb. Univ., trilob., sphaeroidinellopsis semilunina semilunina, recryst.	Tortonian (Middle Miocene) to Zanclean (Early Pliocene)
Papua New Guinea	unspecified	Muabu	1	4290-4300	N/A	Picked Slides	5.4(38C)	A	Slide 1; sacculifer with sac-like chamber, orb. Univ, venez., recryst, Late Miocene - E. Pl, sphaeronidella disjuncta.	Burdigalian (Early Miocene) to Serravallian (Middle Miocene)
Papua New Guinea	unspecified	Muabu	1	4290-4300	N/A	Picked Slides	5.4(38C)	B	Slide 2; miscellaneous microfossils, fragments as written on the slide itself, no sign of forams/ foram fragments.	Burdigalian (Early Miocene) to Serravallian (Middle Miocene)
Papua New Guinea	unspecified	Muabu	1	4390-4400	N/A	Picked Slides	5.4(38C)	A	venez., trilob., orb. Univ., probably menardii menardii, tumida tumida?; recryst.	Messinian (Late Miocene) to Recent
Papua New Guinea	unspecified	Muabu	1	4490-4500	N/A	Picked Slides	5.4(38C)	A	Slide 1; glob. Extremus,trilob., venez., sacculifer?, no globorat. Anymore, vrdi.	Tortonian (Middle Miocene) to Zanclean (Early Pliocene)

Papua New Guinea	unspecified	Muabu	1	4490-4500	N/A	Picked Slides	5.4(38C)	A	Sphaeroidinellopsis semilunina semilunina, tumida tumida I think, glob. Miocenica, menardii menardii, recryst.	Zanclean (Early Pliocene) to Piacenzian (Late Pliocene)
Papua New Guinea	unspecified	Muabu	1	4590-4600	N/A	Picked Slides	5.4(38C)	A	trilob. Orb. Univ. Menardii menardii, plesiotumida, recryst.	Tortonian (Late Miocene) to Piacenzian (Late Pliocene)
Papua New Guinea	unspecified	Muabu	1	4690-4700	N/A	Picked Slides	5.4(38C)	A	Slide number 1; trilob., extremuus, venez., orb., plesiotumida, recryst.	Tortonian (Middle Miocene) to Zanclean (Early Pliocene)
Papua New Guinea	unspecified	Muabu	1	4790-4800	N/A	Picked Slides	5.4(38C)	A	Slide number 2; orb. Univ., trilob., venez.?, miocenica, tumida tumida I think, recryst.	Zanclean (Early Pliocene)
Papua New Guinea	unspecified	Muabu	1	4890-4900	N/A	Picked Slides	5.4(38C)	P	trilob., orb. Univ., venez., sphaeroidinellopsis paenedehiscensis, miocenica?, recryst.	Zanclean (Early Pliocene)
Papua New Guinea	unspecified	Muabu	1	4990-5000	N/A	Picked Slides	5.4(38C)	P	trilpo., orb. Univ., miocenica, venez., recryst.	Zanclean (Early Pliocene)
Papua New Guinea	unspecified	Muabu	1	5090-5100	N/A	Picked Slides	5.4(38C)	P	orb. Univ., sphaeroidinellopsis semilunina semilunina, recryst., venez., tumida tumida¬	Zanclean (Early Pliocene) to Piacenzian (Late Pliocene)

Papua New Guinea	unspecified	Muabu	1	5200-5210	N/A	Picked Slides	5.4(38C)	A	trilob. Orb. Univ., sphaeroidinellopsis semilunina semilunina, venez., merotumida, recryst.	Zanclean (Early Pliocene)
Papua New Guinea	unspecified	Muabu	1	5290-5300	N/A	Picked Slides	5.4(38C)	A	trilob. Orb. Univ., ss. Disjuncta, venez., tumida tumida, recryst.	Langhian (Early Miocene) to Serravallian (Middle Miocene)
Papua New Guinea	unspecified	Muabu	1	5390-5400	N/A	Picked Slides	5.4(38C)	P	Slide 1; venez., trilob., orb. Univ., menardii menardii I think, tumida tumida I think, ss. Semilunina semilunina, sacculifer, recryst.	Messinian (Late Miocene) to Zanclean (Early Pliocene)
Papua New Guinea	unspecified	Muabu	1	5390-5400	N/A	Picked Slides	5.4(38C)	P	Slide 2; orb. Univ., venez., tumida tumida, vrdi.	Messinian (Late Miocene) to Zanclean (Early Pliocene)
Papua New Guinea	unspecified	Muabu	1	5490-5500	N/A	Picked Slides	5.4(38C)	A	Slide 1; orb. Univ., tumida tumida, some pyritised, vrdi.	Messinian (Late Miocene) to Recent
Papua New Guinea	unspecified	Muabu	1	5490-5500	N/A	Picked Slides	5.4(38C)	P	Slide 2; vebnez., trilob., not many specimens, some pyritised, vrdi.	Chattian (Late Oligocene) to Zanclean (Early Pliocene)
Papua New Guinea	unspecified	Muabu	1	5490-5500	N/A	Picked Slides	5.4(38C)	P	Slide 3; venez., mainly benthics, some pyritised; recryst.	Chattian (Late Oligocene) to Zanclean (Early Pliocene)
Papua New Guinea	unspecified	Muabu	1	5590-5600	N/A	Picked Slides	5.4(38C)	P	orb. Univ., trilob., some pyritised, tumida tumida, vrdi.	Messinian (Late Miocene) to Recent
Papua New Guinea	unspecified	Muabu	1	5680-5682	N/A	Picked Slides	5.4(38C)	A	orb. Univ., trilob., tumida tumida, vrdi.	Messinian (Late Miocene) to Recent

Papua New Guinea	unspecified	Muabu	1	5790-5800	N/A	Picked Slides	5.4(38C)	P	tumida tumida, venez., miocenica; vrdi.	Messinian (Late Miocene) to Zanclean (Early Pliocene)
Papua New Guinea	unspecified	Muabu	1	5890-5900	N/A	Picked Slides	5.4(38C)	P	trilob. Orb. Univ., vrdi!!	Langhian (Middle Miocene) to Recent
Papua New Guinea	unspecified	Muabu	1	5990-6000	N/A	Picked Slides	5.4(38C)	P	orb. Univ. Trilob., maybe praoerb. Form? Like praeorb. Glomerosa, vrdi.	Burdigalian (Early Miocene) to Langhian (Middle Miocene)
Papua New Guinea	unspecified	Muabu	1	6090-6100	N/A	Picked Slides	5.4(38C)	A	orb. Univ., trilob. Vrdi!!	Langhian (Middle Miocene) to Recent
Papua New Guinea	unspecified	Muabu	1	6190-6200	N/A	Picked Slides	5.4(38C)	A	orb. Univ., trilob., Venez., Praeorb. Forms I think, vrdi.	Langhian (Middle Miocene)
Papua New Guinea	unspecified	Muabu	1	6290-6300	N/A	Picked Slides	5.4(38C)	P	orb. Univ., literally vrdi (as in previous slides just above), sutures and chambers barely distinguishable as specimens very "white", recryst.!!	Langhian (Middle Miocene) to Recent
Papua New Guinea	unspecified	Muabu	1	6390-6400	N/A	Picked Slides	5.4(38C)	P	orb. Univ., trilob., glob. Pertenuis-multicamerata transition (because 7 chambers against 8 of multicamerata and miocenica laterally is planoconvex), vrdi.	Messinian (Late Miocene) to Recent
Papua New Guinea	unspecified	Muabu	1	6490-6500	N/A	Picked Slides	5.4(38C)	P	orb. Univ., trilob. Other specimens very recrystallised, not even surte they are planktics, vrdi.	

Papua New Guinea	unspecified	Muabu	1	6690-6700	N/A	Picked Slides	5.4(38C)	P	orb. Univ., specimens very recrystallised, difficult to identify.	Langhian (Middle Miocene) to Recent
Papua New Guinea	unspecified	Muabu	1	6790-6800	N/A	Picked Slides	5.4(38C)	P	orb. Univ., specimens very recrystallised, difficult to identify.	Langhian (Middle Miocene) to Recent
Papua New Guinea	unspecified	Muabu	1	6890-6900	N/A	Picked Slides	5.4(38C)	P	orb. Univ., specimens very recrystallised, difficult to identify.	Langhian (Middle Miocene) to Recent
Papua New Guinea	unspecified	Muabu	1	7090-7100	N/A	Picked Slides	5.4(38C)	P	trilob., specimens very recrystallised, difficult to identify.	Chattian (Late Oligocene) to Recent
Papua New Guinea	unspecified	Muabu	1	7290-7300	N/A	Picked Slides	5.4(38C)	P	trilob., specimens very recrystallised, difficult to identify.	Chattian (Late Oligocene) to Recent
Papua New Guinea	unspecified	Muabu	1	7490-7500	N/A	Picked Slides	5.4(38C)	P	orb. Univ., vrdi.	Langhian (Middle Miocene) to Recent
Papua New Guinea	unspecified	Muabu	1	7690-7700	N/A	Picked Slides	5.4(38C)	P	vrdi.	
Papua New Guinea	unspecified	Muabu	1	7700-7708	N/A	Picked Slides	5.4(38C)	P	orb. Univ., vrdi.	Langhian (Middle Miocene) to Recent
Papua New Guinea	unspecified	Muabu	1	7790-7800	N/A	Picked Slides	5.4(38C)	P	orb. Univ., trilob., venez., vrdi.	Langhian (Middle Miocene) to Zanclean (Early Pliocene)
Papua New Guinea	unspecified	Muabu	1	7990-8000	N/A	Picked Slides	5.4(38C)	P	orb. Univ. Trilob., venez., vrdi.	Langhian (Middle Miocene) to Zanclean (Early Pliocene)
Papua New Guinea	unspecified	Muabu	1	8190-8200	N/A	Picked Slides	5.4(38C)	P	orb. Univ., vrdi.	Langhian (Middle Miocene) to Recent
Papua New Guinea	unspecified	Muabu	1	8390-8400	N/A	Picked Slides	5.4(38C)	R	orb. Univ., maybe trilob., few specimens and	Langhian (Middle Miocene) to Recent

									very recrystallised, difficult to identify.	
Papua New Guinea	unspecified	Muabu	1	8590-8600	N/A	Picked Slides	5.4(38C)	P	orb. Univ., miocenica I think, vrdi.	Langhian (Middle Miocene) to Recent
Papua New Guinea	unspecified	Muabu	1	8790-8800	N/A	Picked Slides	5.4(38C)	A	vrdi!!	
Papua New Guinea	unspecified	Muabu	1	8990-9000	N/A	Picked Slides	5.4(38C)	P	orb. Univ., vrdi.	Langhian (Middle Miocene) to Recent
Papua New Guinea	unspecified	Muabu	1	9190-9200	N/A	Picked Slides	5.4(38C)	P	orb. Univ., maybe trilob., vrdi.	Langhian (Middle Miocene) to Recent
Papua New Guinea	unspecified	Muabu	1	9390-9400	N/A	Picked Slides	5.4(38C)	P	orb. Univ., vrdi.	Langhian (Middle Miocene) to Recent
Papua New Guinea	unspecified	Muabu	1	9590-9600	N/A	Picked Slides	5.4(38C)	P	orb. Univ., trilob., vrdi.	Langhian (Middle Miocene) to Recent
Papua New Guinea	unspecified	Muabu	1	9780-9800	N/A	Picked Slides	5.4(38C)	P	trilob., venez., vrdi	Chattian (Late Oligocene) to Zanclean (Early Pliocene)
Papua New Guinea	unspecified	Muabu	1	9900-10000	N/A	Picked Slides	5.4(38C)	P	orb. Univ., maybe trilob., vrdi.	Langhian (Middle Miocene) to Recent
Papua New Guinea	unspecified	Muabu	1	10190-10200	N/A	Picked Slides	5.4(38C)	R	few specimens and specimens vrdi.	
Papua New Guinea	unspecified	Muabu	1	10390-10490	N/A	Picked Slides	5.4(38C)	P	orb. Univ., trilobus, vrdi.	Langhian (Middle Miocene) to Recent
Papua New Guinea	unspecified	Muabu	1	11390-11400	N/A	Picked Slides	5.4(38C)	R	orb. univ., few specimens and specimens vrdi.	Langhian (Middle Miocene) to Recent
Papua New Guinea	unspecified	Muabu	1	11590-11600	N/A	Picked Slides	5.4(38C)	P	trilob. vrdi.	Chattian (Late Oligocene) to Recent

Papua New Guinea	unspecified	Hides	1	1110 - 2583	N/A	Picked Slides	17.2(87H)	N/A	N/A	
Papua New Guinea	unspecified	Hides	1	1110	N/A	Picked Slides	17.2(87H)	R	few specimens, vrdi.	
Papua New Guinea	unspecified	Hides	1	1110	N/A	Picked Slides	17.2(87H)	R	few specimens, vrdi.	
Papua New Guinea	unspecified	Hides	1	1131	N/A	Picked Slides	17.2(87H)	A	Most pyritised and very recrystallised, difficult to identify, probably glob. flexuosa (pyritised) and maybe orb. Univ. (but pyritised and quite small), vrdi.	Ionian (Late Pleistocene) to Holocene (0.1 Ma)
Papua New Guinea	unspecified	Hides	1	1182	N/A	Picked Slides	17.2(87H)	R	Under 10 specimens, some pyritised, vrdi.	
Papua New Guinea	unspecified	Hides	1	1230	N/A	Picked Slides	17.2(87H)	R	Few specimens, most pyritised, vrdi.	
Papua New Guinea	unspecified	Hides	1	1281	N/A	Picked Slides	17.2(87H)	P	Some pyritised, some red-ish, very recrystallised, difficult to identify.	
Papua New Guinea	unspecified	Hides	1	1329	N/A	Picked Slides	17.2(87H)	R	Under 10 specimens, not even sure they are forams, some pyritised, vrdi.	
Papua New Guinea	unspecified	Hides	1	1380	N/A	Picked Slides	17.2(87H)	R	Under 15 specimens, most pyritised, vrdi.	
Papua New Guinea	unspecified	Hides	1	1431	N/A	Picked Slides	17.2(87H)	R	Few specimens, most pyritised, some red-ish, vrdi.	

Papua New Guinea	unspecified	Hides	1	1452	N/A	Picked Slides	17.2(87H)	P	Most specimens pyritised, some red-ish, maybe some orb. Univ (pyiritised and quite small), vrdi.	
Papua New Guinea	unspecified	Hides	1	1482	N/A	Picked Slides	17.2(87H)	P	Orb. Univ., most specimens are pyritised, marginotruncana in that case Cretaceous, vrdi.	Turonian (Late Cretaceous) to Campanian (Late Cretaceous)
Papua New Guinea	unspecified	Hides	1	1500	N/A	Picked Slides	17.2(87H)	R	Some sp. Very small, most pyritised, some red-ish, vrdi.	
Papua New Guinea	unspecified	Hides	1	1530	N/A	Picked Slides	17.2(87H)	A	Most pyritised, Marginotruncana, Vrdi.	Turonian (Late Cretaceous) to Campanian (Late Cretaceous)
Papua New Guinea	unspecified	Hides	1	1551	N/A	Picked Slides	17.2(87H)	R	Few specimens and most pyritiserd, vrdi.	
Papua New Guinea	unspecified	Hides	1	1581	N/A	Picked Slides	17.2(87H)	P	Most pyritised, Marginotruncana, vrdi.	Turonian (Upper Cretaceous) to Campanian (Upper Cretaceous)
Papua New Guinea	unspecified	Hides	1	1602	N/A	Picked Slides	17.2(87H)	P	Most red-ish, vrdi.	
Papua New Guinea	unspecified	Hides	1	1629	N/A	Picked Slides	17.2(87H)	P	Rotali., some pyritiased, vrdi.	Cenomanian (Upper Cretaceous)
Papua New Guinea	unspecified	Hides	1	1653	N/A	Picked Slides	17.2(87H)	P	Most pyritised and some red-ish, vrdi.	
Papua New Guinea	unspecified	Hides	1	1680	N/A	Picked Slides	17.2(87H)	P	Most pyritised and some red-ish, vrdi.	

Papua New Guinea	unspecified	Hides	1	1701	N/A	Picked Slides	17.2(87H)	P	Most pyritised and some red-ish, vrdi.	
Papua New Guinea	unspecified	Hides	1	1722	N/A	Picked Slides	17.2(87H)	P	Most pyritised and some red-ish, vrdi.	
Papua New Guinea	unspecified	Hides	1	1722	N/A	Picked Slides	17.2(87H)	A	Most pyritised and some red-ish, Rotalipora genus forms, vrdi.	Cenomanian (Upper Cretaceous)
Papua New Guinea	unspecified	Hides	1	1731	N/A	Picked Slides	17.2(87H)	P	Most pyritised, Rotalip., Vrdi.	Cenomanian (Upper Cretaceous)
Papua New Guinea	unspecified	Hides	1	1761	N/A	Picked Slides	17.2(87H)	P	Most pyritised, some dark red-ish, some orange-ish, vrdi.	
Papua New Guinea	unspecified	Hides	1	1782	N/A	Picked Slides	17.2(87H)	P	Most pyritised, vrdi.	
Papua New Guinea	unspecified	Hides	1	1800	N/A	Picked Slides	17.2(87H)	P	Most pyritised some bright red-ish, vrdi.	
Papua New Guinea	unspecified	Hides	1	1821 ST 2	N/A	Picked Slides	17.2(87H)	P	Most pyritised, vrdi.	
Papua New Guinea	unspecified	Hides	1	1830	N/A	Picked Slides	17.2(87H)	P	Most pyritised, some red-ish, vrdi.	
Papua New Guinea	unspecified	Hides	1	1860 ST 2	N/A	Picked Slides	17.2(87H)	P	Most pyritised, vrdi.	
Papua New Guinea	unspecified	Hides	1	1869	N/A	Picked Slides	17.2(87H)	P	Most pyritised, some red-ish, vrdi.	
Papua New Guinea	unspecified	Hides	1	1869 ST 2	N/A	Picked Slides	17.2(87H)	P	Most pyritised, vrdi.	
Papua New Guinea	unspecified	Hides	1	1880 ST 3	N/A	Picked Slides	17.2(87H)	P	Most pyritised, vrdi.	

Papua New Guinea	unspecified	Hides	1	1913	N/A	Picked Slides	17.2(87H)	P	Most pyritised, vrdi.	
Papua New Guinea	unspecified	Hides	1	1914 ST 4	N/A	Picked Slides	17.2(87H)	P	Most pyritised, vrdi.	
Papua New Guinea	unspecified	Hides	1	1932 ST 4	N/A	Picked Slides	17.2(87H)	P	Most pyritised, some red-ish, vrdi.	
Papua New Guinea	unspecified	Hides	1	1980 ST 4	N/A	Picked Slides	17.2(87H)	P	Most pyritised, some red-ish, vrdi.	
Papua New Guinea	unspecified	Hides	1	2031	N/A	Picked Slides	17.2(87H)	P	Most pyritised, vrdi.	
Papua New Guinea	unspecified	Hides	1	2082 ST 4	N/A	Picked Slides	17.2(87H)	A	Most pyritised, vrdi.	
Papua New Guinea	unspecified	Hides	1	2130 ST 4	N/A	Picked Slides	17.2(87H)	R	About 5 specimens, vrdi.	
Papua New Guinea	unspecified	Hides	1	2181 ST 4	N/A	Picked Slides	17.2(87H)	A	Most pyritised, vrdi.	
Papua New Guinea	unspecified	Hides	1	2229 ST 4	N/A	Picked Slides	17.2(87H)	P	Most pyritised, some red-ish, vrdi.	
Papua New Guinea	unspecified	Hides	1	2232 ST 4	N/A	Picked Slides	17.2(87H)	P	Most pyritised and some red-ish, vrdi.	
Papua New Guinea	unspecified	Hides	1	2280 ST 4	N/A	Picked Slides	17.2(87H)	A	Most pyritised and some red-ish, vrdi.	
Papua New Guinea	unspecified	Hides	1	2331 ST 4	N/A	Picked Slides	17.2(87H)	A	Most pyritised and some red-ish, vrdi.	
Papua New Guinea	unspecified	Hides	1	2382 ST 4	N/A	Picked Slides	17.2(87H)	R	vrdi!!	
Papua New Guinea	unspecified	Hides	1	2451 ST 4	N/A	Picked Slides	17.2(87H)	R	Few specimens, some pyritised, some red-ish, vrdi.	

Papua New Guinea	unspecified	Hides	1	2430 ST 4	N/A	Picked Slides	17.2(87H)	R	Few specimens and some pyritised, vrdi.	
Papua New Guinea	unspecified	Hides	1	2469 ST 4	N/A	Picked Slides	17.2(87H)	R	Few specimens, some pyritised, some bright red-ish, some red-ish, vrdi.	
Papua New Guinea	unspecified	Hides	1	2475 ST 4	N/A	Picked Slides	17.2(87H)	P	Some pyritised, some bright red-ish, some red-ish, vrdi.	
Papua New Guinea	unspecified	Hides	1	2484 ST 4	N/A	Picked Slides	17.2(87H)	R	Some pyritised, some red-ish, vrdi.	
Papua New Guinea	unspecified	Hides	1	2508 ST 4	N/A	Picked Slides	17.2(87H)	A	Most pyritised, some red-ish, vrdi.	
Papua New Guinea	unspecified	Hides	1	2520 ST 4	N/A	Picked Slides	17.2(87H)	P	Most pyritised, some red-ish, vrdi.	
Papua New Guinea	unspecified	Hides	1	2532 ST 4	N/A	Picked Slides	17.2(87H)	A	Slide 1; Most pyritised, some red-ish, pyritised and very recrystallised, difficult to identify.	
Papua New Guinea	unspecified	Hides	1	2532 ST 4	N/A	Picked Slides	17.2(87H)	P	Slide 2; most pyritised, siome red-ish, vrdi.	
Papua New Guinea	unspecified	Hides	1	2541 ST 4	N/A	Picked Slides	17.2(87H)	P	Most pyritised, vrdi.	
Papua New Guinea	unspecified	Hides	1	2556 ST 4	N/A	Picked Slides	17.2(87H)	A	Check, seems like orb. And trilob. Shapes?; Most pyritised, some red-ish, vrdi.	
Papua New Guinea	unspecified	N/A	N/A	N/A	D 4 - 105	Picked Slides	11.3(88H)	N/A	N/A	

Papua New Guinea	unspecified	N/A	N/A	N/A	D 04	Picked Slides	11.3(88H)	P	Specimens very recryst., some red-ish, diff. To identify.	
Papua New Guinea	unspecified	N/A	N/A	N/A	6	Picked Slides	11.3(88H)	P	Most pyritised, some red-ish, vrdi.	
Papua New Guinea	unspecified	N/A	N/A	N/A	7	Picked Slides	11.3(88H)	P	Slide 1; trilob., vrdi!!	
Papua New Guinea	unspecified	N/A	N/A	N/A	7	Picked Slides	11.3(88H)	G	Slide 2; vrdi, maybe trilob.	
Papua New Guinea	unspecified	N/A	N/A	N/A	26	Picked Slides	11.3(88H)	A	Slide 1; Marginotruncana, some pyritised, recryst.	Turonian (Upper Cretaceous) to Campanian (Upper Cretaceous)
Papua New Guinea	unspecified	N/A	N/A	N/A	26 selected spp.	Picked Slides	11.3(88H)	R	Marginotruncana, Cretaceous.	Turonian (Upper Cretaceous) to Campanian (Upper Cretaceous)
Papua New Guinea	unspecified	N/A	N/A	N/A	26	Picked Slides	11.3(88H)	A	Slide 2; Marginotruncana, some pyritised.	Turonian (Upper Cretaceous) to Campanian (Upper Cretaceous)
Papua New Guinea	unspecified	N/A	N/A	N/A	33A	Picked Slides	11.3(88H)	A	Very recryst., diff. To identify.	
Papua New Guinea	unspecified	N/A	N/A	N/A	36	Picked Slides	11.3(88H)	A	Slide 1; trilo., vrdi.	Chattian (Late Oligocene) to Recent
Papua New Guinea	unspecified	N/A	N/A	N/A	36	Picked Slides	11.3(88H)	A	Slide 2; vrdi!!	
Papua New Guinea	unspecified	N/A	N/A	N/A	37	Picked Slides	11.3(88H)	P	Slide 2; trilob., vrdi	Chattian (Late Oligocene) to Recent
Papua New Guinea	unspecified	N/A	N/A	N/A	37	Picked Slides	11.3(88H)	P	Slide 2; sacculifer, trilob., vrdi.	Chattian (Late Oligocene) to Recent

Papua New Guinea	unspecified	N/A	N/A	N/A	45	Picked Slides	11.3(88H)	R	Miscellaneous microfossils, maybe benthics, no sign of planktics.	
Papua New Guinea	unspecified	N/A	N/A	N/A	46	Picked Slides	11.3(88H)	B	miscellaneous microf. No sign of forams	
Papua New Guinea	unspecified	N/A	N/A	N/A	47	Picked Slides	11.3(88H)	P	But few planktics, very recryst. Some red-ish, diff. To identify.	
Papua New Guinea	unspecified	N/A	N/A	N/A	48	Picked Slides	11.3(88H)	A	Slide 1; orb. Univ., vrdi.	Langhian (Middle Miocene) to Recent
Papua New Guinea	unspecified	N/A	N/A	N/A	48	Picked Slides	11.3(88H)	A	Slide 2; vrdi!	
Papua New Guinea	unspecified	N/A	N/A	N/A	49	Picked Slides	11.3(88H)	A	Slide 1; orb. Univ., trilob., vrdi.	Langhian (Middle Miocene) to Recent
Papua New Guinea	unspecified	N/A	N/A	N/A	49	Picked Slides	11.3(88H)	A	Slide 2; vrdi!!	
Papua New Guinea	unspecified	N/A	N/A	N/A	50	Picked Slides	11.3(88H)	A	Slide 1; vrdi!!	
Papua New Guinea	unspecified	N/A	N/A	N/A	50	Picked Slides	11.3(88H)	A	Slide 2; vrdi!!	
Papua New Guinea	unspecified	N/A	N/A	N/A	52 A	Picked Slides	11.3(88H)	R	Under 5 specimens, vrdi!!	
Papua New Guinea	unspecified	N/A	N/A	N/A	56	Picked Slides	11.3(88H)	P	Slide 1: Maybe trilob., venez., and sacculifer but vrdi!!	Chattian (Late Oligocene) to Zanclean (Early Pliocene)
Papua New Guinea	unspecified	N/A	N/A	N/A	56	Picked Slides	11.3(88H)	P	Slide 2; praeisphonif., vrdi.	Chattian (Late Oligocene) to Serravallian (Late Miocene)

Papua New Guinea	unspecified	N/A	N/A	N/A	57	Picked Slides	11.3(88H)	P	Orb. Univ. Trilob. Vrdi! Some yellow-ish.	Langhian (Middle Miocene) to Recent
Papua New Guinea	unspecified	N/A	N/A	N/A	62	Picked Slides	11.3(88H)	P	Somr broken, very recryst., diff. To identify.	
Papua New Guinea	unspecified	N/A	N/A	N/A	82	Picked Slides	11.3(88H)	A	Slide 1; sacculif. With sac-like chamber, orb. Univ., trilob., plesiotumida, vrdi.	Tortonian (Late Miocene) to Piacenzian (Late Pliocene)
Papua New Guinea	unspecified	N/A	N/A	N/A	82	Picked Slides	11.3(88H)	A	Slide 2; vrdi!!	
Papua New Guinea	unspecified	N/A	N/A	N/A	83	Picked Slides	11.3(88H)	G	orb. Univ., sacculif. With sac-like chamber, merotumida, vrdi.	Tortonian (Middle Miocene) to Zanclean (Early Pliocene)
Papua New Guinea	unspecified	N/A	N/A	N/A	87	Picked Slides	11.3(88H)	R	Under 10 miscell. Microfos. Not even sure they are forams, very small and very ecryst.	
Papua New Guinea	unspecified	N/A	N/A	N/A	88	Picked Slides	11.3(88H)	A	Most specimens are dark red-ish and all very recryst., diff. To identify.	
Papua New Guinea	unspecified	N/A	N/A	N/A	89	Picked Slides	11.3(88H)	R	Few specimens and vrdi.	
Papua New Guinea	unspecified	N/A	N/A	N/A	92	Picked Slides	11.3(88H)	P	vrdi!!	
Papua New Guinea	unspecified	N/A	N/A	N/A	99	Picked Slides	11.3(88H)	P	Mainly benthics, vrdi.	
Papua New Guinea	unspecified	N/A	N/A	N/A	100	Picked Slides	11.3(88H)	P	Slide 1; trilob., vrdi.	Chattian (Late Oligocene) to Recent

Papua New Guinea	unspecified	N/A	N/A	N/A	100	Picked Slides	11.3(88H)	P	Slide 2; vrdi.	
Papua New Guinea	unspecified	N/A	N/A	N/A	101	Picked Slides	11.3(88H)	A	orb. Univ., trilob., vrdi.	Langhian (Middle Miocene) to Recent
Papua New Guinea	unspecified	N/A	N/A	N/A	102	Picked Slides	11.3(88H)	G	trilob., sacculifer with sac-like final chamber, vrdi.	Chattian (Late Oligocene) to Recent
Papua New Guinea	unspecified	N/A	N/A	N/A	103	Picked Slides	11.3(88H)	A	trilob., praesiphonif., vrdi.	Chattian (Late Oligocene) to Serravallian (Late Miocene)
Papua New Guinea	unspecified	N/A	N/A	N/A	104	Picked Slides	11.3(88H)	P	Mainly benthics, trilob., vrdi.	Chattian (Late Oligocene) to Recent
Papua New Guinea	unspecified	N/A	N/A	N/A	104	Picked Slides	11.3(88H)	P	Mainly benthics, trilob., vrdi.	Chattian (Late Oligocene) to Recent
Papua New Guinea	unspecified	N/A	N/A	N/A	104	Picked Slides	11.3(88H)	P	Mainly benthics, trilob., vrdi.	Chattian (Late Oligocene) to Recent
Papua New Guinea	unspecified	N/A	N/A	N/A	105	Picked Slides	11.3(88H)	A	Slide 1; trilob., vrdi!!	Chattian (Late Oligocene) to Recent
Papua New Guinea	unspecified	PPL 27	N/A	N/A	KM 20 - 135	Picked Slides	11.3(88H)	N/A	N/A	
Papua New Guinea	unspecified	PPL 27	N/A	N/A	20A	Picked Slides	11.3(88H)	A	Slide 1; Plesiotumida, orb., trilob., vrdi.	Tortonian (Late Miocene) to Piacenzian (Late Pliocene)
Papua New Guinea	unspecified	PPL 27	N/A	N/A	20A	Picked Slides	11.3(88H)	A	Slide 2; orb. Univ., trilob., aequilateralis, vrdi	Serravallian (Middle Miocene) to Recent
Papua New Guinea	unspecified	PPL 27	N/A	N/A	20A	Picked Slides	11.3(88H)	A	Slide 3; sacculifer with sac-like chamber, vrdi.	Chattian (Late Oligocene) to Recent
Papua New Guinea	unspecified	PPL 27	N/A	N/A	21	Picked Slides	11.3(88H)	A	Slide 1; Globigerinella aequilateralis, vrdi!!	Serravallian (Middle Miocene) to Recent

Papua New Guinea	unspecified	PPL 27	N/A	N/A	21	Picked Slides	11.3(88H)	P	Slide 2; Vrdi!!	
Papua New Guinea	unspecified	PPL 27	N/A	N/A	21	Picked Slides	11.3(88H)	A	Slide 3; vrdi!!	
Papua New Guinea	unspecified	PPL 27	N/A	N/A	23	Picked Slides	11.3(88H)	P	Slide 1; orb. Univ., vrdi!!	langhian (Middle Miocene) to Recent
Papua New Guinea	unspecified	PPL 27	N/A	N/A	23	Picked Slides	11.3(88H)	P	Slide 2; vrdi!!	
Papua New Guinea	unspecified	PPL 27	N/A	N/A	33	Picked Slides	11.3(88H)	A	plesiotumida, bulloides, vrdi.	Tortonian (Late Miocene) to Piacenzian (Late Pliocene)
Papua New Guinea	unspecified	PPL 27	N/A	N/A	34	Picked Slides	11.3(88H)	P	praescitula, vrdi.	Burdigalian (Early Miocene) to Serravallian (Middle Miocene)
Papua New Guinea	unspecified	PPL 27	N/A	N/A	35	Picked Slides	11.3(88H)	A	vrdi!!	
Papua New Guinea	unspecified	PPL 27	N/A	N/A	36	Picked Slides	11.3(88H)	A	some pyritised, vrdi!!	
Papua New Guinea	unspecified	PPL 27	N/A	N/A	37	Picked Slides	11.3(88H)	P	miscellaneous microfossils, vrdi!	
Papua New Guinea	unspecified	PPL 27	N/A	N/A	38	Picked Slides	11.3(88H)	R	some sp. Orange-ish, some red-ish, some pyritised, vrdi!!	
Papua New Guinea	unspecified	PPL 27	N/A	N/A	39	Picked Slides	11.3(88H)	A	Some orange-ish, some lightly pyritisted, vrdi!!	
Papua New Guinea	unspecified	PPL 27	N/A	N/A	41	Picked Slides	11.3(88H)	R	miscellaneous microfossils, under 10 sp., some orange-ish, vrdi!!	

Papua New Guinea	unspecified	PPL 27	N/A	N/A	42	Picked Slides	11.3(88H)	R	miscellaneous microfossils, under 8 sp., vrdi!!	
Papua New Guinea	unspecified	PPL 27	N/A	N/A	73	Picked Slides	11.3(88H)	P	miscellaneous microfossils (including ostracods), vrdi!!	
Papua New Guinea	unspecified	PPL 27	N/A	N/A	73 c	Picked Slides	11.3(88H)	A	Slide 1; vrdi!!	
Papua New Guinea	unspecified	PPL 27	N/A	N/A	73 c	Picked Slides	11.3(88H)	A	Slide 2; vrdi!!	
Papua New Guinea	unspecified	PPL 27	N/A	N/A	74	Picked Slides	11.3(88H)	A	trilob. And bulloides, vrdi and some broken forams too.	Langhian (Middle Miocene) to Recent
Papua New Guinea	unspecified	PPL 27	N/A	N/A	76	Picked Slides	11.3(88H)	P	Some orange-ish, some bright red-ish, some pyritised, vrdi!!	
Papua New Guinea	unspecified	PPL 27	N/A	N/A	80	Picked Slides	11.3(88H)	A	trilob., bulloides, vrdi!!	Langhian (Middle Miocene) to Recent
Papua New Guinea	unspecified	PPL 27	N/A	N/A	82	Picked Slides	11.3(88H)	R	under 10 specimens, some pyritised, vrdi!!	
Papua New Guinea	unspecified	PPL 27	N/A	N/A	83 a	Picked Slides	11.3(88H)	P	Some pyritised, vrdi!!	
Papua New Guinea	unspecified	PPL 27	N/A	N/A	84	Picked Slides	11.3(88H)	A	woodi, vrdi!!	Chattian (Late Oligocene) to Burdigalian (Early Miocene)
Papua New Guinea	unspecified	PPL 27	N/A	N/A	85	Picked Slides	11.3(88H)	A	bulloides, vrdi!!	Langhian (Middle Miocene) to Recent
Papua New Guinea	unspecified	PPL 27	N/A	N/A	86	Picked Slides	11.3(88H)	R	3 specimens, vrdi!!	

Papua New Guinea	unspecified	PPL 27	N/A	N/A	87 A	Picked Slides	11.3(88H)	P	some bright red-ish, some dark red-ish, some pyritised, vrdi!!	
Papua New Guinea	unspecified	PPL 27	N/A	N/A	88	Picked Slides	11.3(88H)	P	some orange-ish, some pyritised, vrdi!!	
Papua New Guinea	unspecified	PPL 27	N/A	N/A	89	Picked Slides	11.3(88H)	P	mainly benthics (some dark red, some black), under 5 specimens, some pyritised, very recrystallised, difficult to identify!!	
Papua New Guinea	unspecified	PPL 27	N/A	N/A	90	Picked Slides	11.3(88H)	P	Some bright red-ish, some dark red-ish, some pyritised, vrdi!!	
Papua New Guinea	unspecified	PPL 27	N/A	N/A	91	Picked Slides	11.3(88H)	P	miscellaneous microfossils, some pyritised, some lightly pyritised, vrdi!!	
Papua New Guinea	unspecified	PPL 27	N/A	N/A	118	Picked Slides	11.3(88H)	P	Slide 1; merotumida and maybe kind of transition between merotumida and plesiotumida since the former is ancestral to plesiotumida, recryst.	Tortonian (Middle Miocene) to Zanclean (Early Pliocene)
Papua New Guinea	unspecified	PPL 27	N/A	N/A	118	Picked Slides	11.3(88H)	A	Slide 2; smaller size fraction than previous slide, woodi, recryst.	Chattian (Late Oligocene) to Piacenzian (Late Pliocene)
Papua New Guinea	unspecified	PPL 27	N/A	N/A	138	Picked Slides	11.3(88H)	P	Slide 1; glob. merotumida, glob. Menardii, woodi, trilobus, orb. Univ., venez., recryst.	Tortonian (Middle Miocene) to Zanclean (Early Pliocene)

Papua New Guinea	unspecified	PPL 28	N/A	N/A		138	Picked Slides	11.3(88H)	P	Slide 2; merotumida, recryst.	Tortonian (Middle Miocene) to Zanclean (Early Pliocene)
Papua New Guinea	unspecified	PPL 29	N/A	N/A		139	Picked Slides	11.3(88H)	A	Slide 1; trilob., sacculifer with sac-like chamber, plesiotumida, recrysrt., some pyritised.	Tortonian (Late Miocene) to Piacenzian (Late Pliocene)
Papua New Guinea	unspecified	PPL 30	N/A	N/A		139	Picked Slides	11.3(88H)	A	Slide 2; smaller size fraction than previous slide, recryst.	Tortonian (Late Miocene) to Piacenzian (Late Pliocene)
Papua New Guinea	unspecified	PPL 31	N/A	N/A		140	Picked Slides	11.3(88H)	R	Miscellaneous microfossils including ostracods, a few forams, recryst.	
Papua New Guinea	unspecified	PPL 32	N/A	N/A		167 A	Picked Slides	11.3(88H)	R	miscellaneous microfossils, vrdi.	
Papua New Guinea	unspecified	PPL 33	N/A	N/A		188	Picked Slides	11.3(88H)	R	Slide 1; miscellaneous microfossils, vrdi.	
Papua New Guinea	unspecified	PPL 34	N/A	N/A		188	Picked Slides	11.3(88H)	P	Slide 2; miscellaneous microfossiuls including ostracods, vrdi.	
Papua New Guinea	unspecified	PPL 35	N/A	N/A		190	Picked Slides	11.3(88H)	A	miscellaneous microfossils including ostracods, trilob.,	Chattian (Late Oligocene) to Recent
Papua New Guinea	unspecified	Elevala	1	3101	3179	N/A	Picked Slides	13.5(74E)	N/A	N/A	
Papua New Guinea	unspecified	Elevala	1	3101		N/A	Picked Slides	13.5(74E)	B	no forams.	

Papua New Guinea	unspecified	Elevala	1	3110	N/A	Picked Slides	13.5(74E)	R	1-10 specimens very recrystallised, some pyritised, not even sure they are forams.	
Papua New Guinea	unspecified	Elevala	1	3119	N/A	Picked Slides	13.5(74E)	R	1-5 specimens, very recryst., some pyritised, not even sure they are forams.	
Papua New Guinea	unspecified	Elevala	1	3131	N/A	Picked Slides	13.5(74E)	R	1-10 specimens very recrystallised, some pyritised, not even sure are forams.	
Papua New Guinea	unspecified	Elevala	1	3140	N/A	Picked Slides	13.5(74E)	B	Miscellaneous microfossils, no forams.	
Papua New Guinea	unspecified	Elevala	1	3149	N/A	Picked Slides	13.5(74E)	R	1-10 specimens, very recryst., some pyritised and some red-ish, not even sure they are forams, difficult to identify.	
Papua New Guinea	unspecified	Elevala	1	3161	N/A	Picked Slides	13.5(74E)	B	Miscellaneous microfossils, no forams.	
Papua New Guinea	unspecified	Elevala	1	3179	N/A	Picked Slides	13.5(74E)	B	Miscellaneous microfossils, no forams.	
Papua New Guinea	unspecified	Mananda	1	3130 - 6900	N/A	Picked Slides	6.1(39A)	N/A	N/A	
Papua New Guinea	unspecified	Mananda	1	3130-3140	N/A	Picked Slides	6.1(39A)	R	About 5 specimens, seems marginotruncana, half glassy!	Turonian (Upper Cretaceous) to Campanian (Upper Cretaceous)

Papua New Guinea	unspecified	Mananda	1	3150-3160	N/A	Picked Slides	6.1(39A)	P	Slide 1, Marginotruncana, some glassy, some pyritised, some recryst.	Turonian (Upper Cretaceous) to Campanian (Upper Cretaceous)
Papua New Guinea	unspecified	Mananda	1	3150-3160	N/A	Picked Slides	6.1(39A)	P	Slide 2; Archaeoglobigerina genera, some glassy, some half glassy, some pyritised.	Turonian (Upper Cretaceous) to Campanian (Upper Cretaceous)
Papua New Guinea	unspecified	Mananda	1	6090-6100	N/A	Picked Slides	6.1(39A)	A	Most pyritisaed, archeoglobigerina, some half glassy, recryst.	Turonian (Upper Cretaceous) to Campanian (Upper Cretaceous)
Papua New Guinea	unspecified	Mananda	1	6190-6200	N/A	Picked Slides	6.1(39A)	P	Ticinella and/or Archeoglobigerina (most likely the latter), depending on overlap in history, some pyritised, some half glassy, recryst.	Albian or Turonian (Upper Cretaceous) to Campanian (Upper Cretaceous)
Papua New Guinea	unspecified	Mananda	1	6900	N/A	Picked Slides	6.1(39A)	P	Very recryst., some orange-ish, some pyritised, diff. To identify.	
Malaysia	unspecified	Kalutan	1	4060 - 6589	N/A	Picked Slides	15.4(61F)	N/A	N/A	
Malaysia	unspecified	Kalutan	1	4060-4070	N/A	Picked Slides	15.4(61F)	R	only benthics, recryst.	
Malaysia	unspecified	Kalutan	1	4540-4550	N/A	Picked Slides	15.4(61F)	P	only benthics, recryst.	
Malaysia	unspecified	Kalutan	1	5050-5060	N/A	Picked Slides	15.4(61F)	P	recryst.	
Malaysia	unspecified	Kalutan	1	5480-5500	N/A	Picked Slides	15.4(61F)	P	recryst.	
Malaysia	unspecified	Kalutan	1	5670-5700	N/A	Picked Slides	15.4(61F)	A	recryst.	

Malaysia	unspecified	Kalutan	1	6070-6090	N/A	Picked Slides	15.4(61F)	P	Trilobus; bulloides; recryst.	Langhian (Middle Miocene) to Recent
Malaysia	unspecified	Kalutan	1	6270-6290	N/A	Picked Slides	15.4(61F)	A	Trilobus; bulloides; recryst.	Langhian (Middle Miocene) to Recent
Malaysia	unspecified	Kalutan	1	6310-6330	N/A	Picked Slides	15.4(61F)	A	slide 1 of 2; recryst.	
Malaysia	unspecified	Kalutan	1	6310-6330	N/A	Picked Slides	15.4(61F)	P	slide 2 of 2; trilobus; sacculifer; recryst.	Chattian (Late Oligocene) to Recent
Malaysia	unspecified	Kalutan	1	6410-6430	N/A	Picked Slides	15.4(61F)	P	orbulina; trilobus; recryst.	Langhian (Middle Miocene) to Recent
Malaysia	unspecified	Kalutan	1	6431-6434	N/A	Picked Slides	15.4(61F)	R	by gc; recryst.	
Malaysia	unspecified	Kalutan	1	6431-6434	N/A	Picked Slides	15.4(61F)	P	by core;	
Malaysia	unspecified	Kalutan	1	6446	N/A	Picked Slides	15.4(61F)	R	recryst.	
Malaysia	unspecified	Kalutan	1	6446-6449	N/A	Picked Slides	15.4(61F)	R	by gc; recryst.	
Malaysia	unspecified	Kalutan	1	6452-6455	N/A	Picked Slides	15.4(61F)	R	by C; recryst.	
Malaysia	unspecified	Kalutan	1	6452-6455	N/A	Picked Slides	15.4(61F)	R	by gc; recryst.	
Malaysia	unspecified	Kalutan	1	6490-6510	N/A	Picked Slides	15.4(61F)	R	orbulina; recryst.	Langhian (Middle Miocene) to Recent
Malaysia	unspecified	Kalutan	1	6570-6589	N/A	Picked Slides	15.4(61F)	P	orbulina, trilobus; recryst.	Langhian (Middle Miocene) to Recent
Malaysia	unspecified	Kudat	1	150-2432.5	N/A	Picked Slides	15.4(61F)	N/A	N/A	
Malaysia	unspecified	Kudat	1	150	N/A	Picked Slides	15.4(61F)	B	1 blue-dyed foram? And 1 other foram?	
Malaysia	unspecified	Kudat	1	200	N/A	Picked Slides	15.4(61F)	A	loads of blue dye	
Malaysia	unspecified	Kudat	1	250	N/A	Picked Slides	15.4(61F)	A	mainly benthics, recryst.; loads of blue dye	

Malaysia	unspecified	Kudat	1	300	N/A	Picked Slides	15.4(61F)	R	mainly benthics; orbulina; recryst.	Langhian (Middle Miocene) to Recent
Malaysia	unspecified	Kudat	1	350	N/A	Picked Slides	15.4(61F)	A	succulifer; orbulina; recryst.	Langhian (Middle Miocene) to Recent
Malaysia	unspecified	Kudat	1	400	N/A	Picked Slides	15.4(61F)	P	recryst.	
Malaysia	unspecified	Kudat	1	450	N/A	Picked Slides	15.4(61F)	P	recryst.	
Malaysia	unspecified	Kudat	1	500	N/A	Picked Slides	15.4(61F)	P	mainly benthics; recryst.	
Malaysia	unspecified	Kudat	1	550	N/A	Picked Slides	15.4(61F)	P	mainly benthics; recryst.	
Malaysia	unspecified	Kudat	1	600	N/A	Picked Slides	15.4(61F)	R	recryst.	
Malaysia	unspecified	Kudat	1	650	N/A	Picked Slides	15.4(61F)	R	mainly benthics; recryst.	
Malaysia	unspecified	Kudat	1	700	N/A	Picked Slides	15.4(61F)	P	recryst.	
Malaysia	unspecified	Kudat	1	750	N/A	Picked Slides	15.4(61F)	P	mainly benthics; recryst.	
Malaysia	unspecified	Kudat	1	800	N/A	Picked Slides	15.4(61F)	P	mainly benthics; 1 orbulina?; recryst.	
Malaysia	unspecified	Kudat	1	850	N/A	Picked Slides	15.4(61F)	R	mainly benthics; recryst.	
Malaysia	unspecified	Kudat	1	900	N/A	Picked Slides	15.4(61F)	R	mainly benthics; recryst.	
Malaysia	unspecified	Kudat	1	950	N/A	Picked Slides	15.4(61F)	P	mainly benthics	
Malaysia	unspecified	Kudat	1	1000	N/A	Picked Slides	15.4(61F)	P	mainly benthics	
Malaysia	unspecified	Kudat	1	1005	N/A	Picked Slides	15.4(61F)	P	trilobus; recryst.	
Malaysia	unspecified	Kudat	1	1050	N/A	Picked Slides	15.4(61F)	R	mainly benthics	
Malaysia	unspecified	Kudat	1	1100	N/A	Picked Slides	15.4(61F)	P	mainly benthics	
Malaysia	unspecified	Kudat	1	1128	N/A	Picked Slides	15.4(61F)	A	recryst.	

Malaysia	unspecified	Kudat	1	1150	N/A	Picked Slides	15.4(61F)	P	mainly benthics	
Malaysia	unspecified	Kudat	1	1200	N/A	Picked Slides	15.4(61F)	P	mainly benthics	
Malaysia	unspecified	Kudat	1	1250	N/A	Picked Slides	15.4(61F)	P	mainly benthics	
Malaysia	unspecified	Kudat	1	1299	N/A	Picked Slides	15.4(61F)	P	recryst.	
Malaysia	unspecified	Kudat	1	1300	N/A	Picked Slides	15.4(61F)	p	bulloides; trilobus; mainly benthics; recryst.	Langhian (Middle Miocene) to Recent
Malaysia	unspecified	Kudat	1	1331	N/A	Picked Slides	15.4(61F)	P	recryst.	
Malaysia	unspecified	Kudat	1	1350	N/A	Picked Slides	15.4(61F)	P	bulloides; trilobus; recryst.	Langhian (Middle Miocene) to Recent
Malaysia	unspecified	Kudat	1	1400	N/A	Picked Slides	15.4(61F)	R	mainly benthics; recryst.	
Malaysia	unspecified	Kudat	1	1421	N/A	Picked Slides	15.4(61F)	R	recryst.	
Malaysia	unspecified	Kudat	1	1450	N/A	Picked Slides	15.4(61F)	P	Trilobus; bulloides; recryst.	Langhian (Middle Miocene) to Recent
Malaysia	unspecified	Kudat	1	1500	N/A	Picked Slides	15.4(61F)	P	mainly benthics; recryst.	
Malaysia	unspecified	Kudat	1	1508	N/A	Picked Slides	15.4(61F)	P	recryst.	
Malaysia	unspecified	Kudat	1	1528	N/A	Picked Slides	15.4(61F)	P	trilobus; recryst.	Chattian (Late Oligocene) to Recent
Malaysia	unspecified	Kudat	1	1550	N/A	Picked Slides	15.4(61F)	P	mainly benthics; recryst.	
Malaysia	unspecified	Kudat	1	1587	N/A	Picked Slides	15.4(61F)	R	recryst.	
Malaysia	unspecified	Kudat	1	1600	N/A	Picked Slides	15.4(61F)	P	trilobus; bulloides; recryst.	Langhian (Middle Miocene) to Recent
Malaysia	unspecified	Kudat	1	1607	N/A	Picked Slides	15.4(61F)	R	recryst.	
Malaysia	unspecified	Kudat	1	1650	N/A	Picked Slides	15.4(61F)	R	bulloides; recryst.	Langhian (Middle Miocene) to Recent

Malaysia	unspecified	Kudat	1	1700	N/A	Picked Slides	15.4(61F)	R	trilobus; 1 biserial foram?; recryst.	chattian (Late Oligocene) to Recent
Malaysia	unspecified	Kudat	1	1715	N/A	Picked Slides	15.4(61F)	R	recryst.	
Malaysia	unspecified	Kudat	1	1750	N/A	Picked Slides	15.4(61F)	P	recryst.	
Malaysia	unspecified	Kudat	1	1800	N/A	Picked Slides	15.4(61F)	P	Trilobus; bulloides; recryst.	Langhian (Middle Miocene) to Recent
Malaysia	unspecified	Kudat	1	1816	N/A	Picked Slides	15.4(61F)	R	recryst.	
Malaysia	unspecified	Kudat	1	1825	N/A	Picked Slides	15.4(61F)	R	recryst.	
Malaysia	unspecified	Kudat	1	1850	N/A	Picked Slides	15.4(61F)	P	Trilobus; bulloides; recryst.	Langhian (Middle Miocene) to Recent
Malaysia	unspecified	Kudat	1	1857	N/A	Picked Slides	15.4(61F)	R	recryst.	
Malaysia	unspecified	Kudat	1	1871	N/A	Picked Slides	15.4(61F)	P	recryst.; some blue dye	
Malaysia	unspecified	Kudat	1	1889	N/A	Picked Slides	15.4(61F)	R	recryst.	
Malaysia	unspecified	Kudat	1	1900	N/A	Picked Slides	15.4(61F)	A	trilobus; orbulina; recryst.	Langhian (Middle Miocene) to Recent
Malaysia	unspecified	Kudat	1	1907	N/A	Picked Slides	15.4(61F)	R	recryst.	
Malaysia	unspecified	Kudat	1	1916	N/A	Picked Slides	15.4(61F)	R	biserial foram?; recryst.	
Malaysia	unspecified	Kudat	1	1930	N/A	Picked Slides	15.4(61F)	P	trilobus; bulloides; biserial foram?; recryst., some pyritised	Langhian (Middle Miocene) to Recent
Malaysia	unspecified	Kudat	1	1940	N/A	Picked Slides	15.4(61F)	P	trilobus; recryst.	Chattian (Late Oligocene) to Recent
Malaysia	unspecified	Kudat	1	1961	N/A	Picked Slides	15.4(61F)	A	Trilobus; bulloides; recryst.	Langhian (Middle Miocene) to Recent
Malaysia	unspecified	Kudat	1	1965.5	N/A	Picked Slides	15.4(61F)	A	recryst.	

Malaysia	unspecified	Kudat	1	1992	N/A	Picked Slides	15.4(61F)	P	uniserial foram?; recryst.	
Malaysia	unspecified	Kudat	1	2003.5	N/A	Picked Slides	15.4(61F)	P	trilobus; recryst.; some blue dye	Chattian (Late Oligocene) to Recent
Malaysia	unspecified	Kudat	1	2021.5	N/A	Picked Slides	15.4(61F)	R	mainly benthics; recryst.	
Malaysia	unspecified	Kudat	1	2033.5	N/A	Picked Slides	15.4(61F)	P	recryst.	
Malaysia	unspecified	Kudat	1	2035.5	N/A	Picked Slides	15.4(61F)	G	trilobus; recryst.	Chattian (Late Oligocene) to Recent
Malaysia	unspecified	Kudat	1	2041	N/A	Picked Slides	15.4(61F)	P	sw50; orbulina?; recryst.	Langhian (Middle Miocene) to Recent
Malaysia	unspecified	Kudat	1	2047	N/A	Picked Slides	15.4(61F)	P	recryst.	
Malaysia	unspecified	Kudat	1	2058.5	N/A	Picked Slides	15.4(61F)	P	orbulina; recryst.	Langhian (Middle Miocene) to Recent
Malaysia	unspecified	Kudat	1	2067.5	N/A	Picked Slides	15.4(61F)	A	orbulina; recryst.	Langhian (Middle Miocene) to Recent
Malaysia	unspecified	Kudat	1	2070	N/A	Picked Slides	15.4(61F)	A	recryst.	
Malaysia	unspecified	Kudat	1	2081.5	N/A	Picked Slides	15.4(61F)	P	orbulina; recryst.	Langhian (Middle Miocene) to Recent
Malaysia	unspecified	Kudat	1	2089	N/A	Picked Slides	15.4(61F)	P	trilobus; bulloides; recryst.	Langhian (Middle Miocene) to Recent
Malaysia	unspecified	Kudat	1	2115.5	N/A	Picked Slides	15.4(61F)	P	orbulina; recryst.	Langhian (Middle Miocene) to Recent
Malaysia	unspecified	Kudat	1	2130	N/A	Picked Slides	15.4(61F)	P	orbulina; recryst.	Langhian (Middle Miocene) to Recent
Malaysia	unspecified	Kudat	1	2138.5	N/A	Picked Slides	15.4(61F)	A	orbulina?; recryst.	Langhian (Middle Miocene) to Recent

Malaysia	unspecified	Kudat	1	2151.5	N/A	Picked Slides	15.4(61F)	A	orbulina; trilobus; recryst.	Langhian (Middle Miocene) to Recent
Malaysia	unspecified	Kudat	1	2161.5	N/A	Picked Slides	15.4(61F)	A	by cr; orbulina; recryst.	Langhian (Middle Miocene) to Recent
Malaysia	unspecified	Kudat	1	2161.5	N/A	Picked Slides	15.4(61F)	P	orbulina; recryst.	Langhian (Middle Miocene) to Recent
Malaysia	unspecified	Kudat	1	2167.4	N/A	Picked Slides	15.4(61F)	A	recryst.	
Malaysia	unspecified	Kudat	1	2200	N/A	Picked Slides	15.4(61F)	A	orbulina; recryst.	Langhian (Middle Miocene) to Recent
Malaysia	unspecified	Kudat	1	2242.6	N/A	Picked Slides	15.4(61F)	A	recryst.	
Malaysia	unspecified	Kudat	1	2299.5	N/A	Picked Slides	15.4(61F)	P	Orbulina?; recryst.	Langhian (Middle Miocene) to Recent
Malaysia	unspecified	Kudat	1	2300	N/A	Picked Slides	15.4(61F)	A	orbulina; recryst.	Langhian (Middle Miocene) to Recent
Malaysia	unspecified	Kudat	1	2313	N/A	Picked Slides	15.4(61F)	P	orbulina; recryst.	Langhian (Middle Miocene) to Recent
Malaysia	unspecified	Kudat	1	2345	N/A	Picked Slides	15.4(61F)	P	orbulina; recryst.	Langhian (Middle Miocene) to Recent
Malaysia	unspecified	Kudat	1	2350	N/A	Picked Slides	15.4(61F)	P	orbulina; black dye present; recryst.	Langhian (Middle Miocene) to Recent
Malaysia	unspecified	Kudat	1	2375.5	N/A	Picked Slides	15.4(61F)	P	orbulina; recryst.	Langhian (Middle Miocene) to Recent
Malaysia	unspecified	Kudat	1	2375.5	N/A	Picked Slides	15.4(61F)	P	by cr; recryst.	
Malaysia	unspecified	Kudat	1	2388.5	N/A	Picked Slides	15.4(61F)	R	by B; bulloides; blue dye present; recryst.	Langhian (Middle Miocene) to Recent
Malaysia	unspecified	Kudat	1	2388.5	N/A	Picked Slides	15.4(61F)	P	trilobus; blue dye; recryst.	Chattian (Late Oligocene) to Recent

Malaysia	unspecified	Kudat	1	2388.5	N/A	Picked Slides	15.4(61F)	P	by mw; trilobus; blue dye; orbulina?; recryst.	Chattian (Late Oligocene) to Recent
Malaysia	unspecified	Kudat	1	2400	N/A	Picked Slides	15.4(61F)	P	orbulina; recryst.	Langhian (Middle Miocene) to Recent
Malaysia	unspecified	Kudat	1	2430	N/A	Picked Slides	15.4(61F)	P	by jc; orbulina; recryst.	Langhian (Middle Miocene) to Recent
Malaysia	unspecified	Kudat	1	2430	N/A	Picked Slides	15.4(61F)	P	by sd; orbulina; trilobus; recryst.; blu dye quite frequent	Langhian (Middle Miocene) to Recent
Malaysia	unspecified	Kudat	1	2430	N/A	Picked Slides	15.4(61F)	R	one-hole slide stating "Eocene"; blue dyed forams and recryst.	Eocene
Malaysia	unspecified	Kudat	1	2438.5	N/A	Picked Slides	15.4(61F)	R	recryst.	
Malaysia	unspecified	Kudat	1	2451	N/A	Picked Slides	15.4(61F)	R	orbulina; uniserial foram?; recryst.	Langhian (Middle Miocene) to Recent
Malaysia	unspecified	Kudat	1	2460	N/A	Picked Slides	15.4(61F)	A	orbulina; bulloides; trilobus; recryst.	Langhian (Middle Miocene) to Recent
Malaysia	unspecified	Kudat	1	2464	N/A	Picked Slides	15.4(61F)	R	recryst.	
Malaysia	unspecified	Kudat	1	2464	N/A	Picked Slides	15.4(61F)	R	by mw; recryst.	
Malaysia	unspecified	Kudat	1	2473	N/A	Picked Slides	15.4(61F)	R	recryst.	
Malaysia	unspecified	Kudat	1	2475	N/A	Picked Slides	15.4(61F)	R	trilobus; bulloides?; recryst.; some blue dyed	Langhian (Middle Miocene) to Recent
Malaysia	unspecified	Sabah	N/A	N/A	CPB 3-51	Picked Slides	8.2(50D)			
Malaysia	unspecified	Sabah	N/A	N/A	3	Picked Slides	8.2(50D)	P	brown-ish; recryst.	
Malaysia	unspecified	Sabah	N/A	N/A	3 rewash	Picked Slides	8.2(50D)	P	brown-ish; recryst.	
Malaysia	unspecified	Sabah	N/A	N/A	6	Picked Slides	8.2(50D)	R	recryst.	

Malaysia	unspecified	Sabah	N/A	N/A	9	Picked Slides	8.2(50D)	P	trilobus; recryst.	Chattian (Late Oligocene) to Recent
Malaysia	unspecified	Sabah	N/A	N/A	11	Picked Slides	8.2(50D)	R	recryst.	
Malaysia	unspecified	Sabah	N/A	N/A	13	Picked Slides	8.2(50D)	R	recryst.	
Malaysia	unspecified	Sabah	N/A	N/A	14	Picked Slides	8.2(50D)	P	brown-ish; recryst.	
Malaysia	unspecified	Sabah	N/A	N/A	20	Picked Slides	8.2(50D)	P	brown-ish; recryst.	
Malaysia	unspecified	Sabah	N/A	N/A	25	Picked Slides	8.2(50D)	R	recryst.	
Malaysia	unspecified	Sabah	N/A	N/A	40	Picked Slides	8.2(50D)	P	recryst.	
Malaysia	unspecified	Sabah	N/A	N/A	50	Picked Slides	8.2(50D)	R	recryst.	
Malaysia	unspecified	Sabah	N/A	N/A	51	Picked Slides	8.2(50D)	R	recryst.	
Malaysia	unspecified	Tigapapan	N/A	210-1541	N/A	Picked Slides	18.1(88A)	Slides not found in the collection	Slides not found in the collection	
Philippines	unspecified	Sarap	1	1220-2586	N/A	Picked Slides	8.5(43G)	N/A	N/A	
Philippines	unspecified	Sarap	1	1220	N/A	Picked Slides	8.5(43G)	P	Slide 1; venez., orb. Univ., Ss. Semilunina, menardii, recryst. And infilled.	Langhian (Middle Miocene) to Zanclean (Early Pliocene)
Philippines	unspecified	Sarap	1	1220	N/A	Picked Slides	8.5(43G)	P	Slide 2; trilob., menardii, recryst. And infilled.	Chattian (Late Oligocene) to Piacenzian (Late Pliocene)
Philippines	unspecified	Sarap	1	1250	N/A	Picked Slides	8.5(43G)	A	Slide 1; extremus, venez., menardii, disjuncta, obliquus, recryst. And infilled.	Burdigalian (Early Miocene) to Zanclean (Early Pliocene)
Philippines	unspecified	Sarap	1	1250	N/A	Picked Slides	8.5(43G)	P	Slide 2; smaller size fraction, trilob., orb., recryst.	Burdigalian (Early Miocene) to Zanclean (Early Pliocene)

Philippines	unspecified	Sarap	1	2583	N/A	Picked Slides	8.5(43G)	A	Slide 1; venez., orb., trilobus, recryst.	Langhian (Middle Miocene) to Zanclean (Early Pliocene)
Philippines	unspecified	Sarap	1	2583	N/A	Picked Slides	8.5(43G)	P	Slide 2; praeisphonif.? Only one, trilob., recryst.	Chattian (Late Oligocene) to Serravallian (Middle Miocene)
Philippines	unspecified	Sarap	1	2583	N/A	Picked Slides	8.5(43G)	P	Slide 3; smaller size fractions, specimens small and recryst.,diff. To identify.	Chattian (Late Oligocene) to Serravallian (Middle Miocene)
Philippines	unspecified	Sarap	1	2586	N/A	Picked Slides	8.5(43G)	A	Slide 1; orb. Univ., venez., recryst.	Langhian (Middle Miocene) to Zanclean (Early Pliocene)
Philippines	unspecified	Sarap	1	2586	N/A	Picked Slides	8.5(43G)	P	Slide 2; trilob., recryst.	Chattian (Late Oligocene) to Recent
Vietnam	unspecified	118-CUX	1X	630 - 2901	N/A	Picked Slides	13.5(74F)			
Vietnam	unspecified	118-CUX	1X	630	N/A	Picked Slides	13.5(74F)	R	Slide 1; benthics only.	
Vietnam	unspecified	118-CUX	1X	630	N/A	Picked Slides	13.5(74F)	A	Slide 2; Sacculifer with sac-like chamber, trilob.; globorotalia menardii lineage, crassaformis species present, recryst.	Seeravallian (Middle Miocene) to Recent
Vietnam	unspecified	118-CUX	1X	640	N/A	Picked Slides	13.5(74F)	R	benthics only, some recryst.	
Vietnam	unspecified	118-CUX	1X	640	N/A	Picked Slides	13.5(74F)	P	orb. Univ., plesiotumiuda, tumida tumida, trilob., recryst.	Messinian (Late Miocene) to Recent
Vietnam	unspecified	118-CUX	1X	2619	N/A	Picked Slides	13.5(74F)	B	empty, orange bits.	

Vietnam	unspecified	118-CUX	1X	2802	N/A	Picked Slides	13.5(74F)	R	not even sure there are forams, orange and bright oranghe-ish bits.	
Vietnam	unspecified	118-CUX	1X	2850	N/A	Picked Slides	13.5(74F)	R	not even sure there are forams, orange and bright oranghe-ish bits.	
Vietnam	unspecified	118-CUX	1X	2901	N/A	Picked Slides	13.5(74F)	R	not even sure there are forams, orange and bright oranghe-ish bits.	
Vietnam	unspecified	119-CH	1X	1190 - 2451	N/A	Picked Slides	7.4(51A)			
Vietnam	unspecified	119-CH	1X	1190	N/A	Picked Slides	7.4(51A)	R	Slide 1; benthics only, some recryst.	
Vietnam	unspecified	119-CH	1X	1190	N/A	Picked Slides	7.4(51A)	P	semilunina semilunina, disjuncta maybe, trilob., praoerb.	Burdigalian (Early Miocene)
Vietnam	unspecified	119-CH	1X	2319	N/A	Picked Slides	7.4(51A)	P	trilob., tumida tumida, some bright orange bits and recryst., not even sure they are forams; sp. Recryst.	Messinian (Late Miocene) to Recent
Vietnam	unspecified	119-CH	1X	2349	N/A	Picked Slides	7.4(51A)	R	orange-ish, few sp. And very recryst., diff. To identify.	
Vietnam	unspecified	119-CH	1X	2370	N/A	Picked Slides	7.4(51A)	R	Very recryst., some pyritised, few sp., diff. To identify.	
Vietnam	unspecified	119-CH	1X	2391	N/A	Picked Slides	7.4(51A)	R	not even sure there are forams, heavily pyritised and recryst., difficult to identify.	

Vietnam	unspecified	119-CH	1X	2412	N/A	Picked Slides	7.4(51A)	R	2 things, not even sure they are forams, one pyritised and one bright orange-ish, very recryst., difficult to identify.	
Vietnam	unspecified	119-CH	1X	2430	N/A	Picked Slides	7.4(51A)	R	not even sure there are forams, heavily pyritised and recryst., difficult to identify.	
Vietnam	unspecified	119-CH	1X	2451	N/A	Picked Slides	7.4(51A)	R	mainly benthics, maybe 1 planktonic, but pyritised and very recryst., diff. Top identify.	
Vietnam	unspecified	119-CH	1X	2472	N/A	Picked Slides	7.4(51A)	R	not even sure they are forams, heavily pyritised.	

Appendix 2

Oxygen and Carbon Isotopes Data from the early Eocene Moogli Mudstones, Papua New Guinea

List of foraminiferal species from the early Eocene used for δ¹⁸O and δ¹³C analyses in Chapter 4, including the part of the specimen (test or infill), size fraction (μm), and estimated temperatures using the palaeotemperature equation by Kim and O'Neil (1997), a latitudinal correction by Hollis et al. (2019), and an ice-volume correction of -0.89‰ after Cramer et al. (2011).

Species Name	Test or infill	Size fraction (μm)	δ¹³C (‰ VPDB)	δ¹⁸O (‰ VPDB)	Estimated Temperature (°C)
Morozovella subbotinae	test	180-212	2.83	-3.81	32.4
Morozovella subbotinae	infill	180-212	2.52	-4.86	
Morozovella marginodentata	test	180-212	2.82	-3.81	32.4
Morozovella marginodentata	infill	180-212	1.86	-5.01	
Subbotina patagonica	test	180-212	1.84	-3.43	30.4
Subbotina patagonica	infill	180-212	1.67	-5.41	
Subbotina hornibrooki	test	180-212	1.87	-3.67	31.7
Subbotina hornibrooki	infill	180-212	2.02	-5.03	
Acarinina wilcoxensis group	test	180-212	3.32	-4.22	34.2
Acarinina wilcoxensis group	infill	180-212	2.03	-5.23	
Subbotina velascoensis	test	180-212	1.83	-3.44	30.1
Subbotina velascoensis	infill	180-212	2.10	-4.88	
Morozovella occlusa	test	180-212	2.96	-3.99	33.0
Morozovella occlusa	infill	180-212	2.67	-4.78	
Morozovella aequa	test	180-212	2.97	-3.57	30.8
Morozovella aequa	infill	180-212	2.11	-4.97	
Morozovella gracilis	test	180-212	2.76	-3.89	32.5
Morozovella gracilis	infill	180-212	2.21	-5.04	
Morozovella acuta	test	180-212	3.08	-4.19	34.1
Morozovella acuta	infill	180-212	3.01	-4.74	

Morozovella pasionensis	test	180-212	3.10	-4.09	33.5
Morozovella pasionensis	infill	180-212	2.69	-4.72	
Subbotina roesnaesensis	test	180-212	1.85	-2.65	26.1
Subbotina roesnaesensis	infill	180-212	1.95	-4.89	
Globoturborotalita bassriverensis	test	180-212	1.94	-2.57	25.7
Globoturborotalita bassriverensis	infill	180-212	2.28	-5.02	
Subbotina patagonica	test	212-250	1.74	-3.30	29.4
Subbotina patagonica	infill	212-250	2.37	-5.18	
Subbotina hornibrooki	test	212-250	1.52	-3.77	31.9
Subbotina hornibrooki	infill	212-250	2.64	-4.72	
Subbotina roesnaesensis	test	212-250	1.69	-3.71	31.6
Subbotina roesnaesensis	infill	212-250	2.15	-5.05	
Morozovella subbotinae	test	212-250	3.30	-3.68	31.4
Morozovella subbotinae	infill	212-250	2.54	-4.77	
Morozovella marginodentata	test	212-250	3.40	-3.84	32.2
Morozovella marginodentata	infill	212-250	3.63	-4.50	
Morozovella acuta	test	212-250	3.14	-4.13	33.8
Morozovella acuta	infill	212-250	2.84	-4.75	
Globoturborotalita bassriverensis	test	212-250	1.96	-2.70	26.4
Globoturborotalita bassriverensis	infill	212-250	2.43	-4.66	
Acarinina wilcoxensis group	test	212-250	3.35	-3.94	32.8
Acarinina wilcoxensis group	infill	212-250	2.96	-4.73	
Morozovella gracilis	test	212-250	3.12	-3.78	31.9
Morozovella gracilis	infill	212-250	2.71	-4.81	
Morozovella velascoensis	test	212-250	3.06	-3.88	32.4
Morozovella velascoensis	infill	212-250	2.70	-4.75	
Morozovella aequa	test	212-250	3.21	-4.03	33.2
Morozovella aequa	infill	212-250	2.15	-4.78	
Morozovella pasionensis	test	212-250	2.97	-3.86	32.3
Morozovella pasionensis	infill	212-250	2.32	-5.04	
Subbotina velascoensis	test	212-250	2.42	-3.66	31.3
Subbotina velascoensis	infill	212-250	2.00	-5.07	
Morozovella occlusa	test	212-250	3.21	-3.91	32.6
Morozovella occlusa	infill	212-250	2.08	-3.75	
Bulimina tuxpamensis	test	212-250	0.65	-1.58	20.9
Bulimina tuxpamensis	infill	212-250	1.64	-2.63	
Morozovella subbotinae	test	250-300	3.44	-4.14	33.8
Morozovella subbotinae	infill	250-300	3.49	-4.65	
Morozovella acuta	test	250-300	3.81	-3.77	31.8
Morozovella acuta	infill	250-300	3.71	-4.55	
Subbotina roesnaesensis	test	250-300	2.02	-2.91	27.5
Subbotina roesnaesensis	infill	250-300	1.98	-4.85	
Morozovella marginodentata	test	250-300	3.08	-3.67	31.3
Morozovella marginodentata	infill	250-300	3.33	-4.51	
Subbotina patagonica	test	250-300	2.12	-3.16	28.7
Subbotina patagonica	infill	250-300	2.42	-4.72	

Globoturborotalita bassriverensis	test	250-300	1.97	-2.56	25.7
Globoturborotalita bassriverensis	infill	250-300	1.95	-5.06	
Subbotina hornibrooki	test	250-300	1.96	-3.34	29.6
Subbotina hornibrooki	infill	250-300	2.67	-4.76	
Morozovella velascoensis	test	250-300	3.11	-4.12	33.7
Morozovella velascoensis	infill	250-300	2.95	-4.76	
Morozovella gracilis	test	250-300	3.31	-4.06	33.4
Morozovella gracilis	infill	250-300	3.15	-4.66	
Acarinina wilcoxensis group	test	250-300	3.51	-4.15	33.8
Acarinina wilcoxensis group	infill	250-300	2.87	-4.76	
Morozovella occlusa	test	250-300	3.25	-3.86	32.3
Morozovella occlusa	infill	250-300	3.21	-4.98	
Morozovella aequa	test	250-300	3.23	-3.63	31.1
Morozovella aequa	infill	250-300	2.86	-4.74	
Morozovella pasionensis	test	250-300	3.31	-3.82	32.1
Morozovella pasionensis	infill	250-300	2.27	-4.91	
Subbotina velascoensis	test	250-300	2.13	-2.69	26.3
Subbotina velascoensis	infill	250-300	2.75	-4.86	
Bulimina tuxpamensis	test	250-300	0.89	-1.08	18.5
Bulimina tuxpamensis	infill	250-300	1.41	-3.61	
Morozovella acuta	test	300-315	3.54	-4.19	34.1
Morozovella acuta	infill	300-315	3.64	-4.61	
Subbotina roesnaesensis	test	300-315	1.77	-3.64	31.2
Subbotina roesnaesensis	infill	300-315	2.27	-4.87	
Globoturborotalita bassriverensis	test	300-315	1.92	-2.28	24.3
Globoturborotalita bassriverensis	infill	300-315	2.51	-4.75	
Morozovella subbotinae	test	300-315	3.21	-4.15	33.8
Morozovella subbotinae	infill	300-315	3.09	-4.63	
Morozovella marginodentata	test	300-315	3.28	-4.09	33.6
Morozovella marginodentata	infill	300-315	3.12	-4.57	
Morozovella velascoensis	test	300-315	3.45	-3.98	33.0
Morozovella velascoensis	infill	300-315	3.20	-4.63	
Subbotina hornibrooki	test	300-315	2.23	-3.44	30.2
Subbotina hornibrooki	infill	300-315	2.74	-4.58	
Morozovella gracilis	test	300-315	3.44	-4.29	34.6
Morozovella gracilis	infill	300-315	2.82	-4.81	
Morozovella pasionensis	test	300-315	3.39	-4.04	33.3
Morozovella pasionensis	infill	300-315	2.90	-4.75	
Subbotina velascoensis	test	300-315	1.93	-2.59	25.8
Subbotina velascoensis	infill	300-315	2.19	-5.16	
Acarinina wilcoxensis group	test	300-315	3.91	-4.04	33.3
Acarinina wilcoxensis group	infill	300-315	4.10	-4.44	
Morozovella gracilis	test	315-355	3.72	-3.77	31.9
Morozovella gracilis	infill	315-355	3.02	-4.62	
Morozovella acuta	test	315-355	3.84	-4.06	33.4
Morozovella acuta	infill	315-355	3.11	-4.59	

Morozovella velascoensis	test	315-355	3.85	-4.07	33.4
Morozovella velascoensis	infill	315-355	2.91	-4.66	
Morozovella occlusa	test	315-355	3.66	-3.84	32.2
Morozovella occlusa	infill	315-355	3.39	-4.62	
Morozovella subbotinae	test	315-355	3.71	-3.59	30.9
Morozovella subbotinae	infill	315-355	2.64	-4.64	
Morozovella marginodentata	test	315-355	3.28	-4.10	33.6
Morozovella marginodentata	infill	315-355	2.96	-4.73	
Globoturborotalita bassriverensis	test	315-355	2.05	-2.56	25.7
Globoturborotalita bassriverensis	infill	315-355	3.14	-4.75	
Subbotina hornibrooki	test	315-355	2.00	-2.78	26.8
Subbotina hornibrooki	infill	315-355	2.70	-4.94	
Subbotina roesnaesensis	test	315-355	2.07	-2.47	25.2
Subbotina roesnaesensis	infill	315-355	2.29	-5.13	
Morozovella pasionensis	test	315-355	3.52	-3.97	32.9
Morozovella pasionensis	infill	315-355	3.33	-4.50	
Bulimina tuxpamensis	test	315-355	0.93	-2.12	23.5
Bulimina tuxpamensis	infill	315-355	1.55	-3.19	
Morozovella aequa	test	315-355	3.52	-3.95	32.8
Morozovella aequa	infill	315-355	N/A, acid error	N/A acid error	
Morozovella gracilis	test	355-425	3.94	-3.85	32.3
Morozovella gracilis	infill	355-425	2.48	-4.62	
Morozovella pasionensis	test	355-425	3.56	-4.04	33.3
Morozovella pasionensis	infill	355-425	3.22	-4.85	
Morozovella velascoensis	test	355-425	4.38	-3.87	32.4
Morozovella velascoensis	infill	355-425	3.62	-4.49	
Subbotina roesnaesensis	test	355-425	2.03	-2.27	24.2
Subbotina roesnaesensis	infill	355-425	1.89	-5.18	
Subbotina hornibrooki	test	355-425	2.24	-2.20	23.9
Subbotina hornibrooki	infill	355-425	3.33	-4.58	
Globoturborotalita bassriverensis	test	355-425	2.18	-2.16	23.7
Globoturborotalita bassriverensis	infill	355-425	3.00	-4.79	
Bulimina tuxpamensis	test	355-425	1.27	-1.34	19.7
Bulimina tuxpamensis	infill	355-425	2.91	-3.26	
Globoturborotalita bassriverensis	test	425-500	1.69	-3.36	29.7
Globoturborotalita bassriverensis	infill	425-500	1.91	-5.09	

Appendix 3

Trace Metal Data from the early Eocene Moogli Mudstones, Papua New Guinea

List of foraminiferal species from the early Eocene used for Mg/Ca analyses in Chapter 4. The Mn/Ca, Al/Ca, and Fe/Ca ratios were also listed as they were used to check on contaminant phases, as well as the size fraction and the part of the shell used (test and infill). The estimated temperatures from Mg/Ca were calculated using the method developed by Evans et al. (2018). The raw Mg/Ca ratios were first pH-corrected and early Eocene Mg/Ca$_{sw}$ adjusted (see Chapter 4 for more details).

Species Name	Size fraction (µm)	Test or infill	Final Mg/Ca ratio (mmol/mol)	pH-corrected Mg/Ca (mmol/mol)	Estimated Temperature (°C)	Mn/Ca (µmol/mol)	Fe/Ca (µmol/mol)	Al/Ca (µmol/mol)
Morozovella subbotinae	212-250	test	5.60	4.16	33.54	3732.44	6313.69	22.10
Subbotina roesnaesensis	212-250	test	4.79	3.56	31.01	2629.20	4948.64	303.35
Subbotina roesnaesensis	212-250	infill	5.54	4.12	33.36	66.87	4889.03	11175.25
Morozovella marginodentata	250-300	test	4.41	3.28	29.66	2813.96	4274.05	160.36
Morozovella acuta	250-300	test	5.98	4.44	34.59	2393.47	3078.92	318.29
Morozovella acuta	250-300	infill	4.66	3.46	30.55	143.35	4617.31	9635.97
Morozovella acuta	212-250	test	4.18	3.11	28.81	2468.74	2805.28	445.63
Acarinina Wilcoxensis group	212-250	test	5.06	3.76	31.87	2922.52	4907.92	978.65
Acarinina Wilcoxensis group	212-250	infill	5.00	3.72	31.69	113.61	4506.08	10191.01
Subbotina patagonica	212-250	test	3.70	2.75	26.81	2078.84	4330.53	394.29
Subbotina patagonica	212-250	infill	5.38	3.99	32.87	175.45	4784.05	10401.21
Subbotina velascoensis	212-250	test	3.76	2.80	27.10	1566.30	3106.09	514.62
Subbotina velascoensis	212-250	infill	5.59	4.16	33.50	97.29	4940.76	10892.83
Subbotina hornibrooki	212-250	test	3.88	2.88	27.58	2016.69	4553.07	432.41
Subbotina hornibrooki	212-250	infill	5.07	3.76	31.90	268.60	4491.74	9682.16
Morozovella marginodentata	212-250	test	4.61	3.43	30.39	2652.67	4000.80	670.67
Morozovella marginodentata	212-250	infill	5.48	4.07	33.18	821.63	4430.23	10639.95
Globoturborotalita bassriverensis	212-250	test	4.68	3.48	30.62	2521.05	4906.77	948.65
Globoturborotalita bassriverensis	212-250	infill	5.33	3.96	32.73	290.77	4927.54	10781.37
Morozovella gracilis	212-250	test	4.99	3.71	31.67	3089.83	5358.66	1385.79
Morozovella gracilis	212-250	infill	5.25	3.90	32.49	187.80	4338.81	10443.60
Morozovella occlusa	212-250	test	5.06	3.76	31.87	5.06	5650.66	818.48
Morozovella occlusa	212-250	infill	5.51	4.09	33.26	114.96	4692.64	10180.74
Globoturborotalita bassriverensis	250-300	test	4.77	3.54	30.94	2261.98	4487.43	122.04
Globoturborotalita bassriverensis	250-300	infill	5.14	3.82	32.15	48.19	4860.87	10274.77
Morozovella subbotinae	250-300	test	4.66	3.46	30.54	2853.04	5402.63	378.67
Morozovella subbotinae	250-300	infill	5.54	4.12	33.36	222.23	4403.49	10392.38

Appendix 4

Oxygen and Carbon Isotopes Data from the late Eocene, Nanggulan Formation, Java

List of foraminiferal species from the late Eocene used for $\delta^{18}O$ and $\delta^{13}C$ analyses in Chapter 5, including the part of the specimen (test or infill), size fraction (µm), and estimated temperatures using the palaeotemperature equation by Kim and O'Neil (1997), a latitudinal correction by Hollis et al. (2019), and an ice-volume correction of -0.75‰ after Cramer et al. (2011).

Species Name	Part of the shell	Size fraction (µm)	$\delta^{13}C$ (‰ VPDB)	$\delta^{18}O$ (‰ VPDB)	Estimated Temperature (°C)
Chiloguembelina cubensis	crushed fragments	63-125	-1.205	-4.828	36.56
Pseudohastigerina micra	crushed fragments	63-125	-1.187	-4.8	36.41
Pseudohastigerina naguewichiensis	crushed fragments	63-125	-1.117	-4.794	36.38
Catapsydrax unicavus	crushed fragments	250-355	0.169	-1.872	21.46
Dentoglobigerina pseudovenezuelana	crushed fragments	250-355	-0.012	-3.706	30.65
Dentoglobigerina galavisi	crushed fragments	250-355	-0.152	-4.004	32.20
Dentoglobigerina tripartita	glassy whole shell	250-355	-0.024	-3.282	28.47
Hantkenina primitiva	crushed fragments	250-355	-0.098	-4.39	34.23
Hantkenina nanggulanensis	crushed fragments	250-355	-0.454	-4.609	35.39
Subbotina angiporoides	glassy whole shell	250-355	0.817	-3.435	29.25
Subbotina corpulenta	crushed fragments	250-355	-0.026	-4.07	32.54
Subbotina linaperta	crushed fragments	250-355	0.678	-3.466	29.41
Turborotalia ampliapertura	glassy whole shell	250-355	0.321	-3.956	31.95

Turborotalia cocoaensis	crushed fragments	250-355	0.515	-2.564	24.86
Turborotalia increbescens	crushed fragments	250-355	0.229	-4.064	32.51
Catapsydrax unicavus	crushed fragments	125-250	-0.151	-1.702	20.64
Chiloguembelina cubensis	crushed fragments	125-250	-1.005	-4.922	37.07
Globigerina officinalis	glassy whole shell	125-250	-0.454	-4.343	33.98
Globoturborotalita martini	crushed fragments	125-250	N/A, sample too small	N/A, sample too small	N/A
Globoturborotalita ouachitaensis	crushed fragments	125-250	N/A, sample too small	N/A, sample too small	N/A
Hantkenina primitiva	crushed fragments	125-250	0.101	-3.96	31.97
Hantkenina nanggulanensis	crushed fragments	125-250	0.037	-3.901	31.66
Paragloborotalia nana	crushed fragments	125-250	-0.311	-4.055	32.46
Pseudohastigerina micra	crushed fragments	125-250	-0.998	-4.817	36.51
Pseudohastigerina naguewichiensis	crushed fragments	125-250	-1.014	-4.881	36.85
Subbotina angiporoides	glassy whole shell	125-250	-0.208	-3.833	31.30
Turborotalia ampliapertura	crushed fragments	125-250	-0.216	-4.28	33.65
Turborotalia increbescens	crushed fragments	≥355	0.285	-4.14	32.91
Subbotina corpulenta	crushed fragments	≥355	-0.251	-2.439	24.24
Hantkenina nanggulanensis	crushed fragments	≥ 355	0.324	-4.2	33.22
Turborotalia ampliapertura	crushed fragments	≥ 355	0.641	-3.858	31.43
Dentoglobigerina pseudovenezuelana	crushed fragments	≥ 355	-0.146	-4.033	32.35
Dentoglobigerina galavisi	crushed fragments	≥ 355	0.251	-3.446	29.31
Dentoglobigerina tripartita	glassy whole shell	≥ 355	0.713	-2.638	25.22
Turborotalia cocoaensis	crushed fragments	≥ 355	0.606	-1.996	22.06
Catapsydrax unicavus	crushed fragments	≥ 355	0.264	-2.029	22.22

Appendix **5**

Species and their assigned Ecological Group for the late Eocene and early Oligocene Databases

List of foraminiferal species from the late Eocene and early Oligocene, and associated ecological group used for the late Eocene and early Oligocene database in Chapter 5.

Old species name	Updated species name	Old ecology group assigned	Updated ecology group assigned
Acarinina appressocamerata	*Acarinina collactea*	1	1
Catapsydrax unicavus	*Catapsydrax unicavus*	3	3
Cassigerinella spp.	*Cassigerinella* spp.	2	1
Catapsydrax dissimilis	*Catapsydrax dissimilis*	3	3
Catapsydrax echinatus	*Acarinina echinata*	1	1
Catapsydrax spp.	*Catapsydrax* spp.	3	3
Chiloguembelina cubensis	*Chiloguembelina cubensis*	3	1
Cibrohantkenina inflata	*Cibrohantkenina inflata*	2	2
Globigerina ampliapertura	*Turborotalia ampliapertura*	2	2
Globorotalia kugleri	*Paragloborotalia kugleri*	2	2
Globorotalia opima nana	*Paragloborotalia nana*	2	2
Globocassidulina subglobosa	*Subbotina* spp.	3	3
Globigerina tapiurensis	*Dentoglobigerina tapiurensis*	3	3
Globigerina venezuelana	*Dentoglobigerina venezuelana*	3	3
Globigerapsis index	*Globigerinatheka index*	2	2
Globigerapsis mexicana	*Globigerinatheka mexicana*	2	2
Globigerina angustiumbilicata	*Tenuitella angustiumbilicata*	2	2
Globigerina cerroazulensis	*Turborotalia cerroazulensis*	2	2

Globigerina cf. *perus*	*Subbotina corpulenta*	3	3
Globigerina corpulenta	*Subbotina corpulenta*	3	3
Globigerina eocaena	*Subbotina eocaena*	3	3
Globigerina euaperta/euapertura	*Globoturborotalita euapertura*	3	1
Globigerina galavisi	*Dentoglobigerina galavisi*	3	3
Globigerina gortanii	*Subbotina gortanii*	3	3
Globigerina linaperta	*Subbotina linaperta*	3	3
Globigerina officinalis	*Globigerina officinalis*	2	2
Globigerina perus	*Subbotina corpulenta*	3	3
Globigerina pseudoampliapertura	*Turborotalia ampliapertura*	2	2
Globigerina pseudoeocaena	*Subbotina yeguaensis*	3	3
Globigerina spp.	*Globigerina* spp.	2	2
Globigerina utilisindex	*Subbotina utilisindex*	3	3
Globigerina winkleri	*Subbotina corpulenta*	3	3
Globigerinatheka index	*Globigerinatheka index*	2	2
Globigerinatheka semiinvoluta	*Globigerinatheka semiinvoluta*	2	2
Globigerinatheka spp.	*Globigerinatheka* spp.	2	2
Globigerinatheka tropicalis	*Globigerinatheka tropicalis*	2	2
Globigerinoides subconglobatus	*Globigerinatheka subconglobata*	2	2
Globogerinoides index	*Globigerinatheka index*	2	2
Globoquadrina tapiurensis	*Dentoglobigerina tapiurensis*	3	3
Globoquadrina tripartite	*Dentoglobigerina tripartita*	3	3
Globorotalia cerroazulensis	*Turborotalia cerrozulensis*	2	2
Globorotalia opima	*Paragloborotalia opima*	2	2
Globorotalia pomeroli	*Turborotalia pomeroli*	2	2
Globorotalia siakensis	*Paragloborotalia siakensis*	2	2
Globorotaloides suteri	*Globorotaloides suteri*	3	3
Globoturborotalita anguliofficinalis and *Globigerina anguliofficinalis*	*Ciperoella anguliofficinalis*	2 and 1	2
Globoturborotalita martini	*Globoturborotalita martini*	1	1
Globoturborotalita ouachitaensis	*Globoturborotalita ouachitaensis*	1	1
Hantkenina alabamensis	*Hantkenina alabamensis*	2	2
Hantkenina nanggulanensis	*Hantkenina nanggulanensis*	2	2

Hantkenina spp.	*Hantkenina* spp.	2	2
Heterohelicid	*Chiloguembelina* spp.	3	1
juvenile Globorotalia kugleri	*Paragloborotalia* spp.?	2	2
Mixed assemblage of *Globigerina angiporoides* and *G.* aff. *linaperta*	*Subbotina linaperta* and *Subbotina angiporoides*	3	3
Mixed Species of Planktonic Foraminifera	Mixed Species of Planktonic Foraminifera	3	3
Mixed species, dominated by *Globigerapsis index*	Mixed species, dominated by *Globigerinatheka index*	2	2
Pseudohastigerina barbadoensis	*Pseudohastigerina naguewichiensis*	1	1
Praetenuitella gemma	*Tenuitella gemma*	1	2
Paragloborotalia inaequispira	*Subbotina inaequispira*	3	3
Paragloborotalia wilsoni	*Parasubbotina wilsoni*	3	3
Planktonic assemblages	*Planktonic assemblages*	3	3
Pseudohastigerina danvillensis	*Pseudohastigerina micra*	1	1
Pseudohastigerina micra	*Pseudohastigerina micra*	1	1
Pseudohastigerina naguewichiensis	*Pseudohastigerina naguewichiensis*	1	1
Streptochilus cubensis	*Chiloguembelina cubensis*	3	1
Subbotina angiporoides	*Subbotina angiporoides*	3	3
Subbotina eocaena	*Subbotina eocaena*	3	3
Subbotina spp.	*Subbotina* spp.	3	3
Turborotalia/Globorotalia centralis	*Turborotalia cerrozulensis*	2	2
Turborotalia cunialensis	*Turborotalia cunialensis*	2	2
Turborotalia pseudoampliapertura	*Turborotalia ampliapertura*	2	2
Turborotalia increbescens	*Turborotalia increbescens*	2	2
Turborotalia pseudo-ampliapertura	*Turborotalia pseudo-ampliapertura*	2	2

Appendix 6

Global Planktonic Foraminiferal δ^{18}O Database from the late Eocene

Late Eocene database displaying a global δ^{18}O compilation from planktonic foraminifera, along with the name of the site, geographical coordinates, preservation state of the specimens, updated name of the foraminiferal species, ecological group assigned, and the source the data were retrieved from. The palaeolatitude was calculated using the palaeolatitude calculator developed by van Hinsbergen et al. (2015).

Leg	Site	(Bio)zone	Geographical Area	Latitude	Longitude	Palaeolatitude	Author	Age if specified (Ma)	Species name	Updated Species Name	Ecology group	δ¹⁸O value (‰)	Preservation
32	305	P15	Shatsky Rise	32°00.13'N	157°51.00'E	29.24	Douglas and Savin, 1975		Mixed spp. of Planktonic Foraminifera	Mixed spp. of Planktonic Foraminifera	3	0.43	Poor, recrystallised foraminifera.
6	44		Horizon Ridge	19° 18.5'N	169° 00'W	11.85	Douglas and Savin, 1971		*Globigerina corpulenta*	*Subbotina corpulenta*	3	0.18	Poor, recrystallised foraminifera.
17	167	G. gortanii (P.17)	near the crest of the Magellan Rise, in 3176 m of water	7°04.1'N	167°49.5'W	-0.43	Douglas and Savin, 1973		Planktonic assemblages	Planktonic assemblages	3	-0.39	Poor, recrystallised foraminifera.
20	748b		southern Kerguelen Plateau	58°26.45'S	78°58.89'E	-55.3	Mackensen and Ehrmann, 1992		*Chiloguembelina cubensis*	*Chiloguembelina cubensis*	1	1.03	Poor, recrystallised foraminifera.
20	748b		southern Kerguelen Plateau	58°26.45'S	78°58.89'E	-55.3	Zachos et al. 1992		*Chiloguembelina cubensis*	*Chiloguembelina cubensis*	1	0.68	Poor, recrystallised foraminifera.
20	748b		southern Kerguelen Plateau	58°26.45'S	78°58.89'E	-55.3	Zachos et al. 1992		*Chiloguembelina cubensis*	*Chiloguembelina cubensis*	1	0.59	Poor, recrystallised foraminifera.
20	748b		southern Kerguelen Plateau	58°26.45'S	78°58.89'E	-55.3	Zachos et al. 1992		*Chiloguembelina cubensis.*	*Chiloguembelina cubensis*	1	0.38	Poor, recrystallised foraminifera.

20	748b		southern Kerguelen Plateau	58°26.45' S	78°58.89' E	-55.3	Zachos et al. 1992		*Chiloguembelina cubensis*	*Chiloguembelina cubensis*	1	0.43	Poor, recrystallised foraminifera.
20	748b		southern Kerguelen Plateau	58°26.45' S	78°58.89' E	-55.3	Zachos et al. 1992		*Chiloguembelina cubensis*	*Chiloguembelina cubensis*	1	0.64	Poor, recrystallised foraminifera.
20	748b		southern Kerguelen Plateau	58°26.45' S	78°58.89' E	-55.3	Zachos et al. 1992		Mixed *planktonics*	Mixed *planktonics*	3	0.78	Poor, recrystallised foraminifera.
20	748b		southern Kerguelen Plateau	58°26.45' S	78°58.89' E	-55.3	Zachos et al. 1992		*Chiloguembelina cubensis*	*Chiloguembelina cubensis*	1	0.43	Poor, recrystallised foraminifera.
20	748b		southern Kerguelen Plateau	58°26.45' S	78°58.89' E	-55.3	Zachos et al. 1992		*Subbotina angiporoides*	*Subbotina angiporoides*	3	0.87	Poor, recrystallised foraminifera.
74	526		Walvis Ridge	30°07.36' S	03°08.28' E	-38.51	Shackleton and Boersma, 1984	35.486	*Globigerinatheka index*	*Globigerinatheka index*	2	0.14	Poor, recrystallised foraminifera.
74	526		Walvis Ridge	30°07.36' S	03°08.28' E	-38.51	Shackleton and Boersma, 1984	35.486	*Catapsydrax* spp.	*Catapsydrax* spp.	3	0.55	Poor, recrystallised foraminifera.
74	526		Walvis Ridge	30°07.36' S	03°08.28' E	-38.51	Shackleton and Boersma, 1984	35.753	*Globorotalia cerroazulensis*	*Turborotalia cerroazulensis*	2	0.39	Poor, recrystallised foraminifera.
74	526		Walvis Ridge	30°07.36' S	03°08.28' E	-38.51	Shackleton and Boersma, 1984	35.753	*Globigerinatheka index*	*Globigerinatheka index*	2	0.24	Poor, recrystallised foraminifera.

74	526		Walvis Ridge	30°07.36' S	03°08.28' E	-38.51	Shackleton and Boersma, 1984	35.753	*Catapsydrax* spp.	*Catapsydrax* spp.	3	0.19	Poor, recrystallised foraminifera.
74	528		Walvis Ridge	28°31.49' S	02°19.44' E	-36.9	Shackleton and Boersma, 1984	37.285	*Globigerinatheka* spp.	*Globigerinatheka* spp.	2	0.02	Poor, recrystallised foraminifera.
74	529		Walvis Ridge	28°55.83' S	02°46.08' E	-37.31	Shackleton and Boersma, 1984	34.735	*Globigerina pseudoampliapertura*	*Turborotalia ampliapertura*	2	1.35	Poor, recrystallised foraminifera.
74	529		Walvis Ridge	28°55.83' S	02°46.08' E	-37.31	Shackleton and Boersma, 1984	34.735	*Catapsydrax* spp.	*Catapsydrax* spp.	3	1.13	Poor, recrystallised foraminifera.
74	529		Walvis Ridge	28°55.83' S	02°46.08' E	-37.31	Shackleton and Boersma, 1984	34.873	*Globigerina pseudoampliapertura*	*Turborotalia ampliapertura*	2	1.25	Poor, recrystallised foraminifera.
74	529		Walvis Ridge	28°55.83' S	02°46.08' E	-37.31	Shackleton and Boersma, 1984	34.873	*Turborotalia* spp.	*Turborotalia* spp.	2	1.41	Poor, recrystallised foraminifera.
74	529		Walvis Ridge	28°55.83' S	02°46.08' E	-37.31	Shackleton and Boersma, 1984	34.873	*Globigerina euaperta*	*Globoturborotalita euapertura*	1	1.34	Poor, recrystallised foraminifera.
74	529		Walvis Ridge	28°55.83' S	02°46.08' E	-37.31	Shackleton and Boersma, 1984	34.873	*Catapsydrax* spp.	*Catapsydrax* spp.	3	1.26	Poor, recrystallised foraminifera.
74	529		Walvis Ridge	28°55.83' S	02°46.08' E	-37.31	Shackleton and Boersma, 1984	34.901	*C.* spp.	*Catapsydrax* spp.	3	1	Poor, recrystallised foraminifera.

74	529		Walvis Ridge	28°55.83'S	02°46.08'E	-37.31	Shackleton and Boersma, 1984	35.043	*Globigerina cerroazulensis*	*Turborotalia cerroazulensis*	2	1.41	Poor, recrystallised foraminifera.
74	529		Walvis Ridge	28°55.83'S	02°46.08'E	-37.31	Shackleton and Boersma, 1984	35.043	*Catapsydrax* spp.	*Catapsydrax* spp.	3	1.19	Poor, recrystallised foraminifera.
74	529		Walvis Ridge	28°55.83'S	02°46.08'E	-37.31	Shackleton and Boersma, 1984	35.048	*C. unicavus*	*Catapsydrax unicavus*	3	1.3	Poor, recrystallised foraminifera.
74	529		Walvis Ridge	28°55.83'S	02°46.08'E	-37.31	Shackleton and Boersma, 1984	36.037	*C.* spp.	*Catapsydrax* spp.	3	1.15	Poor, recrystallised foraminifera.
74	529		Walvis Ridge	28°55.83'S	02°46.08'E	-37.31	Shackleton and Boersma, 1984	36.79	*C.* spp.	*Catapsydrax* spp.	3	1.33	Poor, recrystallised foraminifera.
74	529		Walvis Ridge	28°55.83'S	02°46.08'E	-37.31	Shackleton and Boersma, 1984	36.823	*Globigerina pseudoeocaena*	*Subbotina yeguaensis*	3	1.17	Poor, recrystallised foraminifera.
74	529		Walvis Ridge	28°55.83'S	02°46.08'E	-37.31	Shackleton and Boersma, 1984	36.823	*Catapsydrax* spp.	*Catapsydrax* spp.	3	1.21	Poor, recrystallised foraminifera.
74	529		Walvis Ridge	28°55.83'S	02°46.08'E	-37.31	Shackleton and Boersma, 1984	37.017	*Globigerina cerroazulensis*	*Turborotalia cerroazulensis*	2	0.28	Poor, recrystallised foraminifera.
74	529		Walvis Ridge	28°55.83'S	02°46.08'E	-37.31	Shackleton and Boersma, 1984	37.059	*G. cerroazulensis*	*Turborotalia cerroazulensis*	2	0.46	Poor, recrystallised foraminifera.

74	529		Walvis Ridge	28°55.83'S	02°46.08'E	-37.31	Shackleton and Boersma, 1984	37.059	*Turborotalia increbescens*	*Turborotalia increbescens*	2	0.37	Poor, recrystallised foraminifera.
74	529		Walvis Ridge	28°55.83'S	02°46.08'E	-37.31	Shackleton and Boersma, 1984	37.059	*Globigerinatheka index*	*Globigerinatheka index*	2	0.52	Poor, recrystallised foraminifera.
74	529		Walvis Ridge	28°55.83'S	02°46.08'E	-37.31	Shackleton and Boersma, 1984	37.059	*Globigerina winkleri*	*Subbotina corpulenta*	3	0.66	Poor, recrystallised foraminifera.
74	529		Walvis Ridge	28°55.83'S	02°46.08'E	-37.31	Shackleton and Boersma, 1984	37.059	*Catapsydrax* spp.	*Catapsydrax* spp.	3	0.52	Poor, recrystallised foraminifera.
74	529		Walvis Ridge	28°55.83'S	02°46.08'E	-37.31	Shackleton and Boersma, 1984	37.362	*Hantkenina* spp.	*Hantkenina* spp.	2	0.3	Poor, recrystallised foraminifera.
74	529		Walvis Ridge	28°55.83'S	02°46.08'E	-37.31	Shackleton and Boersma, 1984	37.362	*Globigerinatheka index*	*Globigerinatheka* spp.	2	0.21	Poor, recrystallised foraminifera.
74	529		Walvis Ridge	28°55.83'S	02°46.08'E	-37.31	Shackleton and Boersma, 1984	37.362	*Catapsydrax* spp.	*Catapsydrax* spp.	3	0.59	Poor, recrystallised foraminifera.
74	529		Walvis Ridge	28°55.83'S	02°46.08'E	-37.31	Shackleton and Boersma, 1984	37.362	*Globigerina cerroazulensis*	*Turborotalia cerroazulensis*	2	0.37	Poor, recrystallised foraminifera.
74	529		Walvis Ridge	28°55.83'S	02°46.08'E	-37.31	Shackleton and Boersma, 1984	37.647	*Catapsydrax* spp.	*Catapsydrax* spp.	3	0.62	Poor, recrystallised foraminifera.

74	529		Walvis Ridge	28°55.83' S	02°46.08' E	-37.31	Shackleton and Boersma, 1984	37.647	*Globigerinatheka index*	*Globigerinatheka index*	2	0.37	Poor, recrystallised foraminifera.
74	529		Walvis Ridge	28°55.83' S	02°46.08' E	-37.31	Shackleton and Boersma, 1984	37.647	*Catapsydrax unicavus*	*Catapsydrax unicavus*	3	0.72	Poor, recrystallised foraminifera.
74	529		Walvis Ridge	28°55.83' S	02°46.08' E	-37.31	Shackleton and Boersma, 1984	37.712	*Globigerina gortanii*	*Subbotina gortanii*	3	0.97	Poor, recrystallised foraminifera.
74	529		Walvis Ridge	28°55.83' S	02°46.08' E	-37.31	Shackleton and Boersma, 1984	37.712	*G. cerroazulensis*	*Turborotalia cerroazulensis*	2	0.27	Poor, recrystallised foraminifera.
74	529		Walvis Ridge	28°55.83' S	02°46.08' E	-37.31	Shackleton and Boersma, 1984	37.712	*Catapsydrax* spp.	*Catapsydrax* spp.	3	0.41	Poor, recrystallised foraminifera.
74	529		Walvis Ridge	28°55.83' S	02°46.08' E	-37.31	Shackleton and Boersma, 1984	38.202	*Globigerina cerroazulensis*	*Turborotalia cerroazulensis*	2	0.57	Poor, recrystallised foraminifera.
74	529		Walvis Ridge	28°55.83' S	02°46.08' E	-37.31	Shackleton and Boersma, 1984	38.202	*Catapsydrax* spp.	*Catapsydrax* spp.	3	0.77	Poor, recrystallised foraminifera.
74	529		Walvis Ridge	28°55.83' S	02°46.08' E	-37.31	Shackleton and Boersma, 1984	39.424	*Globigerinatheka index*	*Globigerinatheka index*	2	0.59	Poor, recrystallised foraminifera.
74	529		Walvis Ridge	28°55.83' S	02°46.08' E	-37.31	Shackleton and Boersma, 1984	39.424	*Globigerina cerroazulensis*	*Turborotalia cerroazulensis*	2	0.6	Poor, recrystallised foraminifera.

74	529		Walvis Ridge	28°55.83' S	02°46.08' E	-37.31	Shackleton and Boersma, 1984	39.424	*Catapsydrax echinatus*	*Acarinina echinatus*	1	0.15	Poor, recrystallised foraminifera.
74	529		Walvis Ridge	28°55.83' S	02°46.08' E	-37.31	Shackleton and Boersma, 1984	39.424	*C.* spp.	*Catapsydrax* spp.	3	0.6	Poor, recrystallised foraminifera.
74	529		Walvis Ridge	28°55.83' S	02°46.08' E	-37.31	Shackleton and Boersma, 1984	39.424	*Turborotalia increbescens*	*Turborotalia increbescens*	2	0.54	Poor, recrystallised foraminifera.
74	529		Walvis Ridge	28°55.83' S	02°46.08' E	-37.31	Shackleton and Boersma, 1984	39.424	*Globigerina winkleri*	*Subbotina corpulenta*	3	0.64	Poor, recrystallised foraminifera.
74	529		Walvis Ridge	28°55.83' S	02°46.08' E	-37.31	Shackleton and Boersma, 1984	40.428	*Globigerinatheka index*	*Globigerinatheka index*	2	0.6	Poor, recrystallised foraminifera.
74	529		Walvis Ridge	28°55.83' S	02°46.08' E	-37.31	Shackleton and Boersma, 1984	40.428	*Globigerina cerroazulensis*	*Turborotalia cerroazulensis*	2	0.54	Poor, recrystallised foraminifera.
74	529		Walvis Ridge	28°55.83' S	02°46.08' E	-37.31	Shackleton and Boersma, 1984	40.428	*G. corpulenta*	*Subbotina corpulenta*	3	0.65	Poor, recrystallised foraminifera.
74	529		Walvis Ridge	28°55.83' S	02°46.08' E	-37.31	Shackleton and Boersma, 1984	40.428	*Catapsydrax* spp.	*Catapsydrax* spp.	3	0.71	Poor, recrystallised foraminifera.
74	529		Walvis Ridge	28°55.83' S	02°46.08' E	-37.31	Shackleton and Boersma, 1984	40.428	*Globigerinatheka subconglobata*	*Globigerinatheka subconglobata*	2	0.4	Poor, recrystallised foraminifera.

74	529		Walvis Ridge	28°55.83'S	02°46.08'E	-37.31	Shackleton and Boersma, 1984	40.428	*Globigerina winkleri*	*Subbotina corpulenta*	3	0.57	Poor, recrystallised foraminifera.
73	522		southern Angola Abyssal Plain	26°06.843'S	5°07.78'W	-34.34	Oberhansli et al., 1984		*Glob. venezuelana*	*Dentoglobigerina venezuelana*	3	0.43	Poor, recrystallised foraminifera.
73	522		southern Angola Abyssal Plain	26°06.843'S	5°07.78'W	-34.34	Oberhansli et al., 1984		*Glob. venezuelana*	*Dentoglobigerina venezuelana*	3	0.84	Poor, recrystallised foraminifera.
73	522		southern Angola Abyssal Plain	26°06.843'S	5°07.78'W	-34.34	Oberhansli et al., 1984		*Glob. venezuelana*	*Dentoglobigerina venezuelana*	3	0.47	Poor, recrystallised foraminifera.
73	522		southern Angola Abyssal Plain	26°06.843'S	5°07.78'W	-34.34	Oberhansli et al., 1984		*Glob. venezuelana*	*Dentoglobigerina venezuelana*	3	0.66	Poor, recrystallised foraminifera.
73	522		southern Angola Abyssal Plain	26°06.843'S	5°07.78'W	-34.34	Oberhansli et al., 1984		*Glob. venezuelana*	*Dentoglobigerina venezuelana*	3	0.57	Poor, recrystallised foraminifera.
73	522		southern Angola Abyssal Plain	26°06.843'S	5°07.78'W	-34.34	Oberhansli et al., 1984		*Glob. venezuelana*	*Dentoglobigerina venezuelana*	3	0.64	Poor, recrystallised foraminifera.
73	522		southern Angola Abyssal Plain	26°06.843'S	5°07.78'W	-34.34	Oberhansli et al., 1984		*Glob. venezuelana*	*Dentoglobigerina venezuelana*	3	0.76	Poor, recrystallised foraminifera.
73	522		southern Angola Abyssal Plain	26°06.843'S	5°07.78'W	-34.34	Oberhansli et al., 1984		*Glob. venezuelana*	*Dentoglobigerina venezuelana*	3	0.63	Poor, recrystallised foraminifera.

73	522		southern Angola Abyssal Plain	26°06.843'S	5°07.78'W	-34.34	Oberhansli et al., 1984		*Glob. venezuelana*	*Dentoglobigerina venezuelana*	3	0.54	Poor, recrystallised foraminifera.
73	522		southern Angola Abyssal Plain	26°06.843'S	5°07.78'W	-34.34	Oberhansli et al., 1984		*Glob. venezuelana*	*Dentoglobigerina venezuelana*	3	0.63	Poor, recrystallised foraminifera.
73	522		southern Angola Abyssal Plain	26°06.843'S	5°07.78'W	-34.34	Oberhansli et al., 1984		*Glob. venezuelana*	*Dentoglobigerina venezuelana*	3	0.62	Poor, recrystallised foraminifera.
73	522		southern Angola Abyssal Plain	26°06.843'S	5°07.78'W	-34.34	Oberhansli et al., 1984		*Catapsydrax dissimilis*	*Catapsydrax dissimilis*	3	1	Poor, recrystallised foraminifera.
73	522		southern Angola Abyssal Plain	26°06.843'S	5°07.78'W	-34.34	Oberhansli et al., 1984		*Catapsydrax dissimilis*	*Catapsydrax dissimilis*	3	0.86	Poor, recrystallised foraminifera.
73	522		southern Angola Abyssal Plain	26°06.843'S	5°07.78'W	-34.34	Oberhansli et al., 1984		*Catapsydrax dissimilis*	*Catapsydrax dissimilis*	3	1.28	Poor, recrystallised foraminifera.
73	522		southern Angola Abyssal Plain	26°06.843'S	5°07.78'W	-34.34	Oberhansli et al., 1984		*Catapsydrax dissimilis*	*Catapsydrax dissimilis*	3	1.05	Poor, recrystallised foraminifera.
73	522		southern Angola Abyssal Plain	26°06.843'S	5°07.78'W	-34.34	Oberhansli et al., 1984		*Catapsydrax dissimilis*	*Catapsydrax dissimilis*	3	1.16	Poor, recrystallised foraminifera.
73	522		southern Angola Abyssal Plain	26°06.843'S	5°07.78'W	-34.34	Oberhansli et al., 1984		*Catapsydrax dissimilis*	*Catapsydrax dissimilis*	3	0.87	Poor, recrystallised foraminifera.

73	522		southern Angola Abyssal Plain	26°06.843'S	5°07.78'W	-34.34	Oberhansli et al., 1984		*Catapsydrax dissimilis*	*Catapsydrax dissimilis*	3	1.15	Poor, recrystallised foraminifera.
73	522		southern Angola Abyssal Plain	26°06.843'S	5°07.78'W	-34.34	Oberhansli et al., 1984		*Catapsydrax dissimilis*	*Catapsydrax dissimilis*	3	0.87	Poor, recrystallised foraminifera.
73	522		southern Angola Abyssal Plain	26°06.843'S	5°07.78'W	-34.34	Oberhansli et al., 1984		*Catapsydrax dissimilis*	*Catapsydrax dissimilis*	3	1.04	Poor, recrystallised foraminifera.
73	522		southern Angola Abyssal Plain	26°06.843'S	5°07.78'W	-34.34	Oberhansli et al., 1984		*Catapsydrax dissimilis*	*Catapsydrax dissimilis*	3	1.06	Poor, recrystallised foraminifera.
73	522		southern Angola Abyssal Plain	26°06.843'S	5°07.78'W	-34.34	Oberhansli et al., 1984		*Catapsydrax dissimilis*	*Catapsydrax dissimilis*	3	1.14	Poor, recrystallised foraminifera.
73	522		southern Angola Abyssal Plain	26°06.843'S	5°07.78'W	-34.34	Oberhansli et al., 1984		*Catapsydrax dissimilis*	*Catapsydrax dissimilis*	3	1.11	Poor, recrystallised foraminifera.
73	522		southern Angola Abyssal Plain	26°06.843'S	5°07.78'W	-34.34	Oberhansli et al., 1984		*Catapsydrax dissimilis*	*Catapsydrax dissimilis*	3	1.06	Poor, recrystallised foraminifera.
73	522		southern Angola Abyssal Plain	26°06.843'S	5°07.78'W	-34.34	Oberhansli et al., 1984		*Catapsydrax dissimilis*	*Catapsydrax dissimilis*	3	1.11	Poor, recrystallised foraminifera.
73	522		southern Angola Abyssal Plain	26°06.843'S	5°07.78'W	-34.34	Oberhansli et al., 1984		*Catapsydrax dissimilis*	*Catapsydrax dissimilis*	3	1.13	Poor, recrystallised foraminifera.

73	522		southern Angola Abyssal Plain	26°06.843'S	5°07.78'W	-34.34	Oberhansli et al., 1984		*Catapsydrax dissimilis*	*Catapsydrax dissimilis*	3	0.93	Poor, recrystallised foraminifera.
73	522		southern Angola Abyssal Plain	26°06.843'S	5°07.78'W	-34.34	Oberhansli et al., 1984		*Catapsydrax dissimilis*	*Catapsydrax dissimilis*	3	1	Poor, recrystallised foraminifera.
73	522		southern Angola Abyssal Plain	26°06.843'S	5°07.78'W	-34.34	Oberhansli et al., 1984		*Catapsydrax dissimilis*	*Catapsydrax dissimilis*	3	0.94	Poor, recrystallised foraminifera.
73	522		southern Angola Abyssal Plain	26°06.843'S	5°07.78'W	-34.34	Oberhansli et al., 1984		*Catapsydrax dissimilis*	*Catapsydrax dissimilis*	3	0.94	Poor, recrystallised foraminifera.
73	522		southern Angola Abyssal Plain	26°06.843'S	5°07.78'W	-34.34	Oberhansli et al., 1984		*Catapsydrax dissimilis*	*Catapsydrax dissimilis*	3	1.03	Poor, recrystallised foraminifera.
73	522		southern Angola Abyssal Plain	26°06.843'S	5°07.78'W	-34.34	Oberhansli et al., 1984		*Catapsydrax dissimilis*	*Catapsydrax dissimilis*	3	0.9	Poor, recrystallised foraminifera.
73	522		southern Angola Abyssal Plain	26°06.843'S	5°07.78'W	-34.34	Oberhansli et al., 1984		*Catapsydrax dissimilis*	*Catapsydrax dissimilis*	3	1.42	Poor, recrystallised foraminifera.
73	522		southern Angola Abyssal Plain	26°06.843'S	5°07.78'W	-34.34	Oberhansli et al., 1984		*Catapsydrax dissimilis*	*Catapsydrax dissimilis*	3	1.05	Poor, recrystallised foraminifera.

			Location	Lat	Long	Age	Reference		Original	Revised		δ	Preservation
	548A		Near the seaward edge of a tilted block of Hercynian basement at the shallowest site on the Goban Spur transect	48°54.95' N	12°09.84' W	41.47	Boersma et al. 1987		*Turborotalia cerroazulensis*	*Turborotalia cerroazulensis*	2	-0.42	Poor, recrystallised foraminifera.
10	95		Northeasterly facing Campeche Scarp face	24°09.00' N	86°23.85' W	20.02	Boersma et al. 1987		*Globigerina* spp.	*Globigerina* spp.	2	0.33	Poor, recrystallised foraminifera.
10	95		Northeasterly facing Campeche Scarp face	24°09.00' N	86°23.85' W	20.02	Boersma et al. 1987		*Turborotalia/globorotalia centrali*	*Turborotalia cerroazulensis*	2	-0.84	Poor, recrystallised foraminifera.
74	528		Down the western slope of a NNW-SSE-trending block in the Walvis Ridge.	28°31.49' S	02°19.44' E	-36.9	Boersma et al. 1987		*Globigerinatheka sp*	*Globigerinatheka* spp.	2	0.42	Poor, recrystallised foraminifera.
	V29						Boersma et al. 1987		juvenile *Globorotalia kugleri*	*Paragloborotalia?*	2	-0.06	Poor, recrystallised foraminifera.
	V29						Boersma et al. 1987		globigerinids	*Globigerina* spp.		-0.05	Poor, recrystallised foraminifera.
	V29						Boersma et al. 1987		*Hantkenina alabamensis*	*Hantkenina alabamensis*	2	0.18	Poor, recrystallised foraminifera.

				Lat	Long	Temp	Reference		Species A	Species B			Preservation
	V29						Boersma et al. 1987		*Turborotalia cerroazulensis*	*Turborotalia cerroazulensis*	2	0.23	Poor, recrystallised foraminifera.
39	359		Walvis Ridge (Seamount)	34°59.10'S	04°29.83'W	-43.23	Boersma et al. 1987		*Hantkenina alabamensis*	*Hantkenina alabamensis*	2	-0.4	Poor, recrystallised foraminifera.
39	357		eastern flank of the Rio Grande Rise, South Atlantic	3O°00.25'S	35°33.59'W	-36.74	Boersma et al. 1987		*Turborotalia cerroazulensis*	*Turborotalia cerroazulensis*	2	-0.48	Poor, recrystallised foraminifera.
39	357		eastern flank of the Rio Grande Rise, South Atlantic	3O°00.25'S	35°33.59'W	-36.74	Boersma et al. 1987		*Streptochilus cubensis*	*Chiloguembelina cubensis*	1	0.08	Poor, recrystallised foraminifera.
39	357		eastern flank of the Rio Grande Rise, South Atlantic	3O°00.25'S	35°33.59'W	-36.74	Boersma et al. 1987		*Globigerapsis index*	*Globigerinatheka index*	2	0.22	Poor, recrystallised foraminifera.
39	357		eastern flank of the Rio Grande Rise, South Atlantic	3O°00.25'S	35°33.59'W	-36.74	Boersma et al. 1987		*Globigerapsis index*	*Globigerinatheka index*	2	0.08	Poor, recrystallised foraminifera.
	v27		In the southern Atlantic Cape Basin				Boersma et al. 1987		*Turborotalia cerroazulensis*	*Turborotalia cerroazulensis*	2	-0.47	Poor, recrystallised foraminifera.
22	214		Crest of Ninetyeast Ridge	11°20.21'S	88°43.08'E	-24.6	Boersma et al. 1987		*Globigerina* spp.	*Globigerina* spp.	2	0.46	Poor, recrystallised foraminifera.

74	526		Walvis Ridge	30°07.36'S	03°08.28'E	-38.51	Boersma et al. 1987		*Globogerinoides index*	*Globigerinatheka index*	2	0.15	Poor, recrystallised foraminifera.
74	526		Walvis Ridge	30°07.36'S	03°08.28'E	-38.51	Boersma et al. 1987		*Catapsydrax* spp.	*Catapsydrax* spp.	3	0.56	Poor, recrystallised foraminifera.
74	526		Walvis Ridge	30°07.36'S	03°08.28'E	-38.51	Boersma et al. 1987		*Globogerinoides index*	*Globigerinatheka index*	2	0.25	Poor, recrystallised foraminifera.
74	526		Walvis Ridge	30°07.36'S	03°08.28'E	-38.51	Boersma et al. 1987		*Catapsydrax* spp.	*Catapsydrax* spp.	3	0.2	Poor, recrystallised foraminifera.
74	526		Walvis Ridge	30°07.36'S	03°08.28'E	-38.51	Boersma et al. 1987		*Turborotalia cerroazulensis*	*Turborotalia cerroazulensis*	2	0.4	Poor, recrystallised foraminifera.
3	20C		Mid-Atlantic Ridge, western flank.	28°31.57'S	26°50.58'W	-34.58	Boersma et al. 1987		*Globogerinoides index*	*Globigerinatheka index*	2	-0.14	Poor, recrystallised foraminifera.
74	528		Down the western slope of a NNW-SSE-trending block in the Walvis Ridge.	28°31.49'S	02°19.44'E	-36.9	Boersma et al. 1987		*Globigerinatheka* spp.	*Globigerinatheka* spp.	2	0.02	Poor, recrystallised foraminifera.
74	529		Down the western slope of a NNW-SSE-trending block in the Walvis Ridge.	28°55.83'S	02°46.08'E	-37.31	Boersma et al. 1987		*Globigerapsis mexicana*	*Globigerinatheka mexicana*	2	0.41	Poor, recrystallised foraminifera.

74	529		Down the western slope of a NNW-SSE-trending block in the Walvis Ridge.	28°55.83'S	02°46.08'E	-37.31	Boersma et al. 1987		*Globigerinoides subconglobatus*	*Globigerinatheka subconglobata*	2	0.47	Poor, recrystallised foraminifera.
74	529		Down the western slope of a NNW-SSE-trending block in the Walvis Ridge.	28°55.83'S	02°46.08'E	-37.31	Boersma et al. 1987		*Turborotalia cerroazulensis*	*Turborotalia cerroazulensis*	2	0.47	Poor, recrystallised foraminifera.
74	529		Down the western slope of a NNW-SSE-trending block in the Walvis Ridge.	28°55.83'S	02°46.08'E	-37.31	Boersma et al. 1987		*G. winkleri*	*Subbotina corpulenta*	3	0.66	Poor, recrystallised foraminifera.
74	529		Down the western slope of a NNW-SSE-trending block in the Walvis Ridge.	28°55.83'S	02°46.08'E	-37.31	Boersma et al. 1987		*Turborotalia increbescens*	*Turborotalia increbescens*	2	0.38	Poor, recrystallised foraminifera.
74	529		Down the western slope of a NNW-SSE-trending block in the Walvis Ridge.	28°55.83'S	02°46.08'E	-37.31	Boersma et al. 1987		*Turborotalia cerroazulensis*	*Turborotalia cerroazulensis*	2	0.47	Poor, recrystallised foraminifera.

74	529		Down the western slope of a NNW-SSE-trending block in the Walvis Ridge.	28°55.83'S	02°46.08'E	-37.31	Boersma et al. 1987		*G. index*	*Globigerinatheka index*	2	0.53	Poor, recrystallised foraminifera.
74	529		Down the western slope of a NNW-SSE-trending block in the Walvis Ridge.	28°55.83'S	02°46.08'E	-37.31	Boersma et al. 1987		*Catapsydrax* spp.	*Catapsydrax* spp.	3	0.53	Poor, recrystallised foraminifera.
74	529		Down the western slope of a NNW-SSE-trending block in the Walvis Ridge.	28°55.83'S	02°46.08'E	-37.31	Boersma et al. 1987		*S. corpulenta*	*Subbotina corpulenta*	3	0.67	Poor, recrystallised foraminifera.
74	529		Down the western slope of a NNW-SSE-trending block in the Walvis Ridge.	28°55.83'S	02°46.08'E	-37.31	Boersma et al. 1987		*Turborotalia cerroazulensis*	*Turborotalia cerroazulensis*	2	0.58	Poor, recrystallised foraminifera.
74	529		Down the western slope of a NNW-SSE-trending block in the Walvis Ridge.	28°55.83'S	02°46.08'E	-37.31	Boersma et al. 1987		*Catapsydrax* spp.	*Catapsydrax* spp.	3	0.78	Poor, recrystallised foraminifera.

74	529		Down the western slope of a NNW-SSE-trending block in the Walvis Ridge.	28°55.83' S	02°46.08' E	-37.31	Boersma et al. 1987		*Turborotalia increbescens*	*Turborotalia increbescens*	2	0.55	Poor, recrystallised foraminifera.
74	529		Down the western slope of a NNW-SSE-trending block in the Walvis Ridge.	28°55.83' S	02°46.08' E	-37.31	Boersma et al. 1987		*G. winkleri*	*Subbotina corpulenta*	3	0.65	Poor, recrystallised foraminifera.
74	529		Down the western slope of a NNW-SSE-trending block in the Walvis Ridge.	28°55.83' S	02°46.08' E	-37.31	Boersma et al. 1987		*G. subconglobatus*	*Globigerinatheka subconglobata*	2	0.41	Poor, recrystallised foraminifera.
74	529		Down the western slope of a NNW-SSE-trending block in the Walvis Ridge.	28°55.83' S	02°46.08' E	-37.31	Boersma et al. 1987		*G. winkleri*	*Subbotina corpulenta*	3	0.58	Poor, recrystallised foraminifera.
10	94		Campeche Scarp, Yucatan Shelf, Gulf of Mexico	24°31.64' N	88°28.16' W	20.68	Boersma et al. 1987		*Turborotalia cerroazulensis*	*Turborotalia cerroazulensis*	2	-0.42	Poor, recrystallised foraminifera.
10	94		Campeche Scarp, Yucatan Shelf, Gulf of Mexico	24°31.64' N	88°28.16' W	20.68	Boersma et al. 1987		*Catapsydrax* spp.	*Catapsydrax* spp.	3	0.24	Poor, recrystallised foraminifera.

24	237		Mascarene Plateau, in a saddle between the Seychelles and Saya de Malha Bank	07°04.99' S	58°07.48' E	-12.14	Boersma et al. 1987		*Turborotalia cerroazulensis*	*Turborotalia cerroazulensis*	2	0.24	Poor, recrystallised foraminifera.
24	237		Mascarene Plateau, in a saddle between the Seychelles and Saya de Malha Bank	07°04.99' S	58°07.48' E	-12.14	Boersma et al. 1987		*Globigerina* spp.	*Globigerina* spp.	2	0.74	Poor, recrystallised foraminifera.
80	548A		Near the seaward edge of a tilted block of Hercynian basement at the shallowest site on the Goban Spur transect	48°54.95' N	12°09.84' W	41.47	Boersma et al. 1987		*Turborotalia cerroazulensis*	*Turborotalia cerroazulensis*	2	-0.06	Poor, recrystallised foraminifera.
80	548A		Near the seaward edge of a tilted block of Hercynian basement at the shallowest site on the Goban Spur transect	48°54.95' N	12°09.84' W	41.47	Boersma et al. 1987		*Turborotalia pseudoampliapertura*	*Turborotalia ampliapertura*	2	0.63	Poor, recrystallised foraminifera.

80	548A			Near the seaward edge of a tilted block of Hercynian basement at the shallowest site on the Goban Spur transect	48°54.95' N	12°09.84' W	41.47	Boersma et al. 1987		*Catapsydrax* spp.	*Catapsydrax* spp.	3	0.55	Poor, recrystallised foraminifera.
	v20							Boersma et al. 1987		*Catapsydrax*	*Catapsydrax* spp.	3	0.82	Poor, recrystallised foraminifera.
	v20							Boersma et al. 1987		*Turborotalia pseudoampliapertura*	*Turborotalia ampliapertura*	2	0.81	Poor, recrystallised foraminifera.
40	363			Isolated basement high on north-facing escarpment of Frio Ridge portion of Walvis Ridge	19°38.75' S	09°02.80' E	-28.03	Boersma et al. 1987		*heterohelicid*	*Chiloguembelina* spp.	1	-0.35	Poor, recrystallised foraminifera.
40	363			Isolated basement high on north-facing escarpment of Frio Ridge portion of Walvis Ridge	19°38.75' S	09°02.80' E	-28.03	Boersma et al. 1987		*Turborotalia cerroazulensis*	*Turborotalia cerroazulensis*	2	-0.28	Poor, recrystallised foraminifera.

40	363		Isolated basement high on north-facing escarpment of Frio Ridge portion of Walvis Ridge	19°38.75'S	09°02.80'E	-28.03	Boersma et al. 1987		*Turborotalia pseudoampliapertura*	*Turborotalia ampliapertura*	2	-0.51	Poor, recrystallised foraminifera.
40	363		Isolated basement high on north-facing escarpment of Frio Ridge portion of Walvis Ridge	19°38.75'S	09°02.80'E	-28.03	Boersma et al. 1987		*Turborotalia p seudoampliapertura*	*Turborotalia ampliapertura*	2	-0.28	Poor, recrystallised foraminifera.
	V27						Boersma et al. 1987		*Turborotalia cunialensis*	*Turborotalia cunialensis*	2	-0.47	Poor, recrystallised foraminifera.
	V27						Boersma et al. 1987		*G. mexicana*	*Globigerinatheka mexicana*	2	-0.2	Poor, recrystallised foraminifera.
	V27						Boersma et al. 1987		*Turborotalia cerroazulensis*	*Turborotalia cerroazulensis*	2	0.27	Poor, recrystallised foraminifera.
	V27						Boersma et al. 1987		*G. kugleri*	*Paragloborotalia?*	2	0.42	Poor, recrystallised foraminifera.
10	94		Campeche Scarp, Yucatan Shelf, Gulf of Mexico	24°31.64'N	88°28.16'W	20.67	Keigwin and Corliss, 1986		*P. micra*	*Pseudohastigerina micra*	1	-0.84	Poor, recrystallised foraminifera.

23	219		On the crest of the Laccadive-Chagos Ridge	9°01.75'N	72°52.67'E	-2.06	Keigwin and Corliss, 1986		*G. subglobosa*	*Subbotina* spp.	3	0.84	Poor, recrystallised foraminifera.
23	219		On the crest of the Laccadive-Chagos Ridge	9°01.75'N	72°52.67'E	-2.06	Keigwin and Corliss, 1986		*G. ampliapertura*	*Turborotalia ampliapertura*	2	-0.3	Poor, recrystallised foraminifera.
113	689b		Maud Rise, Weddel Sea, off the coast of East Antarctica	64°31'S	03°06'E	-68.06	Stott et al. 1990	33.9 Ma to 41.2 Ma	*Subbotina angiporoides*	*Subbotina angiporoides*	3	2.18	Poor, recrystallised foraminifera.
113	689b		Maud Rise, Weddel Sea, off the coast of East Antarctica	64°31'S	03°06'E	-68.06	Stott et al. 1990	33.9 Ma to 41.2 Ma	*Subbotina angiporoides*	*Subbotina angiporoides*	3	2.54	Poor, recrystallised foraminifera.
113	689b		Maud Rise, Weddel Sea, off the coast of East Antarctica	64°31'S	03°06'E	-68.06	Stott et al. 1990	33.9 Ma to 41.2 Ma	*Subbotina angiporoides*	*Subbotina angiporoides*	3	2.22	Poor, recrystallised foraminifera.
113	689b		Maud Rise, Weddel Sea, off the coast of East Antarctica	64°31'S	03°06'E	-68.06	Stott et al. 1990	33.9 Ma to 41.2 Ma	*Subbotina angiporoides*	*Subbotina angiporoides*	3	2.28	Poor, recrystallised foraminifera.
113	689b		Maud Rise, Weddel Sea, off the coast of East Antarctica	64°31'S	03°06'E	-68.06	Stott et al. 1990	33.9 Ma to 41.2 Ma	*Subbotina angiporoides*	*Subbotina angiporoides*	3	2.53	Poor, recrystallised foraminifera.

113	689b		Maud Rise, Weddel Sea, off the coast of East Antarctica	64°31'S	03°06'E	-68.06	Stott et al. 1990	33.9 Ma to 41.2 Ma	*Subbotina angiporoides*	*Subbotina angiporoides*	3	2.47	Poor, recrystallised foraminifera.
113	689b		Maud Rise, Weddel Sea, off the coast of East Antarctica	64°31'S	03°06'E	-68.06	Stott et al. 1990	33.9 Ma to 41.2 Ma	*Subbotina angiporoides*	*Subbotina angiporoides*	3	2.45	Poor, recrystallised foraminifera.
113	689b		Maud Rise, Weddel Sea, off the coast of East Antarctica	64°31'S	03°06'E	-68.06	Stott et al. 1990	33.9 Ma to 41.2 Ma	*Subbotina angiporoides*	*Subbotina angiporoides*	3	2.59	Poor, recrystallised foraminifera.
113	689b		Maud Rise, Weddel Sea, off the coast of East Antarctica	64°31'S	03°06'E	-68.06	Stott et al. 1990	33.9 Ma to 41.2 Ma	*Subbotina angiporoides*	*Subbotina angiporoides*	3	2.37	Poor, recrystallised foraminifera.
113	689b		Maud Rise, Weddel Sea, off the coast of East Antarctica	64°31'S	03°06'E	-68.06	Stott et al. 1990	33.9 Ma to 41.2 Ma	*Subbotina angiporoides*	*Subbotina angiporoides*	3	2.67	Poor, recrystallised foraminifera.
113	689b		Maud Rise, Weddel Sea, off the coast of East Antarctica	64°31'S	03°06'E	-68.06	Stott et al. 1990	33.9 Ma to 41.2 Ma	*Subbotina angiporoides*	*Subbotina angiporoides*	3	2.67	Poor, recrystallised foraminifera.
113	689b		Maud Rise, Weddel Sea, off the coast	64°31'S	03°06'E	-68.06	Stott et al. 1990	33.9 Ma to 41.2 Ma	*Subbotina angiporoides*	*Subbotina angiporoides*	3	2.68	Poor, recrystallised foraminifera.

			of East Antarctica										
113	689b		Maud Rise, Weddel Sea, off the coast of East Antarctica	64°31'S	03°06'E	-68.06	Stott et al. 1990	33.9 Ma to 41.2 Ma	*Subbotina angiporoides*	*Subbotina angiporoides*	3	2.56	Poor, recrystallised foraminifera.
113	689b		Maud Rise, Weddel Sea, off the coast of East Antarctica	64°31'S	03°06'E	-68.06	Stott et al. 1990	33.9 Ma to 41.2 Ma	*Subbotina angiporoides*	*Subbotina angiporoides*	3	1.94	Poor, recrystallised foraminifera.
113	689b		Maud Rise, Weddel Sea, off the coast of East Antarctica	64°31'S	03°06'E	-68.06	Stott et al. 1990	33.9 Ma to 41.2 Ma	*Subbotina angiporoides*	*Subbotina angiporoides*	3	0.28	Poor, recrystallised foraminifera.
113	689b		Maud Rise, Weddel Sea, off the coast of East Antarctica	64°31'S	03°06'E	-68.06	Stott et al. 1990	33.9 Ma to 41.2 Ma	*Subbotina angiporoides*	*Subbotina angiporoides*	3	1.68	Poor, recrystallised foraminifera.
113	689b		Maud Rise, Weddel Sea, off the coast of East Antarctica	64°31'S	03°06'E	-68.06	Stott et al. 1990	33.9 Ma to 41.2 Ma	*Subbotina angiporoides*	*Subbotina angiporoides*	3	0.52	Poor, recrystallised foraminifera.
113	689b		Maud Rise, Weddel Sea, off the coast of East Antarctica	64°31'S	03°06'E	-68.06	Stott et al. 1990	33.9 Ma to 41.2 Ma	*Subbotina angiporoides*	*Subbotina angiporoides*	3	1.64	Poor, recrystallised foraminifera.

113	689b		Maud Rise, Weddel Sea, off the coast of East Antarctica	64°31'S	03°06'E	-68.06	Stott et al. 1990	33.9 Ma to 41.2 Ma	*Subbotina angiporoides*	*Subbotina angiporoides*	3	1.71	Poor, recrystallised foraminifera.
113	689b		Maud Rise, Weddel Sea, off the coast of East Antarctica	64°31'S	03°06'E	-68.06	Stott et al. 1990	33.9 Ma to 41.2 Ma	*Subbotina angiporoides*	*Subbotina angiporoides*	3	1.73	Poor, recrystallised foraminifera.
113	689b		Maud Rise, Weddel Sea, off the coast of East Antarctica	64°31'S	03°06'E	-68.06	Stott et al. 1990	33.9 Ma to 41.2 Ma	*Subbotina angiporoides*	*Subbotina angiporoides*	3	1.84	Poor, recrystallised foraminifera.
113	689b		Maud Rise, Weddel Sea, off the coast of East Antarctica	64°31'S	03°06'E	-68.06	Stott et al. 1990	33.9 Ma to 41.2 Ma	*Subbotina angiporoides*	*Subbotina angiporoides*	3	1.3	Poor, recrystallised foraminifera.
113	689b		Maud Rise, Weddel Sea, off the coast of East Antarctica	64°31'S	03°06'E	-68.06	Stott et al. 1990	33.9 Ma to 41.2 Ma	*Subbotina angiporoides*	*Subbotina angiporoides*	3	1.4	Poor, recrystallised foraminifera.
113	689b		Maud Rise, Weddel Sea, off the coast of East Antarctica	64°31'S	03°06'E	-68.06	Stott et al. 1990	33.9 Ma to 41.2 Ma	*Subbotina angiporoides*	*Subbotina angiporoides*	3	1.53	Poor, recrystallised foraminifera.
113	689b		Maud Rise, Weddel Sea, off the coast	64°31'S	03°06'E	-68.06	Stott et al. 1990	33.9 Ma to 41.2 Ma	*Subbotina angiporoides*	*Subbotina angiporoides*	3	1.3	Poor, recrystallised foraminifera.

			of East Antarctica										
113	689b		Maud Rise, Weddel Sea, off the coast of East Antarctica	64°31'S	03°06'E	-68.06	Stott et al. 1990	33.9 Ma to 41.2 Ma	*Subbotina angiporoides*	*Subbotina angiporoides*	3	1.58	Poor, recrystallised foraminifera.
113	689b		Maud Rise, Weddel Sea, off the coast of East Antarctica	64°31'S	03°06'E	-68.06	Stott et al. 1990	33.9 Ma to 41.2 Ma	*Subbotina angiporoides*	*Subbotina angiporoides*	3	1.41	Poor, recrystallised foraminifera.
113	689b		Maud Rise, Weddel Sea, off the coast of East Antarctica	64°31'S	03°06'E	-68.06	Stott et al. 1990	33.9 Ma to 41.2 Ma	*Subbotina angiporoides*	*Subbotina angiporoides*	3	1.57	Poor, recrystallised foraminifera.
113	689b		Maud Rise, Weddel Sea, off the coast of East Antarctica	64°31'S	03°06'E	-68.06	Stott et al. 1990	33.9 Ma to 41.2 Ma	*Subbotina angiporoides*	*Subbotina angiporoides*	3	0.39	Poor, recrystallised foraminifera.
113	689b		Maud Rise, Weddel Sea, off the coast of East Antarctica	64°31'S	03°06'E	-68.06	Stott et al. 1990	33.9 Ma to 41.2 Ma	*Subbotina angiporoides*	*Subbotina angiporoides*	3	1.47	Poor, recrystallised foraminifera.
113	689b		Maud Rise, Weddel Sea, off the coast of East Antarctica	64°31'S	03°06'E	-68.06	Stott et al. 1990	33.9 Ma to 41.2 Ma	*Subbotina angiporoides*	*Subbotina angiporoides*	3	1.63	Poor, recrystallised foraminifera.

113	689b		Maud Rise, Weddel Sea, off the coast of East Antarctica	64°31'S	03°06'E	-68.06	Stott et al. 1990	33.9 Ma to 41.2 Ma	*Subbotina angiporoides*	*Subbotina angiporoides*	3	1.56	Poor, recrystallised foraminifera.
113	689b		Maud Rise, Weddel Sea, off the coast of East Antarctica	64°31'S	03°06'E	-68.06	Stott et al. 1990	33.9 Ma to 41.2 Ma	*Subbotina angiporoides*	*Subbotina angiporoides*	3	1.57	Poor, recrystallised foraminifera.
113	689b		Maud Rise, Weddel Sea, off the coast of East Antarctica	64°31'S	03°06'E	-68.06	Stott et al. 1990	33.9 Ma to 41.2 Ma	*Subbotina angiporoides*	*Subbotina angiporoides*	3	1.43	Poor, recrystallised foraminifera.
113	689b		Maud Rise, Weddel Sea, off the coast of East Antarctica	64°31'S	03°06'E	-68.06	Stott et al. 1990	33.9 Ma to 41.2 Ma	*Subbotina angiporoides*	*Subbotina angiporoides*	3	1.48	Poor, recrystallised foraminifera.
113	689b		Maud Rise, Weddel Sea, off the coast of East Antarctica	64°31'S	03°06'E	-68.06	Stott et al. 1990	33.9 Ma to 41.2 Ma	*Subbotina angiporoides*	*Subbotina angiporoides*	3	1.61	Poor, recrystallised foraminifera.
113	689b		Maud Rise, Weddel Sea, off the coast of East Antarctica	64°31'S	03°06'E	-68.06	Stott et al. 1990	33.9 Ma to 41.2 Ma	*Subbotina angiporoides*	*Subbotina angiporoides*	3	1.63	Poor, recrystallised foraminifera.
113	689b		Maud Rise, Weddel Sea, off the coast	64°31'S	03°06'E	-68.06	Stott et al. 1990	33.9 Ma to 41.2 Ma	*Subbotina angiporoides*	*Subbotina angiporoides*	3	1.53	Poor, recrystallised foraminifera.

			of East Antarctica										
113	689b		Maud Rise, Weddel Sea, off the coast of East Antarctica	64°31'S	03°06'E	-68.06	Stott et al. 1990	33.9 Ma to 41.2 Ma	*Subbotina angiporoides*	*Subbotina angiporoides*	3	1.44	Poor, recrystallised foraminifera.
113	689b		Maud Rise, Weddel Sea, off the coast of East Antarctica	64°31'S	03°06'E	-68.06	Stott et al. 1990	33.9 Ma to 41.2 Ma	*Subbotina angiporoides*	*Subbotina angiporoides*	3	1.53	Poor, recrystallised foraminifera.
113	689b		Maud Rise, Weddel Sea, off the coast of East Antarctica	64°31'S	03°06'E	-68.06	Stott et al. 1990	33.9 Ma to 41.2 Ma	*Subbotina eocaena*	*Subbotina eocaena*	3	1.97	Poor, recrystallised foraminifera.
113	689b		Maud Rise, Weddel Sea, off the coast of East Antarctica	64°31'S	03°06'E	-68.06	Stott et al. 1990	33.9 Ma to 41.2 Ma	*Subbotina eocaena*	*Subbotina eocaena*	3	1.94	Poor, recrystallised foraminifera.
113	689b		Maud Rise, Weddel Sea, off the coast of East Antarctica	64°31'S	03°06'E	-68.06	Stott et al. 1990	33.9 Ma to 41.2 Ma	*Subbotina eocaena*	*Subbotina eocaena*	3	1.47	Poor, recrystallised foraminifera.
113	689b		Maud Rise, Weddel Sea, off the coast of East Antarctica	64°31'S	03°06'E	-68.06	Stott et al. 1990	33.9 Ma to 41.2 Ma	*Subbotina eocaena*	*Subbotina eocaena*	3	1.7	Poor, recrystallised foraminifera.

113	689b		Maud Rise, Weddel Sea, off the coast of East Antarctica	64°31'S	03°06'E	-68.06	Stott et al. 1990	33.9 Ma to 41.2 Ma	Subbotina eocaena	Subbotina eocaena	3	1.64	Poor, recrystallised foraminifera.
113	689b		Maud Rise, Weddel Sea, off the coast of East Antarctica	64°31'S	03°06'E	-68.06	Stott et al. 1990	33.9 Ma to 41.2 Ma	Subbotina eocaena	Subbotina eocaena	3	0.82	Poor, recrystallised foraminifera.
113	689b		Maud Rise, Weddel Sea, off the coast of East Antarctica	64°31'S	03°06'E	-68.06	Stott et al. 1990	33.9 Ma to 41.2 Ma	Subbotina eocaena	Subbotina eocaena	3	0.83	Poor, recrystallised foraminifera.
113	689b		Maud Rise, Weddel Sea, off the coast of East Antarctica	64°31'S	03°06'E	-68.06	Stott et al. 1990	33.9 Ma to 41.2 Ma	Subbotina eocaena	Subbotina eocaena	3	1.21	Poor, recrystallised foraminifera.
113	689b		Maud Rise, Weddel Sea, off the coast of East Antarctica	64°31'S	03°06'E	-68.06	Stott et al. 1990	33.9 Ma to 41.2 Ma	Subbotina eocaena	Subbotina eocaena	3	1.39	Poor, recrystallised foraminifera.
113	689b		Maud Rise, Weddel Sea, off the coast of East Antarctica	64°31'S	03°06'E	-68.06	Stott et al. 1990	33.9 Ma to 41.2 Ma	Subbotina eocaena	Subbotina eocaena	3	1.2	Poor, recrystallised foraminifera.
113	689b		Maud Rise, Weddel Sea, off the coast	64°31'S	03°06'E	-68.06	Stott et al. 1990	33.9 Ma to 41.2 Ma	Subbotina eocaena	Subbotina eocaena	3	1.27	Poor, recrystallised foraminifera.

			of East Antarctica										
113	689b		Maud Rise, Weddel Sea, off the coast of East Antarctica	64°31'S	03°06'E	-68.06	Stott et al. 1990	33.9 Ma to 41.2 Ma	*Subbotina eocaena*	*Subbotina eocaena*	3	1.3	Poor, recrystallised foraminifera.
113	689b		Maud Rise, Weddel Sea, off the coast of East Antarctica	64°31'S	03°06'E	-68.06	Stott et al. 1990	33.9 Ma to 41.2 Ma	*Subbotina eocaena*	*Subbotina eocaena*	3	1.22	Poor, recrystallised foraminifera.
113	689b		Maud Rise, Weddel Sea, off the coast of East Antarctica	64°31'S	03°06'E	-68.06	Stott et al. 1990	33.9 Ma to 41.2 Ma	*Subbotina eocaena*	*Subbotina eocaena*	3	1.41	Poor, recrystallised foraminifera.
113	689b		Maud Rise, Weddel Sea, off the coast of East Antarctica	64°31'S	03°06'E	-68.06	Stott et al. 1990	33.9 Ma to 41.2 Ma	*Subbotina eocaena*	*Subbotina eocaena*	3	1.39	Poor, recrystallised foraminifera.
113	689b		Maud Rise, Weddel Sea, off the coast of East Antarctica	64°31'S	03°06'E	-68.06	Stott et al. 1990	33.9 Ma to 41.2 Ma	*Subbotina eocaena*	*Subbotina eocaena*	3	1.24	Poor, recrystallised foraminifera.
113	689b		Maud Rise, Weddel Sea, off the coast of East Antarctica	64°31'S	03°06'E	-68.06	Stott et al. 1990	33.9 Ma to 41.2 Ma	*Subbotina* spp.	*Subbotina* spp.	3	1.02	Poor, recrystallised foraminifera.

113	689b		Maud Rise, Weddel Sea, off the coast of East Antarctica	64°31'S	03°06'E	-68.06	Stott et al. 1990	33.9 Ma to 41.2 Ma	*Subbotina* spp.	*Subbotina* spp.	3	1.1	Poor, recrystallised foraminifera.
113	689b		Maud Rise, Weddel Sea, off the coast of East Antarctica	64°31'S	03°06'E	-68.06	Stott et al. 1990	33.9 Ma to 41.2 Ma	*Acarinina appressocamerata*	*Acarinina collactea*	1	-1.16	Poor, recrystallised foraminifera.
113	689b		Maud Rise, Weddel Sea, off the coast of East Antarctica	64°31'S	03°06'E	-68.06	Stott et al. 1990	33.9 Ma to 41.2 Ma	*Acarinina appressocamerata*	*Acarinina collactea*	1	-1.46	Poor, recrystallised foraminifera.
113	689b		Maud Rise, Weddel Sea, off the coast of East Antarctica	64°31'S	03°06'E	-68.06	Stott et al. 1990	33.9 Ma to 41.2 Ma	*Acarinina appressocamerata*	*Acarinina collactea*	1	-0.91	Poor, recrystallised foraminifera.
113	689b		Maud Rise, Weddel Sea, off the coast of East Antarctica	64°31'S	03°06'E	-68.06	Stott et al. 1990	33.9 Ma to 41.2 Ma	*Acarinina appressocamerata*	*Acarinina collactea*	1	-0.8	Poor, recrystallised foraminifera.
113	689b		Maud Rise, Weddel Sea, off the coast of East Antarctica	64°31'S	03°06'E	-68.06	Stott et al. 1990	33.9 Ma to 41.2 Ma	*Acarinina appressocamerata*	*Acarinina collactea*	1	-0.95	Poor, recrystallised foraminifera.
113	689b		Maud Rise, Weddel Sea, off the coast	64°31'S	03°06'E	-68.06	Stott et al. 1990	33.9 Ma to 41.2 Ma	*Acarinina appressocamerata*	*Acarinina collactea*	1	-1	Poor, recrystallised foraminifera.

113	690C		of East Antarctica									
113	690C		Maud Rise, Weddel Sea, off the coast of East Antarctica	65°10'S	01°12'E	-68.85	Stott et al. 1990	33.9 Ma to 41.2 Ma	*Subbotina angiporoides*	*Subbotina angiporoides*	3	1.75	Poor, recrystallised foraminifera.
113	690C		Maud Rise, Weddel Sea, off the coast of East Antarctica	65°10'S	01°12'E	-68.85	Stott et al. 1990	33.9 Ma to 41.2 Ma	*Subbotina angiporoides*	*Subbotina angiporoides*	3	1.14	Poor, recrystallised foraminifera.
113	690C		Maud Rise, Weddel Sea, off the coast of East Antarctica	65°10'S	01°12'E	-68.85	Stott et al. 1990	33.9 Ma to 41.2 Ma	*Subbotina angiporoides*	*Subbotina angiporoides*	3	1.56	Poor, recrystallised foraminifera.
113	690C		Maud Rise, Weddel Sea, off the coast of East Antarctica	65°10'S	01°12'E	-68.85	Stott et al. 1990	33.9 Ma to 41.2 Ma	*Subbotina angiporoides*	*Subbotina angiporoides*	3	1.68	Poor, recrystallised foraminifera.
113	690C		Maud Rise, Weddel Sea, off the coast of East Antarctica	65°10'S	01°12'E	-68.85	Stott et al. 1990	33.9 Ma to 41.2 Ma	*Subbotina angiporoides*	*Subbotina angiporoides*	3	1.46	Poor, recrystallised foraminifera.
113	690C		Maud Rise, Weddel Sea, off the coast of East Antarctica	65°10'S	01°12'E	-68.85	Stott et al. 1990	33.9 Ma to 41.2 Ma	*Subbotina angiporoides*	*Subbotina angiporoides*	3	1.57	Poor, recrystallised foraminifera.

113	690C		Maud Rise, Weddel Sea, off the coast of East Antarctica	65°10'S	01°12'E	-68.85	Stott et al. 1990	33.9 Ma to 41.2 Ma	*Subbotina angiporoides*	*Subbotina angiporoides*	3	1.42	Poor, recrystallised foraminifera.
113	690C		Maud Rise, Weddel Sea, off the coast of East Antarctica	65°10'S	01°12'E	-68.85	Stott et al. 1990	33.9 Ma to 41.2 Ma	*Subbotina angiporoides*	*Subbotina angiporoides*	3	1.15	Poor, recrystallised foraminifera.
113	690C		Maud Rise, Weddel Sea, off the coast of East Antarctica	65°10'S	01°12'E	-68.85	Stott et al. 1990	33.9 Ma to 41.2 Ma	*Subbotina angiporoides*	*Subbotina angiporoides*	3	1.48	Poor, recrystallised foraminifera.
113	690C		Maud Rise, Weddel Sea, off the coast of East Antarctica	65°10'S	01°12'E	-68.85	Stott et al. 1990	33.9 Ma to 41.2 Ma	*Subbotina angiporoides*	*Subbotina angiporoides*	3	1.63	Poor, recrystallised foraminifera.
113	690C		Maud Rise, Weddel Sea, off the coast of East Antarctica	65°10'S	01°12'E	-68.85	Stott et al. 1990	33.9 Ma to 41.2 Ma	*Subbotina angiporoides*	*Subbotina angiporoides*	3	1.54	Poor, recrystallised foraminifera.
113	690C		Maud Rise, Weddel Sea, off the coast of East Antarctica	65°10'S	01°12'E	-68.85	Stott et al. 1990	33.9 Ma to 41.2 Ma	*Subbotina angiporoides*	*Subbotina angiporoides*	3	1.77	Poor, recrystallised foraminifera.
113	690C		Maud Rise, Weddel Sea, off the coast	65°10'S	01°12'E	-68.85	Stott et al. 1990	33.9 Ma to 41.2 Ma	*Subbotina angiporoides*	*Subbotina angiporoides*	3	1.59	Poor, recrystallised foraminifera.

			of East Antarctica										
113	690C		Maud Rise, Weddel Sea, off the coast of East Antarctica	65°10'S	01°12'E	-68.85	Stott et al. 1990	33.9 Ma to 41.2 Ma	*Subbotina angiporoides*	*Subbotina angiporoides*	3	1.53	Poor, recrystallised foraminifera.
113	690C		Maud Rise, Weddel Sea, off the coast of East Antarctica	65°10'S	01°12'E	-68.85	Stott et al. 1990	33.9 Ma to 41.2 Ma	*Subbotina eocaena*	*Subbotina eocaena*	3	1.57	Poor, recrystallised foraminifera.
22	214		Crest of Ninetyeast Ridge	11°20.21' S	88°43.08' E	-24.59	Not found, anyway it's 18 S so very close to 253 and at the same longitude which is 30 S.						Poor, recrystallised foraminifera.
26	253	NP19, NP20	Southern end of the Ninetyeast Ridge	24°52.65' S	87°21.97' E	-37.26	Oberhansli, 1986		*Globigerina eocaena*	*Subbotina eocaena*	3	1.09	Poor, recrystallised foraminifera.
26	253	NP19, NP20	Southern end of the Ninetyeast Ridge	24°52.65' S	87°21.97' E	-37.26	Oberhansli, 1986		*Globigerina eocaena*	*Subbotina eocaena*	3	0.84	Poor, recrystallised foraminifera.
26	253	NP19, NP20	Southern end of the Ninetyeast Ridge	24°52.65' S	87°21.97' E	-37.26	Oberhansli, 1986		*Globigerina eocaena*	*Subbotina eocaena*	3	0.69	Poor, recrystallised foraminifera.
26	253	NP19, NP20	Southern end of the Ninetyeast Ridge	24°52.65' S	87°21.97' E	-37.26	Oberhansli, 1986		*Globigerina eocaena*	*Subbotina eocaena*	3	0.43	Poor, recrystallised foraminifera.

26	253	NP19, NP20	Southern end of the Ninetyeast Ridge	24°52.65' S	87°21.97' E	-37.26	Oberhansli, 1986		*Globigertnatheka* spp.	*Globigerinatheka* spp.	2	0.29	Poor, recrystallised foraminifera.
26	253	NP19, NP20	Southern end of the Ninetyeast Ridge	24°52.65' S	87°21.97' E	-37.26	Oberhansli, 1986		*Globigerina eocaena*	*Subbotina eocaena*	3	0.49	Poor, recrystallised foraminifera.
26	253	NP19, NP20	Southern end of the Ninetyeast Ridge	24°52.65' S	87°21.97' E	-37.26	Oberhansli, 1986		*Globigertnatheka* spp.	*Globigerinatheka* spp.	2	0.33	Poor, recrystallised foraminifera.
26	253	NP19, NP20	Southern end of the Ninetyeast Ridge	24°52.65' S	87°21.97' E	-37.26	Oberhansli, 1986		*Globigerina eocaena*	*Subbotina eocaena*	3	0.51	Poor, recrystallised foraminifera.
26	253	NP19, NP20	Southern end of the Ninetyeast Ridge	24°52.65' S	87°21.97' E	-37.26	Oberhansli, 1986		*Globigerina eocaena*	*Subbotina eocaena*	3	0.45	Poor, recrystallised foraminifera.
26	253	NP19, NP20	Southern end of the Ninetyeast Ridge	24°52.65' S	87°21.97' E	-37.26	Oberhansli, 1986		*Globigerina eocaena*	*Subbotina eocaena*	3	0.04	Poor, recrystallised foraminifera.
26	253	NP19, NP20	Southern end of the Ninetyeast Ridge	24°52.65' S	87°21.97' E	-37.26	Oberhansli, 1986		*Globigerina eocaena*	*Subbotina eocaena*	3	0.72	Poor, recrystallised foraminifera.
26	253	NP19, NP20	Southern end of the Ninetyeast Ridge	24°52.65' S	87°21.97' E	-37.26	Oberhansli, 1986		*Globigerina eocaena*	*Subbotina eocaena*	3	0.54	Poor, recrystallised foraminifera.
24	237		Mascarene Plateau, in a saddle between the Seychelles and Saya	07°04.99' S	58°07.48' E	-12.14							Poor, recrystallised foraminifera.

			de Malha Bank											
24	237		Mascarene Plateau, in a saddle between the Seychelles and Saya de Malha Bank	07°04.99' S	58°07.48' E	-12.14								Poor, recrystallised foraminifera.
24	237		Mascarene Plateau, in a saddle between the Seychelles and Saya de Malha Bank	07°04.99' S	58°07.48' E	-12.14								Poor, recrystallised foraminifera.
24	237		Mascarene Plateau, in a saddle between the Seychelles and Saya de Malha Bank	07°04.99' S	58°07.48' E	-12.14								Poor, recrystallised foraminifera.
77	540		Gulf of Mexico	23°49.73' N	84°22.25' W	19.43	Belanger and Matthews, 1984		*Globigerinatheka* spp.	*Globigerinatheka* spp.	2	-0.07		Poor, recrystallised foraminifera.
77	540		Gulf of Mexico	23°49.73' N	84°22.25' W	19.43	Belanger and Matthews, 1984		*Globigerinatheka* spp.	*Globigerinatheka* spp.	2	0.02		Poor, recrystallised foraminifera.
77	540		Gulf of Mexico	23°49.73' N	84°22.25' W	19.43	Belanger and Matthews, 1984		*Hantkenina* spp.	*Hantkenina* spp.	2	0.22		Poor, recrystallised foraminifera.

77	540		Gulf of Mexico	23°49.73'N	84°22.25'W	19.43	Belanger and Matthews, 1984		*G. ampliapertura*	*Turborotalia ampliapertura*	2	-0.07	Poor, recrystallised foraminifera
77	540		Gulf of Mexico	23°49.73'N	84°22.25'W	19.43	Belanger and Matthews, 1984		*Globigerinatheka* spp.	*Globigerinatheka* spp.	2	0.15	Poor, recrystallised foraminifera
77	540		Gulf of Mexico	23°49.73'N	84°22.25'W	19.43	Belanger and Matthews, 1984		*Pseudohastigerina sp*	*Pseudohastigerina* spp.	1	-0.8	Poor, recrystallised foraminifera.
77	540		Gulf of Mexico	23°49.73'N	84°22.25'W	19.43	Belanger and Matthews, 1984		*G. ampliapertura*	*Turborotalia ampliapertura*	2	-0.61	Poor, recrystallised foraminifera.
77	540		Gulf of Mexico	23°49.73'N	84°22.25'W	19.43	Belanger and Matthews, 1984		*Globigerinatheka spp*	*Globigerinatheka* spp.	2	-0.04	Poor, recrystallised foraminifera.
29	277		Campbell Plateau in the south-west Pacific	52°13.43'S	166°11.48'E	-55	Keigwin, 1980		*Globigerina angiporoides*	*Subbotina angiporoides*	3	0.03	Poor, recrystallised foraminifera.
31	292		Bneham Rise in the west Philippine Sea	15°49.11'N	124°39.05'E	5.78	Keigwin, 1980		*Globigerina ampliapertura*	*Turborotalia ampliapertura*	2	-1.44	Poor, recrystallised foraminifera.
71	511		Westerrn margin of the Maurice Ewing Bank	51°00.28'S	46°58.30'W	-58.36	Muza et al., 1983		Mixed *assemblage of Globigerina angiporoides and G. aff. Linaperta*	*Subbotina linaperta and Subbotina angiporoides*	3	0.78	Poor, recrystallised foraminifera.
71	511		Westerrn margin of the Maurice Ewing Bank	51°00.28'S	46°58.30'W	-58.36	Muza et al., 1983		Mixed *assemblage of Globigerina angiporoides and G. aff. Linaperta*	*Subbotina linaperta and Subbotina angiporoides*	3	-0.16	Poor, recrystallised foraminifera.

71	511		Westerrn margin of the Maurice Ewing Bank	51°00.28'S	46°58.30'W	-58.36	Muza et al., 1983		Mixed *assemblage of Globigerina angiporoides and G. aff. Linaperta*	*Subbotina linaperta and Subbotina angiporoides*	3	0.22	Poor, recrystallised foraminifera.
71	511		Westerrn margin of the Maurice Ewing Bank	51°00.28'S	46°58.30'W	-58.36	Muza et al., 1983		Mixed *assemblage of Globigerina angiporoides and G. aff. Linaperta*	*Subbotina linaperta and Subbotina angiporoides*	3	0.25	Poor, recrystallised foraminifera.
29	277		Campbell Plateau in the south-west Pacific	52°13.43'S	166°11.48'E	-55	Schackleton and Kennett, 1975		Mixed *Globigerina*	Mixed *Globigerina*	2	0.35	Poor, recrystallised foraminifera.
29	277		Campbell Plateau in the south-west Pacific	52°13.43'S	166°11.48'E	-55	Schackleton and Kennett, 1975		*Globigerapsis index*	*Globigerinatheka index*	2	0.23	Poor, recrystallised foraminifera.
29	277		Campbell Plateau in the south-west Pacific	52°13.43'S	166°11.48'E	-55	Schackleton and Kennett, 1975		Mixed *Globigerina and Globigerapsis index*	Mixed *Globigerina and Globigerinatheka index*	2	0.17	Poor, recrystallised foraminifera.
29	277		Campbell Plateau in the south-west Pacific	52°13.43'S	166°11.48'E	-55	Schackleton and Kennett, 1975		Mixed *Globigerina and Globigerapsis index*	Mixed *Globigerina and Globigerinatheka index*	2	0.2	Poor, recrystallised foraminifera.
29	277		Campbell Plateau in the south-west Pacific	52°13.43'S	166°11.48'E	-55	Schackleton and Kennett, 1975		*Globigerapsis index*	*Globigerinatheka index*	2	-0.17	Poor, recrystallised foraminifera.
41	366		Sierra Leone Rise	05°40.7'N	19°51.1'W	-1.9	Poore and Matthews, 1984 (a)		*Globorotalia pomeroli*	*Turborotalia pomeroli*	2	-1.5	Poor, recrystallised foraminifera.
41	366		Sierra Leone Rise	05°40.7'N	19°51.1'W	-1.9	Poore and Matthews, 1984 (a)		*Pseudohastigerina danvillensis*	*Pseudohastigerina micra*	1	-1.45	Poor, recrystallised foraminifera.

41	366		Sierra Leone Rise	05°40.7'N	19°51.1'W	-1.9	Poore and Matthews, 1984 (a)		*Chiloguembelina cubensis*	*Chiloguembelina cubensis*	1	-1.38	Poor, recrystallised foraminifera.
41	366		Sierra Leone Rise	05°40.7'N	19°51.1'W	-1.9	Poore and Matthews, 1984 (a)		*Hantkenina*	*Hantkenina* spp.	2	-1.28	Poor, recrystallised foraminifera.
41	366		Sierra Leone Rise	05°40.7'N	19°51.1'W	-1.9	Poore and Matthews, 1984 (a)		*Globigerina utilisindex*	*Subbotina utilisindex*	3	0.01	Poor, recrystallised foraminifera.
Eureka	E-67-128		Gulf of Mexico	25°N	-90	21.36	Poore and Matthews, 1984 (a)		*Globigerinatheka semiinvoluta*	*Globigerinatheka semiinvoluta*	2	-2.36	Poor, recrystallised foraminifera.
Eureka	E-67-128		Gulf of Mexico	25°N	-90	21.36	Poore and Matthews, 1984 (a)		*Globigerinatheka semiinvoluta*	*Globigerinatheka semiinvoluta*	2	-1.04	Poor, recrystallised foraminifera.
Eureka	E-67-128		Gulf of Mexico	25°N	-90	21.36	Poore and Matthews, 1984 (a)		*Globigerina cf. perus*	*Subbotina corpulenta*	3	-1.44	Poor, recrystallised foraminifera.
Eureka	E-67-128		Gulf of Mexico	25°N	-90	21.36	Poore and Matthews, 1984 (a)		*Hantkenina alabamensis*	*Hantkenina alabamensis*	2	1.32	Poor, recrystallised foraminifera.
Eureka	E-67-128		Gulf of Mexico	25°N	-90	21.36	Poore and Matthews, 1984 (a)		*Cribrohantkenina inflata*	*Cibrohantkenina inflata*	2	-1.23	Poor, recrystallised foraminifera.
Eureka	E-67-128		Gulf of Mexico	25°N	-90	21.36	Poore and Matthews, 1984 (a)		*Globigerina galavisi*	*Dentoglobigerina galavisi*	3	-1.21	Poor, recrystallised foraminifera.

Eureka	E-67-128		Gulf of Mexico	25°N	-90	21.36	Poore and Matthews, 1984 (a)		*Pseudohastigerina danvillensis*	*Pseudohastigerina micra*	1	-1.19	Poor, recrystallised foraminifera.
Eureka	E-67-128		Gulf of Mexico	25°N	-90	21.36	Poore and Matthews, 1984 (a)		*Globigerina linaperta*	*Subbotina linaperta*	3	-1.15	Poor, recrystallised foraminifera.
Eureka	E-67-128		Gulf of Mexico	25°N	-90	21.36	Poore and Matthews, 1984 (a)		*Globorotalia cerroazulensis*	*Turborotalia cerroazulensis*	2	-1.14	Poor, recrystallised foraminifera.
Eureka	E-67-128		Gulf of Mexico	25°N	-90	21.36	Poore and Matthews, 1984 (a)		*Globorotalia cerroazulensis*	*Turborotalia cerroazulensis*	2	-1.03	Poor, recrystallised foraminifera.
Eureka	E-67-128		Gulf of Mexico	25°N	-90	21.36	Poore and Matthews, 1984 (a)		*Globigerina eocaena*	*Subbotina eocaena*	3	-0.9	Poor, recrystallised foraminifera.
Eureka	E-67-128		Gulf of Mexico	25°N	-90	21.36	Poore and Matthews, 1984 (a)		*Globorotalia pomeroli*	*Turborotalia pomeroli*	2	-1.19	Poor, recrystallised foraminifera.
Eureka	E-67-128		Gulf of Mexico	25°N	-90	21.36	Poore and Matthews, 1984 (a)		*Globigerinatheka semiinvoluta*	*Globigerinatheka semiinvoluta*	2	-0.92	Poor, recrystallised foraminifera.
Eureka	E-67-128		Gulf of Mexico	25°N	-90	21.36	Poore and Matthews, 1984 (a)		*Globigerinatheka semiinvoluta*	*Globigerinatheka semiinvoluta*	2	-0.85	Poor, recrystallised foraminifera.
Eureka	E-67-128		Gulf of Mexico	25°N	-90	21.36	Poore and Matthews, 1984 (a)		*Globorotalia cerroazulensis*	*Turborotalia cerroazulensis*	2	-0.88	Poor, recrystallised foraminifera.

Eureka	E-67-128		Gulf of Mexico	25°N	-90	21.36	Poore and Matthews, 1984 (a)		*Hantkenina alabamensis*	*Hantkenina alabamensis*	2	-0.88	Poor, recrystallised foraminifera.
Eureka	E-67-128		Gulf of Mexico	25°N	-90	21.36	Poore and Matthews, 1984 (a)		*Cribrohantkenina inflata*	*Cibrohantkenina inflata*	2	-0.85	Poor, recrystallised foraminifera.
Eureka	E-67-128		Gulf of Mexico	25°N	-90	21.36	Poore and Matthews, 1984 (a)		*Pseudohastigerina danvillensis*	*Pseudohastigerina micra*	1	-0.82	Poor, recrystallised foraminifera.
Eureka	E-67-128		Gulf of Mexico	25°N	-90	21.36	Poore and Matthews, 1984 (a)		*Globigerina pseudovenezuelana*	*Dentoglobigerina pseudovenezuelana*	3	-0.81	Poor, recrystallised foraminifera.
Eureka	E-67-128		Gulf of Mexico	25°N	-90	21.36	Poore and Matthews, 1984 (a)		*Globigerina pseudovenezuelana*	*Dentoglobigerina pseudovenezuelana*	3	-0.57	Poor, recrystallised foraminifera.
Eureka	E-67-128		Gulf of Mexico	25°N	-90	21.36	Poore and Matthews, 1984 (a)		*Globigerina cf. winkleri*	*Subbotina corpulenta*	3	-0.76	Poor, recrystallised foraminifera.
Eureka	E-67-128		Gulf of Mexico	25°N	-90	21.36	Poore and Matthews, 1984 (a)		*Globigerina linaperta*	*Subbotina linaperta*	3	-0.72	Poor, recrystallised foraminifera.
Eureka	E-67-128		Gulf of Mexico	25°N	-90	21.36	Poore and Matthews, 1984 (a)		*Globigerinatheka tropicalis*	*Globigerinatheka tropicalis*	2	-0.58	Poor, recrystallised foraminifera.
73	522		southern Angola Abyssal Plain	26°06.843'S	5°07.78'W	-34.34	Poore and Matthews, 1984 (a)		*Hantkenina alabamensis*	*Hantkenina alabamensis*	2	0.25	Poor, recrystallised foraminifera.

73	522		southern Angola Abyssal Plain	26°06.843'S	5°07.78'W	-34.34	Poore and Matthews, 1984 (a)		*Globigerinatheka tropicalis*	*Globigerinatheka tropicalis*	2	0.28	Poor, recrystallised foraminifera
73	522		southern Angola Abyssal Plain	26°06.843'S	5°07.78'W	-34.34	Poore and Matthews, 1984 (a)		*Globigerinatheka luterbacheri*	*Globigerinatheka luterbacheri*	2	0.5	Poor, recrystallised foraminifera
73	522		southern Angola Abyssal Plain	26°06.843'S	5°07.78'W	-34.34	Poore and Matthews, 1984 (a)		*Chiloguembelina martini*	*Streptochilus martini*	3	0.61	Poor, recrystallised foraminifera.
73	522		southern Angola Abyssal Plain	26°06.843'S	5°07.78'W	-34.34	Poore and Matthews, 1984 (a)		*Globigerina pseudovenezuelana*	*Dentoglobigerina pseudovenezuelana*	3	0.75	Poor, recrystallised foraminifera.
73	522		southern Angola Abyssal Plain	26°06.843'S	5°07.78'W	-34.34	Poore and Matthews, 1984 (a)		*Globigerina galavisi*	*Dentoglobigerina galavisi*	3	0.86	Poor, recrystallised foraminifera.
73	522		southern Angola Abyssal Plain	26°06.843'S	5°07.78'W	-34.34	Poore and Matthews, 1984 (a)		*Globigerina cf. perus*	*Subbotina corpulenta*	3	1.29	Poor, recrystallised foraminifera.
3	19		East flank of a N-S trending ridge, Mid-Atlantic ridge	28° 32.08'S	23° 40.63'W	-34.29	Keigwin and Corliss, 1986		*G. subglobosa*	*Subbotina* spp.	3	0.82	Poor, recrystallised foraminifera.
10	94		Campeche Scarp, Yucatan Shelf	24°31.64'N	88°28.16'W	20.68	Keigwin and Corliss, 1986		*Pseudohastigerina micra*	*Pseudohastigerina micra*	1	-0.84	Poor, recrystallised foraminifera.
23	219		On the crest of the Laccadive-Chagos Ridge	9°01.75'N	72°52.67'E	-2.06	Keigwin and Corliss, 1986		*G. subglobosa*	*Subbotina* spp.	3	0.84	Poor, recrystallised foraminifera.

23	219		On the crest of the Laccadive-Chagos Ridge	9°01.75' N	72°52.67' E	-2.06	Keigwin and Corliss, 1986		*G. ampliapertura*	*Turborotalia ampliapertura*	2	-0.3	Poor, recrystallised foraminifera.
26	253		On the top of the Ninetyeast Ridge, Indian Ocean	24°52.65' S	87°21.97' E	-37.26	Keigwin and Corliss, 1986		*Chiloguembelina* spp.	*Chiloguembelina* spp.	1	0.45	Poor, recrystallised foraminifera.
29	277		Campbell Plateau in the south-west Pacific	52°13.43' S	166°11.48' E	-55	Keigwin and Corliss, 1986		*G. subglobosa*	*Subbotina* spp.	3	0.42	Poor, recrystallised foraminifera.
29	277		Campbell Plateau in the south-west Pacific	52°13.43' S	166°11.48' E	-55	Keigwin and Corliss, 1986		*Chiloguembelina* spp.	*Chiloguembelina* spp.	1	-0.13	Poor, recrystallised foraminifera.
31	292		Bneham Rise in the west Philippine Sea	15°49.11' N	124°39.05' E	5.78	Keigwin and Corliss, 1986		*G. ampliapertura*	*Turborotalia ampliapertura*	2	-1.01	Poor, recrystallised foraminifera.
40	363		Isolated basement high on north-facing escarpment of Frio Ridge portion of Walvis Ridge	19°38.75' S	09°02.80' E	-28.03	Keigwin and Corliss, 1986		*G. ampliapertura*	*Turborotalia ampliapertura*	2	-0.48	Poor, recrystallised foraminifera.
48	401		On the planated edge of a tilted fault block underlying the southern edge of the	47°25.65' N	08°48.62' W	40.07	Keigwin and Corliss, 1986 who found it in Miller and Curry (1982)		*Pseudohastigerina*	*Pseudohastigerina* spp.	1	0.2	Poor, recrystallised foraminifera.

			Meriadzek Terrace on the north Biscay margin										
71	511		In the basin province of the Falkand Plateau, on Maurice Ewing Bank	51°00.28'S	46°58.30'W	-58.36	Keigwin and Corliss, 1986 who found it in Muza and others (1983)		*G. angiporoides, G. af.. linaperta*	*Subbotina angiporoides and Subbotina linaperta*	3	0.4	Poor, recrystallised foraminifera.
90	592		On the southern Lord Howe Rise	36°28.40'S	165°26.53'E	-46.21	Keigwin and Corliss, 1986		*Chiloguembelina* spp.	*Chiloguembelina* spp.	1	-0.06	Poor, recrystallised foraminifera.
90	593		On the Challenger Plateau, a western extension of the New Zealand Plateau.	40°30.47'S	167°40.47'E	-49.58	Keigwin and Corliss, 1986		*Chiloguembelina* spp.	*Chiloguembelina*	1	-0.22	Poor, recrystallised foraminifera.
95	612		On the middle part of the New Jersey continental slope.	38°49.21'N	72°46.43'W	32.84	Keigwin and Corliss, 1986		*P. micra*	*Pseudohastigerina micra*	1	-0.75	Poor, recrystallised foraminifera.
Eureka	E-67-128		Gulf of Mexico	25°N	90°S	21.36	Keigwin and Corliss, 1986		*G. ampliapertura*	*Turborotalia ampliapertura*	2	-1.39	Poor, recrystallised foraminifera.

73	522	NP20	southern Angola Abyssal Plain	26°06.843'S	5°07.78'W	-34.34	Poore and Matthews(b)		Globigerina galavisi	Dentoglobigerina galavisi	3	0.96	Poor, recrystallised foraminifera.
73	522		southern Angola Abyssal Plain	26°06.843'S	5°07.78'W	-34.34	Poore and Matthews(b)		Globigerinatheka tropicalis	Globigerinatheka tropicalis	2	0.28	Poor, recrystallised foraminifera.
73	522		southern Angola Abyssal Plain	26°06.843'S	5°07.78'W	-34.34	Poore and Matthews(b)		Globigerina galavisi	Dentoglobigerina galavisi	3	0.86	Poor, recrystallised foraminifera.
119	744a	CP15a, AP12	southern end of the Kerguelen Plateau	61°34.66'S	80°35.46'E	-58.29	Barrera and Huber, 1991		Chiloguembelina cubensis	Chiloguembelina cubensis	1	0.38	Poor, recrystallised foraminifera.
119	744a	CP15a, AP12	southern end of the Kerguelen Plateau	61°34.66'S	80°35.46'E	-58.29	Barrera and Huber, 1991		Chiloguembelina cubensis	Chiloguembelina cubensis	1	0.54	Poor, recrystallised foraminifera.
119	744a	CP15a, AP12	southern end of the Kerguelen Plateau	61°34.66'S	80°35.46'E	-58.29	Barrera and Huber, 1991		Chiloguembelina cubensis	Chiloguembelina cubensis	1	0.54	Poor, recrystallised foraminifera.
119	744a	CP15a, AP12	southern end of the Kerguelen Plateau	61°34.66'S	80°35.46'E	-58.29	Barrera and Huber, 1991		Chiloguembelina cubensis	Chiloguembelina cubensis	1	0.32	Poor, recrystallised foraminifera.
119	744a	CP15b, AP12	southern end of the Kerguelen Plateau	61°34.66'S	80°35.46'E	-58.29	Barrera and Huber, 1991		Chiloguembelina cubensis	Chiloguembelina cubensis	1	0.72	Poor, recrystallised foraminifera.
119	744a	CP15b, AP12	southern end of the Kerguelen Plateau	61°34.66'S	80°35.46'E	-58.29	Barrera and Huber, 1991		Chiloguembelina cubensis	Chiloguembelina cubensis	1	1.13	Poor, recrystallised foraminifera.

119	744a	CP15b, AP12	southern end of the Kerguelen Plateau	61°34.66' S	80°35.46' E	-58.29	Barrera and Huber, 1991		*Chiloguembelina cubensis*	*Chiloguembelina cubensis*	1	0.54	Poor, recrystallised foraminifera.
119	744a	CP15b, AP12	southern end of the Kerguelen Plateau	61°34.66' S	80°35.46' E	-58.29	Barrera and Huber, 1991		*Chiloguembelina cubensis*	*Chiloguembelina cubensis*	1	0.36	Poor, recrystallised foraminifera.
119	744a	CP15b, AP12	southern end of the Kerguelen Plateau	61°34.66' S	80°35.46' E	-58.29	Barrera and Huber, 1991		*Chiloguembelina cubensis*	*Chiloguembelina cubensis*	1	0.52	Poor, recrystallised foraminifera.
119	744a	CP15b, AP12	southern end of the Kerguelen Plateau	61°34.66' S	80°35.46' E	-58.29	Barrera and Huber, 1991		*Chiloguembelina cubensis*	*Chiloguembelina cubensis*	1	0.38	Poor, recrystallised foraminifera.
119	744a	CP16, AP12	southern end of the Kerguelen Plateau	61°34.66' S	80°35.46' E	-58.29	Barrera and Huber, 1991		*Chiloguembelina cubensis*	*Chiloguembelina cubensis*	1	0.91	Poor, recrystallised foraminifera.
119	744a	CP16, AP12	southern end of the Kerguelen Plateau	61°34.66' S	80°35.46' E	-58.29	Barrera and Huber, 1991		*Chiloguembelina cubensis*	*Chiloguembelina cubensis*	1	0.83	Poor, recrystallised foraminifera.
119	744a	CP16, AP12	southern end of the Kerguelen Plateau	61°34.66' S	80°35.46' E	-58.29	Barrera and Huber, 1991		*Chiloguembelina cubensis*	*Chiloguembelina cubensis*	1	1.01	Poor, recrystallised foraminifera.
119	744a	CP16, AP12	southern end of the Kerguelen Plateau	61°34.66' S	80°35.46' E	-58.29	Barrera and Huber, 1991		*Chiloguembelina cubensis*	*Chiloguembelina cubensis*	1	0.88	Poor, recrystallised foraminifera.
119	744a	CP16, AP12	southern end of the Kerguelen Plateau	61°34.66' S	80°35.46' E	-58.29	Barrera and Huber, 1991		*Chiloguembelina cubensis*	*Chiloguembelina cubensis*	1	0.58	Poor, recrystallised foraminifera.

119	744a	CP16, AP12	southern end of the Kerguelen Plateau	61°34.66' S	80°35.46' E	-58.29	Barrera and Huber, 1991		*Chiloguembelina cubensis*	*Chiloguembelina cubensis*	1	0.91	Poor, recrystallised foraminifera.
119	744a	CP15a, AP12	southern end of the Kerguelen Plateau	61°34.66' S	80°35.46' E	-58.29	Barrera and Huber, 1991		*Globorotaloides suteri*	*Globorotaloides suteri*	3	1.17	Poor, recrystallised foraminifera.
119	744a	CP15a, AP12	southern end of the Kerguelen Plateau	61°34.66' S	80°35.46' E	-58.29	Barrera and Huber, 1991		*Globorotaloides suteri*	*Globorotaloides suteri*	3	1.27	Poor, recrystallised foraminifera.
119	744a	CP15a, AP12	southern end of the Kerguelen Plateau	61°34.66' S	80°35.46' E	-58.29	Barrera and Huber, 1991		*Globorotaloides suteri*	*Globorotaloides suteri*	3	1.1	Poor, recrystallised foraminifera.
119	744a	CP15a, AP12	southern end of the Kerguelen Plateau	61°34.66' S	80°35.46' E	-58.29	Barrera and Huber, 1991		*Globorotaloides suteri*	*Globorotaloides suteri*	3	1.22	Poor, recrystallised foraminifera.
119	744a	CP15b, AP12	southern end of the Kerguelen Plateau	61°34.66' S	80°35.46' E	-58.29	Barrera and Huber, 1991		*Globorotaloides suteri*	*Globorotaloides suteri*	3	1.08	Poor, recrystallised foraminifera.
119	744a	CP15b, AP12	southern end of the Kerguelen Plateau	61°34.66' S	80°35.46' E	-58.29	Barrera and Huber, 1991		*Globorotaloides suteri*	*Globorotaloides suteri*	3	1.26	Poor, recrystallised foraminifera.
119	744a	CP15b, AP12	southern end of the Kerguelen Plateau	61°34.66' S	80°35.46' E	-58.29	Barrera and Huber, 1991		*Globorotaloides suteri*	*Globorotaloides suteri*	3	1.36	Poor, recrystallised foraminifera.
119	744a	CP15b, AP12	southern end of the Kerguelen Plateau	61°34.66' S	80°35.46' E	-58.29	Barrera and Huber, 1991		*Globorotaloides suteri*	*Globorotaloides suteri*	3	1.03	Poor, recrystallised foraminifera.

119	744a	CP16, AP12	southern end of the Kerguelen Plateau	61°34.66' S	80°35.46' E	-58.29	Barrera and Huber, 1991		*Globorotaloides suteri*	*Globorotaloides suteri*	3	1.47	Poor, recrystallised foraminifera.
119	744a	CP16, AP12	southern end of the Kerguelen Plateau	61°34.66' S	80°35.46' E	-58.29	Barrera and Huber, 1991		*Globorotaloides suteri*	*Globorotaloides suteri*	3	1.6	Poor, recrystallised foraminifera.
119	744a	CP16, AP12	southern end of the Kerguelen Plateau	61°34.66' S	80°35.46' E	-58.29	Barrera and Huber, 1991		*Globorotaloides suteri*	*Globorotaloides suteri*	3	1.13	Poor, recrystallised foraminifera.
119	738B		southern end of the Kerguelen Plateau	62°42.54' S	82°47.25' E	-59.41	Barrera and Huber, 1991		*Globorotaloides suteri*	*Globorotaloides suteri*	3	2.16	Poor, recrystallised foraminifera.
119	738B		southern end of the Kerguelen Plateau	62°42.54' S	82°47.25' E	-59.41	Barrera and Huber, 1991		*Globorotaloides suteri*	*Globorotaloides suteri*	3	1.35	Poor, recrystallised foraminifera.
119	738B		southern end of the Kerguelen Plateau	62°42.54' S	82°47.25' E	-59.41	Barrera and Huber, 1991		*Globorotaloides suteri*	*Globorotaloides suteri*	3	1.35	Poor, recrystallised foraminifera.
119	738B		southern end of the Kerguelen Plateau	62°42.54' S	82°47.25' E	-59.41	Barrera and Huber, 1991		*Globorotaloides suteri*	*Globorotaloides suteri*	3	1.49	Poor, recrystallised foraminifera.
119	738B		southern end of the Kerguelen Plateau	62°42.54' S	82°47.25' E	-59.41	Barrera and Huber, 1991		*Globorotaloides suteri*	*Globorotaloides suteri*	3	1.25	Poor, recrystallised foraminifera.
119	738B		southern end of the Kerguelen Plateau	62°42.54' S	82°47.25' E	-59.41	Barrera and Huber, 1991		*Globorotaloides suteri*	*Globorotaloides suteri*	3	1.46	Poor, recrystallised foraminifera.

119	738B		southern end of the Kerguelen Plateau	62°42.54'S	82°47.25'E	-59.41	Barrera and Huber, 1991		*Globorotaloides suteri*	*Globorotaloides suteri*	3	1.49	Poor, recrystallised foraminifera.
119	738B		southern end of the Kerguelen Plateau	62°42.54'S	82°47.25'E	-59.41	Barrera and Huber, 1991		*Globorotaloides suteri*	*Globorotaloides suteri*	3	1.31	Poor, recrystallised foraminifera.
119	738B		southern end of the Kerguelen Plateau	62°42.54'S	82°47.25'E	-59.41	Barrera and Huber, 1991		*Globorotaloides suteri*	*Globorotaloides suteri*	3	1.28	Poor, recrystallised foraminifera.
119	738B		southern end of the Kerguelen Plateau	62°42.54'S	82°47.25'E	-59.41	Barrera and Huber, 1991		*Globorotaloides suteri*	*Globorotaloides suteri*	3	1.21	Poor, recrystallised foraminifera.
119	738B		southern end of the Kerguelen Plateau	62°42.54'S	82°47.25'E	-59.41	Barrera and Huber, 1991		*Globorotaloides suteri*	*Globorotaloides suteri*	3	0.99	Poor, recrystallised foraminifera.
119	738B		southern end of the Kerguelen Plateau	62°42.54'S	82°47.25'E	-59.41	Barrera and Huber, 1991		*Globorotaloides suteri*	*Globorotaloides suteri*	3	1.53	Poor, recrystallised foraminifera.
119	738B		southern end of the Kerguelen Plateau	62°42.54'S	82°47.25'E	-59.41	Barrera and Huber, 1991		*Globorotaloides suteri*	*Globorotaloides suteri*	3	1.31	Poor, recrystallised foraminifera.
119	738B		southern end of the Kerguelen Plateau	62°42.54'S	82°47.25'E	-59.41	Barrera and Huber, 1991		*Globorotaloides suteri*	*Globorotaloides suteri*	3	1.32	Poor, recrystallised foraminifera.
119	738B		southern end of the Kerguelen Plateau	62°42.54'S	82°47.25'E	-59.41	Barrera and Huber, 1991		*Globorotaloides suteri*	*Globorotaloides suteri*	3	1.49	Poor, recrystallised foraminifera.

119	738B		southern end of the Kerguelen Plateau	62°42.54' S	82°47.25' E	-59.41	Barrera and Huber, 1991		*Globorotaloides suteri*	*Globorotaloides suteri*	3	1.4	Poor, recrystallised foraminifera.
119	738B		southern end of the Kerguelen Plateau	62°42.54' S	82°47.25' E	-59.41	Barrera and Huber, 1991		*Subbotina angiporoides*	*Subbotina angiporoides*	3	1.29	Poor, recrystallised foraminifera.
119	738B		southern end of the Kerguelen Plateau	62°42.54' S	82°47.25' E	-59.41	Barrera and Huber, 1991		*Subbotina angiporoides*	*Subbotina angiporoides*	3	1.33	Poor, recrystallised foraminifera.
119	738B		southern end of the Kerguelen Plateau	62°42.54' S	82°47.25' E	-59.41	Barrera and Huber, 1991		*Subbotina angiporoides*	*Subbotina angiporoides*	3	1.46	Poor, recrystallised foraminifera.
119	738B		southern end of the Kerguelen Plateau	62°42.54' S	82°47.25' E	-59.41	Barrera and Huber, 1991		*Subbotina angiporoides*	*Subbotina angiporoides*	3	1.51	Poor, recrystallised foraminifera.
119	738B		southern end of the Kerguelen Plateau	62°42.54' S	82°47.25' E	-59.41	Barrera and Huber, 1991		*Subbotina linaperta*	*Subbotina linaperta*	3	1.68	Poor, recrystallised foraminifera.
119	738B		southern end of the Kerguelen Plateau	62°42.54' S	82°47.25' E	-59.41	Barrera and Huber, 1991		*Subbotina linaperta*	*Subbotina linaperta*	3	1.48	Poor, recrystallised foraminifera.
119	738B		southern end of the Kerguelen Plateau	62°42.54' S	82°47.25' E	-59.41	Barrera and Huber, 1991		*Subbotina linaperta*	*Subbotina linaperta*	3	1.17	Poor, recrystallised foraminifera.
119	738B		southern end of the Kerguelen Plateau	62°42.54' S	82°47.25' E	-59.41	Barrera and Huber, 1991		*Subbotina linaperta*	*Subbotina linaperta*	3	1.59	Poor, recrystallised foraminifera.

119	738B		southern end of the Kerguelen Plateau	62°42.54' S	82°47.25' E	-59.41	Barrera and Huber, 1991		*Globorotaloides suteri*	*Globorotaloides suteri*	3	1.57	Poor, recrystallised foraminifera.
119	738B		southern end of the Kerguelen Plateau	62°42.54' S	82°47.25' E	-59.41	Barrera and Huber, 1991		*Globigerinatheka index*	*Globigerinatheka index*	2	1	Poor, recrystallised foraminifera.
119	738B		southern end of the Kerguelen Plateau	62°42.54' S	82°47.25' E	-59.41	Barrera and Huber, 1991		*Globigerinatheka index*	*Globigerinatheka index*	2	1.53	Poor, recrystallised foraminifera.
34 (Sample number)	Browns Creek (Australia)		Browns Creek, southern Victoria, Australia	38 S	142 E	-51.79	Kamp et al., 1990		Mixed spp., dominated by *Globigerapsis index*	Mixed spp., dominated by *Globigerinatheka index*	2	-1.06	Excellent, glassy foraminifera
35 (Sample number)	Browns Creek (Australia)		Browns Creek, southern Victoria, Australia	38 S	142 E	-51.79	Kamp et al., 1990		Mixed spp., dominated by *Globigerapsis index*	Mixed spp., dominated by *Globigerinatheka index*	2	-1.22	Excellent, glassy foraminifera
36 (Sample number)	Browns Creek (Australia)		Browns Creek, southern Victoria, Australia	38 S	142 E	-51.79	Kamp et al., 1990		Mixed spp., dominated by *Globigerapsis index*	Mixed spp., dominated by *Globigerinatheka index*	2	-2.77	Excellent, glassy foraminifera
37 (Sample number)	Browns Creek (Australia)		Browns Creek, southern Victoria, Australia	38 S	142 E	-51.79	Kamp et al., 1990		Mixed spp., dominated by *Globigerapsis index*	Mixed spp., dominated by *Globigerinatheka index*	2	-1.51	Excellent, glassy foraminifera

38 (Sample number)	Browns Creek (Australia)		Browns Creek, southern Victoria, Australia	38 S	142 E	-51.79	Kamp et al., 1990		Mixed spp., dominated by *Globigerapsis index*	Mixed spp., dominated by *Globigerinatheka index*	2	-1.7	Excellent, glassy foraminifera
39 (Sample number)	Browns Creek (Australia)		Browns Creek, southern Victoria, Australia	38 S	142 E	-51.79	Kamp et al., 1990		Mixed spp., dominated by *Globigerapsis index*	Mixed spp., dominated by *Globigerinatheka index*	2	-0.99	Excellent, glassy foraminifera
40 (Sample number)	Browns Creek (Australia)		Browns Creek, southern Victoria, Australia	38 S	142 E	-51.79	Kamp et al., 1990		Mixed spp., dominated by *Globigerapsis index*	Mixed spp., dominated by *Globigerinatheka index*	2	-1.25	Excellent, glassy foraminifera
41 (Sample number)	Browns Creek (Australia)		Browns Creek, southern Victoria, Australia	38 S	142 E	-51.79	Kamp et al., 1990		Mixed spp., dominated by *Globigerapsis index*	Mixed spp., dominated by *Globigerinatheka index*	2	-1.72	Excellent, glassy foraminifera
42 (Sample number)	Browns Creek (Australia)		Browns Creek, southern Victoria, Australia	38 S	142 E	-51.79	Kamp et al., 1990		Mixed spp., dominated by *Globigerapsis index*	Mixed spp., dominated by *Globigerinatheka index*	2	-1.85	Excellent, glassy foraminifera
TDP	TDP 12		Kilwa Group clays, Tanzania	8.7 S	39.4 E	-15.59	Pearson et al., 2008, data from supplementary information, found in the GSA repository, online.		*Turborotalia ampliapertura*	*Turborotalia ampliapertura*	2	-2.635	Excellent, glassy foraminifera

TDP	TDP 12		Kilwa Group clays, Tanzania	8.7 S	39.4 E	-15.59	Pearson et al., 2008, data from supplementary information, found in the GSA repository, online.		*Turborotalia ampliapertura*	*Turborotalia ampliapertura*	2	-2.907	Excellent, glassy foraminifera
TDP	TDP 12		Kilwa Group clays, Tanzania	8.7 S	39.4 E	-15.59	Pearson et al., 2008, data from supplementary information, found in the GSA repository, online.		*Turborotalia ampliapertura*	*Turborotalia ampliapertura*	2	-3.246	Excellent, glassy foraminifera
TDP	TDP 12		Kilwa Group clays, Tanzania	8.7 S	39.4 E	-15.59	Pearson et al., 2008, data from supplementary information, found in the GSA repository, online.		*Turborotalia ampliapertura*	*Turborotalia ampliapertura*	2	-3.227	Excellent, glassy foraminifera
TDP	TDP 12		Kilwa Group clays, Tanzania	8.7 S	39.4 E	-15.59	Pearson et al., 2008, data from supplementary information, found in the GSA repository, online.		*Turborotalia ampliapertura*	*Turborotalia ampliapertura*	2	-3.121	Excellent, glassy foraminifera
TDP	TDP 12		Kilwa Group clays, Tanzania	8.7 S	39.4 E	-15.59	Pearson et al., 2008, data from supplementary information, found in the GSA		*Turborotalia ampliapertura*	*Turborotalia ampliapertura*	2	-2.983	Excellent, glassy foraminifera

							repository, online.					
TDP	TDP 12		Kilwa Group clays, Tanzania	8.7 S	39.4 E	-15.59	Pearson et al., 2008, data from supplementary information, found in the GSA repository, online.		*Turborotalia ampliapertura*	*Turborotalia ampliapertura*	2	-2.951	Excellent, glassy foraminifera
TDP	TDP 12		Kilwa Group clays, Tanzania	8.7 S	39.4 E	-15.59	Pearson et al., 2008, data from supplementary information, found in the GSA repository, online.		*Turborotalia ampliapertura*	*Turborotalia ampliapertura*	2	-2.973	Excellent, glassy foraminifera
TDP	TDP 12		Kilwa Group clays, Tanzania	8.7 S	39.4 E	-15.59	Pearson et al., 2008, data from supplementary information, found in the GSA repository, online.		*Turborotalia ampliapertura*	*Turborotalia ampliapertura*	2	-3.076	Excellent, glassy foraminifera
TDP	TDP 12		Kilwa Group clays, Tanzania	8.7 S	39.4 E	-15.59	Pearson et al., 2008, data from supplementary information, found in the GSA repository, online.		*Turborotalia ampliapertura*	*Turborotalia ampliapertura*	2	-3.05	Excellent, glassy foraminifera

TDP	TDP 12		Kilwa Group clays, Tanzania	8.7 S	39.4 E	-15.59	Pearson et al., 2008, data from supplementary information, found in the GSA repository, online.		*Turborotalia ampliapertura*	*Turborotalia ampliapertura*	2	-2.883	Excellent, glassy foraminifera
TDP	TDP 12		Kilwa Group clays, Tanzania	8.7 S	39.4 E	-15.59	Pearson et al., 2008, data from supplementary information, found in the GSA repository, online.		*Turborotalia ampliapertura*	*Turborotalia ampliapertura*	2	-3.188	Excellent, glassy foraminifera
TDP	TDP 12		Kilwa Group clays, Tanzania	8.7 S	39.4 E	-15.59	Pearson et al., 2008, data from supplementary information, found in the GSA repository, online.		*Turborotalia ampliapertura*	*Turborotalia ampliapertura*	2	-3.049	Excellent, glassy foraminifera
TDP	TDP 12		Kilwa Group clays, Tanzania	8.7 S	39.4 E	-15.59	Pearson et al., 2008, data from supplementary information, found in the GSA repository, online.		*Turborotalia ampliapertura*	*Turborotalia ampliapertura*	2	-2.956	Excellent, glassy foraminifera
TDP	TDP 12		Kilwa Group clays, Tanzania	8.7 S	39.4 E	-15.59	Pearson et al., 2008, data from supplementary information, found in the GSA		*Turborotalia ampliapertura*	*Turborotalia ampliapertura*	2	-3.005	Excellent, glassy foraminifera

							repository, online.						
TDP	TDP 12		Kilwa Group clays, Tanzania	8.7 S	39.4 E	-15.59	Pearson et al., 2008, data from supplementary information, found in the GSA repository, online.		*Turborotalia ampliapertura*	*Turborotalia ampliapertura*	2	-3.176	Excellent, glassy foraminifera
TDP	TDP 12		Kilwa Group clays, Tanzania	8.7 S	39.4 E	-15.59	Pearson et al., 2008, data from supplementary information, found in the GSA repository, online.		*Turborotalia ampliapertura*	*Turborotalia ampliapertura*	2	-3.006	Excellent, glassy foraminifera
TDP	TDP 12		Kilwa Group clays, Tanzania	8.7 S	39.4 E	-15.59	Pearson et al., 2008, data from supplementary information, found in the GSA repository, online.		*Turborotalia ampliapertura*	*Turborotalia ampliapertura*	2	-3.158	Excellent, glassy foraminifera
TDP	TDP 12		Kilwa Group clays, Tanzania	8.7 S	39.4 E	-15.59	Pearson et al., 2008, data from supplementary information, found in the GSA repository, online.		*Turborotalia ampliapertura*	*Turborotalia ampliapertura*	2	-3.027	Excellent, glassy foraminifera

TDP	TDP 12		Kilwa Group clays, Tanzania	8.7 S	39.4 E	-15.59	Pearson et al., 2008, data from supplementary information, found in the GSA repository, online.		*Turborotalia ampliapertura*	*Turborotalia ampliapertura*	2	-2.798	Excellent, glassy foraminifera
TDP	TDP 12		Kilwa Group clays, Tanzania	8.7 S	39.4 E	-15.59	Pearson et al., 2008, data from supplementary information, found in the GSA repository, online.		*Turborotalia ampliapertura*	*Turborotalia ampliapertura*	2	-2.871	Excellent, glassy foraminifera
TDP	TDP 12		Kilwa Group clays, Tanzania	8.7 S	39.4 E	-15.59	Pearson et al., 2008, data from supplementary information, found in the GSA repository, online.		*Turborotalia ampliapertura*	*Turborotalia ampliapertura*	2	-3.159	Excellent, glassy foraminifera
TDP	TDP 12		Kilwa Group clays, Tanzania	8.7 S	39.4 E	-15.59	Pearson et al., 2008, data from supplementary information, found in the GSA repository, online.		*Turborotalia ampliapertura*	*Turborotalia ampliapertura*	2	-3.158	Excellent, glassy foraminifera
TDP	TDP 12		Kilwa Group clays, Tanzania	8.7 S	39.4 E	-15.59	Pearson et al., 2008, data from supplementary information, found in the GSA		*Turborotalia ampliapertura*	*Turborotalia ampliapertura*	2	-3.026	Excellent, glassy foraminifera

							repository, online.						
TDP	TDP 12		Kilwa Group clays, Tanzania	8.7 S	39.4 E	-15.59	Pearson et al., 2008, data from supplementary information, found in the GSA repository, online.		*Turborotalia ampliapertura*	*Turborotalia ampliapertura*	2	-3.114	Excellent, glassy foraminifera
TDP	TDP 12		Kilwa Group clays, Tanzania	8.7 S	39.4 E	-15.59	Pearson et al., 2008, data from supplementary information, found in the GSA repository, online.		*Turborotalia ampliapertura*	*Turborotalia ampliapertura*	2	-2.795	Excellent, glassy foraminifera
TDP	TDP 12		Kilwa Group clays, Tanzania	8.7 S	39.4 E	-15.59	Pearson et al., 2008, data from supplementary information, found in the GSA repository, online.		*Turborotalia ampliapertura*	*Turborotalia ampliapertura*	2	-2.783	Excellent, glassy foraminifera
TDP	TDP 12		Kilwa Group clays, Tanzania	8.7 S	39.4 E	-15.59	Pearson et al., 2008, data from supplementary information, found in the GSA repository, online.		*Turborotalia ampliapertura*	*Turborotalia ampliapertura*	2	-2.963	Excellent, glassy foraminifera

TDP	TDP 12			Kilwa Group clays, Tanzania	8.7 S	39.4 E	-15.59	Pearson et al., 2008, data from supplementary information, found in the GSA repository, online.		*Turborotalia ampliapertura*	*Turborotalia ampliapertura*	2	-3.161	Excellent, glassy foraminifera
TDP	TDP 12			Kilwa Group clays, Tanzania	8.7 S	39.4 E	-15.59	Pearson et al., 2008, data from supplementary information, found in the GSA repository, online.		*Turborotalia ampliapertura*	*Turborotalia ampliapertura*	2	-3.087	Excellent, glassy foraminifera
TDP	TDP 12			Kilwa Group clays, Tanzania	8.7 S	39.4 E	-15.59	Pearson et al., 2008, data from supplementary information, found in the GSA repository, online.		*Turborotalia ampliapertura*	*Turborotalia ampliapertura*	2	-2.926	Excellent, glassy foraminifera
TDP	TDP 12			Kilwa Group clays, Tanzania	8.7 S	39.4 E	-15.59	Pearson et al., 2008, data from supplementary information, found in the GSA repository, online.		*Turborotalia ampliapertura*	*Turborotalia ampliapertura*	2	-3.205	Excellent, glassy foraminifera
TDP	TDP 12			Kilwa Group clays, Tanzania	8.7 S	39.4 E	-15.59	Pearson et al., 2008, data from supplementary information, found in the GSA		*Turborotalia ampliapertura*	*Turborotalia ampliapertura*	2	-3.06	Excellent, glassy foraminifera

								repository, online.				
TDP	TDP 12		Kilwa Group clays, Tanzania	8.7 S	39.4 E	-15.59	Pearson et al., 2008, data from supplementary information, found in the GSA repository, online.		*Turborotalia ampliapertura*	*Turborotalia ampliapertura*	2	-2.896	Excellent, glassy foraminifera
TDP	TDP 12		Kilwa Group clays, Tanzania	8.7 S	39.4 E	-15.59	Pearson et al., 2008, data from supplementary information, found in the GSA repository, online.		*Turborotalia ampliapertura*	*Turborotalia ampliapertura*	2	-2.807	Excellent, glassy foraminifera
TDP	TDP 12		Kilwa Group clays, Tanzania	8.7 S	39.4 E	-15.59	Pearson et al., 2008, data from supplementary information, found in the GSA repository, online.		*Turborotalia ampliapertura*	*Turborotalia ampliapertura*	2	-2.689	Excellent, glassy foraminifera
TDP	TDP 12		Kilwa Group clays, Tanzania	8.7 S	39.4 E	-15.59	Pearson et al., 2008, data from supplementary information, found in the GSA repository, online.		*Turborotalia ampliapertura*	*Turborotalia ampliapertura*	2	-2.818	Excellent, glassy foraminifera

TDP	TDP 12		Kilwa Group clays, Tanzania	8.7 S	39.4 E	-15.59	Pearson et al., 2008, data from supplementary information, found in the GSA repository, online.		*Turborotalia ampliapertura*	*Turborotalia ampliapertura*	2	-2.773	Excellent, glassy foraminifera
TDP	TDP 12		Kilwa Group clays, Tanzania	8.7 S	39.4 E	-15.59	Pearson et al., 2008, data from supplementary information, found in the GSA repository, online.		*Turborotalia ampliapertura*	*Turborotalia ampliapertura*	2	-2.872	Excellent, glassy foraminifera
TDP	TDP 12		Kilwa Group clays, Tanzania	8.7 S	39.4 E	-15.59	Pearson et al., 2008, data from supplementary information, found in the GSA repository, online.		*Turborotalia ampliapertura*	*Turborotalia ampliapertura*	2	-2.815	Excellent, glassy foraminifera
TDP	TDP 12		Kilwa Group clays, Tanzania	8.7 S	39.4 E	-15.59	Pearson et al., 2008, data from supplementary information, found in the GSA repository, online.		*Turborotalia ampliapertura*	*Turborotalia ampliapertura*	2	-2.929	Excellent, glassy foraminifera
TDP	TDP 12		Kilwa Group clays, Tanzania	8.7 S	39.4 E	-15.59	Pearson et al., 2008, data from supplementary information, found in the GSA		*Turborotalia ampliapertura*	*Turborotalia ampliapertura*	2	-3.017	Excellent, glassy foraminifera

							repository, online.						
TDP	TDP 12		Kilwa Group clays, Tanzania	8.7 S	39.4 E	-15.59	Pearson et al., 2008, data from supplementary information, found in the GSA repository, online.		*Turborotalia ampliapertura*	*Turborotalia ampliapertura*	2	-3.001	Excellent, glassy foraminifera
TDP	TDP 12		Kilwa Group clays, Tanzania	8.7 S	39.4 E	-15.59	Pearson et al., 2008, data from supplementary information, found in the GSA repository, online.		*Turborotalia ampliapertura*	*Turborotalia ampliapertura*	2	-3.535	Excellent, glassy foraminifera
TDP	TDP 12		Kilwa Group clays, Tanzania	8.7 S	39.4 E	-15.59	Pearson et al., 2008, data from supplementary information, found in the GSA repository, online.		*Turborotalia ampliapertura*	*Turborotalia ampliapertura*	2	-3.377	Excellent, glassy foraminifera
TDP	TDP 12		Kilwa Group clays, Tanzania	8.7 S	39.4 E	-15.59	Pearson et al., 2008, data from supplementary information, found in the GSA repository, online.		*Turborotalia ampliapertura*	*Turborotalia ampliapertura*	2	-3.646	Excellent, glassy foraminifera

TDP	TDP 12		Kilwa Group clays, Tanzania	8.7 S	39.4 E	-15.59	Pearson et al., 2008, data from supplementary information, found in the GSA repository, online.		Turborotalia ampliapertura	Turborotalia ampliapertura	2	-3.221	Excellent, glassy foraminifera
TDP	TDP 12		Kilwa Group clays, Tanzania	8.7 S	39.4 E	-15.59	Pearson et al., 2008, data from supplementary information, found in the GSA repository, online.		Turborotalia ampliapertura	Turborotalia ampliapertura	2	-3.052	Excellent, glassy foraminifera
TDP	TDP 12		Kilwa Group clays, Tanzania	8.7 S	39.4 E	-15.59	Pearson et al., 2008, data from supplementary information, found in the GSA repository, online.		Turborotalia ampliapertura	Turborotalia ampliapertura	2	-3.008	Excellent, glassy foraminifera
TDP	TDP 12		Kilwa Group clays, Tanzania	8.7 S	39.4 E	-15.59	Pearson et al., 2008, data from supplementary information, found in the GSA repository, online.		Turborotalia ampliapertura	Turborotalia ampliapertura	2	-3.159	Excellent, glassy foraminifera
TDP	TDP 12		Kilwa Group clays, Tanzania	8.7 S	39.4 E	-15.59	Pearson et al., 2008, data from supplementary information, found in the GSA		Turborotalia ampliapertura	Turborotalia ampliapertura	2	-3.059	Excellent, glassy foraminifera

							repository, online.						
TDP	TDP 12		Kilwa Group clays, Tanzania	8.7 S	39.4 E	-15.59	Pearson et al., 2008, data from supplementary information, found in the GSA repository, online.		*Turborotalia ampliapertura*	*Turborotalia ampliapertura*	2	-3.092	Excellent, glassy foraminifera
TDP	TDP 12	From below the Hantkenina extinction	Kilwa Group clays, Tanzania	8.7 S	39.4 E	-15.59	Pearson et al. 2007, additional information from the Gsa repository	33.75 Ma	*Globoturborotalita ouachitaensis*	*Globoturborotalita ouachitaensis*	1	-3.42	Excellent, glassy foraminifera
TDP	TDP 12	From below the Hantkenina extinction	Kilwa Group clays, Tanzania	8.7 S	39.4 E	-15.59	Pearson et al. 2007, additional information from the Gsa repository	33.75 Ma	*Subbotina gortanii*	*Subbotina gortanii*	3	-3.42	Excellent, glassy foraminifera
TDP	TDP 12	From below the Hantkenina extinction	Kilwa Group clays, Tanzania	8.7 S	39.4 E	-15.59	Pearson et al. 2007, additional information from the Gsa repository	33.75 Ma	*Pseudohastigerina naguewichiensis*	*Pseudohastigerina naguewichiensis*	1	-3.23	Excellent, glassy foraminifera
TDP	TDP 12	From below the Hantkenina extinction	Kilwa Group clays, Tanzania	8.7 S	39.4 E	-15.59	Pearson et al. 2007, additional information from the Gsa repository	33.75 Ma	*Pseudohastigerina naguewichiensis*	*Pseudohastigerina naguewichiensis*	1	-3.23	Excellent, glassy foraminifera

TDP	TDP 12	From below the Hantkenina extinction	Kilwa Group clays, Tanzania	8.7 S	39.4 E	-15.59	Pearson et al. 2007, additional information from the Gsa repository	33.75 Ma	*Subbotina eocaena*	*Subbotina eocaena*	3	-3.07	Excellent, glassy foraminifera
TDP	TDP 12	From below the Hantkenina extinction	Kilwa Group clays, Tanzania	8.7 S	39.4 E	-15.59	Pearson et al. 2007, additional information from the Gsa repository	33.75 Ma	*Subbotina corpulenta*	*Subbotina corpulenta*	3	-3.02	Excellent, glassy foraminifera
TDP	TDP 12	From below the Hantkenina extinction	Kilwa Group clays, Tanzania	8.7 S	39.4 E	-15.59	Pearson et al. 2007, additional information from the Gsa repository	33.75 Ma	*Turborotalia ampliapertura*	*Turborotalia ampliapertura*	2	-3	Excellent, glassy foraminifera
TDP	TDP 12	From below the Hantkenina extinction	Kilwa Group clays, Tanzania	8.7 S	39.4 E	-15.59	Pearson et al. 2007, additional information from the Gsa repository	33.75 Ma	*Hantkenina nanggulanensis*	*Hantkenina nanggulanensis*	2	-2.93	Excellent, glassy foraminifera
TDP	TDP 12	From below the Hantkenina extinction	Kilwa Group clays, Tanzania	8.7 S	39.4 E	-15.59	Pearson et al. 2007, additional information from the Gsa repository	33.75 Ma	*Turborotalia cunialensis*	*Turborotalia cunialensis*	2	-2.89	Excellent, glassy foraminifera
TDP	TDP 12	From below the Hantkenina extinction	Kilwa Group clays, Tanzania	8.7 S	39.4 E	-15.59	Pearson et al. 2007, additional information from the Gsa repository	33.75 Ma	*Turborotalia cerroazuelensis*	*Turborotalia cerroazuelensis*	2	-2.76	Excellent, glassy foraminifera
TDP	TDP 12	From below the Hantkenina	Kilwa Group clays, Tanzania	8.7 S	39.4 E	-15.59	Pearson et al. 2007, additional information from the	33.75 Ma	*Cribrohantkenina inflata*	*Cribrohantkenina inflata*	2	-2.75	Excellent, glassy foraminifera

			extinction					Gsa repository						
	TDP	TDP 12	From below the Hantkenina extinction	Kilwa Group clays, Tanzania	8.7 S	39.4 E	-15.59	Pearson et al. 2007, additional information from the Gsa repository	33.75 Ma	*Dentoglobigerina galavisi*	*Dentoglobigerina galavisi*	3	-2.72	Excellent, glassy foraminifera
	TDP	TDP 12	From below the Hantkenina extinction	Kilwa Group clays, Tanzania	8.7 S	39.4 E	-15.59	Pearson et al. 2007, additional information from the Gsa repository	33.75 Ma	*Hantkenina nanggulanensis*	*Hantkenina nanggulanensis*	2	-2.61	Excellent, glassy foraminifera
	TDP	TDP 12	From below the Hantkenina extinction	Kilwa Group clays, Tanzania	8.7 S	39.4 E	-15.59	Pearson et al. 2007, additional information from the Gsa repository	33.75 Ma	*Dentoglobigerina tripartita*	*Dentoglobigerina tripartita*	3	-2.59	Excellent, glassy foraminifera
	TDP	TDP 12	From below the Hantkenina extinction	Kilwa Group clays, Tanzania	8.7 S	39.4 E	-15.59	Pearson et al. 2007, additional information from the Gsa repository	33.75 Ma	*Dentoglobigerina globularis*	*Dentoglobigerina globularis*	3	-2.52	Excellent, glassy foraminifera
	TDP	TDP 12	From below the Hantkenina extinction	Kilwa Group clays, Tanzania	8.7 S	39.4 E	-15.59	Pearson et al. 2007, additional information from the Gsa repository	33.75 Ma	*Turborotalia cocoaensis*	*Turborotalia cocoaensis*	2	-2.51	Excellent, glassy foraminifera
	TDP	TDP 12	From below the Hantkenina extinction	Kilwa Group clays, Tanzania	8.7 S	39.4 E	-15.59	Pearson et al. 2007, additional information from the Gsa repository	33.75 Ma	*Dentoglobigerina tripartita*	*Dentoglobigerina tripartita*	3	-2.32	Excellent, glassy foraminifera

TDP	TDP 12	From below the Hantkenina extinction	Kilwa Group clays, Tanzania	8.7 S	39.4 E	-15.59	Pearson et al. 2007, additional information from the Gsa repository	33.75 Ma	*Dentoglob. pseudovenezuelana*	*Dentoglob. pseudovenezuelana*	3	-2.31	Excellent, glassy foraminifera
TDP	TDP 12	From below the Hantkenina extinction	Kilwa Group clays, Tanzania	8.7 S	39.4 E	-15.59	Pearson et al. 2007, additional information from the Gsa repository	33.75 Ma	*Dentoglob. pseudovenezuelana*	*Dentoglob. pseudovenezuelana*	3	-1.91	Excellent, glassy foraminifera
	PP98-L11		Outcrop on the lower Kitunda slopes, near Lindi, Tanzania	9°59′35″ S	39°43′54″ E	-16.83	Pearson et al. 2001	36.8 + or - 1.6 Myr	*Pseudohastigerina micra*	*Pseudohastigerina micra*	1	-3.1	Excellent, glassy foraminifera
	PP98-L11		Outcrop on the lower Kitunda slopes, near Lindi, Tanzania	9°59′35″ S	39°42′52″ E	-16.83	Pearson et al. 2001	36.8 + or - 1.6 Myr	*Globigerinatheka semiinvoluta*	*Globigerinatheka semiinvoluta*	2	-3	Excellent, glassy foraminifera
	PP98-L11		Outcrop on the lower Kitunda slopes, near Lindi, Tanzania	9°59′35″ S	39°42′52″ E	-16.83	Pearson et al. 2001	36.8 + or - 1.6 Myr	*Globigerinatheka* spp.	*Globigerinatheka* spp.	2	-3.06	Excellent, glassy foraminifera
	PP98-L11		Outcrop on the lower Kitunda slopes, near Lindi, Tanzania	9°59′35″ S	39°42′52″ E	-16.83	Pearson et al. 2001	36.8 + or - 1.6 Myr	*Globoquadrina tripartita*	*Dentoglobigerina tripartita*	3	-2.61	Excellent, glassy foraminifera
	PP98-L11		Outcrop on the lower Kitunda slopes,	9°59′35″ S	39°42′52″ E	-16.83	Pearson et al. 2001	36.8 + or - 1.6 Myr	*Subbotina* spp.	*Subbotina* spp.	3	-2.59	Excellent, glassy foraminifera

		near Lindi, Tanzania										
	PP98-L11	Outcrop on the lower Kitunda slopes, near Lindi, Tanzania	9°59′35″ S	39°42′52″ E	-16.83	Pearson et al. 2001	36.8 + or - 1.6 Myr	*Turborotalia cerroazulensis*	*Turborotalia cerroazulensis*	2	-2.66	Excellent, glassy foraminifera
	PP98-L11	Outcrop on the lower Kitunda slopes, near Lindi, Tanzania	9°59′35″ S	39°42′52″ E	-16.83	Pearson et al. 2001	36.8 + or - 1.6 Myr	*Hantkenina nanggulanensis*	*Hantkenina nanggulanensis*	2	-2.82	Excellent, glassy foraminifera
	Cocoa Sands formation (Alabama)	Just above Zeuglodon bed, infield 100 yards south of Watervalley-Melvin Road, near old Cocoa Post Office, Alabama	31.93 N	88.5 W	27.99	Pearson et al. 2001	36.8 + or - 1.6 Myr	*Globigerina officinalis*	*Globigerina officinalis*	2	-2.32	Excellent, glassy foraminifera
	Cocoa Sands formation (Alabama)	Just above Zeuglodon bed, infield 100 yards south of Watervalley-Melvin Road, near old Cocoa Post Office, Alabama	31.93 N	88.5 W	27.99	Pearson et al. 2001	36.8 + or - 1.6 Myr	*Globoturborotalita martini*	*Globoturborotalita martini (Blow and Banner 1962)*	1	-2.5	Excellent, glassy foraminifera

Cocoa Sands formation (Alabama)		Just above Zeuglodon bed, infield 100 yards south of Watervalley-Melvin Road, near old Cocoa Post Office, Alabama	31.93 N	88.5 W	27.99	Pearson et al. 2001	36.8 + or - 1.6 Myr	*Subbotina linaperta*	*Subbotina linaperta*	3	-1.53	Excellent, glassy foraminifera
Cocoa Sands formation (Alabama)		Just above Zeuglodon bed, infield 100 yards south of Watervalley-Melvin Road, near old Cocoa Post Office, Alabama	31.93 N	88.5 W	27.99	Pearson et al. 2001	36.8 + or - 1.6 Myr	*Hantkenina primitiva*	*Hantkenina primitiva*	2	-1.76	Excellent, glassy foraminifera
Cocoa Sands formation (Alabama)		Just above Zeuglodon bed, infield 100 yards south of Watervalley-Melvin Road, near old Cocoa Post Office, Alabama	31.93 N	88.5 W	27.99	Pearson et al. 2001	36.8 + or - 1.6 Myr	*Globigerina* spp.	*Globigerina* spp.	2	-2	Excellent, glassy foraminifera

Cocoa Sands formation (Alabama)		Just above Zeuglodon bed, infield 100 yards south of Watervalley-Melvin Road, near old Cocoa Post Office, Alabama	31.93 N	88.5 W	27.99	Pearson et al. 2001	36.8 + or - 1.6 Myr	*Pseudohastigerina micra*	*Pseudohastigerina micra*	1	-2.48	Excellent, glassy foraminifera
Cocoa Sands formation (Alabama)		Just above Zeuglodon bed, infield 100 yards south of Watervalley-Melvin Road, near old Cocoa Post Office, Alabama	31.93 N	88.5 W	27.99	Pearson et al. 2001	36.8 + or - 1.6 Myr	*Globoquadrina tapiurensis*	*Dentoglobigerina tapiurensis*	3	-1.63	Excellent, glassy foraminifera
Cocoa Sands formation (Alabama)		Just above Zeuglodon bed, infield 100 yards south of Watervalley-Melvin Road, near old Cocoa Post Office, Alabama	31.93 N	88.5 W	27.99	Pearson et al. 2001	36.8 + or - 1.6 Myr	*Turborotalia pseudo-ampliapertura*	*Turborotalia pseudo-ampliapertura*	2	-1.53	Excellent, glassy foraminifera

	Cocoa Sands formation (Alabama)		Just above Zeuglodon bed, infield 100 yards south of Watervalley-Melvin Road, near old Cocoa Post Office, Alabama	31.93 N	88.5 W	27.99	Pearson et al. 2001	36.8 + or - 1.6 Myr	*Paragloborotalia inaequispira*	*Subbotina inaequispira*	3	-1.12	Excellent, glassy foraminifera
	Tanzania - NAM99 -01		From beside the Namadingura River, near Lindi, Tanzania	9°54'26"S	39°42'18"E	-16.76	Pearson et al. 2001	34.6 + or - 0.6 Myr	*Globoquadrina tripartita*	*Dentoglobigerina tripartita*	3	-2.48	Excellent, glassy foraminifera
	Tanzania - NAM99 -01		From beside the Namadingura River, near Lindi, Tanzania	9°54'26"S	39°42'18"E	-16.76	Pearson et al. 2001	34.6 + or - 0.6 Myr	*Hantkenina alabamensis*	*Hantkenina alabamensis*	2	-2.94	Excellent, glassy foraminifera
	Tanzania - NAM99 -01		From beside the Namadingura River, near Lindi, Tanzania	9°54'26"S	39°42'18"E	-16.76	Pearson et al. 2001	34.6 + or - 0.6 Myr	*Turborotalia pseudo-ampliapertura*	*Turborotalia pseudo-ampliapertura*	2	-2.95	Excellent, glassy foraminifera
	Tanzania - NAM99 -01		From beside the Namadingura River, near Lindi, Tanzania	9°54'26"S	39°42'18"E	-16.76	Pearson et al. 2001	34.6 + or - 0.6 Myr	*Turborotalia pomeroli*	*Turborotalia pomeroli*	2	-2.72	Excellent, glassy foraminifera
	Tanzania - NAM99 -01		From beside the Namadingura River, near Lindi, Tanzania	9°54'26"S	39°42'18"E	-16.76	Pearson et al. 2001	34.6 + or - 0.6 Myr	*Subbotina linaperta*	*Subbotina linaperta*	3	-2.51	Excellent, glassy foraminifera
	Tanzania - NAM99 -01		From beside the Namadingura River,	9°54'26"S	39°42'18"E	-16.76	Pearson et al. 2001	34.6 + or - 0.6 Myr	*Globoturborotalita* spp.	*Globoturborotalita* spp.	1	-3.41	Excellent, glassy foraminifera

		near Lindi, Tanzania									
	Tanzania - NAM99 -01		From beside the Namadingura River, near Lindi, Tanzania	9°54'26" S	39°42'18" E	- 16. 76	Pearson et al. 2001	34.6 + or - 0.6 Myr	*Pseudohastigerina micra*	*Pseudohastigerina micra*	1	- 3.0 9	Excellent, glassy foraminifera
	Tanzania - NAM99 -01		From beside the Namadingura River, near Lindi, Tanzania	9°54'26" S	39°42'18" E	- 16. 76	Pearson et al. 2001	34.6 + or - 0.6 Myr	*Paragloborotalia wilsoni*	*Parasubbotina wilsoni*	3	- 2.5 3	Excellent, glassy foraminifera
	Tanzania - NAM99 -01		From beside the Namadingura River, near Lindi, Tanzania	9°54'26" S	39°42'18" E	- 16. 76	Pearson et al. 2001	34.6 + or - 0.6 Myr	*Subbotina* spp.	*Subbotina* spp.	3	- 1.6 3	Excellent, glassy foraminifera
	Tanzania - NAM99 -01		From beside the Namadingura River, near Lindi, Tanzania	9°54'26" S	39°42'18" E	- 16. 76	Pearson et al. 2001	34.6 + or - 0.6 Myr	*Turborotalia cerroazulensis*	*Turborotalia cerroazulensis*	2	- 2.1 7	Excellent, glassy foraminifera
	Tanzania - NAM99 -01		From beside the Namadingura River, near Lindi, Tanzania	9°54'26" S	39°42'18" E	- 16. 76	Pearson et al. 2001	34.6 + or - 0.6 Myr	*Globoquadrina pseudo-venezuelana*	*Dentoglobigerina pseudovenezuelana*	3	-1.7	Excellent, glassy foraminifera
	Tanzania - NAM99 -01		From beside the Namadingura River, near Lindi, Tanzania	9°54'26" S	39°42'18" E	- 16. 76	Pearson et al. 2001	34.6 + or - 0.6 Myr	*Turborotalia cocoaensis*	*Turborotalia cocoaensis*	2	- 2.2 1	Excellent, glassy foraminifera
	Tanzania - NAM99 -01		From beside the Namadingura River, near Lindi, Tanzania	9°54'26" S	39°42'18" E	- 16. 76	Pearson et al. 2001	34.6 + or - 0.6 Myr	*Cribrohantkenina inflata*	*Cribrohantkenina inflata*	2	- 2.5 1	Excellent, glassy foraminifera

120	748b		Kerguelen Plateau, Southern Ocean (Indian sector)	58°26.45' S	78°58.89' E	-55.3	Bohaty et al. 2012	34.1 Ma to 35.0 Ma	*Subbotina angiporoides*	*Subbotina angiporoides*	3	0.9	Poor, recrystallised foraminifera.
120	748b		Kerguelen Plateau, Southern Ocean (Indian sector)	58°26.45' S	78°58.89' E	-55.3	Bohaty et al. 2012	34.1 Ma to 35.0 Ma	*Subbotina angiporoides*	*Subbotina angiporoides*	3	0.95	Poor, recrystallised foraminifera.
120	748b		Kerguelen Plateau, Southern Ocean (Indian sector)	58°26.45' S	78°58.89' E	-55.3	Bohaty et al. 2012	34.1 Ma to 35.0 Ma	*Subbotina angiporoides*	*Subbotina angiporoides*	3	0.95	Poor, recrystallised foraminifera.
120	748b		Kerguelen Plateau, Southern Ocean (Indian sector)	58°26.45' S	78°58.89' E	-55.3	Bohaty et al. 2012	34.1 Ma to 35.0 Ma	*Subbotina angiporoides*	*Subbotina angiporoides*	3	0.95	Poor, recrystallised foraminifera.
120	748b		Kerguelen Plateau, Southern Ocean (Indian sector)	58°26.45' S	78°58.89' E	-55.3	Bohaty et al. 2012	34.1 Ma to 35.0 Ma	*Subbotina angiporoides*	*Subbotina angiporoides*	3	0.95	Poor, recrystallised foraminifera.
120	748b		Kerguelen Plateau, Southern Ocean (Indian sector)	58°26.45' S	78°58.89' E	-55.3	Bohaty et al. 2012	34.1 Ma to 35.0 Ma	*Subbotina angiporoides*	*Subbotina angiporoides*	3	0.95	Poor, recrystallised foraminifera.
120	748b		Kerguelen Plateau, Southern Ocean (Indian sector)	58°26.45' S	78°58.89' E	-55.3	Bohaty et al. 2012	34.1 Ma to 35.0 Ma	*Subbotina angiporoides*	*Subbotina angiporoides*	3	1	Poor, recrystallised foraminifera.
120	748b		Kerguelen Plateau, Southern Ocean (Indian sector)	58°26.45' S	78°58.89' E	-55.3	Bohaty et al. 2012	34.1 Ma to 35.0 Ma	*Subbotina angiporoides*	*Subbotina angiporoides*	3	1	Poor, recrystallised foraminifera.

120	748b			Kerguelen Plateau, Southern Ocean (Indian sector)	58°26.45'S	78°58.89'E	-55.3	Bohaty et al. 2012	34.1 Ma to 35.0 Ma	*Subbotina angiporoides*	*Subbotina angiporoides*	3	1.1	Poor, recrystallised foraminifera.
120	748b			Kerguelen Plateau, Southern Ocean (Indian sector)	58°26.45'S	78°58.89'E	-55.3	Bohaty et al. 2012	34.1 Ma to 35.0 Ma	*Subbotina angiporoides*	*Subbotina angiporoides*	3	1.1	Poor, recrystallised foraminifera.
120	748b			Kerguelen Plateau, Southern Ocean (Indian sector)	58°26.45'S	78°58.89'E	-55.3	Bohaty et al. 2012	34.1 Ma to 35.0 Ma	*Subbotina angiporoides*	*Subbotina angiporoides*	3	1.1	Poor, recrystallised foraminifera.
120	748b			Kerguelen Plateau, Southern Ocean (Indian sector)	58°26.45'S	78°58.89'E	-55.3	Bohaty et al. 2012	34.1 Ma to 35.0 Ma	*Subbotina angiporoides*	*Subbotina angiporoides*	3	1.1	Poor, recrystallised foraminifera.
120	748b			Kerguelen Plateau, Southern Ocean (Indian sector)	58°26.45'S	78°58.89'E	-55.3	Bohaty et al. 2012	34.1 Ma to 35.0 Ma	*Subbotina angiporoides*	*Subbotina angiporoides*	3	1.1	Poor, recrystallised foraminifera.
120	748b			Kerguelen Plateau, Southern Ocean (Indian sector)	58°26.45'S	78°58.89'E	-55.3	Bohaty et al. 2012	34.1 Ma to 35.0 Ma	*Subbotina angiporoides*	*Subbotina angiporoides*	3	1.1	Poor, recrystallised foraminifera.
120	748b			Kerguelen Plateau, Southern Ocean (Indian sector)	58°26.45'S	78°58.89'E	-55.3	Bohaty et al. 2012	34.1 Ma to 35.0 Ma	*Subbotina angiporoides*	*Subbotina angiporoides*	3	1.1	Poor, recrystallised foraminifera.
120	748b			Kerguelen Plateau, Southern Ocean (Indian sector)	58°26.45'S	78°58.89'E	-55.3	Bohaty et al. 2012	34.1 Ma to 35.0 Ma	*Subbotina angiporoides*	*Subbotina angiporoides*	3	1.1	Poor, recrystallised foraminifera.

120	748b		Kerguelen Plateau, Southern Ocean (Indian sector)	58°26.45' S	78°58.89' E	-55.3	Bohaty et al. 2012	34.1 Ma to 35.0 Ma	*Subbotina angiporoides*	*Subbotina angiporoides*	3	1.1	Poor, recrystalli sed foraminife ra.
120	748b		Kerguelen Plateau, Southern Ocean (Indian sector)	58°26.45' S	78°58.89' E	-55.3	Bohaty et al. 2012	34.1 Ma to 35.0 Ma	*Subbotina angiporoides*	*Subbotina angiporoides*	3	1.1	Poor, recrystalli sed foraminife ra.
120	748b		Kerguelen Plateau, Southern Ocean (Indian sector)	58°26.45' S	78°58.89' E	-55.3	Bohaty et al. 2012	34.1 Ma to 35.0 Ma	*Subbotina angiporoides*	*Subbotina angiporoides*	3	1.2	Poor, recrystalli sed foraminife ra.
120	748b		Kerguelen Plateau, Southern Ocean (Indian sector)	58°26.45' S	78°58.89' E	-55.3	Bohaty et al. 2012	34.1 Ma to 35.0 Ma	*Subbotina angiporoides*	*Subbotina angiporoides*	3	1.2	Poor, recrystalli sed foraminife ra.
120	748b		Kerguelen Plateau, Southern Ocean (Indian sector)	58°26.45' S	78°58.89' E	-55.3	Bohaty et al. 2012	34.1 Ma to 35.0 Ma	*Subbotina angiporoides*	*Subbotina angiporoides*	3	1.2	Poor, recrystalli sed foraminife ra.
120	748b		Kerguelen Plateau, Southern Ocean (Indian sector)	58°26.45' S	78°58.89' E	-55.3	Bohaty et al. 2012	34.1 Ma to 35.0 Ma	*Subbotina angiporoides*	*Subbotina angiporoides*	3	1.2	Poor, recrystalli sed foraminife ra.
120	748b		Kerguelen Plateau, Southern Ocean (Indian sector)	58°26.45' S	78°58.89' E	-55.3	Bohaty et al. 2012	34.1 Ma to 35.0 Ma	*Subbotina angiporoides*	*Subbotina angiporoides*	3	1.2	Poor, recrystalli sed foraminife ra.
120	748b		Kerguelen Plateau, Southern Ocean (Indian sector)	58°26.45' S	78°58.89' E	-55.3	Bohaty et al. 2012	34.1 Ma to 35.0 Ma	*Subbotina angiporoides*	*Subbotina angiporoides*	3	1.2	Poor, recrystalli sed foraminife ra.

120	748b		Kerguelen Plateau, Southern Ocean (Indian sector)	58°26.45' S	78°58.89' E	-55.3	Bohaty et al. 2012	34.1 Ma to 35.0 Ma	*Subbotina angiporoides*	*Subbotina angiporoides*	3	1.3	Poor, recrystallised foraminifera.
120	748b		Kerguelen Plateau, Southern Ocean (Indian sector)	58°26.45' S	78°58.89' E	-55.3	Bohaty et al. 2012	34.1 Ma to 35.0 Ma	*Subbotina angiporoides*	*Subbotina angiporoides*	3	1.3	Poor, recrystallised foraminifera.
120	748b		Kerguelen Plateau, Southern Ocean (Indian sector)	58°26.45' S	78°58.89' E	-55.3	Bohaty et al. 2012	34.1 Ma to 35.0 Ma	*Subbotina angiporoides*	*Subbotina angiporoides*	3	1.3	Poor, recrystallised foraminifera.
120	748b		Kerguelen Plateau, Southern Ocean (Indian sector)	58°26.45' S	78°58.89' E	-55.3	Bohaty et al. 2012	34.1 Ma to 35.0 Ma	*Subbotina angiporoides*	*Subbotina angiporoides*	3	1.3	Poor, recrystallised foraminifera.
120	748b		Kerguelen Plateau, Southern Ocean (Indian sector)	58°26.45' S	78°58.89' E	-55.3	Bohaty et al. 2012	34.1 Ma to 35.0 Ma	*Subbotina angiporoides*	*Subbotina angiporoides*	3	1.3	Poor, recrystallised foraminifera.
120	748b		Kerguelen Plateau, Southern Ocean (Indian sector)	58°26.45' S	78°58.89' E	-55.3	Bohaty et al. 2012	34.1 Ma to 35.0 Ma	*Subbotina angiporoides*	*Subbotina angiporoides*	3	1.3	Poor, recrystallised foraminifera.
120	748b		Kerguelen Plateau, Southern Ocean (Indian sector)	58°26.45' S	78°58.89' E	-55.3	Bohaty et al. 2012	34.1 Ma to 35.0 Ma	*Subbotina angiporoides*	*Subbotina angiporoides*	3	1.3	Poor, recrystallised foraminifera.
120	748b		Kerguelen Plateau, Southern Ocean (Indian sector)	58°26.45' S	78°58.89' E	-55.3	Bohaty et al. 2012	34.1 Ma to 35.0 Ma	*Subbotina angiporoides*	*Subbotina angiporoides*	3	1.3	Poor, recrystallised foraminifera.

120	748b		Kerguelen Plateau, Southern Ocean (Indian sector)	58°26.45' S	78°58.89' E	-55.3	Bohaty et al. 2012	34.1 Ma to 35.0 Ma	*Subbotina angiporoides*	*Subbotina angiporoides*	3	1.3	Poor, recrystallised foraminifera.
120	748b		Kerguelen Plateau, Southern Ocean (Indian sector)	58°26.45' S	78°58.89' E	-55.3	Bohaty et al. 2012	34.1 Ma to 35.0 Ma	*Subbotina angiporoides*	*Subbotina angiporoides*	3	1.3	Poor, recrystallised foraminifera.
120	748b		Kerguelen Plateau, Southern Ocean (Indian sector)	58°26.45' S	78°58.89' E	-55.3	Bohaty et al. 2012	34.1 Ma to 35.0 Ma	*Subbotina angiporoides*	*Subbotina angiporoides*	3	1.3	Poor, recrystallised foraminifera.
120	748b		Kerguelen Plateau, Southern Ocean (Indian sector)	58°26.45' S	78°58.89' E	-55.3	Bohaty et al. 2012	34.1 Ma to 35.0 Ma	*Subbotina angiporoides*	*Subbotina angiporoides*	3	1.35	Poor, recrystallised foraminifera.
120	748b		Kerguelen Plateau, Southern Ocean (Indian sector)	58°26.45' S	78°58.89' E	-55.3	Bohaty et al. 2012	34.1 Ma to 35.0 Ma	*Subbotina angiporoides*	*Subbotina angiporoides*	3	1.35	Poor, recrystallised foraminifera.
120	748b		Kerguelen Plateau, Southern Ocean (Indian sector)	58°26.45' S	78°58.89' E	-55.3	Bohaty et al. 2012	34.1 Ma to 35.0 Ma	*Subbotina angiporoides*	*Subbotina angiporoides*	3	1.35	Poor, recrystallised foraminifera.
120	748b		Kerguelen Plateau, Southern Ocean (Indian sector)	58°26.45' S	78°58.89' E	-55.3	Bohaty et al. 2012	34.1 Ma to 35.0 Ma	*Subbotina angiporoides*	*Subbotina angiporoides*	3	1.35	Poor, recrystallised foraminifera.
120	748b		Kerguelen Plateau, Southern Ocean (Indian sector)	58°26.45' S	78°58.89' E	-55.3	Bohaty et al. 2012	34.1 Ma to 35.0 Ma	*Subbotina angiporoides*	*Subbotina angiporoides*	3	1.4	Poor, recrystallised foraminifera.

120	748b		Kerguelen Plateau, Southern Ocean (Indian sector)	58°26.45'S	78°58.89'E	-55.3	Bohaty et al. 2012	34.1 Ma to 35.0 Ma	*Subbotina angiporoides*	*Subbotina angiporoides*	3	1.4	Poor, recrystallised foraminifera.
120	748b		Kerguelen Plateau, Southern Ocean (Indian sector)	58°26.45'S	78°58.89'E	-55.3	Bohaty et al. 2012	34.1 Ma to 35.0 Ma	*Subbotina angiporoides*	*Subbotina angiporoides*	3	1.4	Poor, recrystallised foraminifera.
120	748b		Kerguelen Plateau, Southern Ocean (Indian sector)	58°26.45'S	78°58.89'E	-55.3	Bohaty et al. 2012	34.1 Ma to 35.0 Ma	*Subbotina angiporoides*	*Subbotina angiporoides*	3	1.4	Poor, recrystallised foraminifera.
120	748b		Kerguelen Plateau, Southern Ocean (Indian sector)	58°26.45'S	78°58.89'E	-55.3	Bohaty et al. 2012	34.1 Ma to 35.0 Ma	*Subbotina angiporoides*	*Subbotina angiporoides*	3	1.45	Poor, recrystallised foraminifera.
120	748b		Kerguelen Plateau, Southern Ocean (Indian sector)	58°26.45'S	78°58.89'E	-55.3	Bohaty et al. 2012	34.1 Ma to 35.0 Ma	*Subbotina angiporoides*	*Subbotina angiporoides*	3	1.45	Poor, recrystallised foraminifera.
120	748b		Kerguelen Plateau, Southern Ocean (Indian sector)	58°26.45'S	78°58.89'E	-55.3	Bohaty et al. 2012	34.1 Ma to 35.0 Ma	*Subbotina angiporoides*	*Subbotina angiporoides*	3	1.45	Poor, recrystallised foraminifera.
120	748b		Kerguelen Plateau, Southern Ocean (Indian sector)	58°26.45'S	78°58.89'E	-55.3	Bohaty et al. 2012	34.1 Ma to 35.0 Ma	*Subbotina angiporoides*	*Subbotina angiporoides*	3	1.45	Poor, recrystallised foraminifera.
120	748b		Kerguelen Plateau, Southern Ocean (Indian sector)	58°26.45'S	78°58.89'E	-55.3	Bohaty et al. 2012	34.1 Ma to 35.0 Ma	*Subbotina angiporoides*	*Subbotina angiporoides*	3	1.45	Poor, recrystallised foraminifera.

120	748b		Kerguelen Plateau, Southern Ocean (Indian sector)	58°26.45' S	78°58.89' E	-55.3	Bohaty et al. 2012	34.1 Ma to 35.0 Ma	*Subbotina angiporoides*	*Subbotina angiporoides*	3	1.45	Poor, recrystallised foraminifera.
120	748b		Kerguelen Plateau, Southern Ocean (Indian sector)	58°26.45' S	78°58.89' E	-55.3	Bohaty et al. 2012	34.1 Ma to 35.0 Ma	*Subbotina angiporoides*	*Subbotina angiporoides*	3	1.5	Poor, recrystallised foraminifera.
120	748b		Kerguelen Plateau, Southern Ocean (Indian sector)	58°26.45' S	78°58.89' E	-55.3	Bohaty et al. 2012	34.1 Ma to 35.0 Ma	*Subbotina angiporoides*	*Subbotina angiporoides*	3	1.55	Poor, recrystallised foraminifera.
119	744a		Kerguelen Plateau, Southern Ocean (Indian sector)	61°34.66' S	80°35.46' E	-58.29	Bohaty et al. 2012	34.1 Ma to 35.0 Ma	*Subbotina angiporoides*	*Subbotina angiporoides*	3	1.75	Poor, recrystallised foraminifera.
119	744a		Kerguelen Plateau, Southern Ocean (Indian sector)	61°34.66' S	80°35.46' E	-58.29	Bohaty et al. 2012	34.1 Ma to 35.0 Ma	*Subbotina angiporoides*	*Subbotina angiporoides*	3	1.75	Poor, recrystallised foraminifera.
119	744a		Kerguelen Plateau, Southern Ocean (Indian sector)	61°34.66' S	80°35.46' E	-58.29	Bohaty et al. 2012	34.1 Ma to 35.0 Ma	*Subbotina angiporoides*	*Subbotina angiporoides*	3	1.75	Poor, recrystallised foraminifera.
119	744a		Kerguelen Plateau, Southern Ocean (Indian sector)	61°34.66' S	80°35.46' E	-58.29	Bohaty et al. 2012	34.1 Ma to 35.0 Ma	*Subbotina angiporoides*	*Subbotina angiporoides*	3	1.75	Poor, recrystallised foraminifera.
119	744a		Kerguelen Plateau, Southern Ocean (Indian sector)	61°34.66' S	80°35.46' E	-58.29	Bohaty et al. 2012	34.1 Ma to 35.0 Ma	*Subbotina angiporoides*	*Subbotina angiporoides*	3	1.8	Poor, recrystallised foraminifera.

119	744a		Kerguelen Plateau, Southern Ocean (Indian sector)	61°34.66' S	80°35.46' E	-58.29	Bohaty et al. 2012	34.1 Ma to 35.0 Ma	*Subbotina angiporoides*	*Subbotina angiporoides*	3	1.8	Poor, recrystalli sed foraminife ra.
119	744a		Kerguelen Plateau, Southern Ocean (Indian sector)	61°34.66' S	80°35.46' E	-58.29	Bohaty et al. 2012	34.1 Ma to 35.0 Ma	*Subbotina angiporoides*	*Subbotina angiporoides*	3	1.8	Poor, recrystalli sed foraminife ra.
119	744a		Kerguelen Plateau, Southern Ocean (Indian sector)	61°34.66' S	80°35.46' E	-58.29	Bohaty et al. 2012	34.1 Ma to 35.0 Ma	*Subbotina angiporoides*	*Subbotina angiporoides*	3	1.8	Poor, recrystalli sed foraminife ra.
119	744a		Kerguelen Plateau, Southern Ocean (Indian sector)	61°34.66' S	80°35.46' E	-58.29	Bohaty et al. 2012	34.1 Ma to 35.0 Ma	*Subbotina angiporoides*	*Subbotina angiporoides*	3	1.8	Poor, recrystalli sed foraminife ra.
119	744a		Kerguelen Plateau, Southern Ocean (Indian sector)	61°34.66' S	80°35.46' E	-58.29	Bohaty et al. 2012	34.1 Ma to 35.0 Ma	*Subbotina angiporoides*	*Subbotina angiporoides*	3	1.75	Poor, recrystalli sed foraminife ra.
119	744a		Kerguelen Plateau, Southern Ocean (Indian sector)	61°34.66' S	80°35.46' E	-58.29	Bohaty et al. 2012	34.1 Ma to 35.0 Ma	*Subbotina angiporoides*	*Subbotina angiporoides*	3	1.75	Poor, recrystalli sed foraminife ra.
119	744a		Kerguelen Plateau, Southern Ocean (Indian sector)	61°34.66' S	80°35.46' E	-58.29	Bohaty et al. 2012	34.1 Ma to 35.0 Ma	*Subbotina angiporoides*	*Subbotina angiporoides*	3	1.8	Poor, recrystalli sed foraminife ra.
119	744a		Kerguelen Plateau, Southern Ocean (Indian sector)	61°34.66' S	80°35.46' E	-58.29	Bohaty et al. 2012	34.1 Ma to 35.0 Ma	*Subbotina angiporoides*	*Subbotina angiporoides*	3	1.8	Poor, recrystalli sed foraminife ra.

119	744a		Kerguelen Plateau, Southern Ocean (Indian sector)	61°34.66' S	80°35.46' E	-58.29	Bohaty et al. 2012	34.1 Ma to 35.0 Ma	*Subbotina angiporoides*	*Subbotina angiporoides*	3	1.85	Poor, recrystalli sed foraminife ra.
119	744a		Kerguelen Plateau, Southern Ocean (Indian sector)	61°34.66' S	80°35.46' E	-58.29	Bohaty et al. 2012	34.1 Ma to 35.0 Ma	*Subbotina angiporoides*	*Subbotina angiporoides*	3	1.85	Poor, recrystalli sed foraminife ra.
119	744a		Kerguelen Plateau, Southern Ocean (Indian sector)	61°34.66' S	80°35.46' E	-58.29	Bohaty et al. 2012	34.1 Ma to 35.0 Ma	*Subbotina angiporoides*	*Subbotina angiporoides*	3	1.85	Poor, recrystalli sed foraminife ra.
119	744a		Kerguelen Plateau, Southern Ocean (Indian sector)	61°34.66' S	80°35.46' E	-58.29	Bohaty et al. 2012	34.1 Ma to 35.0 Ma	*Subbotina angiporoides*	*Subbotina angiporoides*	3	1.9	Poor, recrystalli sed foraminife ra.
119	744a		Kerguelen Plateau, Southern Ocean (Indian sector)	61°34.66' S	80°35.46' E	-58.29	Bohaty et al. 2012	34.1 Ma to 35.0 Ma	*Subbotina angiporoides*	*Subbotina angiporoides*	3	1.9	Poor, recrystalli sed foraminife ra.
119	744a		Kerguelen Plateau, Southern Ocean (Indian sector)	61°34.66' S	80°35.46' E	-58.29	Bohaty et al. 2012	34.1 Ma to 35.0 Ma	*Subbotina angiporoides*	*Subbotina angiporoides*	3	1.9	Poor, recrystalli sed foraminife ra.
119	744a		Kerguelen Plateau, Southern Ocean (Indian sector)	61°34.66' S	80°35.46' E	-58.29	Bohaty et al. 2012	34.1 Ma to 35.0 Ma	*Subbotina angiporoides*	*Subbotina angiporoides*	3	1.95	Poor, recrystalli sed foraminife ra.
119	744a		Kerguelen Plateau, Southern Ocean (Indian sector)	61°34.66' S	80°35.46' E	-58.29	Bohaty et al. 2012	34.1 Ma to 35.0 Ma	*Subbotina angiporoides*	*Subbotina angiporoides*	3	1.95	Poor, recrystalli sed foraminife ra.

119	744a		Kerguelen Plateau, Southern Ocean (Indian sector)	61°34.66' S	80°35.46' E	-58.29	Bohaty et al. 2012	34.1 Ma to 35.0 Ma	Subbotina angiporoides	Subbotina angiporoides	3	1.95	Poor, recrystallised foraminifera.
119	744a		Kerguelen Plateau, Southern Ocean (Indian sector)	61°34.66' S	80°35.46' E	-58.29	Bohaty et al. 2012	34.1 Ma to 35.0 Ma	Subbotina angiporoides	Subbotina angiporoides	3	1.95	Poor, recrystallised foraminifera.
119	744a		Kerguelen Plateau, Southern Ocean (Indian sector)	61°34.66' S	80°35.46' E	-58.29	Bohaty et al. 2012	34.1 Ma to 35.0 Ma	Subbotina angiporoides	Subbotina angiporoides	3	1.95	Poor, recrystallised foraminifera.
119	744a		Kerguelen Plateau, Southern Ocean (Indian sector)	61°34.66' S	80°35.46' E	-58.29	Bohaty et al. 2012	34.1 Ma to 35.0 Ma	Subbotina angiporoides	Subbotina angiporoides	3	1.95	Poor, recrystallised foraminifera.
119	744a		Kerguelen Plateau, Southern Ocean (Indian sector)	61°34.66' S	80°35.46' E	-58.29	Bohaty et al. 2012	34.1 Ma to 35.0 Ma	Subbotina angiporoides	Subbotina angiporoides	3	1.95	Poor, recrystallised foraminifera.
119	744a		Kerguelen Plateau, Southern Ocean (Indian sector)	61°34.66' S	80°35.46' E	-58.29	Bohaty et al. 2012	34.1 Ma to 35.0 Ma	Subbotina angiporoides	Subbotina angiporoides	3	1.95	Poor, recrystallised foraminifera.
119	744a		Kerguelen Plateau, Southern Ocean (Indian sector)	61°34.66' S	80°35.46' E	-58.29	Bohaty et al. 2012	34.1 Ma to 35.0 Ma	Subbotina angiporoides	Subbotina angiporoides	3	1.95	Poor, recrystallised foraminifera.
119	744a		Kerguelen Plateau, Southern Ocean (Indian sector)	61°34.66' S	80°35.46' E	-58.29	Bohaty et al. 2012	34.1 Ma to 35.0 Ma	Subbotina angiporoides	Subbotina angiporoides	3	1.98	Poor, recrystallised foraminifera.

119	744a		Kerguelen Plateau, Southern Ocean (Indian sector)	61°34.66' S	80°35.46' E	- 58. 29	Bohaty et al. 2012	34.1 Ma to 35.0 Ma	Subbotina angiporoides	Subbotina angiporoides	3	1.9 8	Poor, recrystalli sed foraminife ra.
119	744a		Kerguelen Plateau, Southern Ocean (Indian sector)	61°34.66' S	80°35.46' E	- 58. 29	Bohaty et al. 2012	34.1 Ma to 35.0 Ma	Subbotina angiporoides	Subbotina angiporoides	3	1.9 8	Poor, recrystalli sed foraminife ra.
119	744a		Kerguelen Plateau, Southern Ocean (Indian sector)	61°34.66' S	80°35.46' E	- 58. 29	Bohaty et al. 2012	34.1 Ma to 35.0 Ma	Subbotina angiporoides	Subbotina angiporoides	3	1.9 8	Poor, recrystalli sed foraminife ra.
119	744a		Kerguelen Plateau, Southern Ocean (Indian sector)	61°34.66' S	80°35.46' E	- 58. 29	Bohaty et al. 2012	34.1 Ma to 35.0 Ma	Subbotina angiporoides	Subbotina angiporoides	3	1.9 8	Poor, recrystalli sed foraminife ra.
119	744a		Kerguelen Plateau, Southern Ocean (Indian sector)	61°34.66' S	80°35.46' E	- 58. 29	Bohaty et al. 2012	34.1 Ma to 35.0 Ma	Subbotina angiporoides	Subbotina angiporoides	3	1.9 8	Poor, recrystalli sed foraminife ra.
119	744a		Kerguelen Plateau, Southern Ocean (Indian sector)	61°34.66' S	80°35.46' E	- 58. 29	Bohaty et al. 2012	34.1 Ma to 35.0 Ma	Subbotina angiporoides	Subbotina angiporoides	3	1.5	Poor, recrystalli sed foraminife ra.
119	744a		Kerguelen Plateau, Southern Ocean (Indian sector)	61°34.66' S	80°35.46' E	- 58. 29	Bohaty et al. 2012	34.1 Ma to 35.0 Ma	Subbotina angiporoides	Subbotina angiporoides	3	1.5	Poor, recrystalli sed foraminife ra.
119	744a		Kerguelen Plateau, Southern Ocean (Indian sector)	61°34.66' S	80°35.46' E	- 58. 29	Bohaty et al. 2012	34.1 Ma to 35.0 Ma	Subbotina angiporoides	Subbotina angiporoides	3	1.5 5	Poor, recrystalli sed foraminife ra.

119	744a		Kerguelen Plateau, Southern Ocean (Indian sector)	61°34.66'S	80°35.46'E	-58.29	Bohaty et al. 2012	34.1 Ma to 35.0 Ma	Subbotina angiporoides	Subbotina angiporoides	3	1.55	Poor, recrystallised foraminifera.
119	744a		Kerguelen Plateau, Southern Ocean (Indian sector)	61°34.66'S	80°35.46'E	-58.29	Bohaty et al. 2012	34.1 Ma to 35.0 Ma	Subbotina angiporoides	Subbotina angiporoides	3	1.55	Poor, recrystallised foraminifera.
119	744a		Kerguelen Plateau, Southern Ocean (Indian sector)	61°34.66'S	80°35.46'E	-58.29	Bohaty et al. 2012	34.1 Ma to 35.0 Ma	Subbotina angiporoides	Subbotina angiporoides	3	1.55	Poor, recrystallised foraminifera.
119	744a		Kerguelen Plateau, Southern Ocean (Indian sector)	61°34.66'S	80°35.46'E	-58.29	Bohaty et al. 2012	34.1 Ma to 35.0 Ma	Subbotina angiporoides	Subbotina angiporoides	3	1.6	Poor, recrystallised foraminifera.
119	744a		Kerguelen Plateau, Southern Ocean (Indian sector)	61°34.66'S	80°35.46'E	-58.29	Bohaty et al. 2012	34.1 Ma to 35.0 Ma	Subbotina angiporoides	Subbotina angiporoides	3	1.5	Poor, recrystallised foraminifera.
119	744a		Kerguelen Plateau, Southern Ocean (Indian sector)	61°34.66'S	80°35.46'E	-58.29	Bohaty et al. 2012	34.1 Ma to 35.0 Ma	Subbotina angiporoides	Subbotina angiporoides	3	1.5	Poor, recrystallised foraminifera.
119	744a		Kerguelen Plateau, Southern Ocean (Indian sector)	61°34.66'S	80°35.46'E	-58.29	Bohaty et al. 2012	34.1 Ma to 35.0 Ma	Subbotina angiporoides	Subbotina angiporoides	3	1.5	Poor, recrystallised foraminifera.
119	744a		Kerguelen Plateau, Southern Ocean (Indian sector)	61°34.66'S	80°35.46'E	-58.29	Bohaty et al. 2012	34.1 Ma to 35.0 Ma	Subbotina angiporoides	Subbotina angiporoides	3	1.5	Poor, recrystallised foraminifera.

119	744a		Kerguelen Plateau, Southern Ocean (Indian sector)	61°34.66' S	80°35.46' E	-58.29	Bohaty et al. 2012	34.1 Ma to 35.0 Ma	*Subbotina angiporoides*	*Subbotina angiporoides*	3	1.5	Poor, recrystallised foraminifera.
119	738b		Kerguelen Plateau, Southern Ocean (Indian sector)	62°42.54' S	82°47.25' E	-59.25	Bohaty et al. 2012	34.1 Ma to 35.0 Ma	*Subbotina angiporoides*	*Subbotina angiporoides*	3	1.25	Poor, recrystallised foraminifera.
119	738b		Kerguelen Plateau, Southern Ocean (Indian sector)	62°42.54' S	82°47.25' E	-59.25	Bohaty et al. 2012	34.1 Ma to 35.0 Ma	*Subbotina angiporoides*	*Subbotina angiporoides*	3	1.3	Poor, recrystallised foraminifera.
119	738b		Kerguelen Plateau, Southern Ocean (Indian sector)	62°42.54' S	82°47.25' E	-59.25	Bohaty et al. 2012	34.1 Ma to 35.0 Ma	*Subbotina angiporoides*	*Subbotina angiporoides*	3	1.3	Poor, recrystallised foraminifera.
119	738b		Kerguelen Plateau, Southern Ocean (Indian sector)	62°42.54' S	82°47.25' E	-59.25	Bohaty et al. 2012	34.1 Ma to 35.0 Ma	*Subbotina angiporoides*	*Subbotina angiporoides*	3	1.3	Poor, recrystallised foraminifera.
119	738b		Kerguelen Plateau, Southern Ocean (Indian sector)	62°42.54' S	82°47.25' E	-59.25	Bohaty et al. 2012	34.1 Ma to 35.0 Ma	*Subbotina angiporoides*	*Subbotina angiporoides*	3	1.3	Poor, recrystallised foraminifera.
119	738b		Kerguelen Plateau, Southern Ocean (Indian sector)	62°42.54' S	82°47.25' E	-59.25	Bohaty et al. 2012	34.1 Ma to 35.0 Ma	*Subbotina angiporoides*	*Subbotina angiporoides*	3	1.35	Poor, recrystallised foraminifera.
119	738b		Kerguelen Plateau, Southern Ocean (Indian sector)	62°42.54' S	82°47.25' E	-59.25	Bohaty et al. 2012	34.1 Ma to 35.0 Ma	*Subbotina angiporoides*	*Subbotina angiporoides*	3	1.35	Poor, recrystallised foraminifera.

119	738b			Kerguelen Plateau, Southern Ocean (Indian sector)	62°42.54' S	82°47.25' E	-59.25	Bohaty et al. 2012	34.1 Ma to 35.0 Ma	*Subbotina angiporoides*	*Subbotina angiporoides*	3	1.35	Poor, recrystallised foraminifera.
119	738b			Kerguelen Plateau, Southern Ocean (Indian sector)	62°42.54' S	82°47.25' E	-59.25	Bohaty et al. 2012	34.1 Ma to 35.0 Ma	*Subbotina angiporoides*	*Subbotina angiporoides*	3	1.35	Poor, recrystallised foraminifera.
119	738b			Kerguelen Plateau, Southern Ocean (Indian sector)	62°42.54' S	82°47.25' E	-59.25	Bohaty et al. 2012	34.1 Ma to 35.0 Ma	*Subbotina angiporoides*	*Subbotina angiporoides*	3	1.35	Poor, recrystallised foraminifera.
119	738b			Kerguelen Plateau, Southern Ocean (Indian sector)	62°42.54' S	82°47.25' E	-59.25	Bohaty et al. 2012	34.1 Ma to 35.0 Ma	*Subbotina angiporoides*	*Subbotina angiporoides*	3	1.35	Poor, recrystallised foraminifera.
119	738b			Kerguelen Plateau, Southern Ocean (Indian sector)	62°42.54' S	82°47.25' E	-59.25	Bohaty et al. 2012	34.1 Ma to 35.0 Ma	*Subbotina angiporoides*	*Subbotina angiporoides*	3	1.4	Poor, recrystallised foraminifera.
119	738b			Kerguelen Plateau, Southern Ocean (Indian sector)	62°42.54' S	82°47.25' E	-59.25	Bohaty et al. 2012	34.1 Ma to 35.0 Ma	*Subbotina angiporoides*	*Subbotina angiporoides*	3	1.4	Poor, recrystallised foraminifera.
119	738b			Kerguelen Plateau, Southern Ocean (Indian sector)	62°42.54' S	82°47.25' E	-59.25	Bohaty et al. 2012	34.1 Ma to 35.0 Ma	*Subbotina angiporoides*	*Subbotina angiporoides*	3	1.4	Poor, recrystallised foraminifera.
119	738b			Kerguelen Plateau, Southern Ocean (Indian sector)	62°42.54' S	82°47.25' E	-59.25	Bohaty et al. 2012	34.1 Ma to 35.0 Ma	*Subbotina angiporoides*	*Subbotina angiporoides*	3	1.4	Poor, recrystallised foraminifera.

119	738b		Kerguelen Plateau, Southern Ocean (Indian sector)	62°42.54' S	82°47.25' E	-59.25	Bohaty et al. 2012	34.1 Ma to 35.0 Ma	*Subbotina angiporoides*	*Subbotina angiporoides*	3	1.42	Poor, recrystallised foraminifera.
119	738b		Kerguelen Plateau, Southern Ocean (Indian sector)	62°42.54' S	82°47.25' E	-59.25	Bohaty et al. 2012	34.1 Ma to 35.0 Ma	*Subbotina angiporoides*	*Subbotina angiporoides*	3	1.42	Poor, recrystallised foraminifera.
119	738b		Kerguelen Plateau, Southern Ocean (Indian sector)	62°42.54' S	82°47.25' E	-59.25	Bohaty et al. 2012	34.1 Ma to 35.0 Ma	*Subbotina angiporoides*	*Subbotina angiporoides*	3	1.42	Poor, recrystallised foraminifera.
119	738b		Kerguelen Plateau, Southern Ocean (Indian sector)	62°42.54' S	82°47.25' E	-59.25	Bohaty et al. 2012	34.1 Ma to 35.0 Ma	*Subbotina angiporoides*	*Subbotina angiporoides*	3	1.42	Poor, recrystallised foraminifera.
119	738b		Kerguelen Plateau, Southern Ocean (Indian sector)	62°42.54' S	82°47.25' E	-59.25	Bohaty et al. 2012	34.1 Ma to 35.0 Ma	*Subbotina angiporoides*	*Subbotina angiporoides*	3	1.42	Poor, recrystallised foraminifera.
119	738b		Kerguelen Plateau, Southern Ocean (Indian sector)	62°42.54' S	82°47.25' E	-59.25	Bohaty et al. 2012	34.1 Ma to 35.0 Ma	*Subbotina angiporoides*	*Subbotina angiporoides*	3	1.42	Poor, recrystallised foraminifera.
119	738b		Kerguelen Plateau, Southern Ocean (Indian sector)	62°42.54' S	82°47.25' E	-59.25	Bohaty et al. 2012	34.1 Ma to 35.0 Ma	*Subbotina angiporoides*	*Subbotina angiporoides*	3	1.48	Poor, recrystallised foraminifera.
119	738b		Kerguelen Plateau, Southern Ocean (Indian sector)	62°42.54' S	82°47.25' E	-59.25	Bohaty et al. 2012	34.1 Ma to 35.0 Ma	*Subbotina angiporoides*	*Subbotina angiporoides*	3	1.48	Poor, recrystallised foraminifera.

119	738b		Kerguelen Plateau, Southern Ocean (Indian sector)	62°42.54'S	82°47.25'E	-59.25	Bohaty et al. 2012	34.1 Ma to 35.0 Ma	*Subbotina angiporoides*	*Subbotina angiporoides*	3	1.49	Poor, recrystallised foraminifera.
119	738b		Kerguelen Plateau, Southern Ocean (Indian sector)	62°42.54'S	82°47.25'E	-59.25	Bohaty et al. 2012	34.1 Ma to 35.0 Ma	*Subbotina angiporoides*	*Subbotina angiporoides*	3	1.49	Poor, recrystallised foraminifera.
119	738b		Kerguelen Plateau, Southern Ocean (Indian sector)	62°42.54'S	82°47.25'E	-59.25	Bohaty et al. 2012	34.1 Ma to 35.0 Ma	*Subbotina angiporoides*	*Subbotina angiporoides*	3	1.5	Poor, recrystallised foraminifera.
119	738b		Kerguelen Plateau, Southern Ocean (Indian sector)	62°42.54'S	82°47.25'E	-59.25	Bohaty et al. 2012	34.1 Ma to 35.0 Ma	*Subbotina angiporoides*	*Subbotina angiporoides*	3	1.5	Poor, recrystallised foraminifera.
113	689b, d		Maud Rise, Southern Ocean (Atlantic sector)	64°31'S	03°06'E	-68.06	Bohaty et al. 2012	34.1 Ma to 35.0 Ma	*Subbotina angiporoides*	*Subbotina angiporoides*	3	1.5	Poor, recrystallised foraminifera.
113	689b, d		Maud Rise, Southern Ocean (Atlantic sector)	64°31'S	03°06'E	-68.06	Bohaty et al. 2012	34.1 Ma to 35.0 Ma	*Subbotina angiporoides*	*Subbotina angiporoides*	3	1.51	Poor, recrystallised foraminifera.
113	689b, d		Maud Rise, Southern Ocean (Atlantic sector)	64°31'S	03°06'E	-68.06	Bohaty et al. 2012	34.1 Ma to 35.0 Ma	*Subbotina angiporoides*	*Subbotina angiporoides*	3	1.51	Poor, recrystallised foraminifera.
113	689b, d		Maud Rise, Southern Ocean (Atlantic sector)	64°31'S	03°06'E	-68.06	Bohaty et al. 2012	34.1 Ma to 35.0 Ma	*Subbotina angiporoides*	*Subbotina angiporoides*	3	1.51	Poor, recrystallised foraminifera.

113	689b, d		Maud Rise, Southern Ocean (Atlantic sector)	64°31'S	03°06'E	-68.06	Bohaty et al. 2012	34.1 Ma to 35.0 Ma	*Subbotina angiporoides*	*Subbotina angiporoides*	3	1.51	Poor, recrystallised foraminifera.
113	689b, d		Maud Rise, Southern Ocean (Atlantic sector)	64°31'S	03°06'E	-68.06	Bohaty et al. 2012	34.1 Ma to 35.0 Ma	*Subbotina angiporoides*	*Subbotina angiporoides*	3	1.52	Poor, recrystallised foraminifera.
113	689b, d		Maud Rise, Southern Ocean (Atlantic sector)	64°31'S	03°06'E	-68.06	Bohaty et al. 2012	34.1 Ma to 35.0 Ma	*Subbotina angiporoides*	*Subbotina angiporoides*	3	1.52	Poor, recrystallised foraminifera.
113	689b, d		Maud Rise, Southern Ocean (Atlantic sector)	64°31'S	03°06'E	-68.06	Bohaty et al. 2012	34.1 Ma to 35.0 Ma	*Subbotina angiporoides*	*Subbotina angiporoides*	3	1.52	Poor, recrystallised foraminifera.
113	689b, d		Maud Rise, Southern Ocean (Atlantic sector)	64°31'S	03°06'E	-68.06	Bohaty et al. 2012	34.1 Ma to 35.0 Ma	*Subbotina angiporoides*	*Subbotina angiporoides*	3	1.55	Poor, recrystallised foraminifera.
113	689b, d		Maud Rise, Southern Ocean (Atlantic sector)	64°31'S	03°06'E	-68.06	Bohaty et al. 2012	34.1 Ma to 35.0 Ma	*Subbotina angiporoides*	*Subbotina angiporoides*	3	1.55	Poor, recrystallised foraminifera.
113	689b, d		Maud Rise, Southern Ocean (Atlantic sector)	64°31'S	03°06'E	-68.06	Bohaty et al. 2012	34.1 Ma to 35.0 Ma	*Subbotina angiporoides*	*Subbotina angiporoides*	3	1.55	Poor, recrystallised foraminifera.
113	689b, d		Maud Rise, Southern Ocean (Atlantic sector)	64°31'S	03°06'E	-68.06	Bohaty et al. 2012	34.1 Ma to 35.0 Ma	*Subbotina angiporoides*	*Subbotina angiporoides*	3	1.55	Poor, recrystallised foraminifera.

113	689b, d		Maud Rise, Southern Ocean (Atlantic sector)	64°31'S	03°06'E	-68.06	Bohaty et al. 2012	34.1 Ma to 35.0 Ma	*Subbotina angiporoides*	*Subbotina angiporoides*	3	1.55	Poor, recrystallised foraminifera.
113	689b, d		Maud Rise, Southern Ocean (Atlantic sector)	64°31'S	03°06'E	-68.06	Bohaty et al. 2012	34.1 Ma to 35.0 Ma	*Subbotina angiporoides*	*Subbotina angiporoides*	3	1.55	Poor, recrystallised foraminifera.
113	689b, d		Maud Rise, Southern Ocean (Atlantic sector)	64°31'S	03°06'E	-68.06	Bohaty et al. 2012	34.1 Ma to 35.0 Ma	*Subbotina angiporoides*	*Subbotina angiporoides*	3	1.6	Poor, recrystallised foraminifera.
113	689b, d		Maud Rise, Southern Ocean (Atlantic sector)	64°31'S	03°06'E	-68.06	Bohaty et al. 2012	34.1 Ma to 35.0 Ma	*Subbotina angiporoides*	*Subbotina angiporoides*	3	1.6	Poor, recrystallised foraminifera.
113	689b, d		Maud Rise, Southern Ocean (Atlantic sector)	64°31'S	03°06'E	-68.06	Bohaty et al. 2012	34.1 Ma to 35.0 Ma	*Subbotina angiporoides*	*Subbotina angiporoides*	3	1.6	Poor, recrystallised foraminifera.
113	689b, d		Maud Rise, Southern Ocean (Atlantic sector)	64°31'S	03°06'E	-68.06	Bohaty et al. 2012	34.1 Ma to 35.0 Ma	*Subbotina angiporoides*	*Subbotina angiporoides*	3	1.6	Poor, recrystallised foraminifera.
113	689b, d		Maud Rise, Southern Ocean (Atlantic sector)	64°31'S	03°06'E	-68.06	Bohaty et al. 2012	34.1 Ma to 35.0 Ma	*Subbotina angiporoides*	*Subbotina angiporoides*	3	1.6	Poor, recrystallised foraminifera.
113	689b, d		Maud Rise, Southern Ocean (Atlantic sector)	64°31'S	03°06'E	-68.06	Bohaty et al. 2012	34.1 Ma to 35.0 Ma	*Subbotina angiporoides*	*Subbotina angiporoides*	3	1.6	Poor, recrystallised foraminifera.

113	689b, d		Maud Rise, Southern Ocean (Atlantic sector)	64°31'S	03°06'E	-68.06	Bohaty et al. 2012	34.1 Ma to 35.0 Ma	*Subbotina angiporoides*	*Subbotina angiporoides*	3	1.6	Poor, recrystallised foraminifera.
113	689b, d		Maud Rise, Southern Ocean (Atlantic sector)	64°31'S	03°06'E	-68.06	Bohaty et al. 2012	34.1 Ma to 35.0 Ma	*Subbotina angiporoides*	*Subbotina angiporoides*	3	1.6	Poor, recrystallised foraminifera.
113	689b, d		Maud Rise, Southern Ocean (Atlantic sector)	64°31'S	03°06'E	-68.06	Bohaty et al. 2012	34.1 Ma to 35.0 Ma	*Subbotina angiporoides*	*Subbotina angiporoides*	3	1.7	Poor, recrystallised foraminifera.
113	689b, d		Maud Rise, Southern Ocean (Atlantic sector)	64°31'S	03°06'E	-68.06	Bohaty et al. 2012	34.1 Ma to 35.0 Ma	*Subbotina angiporoides*	*Subbotina angiporoides*	3	1.7	Poor, recrystallised foraminifera.
113	689b, d		Maud Rise, Southern Ocean (Atlantic sector)	64°31'S	03°06'E	-68.06	Bohaty et al. 2012	34.1 Ma to 35.0 Ma	*Subbotina angiporoides*	*Subbotina angiporoides*	3	1.9	Poor, recrystallised foraminifera.
113	689b, d		Maud Rise, Southern Ocean (Atlantic sector)	64°31'S	03°06'E	-68.06	Bohaty et al. 2012	34.1 Ma to 35.0 Ma	*Subbotina angiporoides*	*Subbotina angiporoides*	3	1.9	Poor, recrystallised foraminifera.
113	689b, d		Maud Rise, Southern Ocean (Atlantic sector)	64°31'S	03°06'E	-68.06	Bohaty et al. 2012	34.1 Ma to 35.0 Ma	*Subbotina angiporoides*	*Subbotina angiporoides*	3	1.9	Poor, recrystallised foraminifera.
143	865C		Allison Guyot, Mid-Pacific Mountains, Western central	18°26.425'N	179°33.339'W	12.29	Coxhall et al. 2000	34.3, CK 95 timescale	*Hantkenina* spp.	*Hantkenina* spp.	2	-0.2	Poor, recrystallised foraminifera.

143	865C		Allison Guyot, Mid-Pacific Mountains, Western central Pacific Ocean basin									
143	865C		Allison Guyot, Mid-Pacific Mountains, Western central Pacific Ocean basin	18°26.425'N	179°33.339'W	12.29	Coxhall et al. 2000	34.3, CK 95 timescale	*Cibrohantkenina inflata*	*Cibrohantkenina inflata*	2	0.07	Poor, recrystallised foraminifera.
143	865C		Allison Guyot, Mid-Pacific Mountains, Western central Pacific Ocean basin	18°26.425'N	179°33.339'W	12.29	Coxhall et al. 2000	34.8, CK 95 timescale	*Hantkenina* spp.	*Hantkenina* spp.	2	0.07	Poor, recrystallised foraminifera.
143	865C		Allison Guyot, Mid-Pacific Mountains, Western central Pacific Ocean basin	18°26.425'N	179°33.339'W	12.29	Coxhall et al. 2000	34.8, CK 95 timescale	*Cibrohantkenina inflata*	*Cibrohantkenina inflata*	2	0.2	Poor, recrystallised foraminifera.
143	865C		Allison Guyot, Mid-Pacific Mountains, Western central Pacific Ocean basin	18°26.425'N	179°33.339'W	12.29	Coxhall et al. 2001	34.8, CK 95 timescale	*Subbotina* spp.	*Subbotina* spp.	3	0.48	Poor, recrystallised foraminifera.
143	865C		Allison Guyot, Mid-Pacific Mountains, Western central	18°26.425'N	179°33.339'W	12.29	Coxhall et al. 2000	34.8, CK 95 timescale	*Turborotalia* spp.	*Turborotalia* spp.	2	0.01	Poor, recrystallised foraminifera.

143	865C		Pacific Ocean basin										
143	865C		Allison Guyot, Mid-Pacific Mountains, Western central Pacific Ocean basin	18°26.425'N	179°33.339'W	12.29	Coxhall et al. 2000	34.8, CK 95 timescale	*Subbotina linaperta*	*Subbotina linaperta*	3	0.48	Poor, recrystallised foraminifera.
143	865C		Allison Guyot, Mid-Pacific Mountains, Western central Pacific Ocean basin	18°26.425'N	179°33.339'W	12.29	Coxhall et al. 2000	35.2, CK 95 timescale	*Hantkenina* spp.	*Hantkenina* spp.	2	-0.4	Poor, recrystallised foraminifera.
143	865C		Allison Guyot, Mid-Pacific Mountains, Western central Pacific Ocean basin	18°26.425'N	179°33.339'W	12.29	Coxhall et al. 2000	35.2, CK 95 timescale	*Cibrohantkenina inflata*	*Cibrohantkenina inflata*	2	-0.03	Poor, recrystallised foraminifera.
143	865C		Allison Guyot, Mid-Pacific Mountains, Western central Pacific Ocean basin	18°26.425'N	179°33.339'W	12.29	Coxhall et al. 2000	35.2, CK 95 timescale	*Turborotalia* spp.	*Turborotalia* spp.	2	-0.23	Poor, recrystallised foraminifera.
143	865C		Allison Guyot, Mid-Pacific Mountains, Western central	18°26.425'N	179°33.339'W	12.29	Coxhall et al. 2000	36.3, CK 95 timescale	*Hantkenina* spp.	*Hantkenina* spp.	2	-0.3	Poor, recrystallised foraminifera.

			Pacific Ocean basin										
143	865C		Allison Guyot, Mid-Pacific Mountains, Western central Pacific Ocean basin	18°26.425'N	179°33.339'W	12.29	Coxhall et al. 2000	36.3, CK 95 timescale	*Turborotalia* spp.	*Turborotalia* spp.	2	-0.3	Poor, recrystallised foraminifera.
143	865C		Allison Guyot, Mid-Pacific Mountains, Western central Pacific Ocean basin	18°26.425'N	179°33.339'W	12.29	Coxhall et al. 2000	36.3, CK 95 timescale	*Subbotina linaperta*	*Subbotina linaperta*	3	0.13	Poor, recrystallised foraminifera.
143	865C		Allison Guyot, Mid-Pacific Mountains, Western central Pacific Ocean basin	18°26.425'N	179°33.339'W	12.29	Coxhall et al. 2000	36.3, CK 95 timescale	*Subbotina* spp.	*Subbotina* spp.	3	0.13	Poor, recrystallised foraminifera.
143	865B		Allison Guyot, Mid-Pacific Mountains, Western central Pacific Ocean basin	18°26.415'N	179°33.349'W	12.29	Coxhall et al. 2000	35.3, CK 95 timescale	*Hantkenina* spp.	*Hantkenina* spp.	2	-0.35	Poor, recrystallised foraminifera.
143	865B		Allison Guyot, Mid-Pacific Mountains, Western central	18°26.415'N	179°33.349'W	12.29	Coxhall et al. 2000	35.3, CK 95 timescale	*Cibrohantkenina inflata*	*Cibrohantkenina inflata*	2	-0.42	Poor, recrystallised foraminifera.

			Pacific Ocean basin										
143	865B		Allison Guyot, Mid-Pacific Mountains, Western central Pacific Ocean basin	18°26.415'N	179°33.349'W	12.29	Coxhall et al. 2000	35.3, CK 95 timescale	*Turborotalia* spp.	*Turborotalia* spp.	2	-0.38	Poor, recrystallised foraminifera.
143	865B		Allison Guyot, Mid-Pacific Mountains, Western central Pacific Ocean basin	18°26.415'N	179°33.349'W	12.29	Coxhall et al. 2000	35.3, CK 95 timescale	*Subbotina linaperta*	*Subbotina linaperta*	3	-0.02	Poor, recrystallised foraminifera.
143	865B		Allison Guyot, Mid-Pacific Mountains, Western central Pacific Ocean basin	18°26.415'N	179°33.349'W	12.29	Coxhall et al. 2000	35.3, CK 95 timescale	*Subbotina* spp.	*Subbotina* spp.	3	-0.02	Poor, recrystallised foraminifera.
10	94		Campeche Scarp, Yucatan Shelf, Gulf of Mexico	24°31.64'N	88°28.16'W	20.68	Coxhall et al. 2000	36.6, CK 95 timescale	*Hantkenina alabamensis*	*Hantkenina alabamensis*	2	-0.65	Poor, recrystallised foraminifera.
10	94		Campeche Scarp, Yucatan Shelf, Gulf of Mexico	24°31.64'N	88°28.16'W	20.68	Coxhall et al. 2000	36.6, CK 95 timescale	*Hantkenina* spp.	*Hantkenina* spp.	2	-0.65	Poor, recrystallised foraminifera.
10	94		Campeche Scarp, Yucatan Shelf, Gulf of Mexico	24°31.64'N	88°28.16'W	20.68	Coxhall et al. 2000	36.6, CK 95 timescale	*Subbotina linaperta*	*Subbotina linaperta*	3	0.08	Poor, recrystallised foraminifera.

10	94		Campeche Scarp, Yucatan Shelf, Gulf of Mexico	24°31.64' N	88°28.16' W	20.68	Coxhall et al. 2000	36.6, CK 95 timescale	*Subbotina* spp.	*Subbotina* spp.	3	0.08	Poor, recrystallised foraminifera.
10	94		Campeche Scarp, Yucatan Shelf, Gulf of Mexico	24°31.64' N	88°28.16' W	20.68	Coxhall et al. 2000	36.27 CK 95 timescale	*Hantkenina alabamensis*	*Hantkenina alabamensis*	2	-0.32	Poor, recrystallised foraminifera.
10	94		Campeche Scarp, Yucatan Shelf, Gulf of Mexico	24°31.64' N	88°28.16' W	20.68	Coxhall et al. 2000	36.27 CK 95 timescale	*Hantkenina* spp.	*Hantkenina* spp.	2	-0.32	Poor, recrystallised foraminifera.
10	94		Campeche Scarp, Yucatan Shelf, Gulf of Mexico	24°31.64' N	88°28.16' W	20.68	Coxhall et al. 2000	36.27 CK 95 timescale	*Subbotina* spp.	*Subbotina* spp.	3	0.08	Poor, recrystallised foraminifera.
10	94		Campeche Scarp, Yucatan Shelf, Gulf of Mexico	24°31.64' N	88°28.16' W	20.68	Coxhall et al. 2000	36.03, CK 95 timescale	*Hantkenina alabamensis*	*Hantkenina alabamensis*	2	-0.63	Poor, recrystallised foraminifera.
10	94		Campeche Scarp, Yucatan Shelf, Gulf of Mexico	24°31.64' N	88°28.16' W	20.68	Coxhall et al. 2000	36.03, CK 95 timescale	*Hantkenina* spp.	*Hantkenina* spp.	2	-0.63	Poor, recrystallised foraminifera.
10	94		Campeche Scarp, Yucatan Shelf, Gulf of Mexico	24°31.64' N	88°28.16' W	20.68	Coxhall et al. 2000	36.03, CK 95 timescale	*Subbotina* spp.	*Subbotina* spp.	3	0.31	Poor, recrystallised foraminifera.
10	94		Campeche Scarp, Yucatan Shelf, Gulf of Mexico	24°31.64' N	88°28.16' W	20.68	Coxhall et al. 2000	35.95, CK 95 timescale	*Hantkenina alabamensis*	*Hantkenina alabamensis*	2	-0.94	Poor, recrystallised foraminifera.
10	94		Campeche Scarp, Yucatan Shelf, Gulf of Mexico	24°31.64' N	88°28.16' W	20.68	Coxhall et al. 2000	35.95, CK 95 timescale	*Hantkenina* spp.	*Hantkenina* spp.	2	-0.94	Poor, recrystallised foraminifera.

10	94		Campeche Scarp, Yucatan Shelf, Gulf of Mexico	24°31.64' N	88°28.16' W	20.68	Coxhall et al. 2000	35.95, CK 95 timescale	*Subbotina linaperta*	*Subbotina linaperta*	3	-0.37	Poor, recrystallised foraminifera.
10	94		Campeche Scarp, Yucatan Shelf, Gulf of Mexico	24°31.64' N	88°28.16' W	20.68	Coxhall et al. 2000	35.95, CK 95 timescale	*Subbotina* spp.	*Subbotina* spp.	3	-0.37	Poor, recrystallised foraminifera.
10	94		Campeche Scarp, Yucatan Shelf, Gulf of Mexico	24°31.64' N	88°28.16' W	20.68	Coxhall et al. 2000	35.8, CK 95 timescale	*Hantkenina alabamensis*	*Hantkenina alabamensis*	2	-0.42	Poor, recrystallised foraminifera.
10	94		Campeche Scarp, Yucatan Shelf, Gulf of Mexico	24°31.64' N	88°28.16' W	20.68	Coxhall et al. 2000	35.8, CK 95 timescale	*Hantkenina* spp.	*Hantkenina* spp.	2	-0.42	Poor, recrystallised foraminifera.
10	94		Campeche Scarp, Yucatan Shelf, Gulf of Mexico	24°31.64' N	88°28.16' W	20.68	Coxhall et al. 2000	35.8, CK 95 timescale	*Subbotina linaperta*	*Subbotina linaperta*	3	-0.56	Poor, recrystallised foraminifera.
10	94		Campeche Scarp, Yucatan Shelf, Gulf of Mexico	24°31.64' N	88°28.16' W	20.68	Coxhall et al. 2000	35.8, CK 95 timescale	*Subbotina* spp.	*Subbotina* spp.	3	-0.56	Poor, recrystallised foraminifera.
10	94		Campeche Scarp, Yucatan Shelf, Gulf of Mexico	24°31.64' N	88°28.16' W	20.68	Coxhall et al. 2000	35.77, CK 95 timescale	*Hantkenina alabamensis*	*Hantkenina alabamensis*	2	-0.95	Poor, recrystallised foraminifera.
10	94		Campeche Scarp, Yucatan Shelf, Gulf of Mexico	24°31.64' N	88°28.16' W	20.68	Coxhall et al. 2000	35.77, CK 95 timescale	*Hantkenina* spp.	*Hantkenina* spp.	2	-0.95	Poor, recrystallised foraminifera.
10	94		Campeche Scarp, Yucatan Shelf, Gulf of Mexico	24°31.64' N	88°28.16' W	20.68	Coxhall et al. 2000	35.77, CK 95 timescale	*Subbotina linaperta*	*Subbotina linaperta*	3	-0.38	Poor, recrystallised foraminifera.

10	94		Campeche Scarp, Yucatan Shelf, Gulf of Mexico	24°31.64'N	88°28.16'W	20.68	Coxhall et al. 2000	35.77, CK 95 timescale	*Subbotina* spp.	*Subbotina* spp.	3	-0.38	Poor, recrystallised foraminifera.
	SSQ		St. Stephens Quarry corehole, Alabama	31°33'N	88°02'W	27.55	Wade et al. 2012, data from the Supplemetary Informatio Document, found on the GSA repository online	33.806	*Pseudohastigerina naguewichiensis*	*Pseudohastigerina naguewichiensis*	1	-1.84	Excellent, glassy foraminifera
	SSQ		St. Stephens Quarry corehole, Alabama	31°33'N	88°02'W	27.55	Wade et al. 2012, data from the Supplemetary Informatio Document, found on the GSA repository online	33.839	*Pseudohastigerina naguewichiensis*	*Pseudohastigerina naguewichiensis*	1	-1.96	Excellent, glassy foraminifera
	SSQ		St. Stephens Quarry corehole, Alabama	31°33'N	88°02'W	27.55	Wade et al. 2012, data from the Supplemetary Informatio Document, found on the GSA repository online	33.858	*Pseudohastigerina naguewichiensis*	*Pseudohastigerina naguewichiensis*	1	-1.5	Excellent, glassy foraminifera
	SSQ		St. Stephens Quarry corehole, Alabama	31°33'N	88°02'W	27.55	Wade et al. 2012, data from the Supplemetary Informatio Document, found on the GSA	33.905	*Pseudohastigerina naguewichiensis*	*Pseudohastigerina naguewichiensis*	1	-1.86	Excellent, glassy foraminifera

	SSQ		St. Stephens Quarry corehole, Alabama	31°33'N	88°02'W	27.55	Wade et al. 2012, data from the Supplemetary Informatio Document, found on the GSA repository online						
							repository online						
	SSQ		St. Stephens Quarry corehole, Alabama	31°33'N	88°02'W	27.55	Wade et al. 2012, data from the Supplemetary Informatio Document, found on the GSA repository online	33.927	Pseudohastigerina naguewichiensis	Pseudohastigerina naguewichiensis	1	-1.8	Excellent, glassy foraminifera
	SSQ		St. Stephens Quarry corehole, Alabama	31°33'N	88°02'W	27.55	Wade et al. 2012, data from the Supplemetary Informatio Document, found on the GSA repository online	33.963	Pseudohastigerina naguewichiensis	Pseudohastigerina naguewichiensis	1	-1.87	Excellent, glassy foraminifera
	SSQ		St. Stephens Quarry corehole, Alabama	31°33'N	88°02'W	27.55	Wade et al. 2012, data from the Supplemetary Informatio Document, found on the GSA repository online	33.989	Pseudohastigerina naguewichiensis	Pseudohastigerina naguewichiensis	1	-1.76	Excellent, glassy foraminifera

	SSQ		St. Stephens Quarry corehole, Alabama	31°33'N	88°02'W	27.55	Wade et al. 2012, data from the Supplemetary Informatio Document, found on the GSA repository online	34	*Pseudohastigerina naguewichiensis*	*Pseudohastigerina naguewichiensis*	1	-2.24	Excellent, glassy foraminifera
	SSQ		St. Stephens Quarry corehole, Alabama	31°33'N	88°02'W	27.55	Wade et al. 2012, data from the Supplemetary Informatio Document, found on the GSA repository online	33.806	*Turborotalia ampliapertura*	*Turborotalia ampliapertura*	2	-1.77	Excellent, glassy foraminifera
	SSQ		St. Stephens Quarry corehole, Alabama	31°33'N	88°02'W	27.55	Wade et al. 2012, data from the Supplemetary Informatio Document, found on the GSA repository online	33.839	*Turborotalia ampliapertura*	*Turborotalia ampliapertura*	2	-1.78	Excellent, glassy foraminifera
	SSQ		St. Stephens Quarry corehole, Alabama	31°33'N	88°02'W	27.55	Wade et al. 2012, data from the Supplemetary Informatio Document, found on the GSA repository online	33.839	*Turborotalia ampliapertura*	*Turborotalia ampliapertura*	2	-1.81	Excellent, glassy foraminifera

SSQ		St. Stephens Quarry corehole, Alabama	31°33'N	88°02'W	27.55	Wade et al. 2012, data from the Supplemetary Informatio Document, found on the GSA repository online	33.905	*Turborotalia ampliapertura*	*Turborotalia ampliapertura*	2	-1.55	Excellent, glassy foraminifera
SSQ		St. Stephens Quarry corehole, Alabama	31°33'N	88°02'W	27.55	Wade et al. 2012, data from the Supplemetary Informatio Document, found on the GSA repository online	33.927	*Turborotalia ampliapertura*	*Turborotalia ampliapertura*	2	-1.76	Excellent, glassy foraminifera
SSQ		St. Stephens Quarry corehole, Alabama	31°33'N	88°02'W	27.55	Wade et al. 2012, data from the Supplemetary Informatio Document, found on the GSA repository online	33.963	*Turborotalia ampliapertura*	*Turborotalia ampliapertura*	2	-1.9	Excellent, glassy foraminifera
SSQ		St. Stephens Quarry corehole, Alabama	31°33'N	88°02'W	27.55	Wade et al. 2012, data from the Supplemetary Informatio Document, found on the GSA repository online	33.989	*Turborotalia ampliapertura*	*Turborotalia ampliapertura*	2	-2.02	Excellent, glassy foraminifera

	SSQ		St. Stephens Quarry corehole, Alabama	31º33'N	88°02'W	27.55	Wade et al. 2012, data from the Supplemetary Informatio Document, found on the GSA repository online	34	*Turborotalia ampliapertura*	*Turborotalia ampliapertura*	2	-2.27	Excellent, glassy foraminifera
	SSQ		St. Stephens Quarry corehole, Alabama	31º33'N	88°02'W	27.55	Wade et al. 2012, data from the Supplemetary Informatio Document, found on the GSA repository online	34	*Turborotalia ampliapertura*	*Turborotalia ampliapertura*	2	-2.04	Excellent, glassy foraminifera
105	647 A		Southern flank of Gloria Drift in the Southern Labrador Sea	53°19.878'N	45°15.720'W	44.98	Coxall et al. 2018	34.0693	*Catapsydrax unicavus*	*Catapsydrax unicavus*	3	-0.612	Excellent, glassy foraminifera
105	647 A		Southern flank of Gloria Drift in the Southern Labrador Sea	53°19.878'N	45°15.720'W	44.98	Coxall et al. 2018	34.0733	*Catapsydrax unicavus*	*Catapsydrax unicavus*	3	-0.260	Excellent, glassy foraminifera
105	647 A		Southern flank of Gloria Drift in the Southern Labrador Sea	53°19.878'N	45°15.720'W	44.98	Coxall et al. 2018	34.0778	*Catapsydrax unicavus*	*Catapsydrax unicavus*	3	-0.219	Excellent, glassy foraminifera

105	647 A		Southern flank of Gloria Drift in the Southern Labrador Sea	53°19.878'N	45°15.720'W	44.98	Coxall et al. 2018	34.0834	*Catapsydrax unicavus*	*Catapsydrax unicavus*	3	-0.090	Excellent, glassy foraminifera
105	647 A		Southern flank of Gloria Drift in the Southern Labrador Sea	53°19.878'N	45°15.720'W	44.98	Coxall et al. 2018	34.0874	*Catapsydrax unicavus*	*Catapsydrax unicavus*	3	-0.400	Excellent, glassy foraminifera
105	647 A		Southern flank of Gloria Drift in the Southern Labrador Sea	53°19.878'N	45°15.720'W	44.98	Coxall et al. 2018	34.0907	*Catapsydrax unicavus*	*Catapsydrax unicavus*	3	-0.066	Excellent, glassy foraminifera
105	647 A		Southern flank of Gloria Drift in the Southern Labrador Sea	53°19.878'N	45°15.720'W	44.98	Coxall et al. 2018	34.0930	*Catapsydrax unicavus*	*Catapsydrax unicavus*	3	0.296	Excellent, glassy foraminifera
105	647 A		Southern flank of Gloria Drift in the Southern Labrador Sea	53°19.878'N	45°15.720'W	44.98	Coxall et al. 2018	34.1164	*Catapsydrax unicavus*	*Catapsydrax unicavus*	3	0.044	Excellent, glassy foraminifera
105	647 A		Southern flank of Gloria Drift in the Southern Labrador Sea	53°19.878'N	45°15.720'W	44.98	Coxall et al. 2018	34.1208	*Catapsydrax unicavus*	*Catapsydrax unicavus*	3	-0.308	Excellent, glassy foraminifera
105	647 A		Southern flank of Gloria Drift in the Southern	53°19.878'N	45°15.720'W	44.98	Coxall et al. 2018	34.1208	*Catapsydrax unicavus*	*Catapsydrax unicavus*	3	-0.051	Excellent, glassy foraminifera

			Labrador Sea										
105	647 A		Southern flank of Gloria Drift in the Southern Labrador Sea	53°19.878'N	45°15.720' W	44. 98	Coxall et al. 2018	34.122 2	*Catapsydrax unicavus*	*Catapsydrax unicavus*	3	- 0.3 01	Excellent, glassy foraminife ra
105	647 A		Southern flank of Gloria Drift in the Southern Labrador Sea	53°19.878'N	45°15.720' W	44. 98	Coxall et al. 2018	34.129 8	*Catapsydrax unicavus*	*Catapsydrax unicavus*	3	0.0 81	Excellent, glassy foraminife ra
105	647 A		Southern flank of Gloria Drift in the Southern Labrador Sea	53°19.878'N	45°15.720' W	44. 98	Coxall et al. 2018	34.132 7	*Catapsydrax unicavus*	*Catapsydrax unicavus*	3	- 0.2 31	Excellent, glassy foraminife ra
105	647 A		Southern flank of Gloria Drift in the Southern Labrador Sea	53°19.878'N	45°15.720' W	44. 98	Coxall et al. 2018	34.136 7	*Catapsydrax unicavus*	*Catapsydrax unicavus*	3	- 0.5 95	Excellent, glassy foraminife ra
105	647 A		Southern flank of Gloria Drift in the Southern Labrador Sea	53°19.878'N	45°15.720' W	44. 98	Coxall et al. 2018	34.139 6	*Catapsydrax unicavus*	*Catapsydrax unicavus*	3	- 0.5 08	Excellent, glassy foraminife ra
105	647 A		Southern flank of Gloria Drift in the Southern Labrador Sea	53°19.878'N	45°15.720' W	44. 98	Coxall et al. 2018	34.143 2	*Catapsydrax unicavus*	*Catapsydrax unicavus*	3	- 0.0 25	Excellent, glassy foraminife ra

105	647 A		Southern flank of Gloria Drift in the Southern Labrador Sea	53°19.878'N	45°15.720'W	44.98	Coxall et al. 2018	34.1476	*Catapsydrax unicavus*	*Catapsydrax unicavus*	3	-0.427	Excellent, glassy foraminifera
105	647 A		Southern flank of Gloria Drift in the Southern Labrador Sea	53°19.878'N	45°15.720'W	44.98	Coxall et al. 2018	34.1498	*Catapsydrax unicavus*	*Catapsydrax unicavus*	3	-0.352	Excellent, glassy foraminifera
105	647 A		Southern flank of Gloria Drift in the Southern Labrador Sea	53°19.878'N	45°15.720'W	44.98	Coxall et al. 2018	34.1563	*Catapsydrax unicavus*	*Catapsydrax unicavus*	3	-0.966	Excellent, glassy foraminifera
105	647 A		Southern flank of Gloria Drift in the Southern Labrador Sea	53°19.878'N	45°15.720'W	44.98	Coxall et al. 2018	34.1596	*Catapsydrax unicavus*	*Catapsydrax unicavus*	3	-0.130	Excellent, glassy foraminifera
105	647 A		Southern flank of Gloria Drift in the Southern Labrador Sea	53°19.878'N	45°15.720'W	44.98	Coxall et al. 2018	34.1628	*Catapsydrax unicavus*	*Catapsydrax unicavus*	3	-0.238	Excellent, glassy foraminifera
105	647 A		Southern flank of Gloria Drift in the Southern Labrador Sea	53°19.878'N	45°15.720'W	44.98	Coxall et al. 2018	34.1744	*Catapsydrax unicavus*	*Catapsydrax unicavus*	3	-0.575	Excellent, glassy foraminifera
105	647 A		Southern flank of Gloria Drift in the Southern	53°19.878'N	45°15.720'W	44.98	Coxall et al. 2018	34.1835	*Catapsydrax unicavus*	*Catapsydrax unicavus*	3	-0.049	Excellent, glassy foraminifera

			Labrador Sea										
105	647 A		Southern flank of Gloria Drift in the Southern Labrador Sea	53°19.878'N	45°15.720'W	44.98	Coxall et al. 2018	34.1875	*Catapsydrax unicavus*	*Catapsydrax unicavus*	3	0.122	Excellent, glassy foraminifera
105	647 A		Southern flank of Gloria Drift in the Southern Labrador Sea	53°19.878'N	45°15.720'W	44.98	Coxall et al. 2018	34.1918	*Catapsydrax unicavus*	*Catapsydrax unicavus*	3	-0.564	Excellent, glassy foraminifera
105	647 A		Southern flank of Gloria Drift in the Southern Labrador Sea	53°19.878'N	45°15.720'W	44.98	Coxall et al. 2018	34.1953	*Catapsydrax unicavus*	*Catapsydrax unicavus*	3	-0.079	Excellent, glassy foraminifera
105	647 A		Southern flank of Gloria Drift in the Southern Labrador Sea	53°19.878'N	45°15.720'W	44.98	Coxall et al. 2018	34.1987	*Catapsydrax unicavus*	*Catapsydrax unicavus*	3	-0.270	Excellent, glassy foraminifera
105	647 A		Southern flank of Gloria Drift in the Southern Labrador Sea	53°19.878'N	45°15.720'W	44.98	Coxall et al. 2018	34.2002	*Catapsydrax unicavus*	*Catapsydrax unicavus*	3	-0.279	Excellent, glassy foraminifera
105	647 A		Southern flank of Gloria Drift in the Southern Labrador Sea	53°19.878'N	45°15.720'W	44.98	Coxall et al. 2018	34.2085	*Catapsydrax unicavus*	*Catapsydrax unicavus*	3	-0.021	Excellent, glassy foraminifera

105	647 A		Southern flank of Gloria Drift in the Southern Labrador Sea	53°19.878'N	45°15.720'W	44.98	Coxall et al. 2018	34.2121	*Catapsydrax unicavus*	*Catapsydrax unicavus*	3	0.095	Excellent, glassy foraminifera
105	647 A		Southern flank of Gloria Drift in the Southern Labrador Sea	53°19.878'N	45°15.720'W	44.98	Coxall et al. 2018	34.2194	*Catapsydrax unicavus*	*Catapsydrax unicavus*	3	0.030	Excellent, glassy foraminifera
105	647 A		Southern flank of Gloria Drift in the Southern Labrador Sea	53°19.878'N	45°15.720'W	44.98	Coxall et al. 2018	34.2386	*Catapsydrax unicavus*	*Catapsydrax unicavus*	3	-1.596	Excellent, glassy foraminifera
105	647 A		Southern flank of Gloria Drift in the Southern Labrador Sea	53°19.878'N	45°15.720'W	44.98	Coxall et al. 2018	34.2422	*Catapsydrax unicavus*	*Catapsydrax unicavus*	3	0.106	Excellent, glassy foraminifera
105	647 A		Southern flank of Gloria Drift in the Southern Labrador Sea	53°19.878'N	45°15.720'W	44.98	Coxall et al. 2018	34.2466	*Catapsydrax unicavus*	*Catapsydrax unicavus*	3	-0.263	Excellent, glassy foraminifera
105	647 A		Southern flank of Gloria Drift in the Southern Labrador Sea	53°19.878'N	45°15.720'W	44.98	Coxall et al. 2018	34.2498	*Catapsydrax unicavus*	*Catapsydrax unicavus*	3	0.260	Excellent, glassy foraminifera
105	647 A		Southern flank of Gloria Drift in the Southern	53°19.878'N	45°15.720'W	44.98	Coxall et al. 2018	34.2527	*Catapsydrax unicavus*	*Catapsydrax unicavus*	3	-0.280	Excellent, glassy foraminifera

			Labrador Sea										
105	647 A		Southern flank of Gloria Drift in the Southern Labrador Sea	53°19.878'N	45°15.720' W	44. 98	Coxall et al. 2018	34.257 5	*Catapsydrax unicavus*	*Catapsydrax unicavus*	3	- 0.1 44	Excellent, glassy foraminife ra
105	647 A		Southern flank of Gloria Drift in the Southern Labrador Sea	53°19.878'N	45°15.720' W	44. 98	Coxall et al. 2018	34.264 0	*Catapsydrax unicavus*	*Catapsydrax unicavus*	3	- 0.0 02	Excellent, glassy foraminife ra
105	647 A		Southern flank of Gloria Drift in the Southern Labrador Sea	53°19.878'N	45°15.720' W	44. 98	Coxall et al. 2018	34.267 6	*Catapsydrax unicavus*	*Catapsydrax unicavus*	3	- 0.3 32	Excellent, glassy foraminife ra
105	647 A		Southern flank of Gloria Drift in the Southern Labrador Sea	53°19.878'N	45°15.720' W	44. 98	Coxall et al. 2018	34.271 6	*Catapsydrax unicavus*	*Catapsydrax unicavus*	3	0.0 25	Excellent, glassy foraminife ra
105	647 A		Southern flank of Gloria Drift in the Southern Labrador Sea	53°19.878'N	45°15.720' W	44. 98	Coxall et al. 2018	34.276 3	*Catapsydrax unicavus*	*Catapsydrax unicavus*	3	- 0.5 64	Excellent, glassy foraminife ra
105	647 A		Southern flank of Gloria Drift in the Southern Labrador Sea	53°19.878'N	45°15.720' W	44. 98	Coxall et al. 2018	34.278 1	*Catapsydrax unicavus*	*Catapsydrax unicavus*	3	0.1 53	Excellent, glassy foraminife ra

105	647 A		Southern flank of Gloria Drift in the Southern Labrador Sea	53°19.878'N	45°15.720'W	44.98	Coxall et al. 2018	34.2901	Catapsydrax unicavus	Catapsydrax unicavus	3	-0.835	Excellent, glassy foraminifera
105	647 A		Southern flank of Gloria Drift in the Southern Labrador Sea	53°19.878'N	45°15.720'W	44.98	Coxall et al. 2018	34.2937	Catapsydrax unicavus	Catapsydrax unicavus	3	-1.428	Excellent, glassy foraminifera
105	647 A		Southern flank of Gloria Drift in the Southern Labrador Sea	53°19.878'N	45°15.720'W	44.98	Coxall et al. 2018	34.2963	Catapsydrax unicavus	Catapsydrax unicavus	3	-0.559	Excellent, glassy foraminifera
105	647 A		Southern flank of Gloria Drift in the Southern Labrador Sea	53°19.878'N	45°15.720'W	44.98	Coxall et al. 2018	34.3006	Catapsydrax unicavus	Catapsydrax unicavus	3	-0.768	Excellent, glassy foraminifera
105	647 A		Southern flank of Gloria Drift in the Southern Labrador Sea	53°19.878'N	45°15.720'W	44.98	Coxall et al. 2018	34.3075	Catapsydrax unicavus	Catapsydrax unicavus	3	-0.927	Excellent, glassy foraminifera
105	647 A		Southern flank of Gloria Drift in the Southern Labrador Sea	53°19.878'N	45°15.720'W	44.98	Coxall et al. 2018	34.3146	Catapsydrax unicavus	Catapsydrax unicavus	3	-0.654	Excellent, glassy foraminifera
105	647 A		Southern flank of Gloria Drift in the Southern	53°19.878'N	45°15.720'W	44.98	Coxall et al. 2018	34.3187	Catapsydrax unicavus	Catapsydrax unicavus	3	-0.744	Excellent, glassy foraminifera

			Labrador Sea										
105	647 A		Southern flank of Gloria Drift in the Southern Labrador Sea	53°19.878'N	45°15.720'W	44.98	Coxall et al. 2018	34.3334	*Catapsydrax unicavus*	*Catapsydrax unicavus*	3	-0.339	Excellent, glassy foraminifera
105	647 A		Southern flank of Gloria Drift in the Southern Labrador Sea	53°19.878'N	45°15.720'W	44.98	Coxall et al. 2018	34.3401	*Catapsydrax unicavus*	*Catapsydrax unicavus*	3	-0.646	Excellent, glassy foraminifera
105	647 A		Southern flank of Gloria Drift in the Southern Labrador Sea	53°19.878'N	45°15.720'W	44.98	Coxall et al. 2018	34.3438	*Catapsydrax unicavus*	*Catapsydrax unicavus*	3	-0.605	Excellent, glassy foraminifera
105	647 A		Southern flank of Gloria Drift in the Southern Labrador Sea	53°19.878'N	45°15.720'W	44.98	Coxall et al. 2018	34.3467	*Catapsydrax unicavus*	*Catapsydrax unicavus*	3	-0.244	Excellent, glassy foraminifera
105	647 A		Southern flank of Gloria Drift in the Southern Labrador Sea	53°19.878'N	45°15.720'W	44.98	Coxall et al. 2018	34.3506	*Catapsydrax unicavus*	*Catapsydrax unicavus*	3	-0.172	Excellent, glassy foraminifera
105	647 A		Southern flank of Gloria Drift in the Southern Labrador Sea	53°19.878'N	45°15.720'W	44.98	Coxall et al. 2018	34.3557	*Catapsydrax unicavus*	*Catapsydrax unicavus*	3	0.013	Excellent, glassy foraminifera

105	647 A		Southern flank of Gloria Drift in the Southern Labrador Sea	53°19.878'N	45°15.720'W	44.98	Coxall et al. 2018	34.3586	*Catapsydrax unicavus*	*Catapsydrax unicavus*	3	-0.132	Excellent, glassy foraminifera
105	647 A		Southern flank of Gloria Drift in the Southern Labrador Sea	53°19.878'N	45°15.720'W	44.98	Coxall et al. 2018	34.3615	*Catapsydrax unicavus*	*Catapsydrax unicavus*	3	0.011	Excellent, glassy foraminifera
105	647 A		Southern flank of Gloria Drift in the Southern Labrador Sea	53°19.878'N	45°15.720'W	44.98	Coxall et al. 2018	34.3697	*Catapsydrax unicavus*	*Catapsydrax unicavus*	3	0.026	Excellent, glassy foraminifera
105	647 A		Southern flank of Gloria Drift in the Southern Labrador Sea	53°19.878'N	45°15.720'W	44.98	Coxall et al. 2018	34.3735	*Catapsydrax unicavus*	*Catapsydrax unicavus*	3	-0.063	Excellent, glassy foraminifera
105	647 A		Southern flank of Gloria Drift in the Southern Labrador Sea	53°19.878'N	45°15.720'W	44.98	Coxall et al. 2018	34.3766	*Catapsydrax unicavus*	*Catapsydrax unicavus*	3	-0.038	Excellent, glassy foraminifera
105	647 A		Southern flank of Gloria Drift in the Southern Labrador Sea	53°19.878'N	45°15.720'W	44.98	Coxall et al. 2018	34.3840	*Catapsydrax unicavus*	*Catapsydrax unicavus*	3	0.193	Excellent, glassy foraminifera
105	647 A		Southern flank of Gloria Drift in the Southern	53°19.878'N	45°15.720'W	44.98	Coxall et al. 2018	34.3913	*Catapsydrax unicavus*	*Catapsydrax unicavus*	3	0.358	Excellent, glassy foraminifera

			Labrador Sea										
105	647 A		Southern flank of Gloria Drift in the Southern Labrador Sea	53°19.878'N	45°15.720' W	44. 98	Coxall et al. 2018	34.401 8	*Catapsydrax unicavus*	*Catapsydrax unicavus*	3	0.1 19	Excellent, glassy foraminife ra
105	647 A		Southern flank of Gloria Drift in the Southern Labrador Sea	53°19.878'N	45°15.720' W	44. 98	Coxall et al. 2018	34.420 1	*Catapsydrax unicavus*	*Catapsydrax unicavus*	3	0.1 85	Excellent, glassy foraminife ra
105	647 A		Southern flank of Gloria Drift in the Southern Labrador Sea	53°19.878'N	45°15.720' W	44. 98	Coxall et al. 2018	34.431 7	*Catapsydrax unicavus*	*Catapsydrax unicavus*	3	- 0.2 97	Excellent, glassy foraminife ra
105	647 A		Southern flank of Gloria Drift in the Southern Labrador Sea	53°19.878'N	45°15.720' W	44. 98	Coxall et al. 2018	34.435 5	*Catapsydrax unicavus*	*Catapsydrax unicavus*	3	0.0 09	Excellent, glassy foraminife ra
105	647 A		Southern flank of Gloria Drift in the Southern Labrador Sea	53°19.878'N	45°15.720' W	44. 98	Coxall et al. 2018	34.439 1	*Catapsydrax unicavus*	*Catapsydrax unicavus*	3	- 0.6 22	Excellent, glassy foraminife ra
105	647 A		Southern flank of Gloria Drift in the Southern Labrador Sea	53°19.878'N	45°15.720' W	44. 98	Coxall et al. 2018	34.442 4	*Catapsydrax unicavus*	*Catapsydrax unicavus*	3	- 0.0 76	Excellent, glassy foraminife ra

105	647 A		Southern flank of Gloria Drift in the Southern Labrador Sea	53°19.878'N	45°15.720' W	44.98	Coxall et al. 2018	34.4460	*Catapsydrax unicavus*	*Catapsydrax unicavus*	3	0.045	Excellent, glassy foraminifera
105	647 A		Southern flank of Gloria Drift in the Southern Labrador Sea	53°19.878'N	45°15.720' W	44.98	Coxall et al. 2018	34.4494	*Catapsydrax unicavus*	*Catapsydrax unicavus*	3	0.306	Excellent, glassy foraminifera
105	647 A		Southern flank of Gloria Drift in the Southern Labrador Sea	53°19.878'N	45°15.720' W	44.98	Coxall et al. 2018	34.4533	*Catapsydrax unicavus*	*Catapsydrax unicavus*	3	0.174	Excellent, glassy foraminifera
105	647 A		Southern flank of Gloria Drift in the Southern Labrador Sea	53°19.878'N	45°15.720' W	44.98	Coxall et al. 2018	34.4569	*Catapsydrax unicavus*	*Catapsydrax unicavus*	3	0.117	Excellent, glassy foraminifera
105	647 A		Southern flank of Gloria Drift in the Southern Labrador Sea	53°19.878'N	45°15.720' W	44.98	Coxall et al. 2018	34.4612	*Catapsydrax unicavus*	*Catapsydrax unicavus*	3	-0.348	Excellent, glassy foraminifera
105	647 A		Southern flank of Gloria Drift in the Southern Labrador Sea	53°19.878'N	45°15.720' W	44.98	Coxall et al. 2018	34.4649	*Catapsydrax unicavus*	*Catapsydrax unicavus*	3	-0.144	Excellent, glassy foraminifera
105	647 A		Southern flank of Gloria Drift in the Southern	53°19.878'N	45°15.720' W	44.98	Coxall et al. 2018	34.4717	*Catapsydrax unicavus*	*Catapsydrax unicavus*	3	0.076	Excellent, glassy foraminifera

			Labrador Sea										
105	647 A		Southern flank of Gloria Drift in the Southern Labrador Sea	53°19.878'N	45°15.720' W	44. 98	Coxall et al. 2018	34.475 4	*Catapsydrax unicavus*	*Catapsydrax unicavus*	3	- 0.3 10	Excellent, glassy foraminife ra
105	647 A		Southern flank of Gloria Drift in the Southern Labrador Sea	53°19.878'N	45°15.720' W	44. 98	Coxall et al. 2018	34.477 9	*Catapsydrax unicavus*	*Catapsydrax unicavus*	3	- 0.6 11	Excellent, glassy foraminife ra
105	647 A		Southern flank of Gloria Drift in the Southern Labrador Sea	53°19.878'N	45°15.720' W	44. 98	Coxall et al. 2018	34.480 8	*Catapsydrax unicavus*	*Catapsydrax unicavus*	3	- 0.2 06	Excellent, glassy foraminife ra
105	647 A		Southern flank of Gloria Drift in the Southern Labrador Sea	53°19.878'N	45°15.720' W	44. 98	Coxall et al. 2018	34.489 5	*Catapsydrax unicavus*	*Catapsydrax unicavus*	3	- 0.4 08	Excellent, glassy foraminife ra
105	647 A		Southern flank of Gloria Drift in the Southern Labrador Sea	53°19.878'N	45°15.720' W	44. 98	Coxall et al. 2018	34.492 4	*Catapsydrax unicavus*	*Catapsydrax unicavus*	3	- 0.5 52	Excellent, glassy foraminife ra
105	647 A		Southern flank of Gloria Drift in the Southern Labrador Sea	53°19.878'N	45°15.720' W	44. 98	Coxall et al. 2018	34.500 2	*Catapsydrax unicavus*	*Catapsydrax unicavus*	3	- 0.1 91	Excellent, glassy foraminife ra

105	647 A		Southern flank of Gloria Drift in the Southern Labrador Sea	53°19.878'N	45°15.720'W	44.98	Coxall et al. 2018	34.5065	*Catapsydrax unicavus*	*Catapsydrax unicavus*	3	-0.797	Excellent, glassy foraminifera
105	647 A		Southern flank of Gloria Drift in the Southern Labrador Sea	53°19.878'N	45°15.720'W	44.98	Coxall et al. 2018	34.5102	*Catapsydrax unicavus*	*Catapsydrax unicavus*	3	-0.069	Excellent, glassy foraminifera
105	647 A		Southern flank of Gloria Drift in the Southern Labrador Sea	53°19.878'N	45°15.720'W	44.98	Coxall et al. 2018	34.7689	*Catapsydrax unicavus*	*Catapsydrax unicavus*	3	-0.140	Excellent, glassy foraminifera
105	647 A		Southern flank of Gloria Drift in the Southern Labrador Sea	53°19.878'N	45°15.720'W	44.98	Coxall et al. 2018	34.7848	*Catapsydrax unicavus*	*Catapsydrax unicavus*	3	-0.464	Excellent, glassy foraminifera
105	647 A		Southern flank of Gloria Drift in the Southern Labrador Sea	53°19.878'N	45°15.720'W	44.98	Coxall et al. 2018	34.7921	*Catapsydrax unicavus*	*Catapsydrax unicavus*	3	-1.049	Excellent, glassy foraminifera
105	647 A		Southern flank of Gloria Drift in the Southern Labrador Sea	53°19.878'N	45°15.720'W	44.98	Coxall et al. 2018	34.7921	*Catapsydrax unicavus*	*Catapsydrax unicavus*	3	-0.739	Excellent, glassy foraminifera
105	647 A		Southern flank of Gloria Drift in the Southern	53°19.878'N	45°15.720'W	44.98	Coxall et al. 2018	34.8035	*Catapsydrax unicavus*	*Catapsydrax unicavus*	3	-1.049	Excellent, glassy foraminifera

			Labrador Sea										
105	647 A		Southern flank of Gloria Drift in the Southern Labrador Sea	53°19.878'N	45°15.720'W	44.98	Coxall et al. 2018	34.8075	*Catapsydrax unicavus*	*Catapsydrax unicavus*	3	-0.681	Excellent, glassy foraminifera
105	647 A		Southern flank of Gloria Drift in the Southern Labrador Sea	53°19.878'N	45°15.720'W	44.98	Coxall et al. 2018	34.8142	*Catapsydrax unicavus*	*Catapsydrax unicavus*	3	-1.220	Excellent, glassy foraminifera
105	647 A		Southern flank of Gloria Drift in the Southern Labrador Sea	53°19.878'N	45°15.720'W	44.98	Coxall et al. 2018	34.9384	*Catapsydrax unicavus*	*Catapsydrax unicavus*	3	0.504	Excellent, glassy foraminifera
105	647 A		Southern flank of Gloria Drift in the Southern Labrador Sea	53°19.878'N	45°15.720'W	44.98	Coxall et al. 2018	35.1421	*Catapsydrax unicavus*	*Catapsydrax unicavus*	3	-0.923	Excellent, glassy foraminifera
105	647 A		Southern flank of Gloria Drift in the Southern Labrador Sea	53°19.878'N	45°15.720'W	44.98	Coxall et al. 2018	35.1481	*Catapsydrax unicavus*	*Catapsydrax unicavus*	3	-1.092	Excellent, glassy foraminifera
105	647 A		Southern flank of Gloria Drift in the Southern Labrador Sea	53°19.878'N	45°15.720'W	44.98	Coxall et al. 2018	35.1523	*Catapsydrax unicavus*	*Catapsydrax unicavus*	3	-0.851	Excellent, glassy foraminifera

105	647 A		Southern flank of Gloria Drift in the Southern Labrador Sea	53°19.878'N	45°15.720'W	44.98	Coxall et al. 2018	35.1566	Catapsydrax unicavus	Catapsydrax unicavus	3	-0.624	Excellent, glassy foraminifera
105	647 A		Southern flank of Gloria Drift in the Southern Labrador Sea	53°19.878'N	45°15.720'W	44.98	Coxall et al. 2018	35.1606	Catapsydrax unicavus	Catapsydrax unicavus	3	-0.640	Excellent, glassy foraminifera
105	647 A		Southern flank of Gloria Drift in the Southern Labrador Sea	53°19.878'N	45°15.720'W	44.98	Coxall et al. 2018	35.1644	Catapsydrax unicavus	Catapsydrax unicavus	3	-0.467	Excellent, glassy foraminifera
105	647 A		Southern flank of Gloria Drift in the Southern Labrador Sea	53°19.878'N	45°15.720'W	44.98	Coxall et al. 2018	35.1664	Catapsydrax unicavus	Catapsydrax unicavus	3	-0.691	Excellent, glassy foraminifera
105	647 A		Southern flank of Gloria Drift in the Southern Labrador Sea	53°19.878'N	45°15.720'W	44.98	Coxall et al. 2018	35.1719	Catapsydrax unicavus	Catapsydrax unicavus	3	-0.709	Excellent, glassy foraminifera
105	647 A		Southern flank of Gloria Drift in the Southern Labrador Sea	53°19.878'N	45°15.720'W	44.98	Coxall et al. 2018	35.1751	Catapsydrax unicavus	Catapsydrax unicavus	3	-0.778	Excellent, glassy foraminifera
105	647 A		Southern flank of Gloria Drift in the Southern	53°19.878'N	45°15.720'W	44.98	Coxall et al. 2018	35.1791	Catapsydrax unicavus	Catapsydrax unicavus	3	-0.650	Excellent, glassy foraminifera

			Labrador Sea										
105	647 A		Southern flank of Gloria Drift in the Southern Labrador Sea	53°19.878'N	45°15.720'W	44.98	Coxall et al. 2018	35.1820	*Catapsydrax unicavus*	*Catapsydrax unicavus*	3	-0.928	Excellent, glassy foraminifera
105	647 A		Southern flank of Gloria Drift in the Southern Labrador Sea	53°19.878'N	45°15.720'W	44.98	Coxall et al. 2018	35.4793	*Catapsydrax unicavus*	*Catapsydrax unicavus*	3	-0.154	Excellent, glassy foraminifera
105	647 A		Southern flank of Gloria Drift in the Southern Labrador Sea	53°19.878'N	45°15.720'W	44.98	Coxall et al. 2018	35.4826	*Catapsydrax unicavus*	*Catapsydrax unicavus*	3	-0.501	Excellent, glassy foraminifera
105	647 A		Southern flank of Gloria Drift in the Southern Labrador Sea	53°19.878'N	45°15.720'W	44.98	Coxall et al. 2018	35.8484	*Catapsydrax unicavus*	*Catapsydrax unicavus*	3	-0.298	Excellent, glassy foraminifera
105	647 A		Southern flank of Gloria Drift in the Southern Labrador Sea	53°19.878'N	45°15.720'W	44.98	Coxall et al. 2018	35.8535	*Catapsydrax unicavus*	*Catapsydrax unicavus*	3	-0.345	Excellent, glassy foraminifera
105	647 A		Southern flank of Gloria Drift in the Southern Labrador Sea	53°19.878'N	45°15.720'W	44.98	Coxall et al. 2018	35.8793	*Catapsydrax unicavus*	*Catapsydrax unicavus*	3	-0.636	Excellent, glassy foraminifera

105	647 A		Southern flank of Gloria Drift in the Southern Labrador Sea	53°19.878'N	45°15.720' W	44.98	Coxall et al. 2018	35.8923	*Catapsydrax unicavus*	*Catapsydrax unicavus*	3	-0.347	Excellent, glassy foraminifera
105	647 A		Southern flank of Gloria Drift in the Southern Labrador Sea	53°19.878'N	45°15.720' W	44.98	Coxall et al. 2018	35.8992	*Catapsydrax unicavus*	*Catapsydrax unicavus*	3	-0.586	Excellent, glassy foraminifera
105	647 A		Southern flank of Gloria Drift in the Southern Labrador Sea	53°19.878'N	45°15.720' W	44.98	Coxall et al. 2018	35.9032	*Catapsydrax unicavus*	*Catapsydrax unicavus*	3	-0.366	Excellent, glassy foraminifera
105	647 A		Southern flank of Gloria Drift in the Southern Labrador Sea	53°19.878'N	45°15.720' W	44.98	Coxall et al. 2018	35.9068	*Catapsydrax unicavus*	*Catapsydrax unicavus*	3	-0.722	Excellent, glassy foraminifera
105	647 A		Southern flank of Gloria Drift in the Southern Labrador Sea	53°19.878'N	45°15.720' W	44.98	Coxall et al. 2018	35.9260	*Catapsydrax unicavus*	*Catapsydrax unicavus*	3	-1.342	Excellent, glassy foraminifera
105	647 A		Southern flank of Gloria Drift in the Southern Labrador Sea	53°19.878'N	45°15.720' W	44.98	Coxall et al. 2018	35.9398	*Catapsydrax unicavus*	*Catapsydrax unicavus*	3	-1.481	Excellent, glassy foraminifera
105	647 A		Southern flank of Gloria Drift in the Southern	53°19.878'N	45°15.720' W	44.98	Coxall et al. 2018	35.9460	*Catapsydrax unicavus*	*Catapsydrax unicavus*	3	-1.354	Excellent, glassy foraminifera

			Labrador Sea										
105	647 A		Southern flank of Gloria Drift in the Southern Labrador Sea	53°19.878'N	45°15.720'W	44.98	Coxall et al. 2018	35.9547	*Catapsydrax unicavus*	*Catapsydrax unicavus*	3	-1.627	Excellent, glassy foraminifera
105	647 A		Southern flank of Gloria Drift in the Southern Labrador Sea	53°19.878'N	45°15.720'W	44.98	Coxall et al. 2018	35.9572	*Catapsydrax unicavus*	*Catapsydrax unicavus*	3	-1.025	Excellent, glassy foraminifera
105	647 A		Southern flank of Gloria Drift in the Southern Labrador Sea	53°19.878'N	45°15.720'W	44.98	Coxall et al. 2018	35.9697	*Catapsydrax unicavus*	*Catapsydrax unicavus*	3	-1.010	Excellent, glassy foraminifera
105	647 A		Southern flank of Gloria Drift in the Southern Labrador Sea	53°19.878'N	45°15.720'W	44.98	Coxall et al. 2018	35.9743	*Catapsydrax unicavus*	*Catapsydrax unicavus*	3	-0.937	Excellent, glassy foraminifera
105	647 A		Southern flank of Gloria Drift in the Southern Labrador Sea	53°19.878'N	45°15.720'W	44.98	Coxall et al. 2018	35.9877	*Catapsydrax unicavus*	*Catapsydrax unicavus*	3	-0.702	Excellent, glassy foraminifera
105	647 A		Southern flank of Gloria Drift in the Southern Labrador Sea	53°19.878'N	45°15.720'W	44.98	Coxall et al. 2018	35.9956	*Catapsydrax unicavus*	*Catapsydrax unicavus*	3	-0.250	Excellent, glassy foraminifera

105	647 A		Southern flank of Gloria Drift in the Southern Labrador Sea	53°19.878'N	45°15.720'W	44.98	Coxall et al. 2018	36.1755	Catapsydrax unicavus	Catapsydrax unicavus	3	-1.015	Excellent, glassy foraminifera
105	647 A		Southern flank of Gloria Drift in the Southern Labrador Sea	53°19.878'N	45°15.720'W	44.98	Coxall et al. 2018	36.1816	Catapsydrax unicavus	Catapsydrax unicavus	3	-1.045	Excellent, glassy foraminifera
105	647 A		Southern flank of Gloria Drift in the Southern Labrador Sea	53°19.878'N	45°15.720'W	44.98	Coxall et al. 2018	36.2052	Catapsydrax unicavus	Catapsydrax unicavus	3	-1.188	Excellent, glassy foraminifera
105	647 A		Southern flank of Gloria Drift in the Southern Labrador Sea	53°19.878'N	45°15.720'W	44.98	Coxall et al. 2018	36.2125	Catapsydrax unicavus	Catapsydrax unicavus	3	-0.692	Excellent, glassy foraminifera
105	647 A		Southern flank of Gloria Drift in the Southern Labrador Sea	53°19.878'N	45°15.720'W	44.98	Coxall et al. 2018	36.2368	Catapsydrax unicavus	Catapsydrax unicavus	3	-0.511	Excellent, glassy foraminifera
105	647 A		Southern flank of Gloria Drift in the Southern Labrador Sea	53°19.878'N	45°15.720'W	44.98	Coxall et al. 2018	36.2523	Catapsydrax unicavus	Catapsydrax unicavus	3	-0.666	Excellent, glassy foraminifera
105	647 A		Southern flank of Gloria Drift in the Southern	53°19.878'N	45°15.720'W	44.98	Coxall et al. 2018	36.2571	Catapsydrax unicavus	Catapsydrax unicavus	3	-0.663	Excellent, glassy foraminifera

			Labrador Sea										
105	647 A		Southern flank of Gloria Drift in the Southern Labrador Sea	53°19.878'N	45°15.720'W	44.98	Coxall et al. 2018	36.2629	*Catapsydrax unicavus*	*Catapsydrax unicavus*	3	-0.604	Excellent, glassy foraminifera
105	647 A		Southern flank of Gloria Drift in the Southern Labrador Sea	53°19.878'N	45°15.720'W	44.98	Coxall et al. 2018	36.2701	*Catapsydrax unicavus*	*Catapsydrax unicavus*	3	-1.576	Excellent, glassy foraminifera
105	647 A		Southern flank of Gloria Drift in the Southern Labrador Sea	53°19.878'N	45°15.720'W	44.98	Coxall et al. 2018	36.2732	*Catapsydrax unicavus*	*Catapsydrax unicavus*	3	-1.166	Excellent, glassy foraminifera
105	647 A		Southern flank of Gloria Drift in the Southern Labrador Sea	53°19.878'N	45°15.720'W	44.98	Coxall et al. 2018	36.2810	*Catapsydrax unicavus*	*Catapsydrax unicavus*	3	-1.396	Excellent, glassy foraminifera
105	647 A		Southern flank of Gloria Drift in the Southern Labrador Sea	53°19.878'N	45°15.720'W	44.98	Coxall et al. 2018	36.3017	*Catapsydrax unicavus*	*Catapsydrax unicavus*	3	-0.702	Excellent, glassy foraminifera
105	647 A		Southern flank of Gloria Drift in the Southern Labrador Sea	53°19.878'N	45°15.720'W	44.98	Coxall et al. 2018	36.3049	*Catapsydrax unicavus*	*Catapsydrax unicavus*	3	-0.766	Excellent, glassy foraminifera

105	647 A		Southern flank of Gloria Drift in the Southern Labrador Sea	53°19.878'N	45°15.720'W	44.98	Coxall et al. 2018	36.3140	*Catapsydrax unicavus*	*Catapsydrax unicavus*	3	-0.977	Excellent, glassy foraminifera
105	647 A		Southern flank of Gloria Drift in the Southern Labrador Sea	53°19.878'N	45°15.720'W	44.98	Coxall et al. 2018	36.3214	*Catapsydrax unicavus*	*Catapsydrax unicavus*	3	-1.594	Excellent, glassy foraminifera
105	647 A		Southern flank of Gloria Drift in the Southern Labrador Sea	53°19.878'N	45°15.720'W	44.98	Coxall et al. 2018	36.3314	*Catapsydrax unicavus*	*Catapsydrax unicavus*	3	-1.902	Excellent, glassy foraminifera
105	647 A		Southern flank of Gloria Drift in the Southern Labrador Sea	53°19.878'N	45°15.720'W	44.98	Coxall et al. 2018	36.3341	*Catapsydrax unicavus*	*Catapsydrax unicavus*	3	-1.545	Excellent, glassy foraminifera
105	647 A		Southern flank of Gloria Drift in the Southern Labrador Sea	53°19.878'N	45°15.720'W	44.98	Coxall et al. 2018	36.3423	*Catapsydrax unicavus*	*Catapsydrax unicavus*	3	-1.578	Excellent, glassy foraminifera
105	647 A		Southern flank of Gloria Drift in the Southern Labrador Sea	53°19.878'N	45°15.720'W	44.98	Coxall et al. 2018	36.3564	*Catapsydrax unicavus*	*Catapsydrax unicavus*	3	-1.496	Excellent, glassy foraminifera
105	647 A		Southern flank of Gloria Drift in the Southern	53°19.878'N	45°15.720'W	44.98	Coxall et al. 2018	37.3528	*Catapsydrax unicavus*	*Catapsydrax unicavus*	3	-1.096	Excellent, glassy foraminifera

			Labrador Sea										
105	647 A		Southern flank of Gloria Drift in the Southern Labrador Sea	53°19.878'N	45°15.720'W	44.98	Coxall et al. 2018	34.2002	*Globoturborotalita oachitaensis*	*Globoturborotalita oachitaensis*	1	-2.366	Excellent, glassy foraminifera
105	647 A		Southern flank of Gloria Drift in the Southern Labrador Sea	53°19.878'N	45°15.720'W	44.98	Coxall et al. 2018	34.3042	*Globoturborotalita oachitaensis*	*Globoturborotalita oachitaensis*	1	-1.340	Excellent, glassy foraminifera
105	647 A		Southern flank of Gloria Drift in the Southern Labrador Sea	53°19.878'N	45°15.720'W	44.98	Coxall et al. 2018	34.3075	*Globoturborotalita oachitaensis*	*Globoturborotalita oachitaensis*	1	-1.005	Excellent, glassy foraminifera
105	647 A		Southern flank of Gloria Drift in the Southern Labrador Sea	53°19.878'N	45°15.720'W	44.98	Coxall et al. 2018	34.3146	*Globoturborotalita oachitaensis*	*Globoturborotalita oachitaensis*	1	-1.682	Excellent, glassy foraminifera
105	647 A		Southern flank of Gloria Drift in the Southern Labrador Sea	53°19.878'N	45°15.720'W	44.98	Coxall et al. 2018	34.3187	*Globoturborotalita oachitaensis*	*Globoturborotalita oachitaensis*	1	-1.672	Excellent, glassy foraminifera
105	647 A		Southern flank of Gloria Drift in the Southern Labrador Sea	53°19.878'N	45°15.720'W	44.98	Coxall et al. 2018	34.3224	*Globoturborotalita oachitaensis*	*Globoturborotalita oachitaensis*	1	-2.091	Excellent, glassy foraminifera

105	647 A		Southern flank of Gloria Drift in the Southern Labrador Sea	53°19.878'N	45°15.720'W	44.98	Coxall et al. 2018	34.4808	*Globoturborotalita oachitaensis*	*Globoturborotalita oachitaensis*	1	-1.499	Excellent, glassy foraminifera
105	647 A		Southern flank of Gloria Drift in the Southern Labrador Sea	53°19.878'N	45°15.720'W	44.98	Coxall et al. 2018	34.4924	*Globoturborotalita oachitaensis*	*Globoturborotalita oachitaensis*	1	-1.897	Excellent, glassy foraminifera
105	647 A		Southern flank of Gloria Drift in the Southern Labrador Sea	53°19.878'N	45°15.720'W	44.98	Coxall et al. 2018	34.5002	*Globoturborotalita oachitaensis*	*Globoturborotalita oachitaensis*	1	-1.410	Excellent, glassy foraminifera
105	647 A		Southern flank of Gloria Drift in the Southern Labrador Sea	53°19.878'N	45°15.720'W	44.98	Coxall et al. 2018	35.1481	*Globoturborotalita oachitaensis*	*Globoturborotalita oachitaensis*	1	-3.073	Excellent, glassy foraminifera
105	647 A		Southern flank of Gloria Drift in the Southern Labrador Sea	53°19.878'N	45°15.720'W	44.98	Coxall et al. 2018	35.1820	*Globoturborotalita oachitaensis*	*Globoturborotalita oachitaensis*	1	-2.727	Excellent, glassy foraminifera
105	647 A		Southern flank of Gloria Drift in the Southern Labrador Sea	53°19.878'N	45°15.720'W	44.98	Coxall et al. 2018	35.9877	*Globoturborotalita oachitaensis*	*Globoturborotalita oachitaensis*	1	-2.024	Excellent, glassy foraminifera
105	647 A		Southern flank of Gloria Drift in the Southern	53°19.878'N	45°15.720'W	44.98	Coxall et al. 2018	36.3314	*Globoturborotalita oachitaensis*	*Globoturborotalita oachitaensis*	1	-2.226	Excellent, glassy foraminifera

			Labrador Sea										
105	647 A		Southern flank of Gloria Drift in the Southern Labrador Sea	53°19.878'N	45°15.720' W	44. 98	Coxall et al. 2018	36.334 1	*Globoturborotalita oachitaensis*	*Globoturborotalita oachitaensis*	1	- 0.8 31	Excellent, glassy foraminife ra
105	647 A		Southern flank of Gloria Drift in the Southern Labrador Sea	53°19.878'N	45°15.720' W	44. 98	Coxall et al. 2018	36.342 3	*Globoturborotalita oachitaensis*	*Globoturborotalita oachitaensis*	1	- 2.8 01	Excellent, glassy foraminife ra
105	647 A		Southern flank of Gloria Drift in the Southern Labrador Sea	53°19.878'N	45°15.720' W	44. 98	Coxall et al. 2018	37.352 8	*Globoturborotalita oachitaensis*	*Globoturborotalita oachitaensis*	1	- 1.9 69	Excellent, glassy foraminife ra
105	647 A		Southern flank of Gloria Drift in the Southern Labrador Sea	53°19.878'N	45°15.720' W	44. 98	Coxall et al. 2018	34.073 27	*Turborotalia ampliapertura*	*Turborotalia ampliapertura*	2	- 2.0 35	Excellent, glassy foraminife ra
105	647 A		Southern flank of Gloria Drift in the Southern Labrador Sea	53°19.878'N	45°15.720' W	44. 98	Coxall et al. 2018	34.122 22	*Turborotalia ampliapertura/increbescens*	*Turborotalia ampliapertura/increbescens*	2	- 1.8 16	Excellent, glassy foraminife ra
105	647 A		Southern flank of Gloria Drift in the Southern Labrador Sea	53°19.878'N	45°15.720' W	44. 98	Coxall et al. 2018	34.132 73	*Turborotalia ampliapertura/increbescens*	*Turborotalia ampliapertura/increbescens*	2	- 1.5 40	Excellent, glassy foraminife ra

105	647 A		Southern flank of Gloria Drift in the Southern Labrador Sea	53°19.878'N	45°15.720' W	44. 98	Coxall et al. 2018	34.136 72	*Turborotalia ampliapertura*	*Turborotalia ampliapertura*	2	- 2.6 10	Excellent, glassy foraminife ra
105	647 A		Southern flank of Gloria Drift in the Southern Labrador Sea	53°19.878'N	45°15.720' W	44. 98	Coxall et al. 2018	34.147 60	*Turborotalia ampliapertura*	*Turborotalia ampliapertura*	2	- 1.8 04	Excellent, glassy foraminife ra
105	647 A		Southern flank of Gloria Drift in the Southern Labrador Sea	53°19.878'N	45°15.720' W	44. 98	Coxall et al. 2018	34.149 78	*Turborotalia ampliapertura*	*Turborotalia ampliapertura*	2	- 1.6 42	Excellent, glassy foraminife ra
105	647 A		Southern flank of Gloria Drift in the Southern Labrador Sea	53°19.878'N	45°15.720' W	44. 98	Coxall et al. 2018	34.153 58	*Turborotalia ampliapertura*	*Turborotalia ampliapertura*	2	- 2.4 71	Excellent, glassy foraminife ra
105	647 A		Southern flank of Gloria Drift in the Southern Labrador Sea	53°19.878'N	45°15.720' W	44. 98	Coxall et al. 2018	34.159 56	*Turborotalia ampliapertura/increbescens*	*Turborotalia ampliapertura/increbescens*	2	- 2.0 09	Excellent, glassy foraminife ra
105	647 A		Southern flank of Gloria Drift in the Southern Labrador Sea	53°19.878'N	45°15.720' W	44. 98	Coxall et al. 2018	34.162 83	*Turborotalia ampliapertura/increbescens*	*Turborotalia ampliapertura/increbescens*	2	- 1.8 16	Excellent, glassy foraminife ra
105	647 A		Southern flank of Gloria Drift in the Southern	53°19.878'N	45°15.720' W	44. 98	Coxall et al. 2018	34.167 00	*Turborotalia ampliapertura*	*Turborotalia ampliapertura*	2	- 2.0 49	Excellent, glassy foraminife ra

			Labrador Sea										
105	647 A		Southern flank of Gloria Drift in the Southern Labrador Sea	53°19.878'N	45°15.720' W	44. 98	Coxall et al. 2018	34.170 26	*Turborotalia ampliapertura*	*Turborotalia ampliapertura*	2	- 1.4 49	Excellent, glassy foraminife ra
105	647 A		Southern flank of Gloria Drift in the Southern Labrador Sea	53°19.878'N	45°15.720' W	44. 98	Coxall et al. 2018	34.174 43	*Turborotalia ampliapertura/increbescens*	*Turborotalia ampliapertura/increbescens*	2	- 2.3 79	Excellent, glassy foraminife ra
105	647 A		Southern flank of Gloria Drift in the Southern Labrador Sea	53°19.878'N	45°15.720' W	44. 98	Coxall et al. 2018	34.176 61	*Turborotalia ampliapertura/increbescens*	*Turborotalia ampliapertura/increbescens*	2	- 2.1 44	Excellent, glassy foraminife ra
105	647 A		Southern flank of Gloria Drift in the Southern Labrador Sea	53°19.878'N	45°15.720' W	44. 98	Coxall et al. 2018	34.180 59	*Turborotalia ampliapertura*	*Turborotalia ampliapertura*	2	- 1.5 32	Excellent, glassy foraminife ra
105	647 A		Southern flank of Gloria Drift in the Southern Labrador Sea	53°19.878'N	45°15.720' W	44. 98	Coxall et al. 2018	34.183 49	*Turborotalia ampliapertura*	*Turborotalia ampliapertura*	2	- 2.0 08	Excellent, glassy foraminife ra
105	647 A		Southern flank of Gloria Drift in the Southern Labrador Sea	53°19.878'N	45°15.720' W	44. 98	Coxall et al. 2018	34.187 48	*Turborotalia ampliapertura/increbescens*	*Turborotalia ampliapertura/increbescens*	2	- 1.6 62	Excellent, glassy foraminife ra

105	647 A		Southern flank of Gloria Drift in the Southern Labrador Sea	53°19.878'N	45°15.720' W	44. 98	Coxall et al. 2018	34.191 83	*Turborotalia ampliapertura/increbescens*	*Turborotalia ampliapertura/increbescens*	2	- 1.6 32	Excellent, glassy foraminife ra
105	647 A		Southern flank of Gloria Drift in the Southern Labrador Sea	53°19.878'N	45°15.720' W	44. 98	Coxall et al. 2018	34.195 28	*Turborotalia ampliapertura*	*Turborotalia ampliapertura*	2	- 1.4 38	Excellent, glassy foraminife ra
105	647 A		Southern flank of Gloria Drift in the Southern Labrador Sea	53°19.878'N	45°15.720' W	44. 98	Coxall et al. 2018	34.198 72	*Turborotalia ampliapertura*	*Turborotalia ampliapertura*	2	- 1.9 54	Excellent, glassy foraminife ra
105	647 A		Southern flank of Gloria Drift in the Southern Labrador Sea	53°19.878'N	45°15.720' W	44. 98	Coxall et al. 2018	34.200 17	*Turborotalia ampliapertura*	*Turborotalia ampliapertura*	2	- 1.6 75	Excellent, glassy foraminife ra
105	647 A		Southern flank of Gloria Drift in the Southern Labrador Sea	53°19.878'N	45°15.720' W	44. 98	Coxall et al. 2018	34.208 51	*Turborotalia ampliapertura/increbescens*	*Turborotalia ampliapertura/increbescens*	2	- 1.5 77	Excellent, glassy foraminife ra
105	647 A		Southern flank of Gloria Drift in the Southern Labrador Sea	53°19.878'N	45°15.720' W	44. 98	Coxall et al. 2018	34.212 14	*Turborotalia ampliapertura*	*Turborotalia ampliapertura*	2	- 1.8 29	Excellent, glassy foraminife ra
105	647 A		Southern flank of Gloria Drift in the Southern	53°19.878'N	45°15.720' W	44. 98	Coxall et al. 2018	34.215 58	*Turborotalia ampliapertura*	*Turborotalia ampliapertura*	2	- 1.7 73	Excellent, glassy foraminife ra

			Labrador Sea										
105	647 A		Southern flank of Gloria Drift in the Southern Labrador Sea	53°19.878'N	45°15.720' W	44. 98	Coxall et al. 2018	34.219 39	*Turborotalia ampliapertura/increbescens*	*Turborotalia ampliapertura/increbescens*	2	- 1.9 59	Excellent, glassy foraminife ra
105	647 A		Southern flank of Gloria Drift in the Southern Labrador Sea	53°19.878'N	45°15.720' W	44. 98	Coxall et al. 2018	34.224 47	*Turborotalia ampliapertura/increbescens*	*Turborotalia ampliapertura/increbescens*	2	- 1.4 85	Excellent, glassy foraminife ra
105	647 A		Southern flank of Gloria Drift in the Southern Labrador Sea	53°19.878'N	45°15.720' W	44. 98	Coxall et al. 2018	34.227 73	*Turborotalia ampliapertura*	*Turborotalia ampliapertura*	2	- 1.2 98	Excellent, glassy foraminife ra
105	647 A		Southern flank of Gloria Drift in the Southern Labrador Sea	53°19.878'N	45°15.720' W	44. 98	Coxall et al. 2018	34.231 35	*Turborotalia ampliapertura*	*Turborotalia ampliapertura*	2	- 1.8 09	Excellent, glassy foraminife ra
105	647 A		Southern flank of Gloria Drift in the Southern Labrador Sea	53°19.878'N	45°15.720' W	44. 98	Coxall et al. 2018	34.246 58	*Turborotalia ampliapertura*	*Turborotalia ampliapertura*	2	- 2.1 31	Excellent, glassy foraminife ra
105	647 A		Southern flank of Gloria Drift in the Southern Labrador Sea	53°19.878'N	45°15.720' W	44. 98	Coxall et al. 2018	34.252 75	*Turborotalia ampliapertura/increbescens*	*Turborotalia ampliapertura/increbescens*	2	- 1.5 40	Excellent, glassy foraminife ra

105	647 A		Southern flank of Gloria Drift in the Southern Labrador Sea	53°19.878'N	45°15.720'W	44.98	Coxall et al. 2018	34.25746	*Turborotalia ampliapertura*	*Turborotalia ampliapertura*	2	-1.457	Excellent, glassy foraminifera
105	647 A		Southern flank of Gloria Drift in the Southern Labrador Sea	53°19.878'N	45°15.720'W	44.98	Coxall et al. 2018	34.26399	*Turborotalia ampliapertura*	*Turborotalia ampliapertura*	2	-1.325	Excellent, glassy foraminifera
105	647 A		Southern flank of Gloria Drift in the Southern Labrador Sea	53°19.878'N	45°15.720'W	44.98	Coxall et al. 2018	34.26761	*Turborotalia ampliapertura/increbescens*	*Turborotalia ampliapertura/increbescens*	2	-1.873	Excellent, glassy foraminifera
105	647 A		Southern flank of Gloria Drift in the Southern Labrador Sea	53°19.878'N	45°15.720'W	44.98	Coxall et al. 2018	34.27631	*Turborotalia ampliapertura/increbescens*	*Turborotalia ampliapertura/increbescens*	2	-1.312	Excellent, glassy foraminifera
105	647 A		Southern flank of Gloria Drift in the Southern Labrador Sea	53°19.878'N	45°15.720'W	44.98	Coxall et al. 2018	34.29009	*Turborotalia ampliapertura*	*Turborotalia ampliapertura*	2	-2.285	Excellent, glassy foraminifera
105	647 A		Southern flank of Gloria Drift in the Southern Labrador Sea	53°19.878'N	45°15.720'W	44.98	Coxall et al. 2018	34.29372	*Turborotalia ampliapertura*	*Turborotalia ampliapertura*	2	-1.570	Excellent, glassy foraminifera
105	647 A		Southern flank of Gloria Drift in the Southern	53°19.878'N	45°15.720'W	44.98	Coxall et al. 2018	34.29626	*Turborotalia ampliapertura*	*Turborotalia ampliapertura*	2	-1.968	Excellent, glassy foraminifera

105	647 A		Labrador Sea										
105	647 A		Southern flank of Gloria Drift in the Southern Labrador Sea	53°19.878'N	45°15.720' W	44. 98	Coxall et al. 2018	34.300 61	*Turborotalia ampliapertura/increbescens*	*Turborotalia ampliapertura/increbescens*	2	- 1.8 53	Excellent, glassy foraminife ra
105	647 A		Southern flank of Gloria Drift in the Southern Labrador Sea	53°19.878'N	45°15.720' W	44. 98	Coxall et al. 2018	34.304 23	*Turborotalia ampliapertura*	*Turborotalia ampliapertura*	2	- 1.4 83	Excellent, glassy foraminife ra
105	647 A		Southern flank of Gloria Drift in the Southern Labrador Sea	53°19.878'N	45°15.720' W	44. 98	Coxall et al. 2018	34.325 99	*Turborotalia ampliapertura/increbescens*	*Turborotalia ampliapertura/increbescens*	2	- 2.4 52	Excellent, glassy foraminife ra
105	647 A		Southern flank of Gloria Drift in the Southern Labrador Sea	53°19.878'N	45°15.720' W	44. 98	Coxall et al. 2018	34.333 42	*Turborotalia ampliapertura*	*Turborotalia ampliapertura*	2	- 1.7 73	Excellent, glassy foraminife ra
105	647 A		Southern flank of Gloria Drift in the Southern Labrador Sea	53°19.878'N	45°15.720' W	44. 98	Coxall et al. 2018	34.340 13	*Turborotalia ampliapertura*	*Turborotalia ampliapertura*	2	- 1.8 61	Excellent, glassy foraminife ra
105	647 A		Southern flank of Gloria Drift in the Southern Labrador Sea	53°19.878'N	45°15.720' W	44. 98	Coxall et al. 2018	34.343 75	*Turborotalia ampliapertura/increbescens*	*Turborotalia ampliapertura/increbescens*	2	- 2.1 94	Excellent, glassy foraminife ra

105	647 A		Southern flank of Gloria Drift in the Southern Labrador Sea	53°19.878'N	45°15.720'W	44.98	Coxall et al. 2018	34.34665	*Turborotalia ampliapertura*	*Turborotalia ampliapertura*	2	-1.943	Excellent, glassy foraminifera
105	647 A		Southern flank of Gloria Drift in the Southern Labrador Sea	53°19.878'N	45°15.720'W	44.98	Coxall et al. 2018	34.35572	*Turborotalia ampliapertura*	*Turborotalia ampliapertura*	2	-1.781	Excellent, glassy foraminifera
105	647 A		Southern flank of Gloria Drift in the Southern Labrador Sea	53°19.878'N	45°15.720'W	44.98	Coxall et al. 2018	34.35862	*Turborotalia ampliapertura/increbescens*	*Turborotalia ampliapertura/increbescens*	2	-1.609	Excellent, glassy foraminifera
105	647 A		Southern flank of Gloria Drift in the Southern Labrador Sea	53°19.878'N	45°15.720'W	44.98	Coxall et al. 2018	34.36152	*Turborotalia ampliapertura*	*Turborotalia ampliapertura*	2	-1.740	Excellent, glassy foraminifera
105	647 A		Southern flank of Gloria Drift in the Southern Labrador Sea	53°19.878'N	45°15.720'W	44.98	Coxall et al. 2018	34.37348	*Turborotalia ampliapertura*	*Turborotalia ampliapertura*	2	-1.586	Excellent, glassy foraminifera
105	647 A		Southern flank of Gloria Drift in the Southern Labrador Sea	53°19.878'N	45°15.720'W	44.98	Coxall et al. 2018	34.40177	*Turborotalia ampliapertura*	*Turborotalia ampliapertura*	2	-1.193	Excellent, glassy foraminifera
105	647 A		Southern flank of Gloria Drift in the Southern	53°19.878'N	45°15.720'W	44.98	Coxall et al. 2018	34.42008	*Turborotalia ampliapertura*	*Turborotalia ampliapertura*	2	-2.044	Excellent, glassy foraminifera

			Labrador Sea										
105	647 A		Southern flank of Gloria Drift in the Southern Labrador Sea	53°19.878'N	45°15.720'W	44.98	Coxall et al. 2018	34.42751	*Turborotalia ampliapertura/increbescens*	*Turborotalia ampliapertura/increbescens*	2	-2.553	Excellent, glassy foraminifera
105	647 A		Southern flank of Gloria Drift in the Southern Labrador Sea	53°19.878'N	45°15.720'W	44.98	Coxall et al. 2018	34.43168	*Turborotalia ampliapertura*	*Turborotalia ampliapertura*	2	-2.365	Excellent, glassy foraminifera
105	647 A		Southern flank of Gloria Drift in the Southern Labrador Sea	53°19.878'N	45°15.720'W	44.98	Coxall et al. 2018	34.43548	*Turborotalia ampliapertura*	*Turborotalia ampliapertura*	2	-2.586	Excellent, glassy foraminifera
105	647 A		Southern flank of Gloria Drift in the Southern Labrador Sea	53°19.878'N	45°15.720'W	44.98	Coxall et al. 2018	34.43548	*Turborotalia ampliapertura*	*Turborotalia ampliapertura*	2	-1.919	Excellent, glassy foraminifera
105	647 A		Southern flank of Gloria Drift in the Southern Labrador Sea	53°19.878'N	45°15.720'W	44.98	Coxall et al. 2018	34.43911	*Turborotalia ampliapertura*	*Turborotalia ampliapertura*	2	-1.884	Excellent, glassy foraminifera
105	647 A		Southern flank of Gloria Drift in the Southern Labrador Sea	53°19.878'N	45°15.720'W	44.98	Coxall et al. 2018	34.47537	*Turborotalia ampliapertura/increbescens*	*Turborotalia ampliapertura/increbescens*	2	-1.125	Excellent, glassy foraminifera

105	647 A		Southern flank of Gloria Drift in the Southern Labrador Sea	53°19.878'N	45°15.720'W	44.98	Coxall et al. 2018	34.47791	*Turborotalia ampliapertura*	*Turborotalia ampliapertura*	2	-2.046	Excellent, glassy foraminifera
105	647 A		Southern flank of Gloria Drift in the Southern Labrador Sea	53°19.878'N	45°15.720'W	44.98	Coxall et al. 2018	35.17514	*Turborotalia ampliapertura/increbescens*	*Turborotalia ampliapertura/increbescens*	2	-1.965	Excellent, glassy foraminifera
105	647 A		Southern flank of Gloria Drift in the Southern Labrador Sea	53°19.878'N	45°15.720'W	44.98	Coxall et al. 2018	35.92603	*Turborotalia cocoaensis/cunialensis*	*Turborotalia cocoaensis/cunialensis*	2	-2.655	Excellent, glassy foraminifera
105	647 A		Southern flank of Gloria Drift in the Southern Labrador Sea	53°19.878'N	45°15.720'W	44.98	Coxall et al. 2018	35.95395	*Turborotalia cocoaensis/cunialensis*	*Turborotalia cocoaensis/cunialensis*	2	-2.243	Excellent, glassy foraminifera
105	647 A		Southern flank of Gloria Drift in the Southern Labrador Sea	53°19.878'N	45°15.720'W	44.98	Coxall et al. 2018	36.18165	*Turborotalia ampliapertura*	*Turborotalia ampliapertura*	2	-3.094	Excellent, glassy foraminifera
105	647 A		Southern flank of Gloria Drift in the Southern Labrador Sea	53°19.878'N	45°15.720'W	44.98	Coxall et al. 2018	36.21247	*Turborotalia ampliapertura*	*Turborotalia ampliapertura*	2	-3.098	Excellent, glassy foraminifera
105	647 A		Southern flank of Gloria Drift in the Southern	53°19.878'N	45°15.720'W	44.98	Coxall et al. 2018	36.25235	*Turborotalia ampliapertura*	*Turborotalia ampliapertura*	2	-3.038	Excellent, glassy foraminifera

105	647 A		Labrador Sea										
105	647 A		Southern flank of Gloria Drift in the Southern Labrador Sea	53°19.878'N	45°15.720'W	44.98	Coxall et al. 2018	36.25706	*Turborotalia cerroazulensis*	*Turborotalia cerroazulensis*	2	-3.000	Excellent, glassy foraminifera
105	647 A		Southern flank of Gloria Drift in the Southern Labrador Sea	53°19.878'N	45°15.720'W	44.98	Coxall et al. 2018	36.26286	*Turborotalia ampliapertura*	*Turborotalia ampliapertura*	2	-2.639	Excellent, glassy foraminifera
105	647 A		Southern flank of Gloria Drift in the Southern Labrador Sea	53°19.878'N	45°15.720'W	44.98	Coxall et al. 2018	36.27011	*Turborotalia cocoaensis/cunialensis/cerro azulensis*	*Turborotalia cocoaensis/cunialensis/cerro azulensis*	2	-2.635	Excellent, glassy foraminifera
105	647 A		Southern flank of Gloria Drift in the Southern Labrador Sea	53°19.878'N	45°15.720'W	44.98	Coxall et al. 2018	36.27320	*Turborotalia ampliapertura*	*Turborotalia ampliapertura*	2	-2.672	Excellent, glassy foraminifera
105	647 A		Southern flank of Gloria Drift in the Southern Labrador Sea	53°19.878'N	45°15.720'W	44.98	Coxall et al. 2018	36.30166	*Turborotalia ampliapertura*	*Turborotalia ampliapertura*	2	-2.872	Excellent, glassy foraminifera
105	647 A		Southern flank of Gloria Drift in the Southern Labrador Sea	53°19.878'N	45°15.720'W	44.98	Coxall et al. 2018	36.30492	*Turborotalia ampliapertura*	*Turborotalia ampliapertura*	2	-2.647	Excellent, glassy foraminifera

105	647 A		Southern flank of Gloria Drift in the Southern Labrador Sea	53°19.878'N	45°15.720'W	44.98	Coxall et al. 2018	36.35351	*Turborotalia ampliapertura*	*Turborotalia ampliapertura*	2	-2.541	Excellent, glassy foraminifera
105	647 A		Southern flank of Gloria Drift in the Southern Labrador Sea	53°19.878'N	45°15.720'W	44.98	Coxall et al. 2018	36.70329	*Turborotalia ampliapertura*	*Turborotalia ampliapertura*	2	-3.348	Excellent, glassy foraminifera
105	647 A		Southern flank of Gloria Drift in the Southern Labrador Sea	53°19.878'N	45°15.720'W	44.98	Coxall et al. 2018	36.87432	*Turborotalia ampliapertura*	*Turborotalia ampliapertura*	2	-3.174	Excellent, glassy foraminifera
105	647 A		Southern flank of Gloria Drift in the Southern Labrador Sea	53°19.878'N	45°15.720'W	44.98	Coxall et al. 2018	37.04870	*Turborotalia ampliapertura*	*Turborotalia ampliapertura*	2	-1.871	Excellent, glassy foraminifera
105	647 A		Southern flank of Gloria Drift in the Southern Labrador Sea	53°19.878'N	45°15.720'W	44.98	Coxall et al. 2018	37.20933	*Turborotalia ampliapertura*	*Turborotalia ampliapertura*	2	-4.194	Excellent, glassy foraminifera
105	647 A		Southern flank of Gloria Drift in the Southern Labrador Sea	53°19.878'N	45°15.720'W	44.98	Coxall et al. 2018	37.35285	*Turborotalia ampliapertura*	*Turborotalia ampliapertura*	2	-2.390	Excellent, glassy foraminifera
342	U1411		Southeast Newfoundland Ridge in the northwest	41.6°N	49.0ºW	33.51	Coxall et al. 2018	34.31900	*Catapsydrax unicavus*	*Catapsydrax unicavus*	3	-0.400	Excellent, glassy foraminifera

			Atlantic Ocean										
342	U1411		Southeast Newfoundland Ridge in the northwest Atlantic Ocean	41.6°N	49.0ºW	33.51	Coxall et al. 2018	34.3218	*Catapsydrax unicavus*	*Catapsydrax unicavus*	3	-0.39	Excellent, glassy foraminifera
342	U1411		Southeast Newfoundland Ridge in the northwest Atlantic Ocean	41.6°N	49.0ºW	33.51	Coxall et al. 2018	34.3229	*Turborotalia ampliapertura*	*Turborotalia ampliapertura*	2	-1.43	Excellent, glassy foraminifera
342	U1411		Southeast Newfoundland Ridge in the northwest Atlantic Ocean	41.6°N	49.0ºW	33.51	Coxall et al. 2018	34.3229	*Catapsydrax unicavus*	*Catapsydrax unicavus*	3	-0.44	Excellent, glassy foraminifera
342	U1411		Southeast Newfoundland Ridge in the northwest Atlantic Ocean	41.6°N	49.0ºW	33.51	Coxall et al. 2018	34.3524	*Catapsydrax unicavus*	*Catapsydrax unicavus*	3	-0.24	Excellent, glassy foraminifera
342	U1411		Southeast Newfoundland Ridge in the northwest Atlantic Ocean	41.6°N	49.0ºW	33.51	Coxall et al. 2018	34.3942	*Catapsydrax unicavus*	*Catapsydrax unicavus*	3	-0.27	Excellent, glassy foraminifera
342	U1411		Southeast Newfoundland Ridge in the northwest Atlantic Ocean	41.6°N	49.0ºW	33.51	Coxall et al. 2018	34.4177	*Turborotalia ampliapertura*	*Turborotalia ampliapertura*	2	-1.87	Excellent, glassy foraminifera

342	U1411		Southeast Newfoundl and Ridge in the northwest Atlantic Ocean	41.6°N	49.0ºW	33. 51	Coxall et al. 2018	34.417 7	*Catapsydrax unicavus*	*Catapsydrax unicavus*	3	- 0.0 6	Excellent, glassy foraminife ra
342	U1411		Southeast Newfoundl and Ridge in the northwest Atlantic Ocean	41.6°N	49.0ºW	33. 51	Coxall et al. 2018	34.435 9	*Catapsydrax unicavus*	*Catapsydrax unicavus*	3	- 0.2 7	Excellent, glassy foraminife ra
342	U1411		Southeast Newfoundl and Ridge in the northwest Atlantic Ocean	41.6°N	49.0ºW	33. 51	Coxall et al. 2018	34.675 3	*Turborotalia ampliapertura*	*Turborotalia ampliapertura*	2	- 1.4 1	Excellent, glassy foraminife ra
342	U1411		Southeast Newfoundl and Ridge in the northwest Atlantic Ocean	41.6°N	49.0ºW	33. 51	Coxall et al. 2018	34.675 3	*Catapsydrax unicavus*	*Catapsydrax unicavus*	3	- 0.0 8	Excellent, glassy foraminife ra
342	U1411		Southeast Newfoundl and Ridge in the northwest Atlantic Ocean	41.6°N	49.0ºW	33. 51	Coxall et al. 2018	34.680 3	*Catapsydrax unicavus*	*Catapsydrax unicavus*	3	- 0.2 9	Excellent, glassy foraminife ra
342	U1411		Southeast Newfoundl and Ridge in the northwest Atlantic Ocean	41.6°N	49.0ºW	33. 51	Coxall et al. 2018	34.714 3	*Turborotalia ampliapertura*	*Turborotalia ampliapertura*	2	- 1.7 3	Excellent, glassy foraminife ra
342	U1411		Southeast Newfoundl and Ridge in the northwest	41.6°N	49.0ºW	33. 51	Coxall et al. 2018	34.714 3	*Catapsydrax unicavus*	*Catapsydrax unicavus*	3	0.0 1	Excellent, glassy foraminife ra

342	U1411		Atlantic Ocean										
342	U1411		Southeast Newfoundland Ridge in the northwest Atlantic Ocean	41.6°N	49.0ºW	33.51	Coxall et al. 2018	34.7560	*Turborotalia ampliapertura*	*Turborotalia ampliapertura*	2	-1.60	Excellent, glassy foraminifera
342	U1411		Southeast Newfoundland Ridge in the northwest Atlantic Ocean	41.6°N	49.0ºW	33.51	Coxall et al. 2018	34.7560	*Catapsydrax unicavus*	*Catapsydrax unicavus*	3	0.19	Excellent, glassy foraminifera
342	U1411		Southeast Newfoundland Ridge in the northwest Atlantic Ocean	41.6°N	49.0ºW	33.51	Coxall et al. 2018	34.7583	*Turborotalia ampliapertura*	*Turborotalia ampliapertura*	2	-1.41	Excellent, glassy foraminifera
342	U1411		Southeast Newfoundland Ridge in the northwest Atlantic Ocean	41.6°N	49.0ºW	33.51	Coxall et al. 2018	34.7583	*Catapsydrax unicavus*	*Catapsydrax unicavus*	3	-0.28	Excellent, glassy foraminifera
342	U1411		Southeast Newfoundland Ridge in the northwest Atlantic Ocean	41.6°N	49.0ºW	33.51	Coxall et al. 2018	34.7814	*Turborotalia ampliapertura*	*Turborotalia ampliapertura*	2	-1.49	Excellent, glassy foraminifera
342	U1411		Southeast Newfoundland Ridge in the northwest Atlantic Ocean	41.6°N	49.0ºW	33.51	Coxall et al. 2018	34.7814	*Catapsydrax unicavus*	*Catapsydrax unicavus*	3	-0.23	Excellent, glassy foraminifera

Appendix 7

Global Planktonic Foraminiferal δ^{18}O Database from the early Oligocene

Early Oligocene database displaying a global δ^{18}O compilation from planktonic foraminifera, along with the name of the site, geographical coordinates, preservation state of the specimens, updated name of the foraminiferal species, ecological group assigned, and the source the data were retrieved from. The palaeolatitude was calculated using the palaeolatitude calculator developed by van Hinsbergen (2015).

Leg	Site	(Bio)zone	Geographical Area	Latitude	Longitude	Palaeolatitude	Author	Age if specified (Ma)	Species name	Updated Name	Ecology group	$\delta^{18}O$ Value (‰)	Preservation
17	167	P18	Shatsky Rise	7°04.1'N	167°49.5' W	0.8	Douglas and Savin, 1973		*Globigerina tapiurensis*	*Dentoglobigerina tapiurensis*	3	-0.37	
17	167	P19/P20	Shatsky Rise	7°04.1'N	167°49.5' W	0.8	Douglas and Savin, 1973		*Pseudohastigerina barbadoensis*	*Pseudohastigerina naguewichiensis*	1	1.95	
17	167	P19/P20	Shatsky Rise	7°04.1'N	167°49.5' W	0.8	Douglas and Savin, 1973		*Pseudohastigerina barbadoensis*	*Pseudohastigerina naguewichiensis*	1	-0.02	
17	167	P19/P20	Shatsky Rise	7°04.1'N	167°49.5' W	0.8	Douglas and Savin, 1973		*Pseudohastigerina barbadoensis*	*Pseudohastigerina naguewichiensis*	1	-0.25	
17	167	P19/P20	Shatsky Rise	7°04.1'N	167°49.5' W	0.8	Douglas and Savin, 1973		*Globigerina ampliapertura*	*Turborotalia ampliapertura*	2	-0.32	
17	171	P18	Shatsky Rise	7°04.1'N	167°49.5' W	0.8	Douglas and Savin, 1973		*Globigerina tapiurensis*	*Dentoglobigerina tapiurensis*	3	0.43	
6	44		Horizon Ridge	19° 18.5'N	169° 00'W	13.1	Douglas and Savin, 1971	Lower Oligocene	*Globigerina ampliapertura*	*Turborotalia ampliapertura*	2	0.5	

6	44		Horizon Ridge	19° 18.5'N	169° 00'W	13.1	Douglas and Savin, 1971	Lower Oligocene	*Globigerina ampliapertura*	*Turborotalia ampliapertura*	2	0.49	
32	305	P18	Shatsky Rise	32°00.13'N	157°51.00'E	29.78	Douglas and Savin, 1975	early Oligocene	Mixed spp. *of Planktonic Foraminifera*	Mixed spp. *of Planktonic Foraminifera*	3	0.78	
113	689b	It only says early Oligocene	Maud Rise	64 31.01"S	03 06.00"E	-67.64	Mackensen and Ehrmann, 1992		Subbotinids	*Subbotina* spp.	3	2.41	
113	689b	It only says early Oligocene	Maud Rise	64 31.01"S	03 06.00"E	-67.64	Mackensen and Ehrmann, 1992		Subbotinids	*Subbotina* spp.	3	2.36	
113	689b	It only says early Oligocene	Maud Rise	64 31.01"S	3 06.00"E	-67.64	Mackensen and Ehrmann, 1992		Subbotinids	*Subbotina* spp.	3	2.2	
113	689b	It only says early Oligocene	Maud Rise	64 31.01"S	3 06.00"E	-67.64	Mackensen and Ehrmann, 1992		Subbotinids	*Subbotina* spp.	3	2.12	
113	689b	It only says early Oligocene	Maud Rise	64 31.01"S	3 06.00"E	-67.64	Mackensen and Ehrmann, 1992		Subbotinids	*Subbotina* spp.	3	2.5	
113	689b	It only says early Oligocene	Maud Rise	64 31.01"S	3 06.00"E	-67.64	Mackensen and Ehrmann, 1992		Subbotinids	*Subbotina* spp.	3	2.33	
113	690b	It only says early Oligocene	Maud Rise	65' 09.63"S	01 '12.30"E	-68.41	Mackensen and Ehrmann, 1992		Subbotinids	*Subbotina* spp.	3	2.12	

113	690b	It only says early Oligocene	Maud Rise	65' 09.63"S	01 '12.30"E	-68.4 1	Mackensen and Ehrmann, 1992		Subbotinids	*Subbotina* spp.	3	2.39	
113	690b	It only says early Oligocene	Maud Rise	65' 09.63"S	1 '12.30"E	-68.4 1	Mackensen and Ehrmann, 1992		Subbotinids	*Subbotina* spp.	3	2.42	
113	690b	It only says early Oligocene	Maud Rise	65' 09.63"S	1 '12.30"E	-68.4 1	Mackensen and Ehrmann, 1992		Subbotinids	*Subbotina* spp.	3	1.96	
113	690b	It only says early Oligocene	Maud Rise	65' 09.63"S	1 '12.30"E	-68.4 1	Mackensen and Ehrmann, 1992		Subbotinids	*Subbotina* spp.	3	1.7	
113	690b	It only says early Oligocene	Maud Rise	65' 09.63"S	1 '12.30"E	-68.4 1	Mackensen and Ehrmann, 1992		Subbotinids	*Subbotina* spp.	3	1.78	
113	690b	It only says early Oligocene	Maud Rise	65' 09.63"S	1 '12.30"E	-68.4 1	Mackensen and Ehrmann, 1992		Subbotinids	*Subbotina* spp.	3	2.03	
117	738b	It only says early Oligocene	Kerguelen Plateau	62"42.54" S 82'47.25" E		-59.5	Mackensen and Ehrmann, 1992		Subbotinids	*Subbotina* spp.	3	1.49	
117	738b	It only says early Oligocene	Kerguelen Plateau	62"42.54" S 82'47.25" E		-59.5	Mackensen and Ehrmann, 1992		*Globigerinids*	*Globigerina* spp.	2	1.46	
117	738b	It only says early Oligocene	Kerguelen Plateau	62"42.54" S 82'47.25" E		-59.5	Mackensen and Ehrmann, 1992		Subbotinids	*Subbotina* spp.	3	1.18	

119	744b	It only says early Oligocene	Kerguelen Plateau	61 '34.66"S 80 35.46"E		-58.36	Mackensen and Ehrmann, 1992		*Globigerinids*	*Globigerina* spp.	2	2.13	
119	744b	It only says early Oligocene	Kerguelen Plateau	61 '34.66"S 80 35.46"E		-58.36	Mackensen and Ehrmann, 1992		Subbotinids	*Subbotina* spp.	3	1.98	
119	744b	It only says early Oligocene	Kerguelen Plateau	61 '34.66"S 80 35.46"E		-58.36	Mackensen and Ehrmann, 1992		Subbotinids	*Subbotina* spp.	3	1.86	
119	744b	It only says early Oligocene	Kerguelen Plateau	61 '34.66"S 80 35.46"E		-58.36	Mackensen and Ehrmann, 1992		Subbotinids	*Subbotina* spp.	3	1.87	
119	744b	It only says early Oligocene	Kerguelen Plateau	61 '34.66"S 80 35.46"E		-58.36	Mackensen and Ehrmann, 1992		Subbotinids	*Subbotina* spp.	3	1.68	
120	749b	It only says early Oligocene	Kerguelen Plateau	58 '43.03"S	76 '24.45'E	-55.81	Mackensen and Ehrmann, 1992		*Globigerinids*	*Globigerina* spp.	2	1.87	
120	749b	It only says early Oligocene	Kerguelen Plateau	58 '43.03"S	76 '24.45'E	-55.81	Mackensen and Ehrmann, 1992		*Globigerinids*	*Globigerina* spp.	2	1.73	
120	749b	It only says early Oligocene	Kerguelen Plateau	58 '43.03"S	76 '24.45'E	-55.81	Mackensen and Ehrmann, 1992		Subbotinids	*Subbotina* spp.	3	1.72	
120	748b	It only says early Oligocene	southern Kerguelen Plateau	58°26.45'S	78°58.89'E	-55.36	Zachos et al. 1992		Mixed planktonic foraminifers	Mixed planktonic foraminifers	3	1.4	

120	748b	It only says early Oligocene	southern Kerguelen Plateau	58°26.45'S	78°58.89'E	-55.36	Zachos et al. 1992		Mixed planktonic foraminifers	Mixed planktonic foraminifers	3	2.03	
120	748b	It only says early Oligocene	southern Kerguelen Plateau	58°26.45'S	78°58.89'E	-55.36	Zachos et al. 1992		*S. angiporoides*	*S. angiporoides*	3	2.1	
120	748b	It only says early Oligocene	southern Kerguelen Plateau	58°26.45'S	78°58.89'E	-55.36	Zachos et al. 1992		*C. cubensis*	*C. cubensis*	3	1.35	
120	748b	It only says early Oligocene	southern Kerguelen Plateau	58°26.45'S	78°58.89'E	-55.36	Zachos et al. 1992		*S. angiporoides*	*S. angiporoides*	3	2.05	
120	748b	It only says early Oligocene	southern Kerguelen Plateau	58°26.45'S	78°58.89'E	-55.36	Zachos et al. 1992		*C. cubensis*	*C. cubensis*	3	1.76	
120	748b	It only says early Oligocene	southern Kerguelen Plateau	58°26.45'S	78°58.89'E	-55.36	Zachos et al. 1992		*S. angiporoides*	*S. angiporoides*	3	1.72	
120	748b	It only says early Oligocene	southern Kerguelen Plateau	58°26.45'S	78°58.89'E	-55.36	Zachos et al. 1992		*C. cubensis*	*C. cubensis*	3	1.33	
120	748b	It only says early Oligocene	southern Kerguelen Plateau	58°26.45'S	78°58.89'E	-55.36	Zachos et al. 1992		*C. cubensis*	*C. cubensis*	3	1.17	
120	748b	It only says early Oligocene	southern Kerguelen Plateau	58°26.45'S	78°58.89'E	-55.36	Zachos et al. 1992		*C. cubensis*	*C. cubensis*	3	0.99	

120	748b	It only says early Oligocene	southern Kerguelen Plateau	58°26.45'S	78°58.89'E	-55.36	Zachos et al. 1992		Mixed *planktonic foraminifers*	Mixed *planktonic foraminifers*	3	1.58
120	748b	It only says early Oligocene	southern Kerguelen Plateau	58°26.45'S	78°58.89'E	-55.36	Zachos et al. 1992		*C. cubensis*	*C. cubensis*	3	1.16
120	748b	It only says early Oligocene	southern Kerguelen Plateau	58°26.45'S	78°58.89'E	-55.36	Zachos et al. 1992		*C. cubensis*	*C. cubensis*	3	1.61
120	748b	It only says early Oligocene	southern Kerguelen Plateau	58°26.45'S	78°58.89'E	-55.36	Zachos et al. 1992		*C. cubensis*	*C. cubensis*	3	1.48
120	748b	It only says early Oligocene	southern Kerguelen Plateau	58°26.45'S	78°58.89'E	-55.36	Zachos et al. 1992		*C. cubensis*	*C. cubensis*	3	1.61
74	526A	It only says early Oligocene	Walvis Ridge	30°07.36'S	03°08.28'E	-37.4	Shackleton et al, 1984	29.002	*Globorotalia opima*	*Paragloborotalia opima*	2	1.12
74	526A	It only says early Oligocene	Walvis Ridge	30°07.36'S	03°08.28'E	-37.4	Shackleton et al, 1984	29.143	*G. opima nana*	*Paragloborotalia nana*	2	1.17
74	526A	It only says early Oligocene	Walvis Ridge	30°07.36'S	03°08.28'E	-37.4	Shackleton et al, 1984	29.143	*Globigerina ampliapertura*	*Turborotalia ampliapertura*	2	1.15
74	529	It only says early Oligocene	Walvis Ridge	28°55.83'S	02°46.08'E	-36.21	Shackleton et al, 1984	28.982	*Catapsydrax* spp.	*Catapsydrax* spp.	3	1.69

74	529	It only says early Oligocene	Walvis Ridge	28°55.83'S	02°46.08'E	-36.21	Shackleton et al, 1984	31.611	*Catapsydrax* spp.	*Catapsydrax* spp.	3	1.64	
74	529	It only says early Oligocene	Walvis Ridge	28°55.83'S	02°46.08'E	-36.21	Shackleton et al, 1984	31.611	*Turborotalia* spp.	*Turborotalia* spp.	2	1.38	
74	529	It only says early Oligocene	Walvis Ridge	28°55.83'S	02°46.08'E	-36.21	Shackleton et al, 1984	32.911	*Catapsydrax* spp.	*Catapsydrax* spp.	3	1.33	
74	529	It only says early Oligocene	Walvis Ridge	28°55.83'S	02°46.08'E	-36.21	Shackleton et al, 1984	32.911	*Globorotalia siakensis*	*Paragloborotalia siakensis*	2	1.34	
73	522		southern Angola Abyssal Plain	26°06.843'S	5°07.784'W		Oberhansli et al., 1984					No Data Available	
73	524		southern Angola Abyssal Plain	29°29.055'S	3°30.74'E		Oberhansli et al., 1984					No Data Available	
73	523	NP22	southern Angola Abyssal Plain	28°33.131'S	2°15.078'W		Oberhansli et al., 1984					No Data Available	
	V20-220	P18	Southwestern Atlantic Ocean	28°36' S	29°01' W	-34.14	Boersma et al., 1987	P18 in this article is: 36-34.8 Ma	*P. micra*	*Pseudohastigerina micra*	1	1.1	
	V20-220	P18	Southwestern Atlantic Ocean	28°36' S	29°01' W	-34.14	Boersma et al., 1987	P18 in this article is: 36-34.8 Ma	*S. corpulenta*	*Subbotina corpulenta*	3	1.13	

	V20-220	P18	Southwestern Atlantic Ocean	28°36' S	29°01' W	-34.14	Boersma et al., 1987	P18 in this article is: 36-34.8 Ma	*Catapsydrax* spp.	*Catapsydrax* spp.	3	1.19	
	V20-220	P18	Southwestern Atlantic Ocean	28°36' S	29°01' W	-34.14	Boersma et al., 1987	P18 in this article is: 36-34.8 Ma	*Turborotalia ampliapertura.*	*Turborotalia ampliapertura*	2	1.21	
	V20-220	P18	Southwestern Atlantic Ocean	28°36' S	29°01' W	-34.14	Boersma et al., 1987	P18 in this article is: 36-34.8 Ma	*S. gortanii*	*Subbotina gortanii*	3	1.22	
	V20-220	P18	Southwestern Atlantic Ocean	28°36' S	29°01' W	-34.14	Boersma et al., 1987	P18 in this article is: 36-34.8 Ma	*G. pseudoeocaena*	*Subbotina yeguaensis*	3	1.22	
40	363	P18	Isolated basement high on north-facing escarpment of Frio Ridge portion of Walvis Ridge	19°38.75' S	09°02.80'E	-26.86	Boersma et al., 1987	P18 in this article is: 36-34.8 Ma	*Turborotalia pseudoampl.*	*Turborotalia ampliapertura*	2	0	
40	363	P18	Isolated basement high on north-facing escarpment of Frio Ridge portion of Walvis Ridge	19°38.75' S	09°02.80'E	-26.86	Boersma et al., 1987	P18 in this article is: 36-34.8 Ma	*Turborotalia pseudoampl.*	*Turborotalia ampliapertura*	2	-0.01	

40	363	P18	Isolated basement high on north-facing escarpment of Frio Ridge portion of Walvis Ridge	19°38.75'S	09°02.80'E	-26.86	Boersma et al., 1987	P18 in this article is: 36-34.8 Ma	*Turborotalia pseudoampl.*	*Turborotalia ampliapertura*	2	0.12	
74	529	P18	Walvis Ridge	28°55.83'S	02°46.08'E	-36.21	Boersma et al., 1987	P18 in this article is: 36-34.8 Ma	*Catapsydrax* spp.	*Catapsydrax* spp.	3	1.19	
74	529	P18	Walvis Ridge	28°55.83'S	02°46.08'E	-36.21	Boersma et al., 1987	P18 in this article is: 36-34.8 Ma	*Turborotalia pseudoampl.*	*Turborotalia ampliapertura*	2	1.41	
	77B	It only says early Oligocene	Equatorial Pacific Ocean	00°28.90'N	133°13.70'W	-7.74	Keigwin and Corliss, 1986		*Chiloguembelina Cubensis*	*Chiloguembelina cubensis*	1	-0.18	
	77B	P21	Equatorial Pacific Ocean	00°28.90'N	133°13.70'W	-7.74	Keller, 1983		*Globigerina angustiumbilicata*	*Tenuitella angustiumbilicata*	1	-0.61	
	77B	P20	Equatorial Pacific Ocean	00°28.90'N	133°13.70'W	-7.74	Keller, 1983		*Globigerina angustiumbilicata*	*Tenuitella angustiumbilicata*	1	-0.58	
	77B	P18/P19	Equatorial Pacific Ocean	00°28.90'N	133°13.70'W	-7.74	Keller, 1983		*Globigerina angustiumbilicata*	*Tenuitella angustiumbilicata*	1	-0.485	

	77B	P20	Equatorial Pacific Ocean	00°28.90' N	133°13.70' W	-7.74	Keller, 1983		*Chiloguembelin a cubensis*	*Chiloguembelin a cubensis*	1	-0.31	
	77B	P18/P19	Equatorial Pacific Ocean	00°28.90' N	133°13.70' W	-7.74	Keller, 1983		*Chiloguembelin a cubensis*	*Chiloguembelin a cubensis*	1	-0.535	
	77B	P18/P19	Equatorial Pacific Ocean	00°28.90' N	133°13.70' W	-7.74	Keller, 1983		*Globigerina ampliapertura*	*Turborotalia ampliapertura*	2	-0.14	
	77B	P18/P19	Equatorial Pacific Ocean	00°28.90' N	133°13.70' W	-7.74	Keller, 1983		*Globigerina ampliapertura*	*Turborotalia ampliapertura*	2	-0.17	
	77B	P18/P19	Equatorial Pacific Ocean	00°28.90' N	133°13.70' W	-7.74	Keller, 1983		*Globigerina euapertura*	*Globoturborotali ta euapertura*	2	0.35	
	77B	P18/P19	Equatorial Pacific Ocean	00°28.90' N	133°13.70' W	-7.74	Keller, 1983		*Globigerina euapertura*	*Globoturborotali ta euapertura*	2	0	
	77B	P18/P19	Equatorial Pacific Ocean	00°28.90' N	133°13.70' W	-7.74	Keller, 1983		*Globigerina linaperta*	*Subbotina linaperta*	3	0.57	
	77B	P18/P19	Equatorial Pacific Ocean	00°28.90' N	133°13.70' W	-7.74	Keller, 1983		*Globigerina linaperta*	*Subbotina linaperta*	3	0.5	
	77B	P18/P19	Equatorial Pacific Ocean	00°28.90' N	133°13.70' W	-7.74	Keller, 1983		*Globigerina linaperta*	*Subbotina linaperta*	3	0.65	

	77B	P18/P19	Equatorial Pacific Ocean	00°28.90' N	133°13.70' W	-7.74	Keller, 1983		*Globigerina linaperta*	*Subbotina linaperta*	3	0.7	
	77B	P18/P19	Equatorial Pacific Ocean	00°28.90' N	133°13.70' W	-7.74	Keller, 1983		*Globigerina linaperta*	*Subbotina linaperta*	3	0.84	
	77B	P20/P21	Equatorial Pacific Ocean	00°28.90' N	133°13.70' W	-7.74	Keller, 1983		*Globorotalia opima*	*Paragloborotalia opima*	2	0.47	
	77B	P20/P21	Equatorial Pacific Ocean	00°28.90' N	133°13.70' W	-7.74	Keller, 1983		*Catapsydrax dissimilis*	*Catapsydrax dissimilis*	3	0.81	
	77B	P18/P19	Equatorial Pacific Ocean	00°28.90' N	133°13.70' W	-7.74	Keller, 1983		*Catapsydrax dissimilis*	*Catapsydrax dissimilis*	3	1.19	
	77B	P18/P19	Equatorial Pacific Ocean	00°28.90' N	133°13.70' W	-7.74	Keller, 1983		*Catapsydrax dissimilis*	*Catapsydrax dissimilis*	3	1.38	
	77B	P18/P19	Equatorial Pacific Ocean	00°28.90' N	133°13.70' W	-7.74	Keller, 1983		*Catapsydrax dissimilis*	*Catapsydrax dissimilis*	3	1.15	
	77B	P18/P19	Equatorial Pacific Ocean	00°28.90' N	133°13.70' W	-7.74	Keller, 1983		*Catapsydrax dissimilis*	*Catapsydrax dissimilis*	3	1.2	
	77B	P18/P19	Equatorial Pacific Ocean	00°28.90' N	133°13.70' W	-7.74	Keller, 1983		*Catapsydrax dissimilis*	*Catapsydrax dissimilis*	3	1.26	

	77B	P18/P19	Equatorial Pacific Ocean	00°28.90' N	133°13.70' W	-7.74	Keller, 1983		*Catapsydrax dissimilis*	*Catapsydrax dissimilis*	3	1.33	
	77B	P18/P19	Equatorial Pacific Ocean	00°28.90' N	133°13.70' W	-7.74	Keller, 1983		*Catapsydrax dissimilis*	*Catapsydrax dissimilis*	3	1.38	
41	366	P20	Sierra Leone Rise	05°40.7' N	19°51.1'W	-1.12	Keller, 1983		*Globigerina ampliapertura*	*Turborotalia ampliapertura*	2	-0.16	
41	366	P20	Sierra Leone Rise	05°40.7' N	19°51.1'W	-1.12	Keller, 1983		*Catapsydrax* spp.	*Catapsydrax* spp.	3	1.02	
41	366	P20	Sierra Leone Rise	05°40.7' N	19°51.1'W	-1.12	Keller, 1983		*Globigerina ampliapertura*	*Turborotalia ampliapertura*	2	0.11	
41	366	P20	Sierra Leone Rise	05°40.7' N	19°51.1'W	-1.12	Keller, 1983		*Globorotalia opima nana*	*Turborotalia ampliapertura*	2	-0.81	
41	366	P19	Sierra Leone Rise	05°40.7' N	19°51.1'W	-1.12	Keller, 1983		*Catapsydrax* spp.	*Catapsydrax* spp.	3	0.54	
41	366	P19	Sierra Leone Rise	05°40.7' N	19°51.1'W	-1.12	Keller, 1983		*Globigerina ampliapertura*	*Turborotalia ampliapertura*	2	-0.87	
41	366	P19	Sierra Leone Rise	05°40.7' N	19°51.1'W	-1.12	Keller, 1983		*Globorotalia opima nana*	*Paragloborotalia nana*	2	-0.07	

41	366	P18/P19	Sierra Leone Rise	05°40.7'N	19°51.1'W	-1.12	Keller, 1983		*Catapsydrax* spp.	*Catapsydrax* spp.	3	1.06	
41	366	P18/P19	Sierra Leone Rise	05°40.7'N	19°51.1'W	-1.12	Keller, 1983		*Globigerina ampliapertura*	*Turborotalia ampliapertura*	2	-0.44	
41	366	P18/P19	Sierra Leone Rise	05°40.7'N	19°51.1'W	-1.12	Keller, 1983		*Chiloguembelina cubensis*	*Chiloguembelina cubensis*	1	-1.33	
41	366	P18/P19	Sierra Leone Rise	05°40.7'N	19°51.1'W	-1.12	Keller, 1983		*Globigerina ampliapertura*	*Turborotalia ampliapertura*	2	0.03	
41	366	P18/P19	Sierra Leone Rise	05°40.7'N	19°51.1'W	-1.12	Keller, 1983		*Catapsydrax* spp.	*Catapsydrax* spp.	3	0.32	
41	366	P18/P19	Sierra Leone Rise	05°40.7'N	19°51.1'W	-1.12	Keller, 1983		*Globigerina ampliapertura*	*Turborotalia ampliapertura*	2	-0.42	
41	366	P18/P19	Sierra Leone Rise	05°40.7'N	19°51.1'W	-1.12	Keller, 1983		*Chiloguembelina cubensis*	*Chiloguembelina cubensis*	1	-1.23	
10	94	It only says early Oligocene	Campeche Scarp, Yucatan Shelf, Gulf of Mexico	24°31.64'N	88°28.16'W	21.2	Keigwin and Corliss, 1986		*Chiloguembelina Cubensis*	*Chiloguembelina cubensis*	1	-0.41	
23	219	It only says early Oligocene	On the crest of the Laccadive-Chagos Ridge	9°01.75'N	72°52.67'E	-0.31	Keigwin and Corliss, 1986		*Chiloguembelina Cubensis*	*Chiloguembelina cubensis*	1	0.21	

26	253	It only says early Oligocene	Southern end of the Ninetyeast Ridge	24°52.65'S	87°21.97'E	-35.57	Keigwin and Corliss, 1986		*Chiloguembelina Cubensis*	*Chiloguembelina cubensis*	1	0.99
29	277	It only says early Oligocene	Campbell Plateau in the south-west Pacific	52°13.43'S	166°11.48'E	-54.74	Keigwin and Corliss, 1986		*G. subglobosa*	*Subbotina* spp.	3	1.27
29	277	It only says early Oligocene	Campbell Plateau in the south-west Pacific	52°13.43'S	166°11.48'E	-54.74	Keigwin and Corliss, 1986		*Chiloguembelina Cubensis*	*Chiloguembelina cubensis*	1	0.39
31	292	It only says early Oligocene	Bneham Rise in the west Philippine Sea	15°49.11'N	124°39.05'E	5.12	Keigwin and Corliss, 1986		*G. ampliapertura*	*Turborotalia ampliapertura*	2	-0.81
39	357	It only says early Oligocene	eastern flank of the Rio Grande Rise, South Atlantic	3O°00.25'S	35°33.59'W	-35.99	Keigwin and Corliss, 1986		*C. cubensis*	*Chiloguembelina cubensis*	1	-0.04
40	363	It only says early Oligocene	Isolated basement high on north-facing escarpment of Frio Ridge portion of Walvis Ridge	19°38.75'S	09°02.80'E	-26.86	Keigwin and Corliss, 1986		*Chiloguembelina Spp.*	*Chiloguembelina cubensis*	1	0.03
41	366	It only says early Oligocene	Sierra Leone Rise	05°40.7'N	19°51.1'W	-1.12	Keigwin and Corliss, 1986		*C. cubensis*	*Chiloguembelina cubensis*	1	-1.13

41	366	CP17, as shown in Figure 2	Sierra Leone Rise	05°40.7'N	19°51.1'W	-1.12	Poore and Matthews (a), 1984		*Globorotalia* spp. *A*	*Paragloborotalia* spp.	2	-1.09	
41	366	CP17, as shown in Figure 2	Sierra Leone Rise	05°40.7'N	19°51.1'W	-1.12	Poore and Matthews (a), 1984		*Globigerina angustiumbilicata*	*Tenuitella angustiumbilicata*	1	-0.97	
41	366	CP17, as shown in Figure 2	Sierra Leone Rise	05°40.7'N	19°51.1'W	-1.12	Poore and Matthews (a), 1984		*Chiloguembelina cubensis*	*Chiloguembelina cubensis*	1	-0.9	
41	366	CP17, as shown in Figure 2	Sierra Leone Rise	05°40.7'N	19°51.1'W	-1.12	Poore and Matthews (a), 1984		*Globigerina pseudovenezuelana*	*Dentoglobigerina pseudovenezuelana*	3	-0.75	
41	366	CP17, as shown in Figure 2	Sierra Leone Rise	05°40.7'N	19°51.1'W	-1.12	Poore and Matthews (a), 1984		*Globigerina euapertura*	*Globoturborotalita euapertura*	2	-0.6	
41	366	CP17, as shown in Figure 2	Sierra Leone Rise	05°40.7'N	19°51.1'W	-1.12	Poore and Matthews (a), 1984		*Globorotalia opima nana*	*Paragloborotalia nana*	2	0.2	
41	366	CP17, as shown in Figure 2	Sierra Leone Rise	05°40.7'N	19°51.1'W	-1.12	Poore and Matthews (a), 1984		*Catapsydrax* spp. *A*	*Catapsydrax* spp.	3	0.59	
41	366	CP17, as shown in Figure 2	Sierra Leone Rise	05°40.7'N	19°51.1'W	-1.12	Poore and Matthews (a), 1984		*Catapsydrax dissimilis*	*Catapsydrax dissimilis*	3	1.17	
41	366	CP17, as shown in Figure 2	Sierra Leone Rise	05°40.7'N	19°51.1'W	-1.12	Poore and Matthews (a), 1984		*Globocassidulina subglobosa*	*Subbotina* spp.	3	1.76	

	EUREKA E-67-128	CP16c, as shown in Figure 2	Gulf of Mexico	25°N	-90	21.86	Poore and Matthews (a), 1984		*Chiloguembelina cubensis*	*Chiloguembelina cubensis*	1	-1.21	
	EUREKA E-67-128	CP16c, as shown in Figure 2	Gulf of Mexico	25°N	-90	21.86	Poore and Matthews (a), 1984		*Globigerina bulloides*	*Globigerina bulloides*	1	-1.17	
	EUREKA E-67-128	CP16c, as shown in Figure 2	Gulf of Mexico	25°N	-90	21.86	Poore and Matthews (a), 1984		*Globigerina ampliapertura*	*Turborotalia ampliapertura*	2	-0.87	
	EUREKA E-67-128	CP16c, as shown in Figure 2	Gulf of Mexico	25°N	-90	21.86	Poore and Matthews (a), 1984		*Globigerina eocaena*	*Subbotina eocaena*	3	-0.81	
	EUREKA E-67-128	CP16c, as shown in Figure 2	Gulf of Mexico	25°N	-90	21.86	Poore and Matthews (a), 1984		*Globorotalia increbescens*	*Turborotalia increbescens*	2	-0.55	
	EUREKA E-67-128	CP16c, as shown in Figure 2			-90	21.86	Poore and Matthews (a), 1984		*Globigerina pseudovenezuelana*	*Dentoglobigerina pseudovenezuelana*	3	-0.44	
73	522	Between CP6c and CP17, as shown in Figure 2	southern Angola Abyssal Plain	26°06.843'S	5°07.78'W	-33.35	Poore and Matthews (a), 1984		*Globigerina ampliapertura*	*Turborotalia ampliapertura*	2	0.69	
73	522	Between CP6c and CP17, as shown in Figure 2	southern Angola Abyssal Plain	26°06.843'S	5°07.78'W	-33.35	Poore and Matthews (a), 1984		*Globigerina ampliapertura*	*Turborotalia ampliapertura*	2	1.07	
73	522	Between CP6c and CP17, as shown in Figure 2	southern Angola Abyssal Plain	26°06.843'S	5°07.78'W	-33.35	Poore and Matthews (a), 1984		*Globigerina perus*	*Subbotina corpulenta*	3	0.75	

73	522	Between CP6c and CP17, as shown in Figure 2	southern Angola Abyssal Plain	26°06.843'S	5°07.78'W	-33.35	Poore and Matthews (a), 1984		*Globigerina perus*	*Subbotina corpulenta*	3	1.05	
73	522	Between CP6c and CP17, as shown in Figure 2	southern Angola Abyssal Plain	26°06.843'S	5°07.78'W	-33.35	Poore and Matthews (a), 1984		*Globigerina angustiumbilicata*	*Tenuitella angustiumbilicata*	1	0.87	
73	522	Between CP6c and CP17, as shown in Figure 2	southern Angola Abyssal Plain	26°06.843'S	5°07.78'W	-33.35	Poore and Matthews (a), 1984		*Globigerina galavisi*	*Dentoglobigerina galavisi*	3	1.16	
73	522	Between CP6c and CP17, as shown in Figure 2	southern Angola Abyssal Plain	26°06.843'S	5°07.78'W	-33.35	Poore and Matthews (a), 1984		*Chiloguembelina cubensis*	*Chiloguembelina cubensis*	1	1.16	
73	522	Between CP6c and CP17, as shown in Figure 2	southern Angola Abyssal Plain	26°06.843'S	5°07.78'W	-33.35	Poore and Matthews (a), 1984		*Globigerina euapertura*	*Globoturborotalita euapertura*	2	1.17	
73	522	Between CP6c and CP17, as shown in Figure 2	southern Angola Abyssal Plain	26°06.843'S	5°07.78'W	-33.35	Poore and Matthews (a), 1984		*Globorotalia opima nana*	*Paragloborotalia nana*	2	1.16	
73	522	Between CP6c and CP17, as shown in Figure 2	southern Angola Abyssal Plain	26°06.843'S	5°07.78'W	-33.35	Poore and Matthews (a), 1984		*Globigerina angiporoides*	*Subbotina angiporoides*	3	1.2	
73	522	Between CP6c and CP17, as shown in Figure 2	southern Angola Abyssal Plain	26°06.843'S	5°07.78'W	-33.35	Poore and Matthews (a), 1984		*Catapsydrax dissimilis*	*Catapsydrax dissimilis*	3	1.72	

73	522	Between CP6c and CP17, as shown in Figure 2	southern Angola Abyssal Plain	26°06.843'S	5°07.78'W	-33.35	Poore and Matthews (a), 1984		*Catapsydrax unicavus*	*Catapsydrax unicavus*	3	1.74
73	522	It only says early Oligocene	southern Angola Abyssal Plain	26°06.843'S	5°07.78'W	-33.35	Poore and Matthews (b), 1984 (found in Keigwin and Corliss, 1986)		*G. ampliapertura*	*Turborotalia ampliapertura*	2	1.21
77	540	It only says early Oligocene	Gulf of Mexico	23°49.73'N	84°22.25'W	20	Belanger and Matthews (1984) (Found in Keigwin and Corliss, 1986)		*C. cubensis*	*C. cubensis*	1	-0.29
90	592	It only says early Oligocene	On the southern Lord Howe Rise	36°28.40'S	165°26.53'E	-45.26	Found in Keigwin and Corliss, 1986		*Chiloguembelina* spp.	*Chiloguembelina* spp.	1	0.44
90	593	It only says early Oligocene	On the Challenger Plateau, a western extension of the New Zealand Plateau.	40°30.47'S	167°40.47'E	-48.77	Found in Keigwin and Corliss, 1986		*Chiloguembelina* spp.	*Chiloguembelina* spp.	1	0.25
95	612	It only says early Oligocene	On the middle part of the New Jersey continental slope.	38°49.21'N	72°46.43'W	33.57	Found in Keigwin and Corliss, 1986		*P. gemma*	*Tenuitella gemma*	1	-0.19

EU RE KA	E-67-128	It only says early Oligocene	Gulf of Mexico	25°N	-90	21.86	Found in Keigwin and Corliss, 1986		*Chiloguembelina* Spp.	*Chiloguembelina* Spp.	1	-1.34	
	SSQ	It only says early Oligocene	St. Stephens Quarry corehole, Alabama	31°33'N	88°02'W	28.1	Found in Keigwin and Corliss, 1986		*Pseudohastigerina* spp.	*Pseudohastigerina* spp.	1	-1.54	
71	511	They only mention about Eocene, Oligocene, etc… but they explain where the E/O boundary is within the core section, I think I could identify the EOGM peak.	Westerrn margin of the Maurice Ewing Bank	51°00.28'S	46°58.30'W	-57.57	Muza et al., 1983		Mixed assemblage *of Globigerina angiporoides* and *G. aff. Linaperta*	*Subbotina linaperta* and *Subbotina angiporoides*	3	0.24	
71	511	They only mention about Eocene, Oligocene, etc… but they explain where the E/O boundary is within the core section, I	Westerrn margin of the Maurice Ewing Bank	51°00.28'S	46°58.30'W	-57.57	Muza et al., 1983		Mixed assemblage *of Globigerina angiporoides* and *G. aff. Linaperta*	*Subbotina linaperta* and *Subbotina angiporoides*	3	0.51	

			think I could identify the EOGM peak.											
71	511	They only mention about Eocene, Oligocene, etc… but they explain where the E/O boundary is within the core section, I think I could identify the EOGM peak.	Westerrn margin of the Maurice Ewing Bank	51°00.28' S	46°58.30' W	-57.57	Muza et al., 1983		Mixed assemblage *of Globigerina angiporoides* and *G. aff. Linaperta*	*Subbotina linaperta* and *Subbotina angiporoides*	3	1.26	
71	511	They only mention about Eocene, Oligocene, etc… but they explain where the E/O boundary is within the core section, I think I could identify the EOGM peak.	Westerrn margin of the Maurice Ewing Bank	51°00.28' S	46°58.30' W	-57.57	Muza et al., 1983		Mixed assemblage *of Globigerina angiporoides* and *G. aff. Linaperta*	*Subbotina linaperta* and *Subbotina angiporoides*	3	1.39	

71	511	They only mention about Eocene, Oligocene, etc… but they explain where the E/O boundary is within the core section, I think I could identify the EOGM peak.	Westerrn margin of the Maurice Ewing Bank	51°00.28' S	46°58.30' W	-57.57	Muza et al., 1983		Mixed assemblage *of Globigerina angiporoides* and *G. aff. Linaperta*	*Subbotina linaperta* and *Subbotina angiporoides*	3	1	
71	511	They only mention about Eocene, Oligocene, etc… but they explain where the E/O boundary is within the core section, I think I could identify the EOGM peak.	Westerrn margin of the Maurice Ewing Bank	51°00.28' S	46°58.30' W	-57.57	Muza et al., 1983		Mixed assemblage *of Globigerina angiporoides* and *G. aff. Linaperta*	*Subbotina linaperta* and *Subbotina angiporoides*	3	1.2	
71	511	They only mention about Eocene, Oligocene,	Westerrn margin of the Maurice	51°00.28' S	46°58.30' W	-57.57	Muza et al., 1983		Mixed assemblage *of Globigerina angiporoides*	*Subbotina linaperta* and *Subbotina angiporoides*	3	1.34	

			Comment	Location	Lat	Long		Reference		Assemblage	Species		Value	
			etc… but they explain where the E/O boundary is within the core section, I think I could identify the EOGM peak.	Ewing Bank						and *G. aff. Linaperta*				
	71	511	They only mention about Eocene, Oligocene, etc… but they explain where the E/O boundary is within the core section, I think I could identify the EOGM peak.	Westerrn margin of the Maurice Ewing Bank	51°00.28' S	46°58.30' W	-57.57	Muza et al., 1983		Mixed assemblage *of Globigerina angiporoides* and *G. aff. Linaperta*	*Subbotina linaperta* and *Subbotina angiporoides*	3	1.26	
	71	511	They only mention about Eocene, Oligocene, etc… but they explain where the E/O	Westerrn margin of the Maurice Ewing Bank	51°00.28' S	46°58.30' W	-57.57	Muza et al., 1983		Mixed assemblage *of Globigerina angiporoides* and *G. aff. Linaperta*	*Subbotina linaperta* and *Subbotina angiporoides*	3	1.17	

		boundary is within the core section, I think I could identify the EOGM peak.										
71	511	They only mention about Eocene, Oligocene, etc… but they explain where the E/O boundary is within the core section, I think I could identify the EOGM peak.	Westerrn margin of the Maurice Ewing Bank	51°00.28' S	46°58.30' W	-57.57	Muza et al., 1983		Mixed assemblage *of Globigerina angiporoides* and *G. aff. Linaperta*	*Subbotina linaperta* and *Subbotina angiporoides*	3	0.98
71	511	They only mention about Eocene, Oligocene, etc… but they explain where the E/O boundary is within the core section, I think I	Western margin of the Maurice Ewing Bank	51°00.28' S	46°58.30' W	-57.57	Muza et al., 1983		Mixed assemblage *of Globigerina angiporoides* and *G. aff. Linaperta*	*Subbotina linaperta* and *Subbotina angiporoides*	3	0.77

		could identify the EOGM peak.										
71	511	They only mention about Eocene, Oligocene, etc… but they explain where the E/O boundary is within the core section, I think I could identify the EOGM peak.	Western margin of the Maurice Ewing Bank	51°00.28' S	46°58.30' W	-57.57	Muza et al., 1983		Mixed assemblage *of Globigerina angiporoides* and *G. aff. Linaperta*	*Subbotina linaperta* and *Subbotina angiporoides*	3	1.06
71	511	They only mention about Eocene, Oligocene, etc… but they explain where the E/O boundary is within the core section, I think I could identify the EOGM peak.	Westerrn margin of the Maurice Ewing Bank	51°00.28' S	46°58.30' W	-57.57	Muza et al., 1983		Mixed assemblage *of Globigerina angiporoides* and *G. aff. Linaperta*	*Subbotina linaperta* and *Subbotina angiporoides*	3	1

71	511	They only mention about Eocene, Oligocene, etc… but they explain where the E/O boundary is within the core section, I think I could identify the EOGM peak.	Westerrn margin of the Maurice Ewing Bank	51°00.28' S	46°58.30' W	-57.57	Muza et al., 1983		Mixed assemblage *of Globigerina angiporoides* and *G. aff. Linaperta*	*Subbotina linaperta* and *Subbotina angiporoides*	3	1.4	
71	511	They only mention about Eocene, Oligocene, etc… but they explain where the E/O boundary is within the core section, I think I could identify the EOGM peak.	Westerrn margin of the Maurice Ewing Bank	51°00.28' S	46°58.30' W	-57.57	Muza et al., 1983		Mixed assemblage *of Globigerina angiporoides* and *G. aff. Linaperta*	*Subbotina linaperta* and *Subbotina angiporoides*	3	1.36	
20 (Sampl e nu	Glen Aire Clays, Castle	NP22	Glen Aire Clays, Castle Cove Section	38 S	142 E	-50.15	Kamp et al., 1990		Mixed assemblage dominated by *Subbotina angiporoides,*	Mixed assemblage dominated by *Subbotina angiporoides,*	3	-0.68	

mb er)	Cove Section								*Subbotina linaperta,* and *Globigerina bulloides*	*Subbotina linaperta,* and *Globigerina bulloides*			
21 (Sa mpl e nu mb er)	Glen Aire Clays, Castle Cove Section	NP22	Glen Aire Clays, Castle Cove Section	38 S	142 E	-50.1 5	Kamp et al., 1990		Mixed assemblage dominated by *Subbotina angiporoides, Subbotina linaperta,* and *Globigerina bulloides*	Mixed assemblage dominated by *Subbotina angiporoides, Subbotina linaperta,* and *Globigerina bulloides*	3	-1.2	
22 (Sa mpl e nu mb er)	Glen Aire Clays, Castle Cove Section	NP22	Glen Aire Clays, Castle Cove Section	38 S	142 E	-50.1 5	Kamp et al., 1990		Mixed assemblage dominated by *Subbotina angiporoides, Subbotina linaperta,* and *Globigerina bulloides*	Mixed assemblage dominated by *Subbotina angiporoides, Subbotina linaperta,* and *Globigerina bulloides*	3	-0.08	
23 (Sa mpl e nu mb er)	Glen Aire Clays, Castle Cove Section	NP22	Glen Aire Clays, Castle Cove Section	38 S	142 E	-50.1 5	Kamp et al., 1990		Mixed assemblage dominated by *Subbotina angiporoides, Subbotina linaperta,* and *Globigerina bulloides*	Mixed assemblage dominated by *Subbotina angiporoides, Subbotina linaperta,* and *Globigerina bulloides*	3	-0.08	
	Java - NKK1		Central Java	7°73844' S	110°18574 'E	-2.14	Coxall et al. (in prep.)		*Turborotalia ampliapertura '1'*	*Turborotalia ampliapertura*	2	-2.982	glas sy

Java - NKK1		Central Java	7°73844' S	110°18574 'E	- 2.14	Coxall et al. (in prep.)		*Turborotalia ampliapertura '1'*	*Turborotalia ampliapertura*	2	-3.324	glas sy
Java - NKK1		Central Java	7°73844' S	110°18574 'E	- 2.14	Coxall et al. (in prep.)		*Turborotalia ampliapertura '1'*	*Turborotalia ampliapertura*	2	-3.025	glas sy
Java - NKK1		Central Java	7°73844' S	110°18574 'E	- 2.14	Coxall et al. (in prep.)		*Turborotalia ampliapertura '2'*	*Turborotalia ampliapertura*	2	-3.310	glas sy
Java - NKK1		Central Java	7°73844' S	110°18574 'E	- 2.14	Coxall et al. (in prep.)		*Turborotalia ampliapertura '2'*	*Turborotalia ampliapertura*	2	-3.252	glas sy
Java - NKK1		Central Java	7°73844' S	110°18574 'E	- 2.14	Coxall et al. (in prep.)		*Catapsydrax unicavus*	*Catapsydrax unicavus*	3	0.691	glas sy
Java - NKK1		Central Java	7°73844' S	110°18574 'E	- 2.14	Coxall et al. (in prep.)		*Catapsydrax unicavus 'smaller'*	*Catapsydrax unicavus*	3	-1.543	glas sy
Java - NKK1		Central Java	7°73844' S	110°18574 'E	- 2.14	Coxall et al. (in prep.)		*Catapsydrax unicavus 'bigger'*	*Catapsydrax unicavus*	3	-0.496	glas sy
Java - NKK1		Central Java	7°73844' S	110°18574 'E	- 2.14	Coxall et al. (in prep.)		*Subbotina utilusindex*	*Subbotina utilisindex*	3	-0.130	glas sy
Java - NKK1		Central Java	7°73844' S	110°18574 'E	- 2.14	Coxall et al. (in prep.)		*Subbotina utilusindex*	*Subbotina utilisindex*	3	-1.867	glas sy

Java - NKK1		Central Java	7°73844'S	110°18574'E	-2.14	Coxall et al. (in prep.)		*Paragloborotalia nana*	*Paragloborotalia nana*	2	-3.533	glassy
Java - NKK1		Central Java	7°73844'S	110°18574'E	-2.14	Coxall et al. (in prep.)		*Paragloborotalia nana*	*Paragloborotalia nana*	2	-3.621	glassy
Java - NKK1		Central Java	7°73844'S	110°18574'E	-2.14	Coxall et al. (in prep.)		*Dentiglobigerina galavisi*	*Dentoglobigerina galavisi*	3	-3.035	glassy
Java - NKK1		Central Java	7°73844'S	110°18574'E	-2.14	Coxall et al. (in prep.)		*Dentiglobigerina galavisi*	*Dentoglobigerina galavisi*	3	-2.925	glassy
Java - NKK1		Central Java	7°73844'S	110°18574'E	-2.14	Coxall et al. (in prep.)		*Dentiglobigerina pseudovenezuelana*	*Dentoglobigerina pseudovenezuelana*	3	-2.743	glassy
Java - NKK1		Central Java	7°73844'S	110°18574'E	-2.14	Coxall et al. (in prep.)		*Dentiglobigerina galavisi*	*Dentoglobigerina galavisi*	3	-3.007	glassy
Java - NKK1		Central Java	7°73844'S	110°18574'E	-2.14	Coxall et al. (in prep.)		*Dentiglobigerina pseudovenezuelana*	*Dentoglobigerina pseudovenezuelana*	3	-2.274	glassy
Java - NKK1		Central Java	7°73844'S	110°18574'E	-2.14	Coxall et al. (in prep.)		*Turborotalia ampliapertura '2'*	*Turborotalia ampliapertura*	2	-2.150	glassy
Java - NKK1		Central Java	7°73844'S	110°18574'E	-2.14	Coxall et al. (in prep.)		*Globoturborotalita anguliofficinanis*	*Globoturborotalita anguliofficinalis*	Ciperoella	-3.787	glassy

Java - NKK1		Central Java	7°73844'S	110°18574'E	-2.14	Coxall et al. (in prep.)		*Globoturborotalita anguliofficinalis*	*Globoturborotalita anguliofficinalis*		-3.382	glassy
Java - NKK1		Central Java	7°73844'S	110°18574'E	-2.14	Coxall et al. (in prep.)		*Globigerina officinalis*	*Globigerina officinalis*	2	-3.289	glassy
Java - NKK1		Central Java	7°73844'S	110°18574'E	-2.14	Coxall et al. (in prep.)		*Pseudohastigerina naguewichiensis*	*Pseudohastigerina naguewichiensis*	1	-3.609	glassy
Java - NKK1		Central Java	7°73844'S	110°18574'E	-2.14	Coxall et al. (in prep.)		*Chiloguembelina cubensis*	*Chiloguembelina cubensis*	1	-4.032	glassy
Java - NKK1		Central Java	7°73844'S	110°18574'E	-2.14	Coxall et al. (in prep.)		*Pseudohastigerina naguewichiensis*	*Pseudohastigerina naguewichiensis*	1	-3.713	glassy
Java - NKK1		Central Java	7°73844'S	110°18574'E	-2.14	Coxall et al. in prep		*Chiloguembelina cubensis*	*Chiloguembelina cubensis*	1	-4.061	glassy
Java - NKK1		Central Java	7°73844'S	110°18574'E	-2.14	Coxall et al. (in prep.)		*Globoturborotalita anguliofficinanis*	*Ciperoella anguliofficinalis*	2	-4.034	glassy
Java - NKK1		Central Java	7°73844'S	110°18574'E	-2.14	Coxall et al. (in prep.)		*Globoturborotalita martini*	*Globoturborotalita martini*	1	-3.228	glassy
Java - NKK1		Central Java	7°73844'S	110°18574'E	-2.14	Coxall et al. (in prep.)		*Globoturborotalita martini*	*Globoturborotalita martini*	1	-3.477	glassy

Java - NKK1		Central Java	7°73844'S	110°18574'E	-2.14	Coxall et al. (in prep.)		*Cassigerinella* spp.	*Cassigerinella* spp.	2	-3.918	glassy
Java - NKK1		Central Java	7°73844'S	110°18574'E	-2.14	Coxall et al. (in prep.)		*Turborotalia ampliapertura*	*Turborotalia ampliapertura*	2	-2.949522553	glassy
Java - NKK1		Central Java	7°73844'S	110°18574'E	-2.14	Coxall et al. (in prep.)		*Turborotalia ampliapertura*	*Turborotalia ampliapertura*	2	-3.957251072	glassy
Java - NKK1		Central Java	7°73844'S	110°18574'E	-2.14	Coxall et al. (in prep.)		*Turborotalia ampliapertura*	*Turborotalia ampliapertura*	2	-3.38042178	glassy
Java - NKK1		Central Java	7°73844'S	110°18574'E	-2.14	Coxall et al. (in prep.)		*Turborotalia ampliapertura*	*Turborotalia ampliapertura*	2	-3.26891083	glassy
Java - NKK1		Central Java	7°73844'S	110°18574'E	-2.14	Coxall et al. (in prep.)		*Turborotalia ampliapertura*	*Turborotalia ampliapertura*	2	-2.982346912	glassy
Java - NKK1		Central Java	7°73844'S	110°18574'E	-2.14	Coxall et al. (in prep.)		*Turborotalia ampliapertura*	*Turborotalia ampliapertura*	2	-3.324272955	glassy
Java - NKK1		Central Java	7°73844'S	110°18574'E	-2.14	Coxall et al. (in prep.)		*Turborotalia ampliapertura*	*Turborotalia ampliapertura*	2	-3.0250474	glassy
Java - NKK1		Central Java	7°73844'S	110°18574'E	-2.14	Coxall et al. (in prep.)		*Turborotalia ampliapertura*	*Turborotalia ampliapertura*	2	-3.309543712	glassy

Java - NKK1		Central Java	7°73844'S	110°18574'E	-2.14	Coxall et al. (in prep.)		*Turborotalia ampliapertura*	*Turborotalia ampliapertura*	2	-3.251697533	glassy
Java - NKK1		Central Java	7°73844'S	110°18574'E	-2.14	Coxall et al. (in prep.)		*Turborotalia ampliapertura*	*Turborotalia ampliapertura*	2	-4.54801432	glassy
Java - NKK1		Central Java	7°73844'S	110°18574'E	-2.14	Coxall et al. (in prep.)		*Turborotalia ampliapertura*	*Turborotalia ampliapertura*	2	-3.38042178	glassy
Java - NKK1		Central Java	7°73844'S	110°18574'E	-2.14	Coxall et al. (in prep.)		*Turborotalia ampliapertura*	*Turborotalia ampliapertura*	2	-2.949522553	glassy
Java - NKK1		Central Java	7°73844'S	110°18574'E	-2.14	Coxall et al. (in prep.)		*Turborotalia ampliapertura*	*Turborotalia ampliapertura*	2	-3.26891083	glassy
Java - NKK1		Central Java	7°73844'S	110°18574'E	-2.14	Coxall et al. (in prep.)		*Turborotalia ampliapertura*	*Turborotalia ampliapertura*	2	-2.982346912	glassy
Java - NKK1		Central Java	7°73844'S	110°18574'E	-2.14	Coxall et al. (in prep.)		*Turborotalia ampliapertura*	*Turborotalia ampliapertura*	2	-3.324272955	glassy
Java - NKK1		Central Java	7°73844'S	110°18574'E	-2.14	Coxall et al. (in prep.)		*Turborotalia ampliapertura*	*Turborotalia ampliapertura*	2	-3.0250474	glassy
Java - NKK1		Central Java	7°73844'S	110°18574'E	-2.14	Coxall et al. (in prep.)		*Turborotalia ampliapertura*	*Turborotalia ampliapertura*	2	-3.309543712	glassy

Java - NKK1		Central Java	7°73844'S	110°18574'E	-2.14	Coxall et al. (in prep.)		*Turborotalia ampliapertura*	*Turborotalia ampliapertura*	2	-3.251697 533	glas sy
Java - NKK1		Central Java	7°73844'S	110°18574'E	-2.14	Coxall et al. (in prep.)		*Turborotalia ampliapertura*	*Turborotalia ampliapertura*	2	-3.957251 072	glas sy
Java - NKK1		Central Java	7°73844'S	110°18574'E	-2.14	Coxall et al. (in prep.)		*Turborotalia ampliapertura*	*Turborotalia ampliapertura*	2	-4.548014 32	glas sy
Java - NKK1		Central Java	7°73844'S	110°18574'E	-2.14	Coxall et al. (in prep.)		*Turborotalia ampliapertura*	*Turborotalia ampliapertura*	2	-2.950	glas sy
Java - NKK1		Central Java	7°73844'S	110°18574'E	-2.14	Coxall et al. (in prep.)		*Turborotalia ampliapertura*	*Turborotalia ampliapertura*	2	-3.957	glas sy
Java - NKK1		Central Java	7°73844'S	110°18574'E	-2.14	Coxall et al. (in prep.)		*Turborotalia ampliapertura*	*Turborotalia ampliapertura*	2	-3.269	glas sy
Java - NKK1		Central Java	7°73844'S	110°18574'E	-2.14	Coxall et al. (in prep.)		*Turborotalia ampliapertura*	*Turborotalia ampliapertura*	2	-4.142	glas sy
Java - NKK1		Central Java	7°73844'S	110°18574'E	-2.14	Coxall et al. (in prep.)		*Turborotalia ampliapertura*	*Turborotalia ampliapertura*	2	-3.328	glas sy
Java - NKK1		Central Java	7°73844'S	110°18574'E	-2.14	Coxall et al. (in prep.)		*Turborotalia ampliapertura*	*Turborotalia ampliapertura*	2	-3.380	glas sy

	Java - NKK1		Central Java	7°73844'S	110°18574'E	-2.14	Coxall et al. (in prep.)		*Turborotalia ampliapertura*	*Turborotalia ampliapertura*	2	-4.548	glassy
	SSQ	Wade et al., 2011 so it's correct as it's an update biozone system	St. Stephens Quarry corehole, Alabama	31°33'N	88°02'W	28.1	Wade et al., 2012, Supplementary Information	32.662	*P. naguewichiensis*	*P. naguewichiensis*	1	-1.15	
	SSQ	Wade et al., 2011 so it's correct as it's an update biozone system	St. Stephens Quarry corehole, Alabama	31°33'N	88°02'W	28.1	Wade et al., 2012, Supplementary Information	32.725	*P. naguewichiensis*	*P. naguewichiensis*	1	-1.14	
	SSQ	Wade et al., 2011 so it's correct as it's an update biozone system	St. Stephens Quarry corehole, Alabama	31°33'N	88°02'W	28.1	Wade et al., 2012, Supplementary Information	32.725	*Turborotalia ampliapertura*	*Turborotalia ampliapertura*	2	-1.03	
	SSQ	Wade et al., 2011 so it's correct as it's an update biozone system	St. Stephens Quarry corehole, Alabama	31°33'N	88°02'W	28.1	Wade et al., 2012, Supplementary Information	32.782	*P. naguewichiensis*	*P. naguewichiensis*	1	-1.1	
	SSQ	Wade et al., 2011 so it's correct as it's an update	St. Stephens Quarry corehole, Alabama	31°33'N	88°02'W	28.1	Wade et al., 2012, Supplementary Information	32.782	*Turborotalia ampliapertura*	*Turborotalia ampliapertura*	2	-1.1	

		biozone system										
	SSQ	Wade et al., 2011 so it's correct as it's an update biozone system	St. Stephens Quarry corehole, Alabama	31°33'N	88°02'W	28.1	Wade et al., 2012, Supplementary Information	32.819	*P. naguewichiensis*	*P. naguewichiensis*	1	-1.44
	SSQ	Wade et al., 2011 so it's correct as it's an update biozone system	St. Stephens Quarry corehole, Alabama	31°33'N	88°02'W	28.1	Wade et al., 2012, Supplementary Information	33.013	*P. naguewichiensis*	*P. naguewichiensis*	1	-1.42
	SSQ	Wade et al., 2011 so it's correct as it's an update biozone system	St. Stephens Quarry corehole, Alabama	31°33'N	88°02'W	28.1	Wade et al., 2012, Supplementary Information	33.013	*Turborotalia ampliapertura*	*Turborotalia ampliapertura*	2	-1.63
	SSQ	Wade et al., 2011 so it's correct as it's an update biozone system	St. Stephens Quarry corehole, Alabama	31°33'N	88°02'W	28.1	Wade et al., 2012, Supplementary Information	33.067	*P. naguewichiensis*	*P. naguewichiensis*	1	-1.32
	SSQ	Wade et al., 2011 so it's correct as it's an update	St. Stephens Quarry corehole, Alabama	31°33'N	88°02'W	28.1	Wade et al., 2012, Supplementary Information	33.12	*P. naguewichiensis*	*P. naguewichiensis*	1	-1.35

		biozone system										
	SSQ	Wade et al., 2011 so it's correct as it's an update biozone system	St. Stephens Quarry corehole, Alabama	31°33'N	88°02'W	28.1	Wade et al., 2012, Supplementary Information	33.131	*P. naguewichiensis*	*P. naguewichiensis*	1	-1.44
	SSQ	Wade et al., 2011 so it's correct as it's an update biozone system	St. Stephens Quarry corehole, Alabama	31°33'N	88°02'W	28.1	Wade et al., 2012, Supplementary Information	33.131	*Turborotalia ampliapertura*	*Turborotalia ampliapertura*	2	-0.82
	SSQ	Wade et al., 2011 so it's correct as it's an update biozone system	St. Stephens Quarry corehole, Alabama	31°33'N	88°02'W	28.1	Wade et al., 2012, Supplementary Information	33.144	*P. naguewichiensis*	*P. naguewichiensis*	1	-1.4
	SSQ	Wade et al., 2011 so it's correct as it's an update biozone system	St. Stephens Quarry corehole, Alabama	31°33'N	88°02'W	28.1	Wade et al., 2012, Supplementary Information	33.144	*Turborotalia ampliapertura*	*Turborotalia ampliapertura*	2	-1.69
	SSQ	Wade et al., 2011 so it's correct as it's an update	St. Stephens Quarry corehole, Alabama	31°33'N	88°02'W	28.1	Wade et al., 2012, Supplementary Information	33.165	*P. naguewichiensis*	*P. naguewichiensis*	1	-1.26

		biozone system											
	SSQ	Wade et al., 2011 so it's correct as it's an update biozone system	St. Stephens Quarry corehole, Alabama	31°33'N	88°02'W	28.1	Wade et al., 2012, Supplementary Information	33.165	*Turborotalia ampliapertura*	*Turborotalia ampliapertura*	2	-0.89	
	SSQ	Wade et al., 2011 so it's correct as it's an update biozone system	St. Stephens Quarry corehole, Alabama	31°33'N	88°02'W	28.1	Wade et al., 2012, Supplementary Information	33.187	*P. naguewichiensis*	*P. naguewichiensis*	1	-1.37	
	U1334		~100 km north of the Clipperton Fracture Zone on abyssal hill topography draped with ~280 m sediment	7°59.998′ N	131°58.408′W	-0.24	Moore et al., 2014		*C. unicavus*	*Catapsydrax unicavus*	3	1.8	
	U1334		~100 km north of the Clipperton Fracture Zone on abyssal hill topography draped with ~280	7°59.998′ N	131°58.408′W	-0.24	Moore et al., 2014		*C. unicavus*	*Catapsydrax unicavus*	3	1.55	

		m sediment									
	U1334		~100 km north of the Clipperton Fracture Zone on abyssal hill topography draped with ~280 m sediment	7°59.998′ N	131°58.408′W	-0.24	Moore et al., 2014		*C. unicavus*	*Catapsydrax unicavus*	3	1.65
	U1334		~100 km north of the Clipperton Fracture Zone on abyssal hill topography draped with ~280 m sediment	7°59.998′ N	131°58.408′W	-0.24	Moore et al., 2014		*C. unicavus*	*Catapsydrax unicavus*	3	1.8
	U1334		~100 km north of the Clipperton Fracture Zone on abyssal hill topography draped with ~280 m sediment	7°59.998′ N	131°58.408′W	-0.24	Moore et al., 2014		*C. unicavus*	*Catapsydrax unicavus*	3	1.7

	U1334		~100 km north of the Clipperton Fracture Zone on abyssal hill topography draped with ~280 m sediment	7°59.998′ N	131°58.408′W	- 0.24	Moore et al., 2014		*C. unicavus*	*Catapsydrax unicavus*	3	1.5	
	U1334		~100 km north of the Clipperton Fracture Zone on abyssal hill topography draped with ~280 m sediment	7°59.998′ N	131°58.408′W	- 0.24	Moore et al., 2014		*C. unicavus*	*Catapsydrax unicavus*	3	2	
	U1334		~100 km north of the Clipperton Fracture Zone on abyssal hill topography draped with ~280 m sediment	7°59.998′ N	131°58.408′W	- 0.24	Moore et al., 2014		*C. unicavus*	*Catapsydrax unicavus*	3	1.3	
	U1334		~100 km north of the Clipperton Fracture Zone on abyssal hill	7°59.998′ N	131°58.408′W	- 0.24	Moore et al., 2014		*C. unicavus*	*Catapsydrax unicavus*	3	1.3	

			topography draped with ~280 m sediment										
	U1334		~100 km north of the Clipperton Fracture Zone on abyssal hill topography draped with ~280 m sediment	7°59.998′N	131°58.408′W	-0.24	Moore et al., 2014		*C. unicavus*	*Catapsydrax unicavus*	3	1.5	
	U1334		~100 km north of the Clipperton Fracture Zone on abyssal hill topography draped with ~280 m sediment	7°59.998′N	131°58.408′W	-0.24	Moore et al., 2014		*C. unicavus*	*Catapsydrax unicavus*	3	1.65	
	U1334		~100 km north of the Clipperton Fracture Zone on abyssal hill topography draped with ~280 m sediment	7°59.998′N	131°58.408′W	-0.24	Moore et al., 2014		*C. unicavus*	*Catapsydrax unicavus*	3	1.5	

U1334		~100 km north of the Clipperton Fracture Zone on abyssal hill topography draped with ~280 m sediment	7°59.998′N	131°58.408′W	-0.24	Moore et al., 2014		*C. unicavus*	*Catapsydrax unicavus*	3	1.7	
U1334		~100 km north of the Clipperton Fracture Zone on abyssal hill topography draped with ~280 m sediment	7°59.998′N	131°58.408′W	-0.24	Moore et al., 2014		*C. dissimilis*	*Catapsydrax dissimilis*	3	1.8	
U1334		~100 km north of the Clipperton Fracture Zone on abyssal hill topography draped with ~280 m sediment	7°59.998′N	131°58.408′W	-0.24	Moore et al., 2014		*C. dissimilis*	*Catapsydrax dissimilis*	3	1.5	
U1334		~100 km north of the Clipperton Fracture Zone on abyssal hill	7°59.998′N	131°58.408′W	-0.24	Moore et al., 2014		*Subbotina utilisindex*	*Subbotina utilisindex*	3	0.82	

		topography draped with ~280 m sediment									
	U1334		~100 km north of the Clipperton Fracture Zone on abyssal hill topography draped with ~280 m sediment	7°59.998′N	131°58.408′W	-0.24	Moore et al., 2014		*Subbotina utilisindex*	*Subbotina utilisindex*	3	0.85
	U1334		~100 km north of the Clipperton Fracture Zone on abyssal hill topography draped with ~280 m sediment	7°59.998′N	131°58.408′W	-0.24	Moore et al., 2014		*Subbotina utilisindex*	*Subbotina utilisindex*	3	1.7
	U1334		~100 km north of the Clipperton Fracture Zone on abyssal hill topography draped with ~280 m sediment	7°59.998′N	131°58.408′W	-0.24	Moore et al., 2014		*Turborotalia ampliapertura*	*Turborotalia ampliapertura*	2	0.092

U1334		~100 km north of the Clipperton Fracture Zone on abyssal hill topography draped with ~280 m sediment	7°59.998′N	131°58.408′W	-0.24	Moore et al., 2014		*Turborotalia ampliapertura*	*Turborotalia ampliapertura*	2	0.3
U1334		~100 km north of the Clipperton Fracture Zone on abyssal hill topography draped with ~280 m sediment	7°59.998′N	131°58.408′W	-0.24	Moore et al., 2014		*Turborotalia ampliapertura*	*Turborotalia ampliapertura*	2	0.37
U1334		~100 km north of the Clipperton Fracture Zone on abyssal hill topography draped with ~280 m sediment	7°59.998′N	131°58.408′W	-0.24	Moore et al., 2014		*Turborotalia ampliapertura*	*Turborotalia ampliapertura*	2	0.12
U1334		~100 km north of the Clipperton Fracture Zone on abyssal hill	7°59.998′N	131°58.408′W	-0.24	Moore et al., 2014		*Turborotalia ampliapertura*	*Turborotalia ampliapertura*	2	-0.05

			topography draped with ~280 m sediment									
	U1334		~100 km north of the Clipperton Fracture Zone on abyssal hill topography draped with ~280 m sediment	7°59.998′N	131°58.408′W	-0.24	Moore et al., 2014		*Turborotalia ampliapertura*	*Turborotalia ampliapertura*	2	-0.25
	U1334		~100 km north of the Clipperton Fracture Zone on abyssal hill topography draped with ~280 m sediment	7°59.998′N	131°58.408′W	-0.24	Moore et al., 2014		*Turborotalia ampliapertura*	*Turborotalia ampliapertura*	2	0.45
	U1334		~100 km north of the Clipperton Fracture Zone on abyssal hill topography draped with ~280 m sediment	7°59.998′N	131°58.408′W	-0.24	Moore et al., 2014		*Turborotalia ampliapertura*	*Turborotalia ampliapertura*	2	0.45

U1334		~100 km north of the Clipperton Fracture Zone on abyssal hill topography draped with ~280 m sediment	7°59.998′N	131°58.408′W	-0.24	Moore et al., 2014		*D. venezuelana*	*Dentoglobigerina venezuelana*	3	0.45
U1334		~100 km north of the Clipperton Fracture Zone on abyssal hill topography draped with ~280 m sediment	7°59.998′N	131°58.408′W	-0.24	Moore et al., 2014		*D. venezuelana*	*Dentoglobigerina venezuelana*	3	-0.1
U1334		~100 km north of the Clipperton Fracture Zone on abyssal hill topography draped with ~280 m sediment	7°59.998′N	131°58.408′W	-0.24	Moore et al., 2014		*D. venezuelana*	*Dentoglobigerina venezuelana*	3	0.3
U1334		~100 km north of the Clipperton Fracture Zone on abyssal hill	7°59.998′N	131°58.408′W	-0.24	Moore et al., 2014		*D. venezuelana*	*Dentoglobigerina venezuelana*	3	0

		topograph y draped with ~280 m sediment										
	U1334		~100 km north of the Clipperton Fracture Zone on abyssal hill topograph y draped with ~280 m sediment	7°59.998′ N	131°58.40 8′W	- 0.24	Moore et al., 2014		*D. venezuelana*	*Dentoglobigerin a venezuelana*	3	0.6
	U1334		~100 km north of the Clipperton Fracture Zone on abyssal hill topograph y draped with ~280 m sediment	7°59.998′ N	131°58.40 8′W	- 0.24	Moore et al., 2014		*D. venezuelana*	*Dentoglobigerin a venezuelana*	3	-0.1
	U1334		~100 km north of the Clipperton Fracture Zone on abyssal hill topograph y draped with ~280 m sediment	7°59.998′ N	131°58.40 8′W	- 0.24	Moore et al., 2014		*D. venezuelana*	*Dentoglobigerin a venezuelana*	3	-0.3

		U1334		~100 km north of the Clipperton Fracture Zone on abyssal hill topography draped with ~280 m sediment	7°59.998′N	131°58.408′W	-0.24	Moore et al., 2014		*D. venezuelana*	*Dentoglobigerina venezuelana*	3	-0.3	
		U1334		~100 km north of the Clipperton Fracture Zone on abyssal hill topography draped with ~280 m sediment	7°59.998′N	131°58.408′W	-0.24	Moore et al., 2014		*D. venezuelana*	*Dentoglobigerina venezuelana*	3	-0.27	
		U1334		~100 km north of the Clipperton Fracture Zone on abyssal hill topography draped with ~280 m sediment	7°59.998′N	131°58.408′W	-0.24	Moore et al., 2014		*D. venezuelana*	*Dentoglobigerina venezuelana*	3	-0.05	
		U1334		~100 km north of the Clipperton Fracture Zone on abyssal hill	7°59.998′N	131°58.408′W	-0.24	Moore et al., 2014		*D. venezuelana*	*Dentoglobigerina venezuelana*	3	-0.05	

		topograph y draped with ~280 m sediment										
U1334		~100 km north of the Clipperton Fracture Zone on abyssal hill topograph y draped with ~280 m sediment	7°59.998′ N	131°58.40 8′W	- 0.24	Moore et al., 2014		*Subbotina eocaena*	*Dentoglobigerin a venezuelana*	3	1.47	